SYNTHESIS AND EVALUATION OF MULTITARGET ANTIBIOTIC ARMENIASPIROL AND ANALOGUES

Michael Darnowski

A Thesis Submitted in Partial Fulfillment
of the Requirements for the Degree of

Doctorate in Philosophy in Chemistry

Department of Chemistry and Biomolecular Sciences

Faculty of Science

University of Ottawa

Supervisor: Christopher N. Boddy

Examining Board: Jeffrey Keillor, PhD, Chemistry and Biomolecular Science
Tony Durst, PhD, Chemistry and Biomolecular Science
Fabien Gagosz, PhD, Chemistry and Biomolecular Science

External Examiner: Chris Vanderwal, PhD, Chemistry, UC Irvine

April 2023

ABSTRACT

Antimicrobial resistance is a human health issue that demands development of new antibiotics with unique mechanisms of action to combat antibiotic failure in the clinic. Methicillin-resistant *Staphylococcus aureus* (MRSA) has emerged as a particular resistant pathogen associated with high levels of incidence and mortality. Isolation and structural elucidation of the antibiotic natural products armeniaspirols A-C was first reported in 2012 by Sanofi. Armeniaspirol possess an unprecedented scaffold and novel multiple mechanisms of action. For these reasons the armeniaspirols were an ideal scaffold to investigate for the development of antibiotics effective against current resistant pathogens.

A series of focused derivatives were synthesized and evaluated for antibiotic activity against clinically relevant pathogens including methicillin-resistant *Staphylococcus aureus* and vancomycin-resistant *Enterococcus*. Replacement of the *N*-methyl with *N*-hexyl and various *N*-benzyl substituents lead to a substantial increase in antibiotic activity and potency for inhibition of both ClpYQ and ClpXP, the intracellular targets of armeniaspirol.

Armeniaspirol is also known to disrupt the proton motive force (PMF) in bacteria, though initial work by the Brönstrup lab suggested this was via shuttling of protons across the membrane. With a library of analogues in hand from our previous study, we sought to characterize their disruption of the PMF. Using a voltage sensitive dye-based assay and checkerboard synergy-based assay we demonstrated that armeniaspirols disrupt the proton motive force by dissipating the electrical potential ($\Delta\Psi$) of the PMF, correcting the previous literature, which suggested they disrupted the transmembrane proton gradient (ΔpH).

Lastly, our efforts toward the total synthesis of armeniaspirol A using an oxidative chlorination transformation led to a constitutional isomer of armeniaspirol by an unexpected

Lewis acid mediated rearrangement in the penultimate step. We characterized the scope of carbonyl derivatives that could undergo successful oxidation generating the key α,β-dichloro-α,β-unsaturated lactam of the armeniaspirol scaffold. Our work led to a mechanistic study demonstrating how simple ketones undergo decomposition via acylium ion formation whereas esters and amides are effectively oxidized to the desired product.

Overall, the research presented here lays the foundation for the future work to confirm safety, efficacy, and toxicity of the armeniaspirols and to synthesize new analogues with improved drug like characteristics. In addition, this thesis previews an evolution-based link between armeniaspirol and its biosynthetic precursor that suggests mid- to late-stage biosynthetic intermediates are likely to possess biological activity but via a different mechanism of action as compared to the parent natural products. Furthermore, this analysis suggests that the intermediate is likely to synergize with the natural product, increasing the fitness of the producing organism as the pathway evolves.

DEDICATION

To George, Sheila, and Robert Darnowski

ACKNOWLEDGEMENTS

It is an absolute pleasure to express my gratitude to the many people who made the completion of this degree possible. First, I must acknowledge my Ph.D. supervisor, Professor Christopher Boddy. I can't imagine completing my PhD with anyone else. You constantly inspire me to be a better scientist and I have never met a more intelligent, curious, and passionate person than you. You allowed me to be myself in every way throughout my degree and for that I can't thank you enough. It is truly a pleasure to have spent the last 4.5 years in your lab. I will always look back on the time I spent in the Boddy lab fondly. I would also like to thank Tony Durst for giving me my first opportunity in a chemistry lab. Your constant encouragement and enthusiasm for research as well as belief in me was a driving force for me attending grad school.

I must also acknowledge all my colleagues in the Boddy Lab, past and present. Thank you for your support. I was very fortunate to work in an environment where there were always people willing and eager to help each other. This degree wouldn't have been possible without the friendship and working alongside André Paquette, Nick Calvert and Eric Gates every day. It made going through grad school easier knowing you guys were by my side. I must also thank Taylor Lanosky, your passion and work ethic were instrumental in finishing so many of the projects that we worked on together.

To my friends outside of science, Jake, Josh, and Mason, you made grad school so much better knowing that no matter how my day went, I had such a supportive and fun group of guys to come home to every day. To Rob and Jess, you have made living in Ottawa for the last 10 years feel like home for me. To George and Sheila, even though you have no idea what the hell I'm doing, your unwavering support for the last ten tears of school has meant the world to me.

Table of Contents

ABSTRACT ii
DEDICATION iv
ACKNOWLEDGEMENTS v
Table of Contents vi
List of Tables ix
List of Figures x
Chapter 1: Introduction 1

1.1 Antimicrobial resistance 1

1.2 Natural product antibiotics 3

1.3 Armeniaspirol discovery and initial pharmacological characterization 6

1.4 Armeniaspirol competitively inhibits ClpXP and ClpYQ 9

1.5 Total synthesis of Armeniasprol and ability to depolarizes cell membranes of Gram-positive bacteria 11

1.6 Thesis overview and Goals Summary and conclusion/ and outlook 16

1.7 References 18

Chapter 2: Armeniaspirol analogues with more potent Gram-positive antibiotic activity show enhanced inhibition of the ATP-dependent proteases ClpXP and ClpYQ 23

2.1 Introduction 23

2.2 References 25

2.4 Copyright 26

2.5 Armeniaspirol analogues with more potent Gram-positive antibiotic activity show enhanced inhibition of the ATP-dependent proteases ClpXP and ClpYQ 27

2.6 Supporting Information 50

Chapter 3: Armeniaspirol analogues disrupt the electrical potential (ΔΨ) of the proton motive force. 139

3.1 Introduction 139

3.2 References 141

3.3 Author contributions 142

3.4 Copyright 142

3.5 Armeniaspirol analogues disrupt the electrical potential (ΔΨ) of the proton motive force. 143

3.6 Supporting Information 155

Chapter 4: Synthesis of a Constitutional Isomer of Armeniaspirol A, Pseudoarmeniaspirol A, via Lewis Acid-Mediated Rearrangement 176

4.1 Introduction 176

4.2 References 177

4.3 Author contributions 178

4.4 Copyright 178

4.5 Synthesis of a constitutional isomer of armeniaspirol A, pseudoarmeniaspirol A, via Lewis acid-mediated rearrangement 179

4.6 Supporting information 196

Chapter 5: Conclusions and future directions 369

5.1 Overview 369

5.2 State of armeniaspirol antibiotic development and outlook 370

5.2 Total synthesis outlook 373

5.3 Perspective on the evolution and genesis of armeniaspirol 377

5.4 Conclusions 379

5.5 References 379

Appendix I: Copyright information and manuscripts 384

List of Tables

RSCMC Table 1.	MIC evaluation of analogues 1–14 against a panel of Gram positive and negative bacteria	34
RSCMC Table 2	Kinetic parameters of potent analogues	35
BMCL Table 1	Antibiotic, membrane disruption, and physicochemical properties of analogs.	149
JOC Table 1	Scope of NCS-Mediated Chlorination of Pyrrole 2- Carbonyl Compounds	183
JOC Table 2.	Biological Evaluation of Constitutional Isomers of Armeniaspirol	191

List of Figures

Figure 1.1.	Structures and mechanisms of action of last line of defense treatment of MRSA infections and three examples of current antibiotics that MRSA has developed resistance to.	2
Figure 1.2	Timeline of natural product antibiotic discovery. Highlighting the golden era of antibiotics and the lag phase from the 1980s onwards.	4
Figure 1.3	Source of FDA approved antibiotics highlighting prominence of natural products as antibiotic therapeutics.	5
Figure 1.4	Source of FDA approved antibiotics highlighting prominence of natural products as antibiotic therapeutics.	8
Figure 1.5	Armeniaspirol inhibits cellular AAA+ proteases ClpXP and ClpYQ competitively to cause cell division arrest.	10
Figure 1.6	Structure of select potent halopyrrole antibiotics which function as protonophores and the proposed biosynthetic precursor of armeniaspirol.	12
Figure 1.7.	Synthesis of armeniaspirol by Arsetti *et al.*	14
Figure 2.1	Figure 2.1 Preliminary SAR studies and new targeted areas for SAR	23
Figure 2.2	Improved inhibition of protein targets ClpXP and ClpYQ by armeniaspirol led to improved antibiotic activity in gram positive pathogens. Armeniaspirol diversification points studied are highlighted in blue.	24
Figure RSCMC-1	Analogues of armeniaspirol to probe antibiotic activity via inhibition of ClpXP and ClpYQ	28
Figure RSCMC-2	Armeniaspirol analogues	32
Figure RSCMC-3	Structure and docking results of S. aureus ClpP (3V5E).	40
Figure RSCMC-4	Structure and docking results of S. aureus ClpQ (6KUI).	42
Figure 3.1	Armeniaspirols rely on disruption of both the PMF and intracellular targets for potent antibiotic activity.	140
Figure BMCL-1	The structure of the armeniaspirol analogues investigated in this study.	143
Figure BMCL-2	**1** dissipates $\Delta\Psi$, not ΔpH	145
Figure 4.1	Oxidative chlorination of pyrrole-2-carbonyls used for attempted synthesis of armeniaspirol	177
Figure JOC-1.	(A) Structures of (±)-pseudoarmeniaspirol A, 1, and (±)-armeniaspirol A, 2. (B) NCS-mediated oxidative chlorination used to generate the skeleton of armeniaspirol along with undesired chlorination at the 5 position. (C) Previous retrosynthetic disconnection of (±)-armeniaspirol A.	181
Figure JOC-2.	Retrosynthetic analysis of (±)-pseudoarmeniaspirol A from early stage oxidation of the pyrrole moiety	182
Figure JOC-3.	(A) Productive ketone oxidative chlorination via intramolecular phenol trapping. (B) Fate of protected phenol in the armeniaspirol system. (C) Fate of pyrrole carboxylic acid derivative under oxidative chlorination conditions. (D) Mechanistic proposal for C–C bond fragmentation when R = alkyl. C–C bond fragmentation does not occur when R = NHR′ or R = OR.	186

Figure JOC-4.	Proposed mechanism of pyrrole ketone oxidative chlorination on the route to (±)- chloro-armeniaspirol	188
Figure JOC-5.	(A) Route to synthesis of (±)-pseudoarmeniaspirol. (B) Proposed Lewis acid-mediated skeletal rearrangement leading to the pseudoarmeniaspirol skeleton. (C) Key HMBC correlation in structure elucidation. (D) Analogues of pseudoarmeniaspirol.	189
Figure 5.1	Design of second-generation aryl analogues of armeniaspirol	371
Figure 5.2	Potential future analogues of armeniaspirol with improved clogP values	373
Figure 5.3	Boger and Wassermans oxidation of pyrrole using singlet oxygen.	374
Figure 5.4	Synthesis of des-chloroarmeniaspirol using singlet oxygen	374
Figure 5.5	Attempts using 3,4 chlorinated pyrroles to access armeniaspirol.	376
Figure 5.6	Biosynthesis of armeniaspirol containing potent antibiotic precursors	378

Chapter 1: Introduction

1.1 Antimicrobial resistance

Antimicrobial resistance is the occurrence of change within a microorganism that causes common drugs treatments to become ineffective. This results in bacterial strains that continue to grow despite the presence of previously effective antibiotics[1]. This phenomenon arises due to horizontal gene transfer as well as rapid rates of genetic mutations when bacteria are subjected to selection pressures by the addition of a drug. The evolutionary pressure rapidly selects for the resistant mutants enabling this mutation to become fixed in the population[2,3].

Some of the highest risk pathogens associated with antimicrobial resistance have been deemed the 'ESKAPE' pathogens. This includes *Enterococcus faecium*, *Staphylococcus aureus*, *Klebsiella pneumoniae*, *Acinetobacter baumannii*, *Pseudomonas aeruginosa* and *Enterobacter spp*[4]. A review of clinical and economic burdens reports that the ESKAPE pathogens are associated with the highest risk of mortality and greater economic costs[5]. The report estimated that 10 million deaths will be attributed to antimicrobial resistance by 2050, and 100 trillion USD of the world's economic outputs will be lost if substantive efforts are not made to contain this threat[4–6].

Methicillin-resistant *Staphylococcus aureus* (MRSA), has emerged as a significant pathogen associated with high levels of morbidity and mortality[7,8]. Government initiatives and programs have been put in place for the continued tracking and monitoring of new resistant strains of MRSA[9]. Recently, new MRSA strains have emerged with resistance as well as lower susceptibility to vancomycin and daptomycin, the current frontline treatment for MRSA infections[10]. As MRSA is resistant to nearly all β-lactam antibiotics, some fluoroquinolone

(levofloxacin), aminoglycosides (kanamycin), and macrolide antibiotics (erythromycin),[8,9,11] few treatment options remain for clinicians to treat these pathogens.

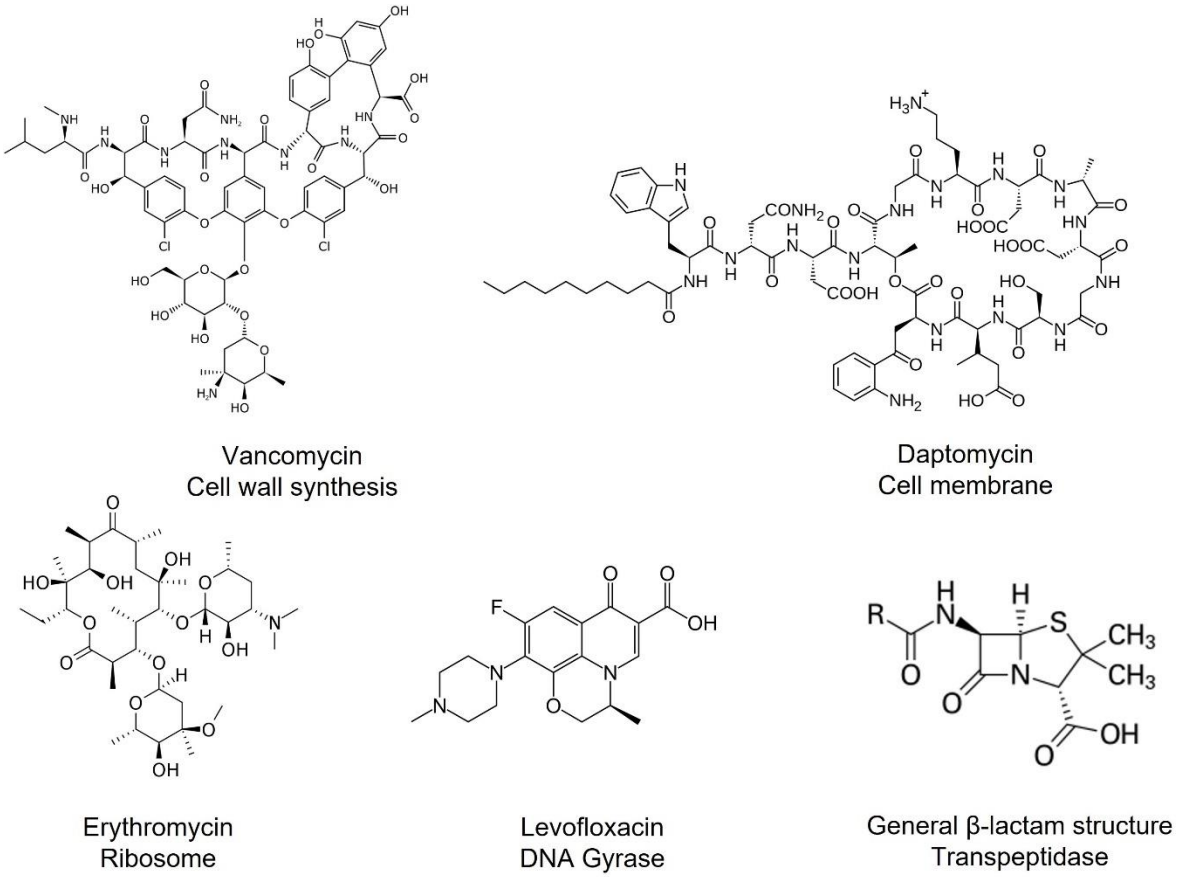

Figure 1.1 Structures and mechanisms of action of last line of defense treatment of MRSA infections and three examples of current antibiotics that MRSA has developed resistance to.

The increased prevalence of antimicrobial resistance (and more resistant organisms being discovered in the clinic) is compounded by the sharp decrease in output of new antibiotic therapeutics from the pharmaceutical industry[12]. Many major companies in the pharmaceutical industry including Novartis, AstraZeneca and Sanofi have closed their antibiotic research programs all together, with Johnson and Johnson (Janssen) the most recent as of February

2023[13]. This comes as little surprise as the cost to develop a drug from a hit compound is generally approximated at close to 1 billion dollars. With antibiotic treatments being single use and having short-term longevity in the clinic due to the rapid emergence of resistance, there are low recovery rates of investment capital and decreased profitability for companies developing antibiotics. This can be seen with the recent example plazomicin, an aminoglycoside derivative that was approved by the FDA in 2018. Achaogen, the company that developed the drug, filed for bankruptcy in 2019 after sales amounted to roughly $80 million dollars, less than one tenth the cost required to bring the drug to market[14].

With rising rates of antimicrobial resistance and decreased pharma presence in the field, a large portion of new antibiotic discovery and development has been placed on the shoulders of academia. Academia now plays a vital role in uncovering both clinically and chemically unique antibiotics that engage new targets to develop therapeutics to combat the threat that multidrug resistant pathogens pose.

1.2 Natural product antibiotics

With the clear need and challenges for antibiotic development highlighted above, a new approach to the problem must be taken. Natural products have been at the forefront of treating antibiotic infections for almost a century, since the discovery of penicillin G in 1928. The "golden age" of antibiotics, from the 1940s to the 1960s, saw over 30 new classes of antibiotics (Figure 1.2) discovered and brought to the clinic[15,16]. The majority of these therapeutic compounds were natural products or of natural product origin (Figure 1.3). Following the "Golden age", synthetic second-generation derivatives were developed that were aimed at improving these natural products' clinical efficacy. During this lag phase, few new classes of

antibiotics were brought to the clinic. Recently, antibiotic research has fallen even further behind as the current antibiotic pipeline is saturated with drug candidates that share substantial structural homology (third and fourth generations) or are in the same class as known antibiotics.

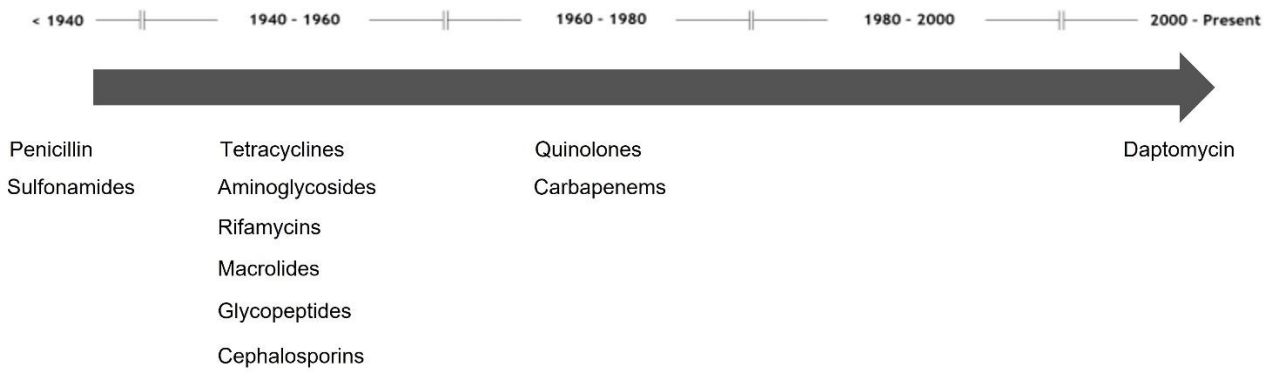

Figure 1.2 Timeline of natural product antibiotic discovery. Highlighting the golden era of antibiotics and the lag phase from the 1980s onwards.

Classes of antibiotics that share distinct structural features often function with similar mechanisms of actions. This often enables resistant bacteria to rapidly evade new developed compounds if they are based on a known scaffold and have a conserved mechanism of action[3]. While 2013-2017 represented an uptick in the number of antibiotics approved by the Food and Drug Administration (FDA), with seven new antibiotics approved, none of these possessed a new mechanism of action[17]. Antibiotics with new or privileged targets that causes resistance to arise at a much slower rate is clearly needed.

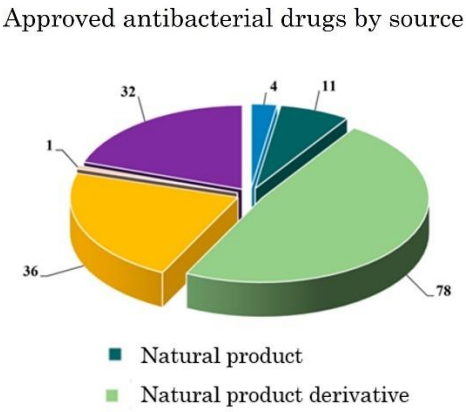

Figure 1.3 Source of FDA approved antibiotics highlighting prominence of natural products as antibiotic therapeutics[17].

Recent advancements in natural product discovery are helping to spur new antibiotic development. For example, a novel cultivation technique coined the iChip enables growth of previously uncultivatable soil bacteria in situ such that the appropriate nutrients and growth factors are present has enabled many new genera of bacteria to be discovered[18]. As current estimates suggest only 1% of bacterial diversity is cultivatable in the lab, this technology opens the door to growing orders of magnitude more bacterial strains, including many that are rich in secondary metabolites. As a proof of principle, this approach was used to discover teixobactin from the previously uncharacterized bacteria *Eleftheria terrae*[18]. Teixobactin is a potent Gram-positive antibiotic, active against MRSA, vancomycin resistant *E. faecalis* (VRE) and penicillin resistant *S. pneumoniae* (PRSP). It displays a similar mechanism of vancomycin by binding to lipid II, a precursor to peptidoglycan. As it binds to a bacterial cell wall building block that is not directly encoded in the genome, development of resistance mutants is much slower, as has been seen for vancomycin.

Another recent approach in drug discovery research has come in the form of polypharmacology. Polypharmacology is the design or use of pharmaceutical agents that act on multiple targets or disease pathways. This trait was deemed undesirable for many years in industry due to concerns over off-target activity leading to toxicity issues[19]. This led to most drug development programs focused on a "one target-one molecule" approach. However, a data mining analysis suggested that each drug with a natural product origin interacts with 2-7 targets[20]. This inherent polypharmacolgy is likely built into natural products as they have been selected for through evolution for desirable biological interactions across a wide spread of organisms. Over half of approved antibiotics since 2015 have multitarget mechanisms of action, likely stemming from the drugs' natural product origins[21]. Polypharmacology may provide a new attractive avenue for the development of antibiotic therapeutics for two reasons. First, resistance will arise at a lower rate since concurrent mutations in multiple targets, which is statistically improbable, is required for resistance[20]. Secondly, inhibiting multiple cellular processes within a cell can lead to synergism, improving potency[22]. These two factors create an intriguing avenue to pursue natural products as a viable option in combatting antimicrobial resistance due to increased potency with multiple cellular targets and lower likelihood of resistance developing.

1.3 Armeniaspirol discovery and initial pharmacological characterization

Isolation and structural elucidation of armeniaspirols A-C was first reported in 2012 by the now defunct Sanofi antibiotic discovery team[23]. Monitoring the metabolite profiles of the growth on ISP-2 by HPLC, the authors describe the emergence of three new peaks in the methanolic extracts of the crude broth. Each peak was collected using preparatory HPLC and analyzed using a suite of NMR, computer aided NMR simulations, mass spectrometry and X-ray

crystallography. This computer-assisted structure elucidation method (CASE) used ^{1}H and ^{13}C chemical shifts, multiplicities, carbon hybridization state, as well as COSY, HSQC and HMBC connectivities to build a molecular connectivity diagram (MCD). A total of 19834 molecules were generated using MCD, which was narrowed down to 9 molecules when checked against chemical feasibility, ring rules, and chemical formula. An extra CASE method using predicted ^{13}C-spectra were used to compare predicted and experimental spectra where the best match resulted in the structure of armeniaspirol. All three structures of armeniaspirols A-C containing the unprecedented spiro-[4.4]non-8-ene skeleton were then confirmed by X-ray crystallography, which also confirmed the *R* stereochemistry contained in the natural product[23].

Biological evaluation of armeniaspirol A-C showed them to be potent Gram-positive antibiotics effective against bacteria including MRSA, PRSP, and VRE. In addition to their potency, no resistant *S. aureus* mutants could be detected even after 30 serial passages with subtherapeutic levels of the compounds. Armeniaspirol A-C showed no inhibition of Gram-negative pathogens (*E. coli* or *P. aeruginosa*) or fungi (*C. albicans*) and showed no toxicity in human hepatocyte HepG2 cells or activity against the hERG cardiac channel. Despite the electrophilic Michael acceptor present in the lactam of the armeniaspirols under physiological conditions the armeniaspirols were stable in PBS buffer for over 24 hours and showed only minor instability in the presence of 10 mM glutathione, 10 mM isobutylamine or cytochromes CYP3A4 and CYP2D6[24].

The Sanofi group furthered the development of the armeniaspirols by conducting a preliminary SAR study by synthesizing semi-synthetic and synthetic derivatives[24]. Their findings showed that substitution of β-chlorine on the Michael accepter with amine, thiol and alcohol nucleophiles rendered no improvements in activity. Reduction of the central ketone, and

alkylation of the phenol led to reduction in activity (Figure 1.4). The only derivatives that were tolerated were the incorporation of halogens into the aromatic moiety, although this did not improve the potency. These analogues arose during attempts to synthesize the natural product, including the challenging *N,O* spiro ketal center. Unfortunately, during the construction of the spiro center using the electrophilic chlorine source, *N*-chlorosuccinimide (NCS), unintended chlorination of the aromatic moiety occurred, yielding Cl-armeniaspirol. Several attempts to change reagent, solvent, and temperature to construct the spiro center were reported; however, unwanted incorporation of the halogen could not be avoided. This was, however, a key finding from a medicinal chemistry perspective as a method of accessing these halogenated analogues was established. The synthesis of a library of armeniaspirol analogues using this chemistry will be discussed in detail in chapter 2.

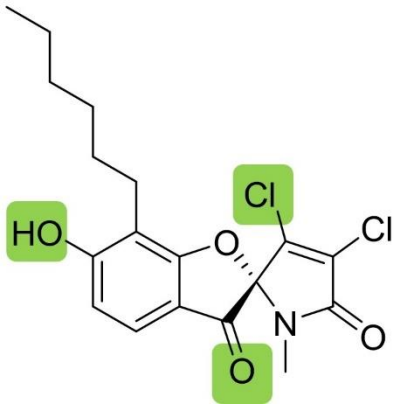

Figure 1.4 Structure of armeniaspirol A. Functional groups required for activity from the initial SAR study are highlighted in green.

Lastly, to further support the safety profile of armeniaspirol, an MRSA-induced sepsis model was done in mice, which showed increased survival rates and reduction of blood bacteremia levels at 15 mg/kg/d using IV administration. With the unique structure, high

potency, and promising safety data coupled to the need for new and novel mechanism of action antibiotics, armeniaspirol made for an obvious candidate for investigation into the mechanism of action and further SAR studies.

1.4 Armeniaspirol competitively inhibits ClpXP and ClpYQ

To determine the mechanism of action of armeniaspirol, a host of proteomic and *in vitro* biochemical assays were conducted[25]. The *B. subtilis* proteome has been extensively fingerprinted in response to known antibiotics of various mechanisms including those that inhibit protein biosynthesis, fatty acid biosynthesis, cell wall biosynthesis, and DNA damaging agents[22,26–29]. Thus, it is known that treatment with varying antibiotics with distinct mechanisms of action causes changes in the abundance of specific protein biomarkers that are characteristic of the drug's mechanism of action. Therefore, when the armeniaspirol treated proteomic profile was compared to the expected changes from known antibiotic treatments, no increase in key associated proteins was observed indicating armeniaspirol may display a unique mechanism of action. To further support this, a checkerboard synergy assay was done comparing armeniaspirol with a panel of known antibiotics. If synergy is observed between two antibiotic compounds, it is often indicative that they function through a similar mechanism of action. However, no synergy was observed when armeniaspirol was co-administered with tetracycline, cerulenin, penicillin or ciprofloxacin.

A competitive activity-based protein profiling experiment using armeniaspirol was conducted in *B. subtilis* to try to discover its potential protein targets. With armeniaspirol's electrophilic Michael acceptor, the cell lysate was first treated with the chlorinated natural product followed by a bioorthogonal alkyne-containing analogue to facilitate a competitive

protein capture using crosslinking with biotin azide and capture on streptavidin beads. This competitive profiling assay facilitates capture of all remaining off target proteins which can be counter screened against the proteins obtained from the pull-down probe alone to rule out false positives. From this pull-down assay, twelve proteins showed a statistically significant (p-value 2) increase in abundance. After ruling out targets associated with the primary metabolism, translation (due to the fingerprinting and synergy assays) and other remaining proteins with no implications in antibiotic activity, this left protein target ClpP with a 3.3-fold increase in the probe only capture experiment.

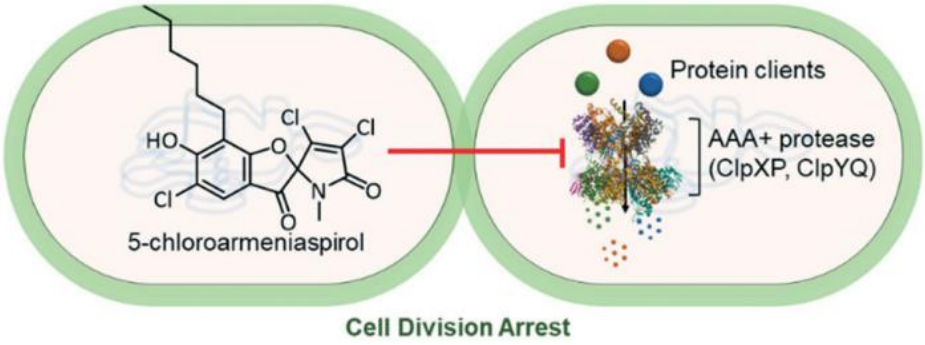

Figure 1.5 Armeniaspirol inhibits cellular AAA+ proteases ClpXP and ClpYQ competitively to cause cell division arrest.

ClpP is the proteolytic component of the ClpXP AAA+ protease that plays a role in bacterial physiology by degrading damaged and misfolded proteins and is associated with virulence in Gram-positive pathogens. In one of the four biological replicates of the probe-only inhibitor capture experiment, ClpQ —another AAA+ protease— was detected in high abundance. The detection of the Clp proteases indicated that these proteases could be a potential target of armeniaspirol. To interrogate this hypothesis, a kinetic *in vitro* evaluation of the

proteolytic activity was conducted using purified protein from *B. subtilis* and *E. coli*. Armeniaspirol showed a dose response towards proteolytic activity of both ClpYQ and ClpXP allowing for a determination of an IC_{50} value for each protein. An increase in apparent K_M and a stable V_{max} in the presence of increasing inhibitor concentrations, showed armeniaspirol functions as a competitive inhibitor of the Clp proteases. Under conditions of competitive inhibition, the Cheng-Prusoff equation allows for the conversion of IC_{50} values to obtain K_i of armeniaspirol for each protease. Lastly, the double knockout mutants of ClpP and ClpQ were synthetically lethal to the organism. Synthetic lethality is a situation in which mutations to two genes together result in cell death, but a knockout of either gene alone does not. This aspect is in line with armeniaspirol inhibiting both ClpXP and ClpYQ which causes cell death. By chemical and quantitative proteomics, biochemical assays, armeniaspirols are shown to competitively inhibit the AAA+ proteases ClpXP and ClpYQ displaying an unprecedented mechanism of action.

1.5 Total synthesis of armeniasprol and ability to depolarize cell membranes of Gram-positive bacteria

The armeniaspirol compounds arise biosynthetically from halogenated pyrroles, which are converted to the spirocyclic armeniaspirol through a flavin-dependent monooxygenase[30,31]. The halogenated biosynthetic precursor to armeniaspirol shares structural and functional group homology (contain a carbonyl linker between the aryl and halogenated pyrrole moiety) to a class of compounds often referred to as halopyrroles including pyoluteorin and the pyrrolomycins (Figure 1.6)[32,33]. These compounds show potent activity against Gram-positive pathogens; however, no clear mechanism of action had been deduced from this family of compounds until a

2019 study on the pyrrolomycins, produced by *Streptomyces vitaminophilus* [34]. The study demonstrated that the pyrrolomycins are "protonophores", compounds that shuttle protons across membranes resulting in membrane depolarization. The transmembrane proton gradient is responsible for powering ATP synthesis in bacteria and is generated through the electron transport chain. When it is disrupted, bacteria can undergo energy depletion and cell death. The authors concluded that the pyrrolomycins are protonophores through a variety of biochemical and biophysical experiments. This included attempting to generate resistant mutants, pH dependent MICs, examining morphology using microscopy, examining charge on either side of a lipid bilayer, testing mitochondrial respiration levels, and using fluorescent cationic dyes to examine changes in membrane potential. The group postulated that ability to transfer protons across the membrane was due to the decreased pK_a of the phenols by the electron withdrawing groups on the ring. This enabled the phenols to be readily ionisable, facilitating transfer of protons through the membrane as a neutral molecule, followed by formation of the phenoxide intracellularly, releasing the proton.

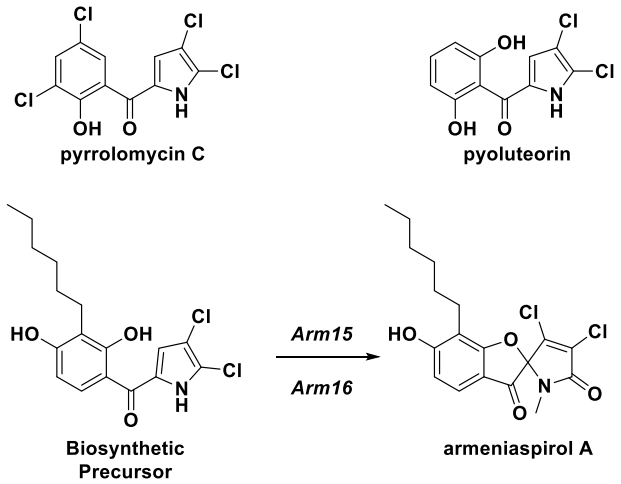

Figure 1.6 Structure of select potent halopyrrole antibiotics which function as protonophores and the proposed biosynthetic precursor of armeniaspirol.

With armeniaspirols' structural similarity to the pyrrolomycins, a 2021 publication reported that armeniaspirols also function as protonophores[35]. In addition, this work also detailed the total synthesis of the natural product. This study used many of the same experiments as the pyrrolomycin study, including assays using voltage sensitive dyes in Gram-positive and -negative bacteria, ion conductance assays across a planar lipid bilayer, and pH-sensitive dyes encapsulated in unilamellar vesicle as well as pH dependent MICs, to demonstrate the protonophore activity of armeniaspirols[35]

In the first part of this study, the authors detailed the first total synthesis of armeniaspirol. The synthesis was based on an early-stage chlorination to avoid the problem of electrophilic substitution of the electron rich aryl moiety that led to the unintended chlorination in all previous syntheses. The synthesis started with methyl addition into the carbonyl of a functionalized α-β unsaturated, α-β dichlorinated maleimide followed by subsequent dehydration to yield the exo-olefin (Figure 1.7). This set the stage for an annulation reaction based on an oxidative radical [3+2] cross coupling between the aryl moiety and pyrrole moiety. DDQ oxidized the corresponding free phenol to the semiquinone with a C4 carbon radical that could then engage the exo double bond of the pyrrole moiety. Only one regioisomer was formed as the addition to the olefin likely generated the more stable carbon radical at the more substituted position as opposed to a primary radical intermediate. This formed the central ring in armeniaspirol. With the full carbon skeleton constructed, the penultimate compound was converted to armeniaspirol after screening a wide variety of benzylic oxidation conditions. The efficient five step synthesis constructed the spiro center with a [3+2] cycloaddition using an exocyclic double bond on a heterocycle.

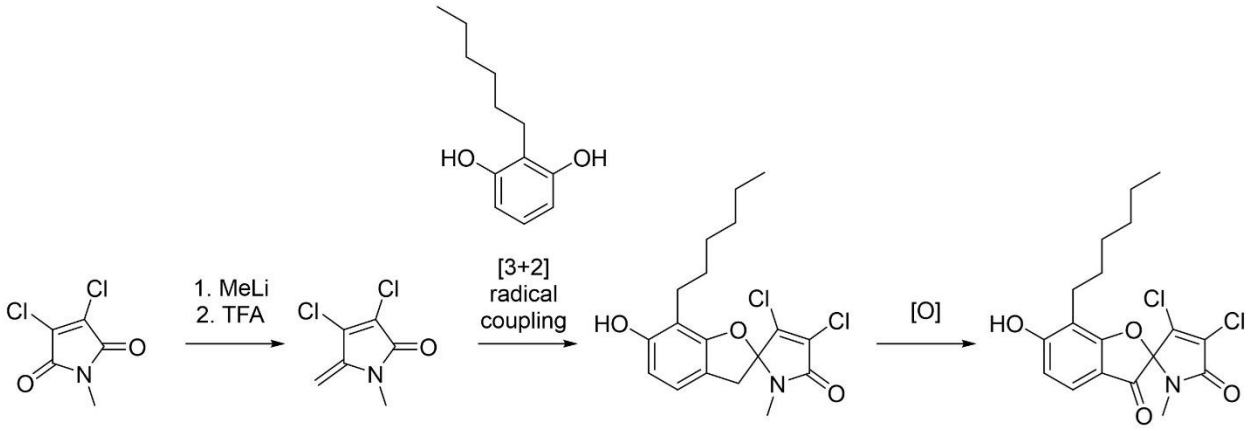

Figure 1.7 Synthesis of armeniaspirol by Arsetti *et al*[35].

The second portion of the study detailed the experiments that led to the conclusion that armeniaspirol functions as a protonophore resulting in membrane depolarization. Akin to the pyrrolomycin work, the initial hypothesis was based on the activity of the natural product compared to the phenol methyl ether. To evaluate the role of the protonation state of the phenol, the MICs of armeniaspirol were determined at varying pH, showing enhanced potency at low pH (MIC = 1.3 μg mL^{-1} at pH 6.5; MIC = 16 μg mL^{-1} at pH 10). However, it is well documented that ionic strength and pH of the medium can have a drastic effect on antibiotic potency due to increase in penetration or accumulation within bacteria.

Next, membrane depolarization was probed using cationic fluorescent dyes in both Gram-positive and genetically manipulated Gram-negative bacteria (*S. aureus*, *Micrococcus luteus*, *E. coli ΔtolC*). These assays showed that bacterial membranes were depolarized at concentrations compared to the known, non-antibiotic protonophore CCCP. This was followed up in the mitochondria of HeLa cells using a fluorescence-based assay where the integrity of mitochondrial membranes was monitored. Armeniaspirol was shown to compromise the

mitochondrial membrane at concentrations as low as 1 μM. A second assay using mitochondria was conducted where oxygen consumption was monitored. If oxidative phosphorylation is uncoupled by membrane depolarization, this breaks the link between electron transport and ATP production, which causes an increase in the flow of electrons through the electron transport chain and results in an increase in oxygen consumption. In this study an increase in oxygen consumption was observed at 10 μM. This is comparable to the positive control CCCP.

The final assays that were conducted measured translocation of ions across a bilayer composed of 1,2-diphytanoyl-sn-glycero-3-phosphocholine (DPhPC) in a protein independent manner. At varying pH levels the flow of ions was monitored and detected as an electric current. The ion conductance values aligned with that of CCCP and at lower pH an increased conductance was observed which supported the conclusion armeniaspirol acted as an ion carrier across the membrane. A second orthogonal method for the detection of proton transport across a membrane was conducted using unilaminar vesicles composed of 1-palmitoyl-2-oleoyl-sn-glycero-3-phosphocholine (POPC). This was done by monitoring the flow of protons on either side of the membrane using a pH sensitive dye in the presence of armeniaspirol at varying pH on either side of the vesicle. It showed proton translocation by armeniaspirol. Interestingly two other synthetic compounds were tested, the methylated phenol and the precursor to the total synthesis with the ketone absent at the benzylic position but with the phenol free. Unexpectedly they reported that both compounds demonstrated proton transport capability but at a reduced ability compared to armeniaspirol, with the anisole compound being a stronger proton translocator than the compound lacking the ketone but with the free phenol. With the key hypothesis being the need for an ionizable free phenol to transport protons for antibiotic activity, it is of great surprise to see a compound with no ionizable groups being capable of proton

translocation. This publication formed the basis for a hypothesis that armeniaspirols interfere with bacterial membranes in a protein-independent manner.

The pyrrolomycin and armeniaspirol mechanism of action studies provided an important preliminary investigation into how armeniaspirol causes cell death. Both studies only showed that the membrane potential was being disrupted but a thorough investigation into how this happened in bacterial organisms was absent. This is highlighted by the lack of discussion or even mention of anything related to the proton motive force (PMF). The proton motive force is the electrochemical potential gradient that bacteria establish to drive ATP synthesis[36]. It is dictated by two components, the electric potential ($\Delta\Psi$) and the transmembrane proton gradient (ΔpH)[37]. Bacteria exhibit tight regulatory control over both factors where changes a change in one are compensated for by adjustment of the other to maintain a constant PMF. This complex interplay between both aspects makes it often difficult to discern which aspect of the PMF is being disrupted. It has been shown extensively through the literature that small molecules can selectively disrupt either aspect of the PMF leading to membrane depolarization[22,38,39]. A more thorough analysis of how armeniaspirol disrupts the PMF is discussed in detail in Chapter 3.

1.6 Thesis overview, goals summary and conclusion/outlook

The need for effective antibiotics against drug resistant Gram-positive bacteria with novel mechanisms of action has been clearly highlighted. A major research and development gap in new clinical antibiotics coupled to the rapid rise in microbial resistance has generated a push to develop innovative ways to overcome antimicrobial resistance. A new approach using compounds displaying polypharmacology could provide a new avenue to develop clinical antibiotics with increased potency and less likely to develop resistance. The potent natural

product antibiotic armeniaspirol, with its unique scaffold, mechanism of action and polypharmacology provide an intriguing opportunity to develop and investigate its potential as an antibiotic therapeutic.

Chapter 2 describes the design and execution of a medicinal chemistry study where a series of armeniaspirol analogues were synthesized to interrogate the effects of structural changes on potency at the two protein targets ClpXP and ClpYQ. We used *in vitro* and *in silico* models to evaluate the analogues and determined that balancing the potency at both targets resulted in the most potent antibiotics that showed no toxicity in human cells.

In chapter 3 we evaluate the armeniaspirol analogues' effect on the PMF. The armeniaspirols disrupt the transmembrane electrical potential ($\Delta\Psi$), not the transmembrane proton gradient (ΔpH) of the PMF. Disruption of the $\Delta\Psi$ is necessary for antibiotic activity but not sufficient. We propose that disruption of the $\Delta\Psi$ and inhibition of the Clp proteases work in concert to effect antibiotic activity.

Chapter 4 explores the scope and mechanism of an oxidative chlorination reaction of pyrrole-2-carbonyl compounds. This reaction was proposed to be used for the total synthesis of armeniaspirol, by utilizing this early-stage chlorination to avoiding unintended chlorination of the electron rich phenyl ring. Surprisingly, this strategy was derailed in the penultimate step which yielded a skeletal rearranged product which was a constitutional isomer of the natural product. These constitiutional isomers were coined pseudoarmeniaspirol and were tested for antibiotic potency as well as were evaluated for known targets of armeniaspirol, ClpXP, ClpYQ, and disruption of the proton motive force.

1.7 References

1. O'Neill, J. Antimicrobial Resistance: Tackling a crisis for the health and wealth of nations The Review on Antimicrobial Resistance Chaired by Jim O. (2014).
2. Rossolini, G. M., Arena, F., Pecile, P. & Pollini, S. Update on the antibiotic resistance crisis. *Current Opinion in Pharmacology* vol. 18 56–60 (2014).
3. Lee Ventola, C. The Antibiotic Resistance Crisis Part 1: Causes and Threats. in vol. 40 (4): 277–283. (2015).
4. Murray, C. J. Antimicrobial Resistance Collaborators. Global burden of bacterial antimicrobial resistance in 2019: a systematic analysis. *Lancet* **399**, 629–655 (2022).
5. Marturano, J. E. & Lowery, T. J. ESKAPE pathogens in bloodstream infections are associated with higher cost and mortality but can be predicted using diagnoses upon admission. *Open Forum Infect. Dis.* **6**, 1–8 (2019).
6. de Kraker, M. E. A., Stewardson, A. J. & Harbarth, S. Will 10 Million People Die a Year due to Antimicrobial Resistance by 2050? *PLoS Med.* **13**, S71–S75 (2016).
7. Stryjewski, M. E. & Corey, G. R. Methicillin-resistant Staphylococcus aureus: An evolving pathogen. *Clin. Infect. Dis.* **58**, 10–19 (2014).
8. Rodvold, K. A. & Mcconeghy, K. W. Methicillin-resistant staphylococcus aureus therapy: Past, present, and future. *Clin. Infect. Dis.* **58**, 20–27 (2014).
9. Diekema, D. J., Pfaller, M. A., Shortridge, D., Zervos, M. & Jones, R. N. Twenty-year trends in antimicrobial susceptibilities among Staphylococcus aureus from the SENTRY Antimicrobial Surveillance Program. *Open Forum Infect. Dis.* **6**, S47–S53 (2019).
10. Roch M, Gagetti P, Davis J, Ceriana P, Errecalde L, Corso A, Rosato Daptomycin resistance in clinical MRSA strains is associated with a high biological fitness cost. *Front.*

Microbiol. **8**, 1–9 (2017).

11. Kurosu, M., Siricilla, S. & Mitachi, K. Advances in MRSA drug discovery: Where are we and where do we need to be? *Expert Opinion on Drug Discovery* vol. 8 1095–1116 (2013).
12. Freire-Moran L, Aronsson B, Manz C, Gyssens IC, So AD, Monnet DL, Cars O; ECDC-EMA Working Group. Critical shortage of new antibiotics in development against multidrug-resistant bacteria - Time to react is now. in *Drug Resistance Updates* vol. 14 118–124 (2011).
13. Wanted: A reward for antibiotic development. *Nat. Biotechnol* vol. 36 555 (2018).
14. Newman, D. J. & Cragg, G. M. Natural Products as Sources of New Drugs over the Nearly Four Decades from 01/1981 to 09/2019. *J. Nat. Prod.* vol. 83 770–803 (2020).
15. Harbarth, S., Theuretzbacher, U. & Hackett, J. Antibiotic research and development: business as usual? 1604–1607 (2015) doi:10.1093/jac/dkv020.
16. Walsh, C. T. & Wencewicz, T. A. Prospects for new antibiotics : a molecule-centered perspective. 7–22 (2014) doi:10.1038/ja.2013.49.
17. Talbot GH, Jezek A, Murray BE, Jones RN, Ebright RH, Nau GJ, Rodvold KA, Newland JG, Boucher HW. The infectious diseases society of America's 10 × '20 initiative (10 new systemic antibacterial agents US food and drug administration approved by 2020): Is 20 × '20 a possibility? *Clinical Infectious Diseases* vol. 69 1–11 (2019).
18. Ling LL, Schneider T, Peoples AJ, Spoering AL, Engels I, Conlon BP, Mueller A, Schäberle TF, Hughes DE, Epstein S, Jones M, Lazarides L, Steadman VA, Cohen DR, Felix CR, Fetterman KA, Millett WP, Nitti AG, Zullo AM, Chen C, Lewis K. A new antibiotic kills pathogens without detectable resistance. Nature. 2015 22; 517, 455-459

(2015).

19. Kabir, A. & Muth, A. Polypharmacology : The science of multi-targeting molecules. *Pharmacol. Res.* **176**, 106055 (2022).

20. Ho, T. T., Tran, Q. T. & Chai, C. L. The polypharmacology of natural products. *Future Med. Chem.* **10**, 1361–1368 (2018).

21. Wetzel, C., Lonneman, M. & Wu, C. European Journal of Medicinal Chemistry Polypharmacological drug actions of recently FDA approved antibiotics. *Eur. J. Med. Chem.* **209**, 112931 (2021).

22. Stepanek, J. J., Lukežič, T., Teichert, I., Petković, H. & Bandow, J. E. Dual mechanism of action of the atypical tetracycline chelocardin. *Biochim. Biophys. Acta - Proteins Proteomics* **1864**, 645–654 (2016).

23. Dufour C, Wink J, Kurz M, Kogler H, Olivan H, Sablé S, Heyse W, Gerlitz M, Toti L, Nußer A, Rey A, Couturier C, Bauer A, Brönstrup M. Isolation and structural elucidation of armeniaspirols A-C: Potent antibiotics against gram-positive pathogens. *Chem. - A Eur. J.* **18**, 16123–16128 (2012).

24. Couturier, C., Bauer, A., Rey, A., Schroif-Dufour, C. & Broenstrup, M. Armeniaspiroles, a new class of antibacterials: Antibacterial activities and total synthesis of 5-chloro-Armeniaspirole A. *Bioorganic Med. Chem. Lett.* **22**, 6292–6296 (2012).

25. Labana P, Dornan MH, Lafrenière M, Czarny TL, Brown ED, Pezacki JP, Boddy CN. Armeniaspirols inhibit the AAA+ proteases ClpXP and ClpYQ leading to cell division arrest in Gram-positive bacteria. *Cell Chem. Biol.* **28**, 1703-1715.e11 (2021).

26. Bandow, J. E., Brötz, H., Leichert, L. I. O., Labischinski, H. & Hecker, M. Proteomic approach to understanding antibiotic action. *Antimicrob. Agents Chemother.* **47**, 948–955

(2003).

27. Wenzel M, Schriek P, Prochnow P, Albada HB, Metzler-Nolte N, Bandow JE. Influence of lipidation on the mode of action of a small RW-rich antimicrobial peptide. *Biochim. Biophys. Acta - Biomembr.* **1858**, 1004–1011 (2016).

28. Wenzel M, Kohl B, Münch D, Raatschen N, Albada HB, Hamoen L, Metzler-Nolte N, Sahl HG, Bandow JE. Proteomic response of Bacillus subtilis to lantibiotics reflects differences in interaction with the cytoplasmic membrane. *Antimicrob. Agents Chemother.* **56**, 5749–5757 (2012).

29. Freiberg, C., Brunner, N., Macko, L. & Fischer, H. P. Discovering antibiotic efficacy biomakers: Toward mechanism-specific high contest compound screening. *Mol. Cell. Proteomics* **5**, 2326–2335 (2006).

30. Qiao Y, Yan J, Jia J, Xue J, Qu X, Hu Y, Deng Z, Bi H, Zhu D. Characterization of the Biosynthetic Gene Cluster for the Antibiotic Armeniaspirols in Streptomyces armeniacus. *J. Nat. Prod.* **82**, 318–323 (2019).

31. Fu C, Xie F, Hoffmann J, Wang Q, Bauer A, Brönstrup M, Mahmud T, Müller Armeniaspirol Antibiotic Biosynthesis: Chlorination and Oxidative Dechlorination Steps Affording Spiro[4.4]non-8-ene. *ChemBioChem* **20**, 764–769 (2019).

32. Takelda, R. Structure of a new antibiotic, pyoluteorin. *J. Am. Chem. Soc.* vol. 80 4749–4750 (1958).

33. Cascioferro S, Raimondi MV, Cusimano MG, Raffa D, Maggio B, Daidone G, Schillaci D. Pharmaceutical potential of synthetic and natural pyrrolomycins. *Molecules* vol. 20 21658–21671 (2015).

34. Valderrama K, Pradel E, Firsov AM, Drobecq H, Bauderlique-le Roy H, Villemagne B,

Antonenko YN, Hartkoorn RC. Pyrrolomycins are potent natural protonophores. *Antimicrob. Agents Chemother.* **63**, 1–15 (2019).

35. Arisetti, N. Arisetti, N.; Fuchs, H. L. S.; Coetzee, J.; Orozco, M.; Ruppelt, D.; Bauer, A.; Heimann, D.; Kuhnert, E.; Bhamidimarri, S. P.; Bafna, J. A.; Hinkelmann, B.; Eckel, K.; Sieber, S. A.; Müller, P. P.; Herrmann, J.; Müller, R.; Winterhalter, M.; Steinem, C.; Brönstrup, . Total synthesis and mechanism of action of the antibiotic armeniaspirol A. *Chem. Sci.* **12**, 16023–16034 (2021).

36. Maloney, P. C., Kashket, E. R. & Wilson, T. H. A protonmotive force drives ATP synthesis in bacteria. *Proc. Natl. Acad. Sci. U. S. A.* **71**, 3896–3900 (1974).

37. Farha, M. A., Verschoor, C. P., Bowdish, D. & Brown, E. D. Collapsing the proton motive force to identify synergistic combinations against staphylococcus aureus. *Chem. Biol.* **20**, 1168–1178 (2013).

38. Ejim L, Farha MA, Falconer SB, Wildenhain J, Coombes BK, Tyers M, Brown ED, Wright GD. Combinations of antibiotics and nonantibiotic drugs enhance antimicrobial efficacy. *Nat. Chem. Biol.* **7**, 348–350 (2011).

39. Cascales, E., Gavioli, M., Sturgis, J. N. & Lloubes, R. Proton motive force drives the interaction of the inner membrane TolA and outer membrane Pal proteins in Escherichia coli. *Mol. Microbiol.* **38**, 904–915 (2000).

Chapter 2: Armeniaspirol analogues with more potent Gram-positive antibiotic activity show enhanced inhibition of the ATP-dependent proteases ClpXP and ClpYQ

2.1 Introduction

The research presented in this chapter was born out of our desire to identify and develop a novel antibiotic for the treatment of antibiotic resistant Gram-positive bacterial infections[1]. As armeniaspirol possess an unprecedented scaffold and a unique mechanism of action it is likely to be effective against current MDR bacteria[2]. It was previously shown that incorporation of a halogen into the 5 position of the phenyl ring still yielded potent antibiotics (Figure 2.1)[3]. By leveraging the chemistry published by the Sanofi group[3] to access the skeleton of armeniaspirol, we set out to conduct a study to answer key medicinal chemistry questions related to structure-activity relationships surrounding armeniaspirol.

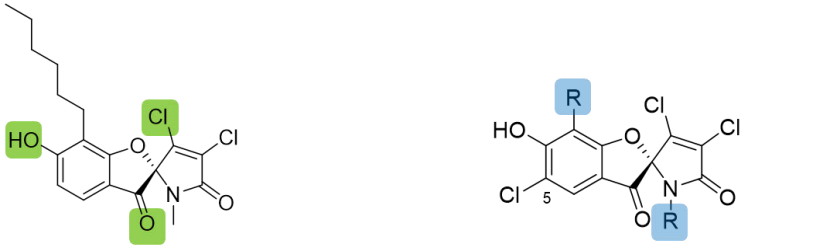

Figure 2.1 Preliminary SAR studies and new targeted areas for SAR

The preliminary SAR study by Sanofi[3] suggested the free phenol, β-chloride, and the central ketone were required for activity (Figure 2.1). This was further supported by preliminary unpublished data from our lab [2,3]. In addition, we knew that alkyl modifications on the amide

nitrogen were tolerated. With these in mind, we set out to design a synthesis where we could use a late-stage diversification to access a wide scope of analogs (Figure 2.1). The alkylation of the amide nitrogen in the penultimate step of the synthesis, provided the ideal opportunity to conduct a SAR study on this chemical space. In addition to probing the functionality on the amide, two parallel analogues were designed to probe the functionality of the aliphatic chain present in armeniaspirol. With N-alkyl chains providing increased lipophilic character, we decided to truncate the native hexyl chain on the aromatic core to a methyl group to probe questions surrounding the lipophilicity of armeniaspirol.

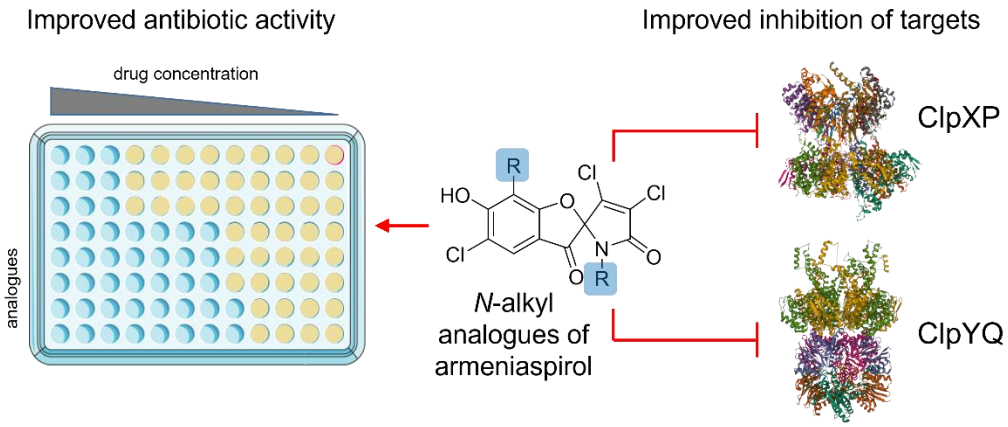

Figure 2.2 Improved inhibition of protein targets ClpXP and ClpYQ by armeniaspirol led to improved antibiotic activity in gram positive pathogens. Armeniaspirol diversification points studied are highlighted in blue.

With the goal of developing antibiotics with improved potency and decreased resistance, this first-generation library of compounds provided the first published improvement in antibiotic potency of the scaffold which allowed for further kinetic evaluation of both protein targets

ClpYQ and ClpXP. Further safety and toxicity assays were conducted confirming the well-established safety profile of armeniaspirol.

2.2 References

1. Freire-Moran L, Aronsson B, Manz C, Gyssens IC, So AD, Monnet DL, Cars O; ECDC-EMA Working Group. Critical shortage of new antibiotics in development against multidrug-resistant bacteria - Time to react is now. in *Drug Resistance Updates* vol. 14 118–124 (2011).
2. Labana, P.; Dornan, M. H.; Lafrenière, M.; Czarny, T. L.; Brown, E. D.; Pezacki, J. P.; Boddy, C. N. Armeniaspirols inhibit the AAA+ proteases ClpXP and ClpYQ leading to cell division arrest in Gram-positive bacteria. *Cell Chem. Biol.* **28**, 1703-1715.e11 (2021).
3. Couturier, C., Bauer, A., Rey, A., Schroif-Dufour, C. & Broenstrup, M. Armeniaspiroles, a new class of antibacterials: Antibacterial activities and total synthesis of 5-chloro-Armeniaspirole A. *Bioorganic Med. Chem. Lett.* **22**, 6292–6296 (2012).

2.3 Author contributions

In this study I was responsible for the synthesis of all compounds. Working with Puneet Labana and Claudia Natola, we collected all the MBC and MIC data. I developed the ClpXP assay and collected all the data regarding ClpXP inhibition. In collaboration with André Paquette, we collected the hemolysis safety data. Taylor Lanosky performed the ClpYQ kinetic assays, Jordan Brazeau-Henrie performed the modelling and Nick Calvert evaluated the toxicity in mammalian cell culture cells. I wrote the first draft of the manuscript.

2.4 Copyright

2.5 Armeniaspirol analogues with more potent Gram-positive antibiotic activity show enhanced inhibition of the ATP-dependent proteases ClpXP and ClpYQ

Michael G. Darnowski, Taylor D. Lanosky, Puneet Labana, Jordan T. Brazeau-Henrie, Nicholas D. Calvert, Mark H. Dornan, Claudia Natola, André R. Paquette, Adam J. Shuhendler and Christopher N. Boddy.

Antibiotics with fundamentally new mechanisms of action such as the armeniaspirols, which target the ATP-dependent proteases ClpXP and ClpYQ, must be developed to combat antimicrobial resistance. While the mechanism of action of armeniaspirol against Gram-positive bacteria is understood, little is known about the structure-activity relationship for its antibiotic activity. Based on the preliminary data showing that modifications of armeniaspirol's *N*-methyl group increased antibiotic potency, we probed the structure-activity relationship of *N*-alkyl armeniaspirol derivatives. A series of focused derivatives were synthesized and evaluated for antibiotic activity against clinically relevant pathogens including methicillin-resistant *Staphylococcus aureus* and vancomycin-resistant *Enterococcus*. Replacement of the N-methyl with *N*-hexyl, various *N*-benzyl, and *N*-phenethyl substituents lead to substantial increases in antibiotic activity and potency for inhibition of both ClpYQ and ClpXP. Docking studies identified binding models for ClpXP and ClpYQ that were consistent with the inhibition data. This work confirms the role of ClpXP and ClpYQ in the mechanism of action of armeniaspirol and provides important lead compounds for further antibiotic development.

Introduction

With the constant threat of increasing antimicrobial resistance, antibiotics with fundamentally new mechanisms of action must be developed and brought to the clinic. The

armeniaspirols discovered in 2012 are hybrid polyketide non-ribosomal peptide natural products produced by *Streptomyces armeniacus*[1,2] that have recently been shown to possess unique pharmacology.[3] The armeniaspirols are potent Gram-positive antibiotics active against methicillin-resistant *Staphylococcus aureus* (MRSA), penicillin-resistant *Streptococcus pneumoniae (*PRSP), and vancomycin-resistant *Enterococcus* (VRE). They competitively inhibit the ATP-dependent proteases ClpXP and ClpYQ (also known as HslVU),[3] whose combined activity is essential,[3] leading to disruption of the divisome and cell division arrest (Figure 1A). While inhibitors of ClpP are known antivirulence compounds, the additional targeting of ClpYQ by armeniaspirol is unprecedented and results in antibiotic activity.

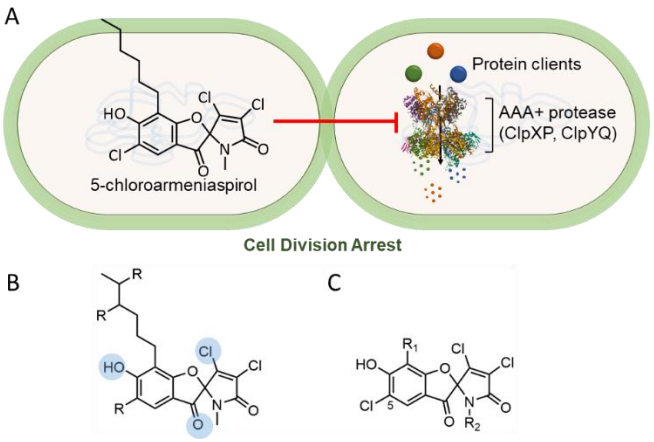

Figure 1. Analogues of armeniaspirol to probe antibiotic activity via inhibition of ClpXP and ClpYQ (A) 5-chloroarmeniaspirol inhibits the ATP-dependent proteases ClpXP and ClpYQ in Gram-positive bacteria, which dysregulates the divisome and leads to cell division arrest. (B) Summary of structure-activity relationships for armeniaspirol. Functional groups highlighted in blue are essential for antibiotic activity. R indicates sites amenable to substitution. (C) 5-chloroarmeniaspirol sites R1 and R2 were selected for detailed structure-activity relationship.

Little is known about the structure-activity relationship for antibiotic activity of armeniaspirol. Initial semi-synthesis work from the isolated natural product showed that substitution of the β-chloride with alcohols, amines, and thiols eliminated antibiotic activity as determined by minimum inhibitory concentrations (MIC).[2] Similarly alkylation of the phenol and reduction of the carbonyl abolished activity (Figure 1B).[2] Via total synthesis, the *N*-methyl moiety proved amenable to replacement with a longer *N*-alkyl chain without loss of activity.[3] However no data is available on how structural modifications impact the activity against ClpXP and ClpYQ. Given that correctly balancing activity at each target is essential for development of effective and potent multi-target drugs, evaluating the impact of structural perturbations on each of these targets is thus essential.

Based on preliminary data showing that modification of armeniaspirol's *N*-methyl group increased antibiotic potency,[3] we probed the structure-activity relationship of *N*-alkyl armeniaspirol derivatives. Fourteen armeniaspirol analogues were synthesized with varying *N*-alkyl groups. To compensate for the additional lipophilic character of extending the *N*-methyl group, the aromatic hexyl chain was simplified to a methyl substituent in a subset of the analogues. All compounds were evaluated for MIC and minimum bactericidal concentration (MBC) against clinically relevant Gram-positive pathogens including MRSA USA300, the most common community acquired MRSA. Potent analogues were evaluated for activity against ClpXP in a cell-based assay and activity against ClpYQ in a biochemical assay. Highly potent armeniaspirol analogues with improved activity against ClpXP and ClpYQ were identified. This data bode well for the further development of the armeniaspirol scaffold as a Gram-positive antibiotic.

Results

The armeniaspirols and their analogues have been isolated from the producing organism,[1,4] generated through semi-synthesis,[3] and accessed via total synthesis.[2,3] Analogues generated from the addition of alcohols like methanol, amines such as isobutyl amine, and thiols like 2-diethylamino-ethanethiol into the Michael acceptor lack antibiotic activity against *S. aureus* in MIC assays.[1] Both diastereomers generated from reduction of the furan ring carbonyl are inactive against *S. aureus* in MIC assays.[1] Methylation of the aromatic phenol also produces inactive compounds.[1,3] However, chlorination ortho to the phenol is tolerated with a slight reduction in antibiotic activity as measured by MIC against MRSA.[1,3] Both the removal of the *N*-methyl[4] and substitution of it with an alkyl chain[3] produce active compounds, with installation of a *N*-hexyl chain boosting potency four fold against *Bacillus subtilis*.[3] Lastly modification of the aromatic alkyl chain via branching produces compounds that are comparatively potent to armeniaspirol A in MIC assays with MRSA.[1]

Based on the known structure-activity relationships, exploring modification of the lactam through *N*-alkylation appeared most promising and likely to yield compounds with improved potency. Thus, we set out to diversify this position by substituting the amide *N* with varying alkyl groups. To evaluate the overall impact of increasing lipophilicity, which typically correlates with an increase in non-selective binding,[5] we planned two series of *N*-alkyl analogues, one with the native hexyl chain on the aromatic ring (Series 1, Figure 1C R_1 = *n*-C_6H_{13}) and a second with a methyl substituent (Series 2, Figure 1C $R_1 = CH_3$).

Synthesis of chloro-armeniaspirol analogues

The synthetic route for generation of the armeniaspirol scaffold relies on a *N*-chlorosuccinimide (NCS)-based chlorination of the pyrrole, which forms the key spirocyclic center and the dichlorinated α,β-unsaturated lactam.[2,3,6] Due to the forcing oxidative conditions,

the electron rich phenyl ring is also chlorinated giving rise to 5-chloroarmeniaspirol analogues (Figure 1C). While the 5-chloro substituent could not be selectively reduced in the presence of the dichloro-α,β-unsaturated lactam, the additional chlorination does not significantly impact the antibiotic activity as measured by MIC.[2] Thus, all analogues synthesized in this study are functionalized with a chloride in the 5-position.

Diversification of the substituent on the phenyl ring (R_1) was implemented in the start of the synthesis. The hexyl chain series of analogues (Series 1) were prepared via a lithium halogen exchange followed by a Suzuki coupling with *N*-hexyl boronic acid (Figure 2A), while the methyl series of analogues (Series 2) were prepared from commercially available 2,6-dimethoxytoluene. The two compounds were elaborated via parallel synthetic routes (Figure 2B). Friedel-Crafts acylation of the electron rich aromatic with the acid chloride of pyrrole carboxylic acid, followed by selective demethylation of methoxy substituent ortho to the carbonyl[7] generated the key precursors for oxidative spirocyclization. NCS in acetic acid chlorinated and oxidized these intermediates generating a mixture of spirocyclic compounds with either the 2,3-dichloro-α,β-unsaturated lactam or the 2,2,3-trichloro lactam. Treatment of this mixture with triethylamine afforded the armeniaspirol scaffolds. Alkylation of the amide with a variety of electrophiles enabled diversification of each series at the R_2 site. Finally, boron tribromide deprotection of the aryl ether generated the final compounds, **1-14** (Figure 2C).

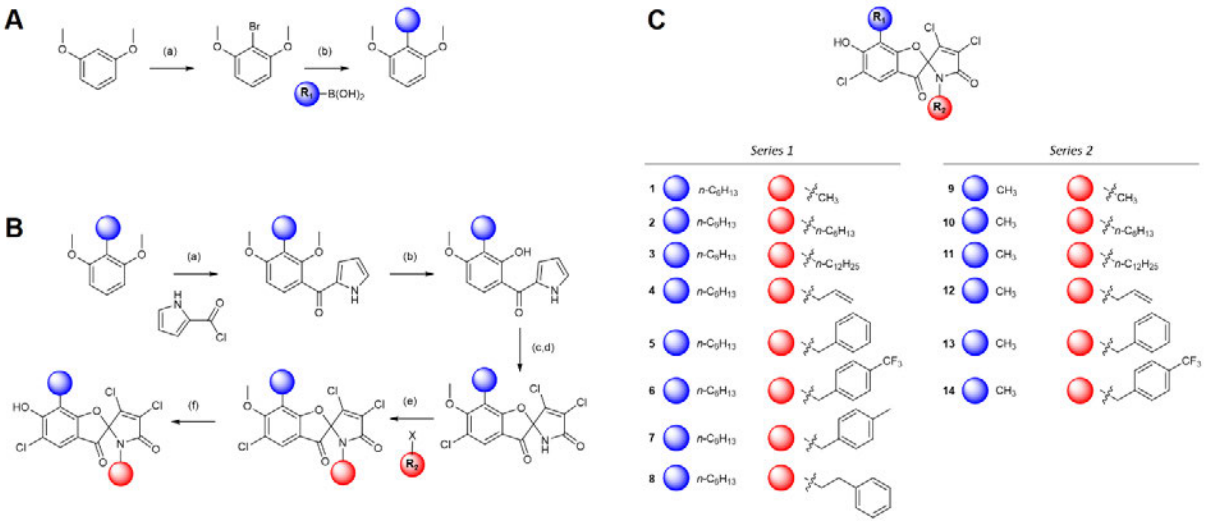

Figure 2 Armeniaspirol analogues. (A) Synthetic route installing the hexyl chain for the starting material used for all series 1 analogues. Reagents and conditions are as follows a) *n*-BuLi, Br_2 b) $Pd(OAc)_2$, SPhos, K_3PO_4. (B) Synthetic route generating series 1 and 2 analogues from dimethyl-2-methylresorcinol and dimethyl-2-hexylresorcinol. Reagents and conditions are as follows a) $SnCl_4$ b) BBr_3 c) NCS d) NEt_3 e) NaH f) BBr_3 (C) Structures of series 1 and 2 analogues used in this study.

MIC evaluation of analogues

The evaluation of antibiotic activity of armeniaspirol analogues was accomplished using the microtiter broth dilution MIC and MBC assays[8] against a panel of clinically relevant Gram-positive pathogens. These include MRSA USA100, the primary lineage responsible for hospital acquired MRSA infections,[9] USA200, responsible for a smaller subset of hospital acquired infections, USA300, the primary community acquired MRSA pathogen, USA400, also responsible for community acquired MRSA infections, [10,11] and the high-priority pathogen VRE.

MIC were also determined with the Gram-negative pathogen *Pseudomonas aeruginosa* PA01, to determine if any analogues had expanded activity against Gram-negative bacteria.

In general, the series 1 hexyl chain analogues exhibited superior potency relative to the methyl derivatives from series 2. The hexyl derivative, **2**, and the benzyl derivative, **5**, showed two- to four-fold more potent MICs compared to **1. 6**, the *p*-trifluorobenzyl derivative consistently showed slightly diminished potency across all strains, while the *p*-methylbenzyl derivative **7** showed some of the most potent activity in this study. Interesting its constitutional isomer **8** also showed comparable activity.

The series 2 analogues, which all possess a methyl substituent at R_1, showed little to no inhibition of bacterial growth except for **10** and **11**. **10** is the constitutional isomer of **1** and shows near identical potency across all six strains. The dodecyl derivative **11** was the most potent of all series 2 compounds and exhibited comparable MIC values to several of the best series 1 derivatives. While derivatives from series 1 were generally more potent than the derivatives from series 2, consistent with the increase in lipophilicity, the *N*-dodecyl derivative in series 2, **11**, was substantially more potent than **3**. In addition to having unique potency in series 2, **11** proved to be bactericidal differentiating it from all the other analogues. The parent compound and all other analogues were bacteriostatic as defined by having MBC greater than four times the MIC (Supplementary Table S1).[12–14]

Table 1. MIC evaluation of analogues **1-14** against a panel of Gram positive and negative bacteria

	Minimum Inhibitory Concentration (μg/mL)													
	1	**2**	**3**	**4**	**5**	**6**	**7**	**8**	**9**	**10**	**11**	**12**	**13**	**14**
Gram-positive														
S. aureus IA116-USA100	4	1	8	4	1	2	1	1	>32	4	2	>32	>32	16
S. aureus MN8-USA200	4	1	16	4	1	2	0.5	0.5	>32	4	2	>32	>32	16
S. aureus LAC-Fitz-USA300	4	1	16	4	1	2	0.5	0.5	>32	4	1	>32	32	16
S. aureus MW2-USA400	4	1	8	4	2	2	0.5	0.5	>32	8	2	>32	32	16
E. faecalis NJ3	8	2	8	8	2	2	1	1	>32	8	0.5	>32	>32	32
Gram-negative														
P. aeruginosa PA01	>32	>32	>32	>32	>32	>32	>32	>32	>32	>32	>32	>32	>32	>32

None of the compounds showed activity against the Gram-negative pathogen *P. aeruginosa*. Previous work has shown that the armeniaspirols are not active against many Gram-negative pathogens including *Acinetobacter baumannii, Klebsiella pneumonia, Salmonella typhimurium, Shigella dysenteriae*.[4] Interestingly while **1** does not inhibit the growth of wild-type *Escherichia coli*, it does inhibit growth of an *E. coli ΔtolC* mutant (Supplemental Table S4), suggesting efflux may be limiting activity in Gram-negative bacteria.[15,16]

Inhibition of recombinant purified ClpYQ

Mechanistically, armeniaspirol functions via inhibition of both the ATP-dependent proteases ClpXP and ClpYQ.[3] We thus evaluated the ability of analogues with enhanced MIC potency relative to **1** for their ability to inhibit peptide hydrolysis by recombinant purified ClpYQ (Table 2, Supplemental Figure S1, Supplemental Table S2). Given that ClpYQ from *S. aureus* was inactive in our in vitro biochemical assays, inhibition kinetics were performed on the characterized *B. subtilis* ClpYQ.[3]

A clear dose response curve was observed with all compounds for ClpYQ hydrolysis of 100 μM fluorogenic substrate Cbz-GGL-AMC. While all compounds exhibited more potent inhibition of ClpYQ,[7] showed the most potent inhibition of ClpYQ, consistent with its highly potent MICs. Given that **1** was shown to be competitive inhibitor of ClpYQ proteolysis activity,[3] we applied the Cheng-Prusoff relationship to determine Ki. **7** inhibits ClpYQ with a K_i = 150 ± 20 nM.

Table 2. Kinetic parameters of potent analogues.

Analogue	R_1 group	R_2 group	MEC_{ClpXP} (μg/mL)	K_i ClpYQ (μM) (± std dev)	MIC (USA300 μg/mL)
1	–*n*-C_6H_{13}	–CH_3	1	3.2 ± 0.2	4
2	–*n*-C_6H_{13}	–*n*-C_6H_{13}	0.067	1.3 ± 0.2	1
5	–*n*-C_6H_{13}	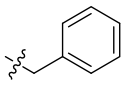	0.25	0.58 ± 0.05	1
6	–*n*-C_6H_{13}	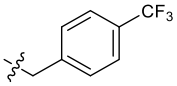	1	0.57 ± 0.10	2
7	–*n*-C_6H_{13}	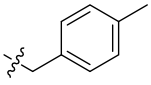	0.25	0.15 ± 0.02	0.5
8	–*n*-C_6H_{13}	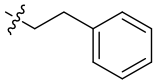	0.25	0.41 ± 0.07	0.5

11	$-CH_3$	$-n\text{-}C_{12}H_{25}$	0.5	1.0 ± 0.2	1

Inhibition of ClpXP activity in S. aureus

To evaluate the inhibition of ClpXP, a cell-based assay was developed. Although we were able to express and purify *S. aureus* ClpXP and the closely related *B. subtilis* ClpXP, we could only achieve single turnover for proteolysis under all conditions investigated. Recombinant purified *E. coli* ClpXP was active and inhibition kinetics could be readily obtained.[3] However, the orthologs from Gram-negative *E. coli* are distantly related to the *S. aureus* proteins. Thus *E. coli* ClpXP inhibition data is expected to be of limited relevance to inhibition of *S. aureus* ClpXP. Because direct ClpP inhibition increases urease activity,[3,17] we were able to determine the minimum effective concentration (MEC) of a ClpXP inhibitor required to increase urease activity above background in MRSA USA300. Thus in Christensen's broth supplemented with phenol red pH indicator, inhibition of ClpXP activity in MRSA USA300 will increase urease activity, hydrolyzing the urea in the media, releasing ammonia, and leading to a colour change from yellow to red as the pH of the broth is increased.[3,17]

Compounds **1-14** were analyzed for their MEC for urease activation from concentrations of 0.067 μg/mL to 1 μg/mL (Supplemental Table S3). As concentrations approached the MIC (within two-fold), bacterial growth slowed. In all cases however, activation of urease by ClpXP inhibition could be detected prior to growth inhibition. The potent benzyl derivatives **5-8** showed similar but improved ClpXP activity compared to **1**. Compound **2** containing a hexyl group at both R_1 and R_2 showed the most potent ClpXP inhibition with a MEC of 0.067 μg/mL.

Discussion

A series of focused derivatives of the natural product antibiotic armeniaspirol were synthesized and evaluated for antibiotic activity against clinically relevant pathogens including MRSA and VRE. Analogues that were more potent than the parent compound **1** were evaluated for their ability to inhibit ClpYQ and ClpXP, the biochemical targets of armeniaspirol.[3] The derivatives focused on diversifying the *N*-methyl moiety (R_2), which proved to be highly amenable to modification. Replacement of the *N*-methyl with *N*-hexyl, various *N*-benzyl, and *N*-phenethyl substituents led to substantial increases in antibiotic activity and potency for inhibition of both ClpYQ and ClpXP. Replacement of the hexyl chain on the aryl core of armeniaspirol (R_1) with a methyl substituent led to a series of analogues substituted on the amide Nitrogen (series 2) that were less active than the corresponding hexyl analogues (series 1), with the exception of **11**.

Armeniaspirol targets both ClpXP and ClpYQ.[3] While single target inhibitors of *Sa*ClpXP are known, without the additional ClpYQ inhibition activity, these compounds are not antibiotic.[17–24] Thus this dual target action is required to intervene sufficiently in the redundant proteolytic pathways that regulate the divisome and cell division. Over half of approved antibiotics since 2015 have multitarget mechanisms of action,[25] likely due to their natural product origins.[26] Optimizing activity of compounds that inhibit multiple targets is challenging. The relevant substrate, cofactor, and allosteric regulator concentrations in the cell can impact the level of inhibition required at each target. Thus it is typically not possible to predict the optimal level of inhibition at each target for maximal effect. Structure-activity relationships at each target are needed as is a structure-activity relationship from an assay that integrates the function of both targets together. In the case of armeniaspirol analogues, the MIC assays provide the data integrating activity at both ClpYQ and ClpXP.

In general, increasing potency at either target appears to correlate with improved overall antibiotic activity. For example, Series 1 analogues **1**, **2**, and **7** show a steady ≈20-fold decrease in K_I for ClpYQ inhibition, which correlates with the 8-fold increase in potency as measured by MIC. Similarly, analogues **1**, **11** and **8** show a steady decrease in MEC, representative of inhibition of ClpXP, which correlates to a decrease in MIC against MRSA USA300. This data is consistent with armeniaspirol antibiotic activity being derived from both ClpXP and ClpYQ inhibition. In addition, the data suggests that inhibitory activity against both targets is balanced, since analogues that possess increased potency against ClpXP or ClpYQ, increase antibiotic activity.

Some analogues however show highly potent inhibition of one of the targets over the other. For example, **7** is a sub-micromolar inhibitor of ClpYQ (K_I = 150 ± 20 nM); however, it is no more active in the MIC assays than the less potent **8** (K_I = 410 ± 70 nM) in MIC assays (MIC = 0.5 μg/mL). This is even more apparent with **2**, which shows ClpXP inhibition at 0.067 μg/mL but is no more active in MIC assays (MIC = 1.0 μg/mL) than **5**, which inhibits ClpXP at 0.25 μg/mL. These data suggest that as analogues become highly potent towards one of the targets, without significantly increasing the potency against the other, little increase in antibiotic activity is obtained.

The enhanced activity of the more lipophilic series 1 analogues over series 2 compounds raised concerns that activity was either a function of aggregation or non-specific lipophilicity-mediated affinity. To evaluate if aggregation of the analogues played a significant role in activity, the MICs for the parent compound **1** and the highly lipophilic **2** were determined in the presence of detergent. Addition of 0.01% v/v triton X-100 had minimal impact on the MICs of either compounds against MRSA USA300 (Supplemental table S4). In further support of

aggregation playing a limited role in activity, fitting of the ClpYQ dose response data to an IC_{50} model where the slope could vary provided Hill coefficients of -1 to -1.5. In cases where aggregation plays a significant role in inhibition, steep slopes are frequently obtained, corresponding to Hill coefficients well below -1.5.[27] As such aggregation was not considered a major source of the increased potency observed for the more lipophilic analogues.

Careful examination of the data shows that activity is not simply a function of increased lipophilicity as the most lipophilic compounds **3** and **6** (highest cLogPs) were not the most potent in any of the assays. Though there does appear to be a correlation between low activity and low lipophilicity since **9** and **12**, two of the library members with the lowest clogP are some of the least active compounds. As the proteolytic chambers of both the ClpYQ and ClpXP must accommodate their unfolded protein clients whose hydrophobic cores are exposed, it stands to reason that moderately lipophilic inhibitors could be well suited to inhibition.

Models rationalizing the observed K_I and MEC data were generated by docking armeniaspirol into ClpP and ClpQ high resolution structures using AutoDock Vina.[28] Armeniaspirol showed two preferred binding sites on the active conformation of the *S. aureus* ClpP heptamer (3V5E),[29] both of which were in the proteolytic cavity (Figure 3 and Supplemental Figure S2A). The most frequent pose from the lowest energy docked structures showed armeniaspirol bound in the same site as seen for the binding of the ClpXP inhibitor bortezomib to *Thermus thermophiles* ClpP (6HWM, Figure 3C).[30] Armeniaspirol, like bortezomib, H-bonds to backbone NHs at the C-terminal end of αC30 via its ketone. In addition, our model shows the ketone H-bonding to the side chain of the active site Ser70. The hexyl chain engages in Van der Waals interactions with the hydrophobic face of αE. Lastly the phenol of armeniaspirol H-bonds to His142 and Thr146 of αE. The second pose showed armeniaspirol

bound closer to the *N*-terminus of ClpP, though still in the proteolytic chamber (Supplemental Figure S2A).

This ClpP binding model is in excellent accordance with the bortezomib *Tt*ClpP structure (Figure 3C, inset 2) and is consistent with all current structure-activity relationship data. For example, both the phenol and ketone are required for antibiotic activity and in this model they both have discrete H-binding interactions with the target. Similarly, our current work shows that the hexyl chain of series 1 analogues is preferred over the methyl chain of series 2 analogues, consistent with the model showing the hexyl to be buried between αE and the loop between β6 and β7. Lastly the model shows significant space available for the *N*-methyl group to be replaced with varying *N*-alkyl groups, consistent with these *N*-alkyl analogues displaying potent inhibition of ClpP. While experimental evidence validating this model is clearly needed, it does provide for testable atomic level hypotheses for inhibitor binding.

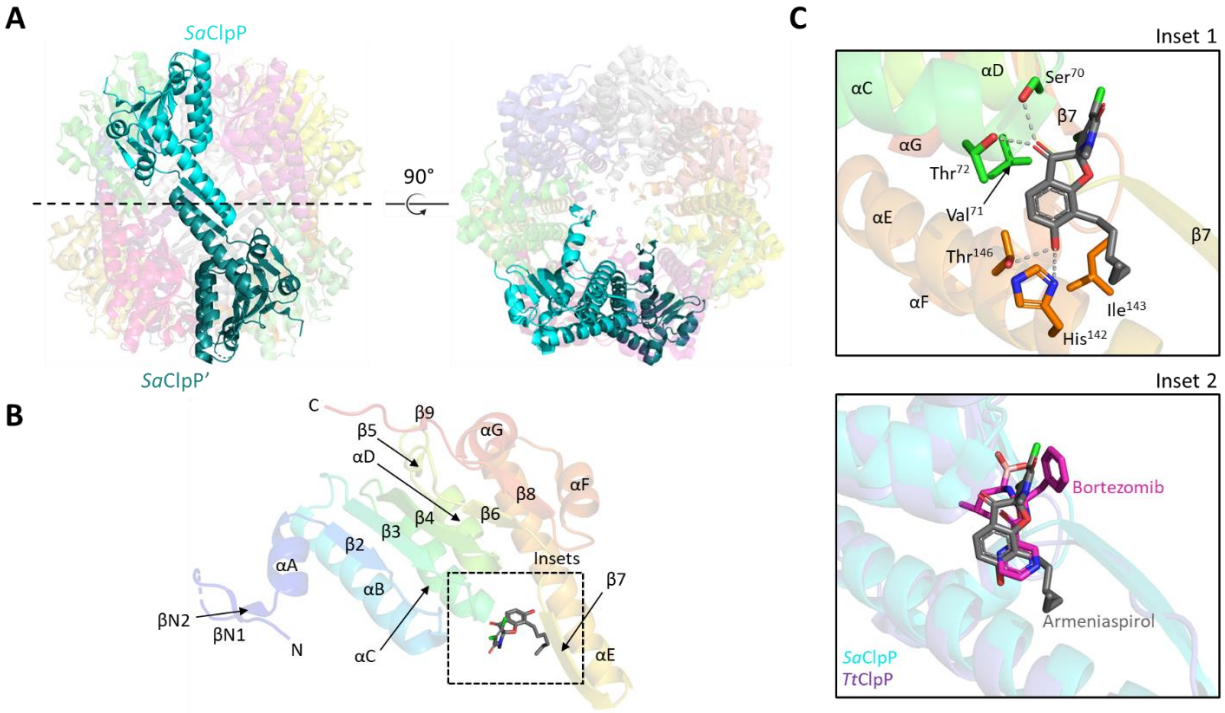

Figure 3. Structure and docking results of *S. aureus* ClpP (3V5E). (A) Side and top views of *S. aureus* ClpP (*Sa*ClpP) tetradecamer. A single monomer per heptameric ring (transparent cartoons) are highlighted in cyan and dark cyan respectively. (B) Cartoon representation of the *Sa*ClpP monomer bound to armeniaspirol. Secondary structures are coloured in rainbow, helices are named by letters while strands are indicated by numbers. The dashed-line box indicates the armeniaspirol binding site predicted by molecular docking. (C) Expanded view of armeniaspirol docking site in *Sa*ClpP. Possible residues involved in armeniaspirol binding are shown as sticks with proposed hydrogen bonds shown as grey dashed lines (inset 1). Overlay of *Thermus thermophilus* ClpP (*Tt*ClpP) bound to bortezomib (PDB: 6HWM) and *Sa*ClpP bound to armeniaspirol is shown (inset 2).

A model of armeniaspirol binding to the dodecamer of *S. aureus* ClpQ (6KUI) was also generated (Figure 4),[31] with two main poses being observed. In the first pose (Figure 4B) armeniaspirol is positioned at the active site, with the phenol hydrogen bonding to the active site Thr1 backbone NH and Thr29 side-chain. This pose is similar to that seen in the high resolution structure of the NLVS inhibitor bound to *Haemophilus influenza* ClpQ (1KYI, Figure 4C).[32] For example, Ser21 of *Hi*ClpQ, analogous to Thr29 of *Sa*ClpQ, H-bonds with the inhibitor. The armeniaspirol hexyl chain fits into the same S1 pocket as the aliphatic *i*Pr group from NLVS and packs against *Sa*ClpQ Val28, in an analogous fashion to *Hi*ClpQ Val20. The ketone of armeniaspirol engages with Gln32, and the amide carbonyl with Glu101, anchoring armeniaspirol in front of the active site. The second pose for armeniaspirol shows the compound bound at the interface between two protomers of one of the hexameric rings (Supplemental

Figure S2B). While the ClpQ binding model agrees with known structure-activity data and the data generated from this study, it remains to be experimentally validated.

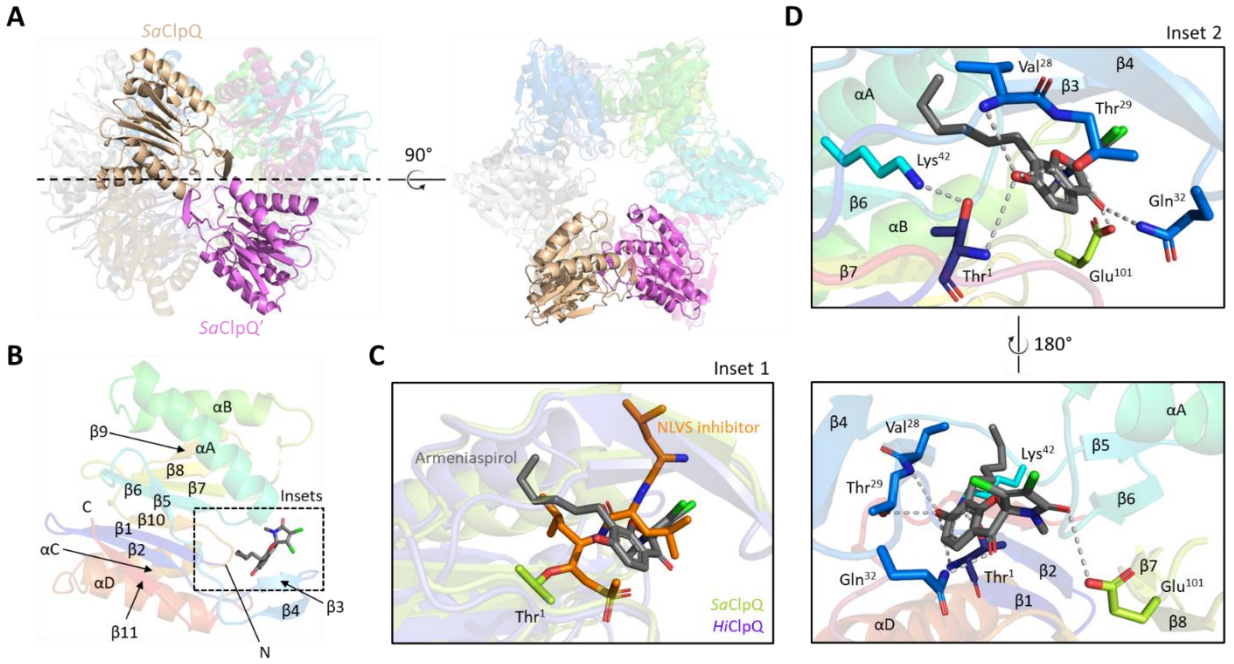

Figure 4. Structure and docking results of *S. aureus* ClpQ (6KUI). (A) Side and top views of *S. aureus* ClpQ (*Sa*ClpQ) dodecamer. A single monomer per hexameric ring (transparent cartoons) are highlighted in sandstone and magenta respectively. (B) Cartoon representation of the *Sa*ClpQ monomer bound to armeniaspirol. Secondary structures are coloured in rainbow, helices are named by letters while strands are indicated by numbers. The dashed-line box indicates the armeniaspirol binding site predicted by molecular docking. (C) Overlay of *Haemophilus influenza* ClpQ (*Hi*ClpQ) covalently bound to a vinyl sulfone inhibitor (PDB: 1KYI) and *Sa*ClpQ bound to armeniaspirol (inset 1). (D) Expanded view of armeniaspirol docking site in *Sa*ClpQ. Possible residues involved in armeniaspirol binding are shown as sticks with proposed hydrogen bonds shown as grey dashed lines (inset 2).

While both bortezomib and NLVS are covalent inhibitors of their respective targets ClpP and ClpQ,[30,32] **1** has been shown to be a competitive inhibitor of the peptide substrate in purified enzyme assays.[3] In the models of armeniaspirol bound to ClpP and ClpQ the electrophilic β-carbon of the α,β-unsaturated lactam is well removed from the active site nucleophiles, consistent with a competitive model for inhibition of proteolysis.

In addition to target binding, lipophilicity can impact off-target interactions.[5,33,34] In particular membrane targeting may be enhanced with increased lipophilicity. As such the hemolytic activity of **1** and two of the most potent and lipophilic analogues **2** and **8** was determined (Figure S3).[35] At 200 μM **1** showed less than 15% lysis of sheep erythrocytes whereas the more lipophilic **2** and **8** showed less than 5% hemolysis. Thus while lypophilic, the armeniaspirols do not destabilize mammalian red blood cell membranes at pharmacologically relevant concentrations. The toxicity of **1**, **2**, and **8** was also evaluated against human lung epithelial carcinoma (A549) cells. The cell culture cells were incubated with up to 100 μM compound, stained with calcein-AM and ethidium homodimer-1, and evaluated by both by confocal microscopy and flow cytometry to determine the fraction of viable and dead cells (Figure S4). All three compounds at 100 μM were indistinguishable from the vehicle control and showed a greater than 95% viable cell population.

Lipophilicity is also an important driver of protein binding, which can impact antibiotic pharmacokinetics and pharamcodynamics.[36] To evaluate the effect of protein binding on antimicrobial activity, we determined the MIC of **1** and the highly lipophilic **2** against MRSA USA300 in the presence of bovine albumin (Table S4). Addition of serum suppressed antibiotic activity, consistent with a high degree of protein binding expected for these lipophilic compounds. For example, the MIC of the parent compound exceeded 32 μg/mL in the presence

of BSA. However armeniaspirol is known to be active in an *in vivo* mouse model of MRSA septicaemia with 10 mg/kg i.v. delivery. Thus while this assay confirms that protein binding is a significant factor in the antibiotic activity of the armeniaspirols, the addition of serum albumin alone does not adequately model the pharmacodynamics behaviour of the drug *in vivo*.[37]

Conclusion

This study has provided new highly potent Gram-positive antibiotics active against clinically relevant strains of MRSA, including USA300 the most common community acquired MRSA infection. Our work has shown that the increased potency of analogues against ClpXP and ClpYQ correlates with increased antibiotic activity, strongly supporting the mechanism of action. We show that activity against both targets is balanced, such that increasing activity at either target increases antibiotic activity. Furthermore, while potency tracks loosely with lipophilicity, this is likely due to binding to the hydrophobic proteolysis chamber rather than non-selective binding interactions. Docking models support this hypothesis and show armeniaspirol may bind at the active site, but in a configuration that does not enable covalent modification of the active site nucleophiles, consistent with competitive inhibition of ClpXP and ClpYQ.

Conflicts of interest

There are no conflicts of interest

Acknowledgements

This work was funded by the Natural Sciences and Engineering Research Council of Canada (NSERC) (A.J.S. RGPIN 2021-03387; C.N.B RGPIN 2019-06859). The authors thank the John L. Holmes Mass Spectrometry Facility for assistance in acquiring mass spectrometry data and

the University of Ottawa Faculty of Science NMR facility for assistance in collecting NMR spectra.

Notes and references

1. Dufour, C.; Wink, J.; Kurz, M.; Kogler, H.; Olivan, H.; Sablé, S.; Heyse, W.; Gerlitz, M.; Toti, L.; Nußer, A. Isolation and structural elucidation of armeniaspirols A-C: Potent antibiotics against gram-positive pathogens. *Chem. - A Eur. J.* **2012**, 18 (50), 16123–16128.
2. Couturier, C.; Bauer, A.; Rey, A.; Schroif-Dufour, C.; Broenstrup, M. Armeniaspiroles, a new class of antibacterials: Antibacterial activities and total synthesis of 5-chloro-Armeniaspirole A. *Bioorg. Med. Chem. Lett*. **2012**, 22 (19), 6292–6296.
3. Labana, P.; Dornan, M. H.; Lafrenière, M.; Czarny, T. L.; Brown, E. D.; Pezacki, J. P.; Boddy, C. N. Armeniaspirols inhibit the AAA+ proteases ClpXP and ClpYQ leading to cell division arrest in Gram-positive bacteria. *Cell Chem. Biol*. **2021**, 28, 12, 1703-1715
4. Qiao, Y.; Yan, J.; Jia, J.; Xue, J.; Qu, X.; Hu, Y.; Deng, Z.; Bi, H.; Zhu, D. Characterization of the biosynthetic gene cluster for the antibiotic armeniaspirols in streptomyces armeniacus. *J. Nat. Prod*. **2019**, 82 (2), 318–323.
5. Leeson, P. D.; Springthorpe, B. The influence of drug-like concepts on decision-making in medicinal chemistry. *Nat. Rev. Drug Discov*. **2007,** 6 (11), 881–890.
6. Durham, D. G.; Rees, A. H. Chlorination of Pyrroles. Part I. *Can. J. Chem*. **1971**, 49 (1), 136–138.
7. Schäfer, W.; Franck, B. Selektive Ätherspaltung von 4-Hydroxy-methoxy-chinolincarbonsäureestern. *Chem. Ber*. **1966**, 99 (1), 160–164.

8. Wiegand, I.; Hilpert, K.; Hancock, R. E. W. Agar and broth dilution methods to determine the minimal inhibitory concentration (MIC) of antimicrobial substances. *Nat. Protoc.* **2008**, 3 (2), 163–175.

9. Chen, Y.; Crosby, H. A.; Oosthuysen, W. F.; Diekema, D. J.; Kelley, S. T.; Horswill, A. R. Draft genome sequence of usa100 methicillin-resistant Staphylococcus aureus strain 209. *Genome Announc*. **2018**, 6 (1).

10. Weber, J. T. Community-associated methicillin-resistant Staphylococcus aureus. *Clinical Infectious Diseases. Clin Infect Dis* August 15**, 2005**.

11. King, J. M.; Kulhankova, K.; Stach, C. S.; Vu, B. G.; Salgado-Pabón, W. Phenotypes and Virulence among Staphylococcus aureus USA100, USA200, USA300, USA400, and USA600 Clonal Lineages . *mSphere* **2016**, 1 (3).

12. Levison, M. E. Pharmacodynamics of antimicrobial drugs. *Infectious Disease Clinics of North America*. September **2004,** pp 451–465.

13. French, G. L. Bactericidal agents in the treatment of MRSA infections-the potential role of daptomycin. *J. Antimicrob. Chemother*. **2006**, 58, 1107–1117.

14. Pankey, G. A.; Sabath, L. D. Clinical relevance of bacteriostatic versus bactericidal mechanisms of action in the treatment of gram-positive bacterial infections. *Clin. Infect. Dis.* **2004**, 38 (6), 864–870.

15. Paulsen, I. T.; Park, J. H.; Choi, P. S.; Saier, M. H. A family of gram-negative bacterial outer membrane factors that function in the export of proteins, carbohydrates, drugs and heavy metals from gram-negative bacteria. *FEMS Microbiol. Lett.* **1997**, 156 (1), 1–8.

16. Koronakis, V.; Eswaran, J.; Hughes, C. Structure and function of TolC: the bacterial exit duct for proteins and drugs. *Annu. Rev. Biochem***. 2004**, 73, 467–489.

17. Gao, P.; Ho, P. L.; Yan, B.; Sze, K. H.; Davies, J.; Kao, R. Y. T. Suppression of Staphylococcus aureus virulence by a small-molecule compound. *Proc. Natl. Acad. Sci*. U. S. A. **2018**, 115 (31), 8003–8008.

18. Böttcher, T.; Sieber, S. A. β-lactones as specific inhibitors of ClpP attenuate the production of extracellular virulence factors of Staphylococcus aureus. *J. Am. Chem. Soc.* **2008**, 130 (44), 14400–14401.

19. Zeiler, E.; Korotkov, V. S.; Lorenz-Baath, K.; Böttcher, T.; Sieber, S. A. Development and characterization of improved β-lactone-based anti-virulence drugs targeting ClpP. *Bioorganic Med. Chem*. **2012**, 20 (2), 583–591.

20. Krysiak, J.; Stahl, M.; Vomacka, J.; Fetzer, C.; Lakemeyer, M.; Fux, A.; Sieber, S. A. Quantitative Map of β-Lactone-Induced Virulence Regulation. J. *Proteome Res.* **2017**, 16 (3), 1180–1192.

21. Hackl MW, Lakemeyer M, Dahmen M, Glaser M, Pahl A, Lorenz-Baath K, Menzel T, Sievers S, Böttcher T, Antes I, Waldmann H, Sieber SA. Phenyl Esters Are Potent Inhibitors of Caseinolytic Protease P and Reveal a Stereogenic Switch for Deoligomerization. *J. Am. Chem. Soc.* **2015**, 137 (26), 8475–8483.

22. Pahl A, Lakemeyer M, Vielberg MT, Hackl MW, Vomacka J, Korotkov VS, Stein ML, Fetzer C, Lorenz-Baath K, Richter K, Waldmann H, Groll M, Sieber SA. Reversible Inhibitors Arrest ClpP in a Defined Conformational State that Can Be Revoked by ClpX Association. *Angew. Chemie - Int. Ed.* **2015**, 54 (52), 15892–15896.

23. Gersch, M.; Kolb, R.; Alte, F.; Groll, M.; Sieber, S. A. Disruption of oligomerization and dehydroalanine formation as mechanisms for ClpP protease inhibition. *J. Am. Chem. Soc.* **2014**, 136 (4), 1360–1366.

24. Moreno-Cinos, C.; Goossens, K.; Salado, I. G.; Van Der Veken, P.; De Winter, H.; Augustyns, K. ClpP protease, a promising antimicrobial target. *Int. J. Mol. Sci*. **2019**, 20 (9).

25. Wetzel, C.; Lonneman, M.; Wu, C. Polypharmacological drug actions of recently FDA approved antibiotics. *European Journal of Medicinal Chemistry*. Elsevier Masson s.r.l. January 1, **2021**, p 112931.

26. Ho, T. T.; Tran, Q. T.; Chai, C. L. The polypharmacology of natural products. *Future Med. Chem.* **2018**, 10 (11), 1361–1368.

27. Shoichet, B. K. Interpreting steep dose-response curves in early inhibitor discovery. *J. Med. Chem.* **2006,** 49 (25), 7274–7277.

28. Trott, O.; Olson, A. J. AutoDock Vina: Improving the speed and accuracy of docking with a new scoring function, efficient optimization, and multithreading. *J. Comput. Chem*. **2009**, 31 (2), NA-NA.

29. Gersch, M.; List, A.; Groll, M.; Sieber, S. A. Insights into structural network responsible for oligomerization and activity of bacterial virulence regulator caseinolytic protease P (ClpP) protein. *J. Biol. Chem***. 2012**, 287 (12), 9484–9494.

30. Felix J, Weinhäupl K, Chipot C, Dehez F, Hessel A, Gauto DF, Morlot C, Abian O, Gutsche I, Velazquez-Campoy A, Schanda P, Fraga H. Mechanism of the allosteric activation of the ClpP protease machinery by substrates and active-site inhibitors. *Sci. Adv. **2019***, 5 (9).

31. Jeong, S.; Ahn, J.; Kwon, A. R.; Ha, N. C. Cleavage-Dependent Activation of ATP-Dependent Protease HslUV from Staphylococcus aureus. *Mol. Cells* **2020**, 43 (8), 694–704.

32. Sousa, M. C.; Kessler, B. M.; Overkleeft, H. S.; McKay, D. B. Crystal Structure of HslUV Complexed with a Vinyl Sulfone Inhibitor: Corroboration of a Proposed Mechanism of Allosteric Activation of HslV by HslU. *J. Mol. Biol*. **2002**, 318 (3), 779–785.

33. Hopkins, A. L.; Mason, J. S.; Overington, J. P. Can we rationally design promiscuous drugs? *Curr. Opin. Struct. Biol.* **2006**, 16 (1), 127-136.

34. Peters, J.-U.; Schnider, P.; Mattei, P.; Kansy, M. Pharmacological Promiscuity: Dependence on Compound Properties and Target Specificity in a Set of Recent Roche Compounds. *ChemMedChem* **2009**, 4 (4), 680-686.

35. Evans, B. C.; Nelson, C. E.; Yu, S. S.; Beavers, K. R.; Kim, A. J.; Li, H.; Nelson, H. M.; Giorgio, T, D.; Duvall, C. L. Ex vivo red blood cell hemolysis assay for the evaluation of pH-responsive endosomolytic agents for cytosolic delivery of biomacromolecular drugs. *J. Vis. Exp.* **2013**, 9 (73), e50166.

36. Zeitlinger, M. A.; Derendorf, H.; Mouton, J. W.; Cars, O.; Craig, W. A.; Andes, D.; Theuretzbacher, U. Protein binding: do we ever learn? *Antimicrob. Agents Chemother*. **2011**, 55 (7), 3067-3074.

37. Beer, J.; Wagner, C. C.; Zeitlinger, M. Protein Binding of Antimicrobials: Methods for Quantification and for Investigation of its Impact on Bacterial Killing. *AAPS J.* **2009**, 11 (1). 1-12.

2.6 Supporting Information

Armeniaspirol analogues with more potent Gram-positive antibiotic activity show enhanced inhibition of the ATP-dependent proteases ClpXP and ClpYQ

Michael G. Darnowski, Taylor Lanosky, Puneet Labana, Jordan Brazeau-Henrie, Nicholas D. Calvert, Mark H. Dornan, Claudia Natola, André R. Paquette, Adam J. Shuhendler, and Christopher N. Boddy*

Experimental

Supplemental Figures and Tables

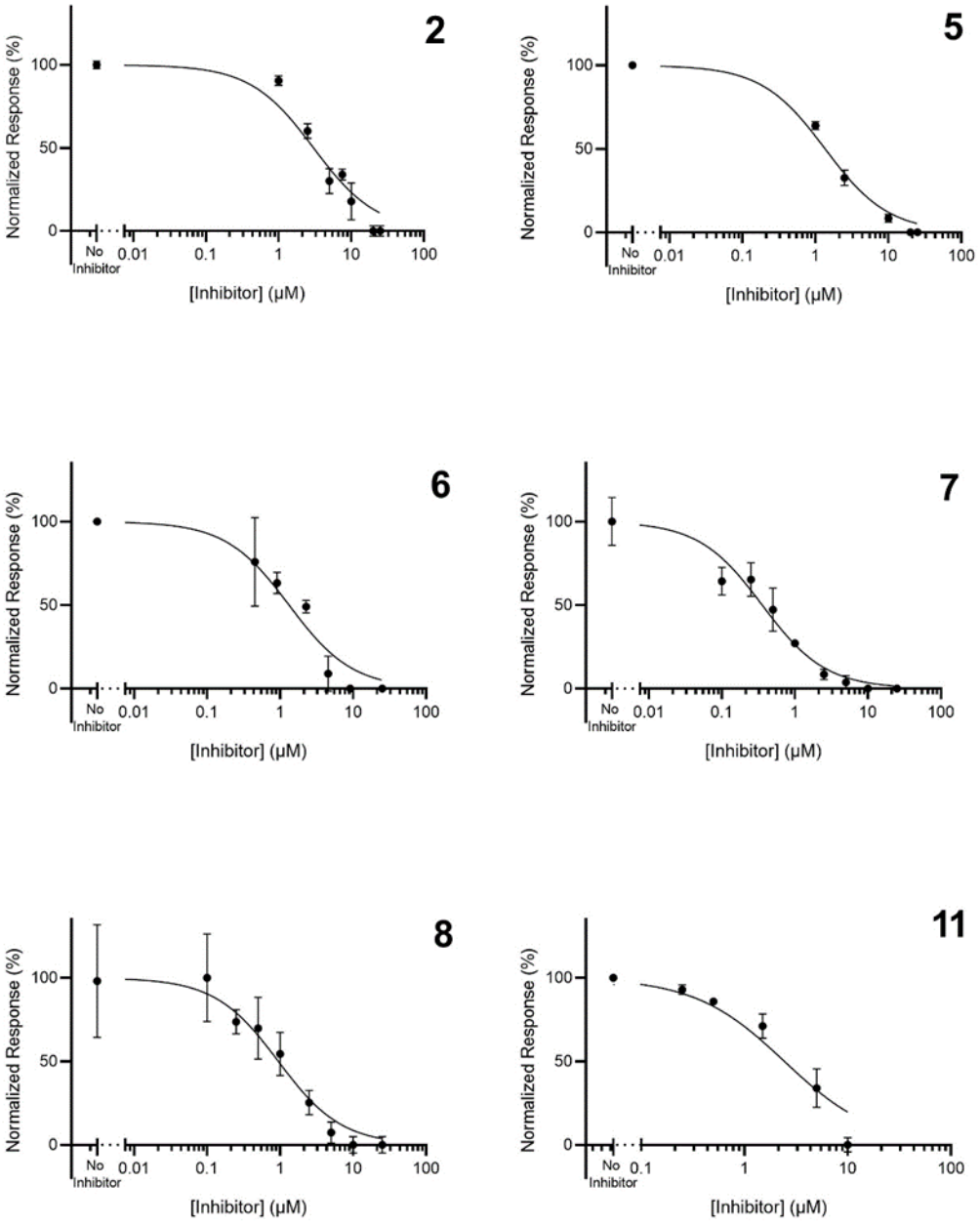

Supplemental Figure S1. ClpYQ inhibition curves showing fit to an IC_{50}

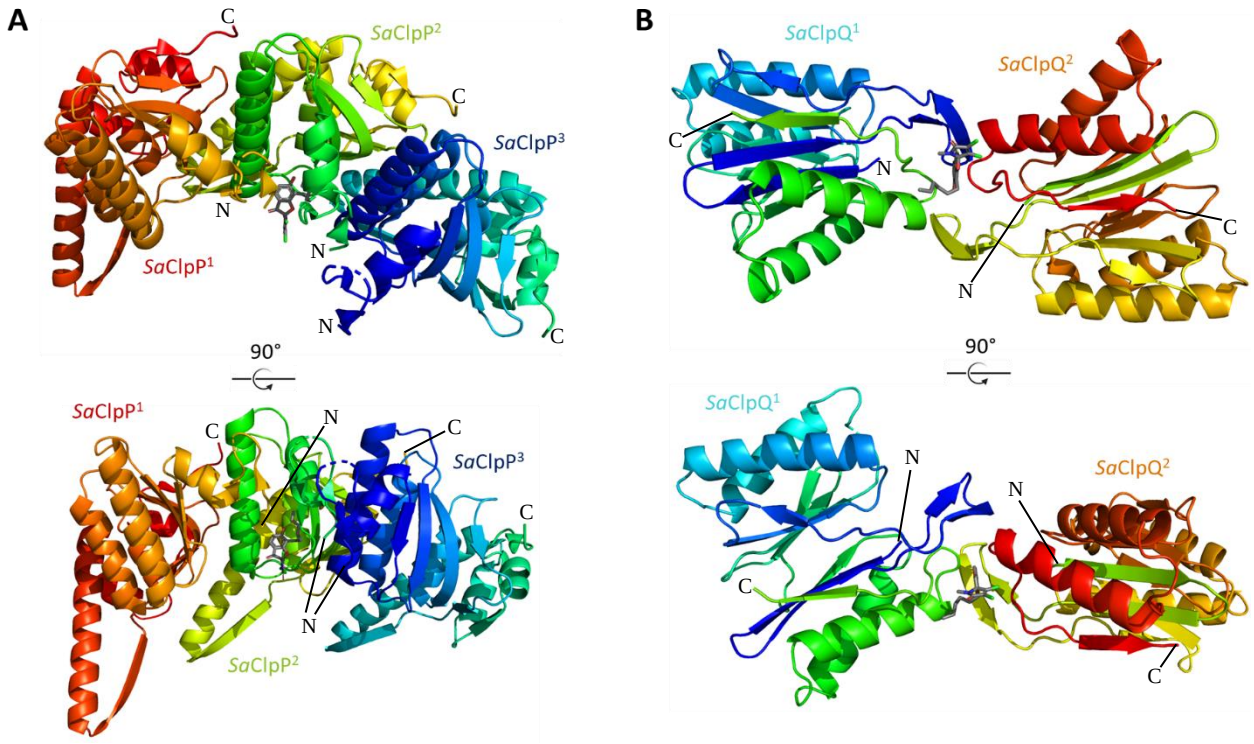

Supplemental Figure S2. Alternate armeniaspirol binding site in *S. aureus* ClpP and ClpQ.

(A) Top and side views of armeniaspirol's alternate binding site on *S. aureus* ClpP (SaClpP) trimer. (B) Top and side views of armeniapsirol's alternate binding site on *S. aureus* ClpQ (*Sa*ClpQ) dimer. In both panels, each monomer is coloured differently and labelled with armeniaspirol shown as grey sticks.

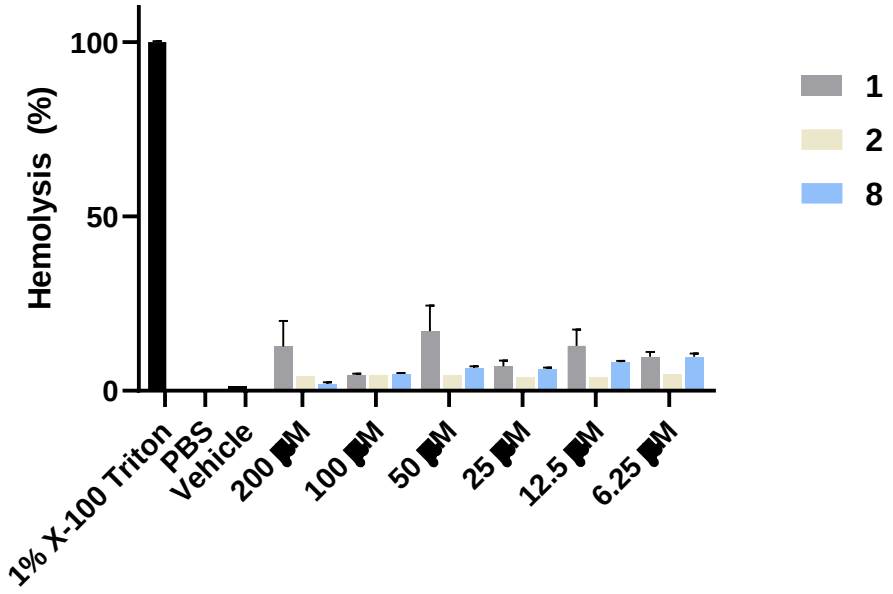

Supplemental Figure S3. Hemolyses of sheep red blood cells by armeniaspirol analogs.

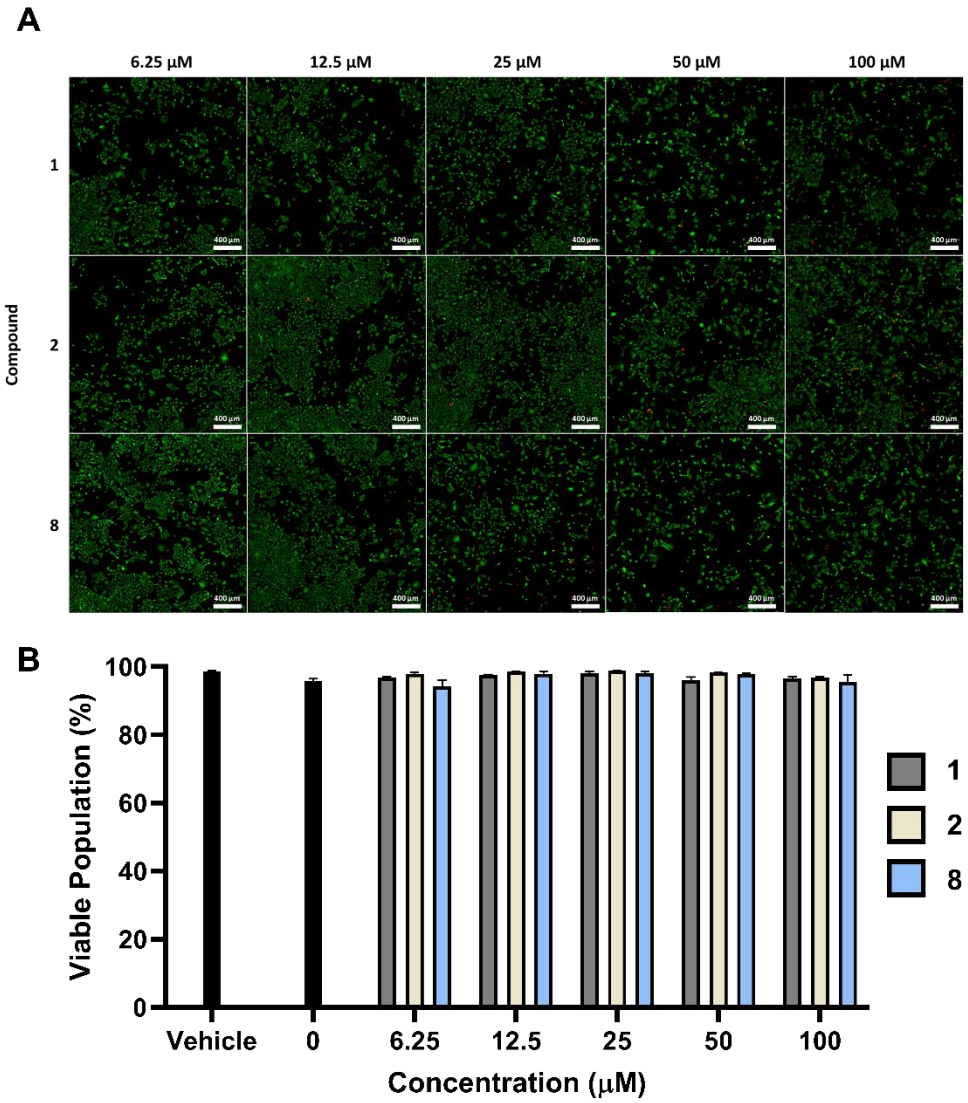

Supplemental Figure S4. Toxicity of armeniaspirol analogues against mammalian A549 cells. (A) Human lung epithelial carcinoma cells (A549) cultured with 100 µM, 50 µM, 25 µM, 12.5 µM, 6.25 µM, or 0 µM of compound **1**, **2**, or **8** for 24 hrs and stained with 1 µM calcein-AM and 2 µM ethidium homodimer-1. Images were acquired on a Zeiss LSM 880 confocal microscope. (B) The viable cell population for each condition, including a 0.5 % DMSO control (vehicle), was determined by comparing the total number of singly-stained, calcein-AM-positive cell counts to the total number of cells that were singly-stained as positive for live or dead as

determined by flow cytometry using a 488 nm excitation with 525/40 bandpass for calcein-AM (live cells, green) and 620/20 bandpass for ethidium homodimer-1 (dead cells, red).

Supplemental Table S1. Minimum bactericidal concentration of analogues.

	Minimum Bactericidal Concentration (μg/ml)													
	1	**2**	**3**	**4**	**5**	**6**	**7**	**8**	**9**	**10**	**11**	**12**	**13**	**14**
Gram-positive														
S. aureus IA116-USA100	32	8	16	32	8	>32	8	8	>32	32	4	>32	>32	>32
S. aureus MN8-USA200	32	16	16	32	>32	32	16	16	>32	>32	8	>32	>32	>32
S. aureus LAC-Fitz-USA300	>32	8	32	>32	>32	16	16	8	>32	>32	2	>32	>32	>32
S. aureus MW2-USA400	>32	8	16	>32	>32	16	16	8	>32	>32	8	>32	>32	>32
E. faecalis NJ3	>32	32	>32	>32	>32	>32	32	32	>32	>32	8	>32	>32	>32
Gram-negative														
P. aeruginosa PA01	>32	>32	>32	>32	>32	>32	>32	>32	>32	>32	>32	>32	>32	>32

Supplemental Table S2. Clp YQ kinetics characterization data

Compound	IC_{50} (± std dev) (μM)	R^2	K_i (μM)
7	0.3562 ± 0.0409	0.9355	0.1532
8	0.9355 ± 0.1663	0.8786	0.4067
6	1.325 ± 0.2319	0.8759	0.5700
5	1.353 ± 0.1131	0.8759	0.5821
2	3.022± 0.3659	0.9209	1.3001
11	2.435 ± 0.3659	0.9095	1.0475

Supplemental Table S3. MEC of Clp XP of analogues in urease assay

Compound	ClpXP MEC (μg/mL)
1	1
2	0.067
3	1
4	1
5	0.25
6	1
7	0.25
8	0.25
9	>1
10	>1

11	0.5
12	>1
13	>1
14	>1

Supplementary Table 4. Additional minimum inhibitory concentration of 1 and 2.

Minimum inhibitory Concentration (µg/ml)		
Bacteria	**1**	**2**
S. aureus LAC-Fitz-USA300	4	1
S. aureus LAC-Fitz-USA300 + 0.5% BSA	>32	32
S. aureus LAC-Fitz-USA300 + 0.01% Triton X-100	8	2
E. coli Δ*tolC*	8	nd
E. coli BW25113	>32	>32

ClpYQ protein purification

The ClpQ expression vector (pPL29, pET21c-based, C-terminal His tag, AmpR) was transformed into chemically competent *E. coli* BL21(DE3) for protein expression. 400 mL LB media was inoculated with 0.5% (*v/v*) of an overnight pre-culture. The culture was grown at 37 °C (200 rpm) and expression was induced with 1 mM isopropyl-1-thio-β-D-galactopyranoside at an optical density (OD_{600}) of 0.5. The culture was grown at 37 °C (200 rpm) for 4 h. The cells were pelleted at 4,000 rpm for 20 min and re-suspended in lysis buffer (50 mM Tris, 100 mM

NaCl, 1 µg/mL leupeptin, 1 µg/mL pepstatin A, 1 mg/mL lysozyme, 10% glycerol, pH 8.0). Mechanical cell lysis was achieved by 3 cycles of 3 s sonication then 2 s incubation on ice followed by a 1 min incubation on ice. The cell debris was pelleted at 10,000 rpm for 60 min and the supernatant was incubated with 800 µL 50% Ni-NTA agarose resin (QIAGEN) for 30 min at 4 °C with gentle shaking. The lysate was loaded onto a column and the flow-through was collected. The resin was washed sequentially with 5 mL elution buffer (100 mM Tris, 300 mM NaCl, pH 8.0) containing 0 mM, 20 mM, 100 mM and 250 mM imidazole. Fractions were analyzed by SDS-PAGE (4-20% Mini-PROTEAN TGX Precast Gels; Bio-Rad). ClpQ-containing fractions were pooled and additionally purified by FPLC size exclusion using a Superdex 200 10/30 GL column (GE Healthcare). Buffer used in FPLC purification included 50 mM Tris, 250 mM NaCl, pH 8.0. ClpQ-containing fractions were concentrated using a 10 kDa Amicon Ultra-15 centrifugal filter unit (Millipore Sigma). The concentrated protein was stored at -80 °C with 30% (*w/w*) glycerol. The *B. subtilis* clpY gene was cloned into pET28B (N-terminal His tag, KanR).

ClpY was expressed and purified from the resulting plasmid (pPL31) as described above with the following modifications. The culture was grown at 16 °C overnight (200 rpm) post-induction. The column fraction containing the highest concentration of ClpY (with 100 mM imidazole) was additionally purified by FPLC size exclusion using a buffer containing 300 mM NaCl, 100 mM Tris, and 100 mM imidazole, pH 8.0. Imidzaole was added to the FPLC buffer to improve protein solubility since ClpY has the tendency to aggregate and must be treated carefully during purification. Accordingly, ClpY-containing fractions obtained from FPLC purification were pooled but not concentrated. All protein concentrations were determined by Bradford assay.

Peptide hydrolysis assays

Peptide hydrolysis was assayed using the Cbz-Gly-Gly-Leu-AMC (Millipore Sigma) substrate. 0.1 mL reaction assays were done in Nunc 96-well microplates for fluorescence-based assays (ThermoFisher Scientific). Assays were composed of purified bsClpQ and bsClpY protein, 0.1 M Tris (pH 8.0), 0.1 mM Cbz-GGL-AMC, 10 mM MgCl2, 1 mM ATP, 1 mM TCEP, and 1 mM EDTA. A continuous assay of AMC release was monitored at 37 °C using a Synergy H4 microplate reader (BioTek). Excitation and emission for Cbz-GGL-AMC were measured at 355 nm and 460 nm, respectively. Inhibition was observed with varying concentrations of analogs.

Minimum inhibitory/bactericidal concentration

Minimum inhibitory concentration (MIC) was carried out in Mueller-Hinton broth with indicated supplements (BSA, Triton X-100) in 100 µL assays in 96-well plates. Sequential concentrations of compound were pipetted into each column through two-fold serial dilutions. 5 µL of bacterial culture (OD_{600} 0.07-0.1) was inoculated into each well and incubated at 37°C for 16 h. Growth was observed by OD_{600} readings using a Synergy H4 microplate reader (BioTek). The MIC was determined by the lowest concentration of compound that prevented bacterial growth.

Minimum bactericidal concentration (MBC) was performed by streaking 100 µL of each MIC bacterial subculture on individual petri dishes of non-antibiotic containing Mueller-Hinton Agar. The MBC was determined by a colony count resulting in a 3-log reduction (99.9%) of bacterial growth. A compound is considered bactericidal if it has an MBC less than 4 × the MIC.

***Staphylococcus aureus* urease activity assay**

Christensen urease broth (pH 6.8) was prepared as follows: 1 g/L peptone, 1 g/L glucose, 5 g/L NaCl, 1.2 g/L Na_2HPO_4, 0.8 g/L KH_2PO_4, 0.004 g/L phenol red. 5 mL of 20% (w/v) urea was then added to a fresh 95 mL of Christensen urease broth. Christensen urease broth was inoculated with 1% (v/v) of an overnight MRSA USA300 pre-culture and 200 µL was added to

each well. Compounds **1-14** were added (1 μg/mL to 0.067 μg/mL). Cultures were grown overnight at 37°C. Cultures were spun down at 4000 rpm for 30 minutes. The supernatant was aspirated into a fresh 96 well plate and resulting colour change was visualized using a Synergy H4 microplate reader (BioTek) at 560 nm.

Preparation of ClpP, ClpQ and ligand structures.

Crystal structures for ClpP and ClpQ (HlsV) from *Staphylococcus aureus* were taken from the PDB database using codes 3V5E and 6KUI respectively. Structures were prepared in the graphical user interface program AutoDock Tools (ADT). ADT removed water molecules, assigned polar hydrogens, computed Gasteiger charges and wrote prepared structures in a PDBQT file format. ChemDraw for armeniaspirol was converted to a MOL2 file format and pre-processed in Avogadro[1] by assigning polar hydrogens and performing structure minimization with default settings. Resulting pre-processed structure was opened in ADT to assign rotatable bonds and convert into a PDBQT file format[2–4].

Docking methodology.

Molecular docking was performed using the AutoDock Vina program[2,4]. Armeniaspirol was docked to both ClpP and ClpQ within grid coordinates (grid centre) and grid boxes centreed around the oligomers axis of symmetry using ADT. Armeniaspirol was in a flexible condition,

with 6 rotatable bonds, when interacting with the proteins under rigid conditions. The grid size for ClpP was set to 70 × 70 × 58 *xyz* points with a grid spacing of 1 Å and a grid centre designated at dimensions -44.762*x*, -12.455*y* and -19.341*z*. The grid size for ClpQ was set to 68 × 46 × 54 *xyz* points with a grid spacing of 1 Å and a grid centre designated at dimensions 1.02*x*, 19.085*y* and 40.824*z*. Ligand-binding affinities were predicted as Gibbs free energy scores (ΔG, kcal/mol) using the AutoDock Vina scoring function. Docked ligand poses with the best score were chosen for post-docking analyses in PyMOL.

Hemolysis assay.

Compounds **1**, **2**, and **8** were diluted to 400 µM in PBS buffer from 50 mM DMSO stock. 1% Triton X-100 was used as the positive control, PBS was used as a negative control and 0.78% DMSO was used as the vehicle control. 75 µL of compound in PBS were added to 75 µL of sheep red blood cells (sRBC) in a 10% suspension in PBS buffer in a flat bottomed black 96-well plate. The plate was sealed and agitated at 37°C for 1 h. The plate was centrifuged for 10 minutes at RT at 1000 x g and 35 µL of the supernatant was removed. A 10 µL aliquot from the supernatant was added to 90 µL PBS in a flat bottomed black 96-well plate and measured absorbance at 414 nm on a Synergy H1 Hybrid Multi-Mode Reader (Biotek, Winooski, VT). % hemolysis was calculated, hemolysis (%) = (abs sample – abs neg average)/(abs pos average – abs neg average) x 100%. The triplicate data was analyzed in GraphPad Prism 8.

Mammalian cell culture toxicity.

Human lung epithelial carcinoma cells (A549) were cultured in Dulbecco's modified Eagle medium (DMEM) supplemented with 10% fetal bovine serum and 1% penicillin-streptomycin were grown and maintained under cell culture conditions (37ºC, 5% CO_2, and in a humidified

environment) in a 24-well plate. At confluency, fresh DMEM was added containing 100 µM, 50 µM, 25 µM, 12.5 µM, 6.25 µM, or 0 µM of compound **1**, **2**, or **8** (from a 50 mM stock in DMSO) in triplicate wells and incubated under cell culture conditions for 24 h. Following incubation, fresh DMEM without phenol red containing 1 µM calcein-AM and 2 µM ethidium homodimer-1 was added and incubated under cell culture conditions for 30 min. Three-by-three tiled images were acquired on a Zeiss LSM 880 confocal microscope while maintaining cell culture conditions. Following microscopy, the media was set aside and cells were detached from the plate with trypsin-EDTA, centrifuged (5min, 1000 × g, 4^{o}C), then resuspended in the dye-containing medum. Cell populations were examined using flow cytometry using a 488 nm excitation with 525/40 bandpass for calcein-AM (live cells, green) and 620/20 bandpass for ethidium homodimer-1 (dead cells, red). The viable cell population for each condition, including a 0.5 % DMSO control (vehicle), was determined by comparing the total number of singly-stained, calcein-AM-positive cell counts to the total number of cells that were singly-stained as positive for live or dead.

Synthesis

General Synthetic Protocols

All reagents were purchased from Sigma-Aldrich at the highest available purity and used without further purification. All solvents were purchased from Fisher Scientific. All reactions were conducted using dry solvents under an argon atmosphere unless otherwise noted. NMR spectroscopy was performed with a Bruker Avance II, operating at 400 MHz for ^{1}H spectra, and 100 MHz for ^{13}C spectra or Bruker Avance III, with cryoprobe operating at 600 MHz for ^{1}H spectra, and 150 MHz for ^{13}C spectra. Preparatory TLC was performed using Merck Millipore 20 x 20 cm silica gel 60 F254 plates. High-resolution mass spectroscopy (HRMS) was conducted on a Micromass Q-TOF I for ESI measurements and a Kratos Concept 1S High Resolution Mass Spectrometer for EI measurements (John L. Holmes Mass Spectroscopy Facility)

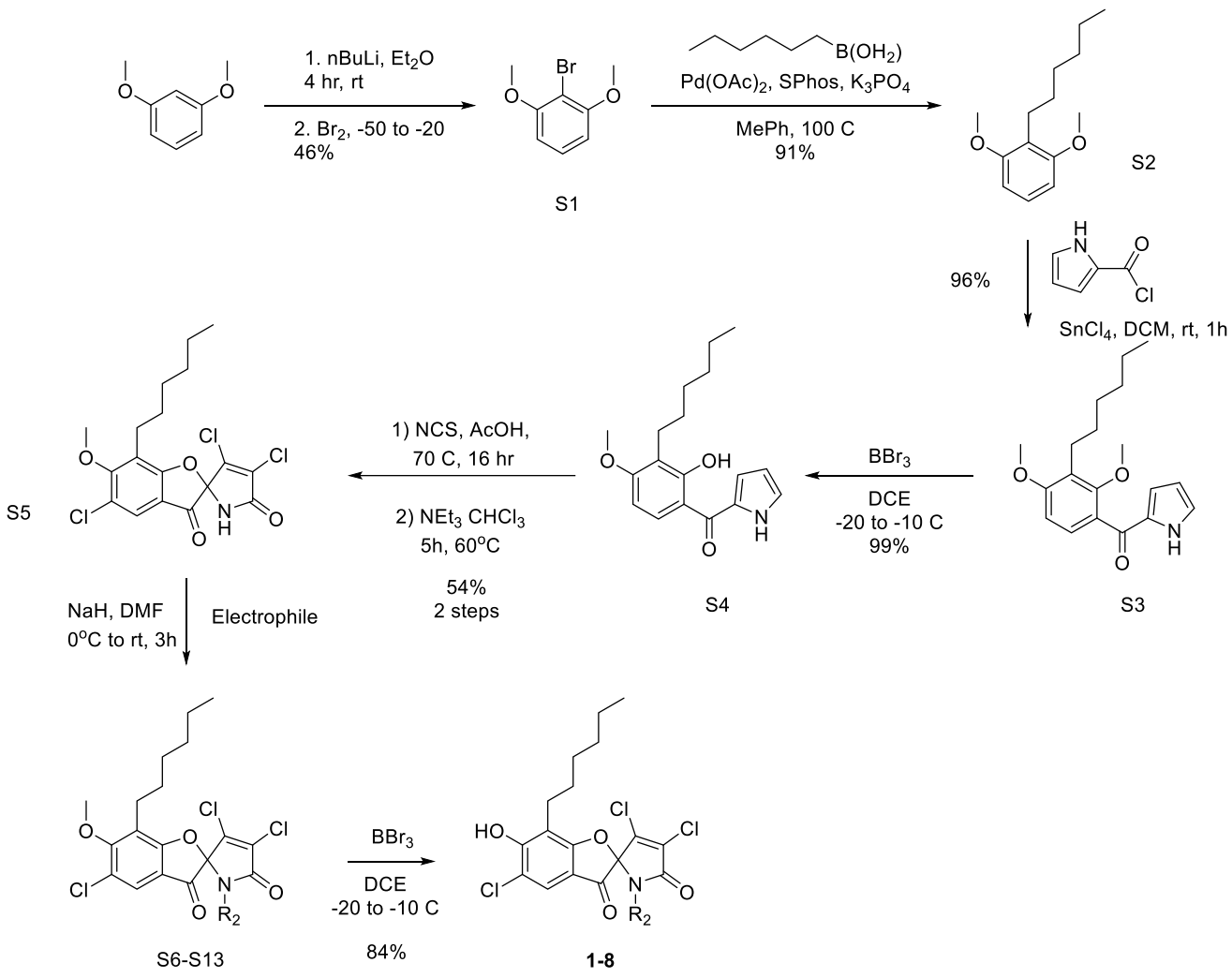

Scheme S1. Synthesis of hexyl R1 series of analogues

S1

1,3-dimethoxybenzene (14.40 g, 0.104 mol, 1.0 equiv.) was dissolved in Et_2O (375 mL) in a round bottom flask. n-BuLi (50 mL of a 2.5 M solution, 1.2 equiv.) was added and the solution was allowed to stir at ambient temperature for 4 hours. The reaction mixture was then cooled to –50 °C using a dry ice/acetone bath. Bromine (18.65 g, 0.117 mol, 1.1 equiv.) was added

dropwise. The solution was then heated to room temperature and allowed to react for another two hours. To the resulting mixture, 250 mL of a 10 % sodium thiosulfate solution was added and the resulting mixture was allowed to stir for 1 hour. The solution was extracted 2 × with Et_2O. The resulting organic fractions were combined and washed with brine. The organic phase was then dried with Na_2SO_4 and concentrated to yield the desired compound **S1** (9.45 g, 43.5 mmol, 42 % yield) which was used without further purification. The NMR data were consistent with literature values.

^{1}H NMR (400 MHz, Chloroform-*d*) δ 7.21 (t, *J* = 8.3 Hz, 1H), 6.56 (d, *J* = 8.4 Hz, 2H), 3.88 (s, 6H).

^{13}C NMR (100 MHz, $CDCl_3$) δ 157.21, 128.24, 104.70, 100.97, 56.45.

S2

In a round-bottom flask, **S1** (5.0 g, 23.0 mmol, 1.0 equiv.) was dissolved in toluene (230 mL). To the resulting solution, n-hexylboronic acid (5.98 g, 46 mmol, 2.0 equiv.), $K_3PO_4 \cdot H_2O$ (10.6 g, 46 mmol, 2.0 equiv.), $Pd(OAc)_2$ (516 mg, 2.3 mmol, 0.1 equiv.), and SPhos (1.89 g, 4.6 mmol, 0.2 equiv.) were added at ambient temperature. The mixture was stirred at 100 °C for 15 hours. After cooling, the reaction mixture was quenched with NH_4Cl (aq) and extracted 3 × with EtOAc. The organic fractions were combined, washed with brine, dried over Na_2SO_4 and concentrated. The desired compound S2 (4.65 g, 20.9 mmol, 91 % yield) was purified from the crude mixture by silica column chromatography (100 % hexanes). The NMR data were consistent with literature values.

^{1}H NMR (400 MHz, Chloroform-*d*) δ 7.08 (t, *J* = 8.3 Hz, 1H), 6.51 (d, *J* = 8.3 Hz, 2H), 3.78 (s, 6H), 2.73 – 2.50 (m, 2H), 1.43 (q, *J* = 7.2 Hz, 2H), 1.37 – 1.22 (m, 6H), 0.89 – 0.81 (m, 3H).

^{13}C NMR (100 MHz, $CDCl_3$) δ 158.30, 126.33, 119.75, 103.71, 55.70, 31.81, 29.53, 29.25, 22.91, 22.71, 14.17.

S3

Pyrrole 2-carboxylic acid (0.721g, 6.49 mmol, 2 eq) was dissolved in 10 mL of DCM, oxalyl chloride (9.7 mL, 19.48 mmol, 3 equiv) was added dropwise, 1 drop of DMF was added. The following mixture was stirred for 1 hour at room temperature. The solvent was removed en vacuo. The intermediate acid chloride was resuspended in DCM in a round-bottom flask, **S2** (0.5 g, 3.246 mmol, 1.0 equiv.) was added and cooled to 0 °C with an ice bath. $SnCl_4$ (16.2 mL of a 1.0 M solution, 5 equiv.) was then added dropwise. The mixture was stirred for 1 hour at 0 °C, then warmed to ambient temperature. The reaction mixture was quenched with a saturated $NaHCO_3$(aq) and extracted 3 × with EtOAc. The organic fractions were combined, washed with brine, dried over Na_2SO_4 and concentrated. The desired compound (0.640 g, 2.519 mmol, 78 % yield) was purified from the crude mixture by silica column chromatography (30 % EtOAc in Hexanes). The NMR data were consistent with literature values.

^{1}H NMR (400 MHz, Acetone-d_6) δ 7.30 (d, *J* = 8.5 Hz, 1H), 7.19 (dq, *J* = 2.9, 1.5 Hz, 1H), 6.80 (d, *J* = 8.6 Hz, 1H), 6.59 (ddd, *J* = 3.8, 2.2, 1.4 Hz, 1H), 6.23 (dt, *J* = 3.8, 2.3 Hz, 1H), 3.89 (s, 3H), 3.67 (s, 3H), 2.70 – 2.57 (m, 2H), 1.52 (q, *J* = 7.7 Hz, 2H), 1.42 – 1.24 (m, 6H), 0.93 – 0.82 (m, 3H).

^{13}C NMR (100 MHz, Acetone-d_6) δ 183.59, 160.13, 157.54, 132.64, 128.20, 125.82, 125.16, 124.37, 118.53, 109.94, 105.12, 61.89, 55.29, 31.56, 29.43, 23.38, 22.43, 13.49.

S4

In a round-bottom flask, **S2** (0.830 g, 2.63 mmol, 1.0 equiv.) was dissolved in 1,2-dichloroethane (3 mL). The solution was cooled to -20 °C using a dry ice/acetone bath. BBr3 (3.13 mL of a 1 M

solution, 1.2 equiv.) was added dropwise, and the reaction mixture was stirred at -20 to – 10 °C for 2 hours. Subsequently, Et_3N / water was added, and the solution was extracted 3 × with EtOAc. The organic fractions were combined, washed with brine, dried over Na2SO4, and concentrated. The desired compound (0.788g, 2.61 mmol, 99 % yield) was used without purification. The NMR data were consistent with literature values.

^{1}H NMR (400 MHz, Acetone-d_6) δ 12.76 (s, 1H), 8.05 (dd, *J* = 8.9, 0.9 Hz, 1H), 7.27 (ddd, *J* = 3.0, 2.5, 1.4 Hz, 1H), 7.05 (dtd, *J* = 4.2, 2.8, 1.3 Hz, 1H), 6.67 (d, *J* = 9.0 Hz, 1H), 6.36 (ddd, *J* = 3.9, 2.9, 2.0 Hz, 1H), 3.93 (s, 3H), 2.73 – 2.58 (m, 2H), 1.59 – 1.42 (m, 2H), 1.40 – 1.26 (m, 6H), 0.91 – 0.82 (m, 3H).

^{13}C NMR (100 MHz, Acetone-d_6) δ 186.18, 162.83, 161.95, 130.68, 129.95, 125.49, 118.54, 117.86, 113.36, 110.70, 102.20, 55.34, 31.64, 29.28, 28.60, 22.45, 22.23, 13.50.

S6- S13 were prepared following the same procedure

In a round-bottom flask, **S4** (1.0 equiv.) was dissolved in acetic acid (0.2M). N-chlorosuccinimide (2.0 equiv.) was added and the mixture was stirred at ambient temperature for 2 hours. Following this, N-chlorosuccinimide (4.0 equiv.) was added and the resulting mixture was heated to 70 °C for 16 hours. The reaction mixture was then quenched with 10 % K_2CO_3(aq) until bubbling ceases and extracted 3 × with EtOAc. The organic fractions were combined, washed with brine, dried over Na_2SO_4 and concentrated. The resulting oil was dissolved in $CHCl_3$ (0.2 M) and Et_3N (3 equiv.) was added. The mixture was heated at 60 °C for 5 hours. The solution was cooled to ambient temperature, concentrated, and the spiro- intermediates were isolated from the crude mixture by silica column chromatography (10 % EtOAc in hexanes). The spiro- intermediate (1.0 equiv.) was dissolved in DMF (0.2 M). The solution was cooled to 0 °C using an ice bath and NaH (1.5 equiv.) was added and allowed to stir for 15 min. Subsequently, the desired electrophile (1.3 equiv.) was added dropwise and stirring was continued at 0 °C to

ambient temperature for 5 hours. The mixture was quenched with NH_4Cl(aq), extracted 3 × with EtOAc, washed with brine, dried over Na_2SO_4, and concentrated. The desired compounds **S6-S13** (41-54%) were purified from the crude mixture by silica column chromatography (25 % EtOAc in hexanes).

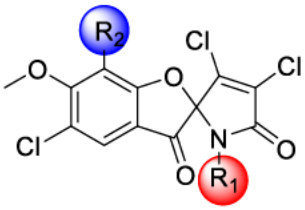

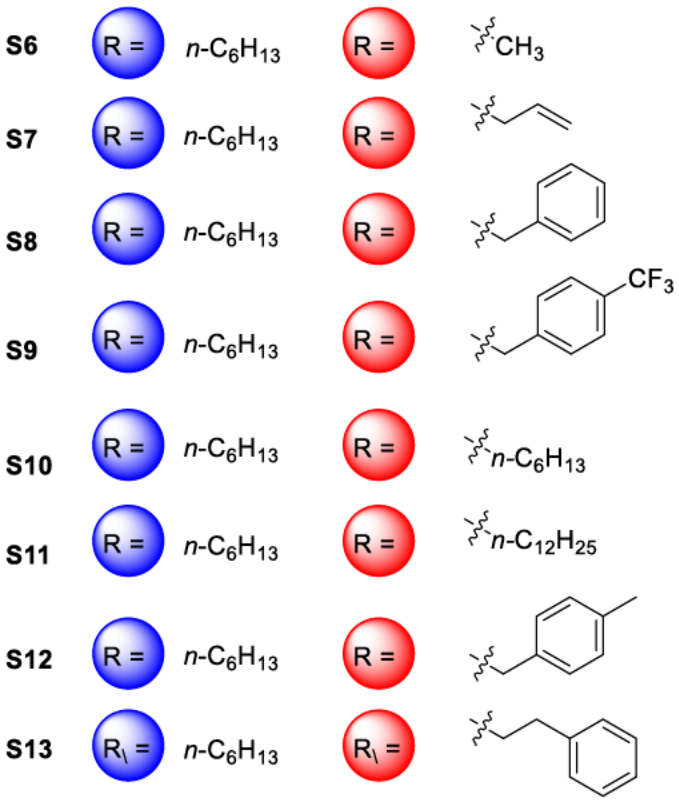

Legend for structures S17-S22

S6

^{1}H NMR (400 MHz, $CDCl_3$) δ 7.63 (s, 1H), 4.00 (s, 3H), 2.79 (s, 3H), 2.76 – 2.70 (m, 2H), 1.64 – 1.55 (m, 3H), 1.41 – 1.24 (m, 6H), 0.88 (t, J = 7.0 Hz, 3H).

^{13}C NMR (100 MHz, $CDCl_3$) δ 189.88, 170.33, 163.79, 163.16, 138.24, 129.38, 124.84, 124.33, 123.73, 115.65, 97.05, 61.92, 31.73, 29.46, 29.38, 25.96, 24.00, 22.71, 14.19.
HRMS (ESI): Exact mass calculated for $C_{19}H_{20}Cl_3NNaO_4$ [M + Na] + : 454.0350. Found: 454.0356

S7

1H NMR (400 MHz, $CDCl_3$) δ 7.63 (s, 1H), 4.00 (s, 3H), 3.42 (dt, J = 14.5, 7.3 Hz, 1H), 3.00 (dt, J = 14.5, 7.3 Hz, 1H), 2.78 – 2.64 (m, 2H), 1.65 – 1.53 (m, 2H), 1.48 – 1.12 (m, 14H), 0.88 (t, J = 6.9 Hz, 3H), 0.83 (t, J = 6.8 Hz, 3H).
13C NMR (100 MHz, $CDCl_3$) δ 190.25, 170.00, 163.71, 163.46, 138.25, 129.29, 124.75, 124.33, 123.72, 115.84, 97.38, 61.93, 41.67, 31.74, 31.36, 29.54, 29.47, 28.76, 26.47, 24.00, 22.71, 22.56, 14.20, 14.10.
HRMS (ESI): Exact mass calculated for $C_{24}H_{30}Cl_3NNaO_4$ [M + Na] + : 524.1133. Found: 524.1134

S8

^{1}H NMR (400 MHz, Chloroform-*d*) δ 7.62 (s, 1H), 3.98 (s, 3H), 3.40 (dt, *J* = 14.7, 7.5 Hz, 1H), 2.98 (dt, *J* = 14.6, 7.5 Hz, 1H), 2.77 – 2.61 (m, 2H), 1.64 – 1.54 (m, 2H), 1.45 – 1.13 (m, 26H), 0.87 (dt, *J* = 5.9, 3.8 Hz, 6H).

^{13}C NMR (150 MHz, $CDCl_3$) δ 190.11, 169.85, 163.55, 163.32, 138.10, 129.14, 124.60, 124.18, 123.58, 115.69, 97.23, 61.79, 41.54, 31.92, 31.61, 31.60, 29.64, 29.63, 29.57, 29.44, 29.41, 29.35, 29.08, 28.66, 26.67, 23.87, 22.70, 22.59, 14.13, 14.08.

HRMS (ESI): Exact mass calculated for $C_{30}H_{42}Cl_3NNaO_4$ [M + Na] + : 608.2077. Found: 608.2056

S9

^{1}H NMR (400 MHz, Acetone-d_6) δ 7.72 (s, 1H), 5.70 (ddt, *J* = 16.7, 10.1, 6.3 Hz, 1H), 5.04 – 4.91 (m, 2H), 4.07 (ddt, *J* = 15.9, 6.3, 1.5 Hz, 1H), 4.02 (s, 3H), 3.81 (ddt, *J* = 15.9, 6.4, 1.4 Hz, 1H), 2.80 – 2.74 (m, 2H), 1.72 – 1.59 (m, 2H), 1.44 – 1.27 (m, 6H), 0.87 (td, *J* = 5.8, 4.7, 2.8 Hz, 3H).

^{13}C NMR (100 MHz, Acetone-d_6) δ 189.69, 169.85, 163.50, 162.05, 138.79, 132.15, 128.57, 124.33, 124.17, 123.24, 118.31, 115.95, 96.66, 61.53, 43.32, 31.44, 29.05, 29.00, 23.48, 22.33, 13.43.

HRMS (ESI): Exact mass calculated for $C_{21}H_{22}Cl_3NNaO_4$ [M + Na] +: 480.0512. Found: 480.0502

S10

^{1}H NMR (400 MHz, Acetone-d_6) δ 7.61 (s, 1H), 7.22 – 7.17 (m, 3H), 7.11 – 7.07 (m, 2H), 4.80 – 4.72 (d, *J* = 15.5 Hz, 1H), 4.23 (d, *J* = 15.5 Hz, 1H), 3.98 (s, 3H), 2.59 (ddd, *J* = 13.3, 9.1, 6.1 Hz, 1H), 2.40 (ddd, *J* = 13.3, 9.2, 6.3 Hz, 1H), 1.49 – 1.38 (m, 2H), 1.27 (d, *J* = 8.2 Hz, 6H), 0.88 – 0.79 (m, 3H).

^{13}C NMR (100 MHz, Acetone-d_6) δ 189.40, 169.73, 163.35, 162.53, 138.86, 135.30, 128.65, 128.49, 128.25, 127.86, 124.23, 124.14, 123.12, 115.70, 96.83, 61.43, 44.58, 31.33, 29.40, 29.01, 23.32, 22.33, 13.44.

HRMS (ESI): Exact mass calculated for $C_{25}H_{24}Cl_3NNaO_4$ [M + Na] +: 530.0669 Found: 530.0685

S11

^{1}H NMR (600 MHz, Acetone-d_6) δ 7.72 (s, 1H), 7.66 – 7.63 (m, 2H), 7.46 (ddt, *J* = 8.1, 1.5, 0.8 Hz, 2H), 5.00 – 4.93 (m, 1H), 4.39 (d, *J* = 16.0 Hz, 1H), 4.04 (s, 3H), 2.64 (ddd, *J* = 13.3, 9.5, 6.0 Hz, 1H), 2.42 (ddd, *J* = 13.3, 9.6, 6.2 Hz, 1H), 1.38 – 1.25 (m, 8H), 0.95 – 0.89 (m, 3H).

^{13}C NMR (150 MHz, Acetone-d_6) δ 189.37, 169.78, 163.55, 162.61, 140.37, 138.98, 128.96, 128.65, 125.21, 125.19, 125.16, 124.44, 124.12, 123.35, 115.58, 96.90, 61.50, 43.98, 31.28, 23.24, 22.35, 13.42.

HRMS (ESI): Exact mass calculated for $C_{26}H_{23}Cl_3F_3NNaO_4$ [M + Na] +: 598.0542 Found: 598.0552

S12

^{1}H NMR (600 MHz, Chloroform-*d*) δ 7.57 (s, 1H), 7.18 – 7.08 (m, 3H), 7.01 – 6.96 (m, 2H), 3.94 (s, 3H), 3.54 (ddd, *J* = 14.5, 10.1, 6.2 Hz, 1H), 3.18 (ddd, *J* = 14.5, 10.1, 5.9 Hz, 1H), 2.82 – 2.69 (m, 2H), 2.66 (dt, *J* = 13.2, 7.4 Hz, 1H), 2.58 (dt, *J* = 13.2, 7.5 Hz, 1H), 1.53 – 1.48 (m, 3H), 1.32 – 1.29 (m, 2H), 1.23 – 1.18 (m, 6H), 0.79 (td, *J* = 5.8, 4.8, 2.4 Hz, 3H).

^{13}C NMR (150 MHz, $CDCl_3$) δ 189.93, 169.85, 163.65, 163.22, 138.31, 137.69, 129.12, 128.56, 128.55, 126.71, 124.72, 124.22, 123.63, 115.64, 97.17, 61.82, 42.89, 34.81, 31.57, 29.41, 29.31, 23.87, 22.56, 14.06.

HRMS (ESI): Exact mass calculated for $C_{26}H_{26}Cl_3NNaO_4$ [M + Na] +: 544.0825 Found: 544.0830

S13

^{1}H NMR (600 MHz, Chloroform-*d*) δ 7.45 (s, 1H), 6.93 – 6.90 (m, 2H), 6.90 – 6.86 (m, 2H), 4.65 (d, *J* = 15.1 Hz, 1H), 4.19 (d, *J* = 15.1 Hz, 1H), 3.95 (s, 3H), 2.53 (ddd, *J* = 13.2, 9.6, 5.8 Hz, 1H), 2.35 (ddd, *J* = 13.2, 9.6, 6.1 Hz, 1H), 2.25 (s, 3H), 1.45 – 1.36 (m, 2H), 1.34 – 1.24 (m, 8H), 0.88 (t, *J* = 6.9 Hz, 3H).

^{13}C NMR (150 MHz, $CDCl_3$) δ 189.67, 169.55, 163.35, 163.13, 138.81, 137.84, 131.25, 129.03, 128.88, 124.23, 124.06, 123.11, 115.75, 96.80, 61.71, 44.93, 31.55, 29.32, 29.12, 23.58, 22.61, 21.10, 14.10.

HRMS (ESI): Exact mass calculated for $C_{26}H_{26}Cl_3NNaO_4$ [M + Na] +: 544.0825 Found: 544.0830

1-8 we prepared following the same procedure

In separate round-bottom flasks, **S6-13**(1.0 equiv.) were dissolved in 1,2- dichloroethane (0.4 M). The mixture was cooled to 0 °C using an ice bath and BBr_3 (3.0 equiv.) was added dropwise. The reaction was allowed to proceed for 4 hours from 0 °C to ambient temperature. Et_3N / water was added, and the solution was extracted 3 × with EtOAc. The organic fractions were combined, washed with brine, dried over Na_2SO_4, and concentrated. The desired compounds **1-8** (63-84%) were purified from the crude mixture using preparative TLC (20 to 30 % EtOAc in hexanes).

1

^{1}H NMR (400 MHz, $CDCl_3$) δ 7.63 (s, 1H), 6.62 (s, 1H), 2.79 (s, 3H), 2.76 (t, J = 7.6 Hz, 2H), 1.66 – 1.56 (m, 2H), 1.39 – 1.24 (m, 6H), 0.87 (t, J = 7.0 Hz, 3H).

^{13}C NMR (100 MHz, $CDCl_3$) δ 188.93, 170.34, 163.21, 158.77, 138.43, 129.27, 122.56, 117.67, 115.79, 112.66, 97.16, 31.77, 29.22, 28.47, 25.91, 23.37, 22.74, 14.21.

HRMS (ESI): Exact mass calculated for $C_{18}H_{17}Cl_3NO_4$ [M - H] - : 416.0229. Found: 416.0223

2

^{1}H NMR (400 MHz, $CDCl_3$) δ 7.62 (s, 1H), 6.51 (s, 1H), 3.46 – 3.36 (m, 1H), 3.04 – 2.91 (m, 1H), 2.80 – 2.63 (m, 2H), 1.65 – 1.11 (m, 16H), 0.86 (t, J = 7.1 Hz, 3H), 0.81 (t, J = 6.9 Hz, 3H).

^{13}C NMR (100 MHz, $CDCl_3$) δ 189.33, 170.01, 163.50, 158.65, 138.42, 129.20, 122.54, 117.57, 115.82, 112.88, 97.50, 41.65, 31.79, 31.39, 29.31, 28.76, 28.56, 26.50, 23.38, 22.74, 22.58, 14.22, 14.10.

HRMS (ESI): Exact mass calculated for $C_{23}H_{27}Cl_3NO_4$ [M - H]- : 486.1001. Found: 486.1006

3

^{1}H NMR (600 MHz, Acetone-d_6) δ 7.42 (s, 1H), 3.58 (dt, *J* = 14.2, 7.5 Hz, 1H), 3.06 (ddd, *J* = 14.1, 7.6, 6.3 Hz, 3H), 2.68 – 2.61 (m, 2H), 1.62 (m, 30H), 1.02 – 0.96 (m, 6H).

^{13}C NMR (150 MHz, Acetone-d_6) δ 180.35, 174.82, 169.38, 162.81, 141.26, 126.57, 125.15, 121.07, 112.12, 100.69, 97.74, 40.79, 31.99, 31.79, 29.52, 29.52, 29.47, 29.38, 29.08, 26.69, 23.18, 22.61, 22.48, 13.63, 13.52.

HRMS (+EI): Exact mass calculated for $C_{29}H_{40}Cl_3NO_4$: 571.2023 Found: 571.2015

4

^{1}H NMR (600 MHz, Acetone-d_6) δ 7.27 (s, 1H), 5.73 (ddt, *J* = 17.1, 10.2, 6.0 Hz, 1H), 5.06 (dq, *J* = 17.1, 1.6 Hz, 1H), 4.96 (dq, *J* = 10.2, 1.4 Hz, 1H), 4.04 (ddt, *J* = 16.0, 5.9, 1.5 Hz, 1H), 3.51 (dd, *J* = 10.9, 5.8 Hz, 1H), 2.52 – 2.47 (m, 2H), 1.51 – 1.47 (m, 2H), 1.29 (q, *J* = 9.0, 8.0 Hz, 8H), 0.86 (td, *J* = 7.1, 2.7 Hz, 3H).

^{13}C NMR (150 MHz, Acetone d_6) δ 179.76, 174.75, 169.29, 162.42, 141.74, 132.94, 126.43, 125.25, 121.00, 116.72, 111.97, 100.57, 97.49, 43.01, 31.95, 29.50, 28.77, 23.11, 22.56, 13.60.

HRMS (+EI): Exact mass calculated for $C_{20}H_{20}Cl_3NO_4$: 443.0458 Found: 443.0460

5

^{1}H NMR (600 MHz, Chloroform-*d*) δ 7.41 (s, 1H), 7.13 – 7.06 (m, 3H), 6.97 – 6.94 (m, 2H), 4.63 (d, *J* = 15.3 Hz, 1H), 4.12 (d, *J* = 15.3 Hz, 1H), 2.48 (ddd, *J* = 13.3, 9.1, 5.9 Hz, 1H), 2.31 (ddd, *J* = 13.2, 9.0, 6.5 Hz, 1H), 1.41 – 1.25 (m, 3H), 1.22 – 1.18 (m, 7H), 0.80 (d, *J* = 7.1 Hz, 3H).

^{13}C NMR (150 MHz, $CDCl_3$) δ 188.67, 169.56, 163.35, 158.19, 138.96, 134.79, 128.95, 128.57, 128.28, 127.98, 122.00, 117.17, 115.58, 112.76, 107.21, 97.00, 44.98, 31.58, 29.13, 28.17, 23.03, 22.61, 14.10.

HRMS (+EI): Exact mass calculated for $C_{24}H_{22}Cl_3NO_4$: 493.0614 Found: 493.0619

6

^{1}H NMR (600 MHz, Acetone-d_6) δ 7.72 – 7.66 (m, 2H), 7.57 – 7.45 (m, 2H), 7.41 – 7.40 (m, 1H), 4.90 (ddd, *J* = 16.0, 7.9, 2.1 Hz, 1H), 4.27 – 4.19 (m, 1H), 2.55 – 2.48 (m, 1H), 2.34 (dddd, *J* = 12.6, 9.0, 6.5, 4.0 Hz, 1H), 1.54 – 1.42 (m, 2H), 1.38 – 1.26 (m, 8H), 0.97 – 0.94 (m, 3H).

^{13}C NMR (150 MHz, Acetone) δ 179.89, 174.72, 169.29, 162.93, 141.85, 128.45, 128.37, 128.10, 126.56, 125.19, 125.05, 125.02, 125.00, 124.14, 121.10, 112.31, 100.87, 97.71, 43.84, 31.80, 29.50, 29.14, 22.97, 22.59, 13.54.

HRMS (+EI): Exact mass calculated for $C_{25}H_{21}Cl_3F_3NO_4$: 561.0488 Found: 561.0479

7

^{1}H NMR (600 MHz, Acetone-d_6) δ 7.33 (s, 1H), 7.16 – 7.12 (m, 2H), 7.10 – 7.06 (m, 2H), 4.69 (d, *J* = 15.5 Hz, 1H), 4.01 (d, *J* = 15.6 Hz, 1H), 2.47 (ddd, *J* = 12.8, 9.4, 5.0 Hz, 1H), 2.38 – 2.33 (m, 1H), 1.50 – 1.41 (m, 2H), 1.32 – 1.25 (m, 7H), 0.90 (t, *J* = 7.0 Hz, 4H).

^{13}C NMR (150 MHz, Acetone) δ 179.91, 174.81, 169.32, 162.77, 141.61, 136.55, 134.05, 128.69, 128.00, 126.54, 125.18, 121.00, 112.20, 100.72, 97.83, 44.20, 31.91, 29.51, 29.12, 23.10, 22.61, 20.27, 13.62.

HRMS (+EI): Exact mass calculated for $C_{25}H_{24}Cl_3NO_4$: 507.0771 Found: 507.0768

8

^{1}H NMR (600 MHz, Acetone-d_6) δ 7.37 (s, 1H), 7.26 – 7.21 (m, 2H), 7.18 – 7.11 (m, 3H), 3.69 – 3.61 (m, 1H), 3.18 (ddd, *J* = 14.2, 9.5, 5.6 Hz, 1H), 2.86 – 2.76 (m, 3H), 2.56 (qdd, *J* = 12.7, 8.5, 6.5 Hz, 2H), 1.59 – 1.47 (m, 2H), 1.31 (ddd, *J* = 6.5, 3.5, 1.5 Hz, 2H), 1.24 – 1.19 (m, 4H), 0.82 – 0.79 (m, 3H).

^{13}C NMR (150 MHz, Acetone) δ 180.64, 174.89, 169.52, 162.60, 141.30, 138.70, 128.61, 128.39, 126.67, 126.32, 125.20, 121.20, 112.37, 100.06, 97.70, 42.21, 34.65, 31.92, 29.38, 28.83, 23.16, 22.54, 13.58.

HRMS (+EI): Exact mass calculated for $C_{25}H_{24}Cl_3NO_4$: 507.0771 Found: 507.0777

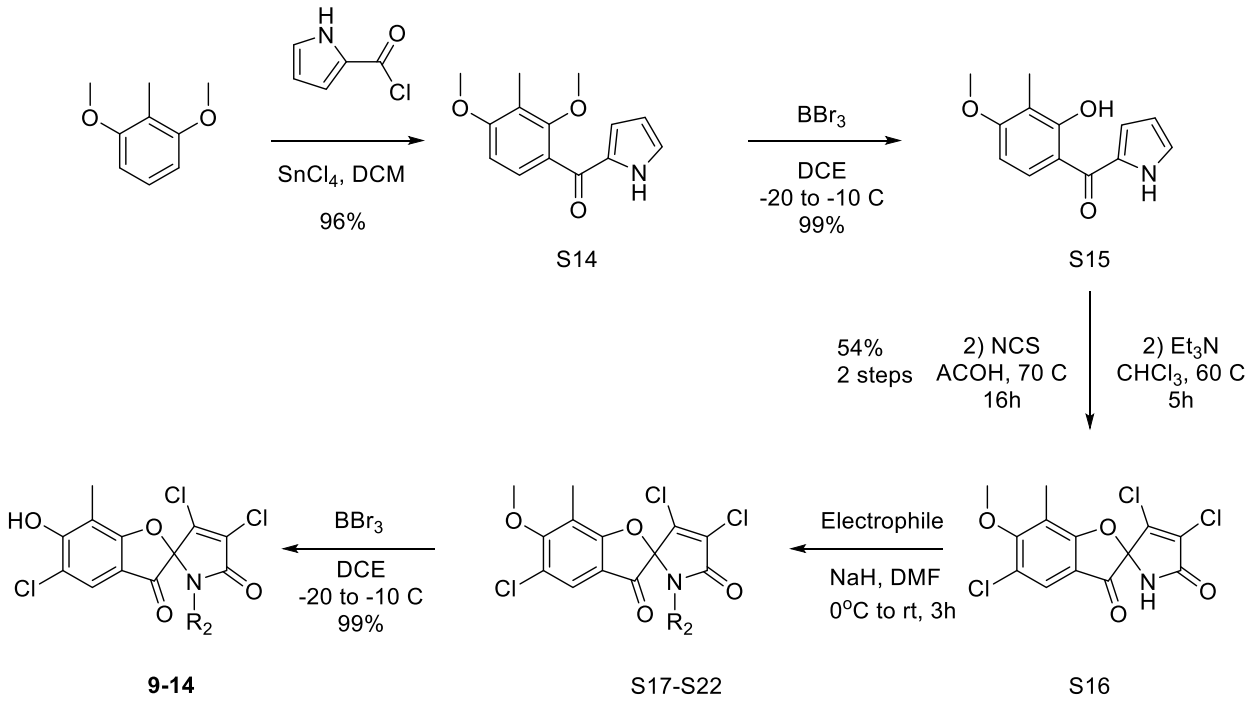

Scheme S2. Synthesis of r1 methyl series of analogues

S14

Pyrrole 2-carboxylic acid (0.721g, 6.49 mmol, 2 eq) was dissolved in 10 mL of DCM. Oxalyl chloride (9.7 mL, 19.48 mmol, 3 equiv) was added dropwise, 1 drop of DMF was added. The following mixture was stirred for 1 hour at room temperature. The solvent was removed *en vacuo*. The intermediate acid chloride was resuspended in DCM in a round-bottom flask, 2,6 dimethoxy toluene (0.5 g, 3.246 mmol, 1.0 equiv.) was added and cooled to 0 °C with an ice bath. $SnCl_4$ (16.2 mL of a 1.0 M solution, 5 equiv.) was then added dropwise. The mixture was

stirred for 1 hour at 0 °C, then warmed to ambient temperature. The reaction mixture was quenched with a saturated $NaHCO_3$(aq) and extracted 3 × with EtOAc. The organic fractions were combined, washed with brine, dried over Na_2SO_4 and concentrated. The desired compound (0.640 g, 2.519 mmol, 78 % yield) was purified from the crude mixture by silica column chromatography (30 % EtOAc in hexanes).

^{1}H NMR (400 MHz, Acetone-d_6) δ 7.30 (dq, *J* = 8.5, 0.6 Hz, 1H), 7.20 (dq, *J* = 2.9, 1.5 Hz, 1H), 6.80 (d, *J* = 8.4 Hz, 1H), 6.57 (ddd, *J* = 3.7, 2.2, 1.4 Hz, 1H), 6.23 (dt, *J* = 3.8, 2.3 Hz, 1H), 3.90 (s, 3H), 3.69 (s, 3H), 2.13 (d, *J* = 0.5 Hz, 3H).

^{13}C NMR (100 MHz, Acetone) δ 183.47, 160.22, 157.53, 132.70, 127.67, 126.21, 125.16, 119.56, 118.55, 109.91, 104.90, 61.41, 55.29, 8.14.

HRMS (+EI) : calcd for: $C_{14}H_{15}NO_3$ Exact Mass: 245.1052. Found: 245.1043

S15

In a round-bottom flask, **S14** (0.641 g, 2.61 mmol, 1.0 equiv.) was dissolved in 1,2-dichloroethane (3 mL). The solution was cooled to -20 °C using a dry ice/acetone bath. BBr_3 (3.13 mL of a 1 M solution, 1.2 equiv.) was added dropwise and the reaction mixture was stirred at -20 to – 10 °C for 2 hours. Subsequently, Et_3N / water was added and the solution was extracted 3 × with EtOAc. The organic fractions were combined, washed with brine, dried over Na_2SO_4, and concentrated. The desired compound (0.600g, 2.586 mmol, 99 % yield) was used without purification.

^{1}H NMR (400 MHz, Acetone-d_6) δ 8.05 (dd, *J* = 9.0, 0.7 Hz, 1H), 7.27 (ddd, *J* = 3.0, 2.5, 1.3 Hz, 1H), 7.05 (ddd, *J* = 3.9, 2.5, 1.3 Hz, 1H), 6.67 (d, *J* = 9.0 Hz, 1H), 6.35 (dt, *J* = 3.8, 2.4 Hz, 1H), 3.93 (s, 3H), 2.06 (d, *J* = 0.5 Hz, 3H).

^{13}C NMR (100 MHz, Acetone) δ 186.09, 162.86, 161.63, 130.47, 129.99, 125.48, 118.52, 113.27, 112.69, 110.67, 100.98, 55.35, 7.00.

HRMS (+EI) : calcd for: $C_{13}H_{13}NO_3$ Exact Mass: 231.0895 Found: 231.0880

S17- S22 were prepared following the same procedure.

In a round-bottom flask, **S15** (1.0 equiv.) was dissolved in acetic acid (0.2 M). N-chlorosuccinimide (2.0 equiv.) was added and the mixture was stirred at ambient temperature for 2 hours. Following this, N-chlorosuccinimide (4.0 equiv.) was added and the resulting mixture was heated to 70 °C for 16 hours. The reaction mixture was then quenched with a 10 % K_2CO_3(aq) and extracted 3 × with EtOAc. The organic fractions were combined, washed with brine, dried over Na_2SO_4 and concentrated. The resulting oil was dissolved in $CHCl_3$ (0.2M) and Et_3N (3 equiv.) was added. The mixture was heated at 60 °C for 5 hours. The solution was cooled to ambient temperature, concentrated, and the spiro- intermediates were isolated from the crude mixture by silica column chromatography (10 % EtOAc in hexanes). The spiro-intermediate (1.0 equiv.) was dissolved in DMF (0.2M). The solution was cooled to 0 °C using an ice bath and NaH (1.5 equiv.) was added and allowed to stir for 15 min. Subsequently, the desired electrophile (1.3 equiv.) was added dropwise and stirring was continued at 0 °C to ambient temperature for 5 hours. The mixture was quenched with NH_4Cl(aq), extracted 3 × with EtOAc, washed with brine, dried over Na_2SO_4, and concentrated. The desired compounds **S17-S22** (44-54% over 2 steps) were purified from the crude mixture by silica column chromatography (25 % EtOAc in hexanes).

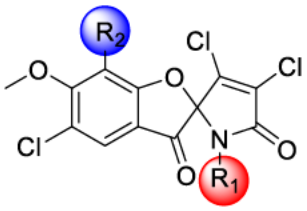

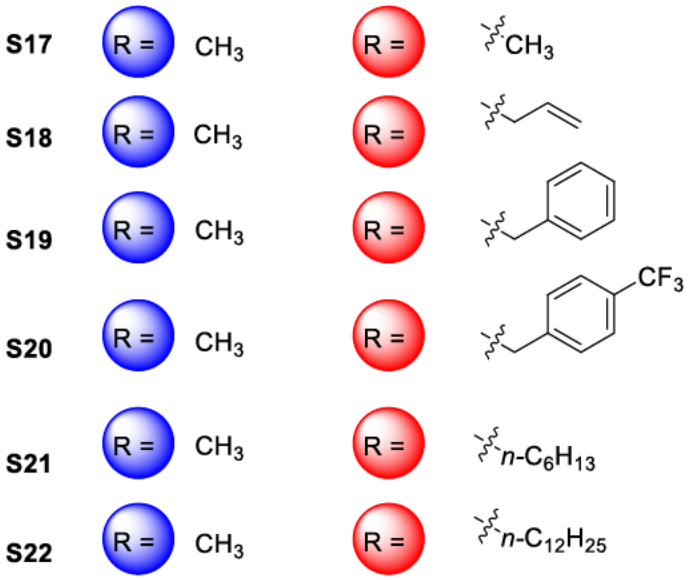

Legend for structures S17-S22

S17

^{1}H NMR (600 MHz, Chloroform-*d*) δ 7.64 (s, 1H), 3.98 (s, 3H), 2.80 (s, 3H), 2.31 (s, 3H).

^{13}C NMR (150 MHz, $CDCl_3$) δ 189.71, 170.16, 163.75, 163.03, 138.08, 129.25, 124.65, 123.36, 119.07, 115.43, 97.00, 61.08, 25.88, 8.75.

HRMS (ESI): Exact mass calculated for $C_{14}H_{10}Cl_3NNaO_4$ [M + Na] +: 383.9573. Found: 383.9566

S18

^{1}H NMR (400 MHz, Chloroform-*d*) δ 7.64 (d, J = 0.7 Hz, 1H), 3.99 (s, 3H), 3.42 (ddd, J = 14.6, 8.3, 6.5 Hz, 1H), 3.00 (ddd, J = 14.5, 8.2, 6.3 Hz, 1H), 2.29 (d, J = 0.7 Hz, 3H), 1.50 – 1.35 (m, 3H), 1.25 – 1.12 (m, 7H), 0.83 (t, J = 6.9 Hz, 3H).

^{13}C NMR (100 MHz, $CDCl_3$) δ 190.24, 170.02, 163.82, 163.43, 138.17, 129.35, 124.72, 123.51, 119.16, 115.74, 97.41, 61.23, 41.67, 31.37, 28.68, 26.41, 22.55, 14.11, 8.82.

HRMS (ESI): Exact mass calculated for $C_{19}H_{20}Cl_3NO_4$ [M + Na]+: 454.0386 Found: 454.0347

S19

^{1}H NMR (600 MHz, Chloroform-*d*) δ 7.64 (d, *J* = 0.8 Hz, 1H), 3.98 (s, 3H), 3.42 (ddd, *J* = 14.7, 8.4, 6.4 Hz, 1H), 3.00 (ddd, *J* = 14.6, 8.3, 6.3 Hz, 1H), 2.29 (d, *J* = 0.6 Hz, 3H), 1.48 – 1.36 (m, 3H), 1.30 – 1.16 (m, 20H), 0.89 – 0.86 (m, 3H).

^{13}C NMR (150 MHz, $CDCl_3$) δ 190.09, 169.86, 163.66, 163.27, 138.01, 129.18, 124.57, 123.36, 119.01, 115.57, 97.24, 61.09, 41.52, 31.91, 29.62, 29.55, 29.40, 29.35, 29.34, 29.06, 28.57, 26.59, 22.69, 14.13, 8.69.

HRMS (ESI): Exact mass calculated for $C_{25}H_{32}Cl_3NO_4$ [M + Na]+: 538.1295 Found: 538.1308

S20

^{1}H NMR (600 MHz, Chloroform-*d*) δ 7.60 (t, *J* = 0.7 Hz, 1H), 5.67 (ddt, *J* = 16.7, 10.1, 6.5 Hz, 1H), 4.97 – 4.84 (m, 2H), 4.04 (ddt, *J* = 15.7, 6.4, 1.4 Hz, 1H), 3.97 (s, 4H), 3.77 (ddt, *J* = 15.8, 6.6, 1.4 Hz, 1H), 2.27 (d, *J* = 0.7 Hz, 3H).

^{13}C NMR (150 MHz, $CDCl_3$) δ 189.95, 169.72, 163.53, 162.87, 138.60, 131.76, 129.08, 124.47, 123.12, 118.97, 118.96, 115.83, 96.74, 61.11, 43.70, 8.65.

HRMS (ESI): Exact mass calculated for $C_{16}H_{12}Cl_3NNaO_4$ [M + Na]+: 409.9730 Found: 409.9709

S21

^{1}H NMR (600 MHz, Chloroform-*d*) δ 7.50 (q, *J* = 0.6 Hz, 1H), 7.17 (d, *J* = 7.3 Hz, 1H), 7.15 – 7.10 (m, 2H), 7.02 – 6.97 (m, 2H), 4.86 (d, *J* = 15.1 Hz, 1H), 4.04 (d, *J* = 15.2 Hz, 1H), 3.91 (s, 3H), 1.93 (d, *J* = 0.6 Hz, 3H).

^{13}C NMR (150 MHz, $CDCl_3$) δ 189.71, 169.68, 163.30, 163.28, 138.69, 134.68, 129.10, 128.73, 128.20, 128.01, 124.31, 122.86, 119.04, 115.54, 96.91, 60.95, 45.10, 8.34.

HRMS (ESI): Exact mass calculated for $C_{20}H_{14}Cl_3NNaO_4$ [M + Na]+: 459.9886 Found: 459.9895

S22

^{1}H NMR (600 MHz, Chloroform-*d*) δ 7.54 (q, *J* = 0.6 Hz, 1H), 7.44 – 7.40 (m, 2H), 7.18 – 7.14 (m, 2H), 5.00 – 4.91 (m, 1H), 4.03 (d, *J* = 15.5 Hz, 1H), 3.91 (s, 3H), 1.91 (d, *J* = 0.6 Hz, 3H).

^{13}C NMR (150 MHz, $CDCl_3$) δ 189.46, 169.56, 163.68, 163.34, 138.96, 138.93, 129.02, 128.89, 125.20, 125.17, 125.15, 125.12, 124.63, 123.03, 118.96, 115.28, 96.90, 61.01, 44.53, 8.19.

HRMS (ESI): Exact mass calculated for $C_{21}H_{13}Cl_3F_3NNaO_4$ [M + Na]+: 527.9760 Found: 527.9769

9-14 we prepared following the same procedure

In separate round-bottom flasks, **S17-22** (1.0 equiv.) were dissolved in 1,2- dichloroethane (0.4 M). The mixture was cooled to 0 °C using an ice bath and BBr_3 (3.0 equiv.) was added dropwise. The reaction was allowed to proceed for 4 hours from 0 ℃ to ambient temperature. Et_3N / water was added, and the solution was extracted 3 × with EtOAc. The organic fractions were combined, washed with brine, dried over Na_2SO_4, and concentrated. The desired compounds **9-14** (88-99%) were purified from the crude mixture using preparative TLC (20 to 40 % EtOAc in hexanes).

9
^{1}H NMR (600 MHz, Acetone-d_6) δ 7.32 (d, *J* = 0.4 Hz, 1H), 2.71 (s, 3H), 1.94 (d, *J* = 0.3 Hz, 3H).

^{13}C NMR (150 MHz, Acetone) δ 180.35, 175.27, 169.69, 162.51, 141.05, 126.79, 124.62, 121.04, 106.96, 100.86, 97.32, 24.83, 7.77.

HRMS (+EI): Exact mass calculated for $C_{13}H_8Cl_3NO_4$: 346.9519 Found: 346.9522

10
^{1}H NMR (600 MHz, Methanol-d_4) δ 7.43 (s, 1H), 3.45 (ddd, *J* = 14.6, 8.0, 6.9 Hz, 1H), 2.98 (ddd, *J* = 14.2, 7.9, 6.1 Hz, 1H), 2.01 (s, 3H), 1.53 – 1.41 (m, 2H), 1.27 – 1.21 (m, 5H), 0.85 (t, *J* = 7.1 Hz, 3H).

^{13}C NMR (150 MHz, MeOD) δ 183.53, 176.13, 170.25, 163.74, 140.58, 127.13, 125.17, 121.35, 108.36, 103.17, 97.82, 40.73, 30.98, 28.04, 26.00, 22.08, 12.96, 7.12.

HRMS (+EI): Exact mass calculated for $C_{18}H_{18}Cl_3NO_4$: 417.0301 Found: 417.0310

11
^{1}H NMR (400 MHz, $CDCl_3$) δ 7.62 (s, 1H), 6.51 (s, 1H), 3.46 – 3.36 (m, 1H), 3.04 – 2.91 (m, 1H), 2.80 – 2.63 (m, 2H), 1.65 – 1.11 (m, 16H), 0.86 (t, J = 7.1 Hz, 3H), 0.81 (t, J = 6.9 Hz, 3H).
^{13}C NMR (100 MHz, $CDCl_3$) δ 189.33, 170.01, 163.50, 158.65, 138.42, 129.20, 122.54, 117.57, 115.82, 112.88, 97.50, 41.65, 31.79, 31.39, 29.31, 28.76, 28.56, 26.50, 23.38, 22.74, 22.58, 14.22, 14.10.
HRMS (+EI): Exact mass calculated for $C_{24}H_{30}Cl_3NO_4$: 501.1240 Found: 501.1233

12

^{1}H NMR (600 MHz, Acetone-d_6) δ 7.30 (s, 1H), 5.71 (dddd, *J* = 17.1, 10.2, 6.3, 5.8 Hz, 1H), 5.03 (dq, *J* = 17.1, 1.6 Hz, 1H), 4.95 (dq, *J* = 10.2, 1.4 Hz, 1H), 4.04 (ddt, *J* = 16.0, 5.9, 1.5 Hz, 1H), 3.60 – 3.58 (m, 1H), 3.57 – 3.55 (m, 1H), 1.91 (s, 3H).

^{13}C NMR (150 MHz, Acetone-d_6) δ 181.25, 176.03, 170.26, 163.20, 142.30, 133.71, 127.50, 125.45, 121.81, 117.55, 107.84, 100.90, 98.30, 43.82, 8.53.

HRMS (+EI): Exact mass calculated for $C_{15}H_{10}Cl_3NO_4$: 372.9675 Found: 372.9675

13

^{1}H NMR (600 MHz, Acetone-d_6) δ 7.30 (s, 1H), 7.21 – 7.16 (m, 5H), 4.74 (d, *J* = 15.5 Hz, 1H), 3.94 (d, *J* = 15.5 Hz, 1H), 1.72 (s, 3H).

^{13}C NMR (150 MHz, Acetone-d_6) δ 180.15, 175.14, 169.30, 162.70, 141.43, 137.04, 128.13, 128.03, 127.14, 126.68, 124.67, 120.94, 107.04, 100.95, 97.79, 44.38, 7.57.

HRMS (+EI): Exact mass calculated for $C_{19}H_{12}Cl_3NO_4$: 422.9832 Found: 422.9840

14

^{1}H NMR (600 MHz, Acetone-d_6) δ 7.56 (dd, *J* = 19.3, 8.2 Hz, 2H), 7.39 (dd, *J* = 22.2, 8.1 Hz, 2H), 7.29 (s, 1H), 4.87 – 4.80 (m, 1H), 4.07 (d, *J* = 15.9 Hz, 1H), 1.68 (s, 3H).

^{13}C NMR (150 MHz, Acetone-d_6) δ 179.74, 175.16, 169.11, 162.80, 141.72, 128.67, 128.55, 126.61, 124.97, 124.94, 124.92, 124.89, 124.80, 120.99, 106.95, 100.76, 97.69, 43.76, 25.31, 7.45.

HRMS (+EI): Exact mass calculated for $C_{20}H_{11}Cl_3F_3NO_4$: 490.9706 Found 490.9701

NMR Spectra

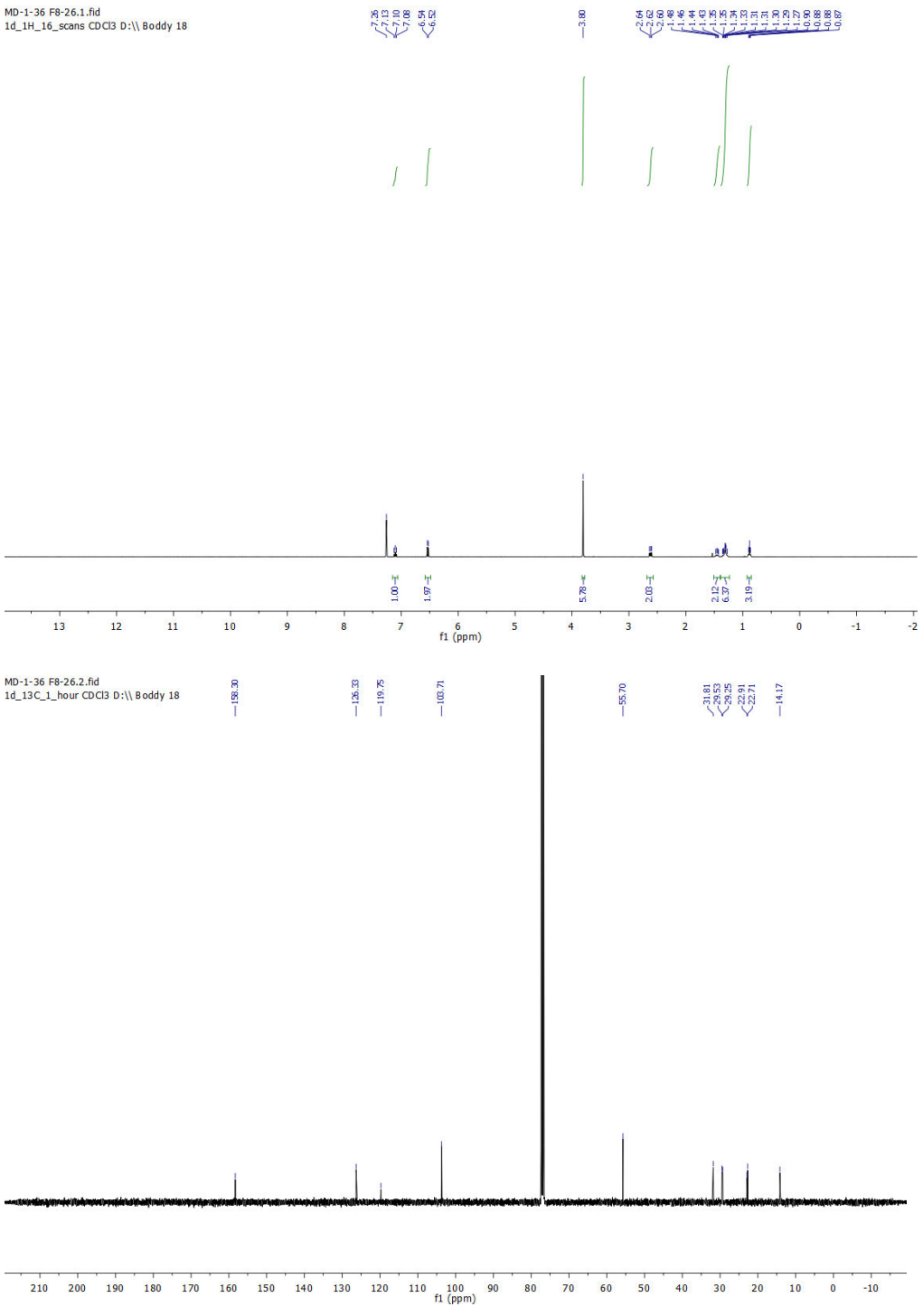

^{1}H NMR (400 MHz, $CDCl_3$) and ^{13}C NMR (100 MHz, $CDCl_3$) of S2

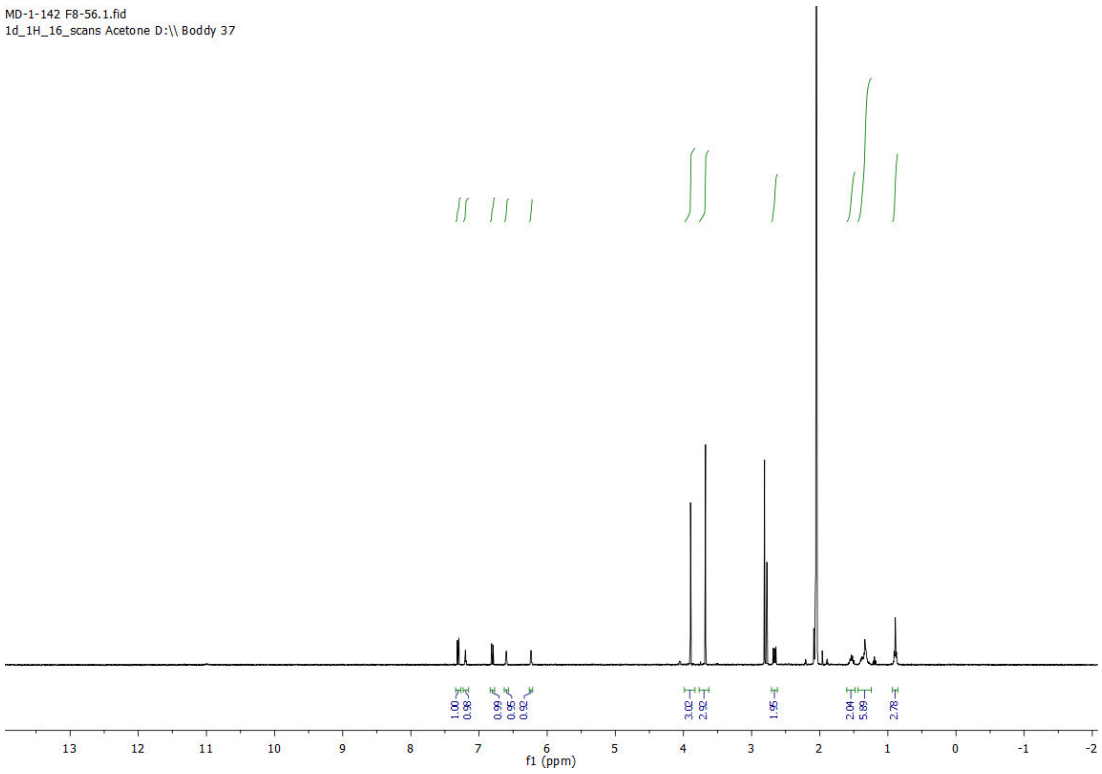
MD-1-142 F8-56.1.fid
1d_1H_16_scans Acetone D:\\ Boddy 37
1.00
0.98
0.99
0.95
0.92
3.02
2.92
1.95
2.04
5.89
2.78
13
12
11
10
9
8
7
6
5
4
3
2
1
0
-1
-2
f1 (ppm)

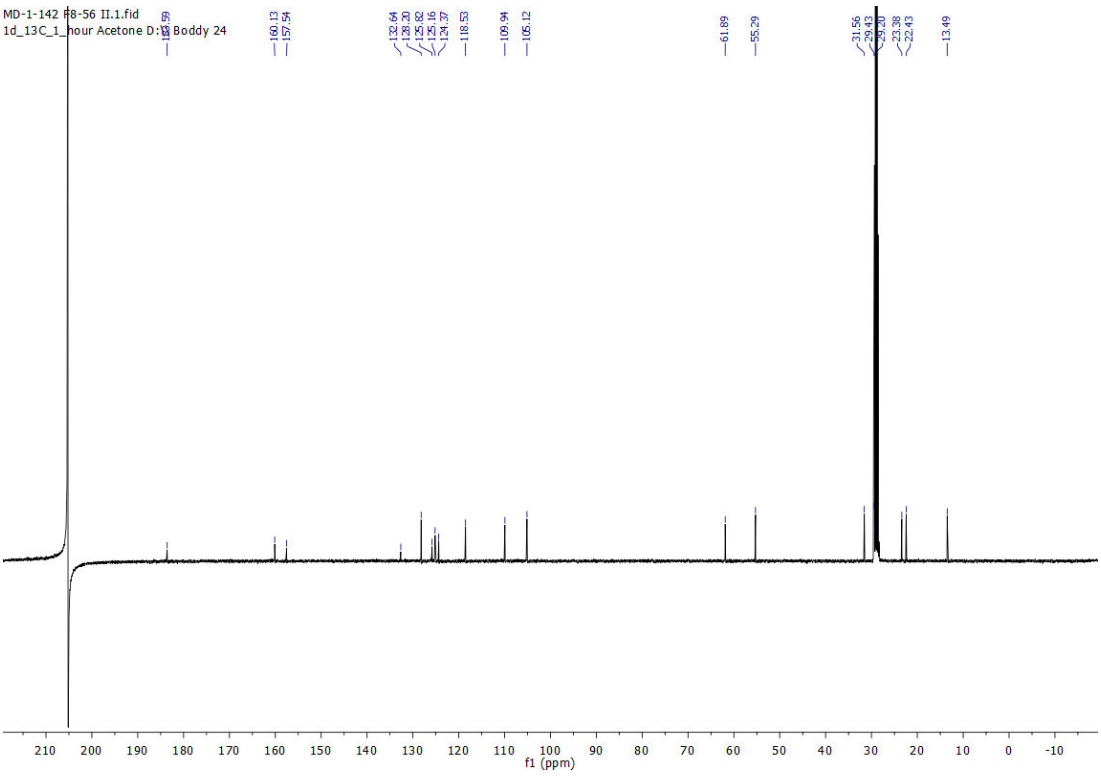

^{1}H NMR (400 MHz, Acetone-D$_6$) and ^{13}C NMR (100 MHz, Acetone-D$_6$) of S3

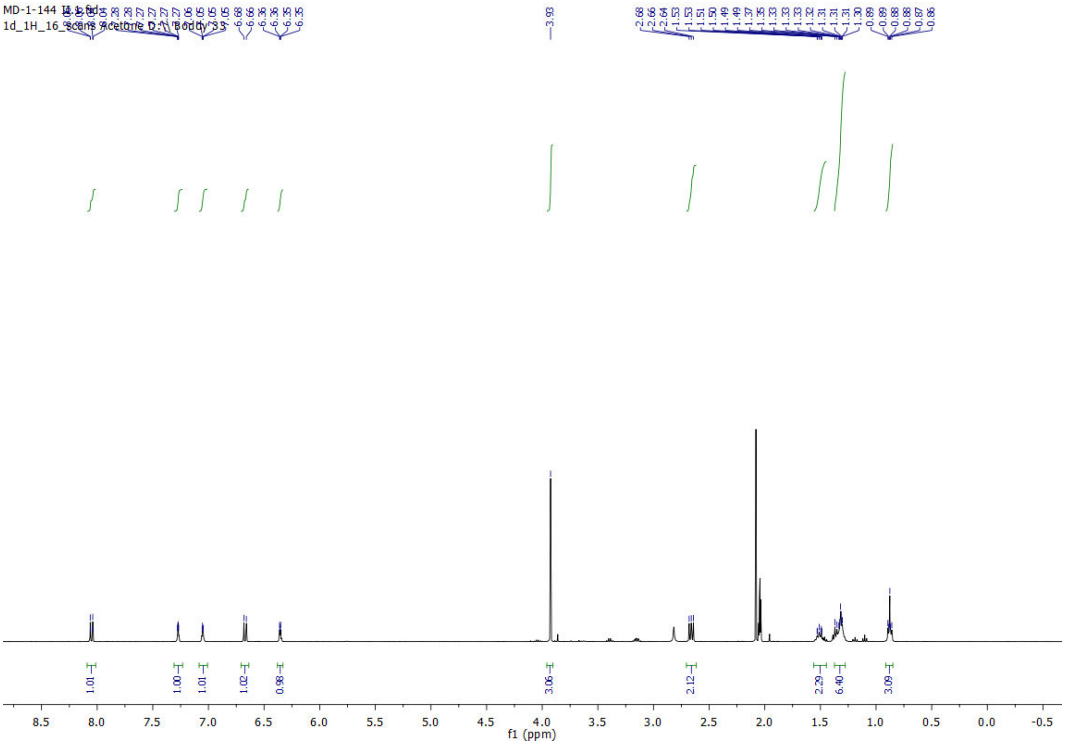
1d_1H_16_scans_Acetone_D_1_Boddy_33
1.01
1.00
1.01
1.02
0.98
3.06
2.12
2.29
6.40
3.09
f1 (ppm)

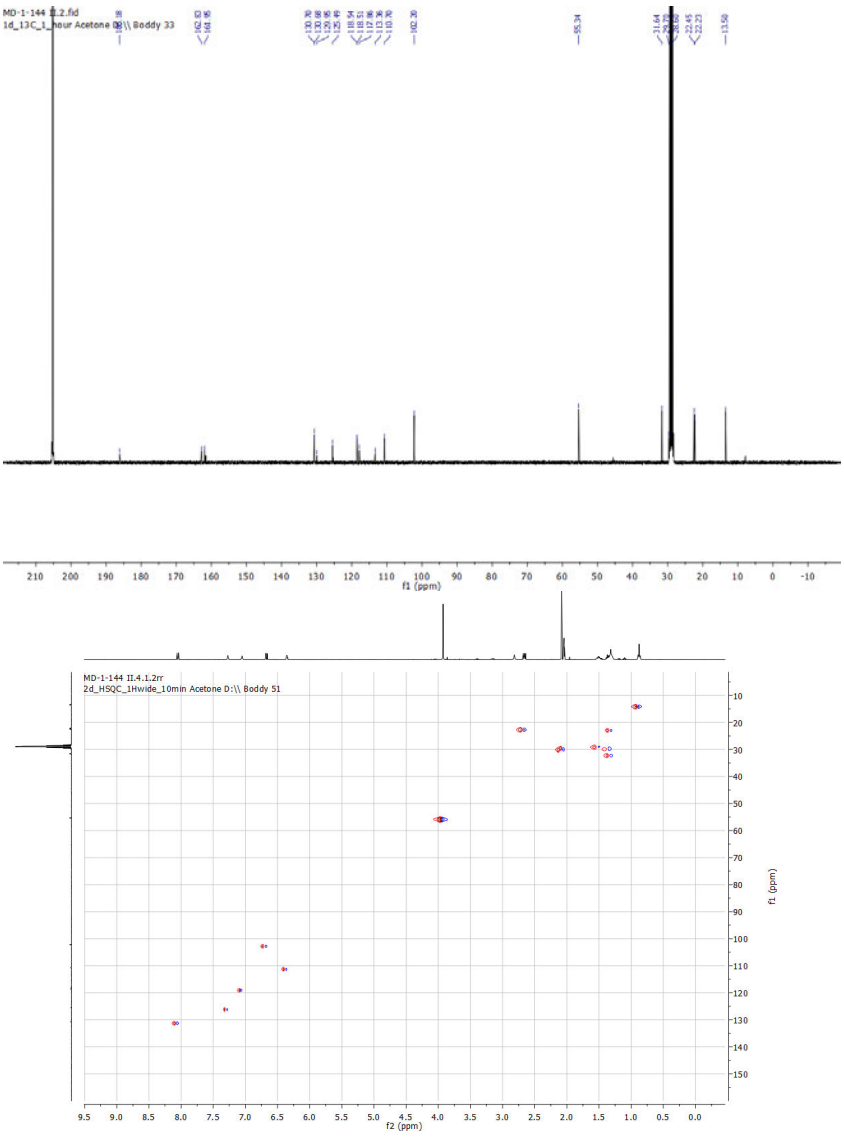

^{1}H NMR (400 MHz, Acetone-D$_6$) and ^{13}C NMR (100 MHz, Acetone-D$_6$) and HSQC of S4

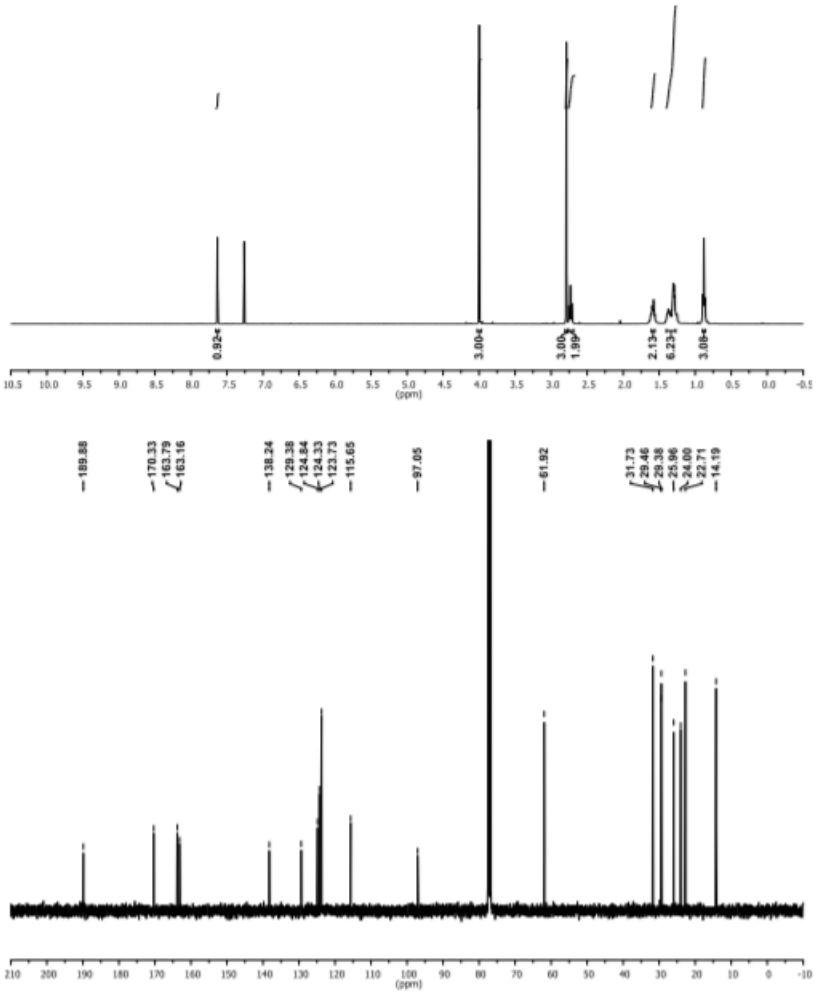

^{1}H NMR (400 MHz, $CDCl_3$) and ^{13}C NMR (100 MHz, $CDCl_3$) of S6

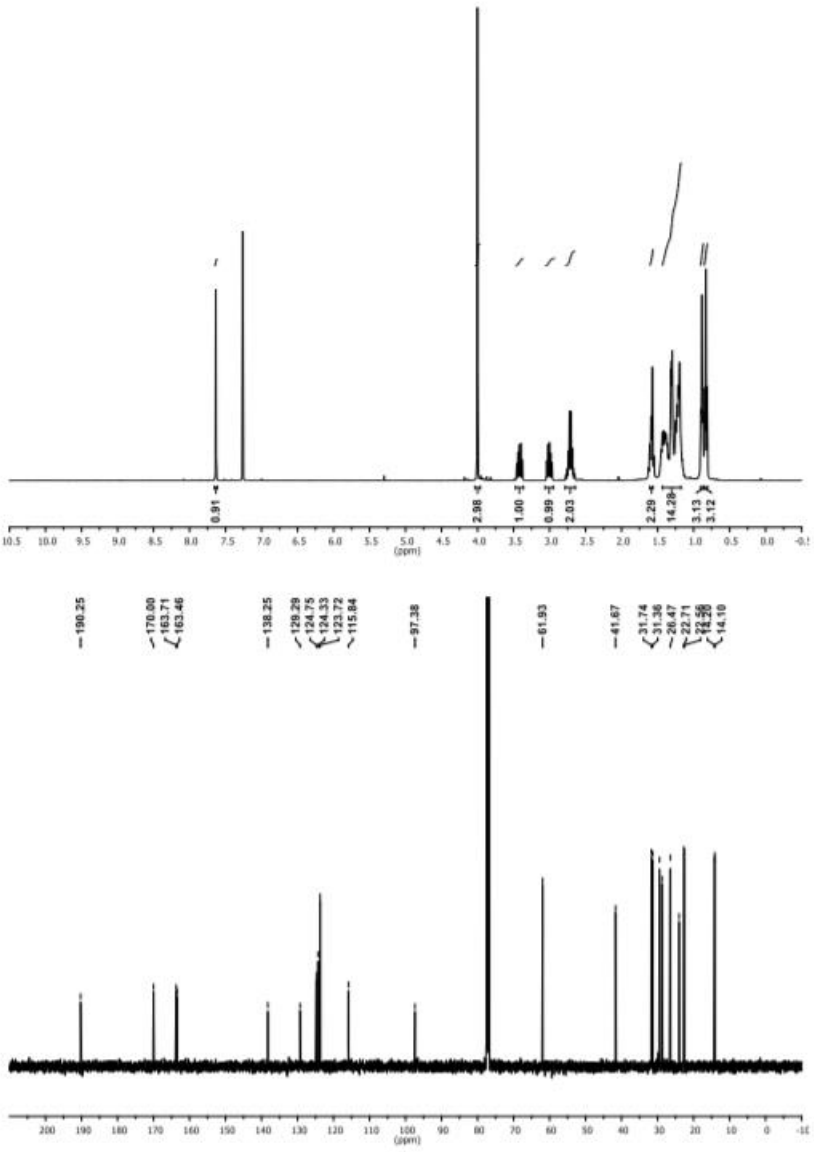

^{1}H NMR (400 MHz, $CDCl_3$) and ^{13}C NMR (100 MHz, $CDCl_3$) of S7

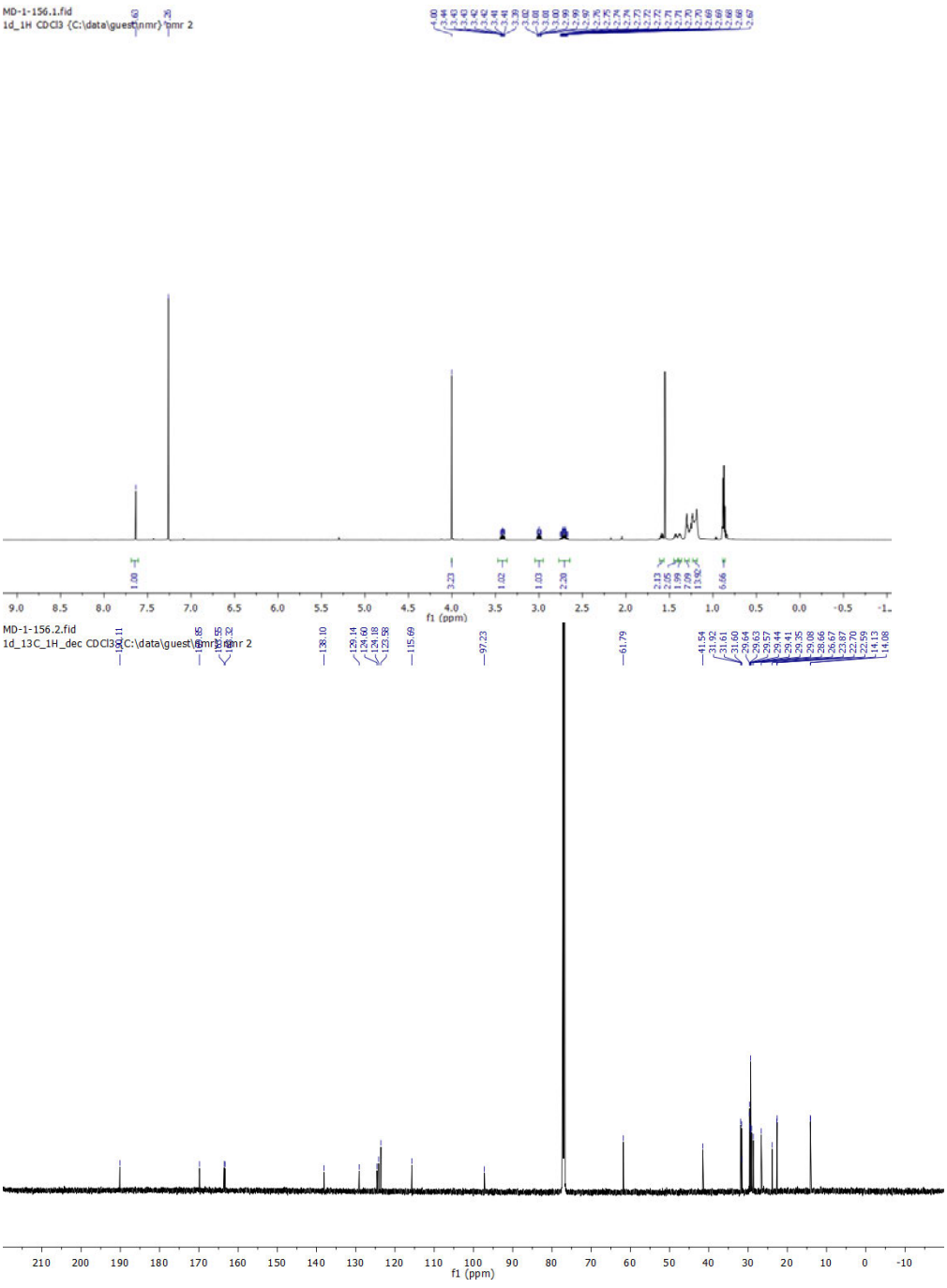
MD-1-156.1.fid
1d_1H CDCl3 {C:\data\guest\nmr} pmr 2
f1 (ppm)
MD-1-156.2.fid
1d_13C_1H_dec CDCl3 {C:\data\guest\6mr} cmr 2
f1 (ppm)

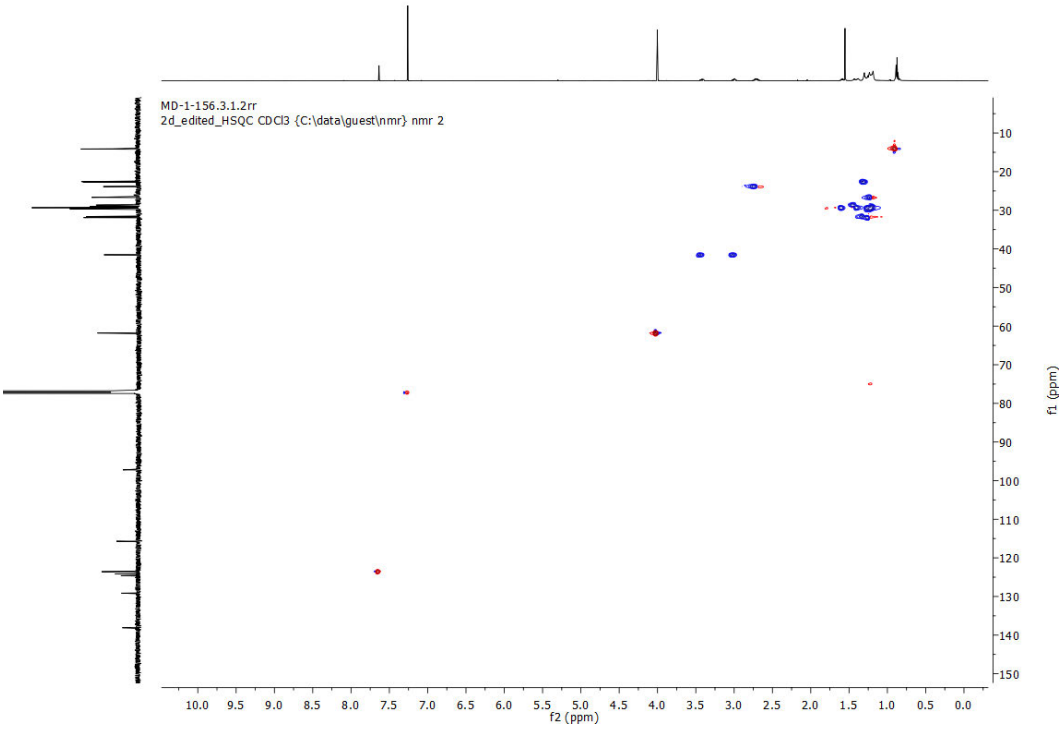

^{1}H NMR (400 MHz, $CDCl_3$) and ^{13}C NMR (100 MHz, $CDCl_3$) and HSQC of S8

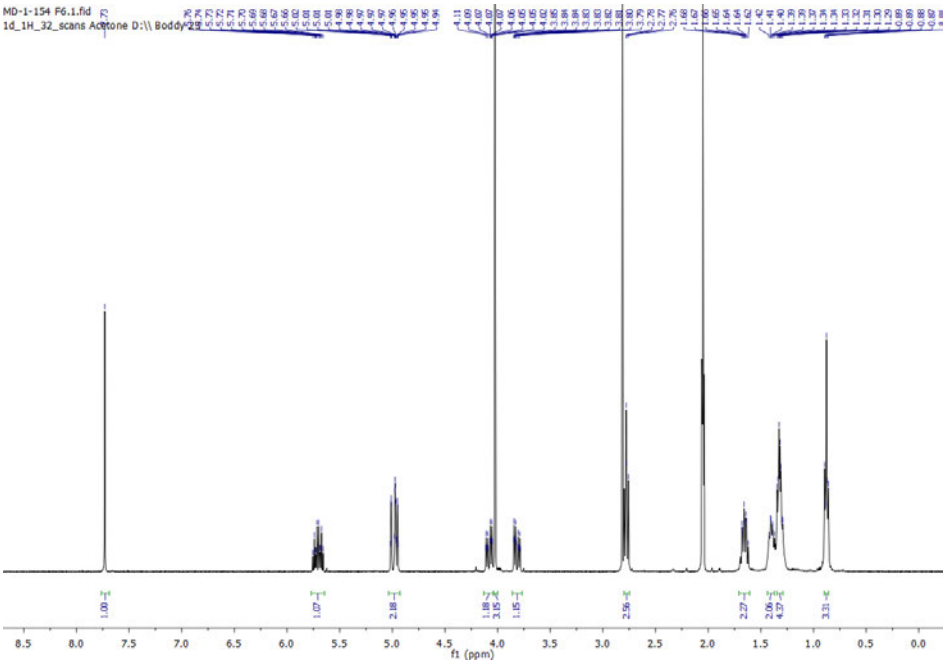
MD-1-154 F6.1.fid
1d_1H_32_scans Acetone D:\\ Boddy 2018
1.00
1.07
2.18
1.18
3.15
1.15
2.56
2.27
2.06
4.37
3.31
8.5
8.0
7.5
7.0
6.5
6.0
5.5
5.0
4.5
4.0
3.5
3.0
2.5
2.0
1.5
1.0
0.5
0.0
f1 (ppm)

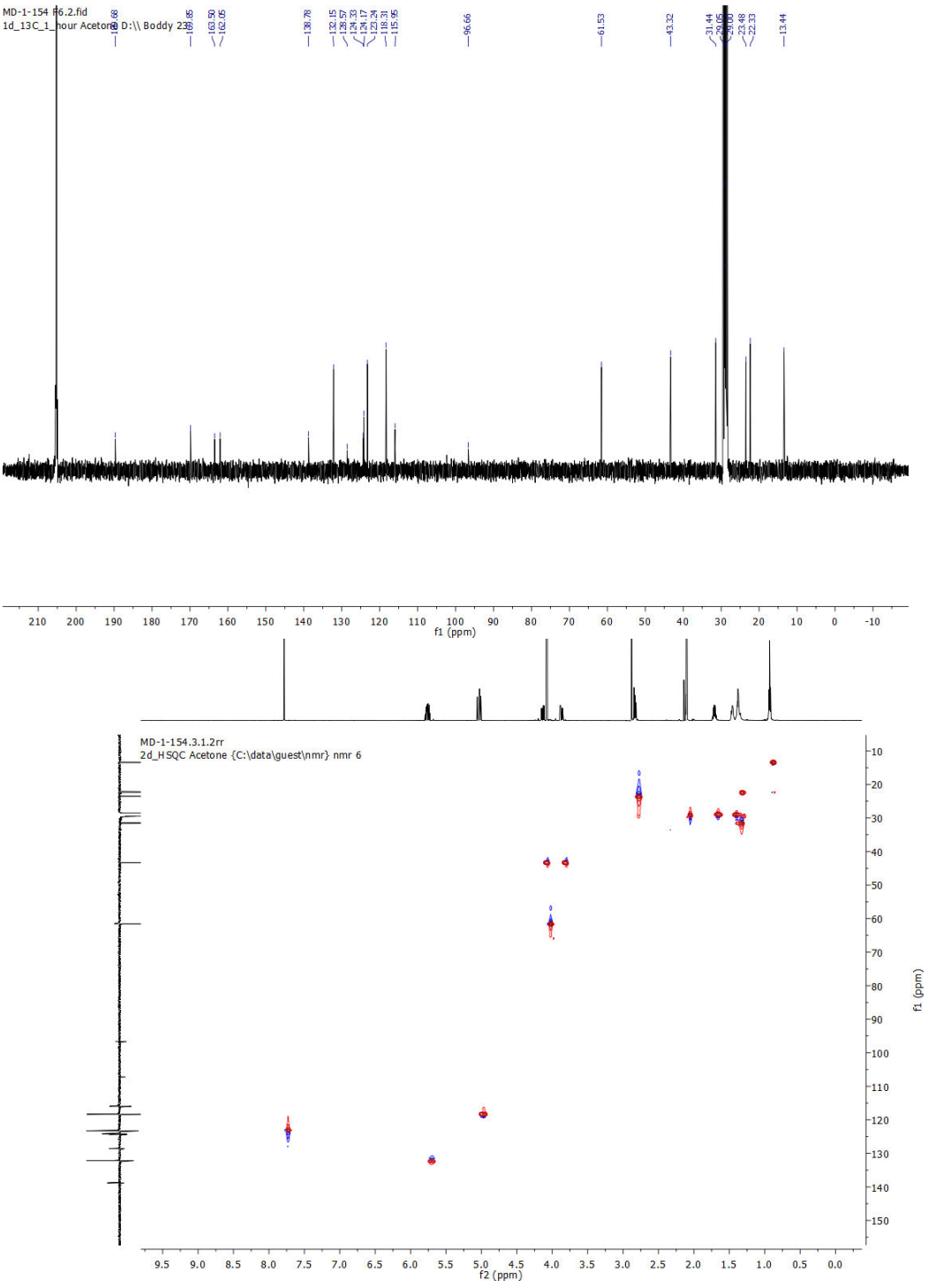

^{1}H NMR (400 MHz, Acetone-D$_6$) and ^{13}C NMR (100 MHz, Acetone-D$_6$) and HSQC of S9

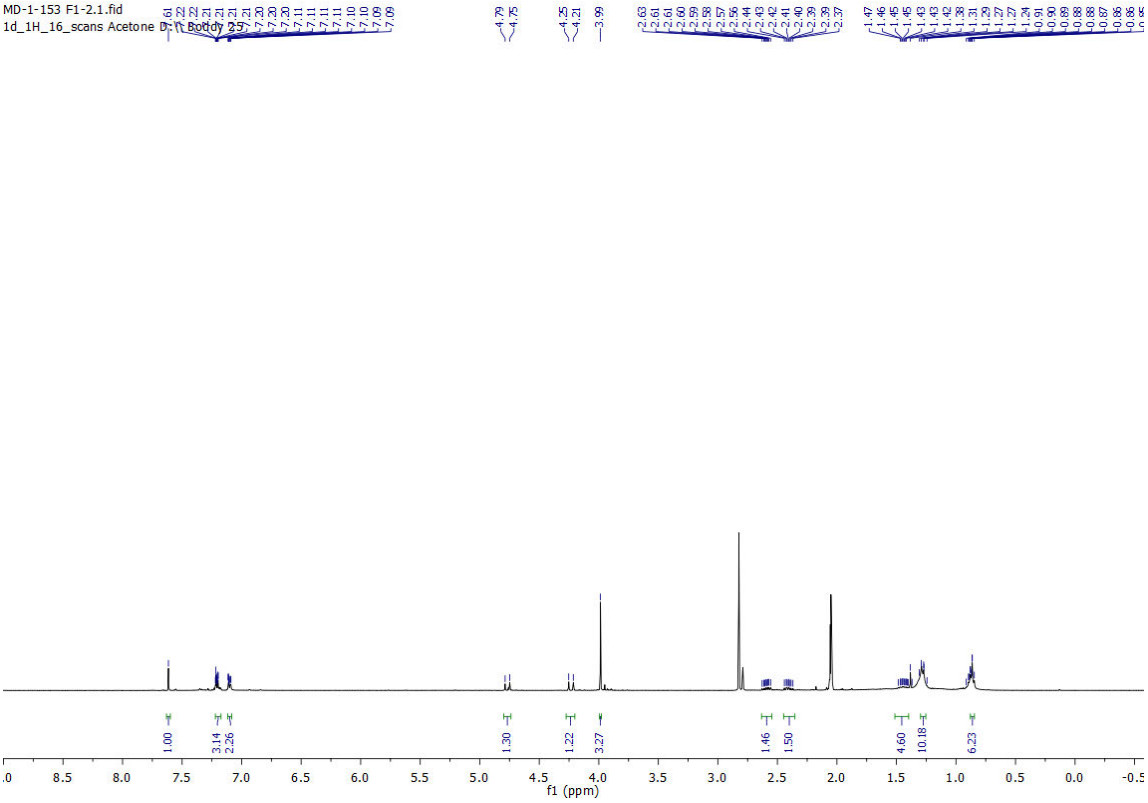
MD-1-153 F1-2.1.fid
1d_1H_16_scans Acetone D:\Users\Buddy 26
1.00
3.14
2.26
1.30
1.22
3.27
1.46
1.50
4.60
10.18
6.23
f1 (ppm)

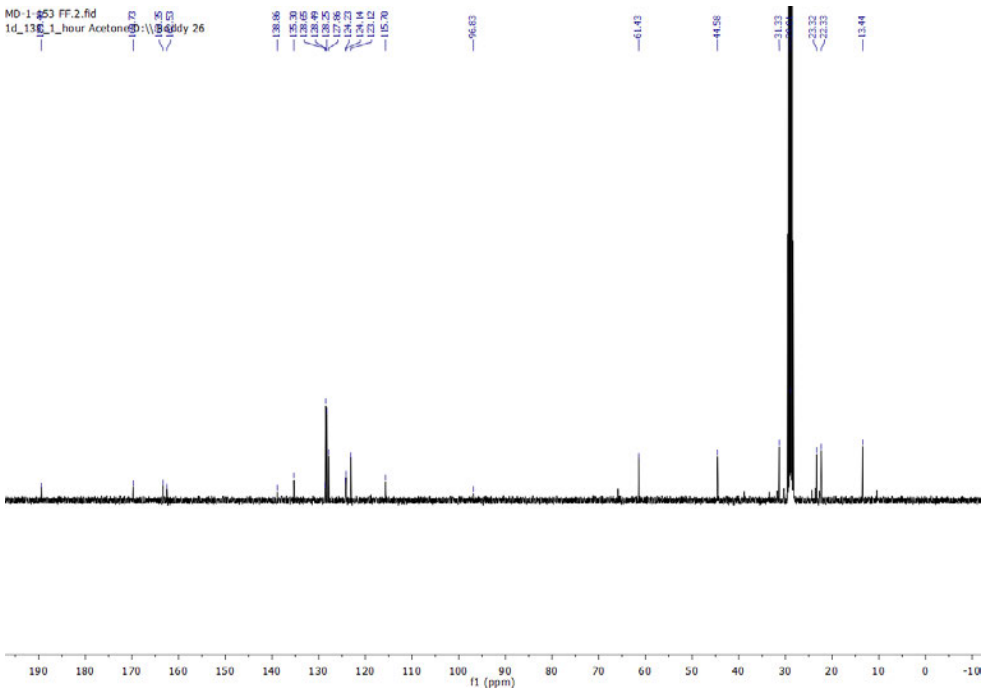
MD-1-153 FF.2.fid
1d_13C_1_hour Acetone D:\Users\Buddy 26
f1 (ppm)

^{1}H NMR (400 MHz, Acetone-D_6) and ^{13}C NMR (100 MHz, Acetone-D_6) of S10

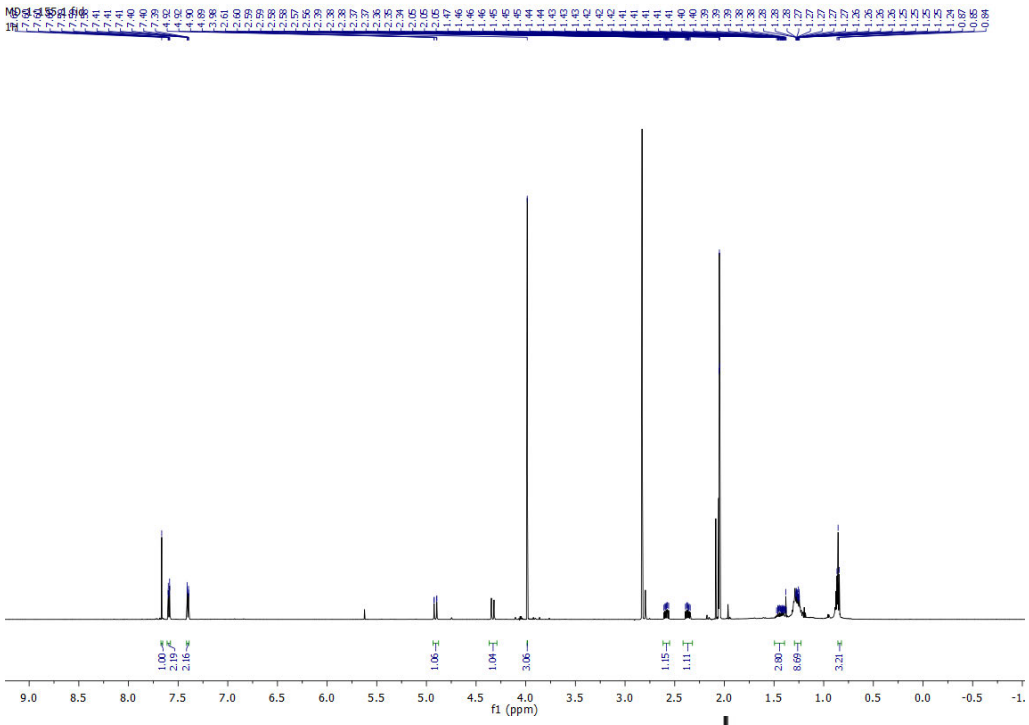
1.00
2.19
2.16
1.06
1.04
3.06
1.15
1.11
2.80
8.69
3.21
f1 (ppm)

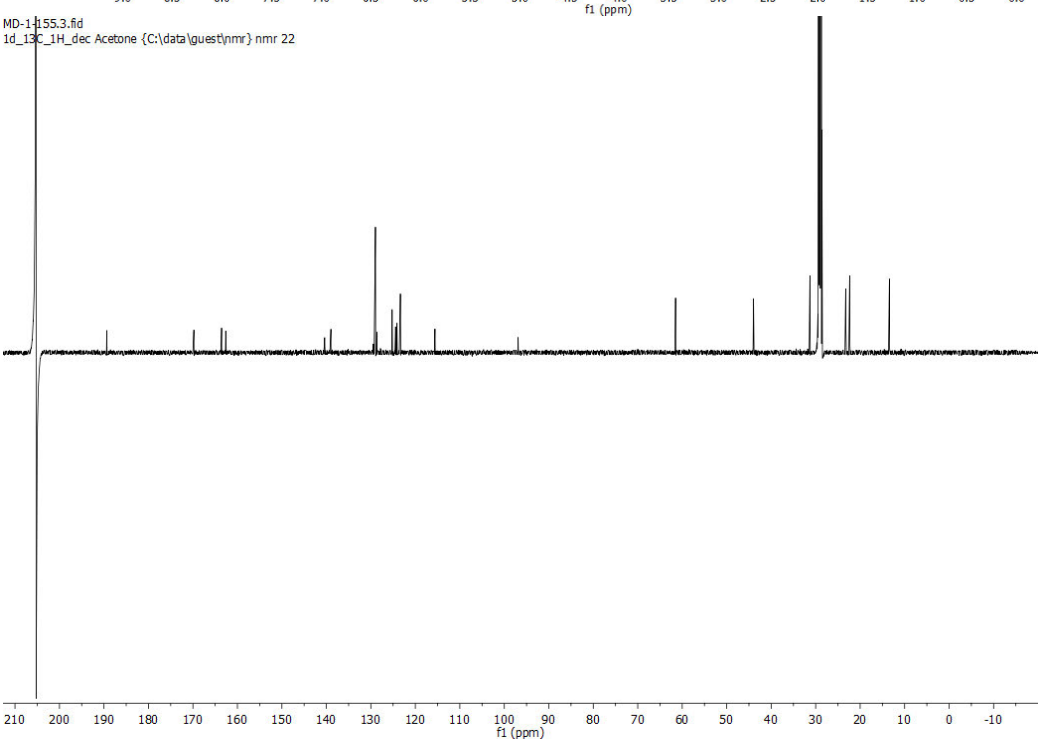
MD-11-155.3.fid
1d_13C_1H_dec Acetone {C:\data\guest\nmr} nmr 22
f1 (ppm)

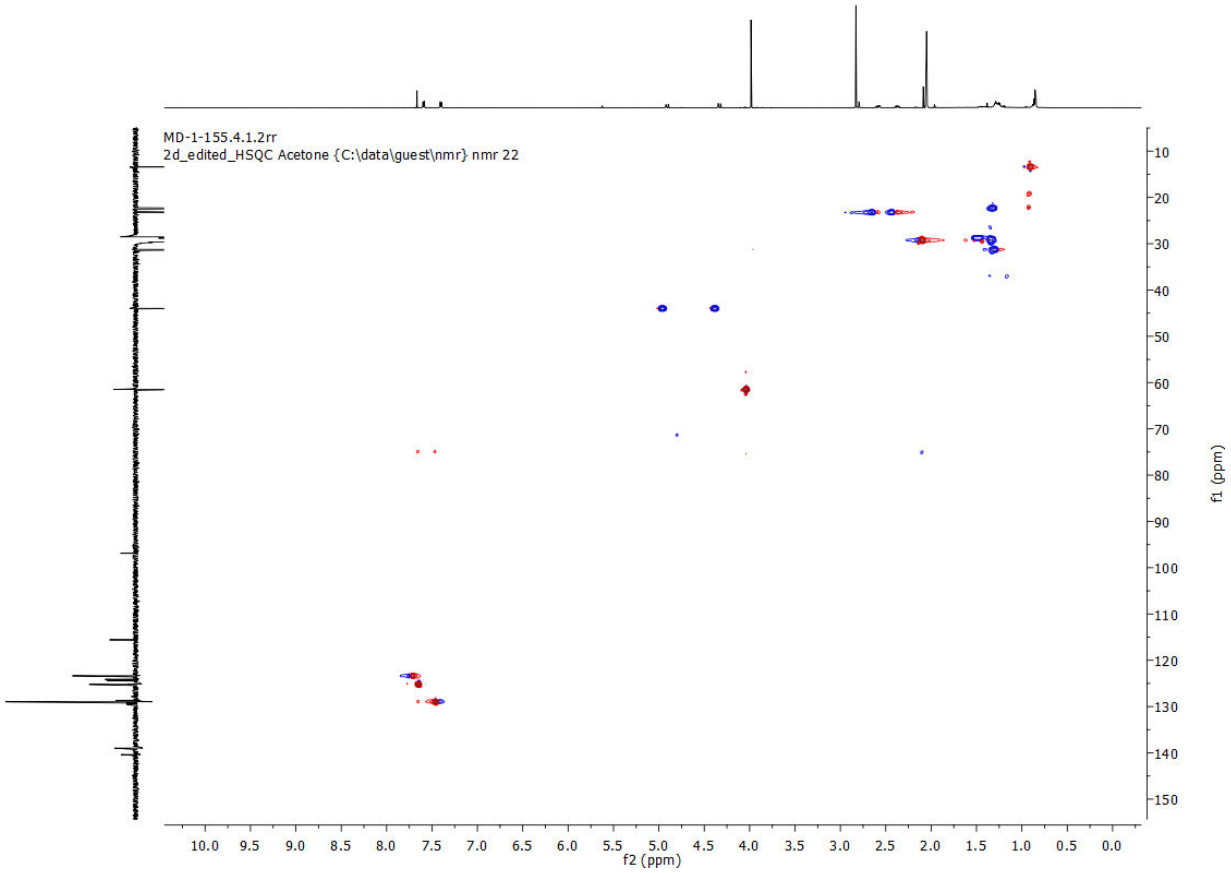

^{1}H NMR (400 MHz, Acetone-D$_6$) and ^{13}C NMR (100 MHz, Acetone-D$_6$) and HSQC of S11

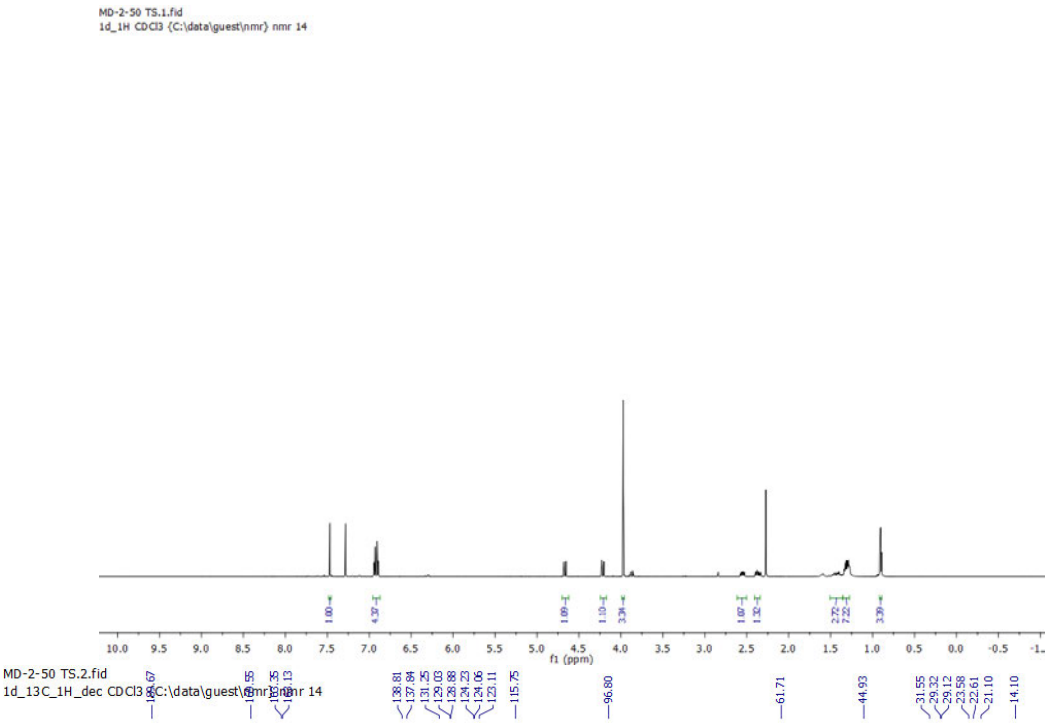
MD-2-50 TS.1.fid
1d_1H CDCl3 {C:\data\guest\nmr} nmr 14
1.00
4.37
1.09
1.10
3.04
1.07
1.32
2.22
2.22
3.39
f1 (ppm)
MD-2-50 TS.2.fid
1d_13C_1H_dec CDCl3 {C:\data\guest\nmr} nmr 14
138.81
137.84
131.25
129.03
128.88
124.23
124.06
123.11
115.75
96.80
61.71
44.93
31.55
29.32
29.12
23.58
22.61
21.10
14.10
f1 (ppm)

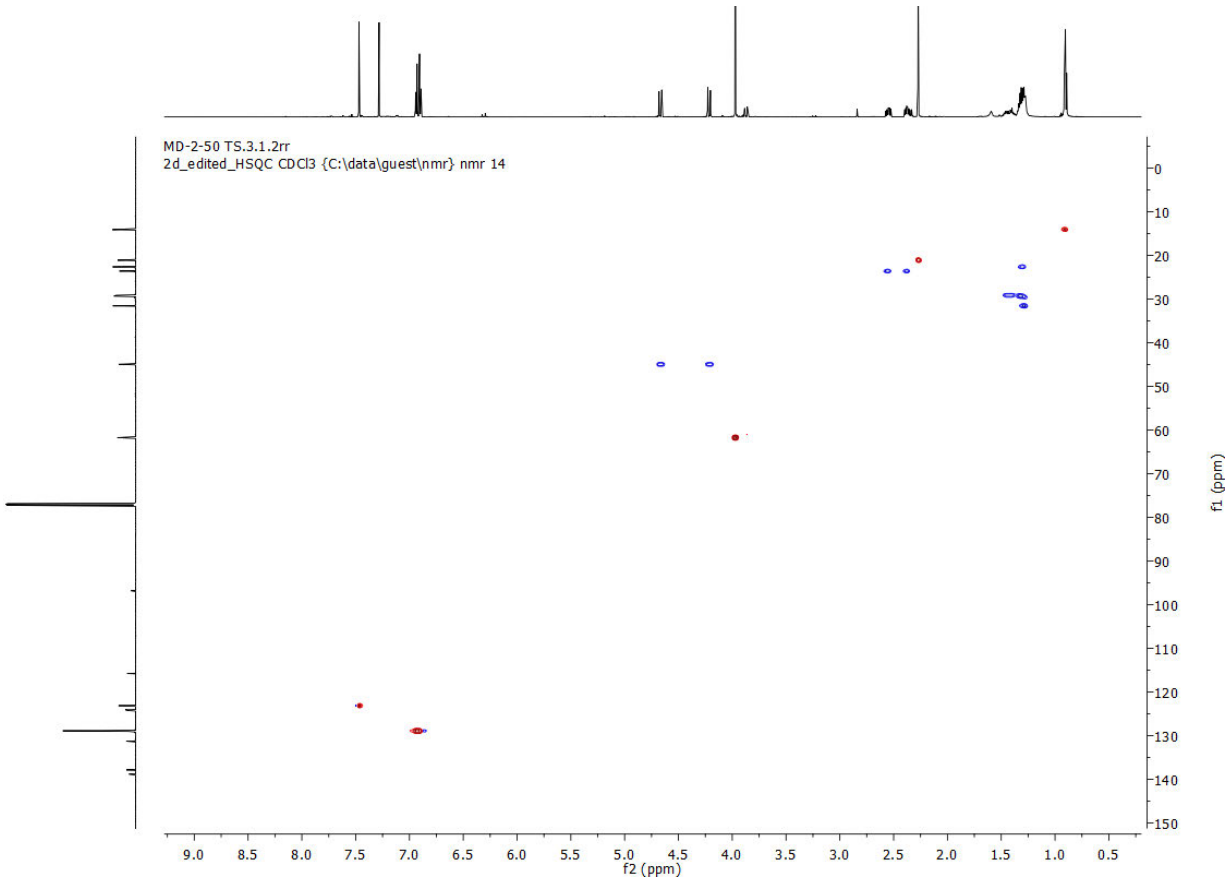

^{1}H NMR (400 MHz, Acetone-D$_6$) and ^{13}C NMR (100 MHz, Acetone-D$_6$) and HSQC of S12

MD-2-48 F7-22.1.fid
1d_1H CDCl3 {C:\data\guest\nmr} nmr 8

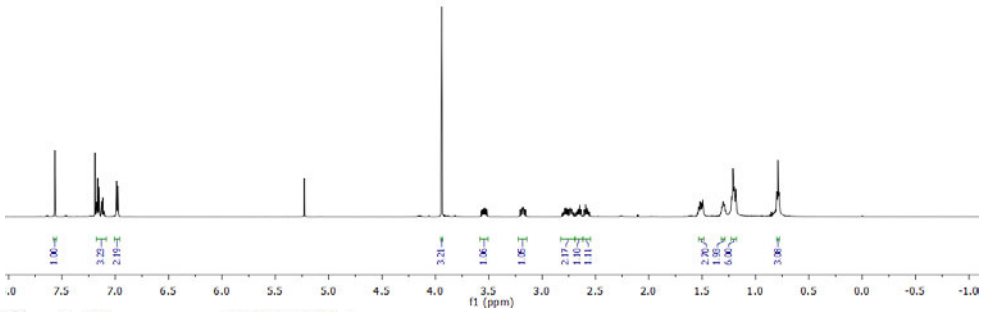

MD-2-48 F7-22.2.fid
1d_13C{1H}_dec CDCl3 {C:\data\guest\nmr} nmr 8

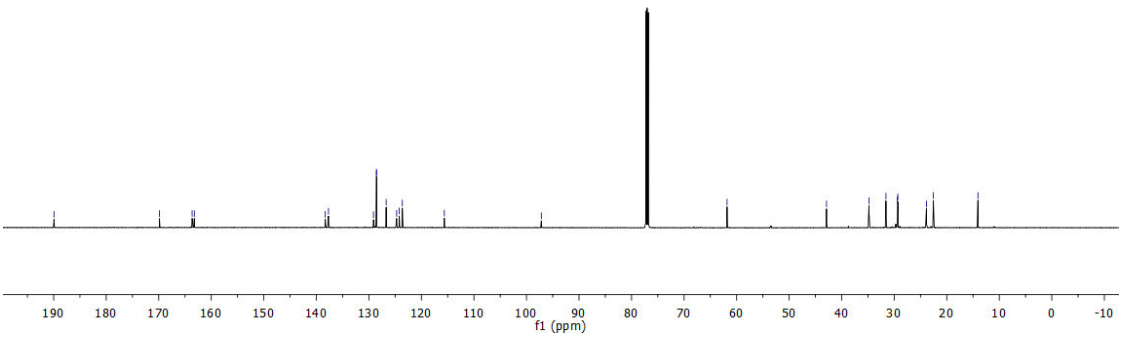

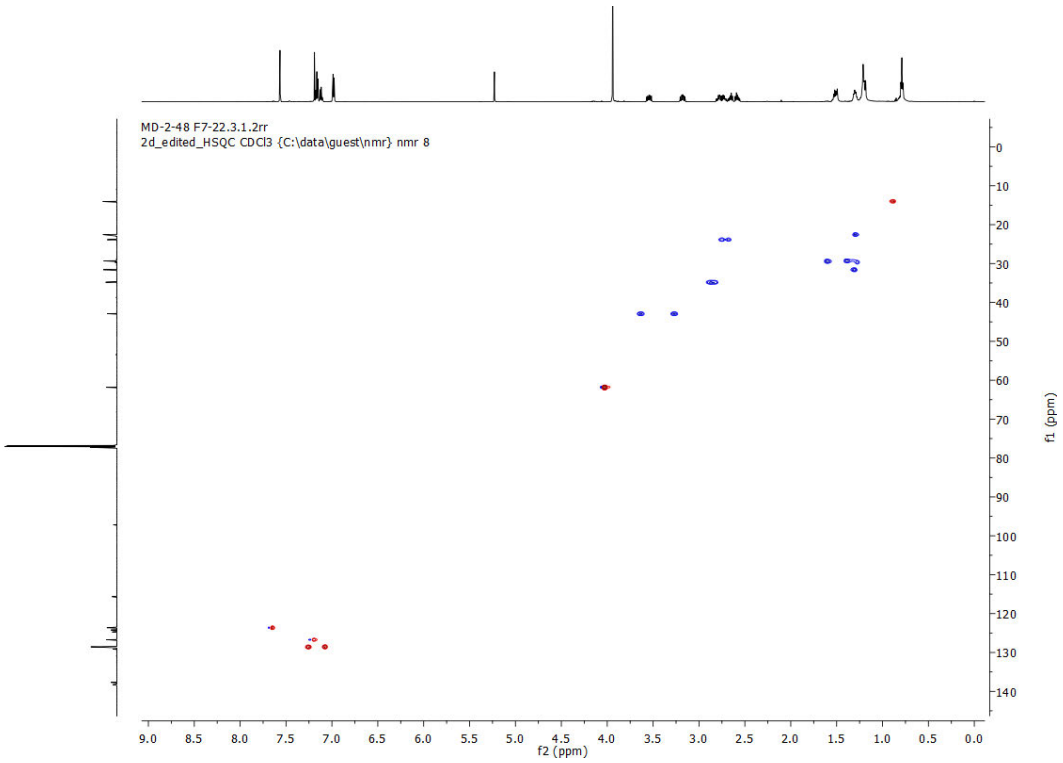

^{1}H NMR (400 MHz, $CDCl_3$) and ^{13}C NMR (100 MHz, $CDCl_3$) and HSQC of S13

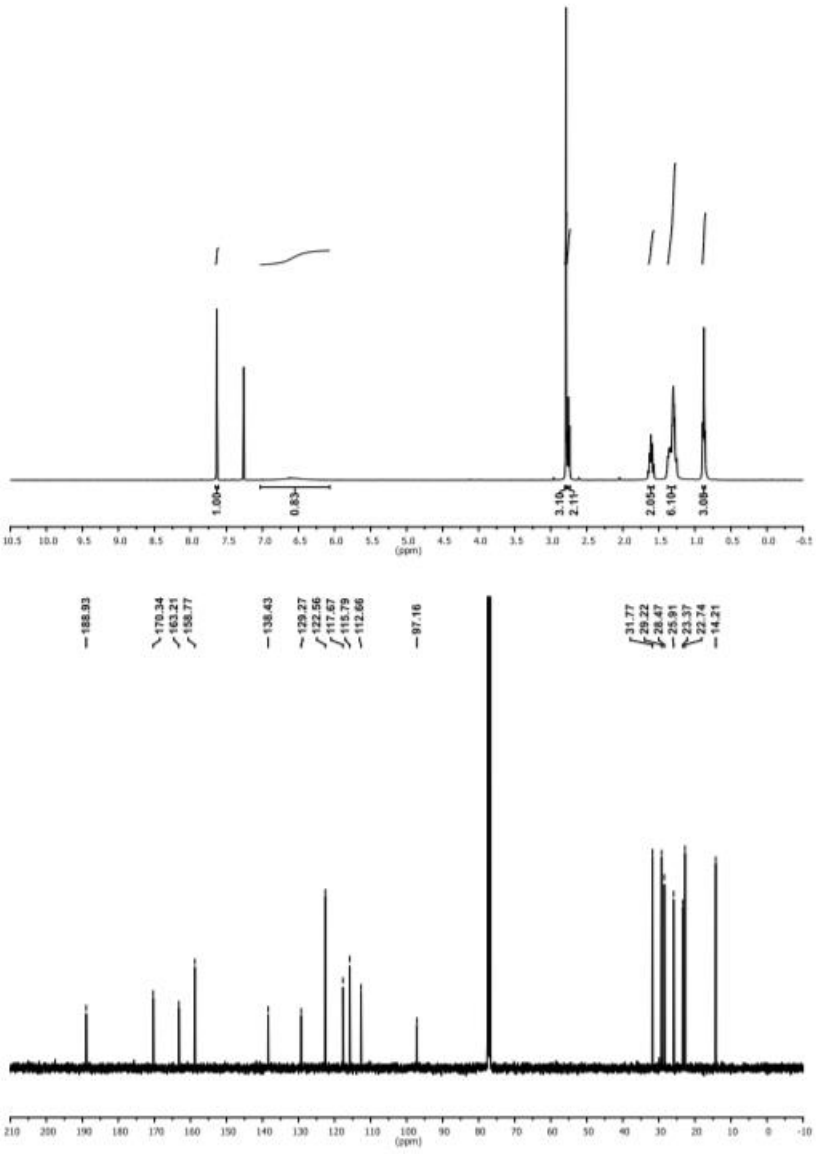

^{1}H NMR (400 MHz, $CDCl_3$) and ^{13}C NMR (100 MHz, $CDCl_3$) of **1**

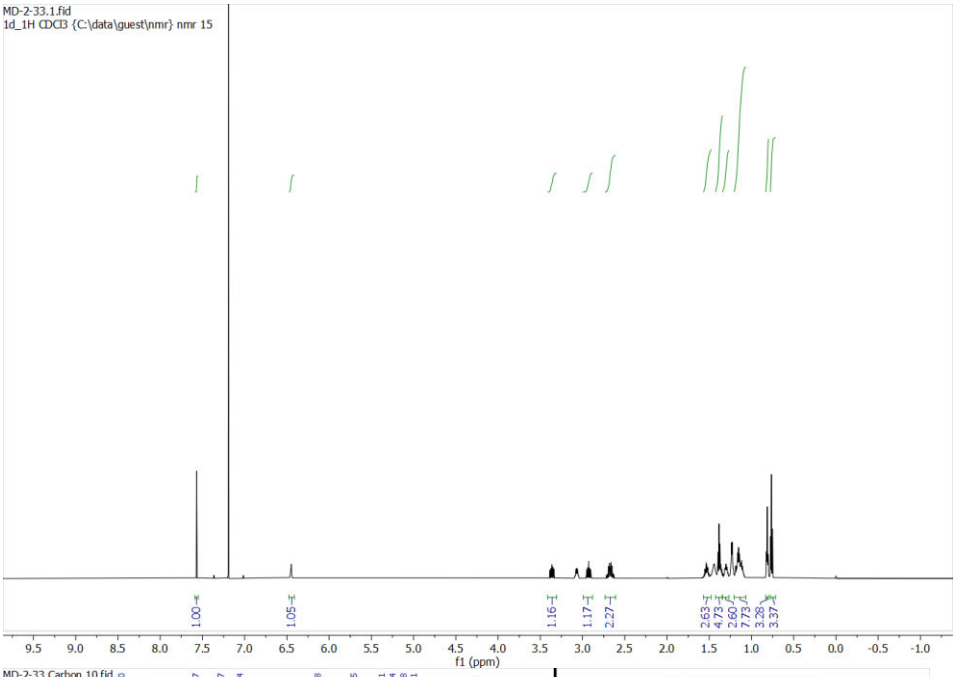
MD-2-33.1.fid
1d_1H CDCl3 {C:\data\guest\nmr} nmr 15
1.00
1.05
1.16
1.17
2.27
2.63
4.73
2.60
7.73
3.28
3.37
f1 (ppm)

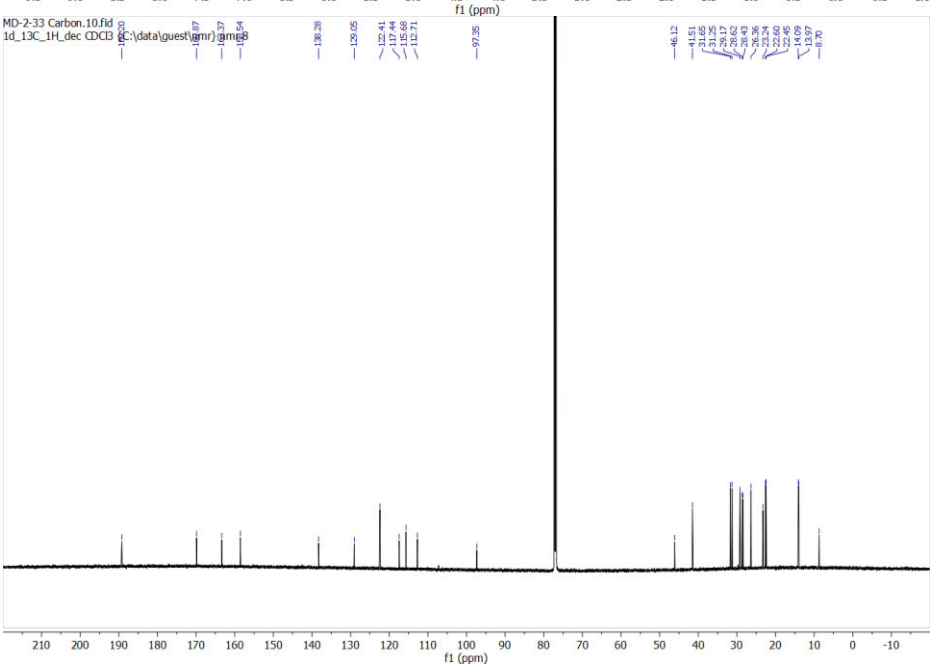
MD-2-33 Carbon.10.fid
1d_13C_1H_dec CDCl3 {C:\data\guest\nmr} nmr 8
f1 (ppm)

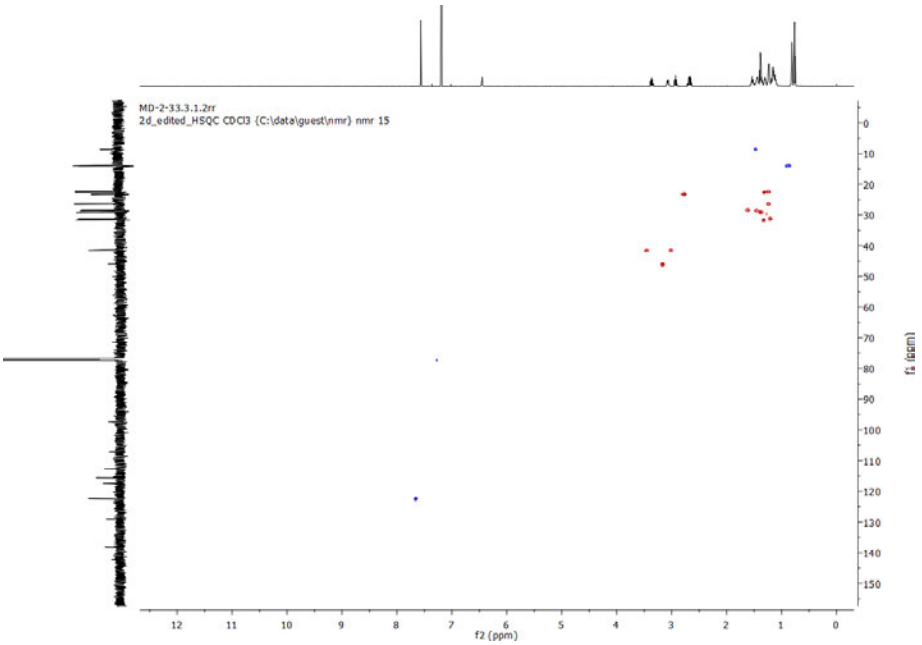

^{1}H NMR (400 MHz, $CDCl_3$) and ^{13}C NMR (100 MHz, $CDCl_3$) and HSQC of **2**

MD-1-170 II.1.fid
1d_1H Acetone {C:\data\guest\nmr} nmr 5

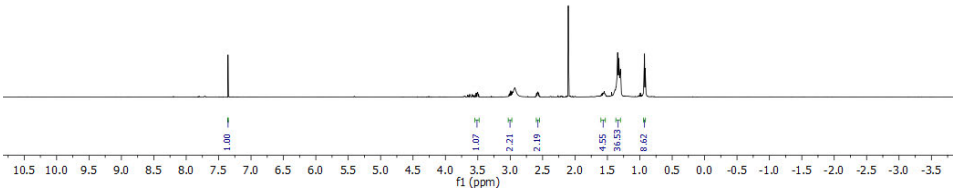

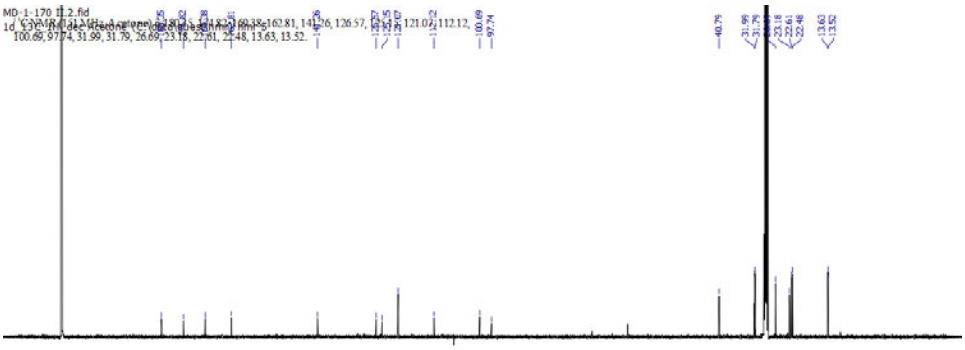

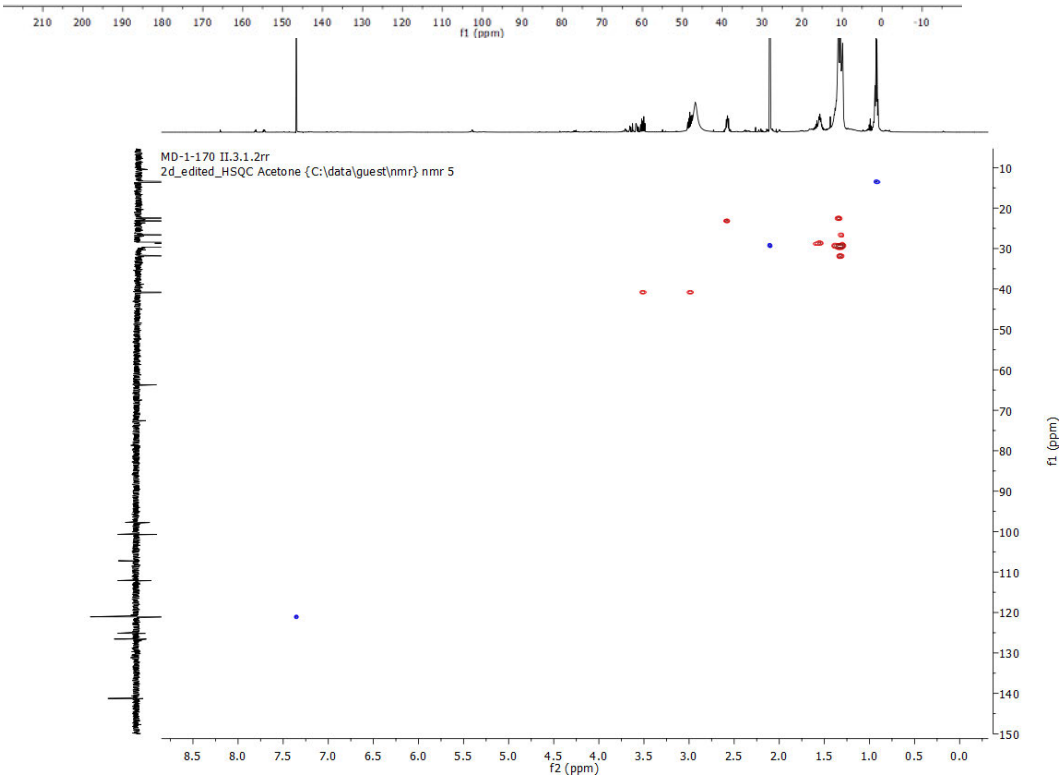

^{1}H NMR (600 MHz, Acetone-D$_6$) and ^{13}C NMR (150 MHz, Acetone-D$_6$) and HSQC of **3**

MD-1-168 III.1.fid
1d_1H Acetone {C:\data\guest\nmr} nmr 19

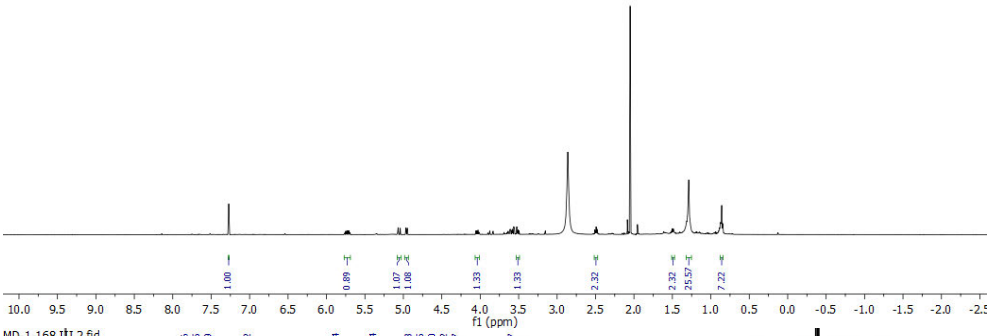

MD-1-168 III.2.fid
1d_13C_1H_dec Acetone {C:\data\guest\nmr} nmr 19

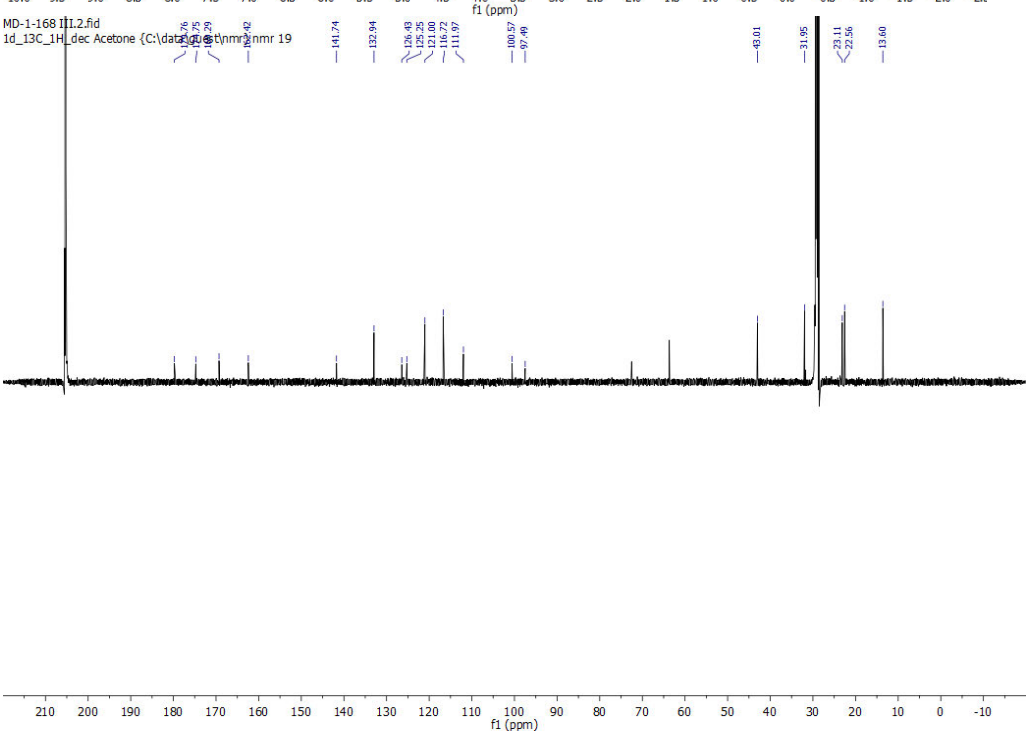

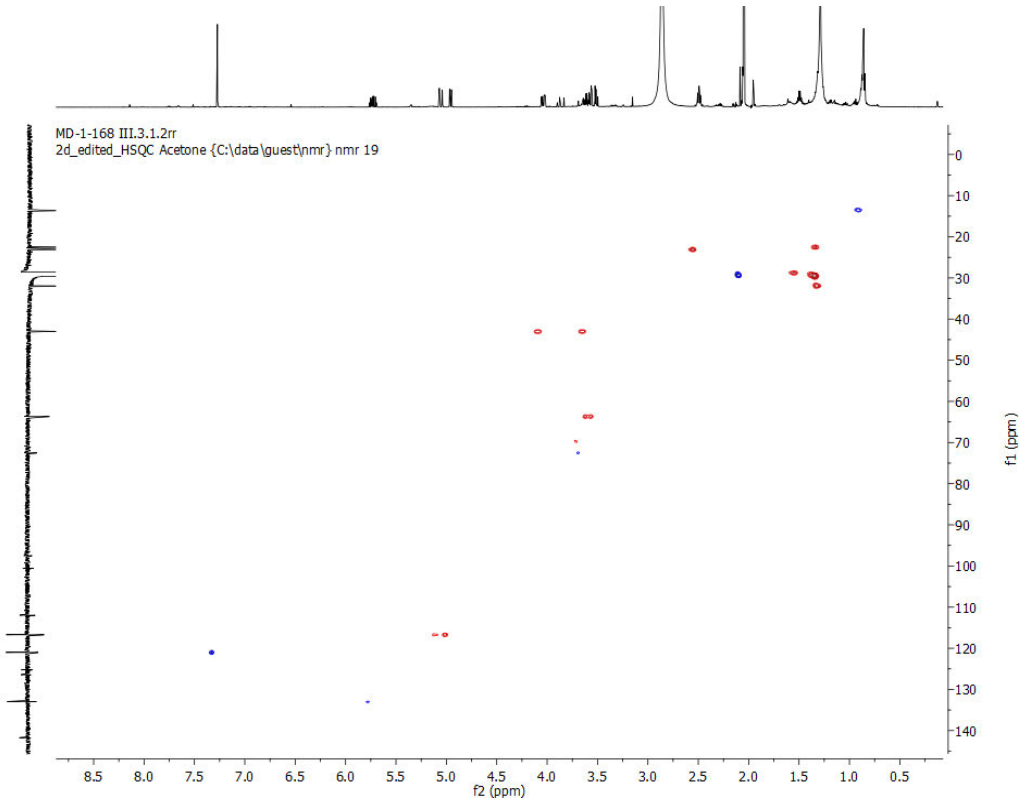

^{1}H NMR (600 MHz, Acetone-D$_6$) and ^{13}C NMR (150 MHz, Acetone-D$_6$) and HSQC of **4**

MD-1-167 F42-52.1.fid
1d_1H CDCl3 {C:\data\guest\nmr} nmr 22

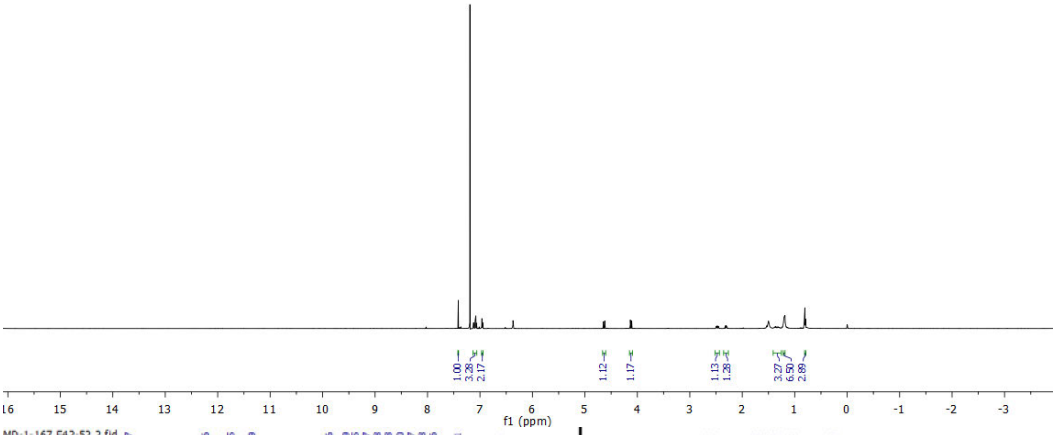

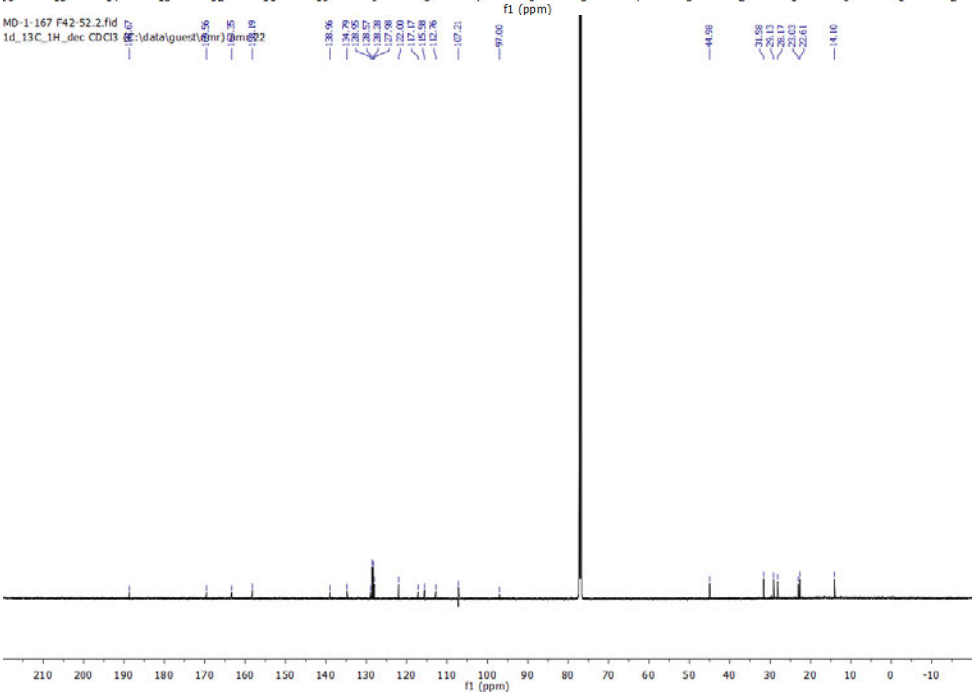

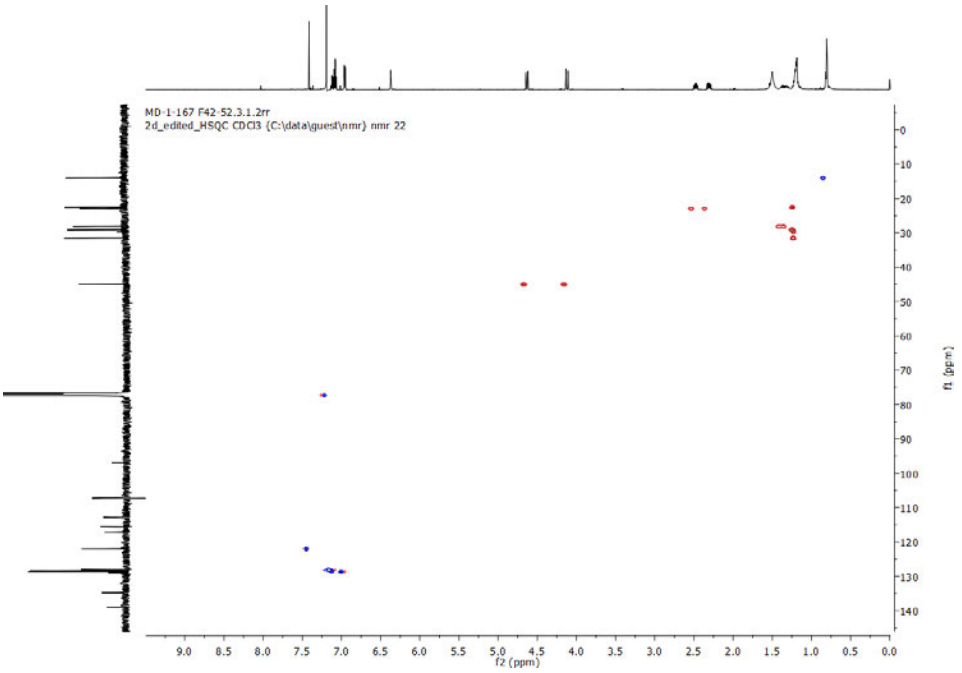

^{1}H NMR (600 MHz, Acetone-D$_6$) and ^{13}C NMR (150 MHz, Acetone-D$_6$) and HSQC of **5**

MD-1-169 II.1.fid
1d_1H Acetone (C:\data\guest\nmr) nmr 4

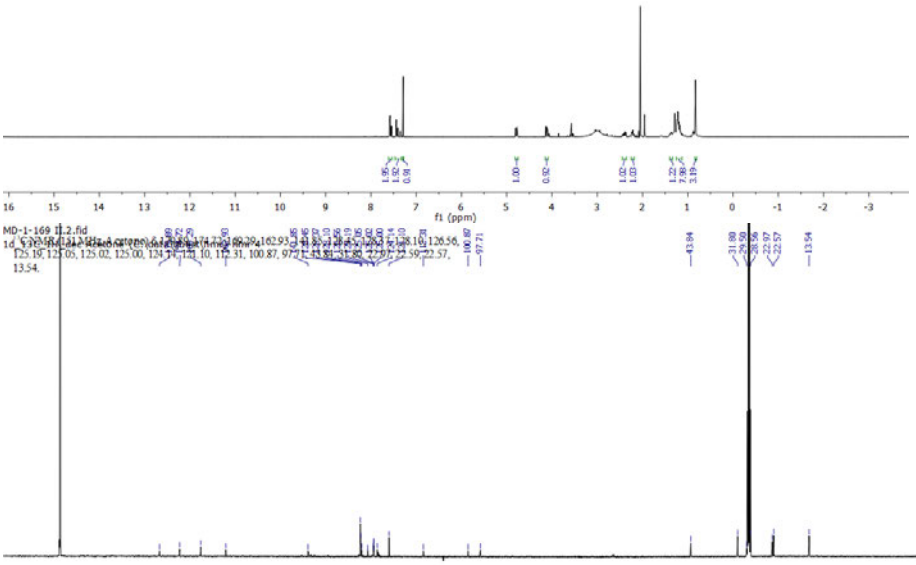

MD-1-169 II.2.fid
1d_13C{1H} (C:\data\guest\nmr) nmr 4

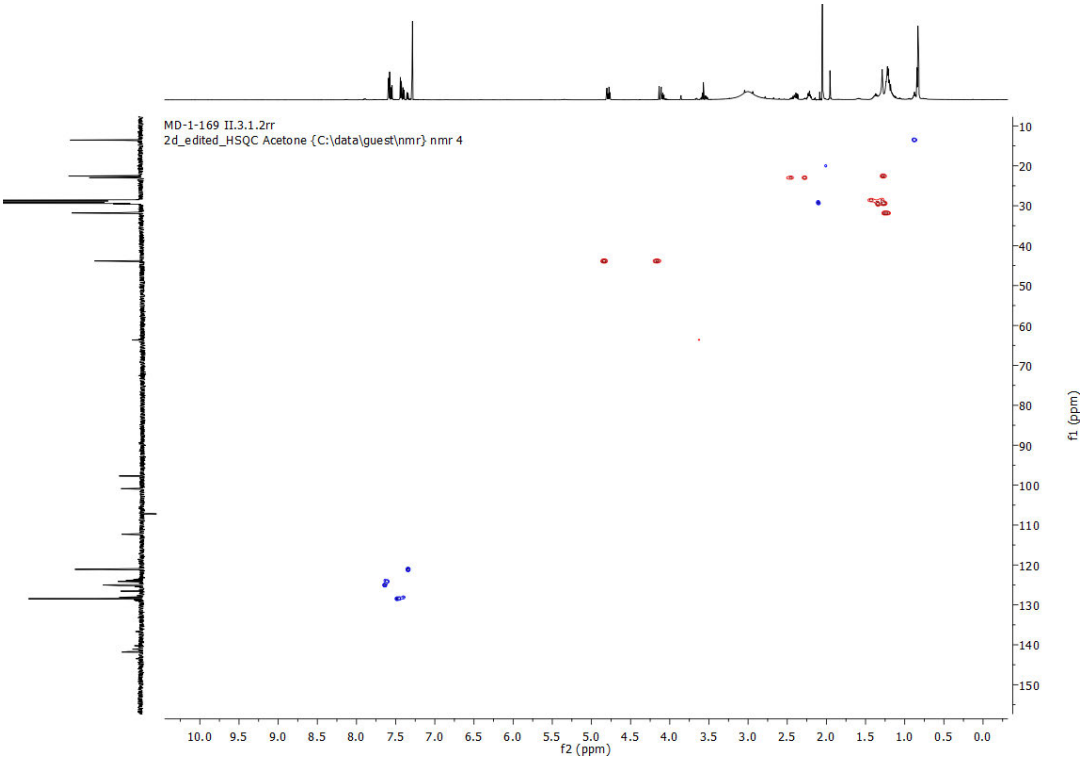

^{1}H NMR (600 MHz, Acetone-D$_6$) and ^{13}C NMR (150 MHz, Acetone-D$_6$) and HSQC of **6**

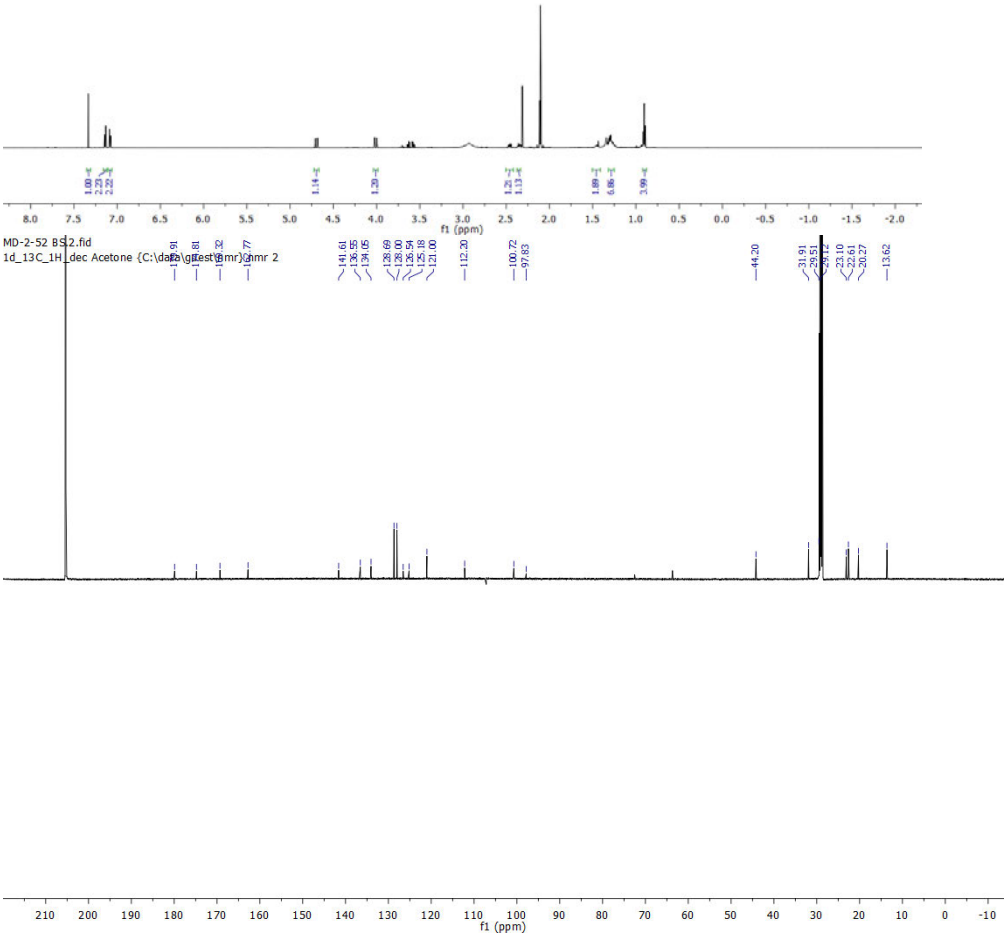
MD-2-52 BS.1.fid
1d_1H Acetone {C:\data\guest\nmr} nmr 2
1.00
2.23
2.22
1.14
1.29
1.25
1.13
1.89
6.86
3.99
f1 (ppm)
MD-2-52 BS2.fid
1d_13C_1H_dec Acetone {C:\data\guest\nmr} nmr 2
141.61
136.55
134.05
128.69
128.00
126.54
125.18
121.00
112.20
100.72
97.83
44.20
31.91
29.51
29.14
23.10
22.61
20.27
13.62
f1 (ppm)

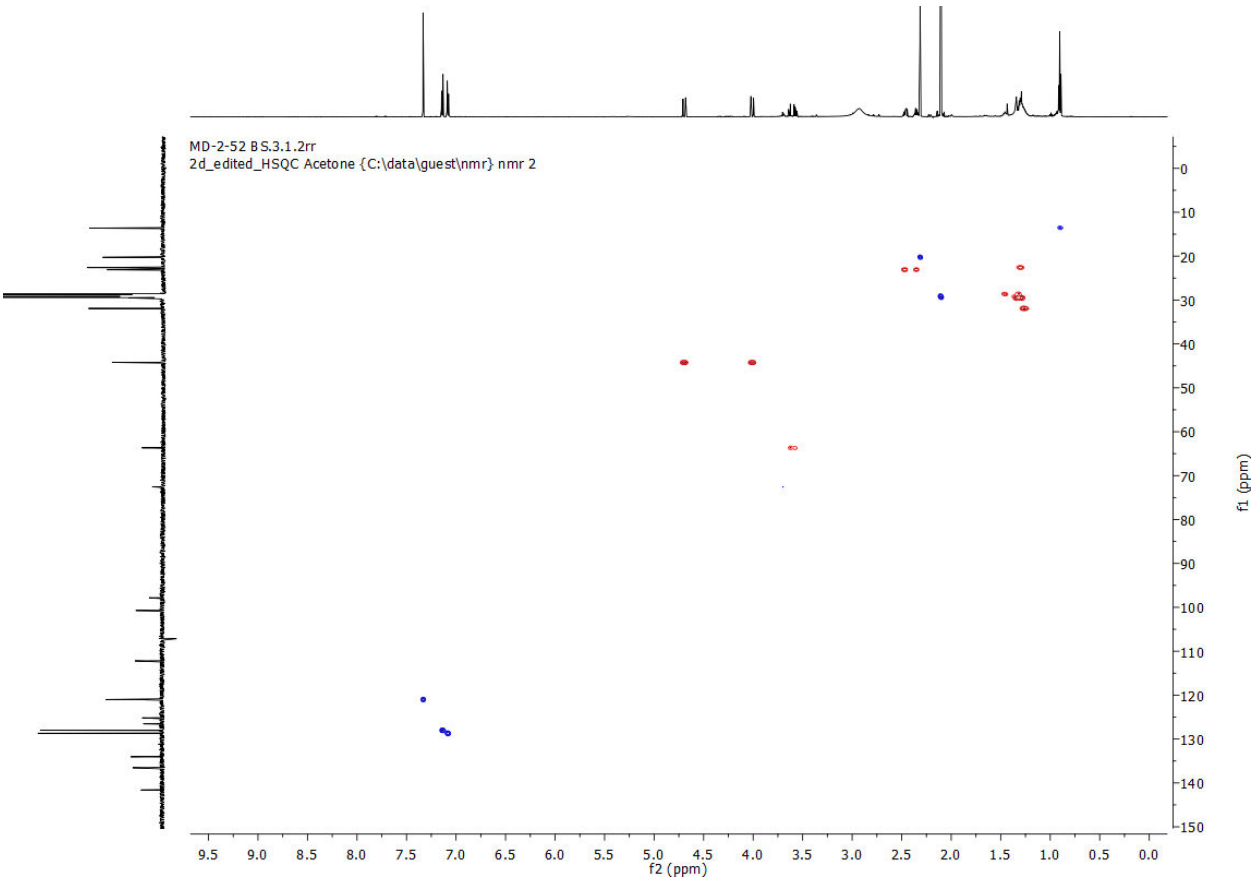

^{1}H NMR (600 MHz, Acetone-D$_6$) and ^{13}C NMR (150 MHz, Acetone-D$_6$) and HSQC of **7**

MD-2-51.1.fid
1d_1H Acetone (C:\data\guest\nmr) nmr 17

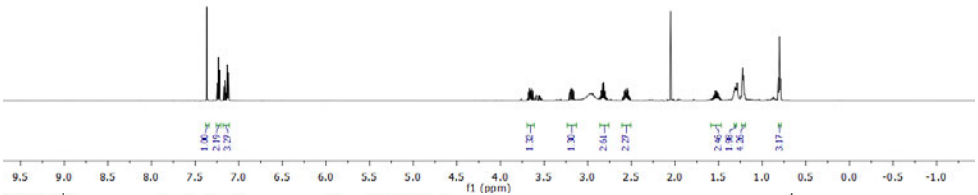

MD-2-51.2.fid
1d_13C_1H_dec Acetone (C:\data\guest\nmr) nmr 17

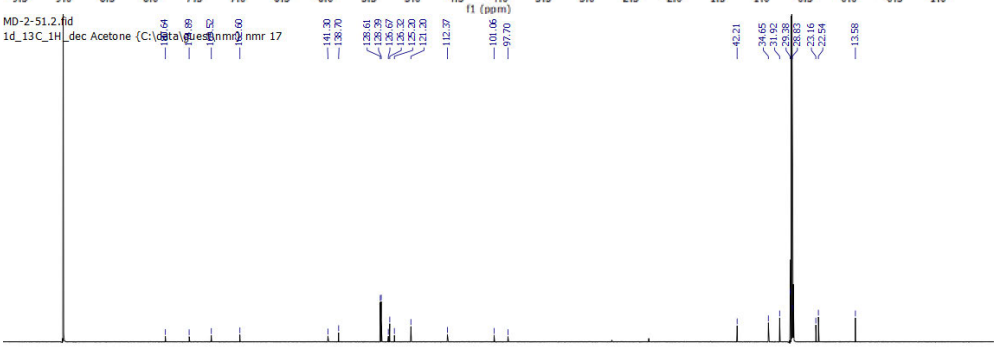

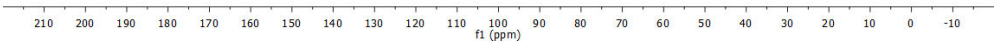

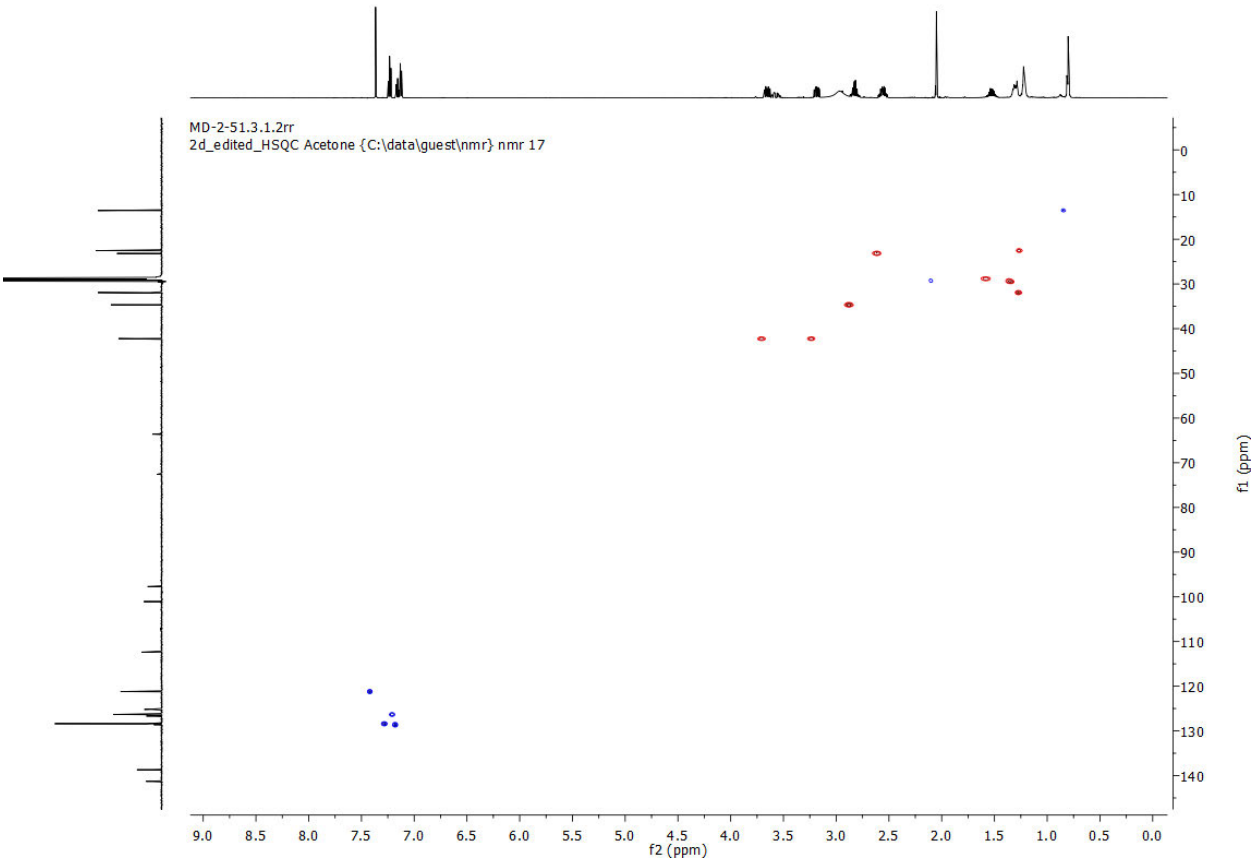

^{1}H NMR (600 MHz, Acetone-D$_6$) and ^{13}C NMR (150 MHz, Acetone-D$_6$) and HSQC of **8**

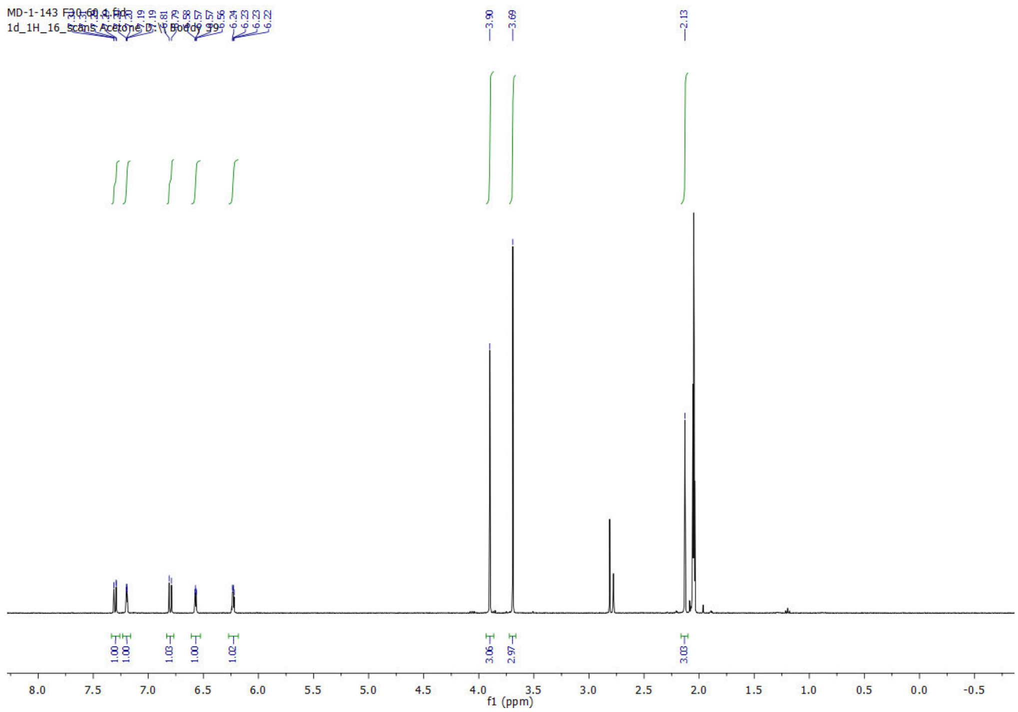
MD-1-143 F30-60 4.fid
1d_1H_16_scans Acetone D:\\ Boddy 39
3.90
3.69
2.13
1.00
1.00
1.03
1.00
1.02
3.06
2.97
3.03
f1 (ppm)

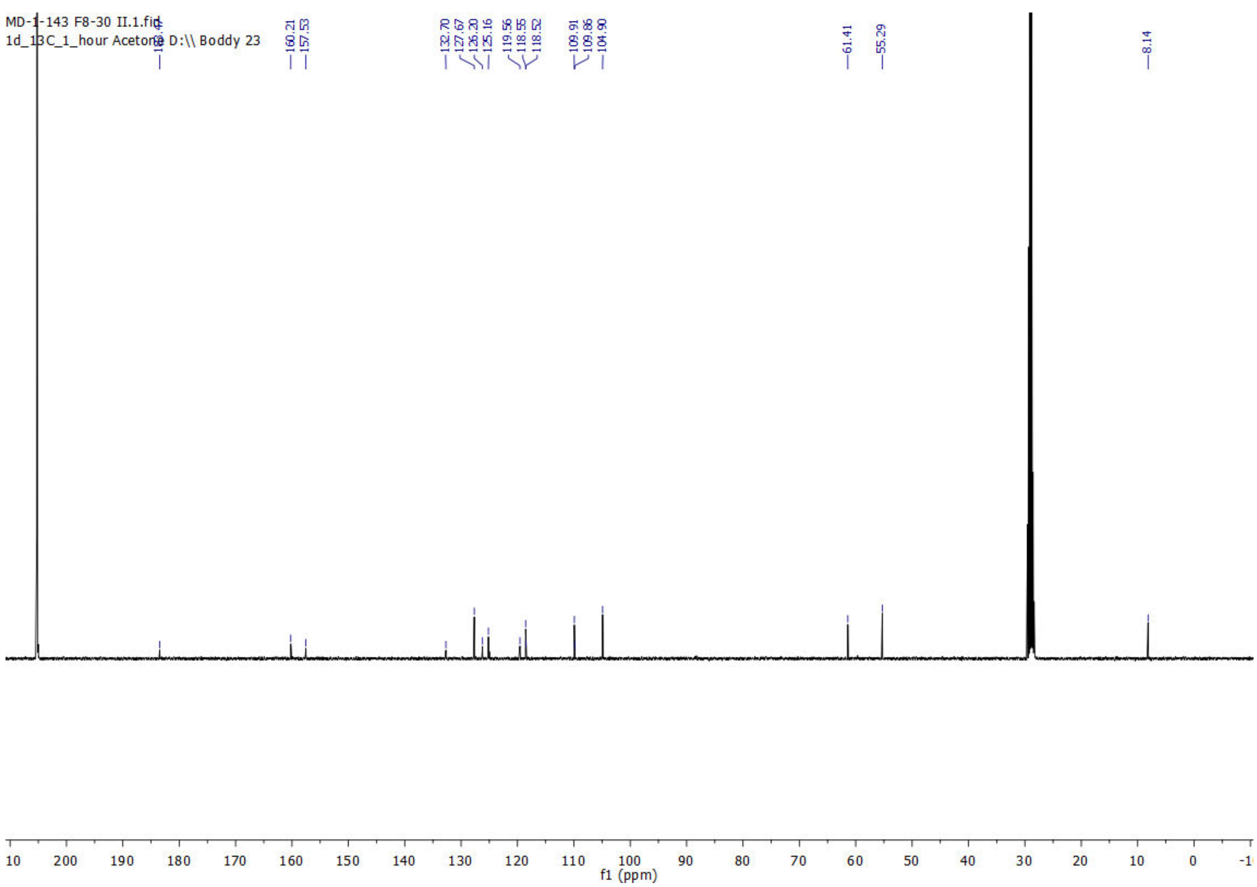
MD-1-143 F8-30 II.1.fid
1d_13C_1_hour Acetone D:\\ Boddy 23
160.21
157.53
132.70
127.67
126.20
125.16
119.56
118.55
118.52
109.91
109.86
104.90
61.41
55.29
8.14
f1 (ppm)

^{1}H NMR (400 MHz, Acetone-D$_6$) and ^{13}C NMR (100 MHz, Acetone-D$_6$) of S14

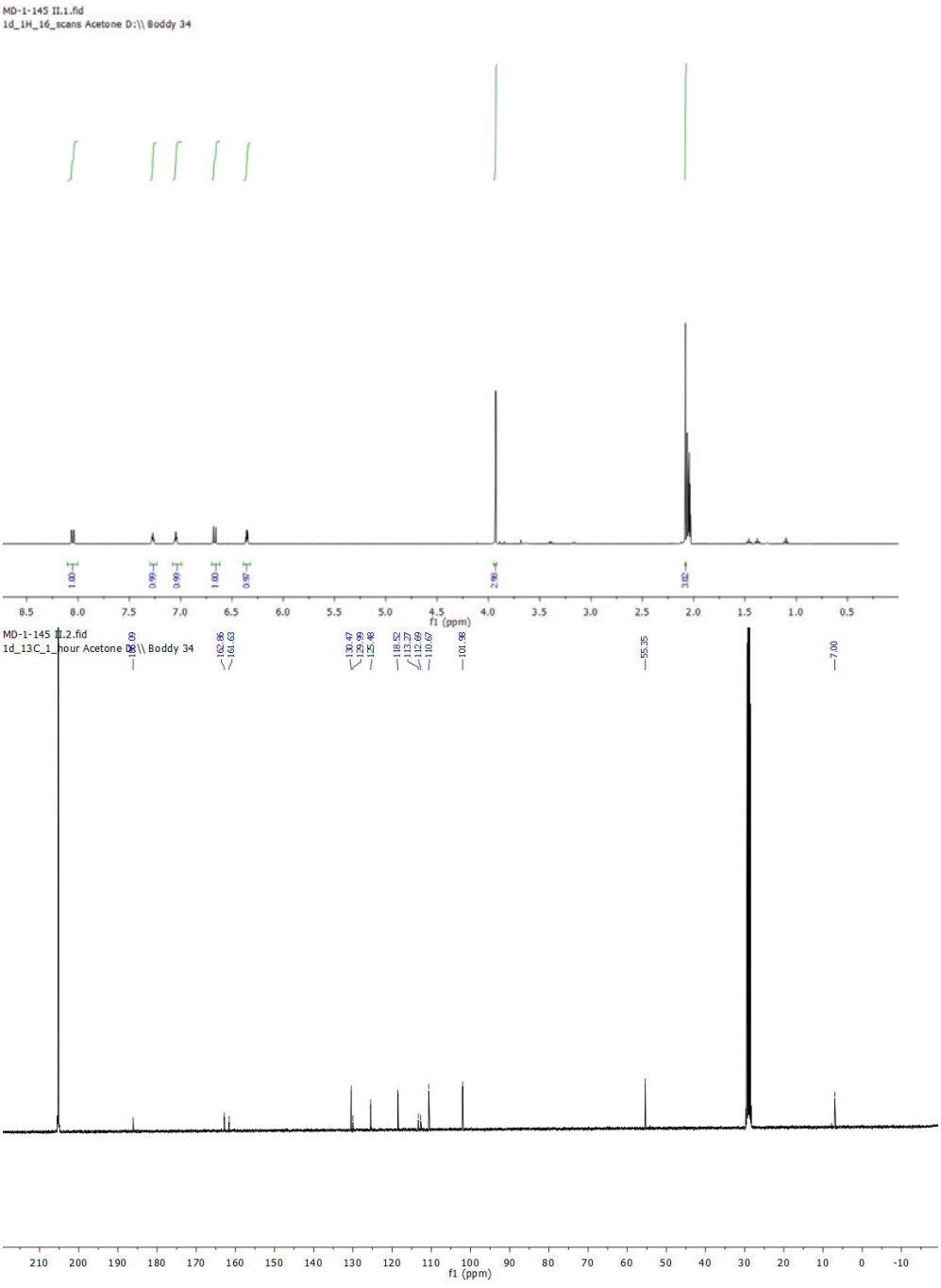

^{1}H NMR (400 MHz, Acetone-D$_6$) and ^{13}C NMR (100 MHz, Acetone-D$_6$) of S15

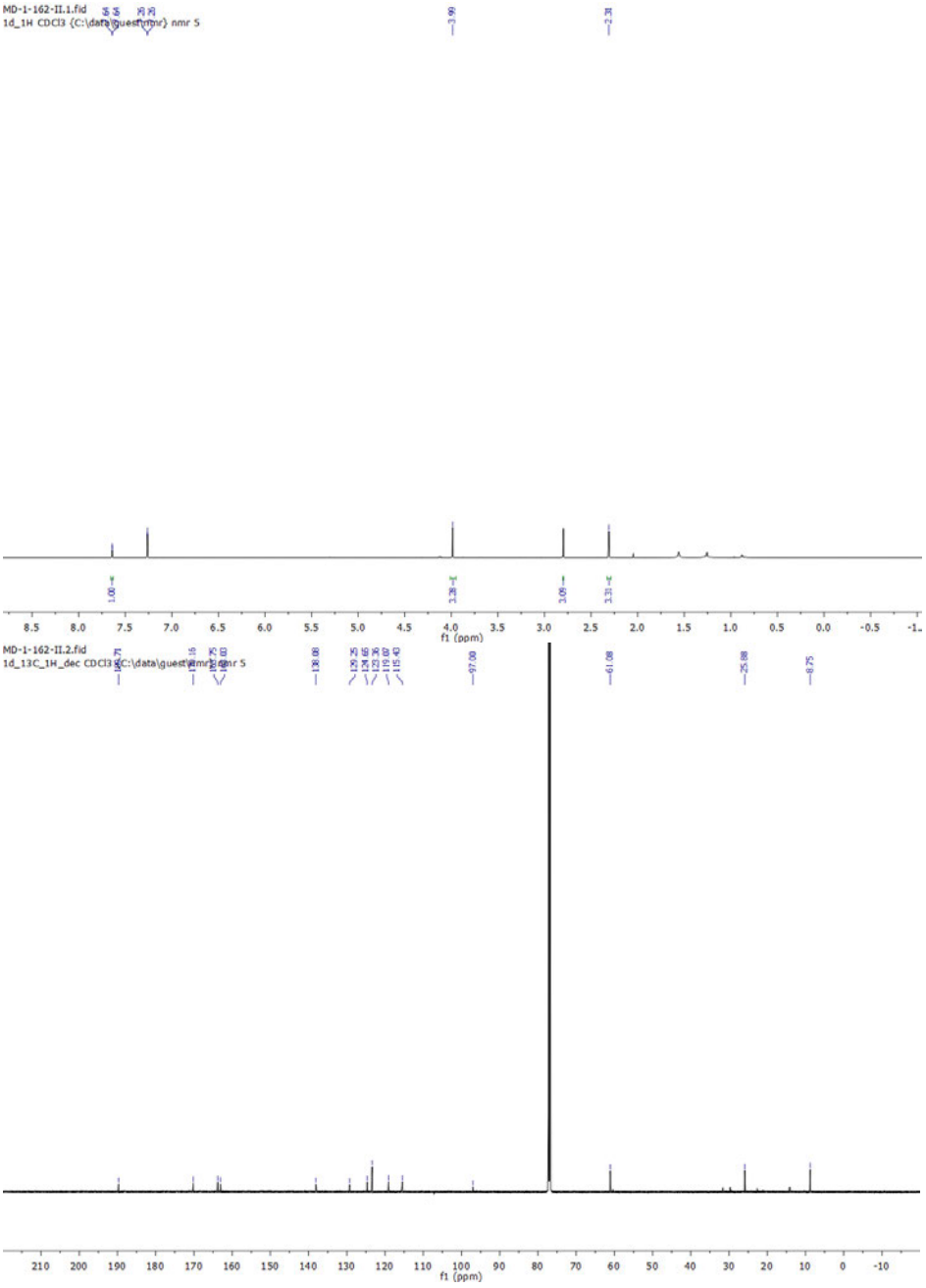
MD-1-162-II.1.fid
1d_1H CDCl3 {C:\data\guest\nmr} nmr 5
MD-1-162-II.2.fid
1d_13C_1H_dec CDCl3 {C:\data\guest\nmr} nmr 5
f1 (ppm)

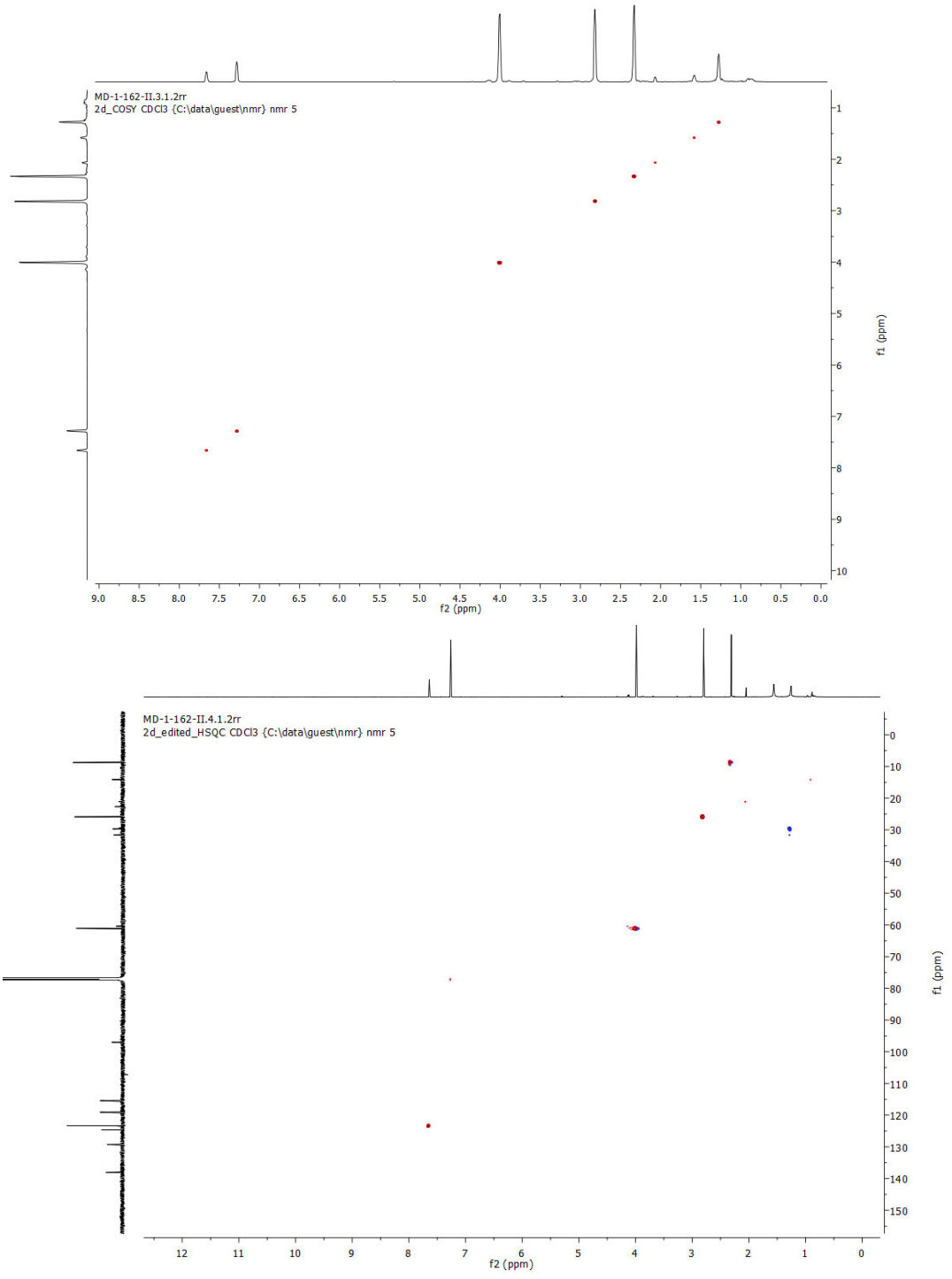

^{1}H NMR (400 MHz, $CDCl_3$) , ^{13}C NMR (100 MHz, $CDCl_3$) COSY and HSQC of S17

MD-2-06.1.fid
1d_1H CDCl3 {C:\data\guest\nmr} nmr 6

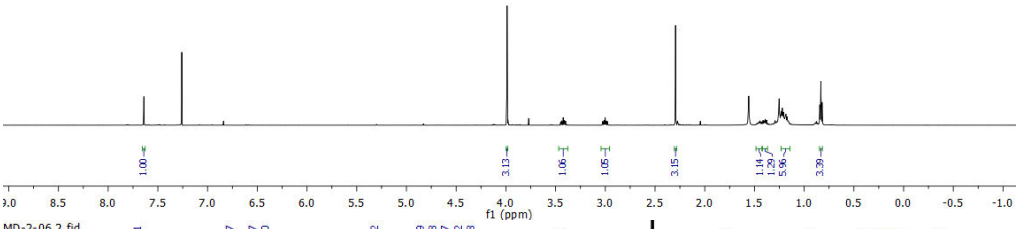

MD-2-06.2.fid
1d_13C_1H_dec CDCl3 {C:\data\guest\nmr} nmr 6

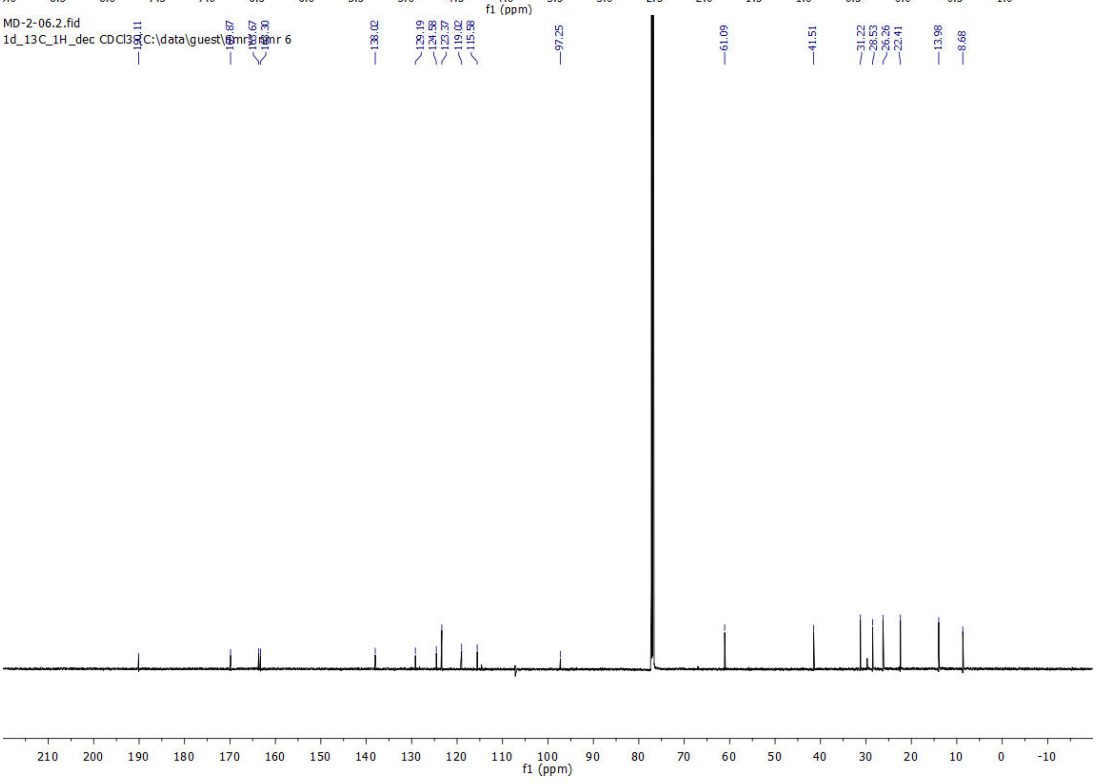

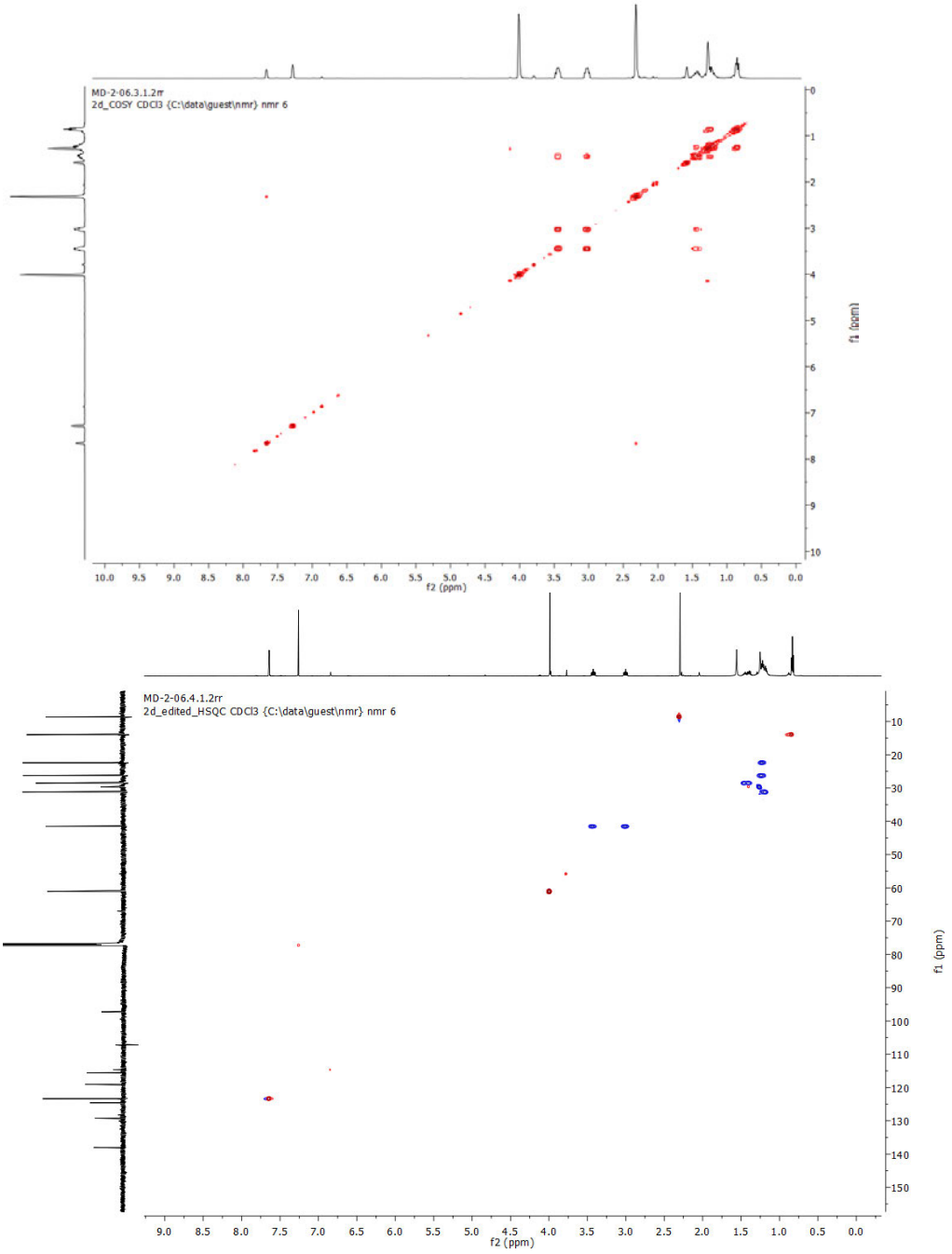

^{1}H NMR (400 MHz, $CDCl_3$) , ^{13}C NMR (100 MHz, $CDCl_3$) COSY and HSQC of S18

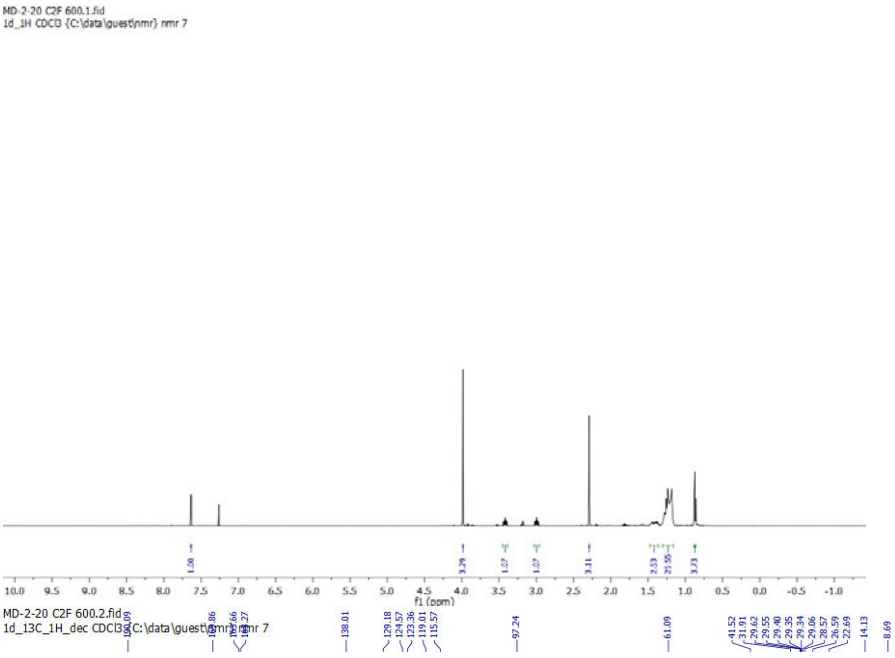
MD-2-20 C2F 600.1.fid
1d_1H CDCl3 {C:\data\guest\nmr} nmr 7
1.00
3.29
1.07
1.07
3.11
2.33
21.55
3.73
10.0 9.5 9.0 8.5 8.0 7.5 7.0 6.5 6.0 5.5 5.0 4.5 4.0 3.5 3.0 2.5 2.0 1.5 1.0 0.5 0.0 -0.5 -1.0
f1 (ppm)
MD-2-20 C2F 600.2.fid
1d_13C_1H_dec CDCl3 C:\data\guest\nmr nmr 7
160.09
138.01
129.18
124.57
123.36
119.01
115.57
97.24
61.09
41.52
31.91
29.62
29.55
29.46
29.35
29.34
29.06
28.57
26.59
22.69
14.13
8.69

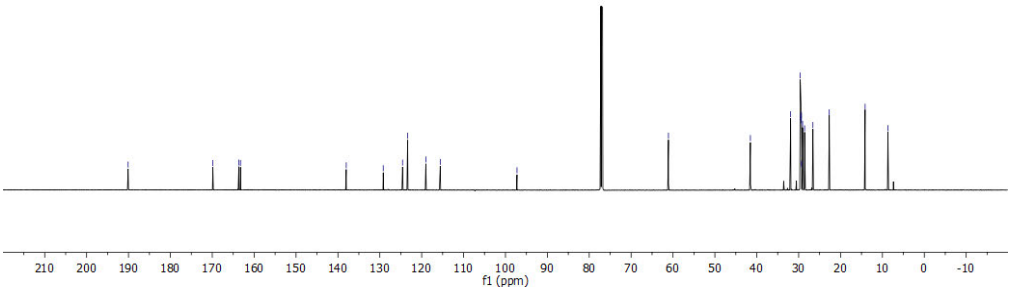
210 200 190 180 170 160 150 140 130 120 110 100 90 80 70 60 50 40 30 20 10 0 -10
f1 (ppm)

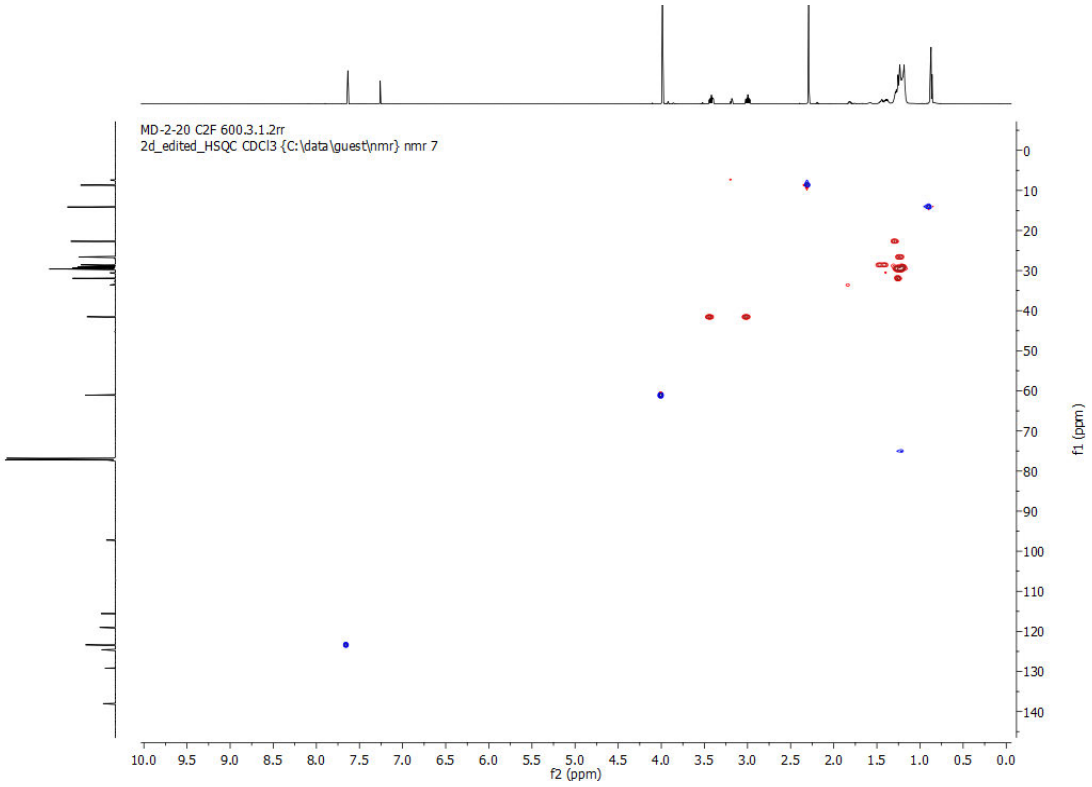

^{1}H NMR (400 MHz, $CDCl_3$) , ^{13}C NMR (100 MHz, $CDCl_3$) and HSQC of S19

MD-1-164.1.fid
1d_1H CDCl3 (C:\data\guest\nmr) nmr 5

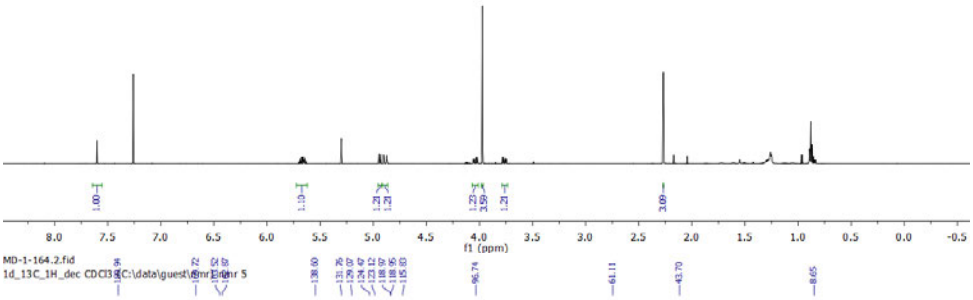

MD-1-164.2.fid
1d_13C_1H_dec CDCl3 (C:\data\guest\nmr) nmr 5

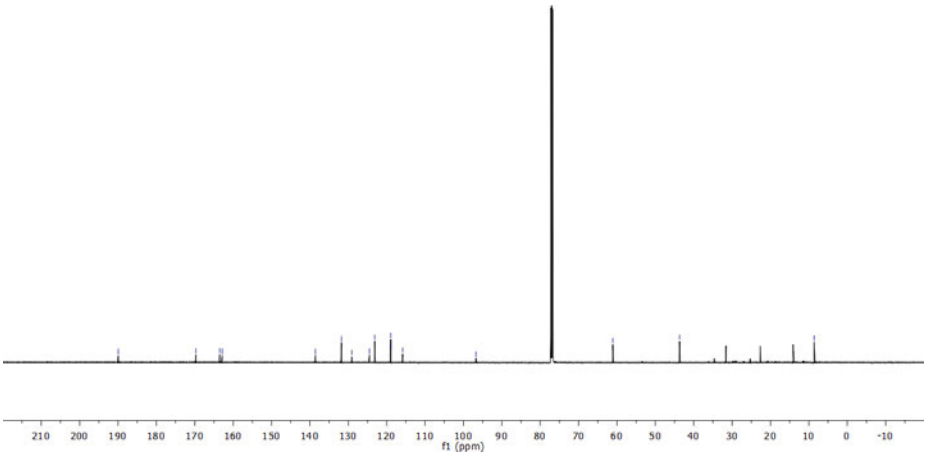

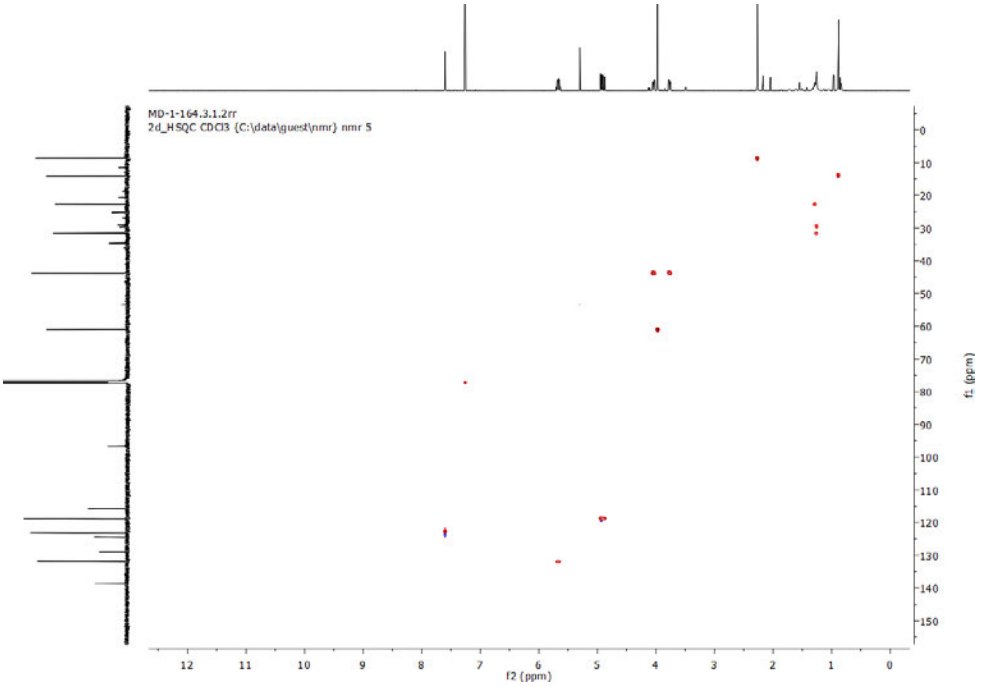

^{1}H NMR (400 MHz, $CDCl_3$) , ^{13}C NMR (100 MHz, $CDCl_3$) and HSQC of S20

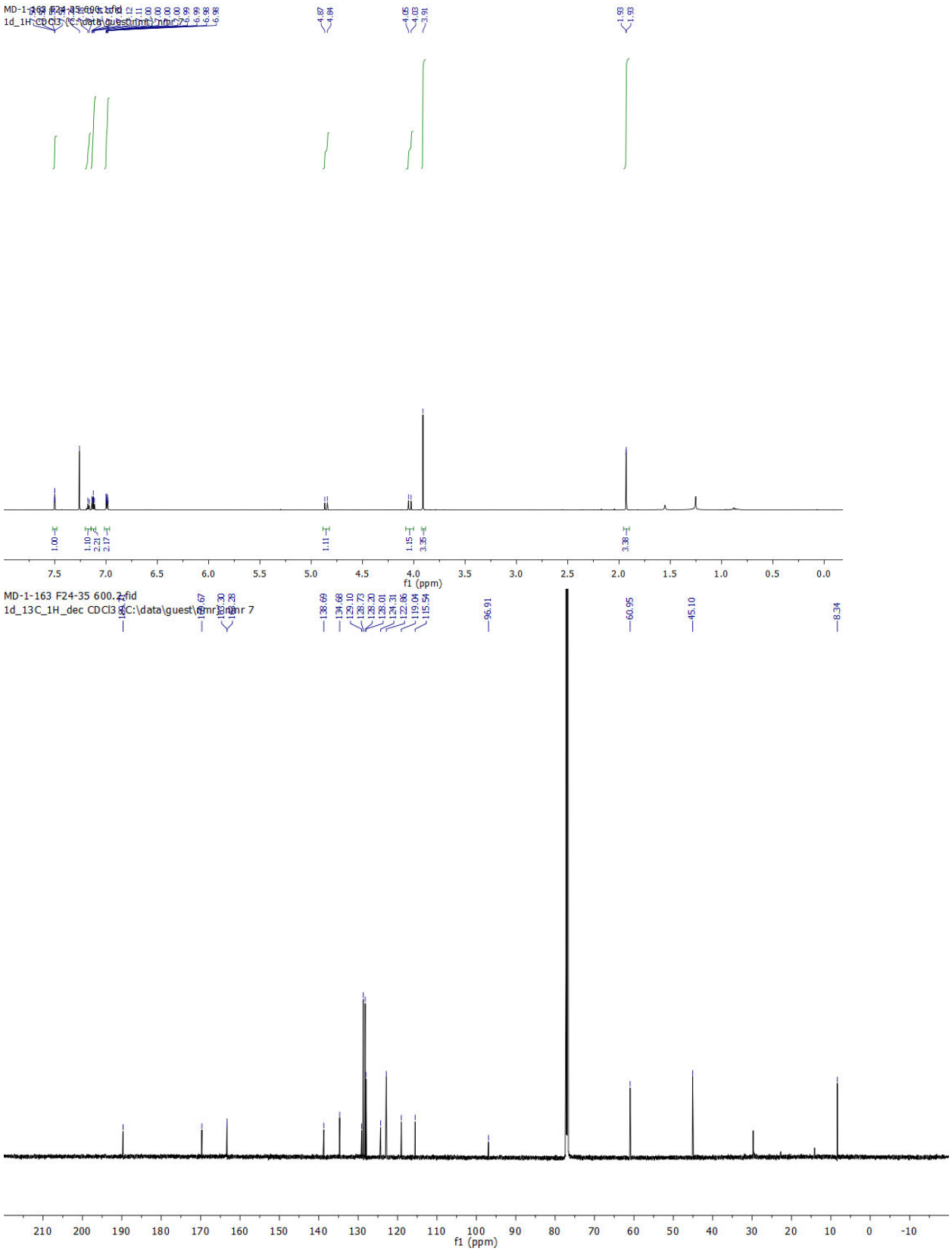
1d_1H_CDCl3 (C:\data\guest\nmr) nmr 7
4.87
4.84
4.05
4.03
3.91
1.93
1.93
1.00
1.10
2.21
2.17
1.11
1.15
3.35
3.38
f1 (ppm)
MD-1-163 F24-35 600.2.fid
1d_13C_1H_dec CDCl3 (C:\data\guest\nmr) nmr 7
138.69
134.68
129.10
128.73
128.20
128.01
124.31
122.86
119.04
115.54
96.91
60.95
45.10
8.34
f1 (ppm)

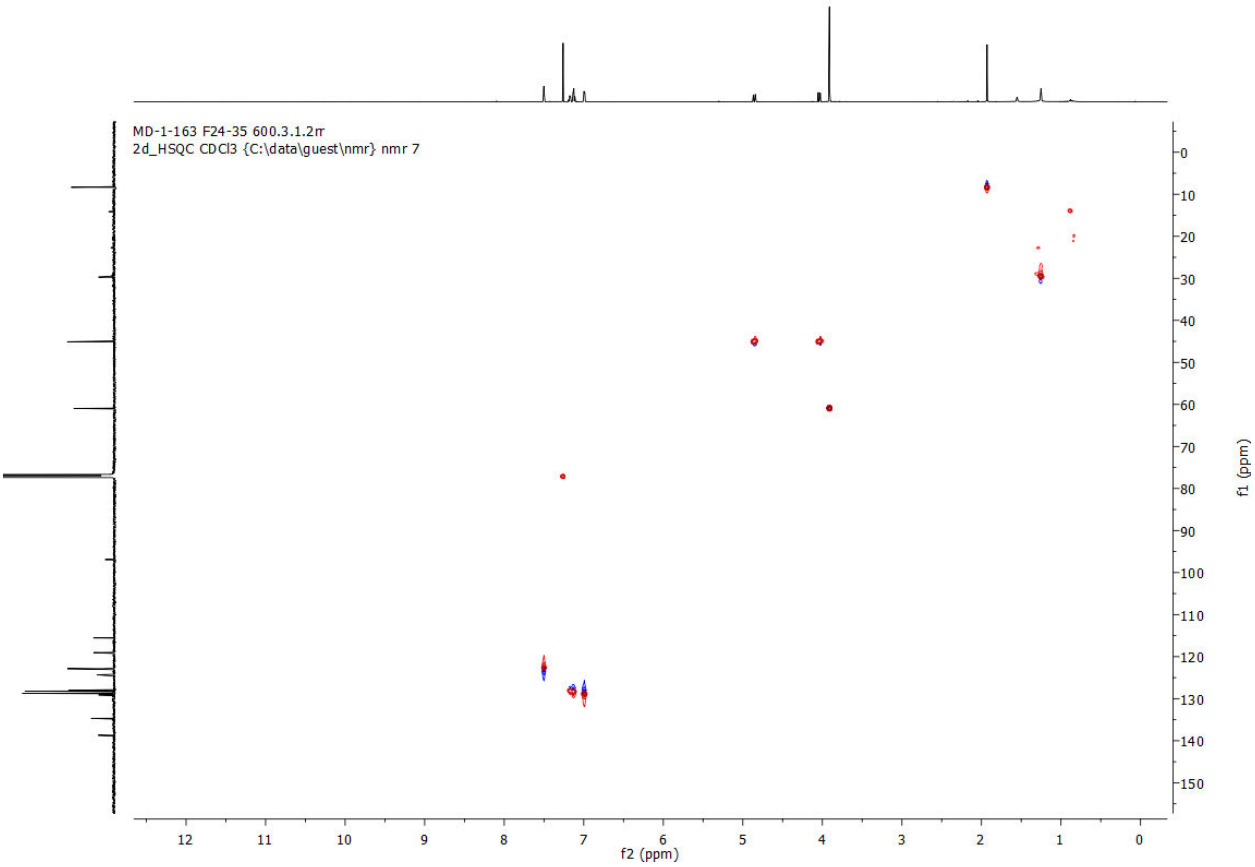

^{1}H NMR (400 MHz, $CDCl_3$) , ^{13}C NMR (100 MHz, $CDCl_3$) and HSQC of S21

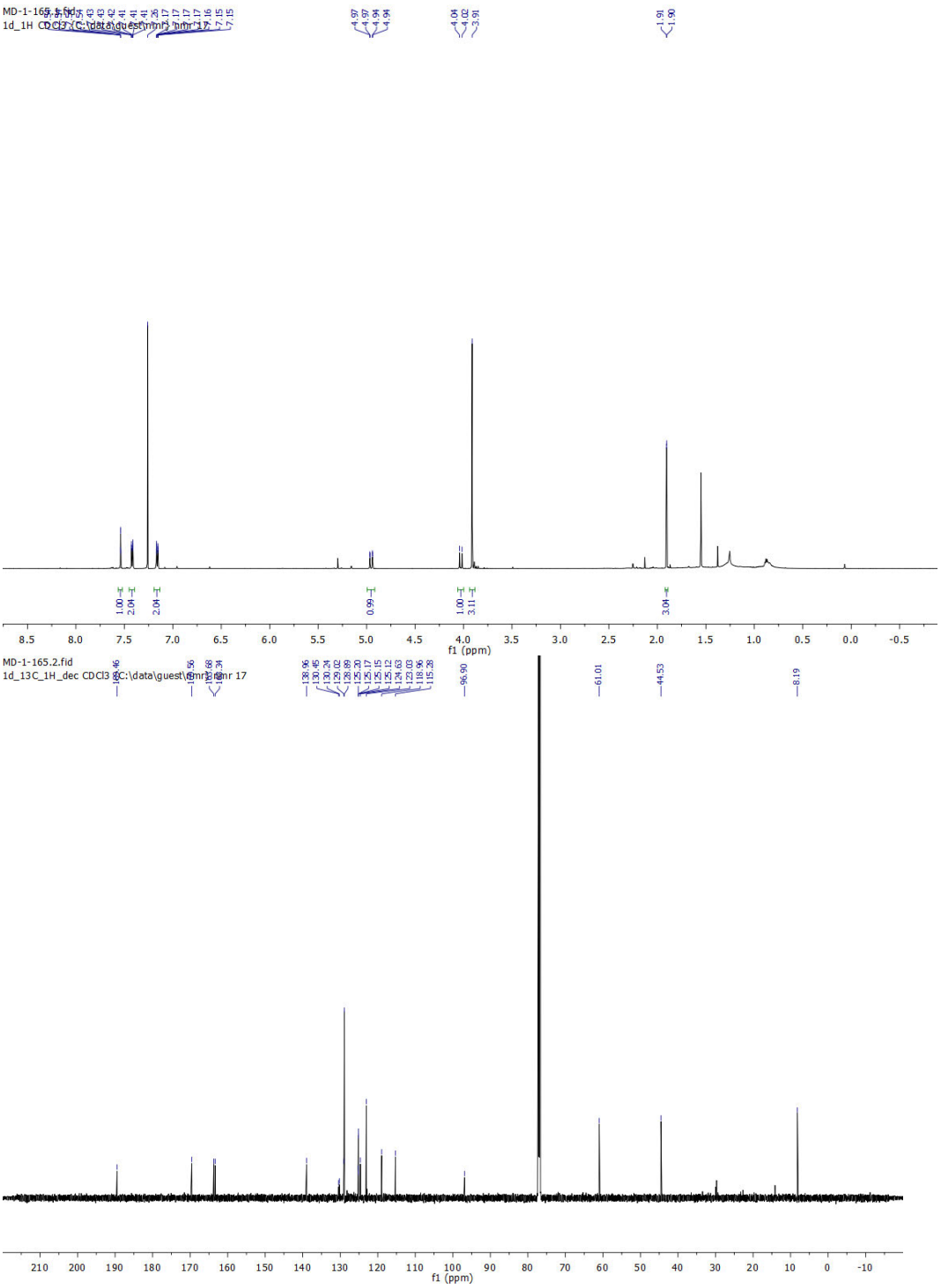

^{1}H NMR (400 MHz, $CDCl_3$) , ^{13}C NMR (100 MHz, $CDCl_3$) and HSQC of S22

MD-2-13 II.1.fid
1d_1H Acetone {C:\data\guest\nmr} nmr 1

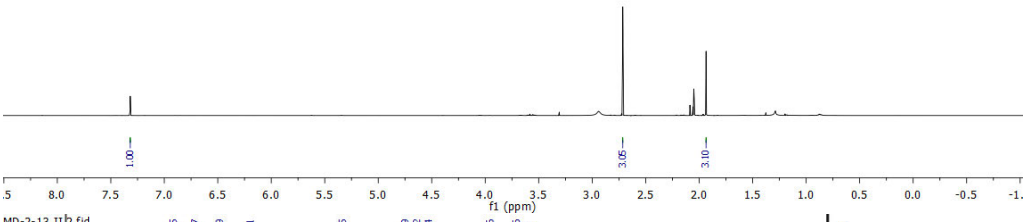

MD-2-13 II.2.fid
1d_13C_1H_dec Acetone {C:\data\guest\nmr} nmr 1

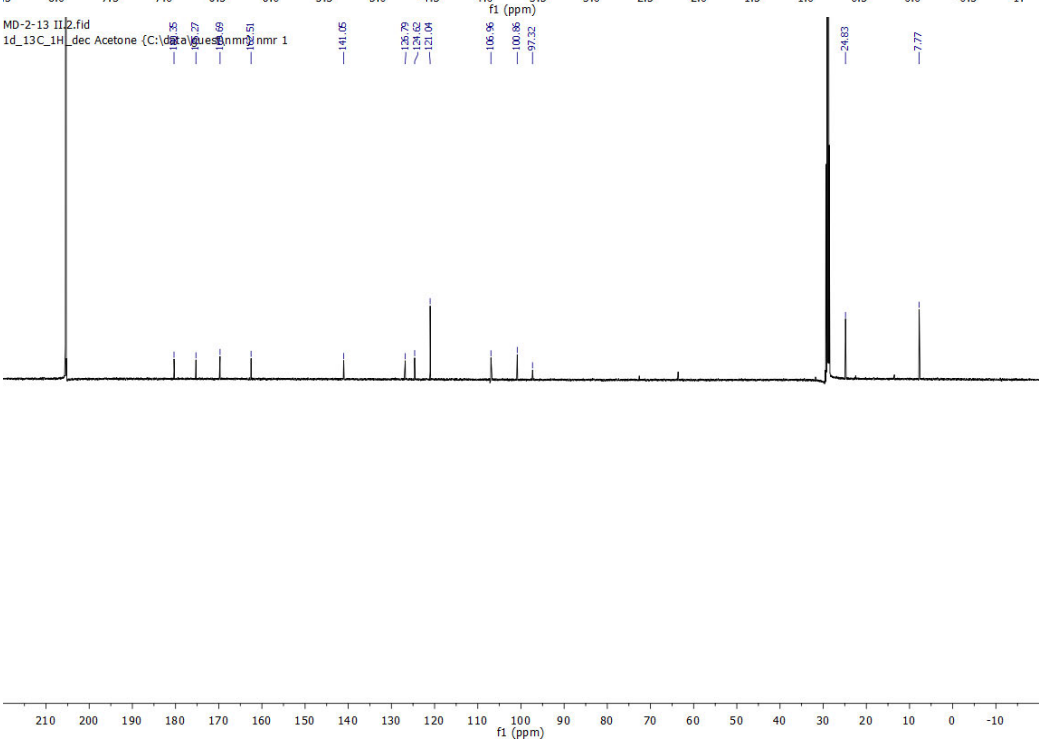

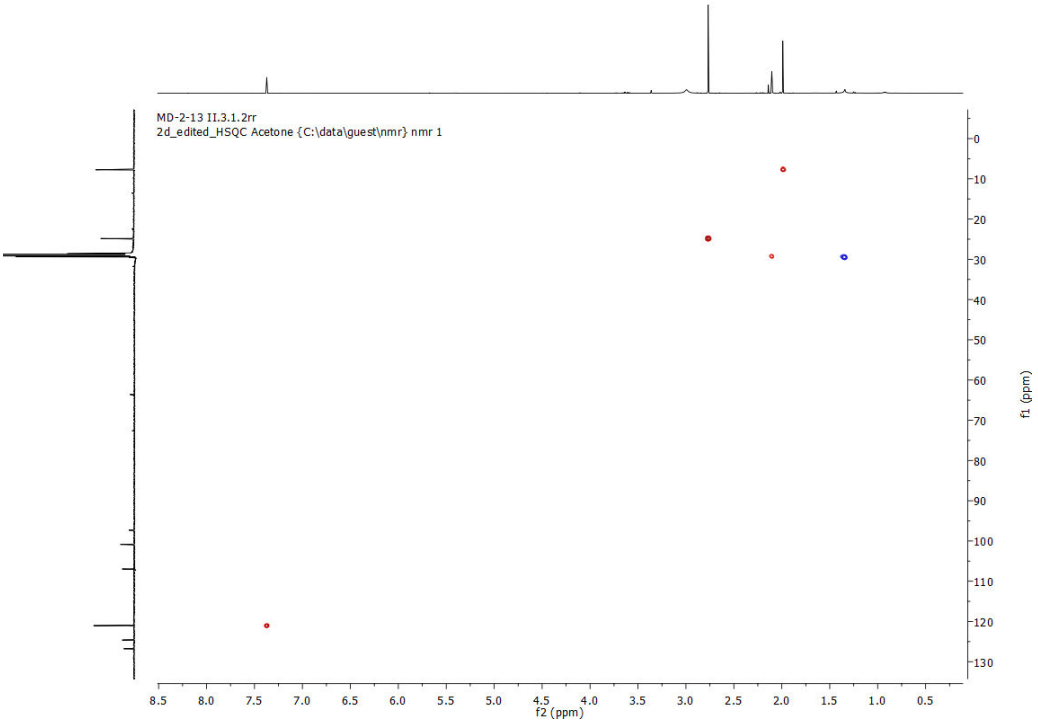

^{1}H NMR (600 MHz, Acetone-D$_6$) , ^{13}C NMR (150 MHz, Acetone-D$_6$) and HSQC of **9**

MD-2-14 II.1.fid
1d_1H MeOD {C:\data\guest\nmr} nmr 2

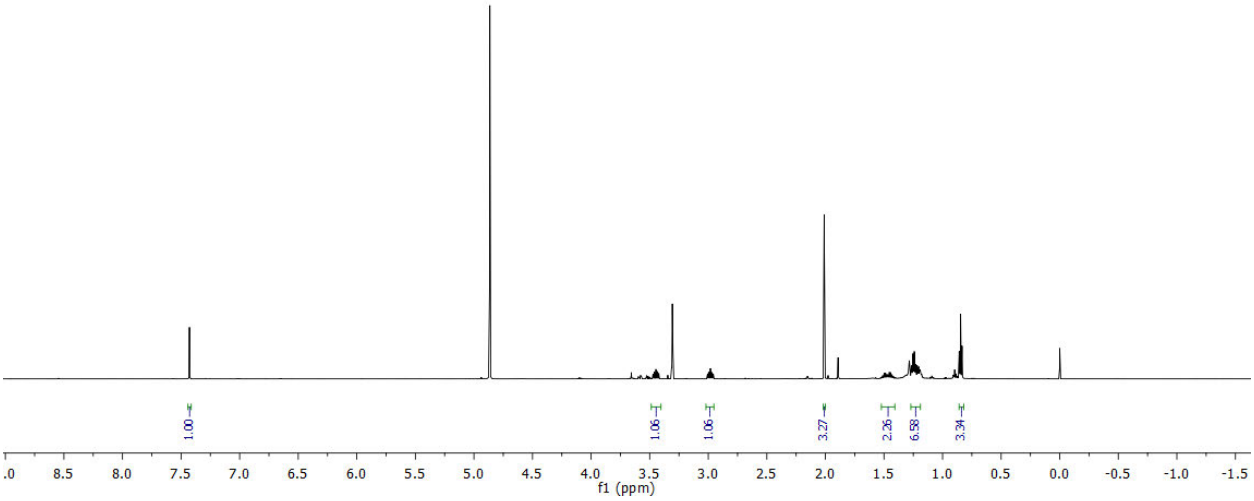

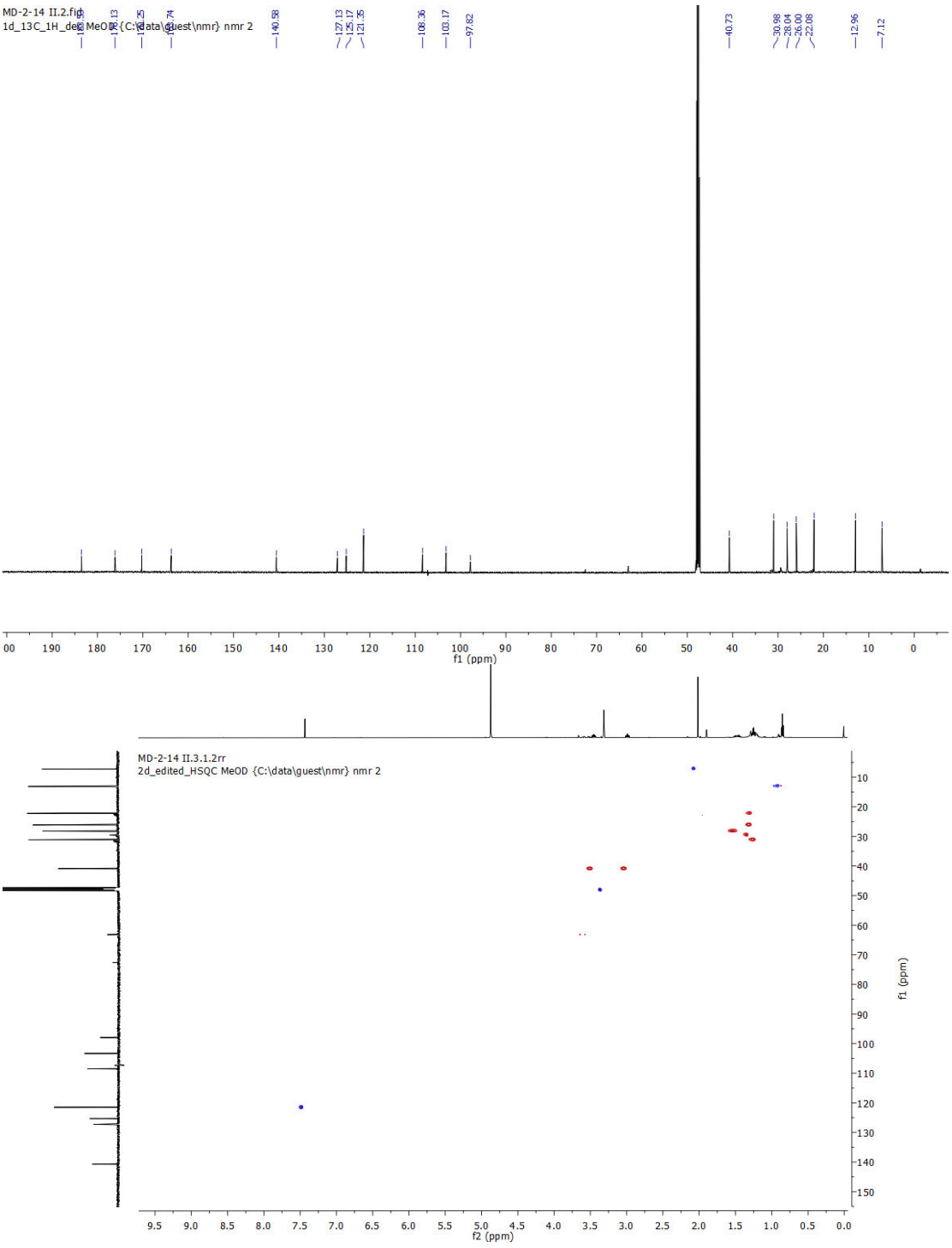

^{1}H NMR (600 MHz, MeOD-d4) , ^{13}C NMR (150 MHz, MeOD – d4) and HSQC of **10**

MD-2-26 II.1.fid
1d_1H Acetone {C:\data\guest\nmr} nmr 8

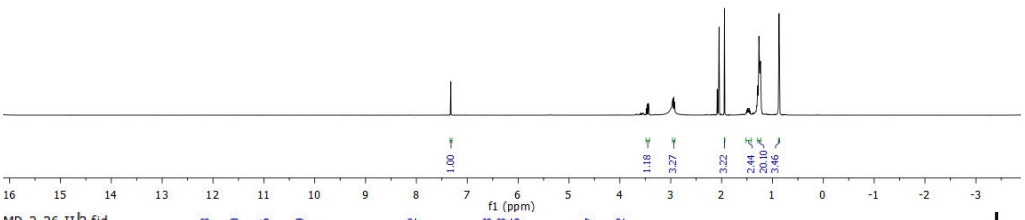

MD-2-26 II.2.fid
1d_13C_1H_dec Acetone {C:\data\guest\nmr} nmr 8

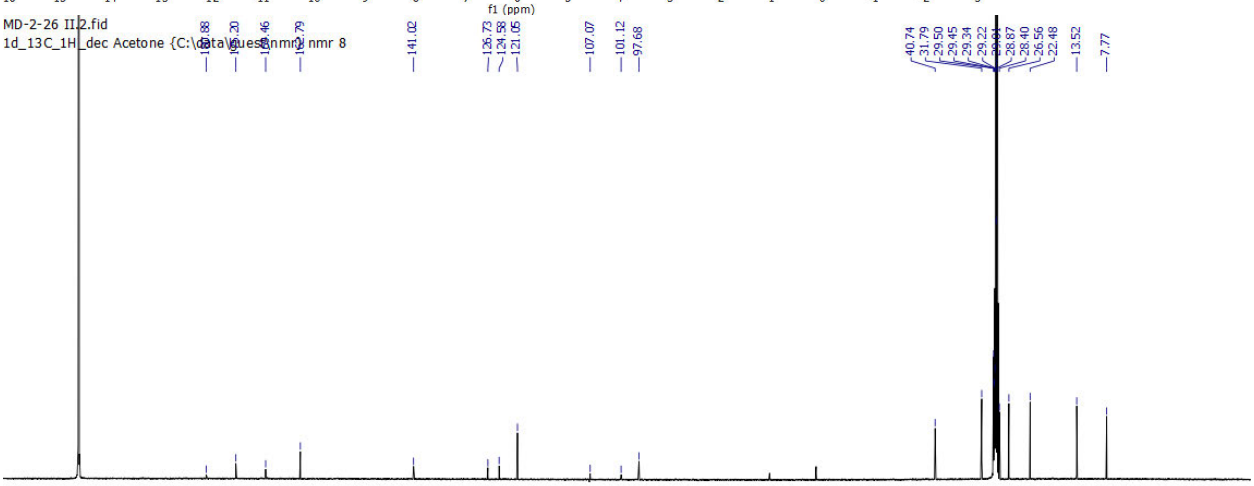

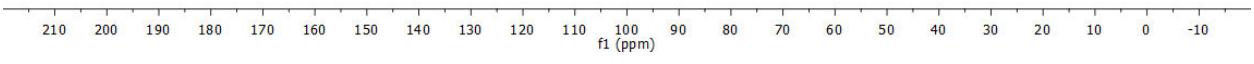

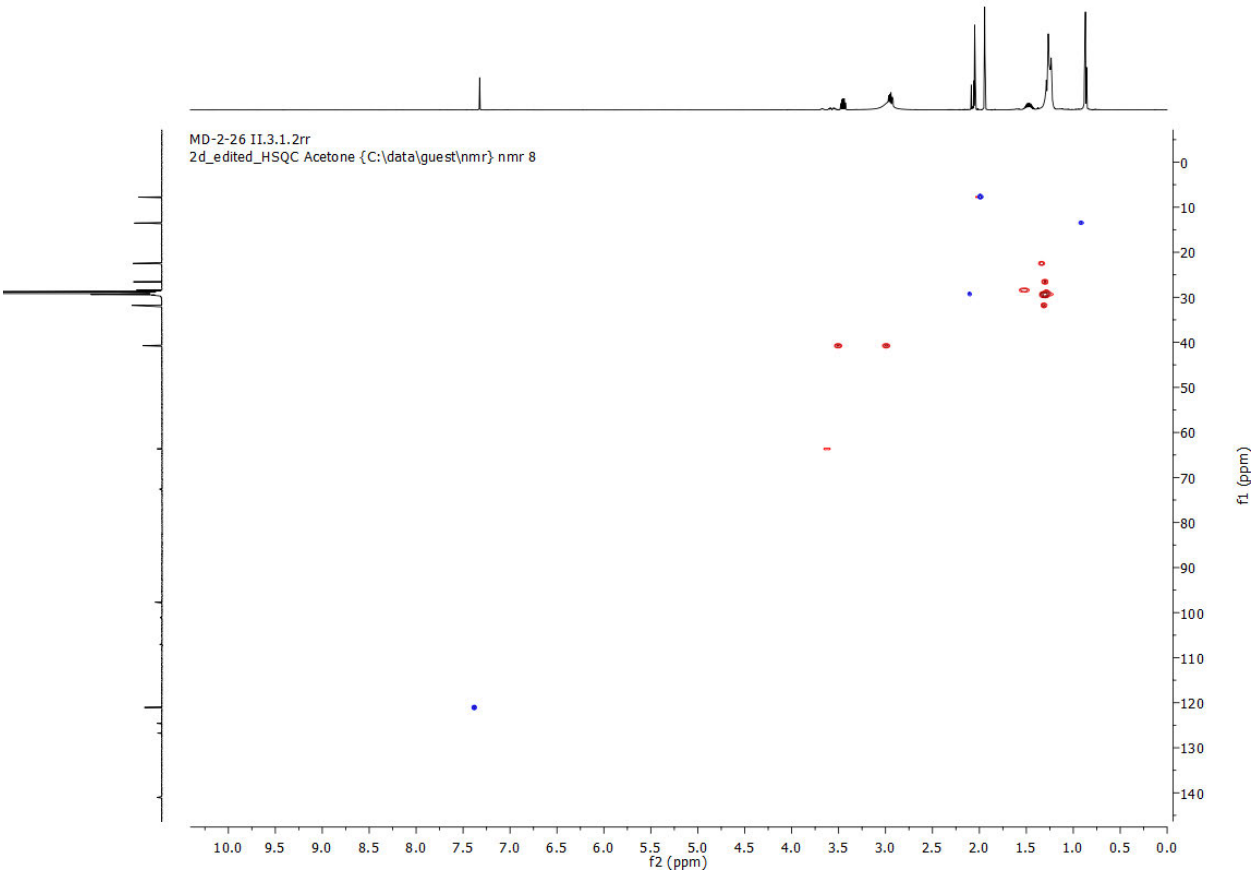

^{1}H NMR (600 MHz, Acetone-D$_6$) , ^{13}C NMR (150 MHz, Acetone-D$_6$) and HSQC of **11**

MD-2-03.1.fid
1d_1H Acetone {C:\data\guest\nmr} nmr 7

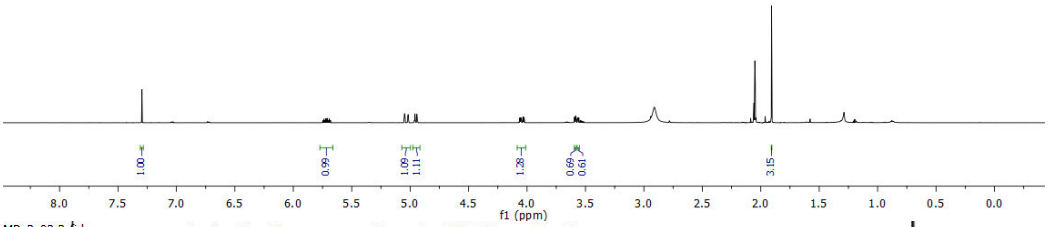

MD-2-03.2.fid
1d_13C_1H_dec Acetone {C:\data\guest\nmr} nmr 7

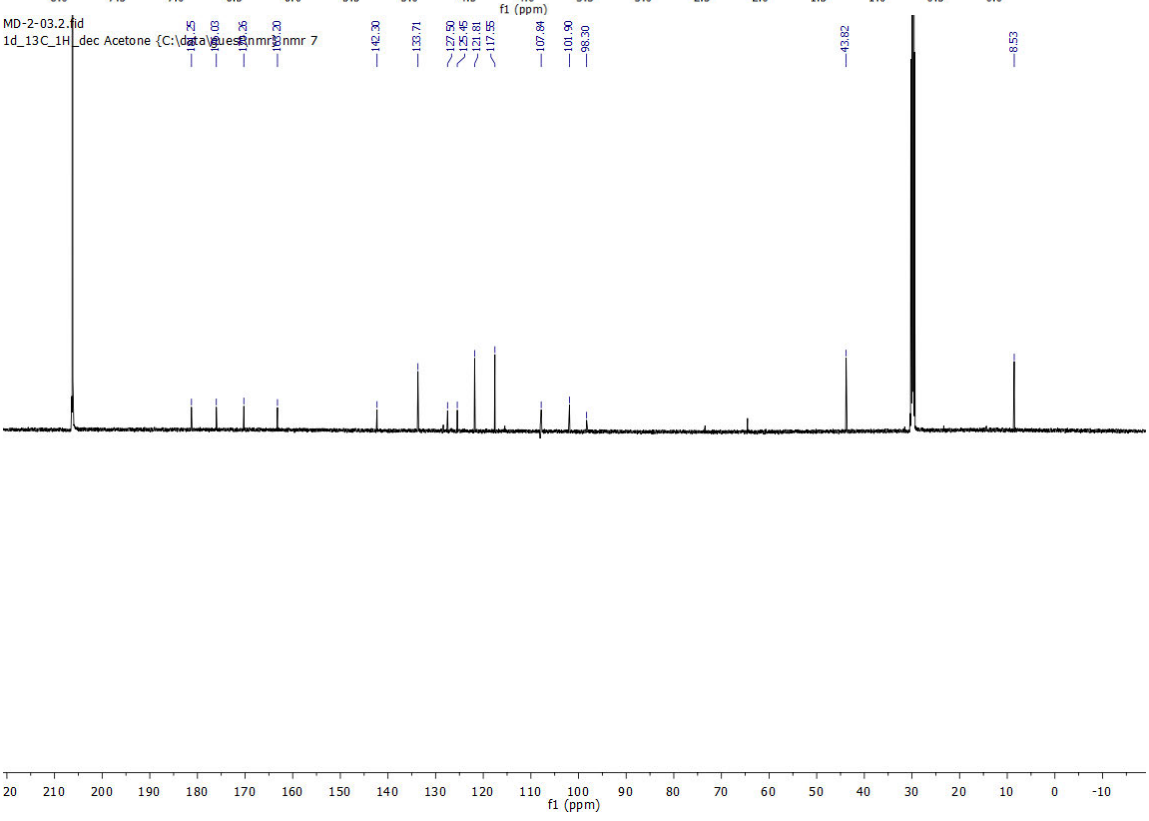

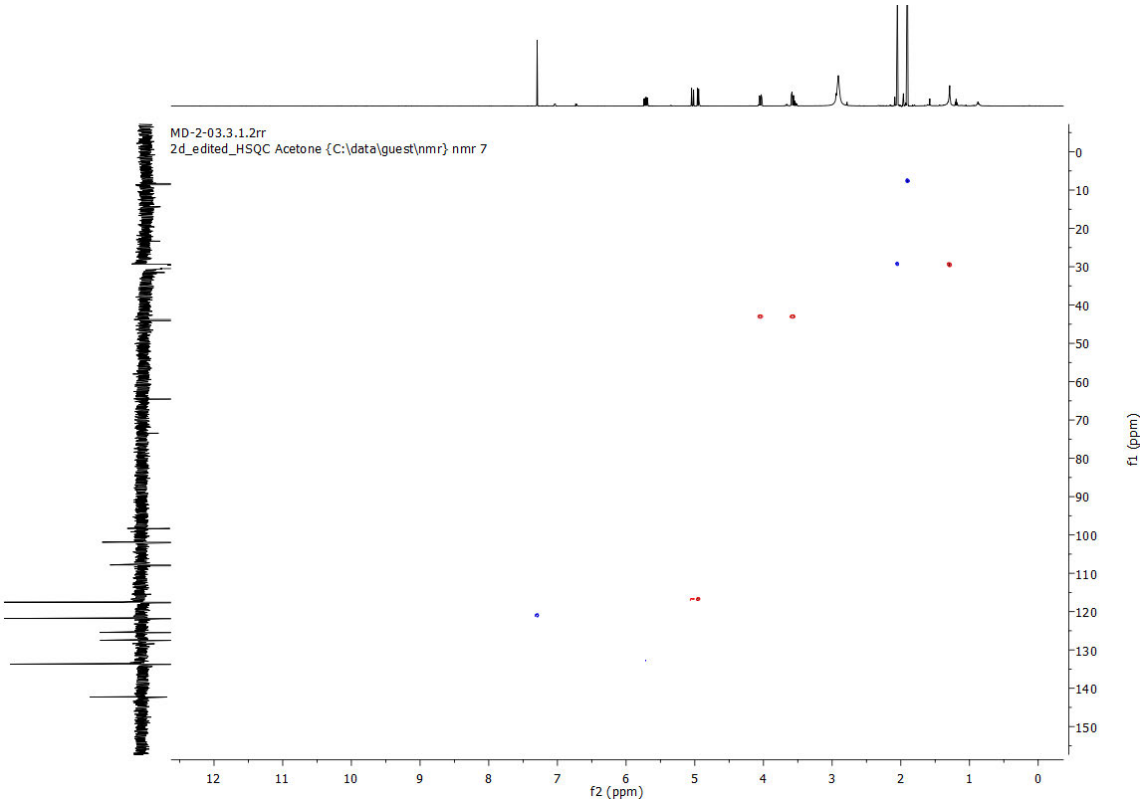

^{1}H NMR (600 MHz, Acetone-D$_6$) , ^{13}C NMR (150 MHz, Acetone-D$_6$) and HSQC of **12**

MD-2-02.1.fid
1d_1H Acetone {C:\data\guest\nmr} nmr 6

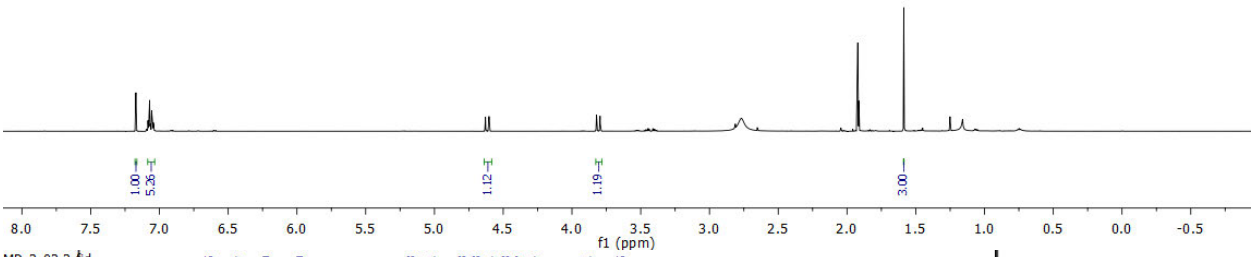

MD-2-02.2.fid
1d_13C_1H_dec Acetone {C:\data\guest\nmr} nmr 6

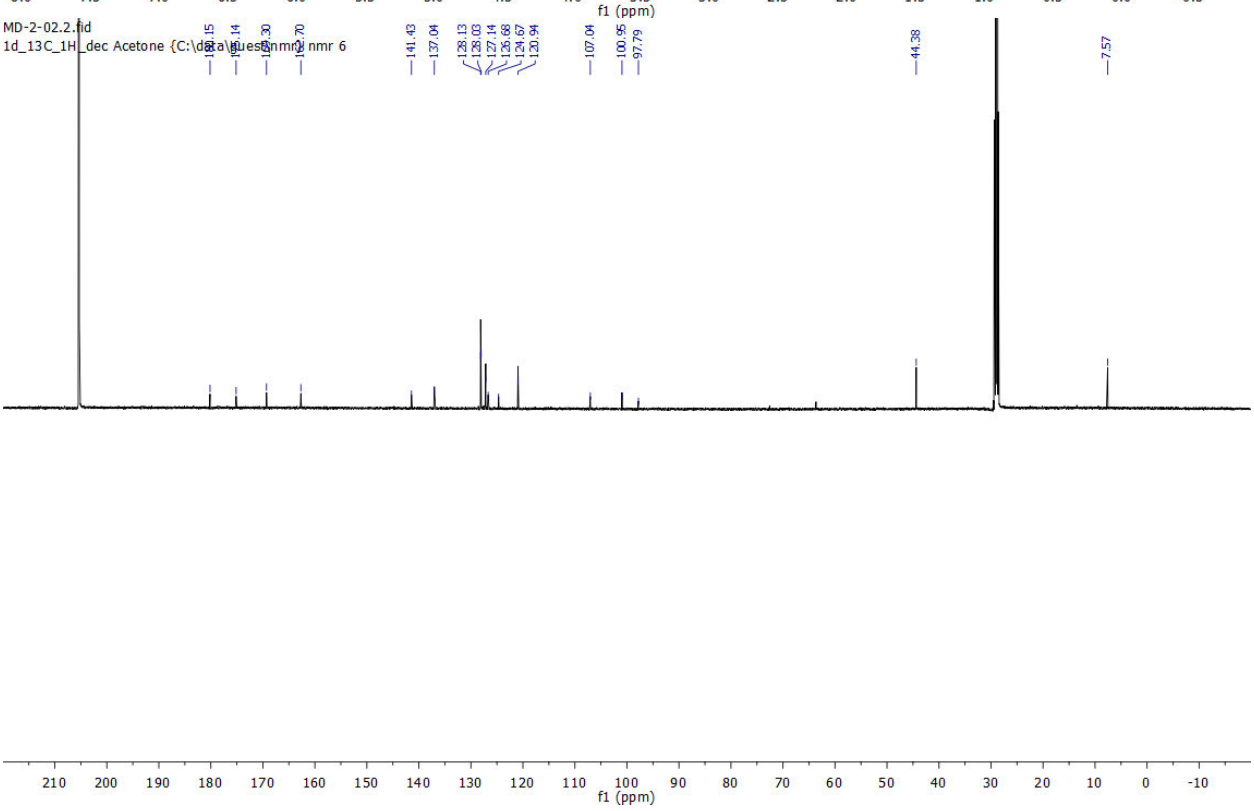

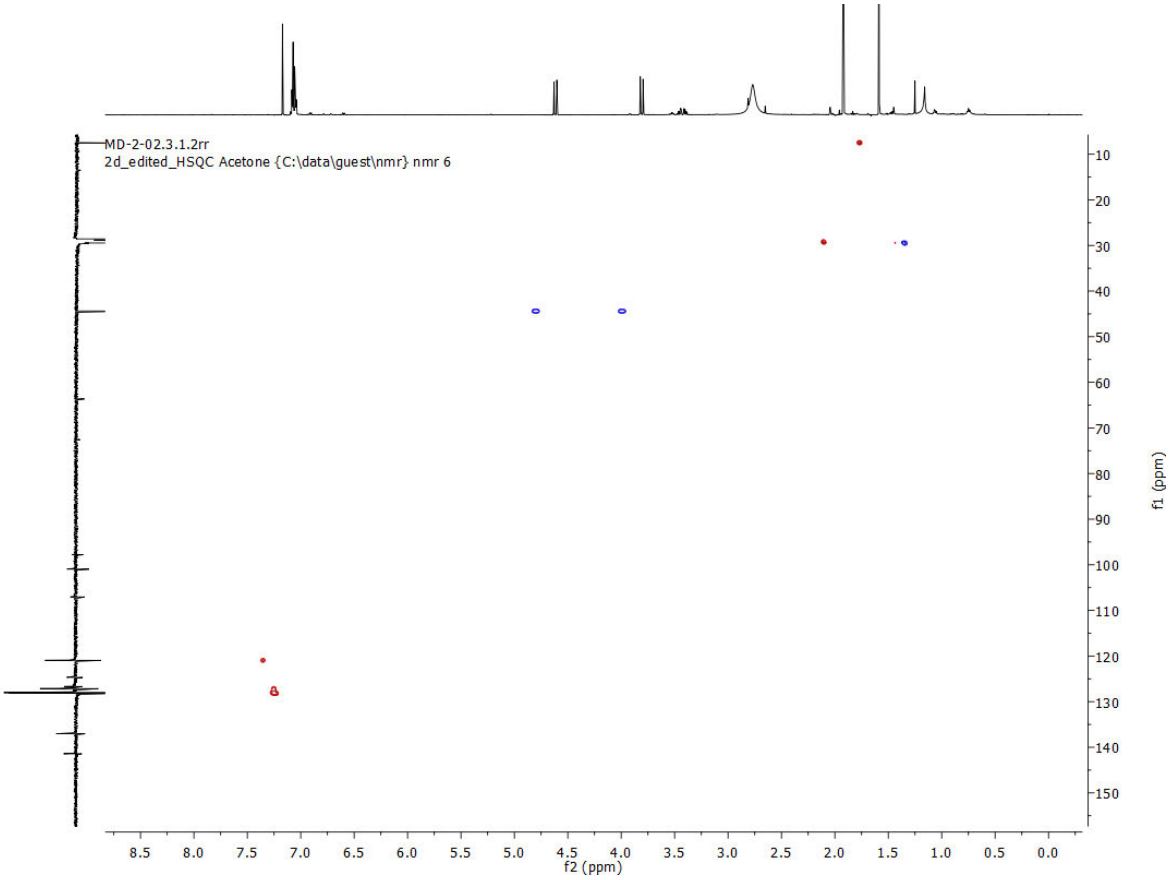

^{1}H NMR (600 MHz, Acetone-D$_6$) , ^{13}C NMR (150 MHz, Acetone-D$_6$) and HSQC of **13**

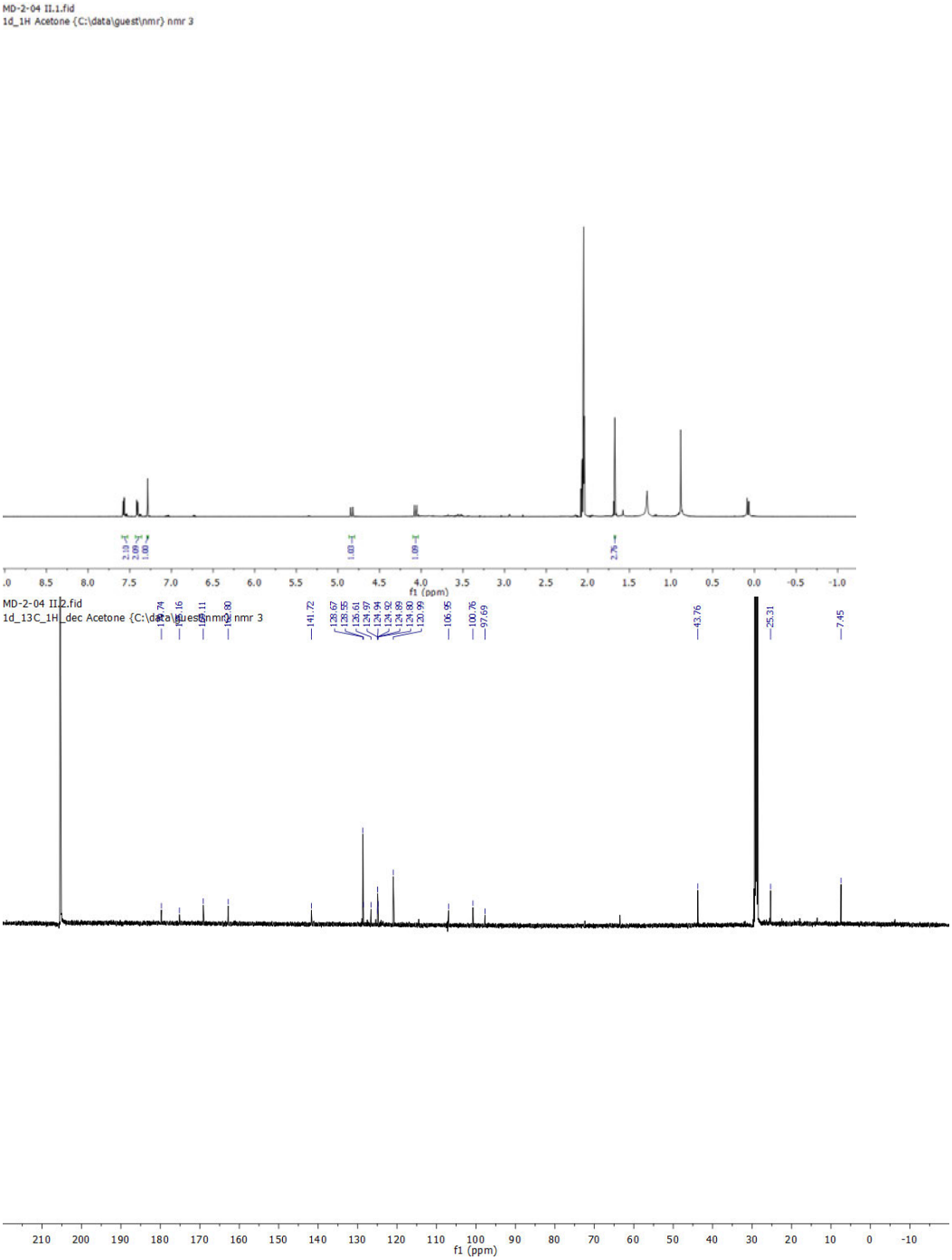
MD-2-04 II.1.fid
1d_1H Acetone {C:\data\guest\nmr} nmr 3
2.19
2.09
1.08
1.03
1.09
2.76
f1 (ppm)
MD-2-04 II2.fid
1d_13C_1H_dec Acetone {C:\data\guest\nmr} nmr 3
174.74
161.16
151.11
140.80
141.72
128.67
128.55
126.61
124.97
124.94
124.92
124.88
124.85
120.99
106.95
100.76
97.69
43.76
25.31
7.45
f1 (ppm)

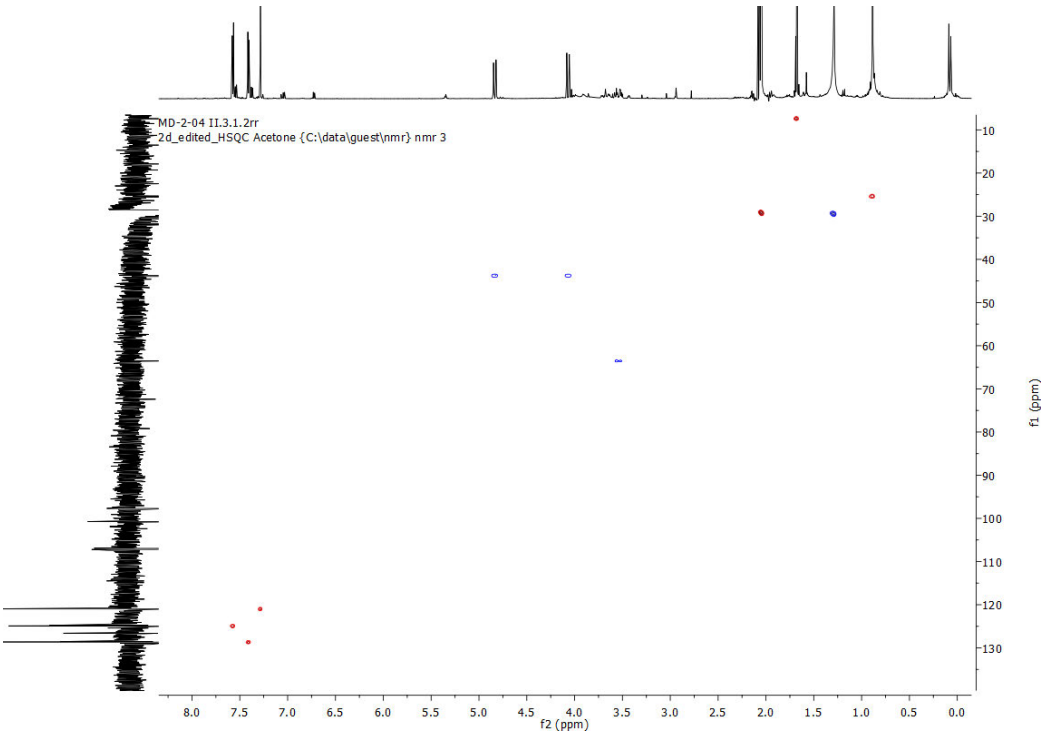

^{1}H NMR (600 MHz, Acetone-D$_6$) , ^{13}C NMR (150 MHz, Acetone-D$_6$) and HSQC of **14**

REFERENCES

(1) Hanwell, M. D.; Curtis, D. E.; Lonie, D. C.; Vandermeersch, T.; Zurek, E.; Hutchison, G. R. Avogadro: An Advanced Semantic Chemical Editor, Visualization, and Analysis Platform. *J. Cheminform.* **2012**, *4* (17), 1–17.

(2) Trott, O.; Olson, A. J. AutoDock Vina: Improving the Speed and Accuracy of Docking with a New Scoring Function, Efficient Optimization, and Multithreading. *J. Comput. Chem.* **2009**, *31* (2), 455–461.

(3) Garrett, M. M.; Huey, R.; Lindstrom, W.; Sanner, M. F.; Belew, R. K.; Goodsell, D. S.; Olson, A. J. AutoDock4 and AutoDockTools4: Automated Docking with Selective Receptor Flexibility. *J. Comput. Chem.* **2009**, *30* (16), 2785–2791.

(4) Jaghoori, M. M.; Bleijlevens, B.; Olabarriaga, S. D. 1001 Ways to Run AutoDock Vina for Virtual Screening. *J. Comput. Aided. Mol. Des.* **2016**, *30* (3), 237–249. h.

Chapter 3: Armeniaspirol analogues disrupt the electrical potential (ΔΨ) of the proton motive force.

3.1 Introduction

The proton motive force is challenging to characterize as it is comprised of at least two important concentration gradients and is often evaluated very differently depending on whether the researchers are biophysicists, biochemists, or biologists. This has led to a wide range of different assays for characterization of PMF disruption[1–5] and has resulted in misused terminology throughout the literature and frequent misinterpretation of data. Our goal was to apply rigorous biochemical characterization of the disruption of the PMF by armeniaspirol analogues. The research presented in this chapter was conducted to further characterize the mechanisms of action of armeniaspirol and how they lead to antibiotic activity. After the publication of our data showing armeniaspirol inhibits ClpXP and ClpYQ leading to cell division arrest, Arisetti *et al*. showed that armeniaspirol can disrupt the proton motive force (PMF) in bacteria through the shuttling of protons across the membrane[6].

Using analogues from the previous study (Chapter 2) allowed us to characterize which component of the PMF was disrupted by armeniaspirols and to evaluate the role of this membrane disruption on antibiotic activity[7]. We conducted two independent assays, a voltage sensitive dye-based assay and checkerboard synergy-based assay that both indicated that armenaispirols disrupt the proton motive force by dissipating the electrical potential (ΔΨ) of the PMF. This is in contrast to Arisetti *et al.* who suggested the armeniaspirols disrupt the proton gradient, ΔpH. Many studies on the PMF point to ionizable groups on small molecules, like the

phenol on armeniaspirol, and conclude that this functionality is responsible for proton transport. However, protected phenol analogues of armeniaspirol still disrupted ΔΨ.

By evaluating sixteen armeniaspirol analogues for antibiotic activity and the ability to disrupt membrane potential, we show that disruption of the ΔΨ by this family of compounds is necessary but not sufficient for potent antibiotic activity. We propose that ClpXP and ClpYQ inhibition in conjunction with disruption of the membrane potential are required for antibiotic activity, akin to the inhibition of translation and membrane disruption of the tetracycline antibiotic chelocardin[8,9]. This is particularly interesting since these two activities likely act synergistically enhancing potency and reducing the susceptibility to emergence of antibiotic resistant mutants. This work provides further understanding of the function and activity of the armeniaspirol analogues and which aspect of the proton motive force is being disrupted in bacterial organisms.

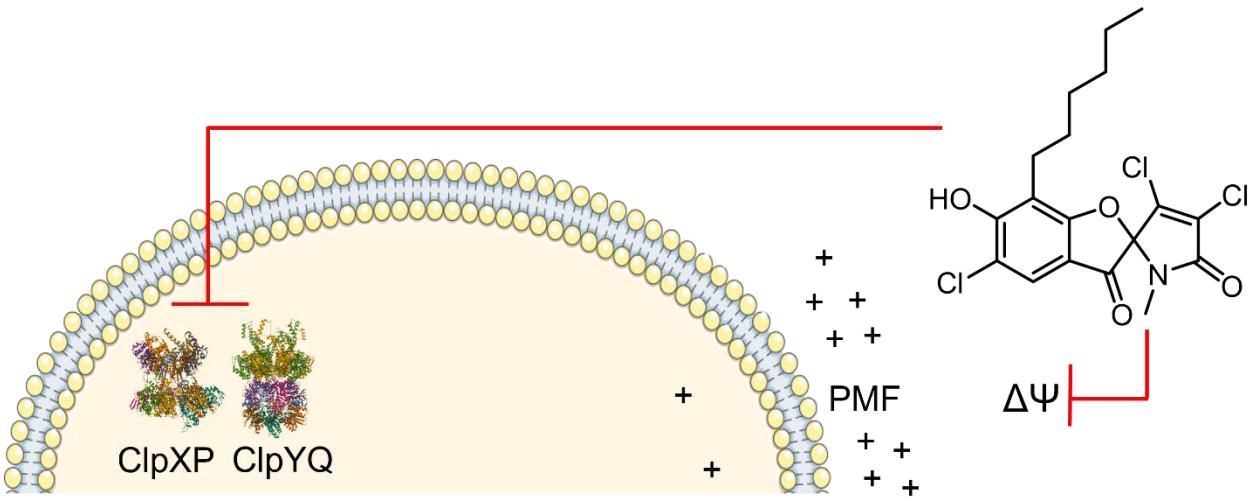

Figure 3.1 Armeniaspirols rely on disruption of both the PMF and intracellular targets for potent antibiotic activity.

3.2 References

1. Chopra, I. Molecular mechanisms involved in the transport of antibiotics into bacteria. *Parasitology* **96**, S25–S44 (**1988**).
2. Benarroch, J. M. & Asally, M. The Microbiologist's Guide to Membrane Potential Dynamics. *Trends Microbiol.* **28**, 304–314 **(2020**).
3. Maloney, P. C., Kashket, E. R. & Wilson, T. H. A protonmotive force drives ATP synthesis in bacteria. *Proc. Natl. Acad. Sci. U. S. A.* **71**, 3896–3900 (**1974**).
4. Valderrama K, Pradel E, Firsov AM, Drobecq H, Bauderlique-le Roy H, Villemagne B, Antonenko YN, Hartkoorn RC. Pyrrolomycins are potent natural protonophores. *Antimicrob. Agents Chemother.* **63**, 1–15 (**2019**).
5. Farha, M. A., Verschoor, C. P., Bowdish, D. & Brown, E. D. Collapsing the proton motive force to identify synergistic combinations against staphylococcus aureus. *Chem. Biol.* **20**, 1168–1178 (**2013**).
6. Arisetti N, Fuchs HLS, Coetzee J, Orozco M, Ruppelt D, Bauer A, Heimann D, Kuhnert E, Bhamidimarri SP, Bafna JA, Hinkelmann B, Eckel K, Sieber SA, Müller PP, Herrmann J, Müller R, Winterhalter M, Steinem C, Brönstrup M. Total synthesis and mechanism of action of the antibiotic armeniaspirol A. *Chem. Sci.* **12**, 16023–16034 (**2021**).
7. Darnowski MG, Lanosky TD, Labana P, Brazeau-Henrie JT, Calvert ND, Dornan MH, Natola C, Paquette AR, Shuhendler AJ, Boddy CN. Armeniaspirol analogues with more potent Gram-positive antibiotic activity show enhanced inhibition of the ATP-dependent proteases ClpXP and ClpYQ. *RSC Med. Chem.* **13**, 436–444 **(2022**).
8. Gray, D. A. & Wenzel, M. Multitarget Approaches against Multiresistant Superbugs. *ACS Infect. Dis.* **6**, 1346 (**2020)**.

9. Stepanek, J. J., Lukežič, T., Teichert, I., Petković, H. & Bandow, J. E. Dual mechanism of action of the atypical tetracycline chelocardin. *Biochim. Biophys. Acta - Proteins Proteomics* **1864**, 645–654 (**2016**).

3.3 Author contributions

I synthesized all the compounds used in this study. In collaboration with Taylor Lanosky, I developed the voltage sensitive dye assays to evaluate membrane disruption by armeniaspirol analogues. We collected all the membrane disruption and checkerboard synergy data together. Andre Paquette helped with data analysis and Christopher Boddy conducted the statistical analyses. I wrote the first draft of the manuscript.

3.4 Copyright

3.5 Armeniaspirol analogues disrupt the electrical potential (ΔΨ) of the proton motive force.

Michael G. Darnowski[#], Taylor D. Lanosky[#], André R. Paquette, Christopher N. Boddy*

Department of Chemistry and Biomolecular Sciences

University of Ottawa

[#] Authors who have equally contributed to work.

Abstract

The armeniaspirol family of natural product antibiotics have been shown to inhibit the ATP-dependent proteases ClpXP and ClpYQ and disrupt membrane potential through shuttling of protons across the membrane. Herein we investigate their ability to disrupt the proton motive force (PMF). We show, using a voltage sensitive dye, that armeniaspirols disrupt the electrical membrane potential (ΔΨ) component of the PMF and not the transmembrane proton gradient (ΔpH). Using checkerboard assays, we confirm this by showing antagonism, with kanamycin, an antibiotic that required ΔΨ for penetration. By evaluating the antibiotic activity and disruption of the PMF by fourteen armeniaspirol analogs, we find that disruption of the PMF is necessary but not sufficient for antibiotic activity. Analogues that are potent disruptors of the PMF without possessing the ability to inhibit ClpXP and ClpYQ are not potent antibiotics. Thus we propose

that the armeniaspirols utilize a dual mechanism of action where they disrupt PMF and inhibit the ATP-dependent proteases ClpXP and ClpYQ. This type of dual mechanism has been observed in other natural product-based antibiotics, most notably chelocardin.

The armeniaspirol family of antibiotics are mixed polyketide non-ribosomal peptide natural products produced by the bacteria *Streptomyces armeniacus*[1–4]. They show potent antibiotic activity against Gram-positive pathogens such as methicillin-resistant *Staphylococcus aureus* (MRSA). Using a combination of chemoproteomics and *in vitro* biochemistry, armeniaspirol was shown to inhibit the AAA+ (ATPases Associated with diverse cellular Activities) bacterial proteases ClpYQ and ClpXP in the Gram-positive bacteria *Bacillus subtilis*, causing cell division arrest[5]. In addition, armeniaspirol has been reported to be a potent membrane depolarizing agent based on data from assays using voltage sensitive dyes in Gram-positive and -negative bacteria, ion conductance assays across a planar lipid bilayer, and pH-sensitive dyes encapsulated in unilamellar vesicles[6]. In this study we investigate disruption of the membrane potential by armeniaspirol and analogues thereof to refine our understanding of the mechanism of action of this class of compounds.

The proton motive force (PMF) in bacteria powers ATP synthesis and secondary active transport[7]. It consists of two components: the transmembrane electrical potential ($\Delta\Psi$) and the transmembrane proton gradient (ΔpH)[8]. Proton pumps, primarily in the electron transport chain, generate the PMF. Because the bacterial cytosolic pH is kept constant, to maintain the PMF over a range of external pHs, $\Delta\Psi$ can vary through the activity of cation-proton antiports[7] and metabolic proton consumption[9]. Thus $\Delta\Psi$ and ΔpH work together to maintain the PMF.

Fluorescence assays based on the voltage sensitive dye $DiSC_3(5)$ can effectively distinguish between agents that disrupt ΔpH or ΔΨ of the PMF[10]. When bacteria are treated with the cationic $DiSC_3(5)$ dye, it accumulates within the membrane where its fluorescence is quenched. When the ΔΨ portion of the PMF is dissipated, the cationic dye is released into the media resulting in an increase in fluorescence. When the ΔpH is dissipated, the cell compensates by increasing ΔΨ and thus maintaining a constant PMF. This further concentrates $DiSC_3(5)$ within the membrane causing additional self quenching and an overall decrease in fluorescence.

Herein we show that the armeniaspirol family of natural products dissipate the ΔΨ of MRSA rather than shuttle protons across the membrane to dissipate ΔpH, as has been proposed[6]. Consistent with this observation, armeniaspirol has antagonistic activity when used with antibiotics that require ΔΨ for uptake and activity. Armeniaspirol analogues with the phenol protected, the proposed site for proton shuttling, still disrupt membrane potential. By evaluating a number of armeniaspirol analogs[11] (Figure 1), we show that potent disruption of the ΔΨ by this family of compounds is not sufficient for antibiotic activity. We hypothesize that disruption of ΔΨ in conjunction with inhibition of ClpXP and ClpYQ activity contributes to the overall mechanism of action of these compounds.

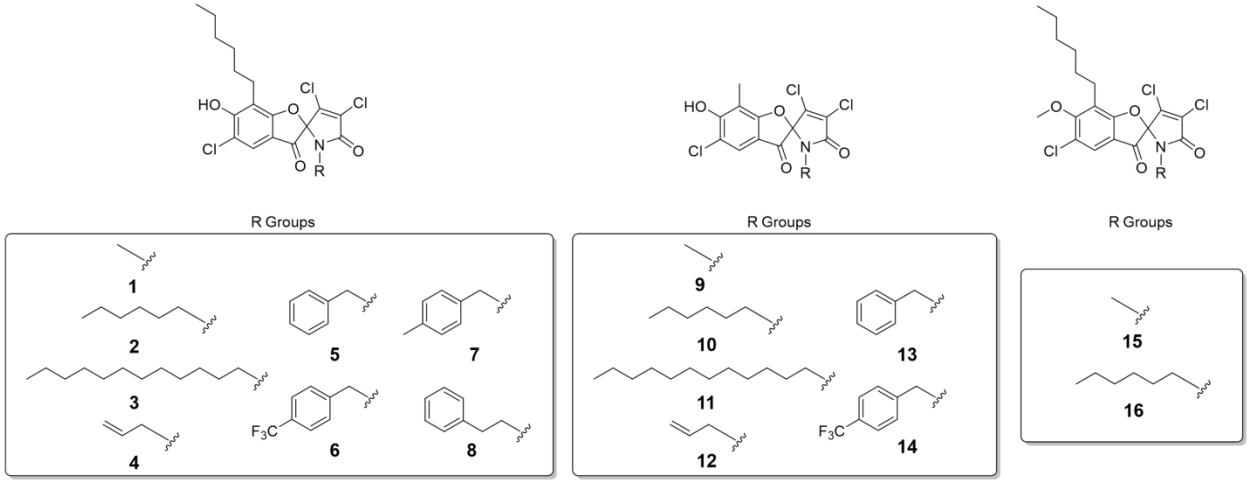

Figure 1. The structure of the armeniaspirol analogues investigated in this study.

Excellent recent work by Arisetti and coworkers has shown that armeniaspirols disrupt the PMF[6]. They conclude that armeniaspirol is a protonophore, a class of molecules that can shuttle protons across the membrane, disrupting the transmembrane proton gradient ΔpH. Consistent with this hypothesis, modification of the phenol and carbonyl of armeniaspirol led to compounds that did not disrupt the PMF, suggesting that deprotonation/protonation of the phenol, whose pKa was sufficiently lowered by electron withdrawing *p*-carbonyl substitution, was required for proton transfer across the membrane.

To evaluate if armeniaspirols were disrupting the PMF via dissipation of ΔΨ or the proton gradient ΔpH, we performed assays with the Nerstian voltage-dependent fluorescent dye $DiSC_3(5)$[12]. Valinomycin, a potent alkali cation transporter that selectively disrupts ΔΨ, leads to an increase in fluorescence when added to $DISC_3(5)$-treated MRSA USA300 (Figure 2a)[10,13]. Like valinomycin, chloro-armeniaspirol, **1**, also showed a significant increase in fluorescence. Treatment with nigericin, which disrupts ΔpH, led to a decrease in fluorescence (Figure 2a)[10]. Based on these data, we suggest that armeniaspirols disrupt ΔΨ rather than ΔpH.

A number of antibiotics rely on either ΔΨ or ΔpH to cross bacterial cell membranes and act on their intracellular targets[14]. For example, aminoglycosides, like kanamycin, require ΔΨ for cell penetration in both Gram-positive bacteria like *S. aureus* and Gram-negatives such as *Escherichia coli*[15]. If **1** is disrupting ΔΨ, then it should act antagonistically when co-administered with kanamycin, reducing the potency of kanamycin. We thus evaluated synergy between potent armeniaspirol analogues **1**, **2,** and **7** and kanamycin in *E. coli ΔtolC*. From checkerboard assays, the fractional inhibitory concentration (FIC) index for **1**, **2**, and **7** with

kanamycin was > 4 (Figure 2b). FICs > 4 are antagonistic[16], further supporting the disruption of ΔΨ by armeniaspirols.

Tetracycline accumulation in *E. coli* is dependent on ΔpH[17]. A checkerboard assay of **1** with tetracycline in *E. coli Δtolc* shows no interaction (FIC = 0.656, Figure 2b). If armeniaspirols were disrupting ΔpH, then they should be antagonistic with tetracycline (FIC > 4). Our data is thus inconsistent with disruption of ΔpH by armeniaspirols. Disruption of ΔΨ is expected to result in no interaction (FIC =0.5 - 4) or a synergistic interaction (FIC < 0.5) between armeniaspirol and tetracycline[18]. Our data is thus consistent with disruption of ΔΨ[19]. We conclude that **1** is dissipating ΔΨ, not ΔpH.

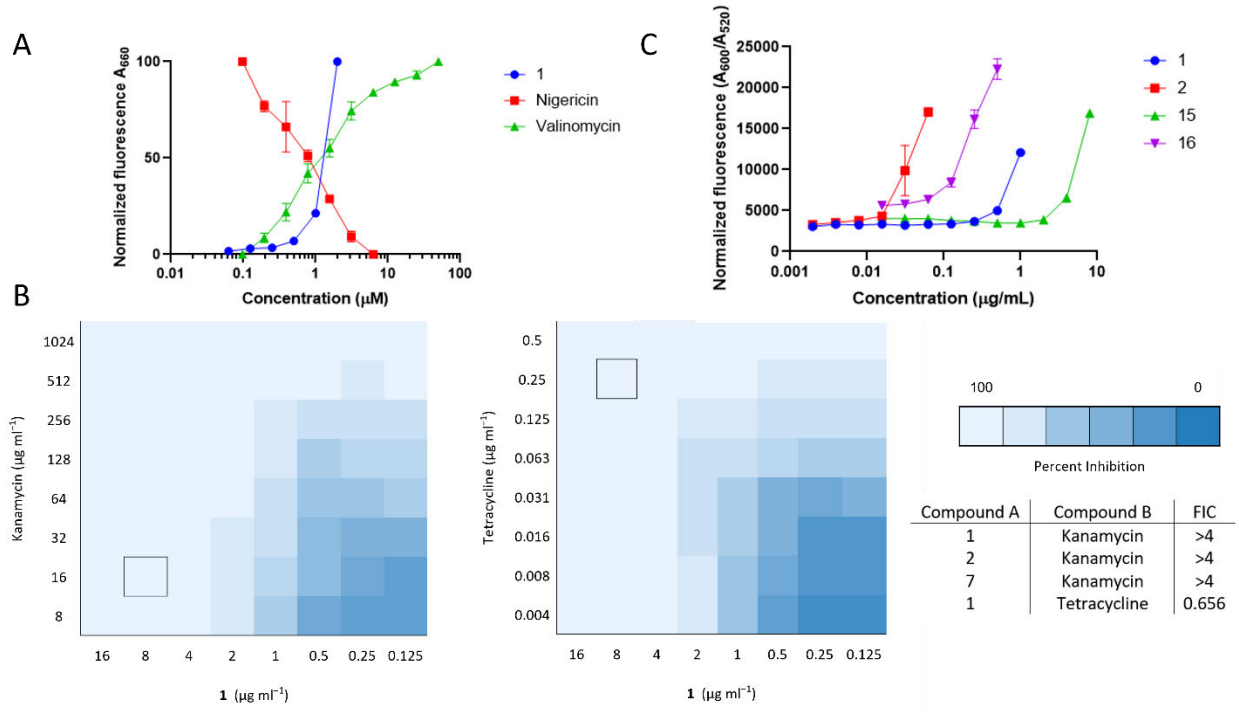

Figure 2. 1 dissipates ΔΨ, not ΔpH. **A** Normalized fluorescence response of MRSA USA300 loaded with the voltage sensitive dye $DiSC_3(5)$ following treatment with **1**, valinomycin, and nigericin. **B** Checkerboard assays showing antagonism of **1** with aminoglycoside kanamycin and

no interaction of **1** and tetracycline in *E. coli ΔtolC*. MICs of **1**, kanamycin, and tetracycline alone are 8 μg ml^{-1}, 16 μg ml^{-1}, and 0.25 μg ml^{-1}, respectively in *E. coli ΔtolC* (MICs are shown as the boxed square on checkerboard asssay). FIC indices for **1**, **2**, and **7** with kanamycin and **1** with tetracycline are reported (see Figure S3). **C**. Normalized fluorescence response of MRSA USA300 loaded with the voltage sensitive dye $DiSC_3(5)$ and treated with **1**, **2**, **15** and **16**. **15** and **16,** which lack an ionizable proton, retained ability to disrupt the PMF.

Because **1** does not disrupt ΔpH, we hypothesized that the phenol, which is proposed to be required for protonophore activity, may not be essential to disrupt the PMF as measured by $DiSC_3(5)$ cell-based assays. We thus synthesized the methyl ether of chloro-armeniaspirol, **15**, and evaluated its ability to disrupt ΔΨ in MRSA. The free phenol, **1,** was a potent disruptor of ΔΨ, with a minimum effective concentration (MEC) of 0.5 μg/mL (Figure 2C). However, **15** was also able to disrupt ΔΨ, though at a higher concentration with an MEC = 4 μg/mL (Figure 2C). **16**, which is the methyl ether of **2**, exhibits more potent disruption of the membrane potential than **1** (Figure 2C). Thus, the phenol does not appear to be required for disruption of the PMF and furthermore is unlikely responsible for shuttling protons across the membrane as previously proposed.

To evaluate if disruption of the PMF is necessary and sufficient for antibiotic activity by the armeniaspirol analogs, we evaluated a panel of 14 armeniaspirol analogs, including **1** and two new analogues where the free phenol was protected as a methyl ether **15** and **16**, removing all ionizable protons. Compounds were evaluated for growth inhibitory activity against MRSA USA300 and the ability to disrupt membrane potential in MRSA USA300, as measured with $DiSC_3(5)$ and $DiOC_2(3)$, two different voltage sensitive dyes (Table 1).

If disruption of the PMF is necessary and sufficient for antibiotic activity, we hypothesized that the MIC and potency of membrane disruption should positively correlate. That is compounds that can disrupt membrane potential at lower concentrations should be antibiotic at lower concentrations. For this analysis we used all the compounds that displayed antibiotic activity (MIC $\leq$ 4 μg/mL) against MRSA USA300. Interestingly, the MEC required to observe membrane depolarization with $DiSC_3(5)$ shows a near-zero correlation with antibiotic activity as measured by MIC (Figure S4). While there is a weak positive correlation between the $DiSC_3(5)$ and MIC data as measured by the Pearson product-moment correlation, it is not statistically significant ($r(10) = 0.41$, $p = 0.23$). Membrane depolarization as measured by the EC_{50} for change in $DiOC_2(3)$ fluorescence shows a similar near-zero correlation (Figure S5) that is not statistically significant ($r(10) = 0.52$, $p = 0.12$). Interestingly, lipophilicity as evaluated by cLogP did not correlate to MIC or $DiOC_2(3)$ EC_{50} values, though did correlate to $DiSC_3(5)$ MEC values (Figures S6-S8).

Table 1. Antibiotic, membrane disruption, and physicochemical properties of analogs.

#	MIC (μg/mL)	$DiSC_3(5)$ MEC (μg/mL)	$DiOC_2(3)$ EC_{50} (μg/mL) ± std error	clogP
1	4	0.5	0.42 ± 0.09	4.94
2	1	0.03125	0.07 ± 0.003	7.39
3	16	>1	> 8	9.23
4	4	0.25	0.23 ± 0.01	5.59
5	1	0.5	0.39 ± 0.03	6.34
6	2	0.125	0.30 ± 0.01	7.24
7	0.5	0.125	0.07 ± 0.002	6.79
8	0.5	0.125	0.12 ± 0.007	6.75
9	>32	8	> 8	2.52
10	4	0.5	0.17 ± 0.01	4.96
11	1	0.25	0.28 ± 0.01	7.99
12	>32	8	> 8	3.16
13	32	4	3.20 ± 0.25	3.91
14	16	2	2.45 ± 0.22	4.81
15	>32	4	2.04 ± 0.09	5.22
16	4	0.125	0.54 ± 0.02	7.67

Careful examination of the analogues shows that compounds with potent ability to disrupt membrane potential do not necessarily possess potent antibiotic activity. For example, **16** is able to disrupt membrane potential at 0.125 μg/mL as measured by the $DiSC_3(5)$ assay but is not antibiotic until 4 μg/mL against MRSA USA300. In contrast other compounds with the ability to disrupt membrane potential at 0.125 μg/mL, such as **7** and **8**, show potent antibiotic activity with MIC of 0.5 μg/mL. It is important to note that none of the non-antibiotic compounds (MIC > 4 μg/mL) are potent disruptors of membrane potential ($DiSC_3(5)$ MEC ≤ 0.5 ug/mL). These data are thus most consistent with the hypothesis that membrane disruption is necessary for antibiotic activity, but it is not sufficient.

Some natural product-based antibiotics have more than one mechanism of action[20]. For example tetracycline binds the 30S ribosomal subunit inhibiting protein synthesis[21] and distorts lipid organization in the membrane in a ribosome binding-independent manner[22]. The tetracycline analogue chelocardin inhibits translation and causes membrane depolarization, with both mechanisms likely contributing to its antibiotic activity[17]. We thus propose that membrane depolarization and inhibition of ClpXP and ClpYQ are both required for antibiotic function of the armeniaspirol family of natural products (Table S3). Consistent with this, **16** is not particularly antibiotic; however, it is a potent depolarizing agent yet shows little to no ability to inhibit ClpYQ activity in an *in vitro* assay or the ability to inhibit ClpXP in a cell-based assay. Intriguingly since ClpXP and ClpYQ are ATP-dependent proteases and membrane potential plays an essential role in ATP synthesis, it is not unreasonable to suggest that reduction of the membrane potential could synergize with inhibition of these cellular targets.

Herein we have used voltage-sensitive dyes to show that the armeniaspirol family of natural products, which are Gram-positive antibiotics, disrupt the proton motive force in MRSA

USA300 by dissipating the transmembrane electrical potential (ΔΨ) rather than the proton gradient (ΔpH). This is supported by armeniaspirol acting antagonistically in checkerboard synergy assays with kanamycin, an antibiotic known to require ΔΨ for penetration in bacteria. Checkerboard assays show armeniaspirol to be indifferent when tested in a synergy assay with tetracycline, an antibiotic known to require the proton gradient to accumulate in Gram-positive bacteria. While all armeniaspirol analogues tested in this study that displayed antibiotic activity were able to disrupt membrane potential, not all compounds that disrupted membrane potential were potent antibiotics. **16** was a potent disruptor of the membrane potential but not an inhibitor of the ATP-dependent proteases ClpXP and ClpYQ, suggesting that both mechanisms may be required for antibiotic activity. This is akin to the inhibition of translation and membrane disruption of chelocardin or the inhibition of dihydrofolate reductase and membrane disruption of SCH-79797[23]. A clear benefit of this dual mechanism is that it should suppress the emergence of armeniaspirol-resistant mutants. This is borne out experimentally since armeniaspirol-resistant MRSA strains cannot be readily generated[2].

References

1. Couturier C, Bauer A, Rey A, Schroif-Dufour C, Broenstrup M. Armeniaspiroles, a new class of antibacterials: Antibacterial activities and total synthesis of 5-chloro-Armeniaspirole A. *Bioorganic Med Chem Lett*. **2012**;22(19):6292-6296.
2. Dufour C, Wink J, Kurz M, Kogler H, Olivan H, Sablé S, Heyse W, Gerlitz M, Toti L, Nußer A, Rey A, Couturier C, Bauer A, Brönstrup M.Isolation and structural elucidation of armeniaspirols A-C: Potent antibiotics against gram-positive pathogens. *Chem - A Eur J*. **2012**;18(50):16123-16128.
3. Fu C, Xie F, Hoffmann J, Wang Q, Bauer A, Brönstrup M, Mahmud T, Müller

Armeniaspirol Antibiotic Biosynthesis: Chlorination and Oxidative Dechlorination Steps Affording Spiro[4.4]non-8-ene. *ChemBioChem*. **2019**;20(6):764-769.

4. Qiao Y, Yan J, Jia J, Xue J, Qu X, Hu Y, Deng Z, Bi H, Zhu D Characterization of the Biosynthetic Gene Cluster for the Antibiotic Armeniaspirols in Streptomyces armeniacus. *J Nat Prod*. **2019**;82:318-323.
5. Labana, P.; Dornan, M. H.; Lafrenière, M.; Czarny, T. L.; Brown, E. D.; Pezacki, J. P.; Boddy, C. N. Armeniaspirols inhibit the AAA+ proteases ClpXP and ClpYQ leading to cell division arrest in Gram-positive bacteria. *Cell Chem Biol*. **2021**;28(12):1703-1715.
6. Arisetti N, Fuchs HLS, Coetzee J, Orozco M, Ruppelt D, Bauer A, Heimann D, Kuhnert E, Bhamidimarri SP, Bafna JA, Hinkelmann B, Eckel K, Sieber SA, Müller PP, Herrmann J, Müller R, Winterhalter M, Steinem C, Brönstrup M. Total synthesis and mechanism of action of the antibiotic armeniaspirol A. *Chem Sci*. **2021**;12(48):16023-16034.
7. Padan E, Bibi E, Ito M, Krulwich TA. Alkaline pH homeostasis in bacteria: New insights. *Biochim Biophys Acta - Biomembr*. **2005**;1717(2):67-88.
8. Benarroch JM, Asally M. The Microbiologist's Guide to Membrane Potential Dynamics. *Trends Microbiol*. **2020;**28(4):304-314.
9. Guan N, Liu L. Microbial response to acid stress: mechanisms and applications. *Appl Microbiol Biotechnol*. **2020**;104(1):51.
10. Farha MA, Verschoor CP, Bowdish D, Brown ED. Collapsing the Proton Motive Force to Identify Synergistic Combinations against Staphylococcus aureus. *Chem Biol*. **2013**;20(9):1168-1178.
11. Darnowski MG, Lanosky TD, Labana P, Brazeau-Henrie JT, Calvert ND, Dornan MH, Natola C, Paquette AR, Shuhendler AJ, Boddy CN. Armeniaspirol analogues with more

potent Gram-positive antibiotic activity show enhanced inhibition of the ATP-dependent proteases ClpXP and ClpYQ. *RSC Med Chem*. **2022**;13(4):436-444.

12. Darnowski MG, Lanosky TD, Paquette AR, Boddy CN. Synthesis of a Constitutional Isomer of Armeniaspirol A, Pseudoarmeniaspirol A, via Lewis Acid-Mediated Rearrangement. *J Org Chem*. **2022**;87(22):15634-15643.
13. King JM, Kulhankova K, Stach CS, Vu BG, Salgado-Pabón W. Phenotypes and Virulence among *Staphylococcus aureus* USA100, USA200, USA300, USA400, and USA600 Clonal Lineages. *mSphere*. **2016**;1(3).
14. Chopra I. Molecular mechanisms involved in the transport of antibiotics into bacteria. *Parasitology*. **1988**;96(S1):S25-S44.
15. Taber HW, Mueller JP, Miller PF, Arrow AS. Bacterial uptake of aminoglycoside antibiotics. *Microbiol Rev*. **1987**;51(4):439.
16. Odds FC. Editorial Synergy, antagonism, and what the chequerboard puts between them. *J Antimicrob Chemother*. **2003**;52:1.
17. Yamaguchi A, Ohmori H, Kaneko-Ohdera M, Nomura T, Sawai T. ΔpH-Dependent accumulation of tetracycline in *Escherichia coli*. *Antimicrob Agents Chemother*. **1991**;35(1):53-56.
18. Meletiadis J, Pournaras S, Roilides E, Walsh TJ. Defining fractional inhibitory concentration index cutoffs for additive interactions based on self-drug additive combinations, Monte Carlo simulation analysis, and *in vitro-in vivo* correlation data for antifungal drug combinations against *Aspergillus fumigatus*. *Antimicrob Agents Chemother*. **2010**;54(2):602-609.
19. Ejim L, Farha MA, Falconer SB, Wildenhain J, Coombes BK, Tyers M, Brown ED,

Wright GD. Combinations of antibiotics and nonantibiotic drugs enhance antimicrobial efficacy. *Nat Chem Biol* ***2011*** *76*. 2011;7(6):348-350.

20. Gray DA, Wenzel M. Multitarget Approaches against Multiresistant Superbugs. *ACS Infect Dis*. **2020**;6(6):1346.

21. Chopra I, Roberts M. Tetracycline Antibiotics: Mode of Action, Applications, Molecular Biology, and Epidemiology of Bacterial Resistance. *Microbiol Mol Biol Rev*. **2001**;65(2):232.

22. Wenzel M, Dekker MP, Wang B, Burggraaf MJ, Bitter W, van Weering JRT, Hamoen LW. A flat embedding method for transmission electron microscopy reveals an unknown mechanism of tetracycline. *Commun Biol*. **2021**;4(1):306.

23. Martin JK 2nd, Sheehan JP, Bratton BP, Moore GM, Mateus A, Li SH, Kim H, Rabinowitz JD, Typas A, Savitski MM, Wilson MZ, Gitai Z. A Dual-Mechanism Antibiotic Kills Gram-Negative Bacteria and Avoids Drug Resistance. *Cell*. **2020**;181(7):1518.

3.6 Supporting Information

Armeniaspirol analogues disrupt the electrical potential (ΔΨ) of the proton motive force.

Michael G. Darnowski[#], Taylor D. Lanosky[#], André R. Paquette, Christopher N. Boddy*

Department of Chemistry and Biomolecular Sciences

University of Ottawa

[#] Authors who have equally contributed to work.

Table of contents

Section 1. General Methods

Minimum inhibitory concentration

Staphylococcus aureus proton motive force assay using $DiSC_3(5)$ fluorescent dye

Staphylococcus aureus protonophore assay to monitor membrane depolarization assay using $DiSC_3(5)$ using Nigericin and Valinomycin.

Staphylococcus aureus proton motive force assay using $DiOC_2(3)$ fluorescent dye

General Synthetic Protocols

Synthesis of **15** and **16**

Section 2. Supplemental figures and tables

Figure S1. (A) $DiSC_3(5)$ assay of methyl chain derivatives (C) $DiSC_3(5)$ assay of Hexyl chain derivatives

Table S1. MIC and EC_{50} of armeniaspirol analogues in $DiSC_3(5)$ assay

Figure S2. (A) $DiOC_2(3)$ assay of methyl chain derivatives (B) $DiOC_2(3)$ assay of hexyl chain derivatives

Table S2. MIC and EC_{50} of armeniaspirol analogues in $DiOC_2(3)$ assay

Figure S3. Heat plot highlighting antibiotic antagonism/synergy against of *E. coli* ΔTolC by **1**, **2**, and **7** with kanamycin and **1** with tetracycline.

Figure S4. Plot of MIC versus $DISC_3(5)$ activity for armeniaspirol analogues with MIC potency ≤ 4 μg/mL

Figure S5. Plot of MIC versus $DIOC_2(3)$ MEC activity for armeniaspirol analogues with MIC potency ≤ 4 μg/mL.

Figure S6. A plot of the lipophilicity (cLogP) versus the antibiotic activity (MIC).

Figure S7. A plot of the lipophilicity (cLogP) versus the minimum effective concentration for disruption of membrane potential as determined by the $DiSC_3(5)$ assay

Figure S8. A plot of the lipophilicity (cLogP) versus the IC_{50} for disruption of membrane potential as determined by the $DiOC_2(3)$ assay

Table S3. Comparing analogues to armeniaspirol for displaying dual mechanism of action. Compounds with improved activity compared to **1** received a check.

Copies of ^{1}H and ^{13}C NMR and EI MS spectra of **15** and **16**

Section 1

Minimum inhibitory concentration and checkerboard assays

Minimum inhibitory concentration (MIC) assays were carried out in Mueller-Hinton broth in 100 µL assays in 96-well plates. Sequential concentrations of compound were pipetted into each column through two-fold serial dilutions. 5 µL of bacterial culture (OD600 0.07-0.1) was inoculated into each well and incubated at 37°C for 16 h. Growth was observed by OD600 readings using a Synergy H4 microplate reader (BioTek). The MIC was determined by the lowest concentration of compound that prevented bacterial growth.

For checkerboard assays, the standard microdilution MIC assay described above was performed with each drug being serially diluted at 8 different concentrations to create an 8 × 8 matrix. At least three replicates were done of each concentration and the means used for calculation. The FIC for each drug combination was determined using the formula shown in Figure S3.

Staphylococcus aureus proton motive force assay using $DiSC_3$ (5) fluorescent dye.

MRSA USA300 cells were grown in 20 mL of LB to an OD_{600} of 0.7. Cells were pelleted at 4,000 rpm for 20 min and resuspended in phosphate-buffered saline (pH 7). The cells were loaded with $DiSC_3(5)$ and allowed to stabilize for 10 minutes while shaking and were protected from light before adding to assay plates containing compounds. The final dye concentration of 1 µM in each well. Compounds were dispensed into 96-well assay plates using sequential two-fold dilutions of concentrations of compound. Fluorescence was monitored at one Synergy H4 microplate reader (BioTek) at an excitation wavelength of 610 nm and an emission wavelength of 660 nm for 10 minutes. Controls for each plate included: no cell control (compounds and dye) to monitor compound quenching fluorescence, no compound control (dye and cells) to monitor fluorescence of non depolarized cells for the baseline reading, no dye control (compounds and

cells) to monitor background fluorescence. Carbonyl cyanide *m*-chlorophenyl hydrazone (CCCP) was run as a positive compound control. All data was run in triplicate. MEC was determined to be at the concentration where an increase in fluorescence by 50% above baseline of untreated cells loaded with dye was observed.

Staphylococcus aureus proton motive force assay to monitor membrane depolarization assay using $DiSC_3(5)$ using Nigericin and Valinomycin.

MRSA USA300 cells were grown in 20 mL of LB to an OD_{600} of 0.7. Cells were pelleted at 4,000 rpm for 20 min and resuspended in 10 mM potassium phosphate, 5 mM MgSO4, and 250 mM sucrose (pH 7.0) to an OD_{600} of 0.085. The cells were loaded with $DiSC_3(5)$ and allowed to stabilize for 10 minutes while shaking and were protected from light before adding to assay plates containing compounds. The final dye concentration was 1 μM in each well. Compounds were dispensed into 96-well assay plates using sequential two-fold dilutions of concentrations of compound. Fluorescence was monitored at one Synergy H4 microplate reader (BioTek) at an excitation wavelength of 610 nm and an emission wavelength of 660 nm for 10 minutes. Controls for each plate included: no cell control (compounds and dye) to monitor compound quenching fluorescence, no compound control (dye and cells) to monitor fluorescence of non depolarized cells, no dye control (compounds and cells) to monitor background fluorescence.

Staphylococcus aureus proton motive force assay using $DiOC_2(3)$ fluorescent dye.

MRSA USA300 cells were grown in 20 mL of LB to an OD600 of 0.7. Cells were pelleted at 4,000 rpm for 20 min and resuspended in phosphate-buffered saline (pH 7). The cells were loaded with $DiOC_2(3)$ and allowed to stabilize for 10 minutes while shaking and were protected from light before adding to assay plates containing compounds. The final dye concentration was 10 μM in each well. Compounds were dispensed into 96-well assay plates using sequential two-

fold dilutions of concentrations of compound. Fluorescence was monitored at one Synergy H4 microplate reader (BioTek) at an excitation wavelength of 485 nm and an emission wavelength of 520 nm as well as an excitation wavelength of 485 nm and an emission wavelength of 600 nm for 10 minutes. The ratio of the fluorescence intensity of A_{600}/A_{520} was plotted. Controls for each plate included: no cell control (compounds and dye) to monitor compound quenching fluorescence, no compound control (dye and cells) to monitor fluorescence of non depolarized cells, no dye control (compounds and cells) to monitor background fluorescence. CCCP was run as a positive compound control. Data was normalized and curves were fit using non-linear regression with 4 parameter fitting.

General Synthetic Protocols

All reagents were purchased from Sigma-Aldrich at the highest available purity and used without further purification. All solvents were purchased from Fisher Scientific and were ACS grade or higher. All reactions were conducted using dry solvents under an argon atmosphere unless otherwise noted. NMR spectroscopy was performed with a Bruker Avance II, operating at 400 MHz for ^{1}H spectra, and 100 MHz for ^{13}C spectra or Bruker Avance III, with cryoprobe operating at 600 MHz for ^{1}H spectra, and 150 MHz for ^{13}C spectra. Structural S5 assignments were made with additional information from gCOSY, gHSQC, and gHMBC experiments. Preparatory TLC was performed using Merck Millipore 20 x 20 cm silica gel 60 F254 plates. High-resolution mass spectroscopy (HRMS) was conducted on a Micromass Q-TOF I for ESI measurements and a Kratos Concept 1S High Resolution Mass Spectrometer for EI measurements (John L. Holmes Mass Spectroscopy Facility)

Synthesis of **15** and **16**

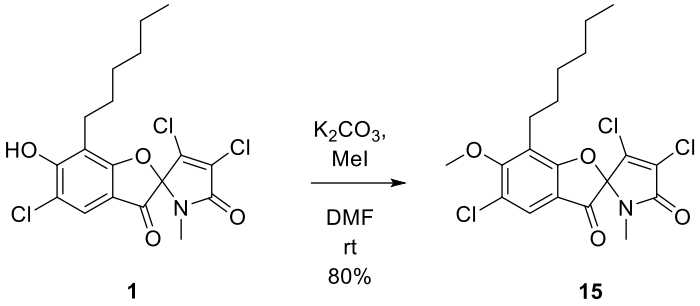

1 (3mg, 0.0076 mmol, 1 equiv) was dissolved in *N*,*N*-dimethyl formamide (DMF) (0.2 M). K_2CO_3 (4.2mg, 0.0225 mmol, 3 equiv) was added and allowed to stir for 15 min. Methyl iodide (2.3 μL, 0.0375 mmol, 5 equiv) was added to the mixture and after 3 h at room temperature, the solution was diluted with ethyl acetate (EtOAc, 10 mL) and washed with a NH_4Cl solution. The aqueous layer was then extracted twice with EtOAc (20 mL). The organic layer was then washed consecutively with brine. The combined EtOAc layers were dried with $MgSO_4$ and concentrated in vacuo. Silica gel chromatography (25 % EtOAc/hexanes) yielded pure **15** (2.6mg, 80%). NMR data were consistent with literature values[1].

^{1}H NMR (400 MHz, $CDCl_3$) δ 7.63 (s, 1H), 4.00 (s, 3H), 2.79 (s, 3H), 2.76 – 2.70 (m, 2H), 1.64 – 1.55 (m, 2H), 1.41 – 1.24 (m, 6H), 0.88 (t, J = 7.0 Hz, 3H).

^{13}C NMR (100 MHz, $CDCl_3$) δ 189.88, 170.33, 163.79, 163.16, 138.24, 129.38, 124.84, 124.33, 123.73, 115.65, 97.05, 61.92, 31.73, 29.46, 29.38, 25.96, 24.00, 22.71, 14.19.

HRMS (ESI): Exact mass calculated for $C_{19}H_{20}Cl_3NNaO_4$ $[M + Na]^+$: 454.0350. Found: 454.0356

HRMS (EI): Exact mass calculated for $C_{19}H_{20}Cl_2NO_4$ $[M\text{-}Cl]^+$: 396.0769 Found 396.0779

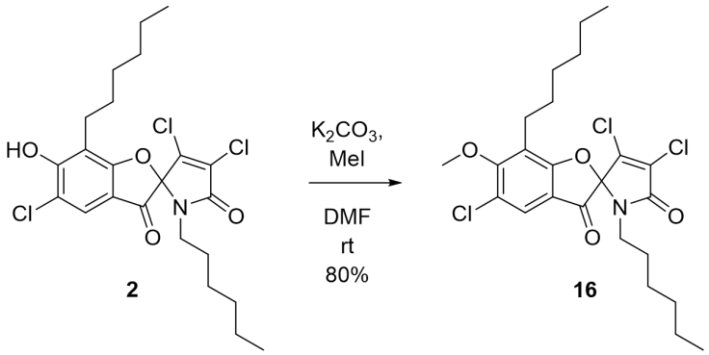

2 (5mg, 0.01 mmol, 1 equiv) was dissolved in DMF (0.2 M). K_2CO_3 (4.2mg, 0.03 mmol, 3 equiv) was added and allowed to stir for 15 min. Methyl iodide (3.7µL, 0.05 mmol, 5 equiv) was added to the mixture and after 3 h at room temperature, the solution was diluted with EtOAc (10 mL) and washed with a NH_4Cl solution. The aqueous layer was then extracted twice with EtOAc (20 mL). The organic layer was then washed consecutively with brine. The combined EtOAc layers were dried with $MgSO_4$ and concentrated in vacuo. Silica gel chromatography (20 % EtOAc/hexanes) yielded pure **16** (4.2mg, 82%). NMR data were consistent with literature values[1].

^{1}H NMR (400 MHz, $CDCl_3$) δ 7.63 (s, 1H), 4.00 (s, 3H), 3.42 (dt, J = 14.5, 7.3 Hz, 1H), 3.00 (dt, J = 14.5, 7.3 Hz, 1H), 2.78 – 2.64 (m, 2H), 1.65 – 1.53 (m, 2H), 1.48 – 1.12 (m, 14H), 0.88 (t, J = 6.9 Hz, 3H), 0.83 (t, J = 6.8 Hz, 3H).

^{13}C NMR (100 MHz, $CDCl_3$) δ 190.25, 170.00, 163.71, 163.46, 138.25, 129.29, 124.75, 124.33, 123.72, 115.84, 97.38, 61.93, 41.67, 31.74, 31.36, 29.54, 29.47, 28.76, 26.47, 24.00, 22.71, 22.56, 14.20, 14.10.

HRMS (ESI): Exact mass calculated for $C_{24}H_{30}Cl_3NNaO_4$ $[M + Na]^+$: 524.1133. Found: 524.1134

HRMS (EI): Exact mass calculated for $C_{24}H_{30}Cl_2NO_4$ $[M-Cl]^+$: 466.1552 Found 466.1554

Section 2

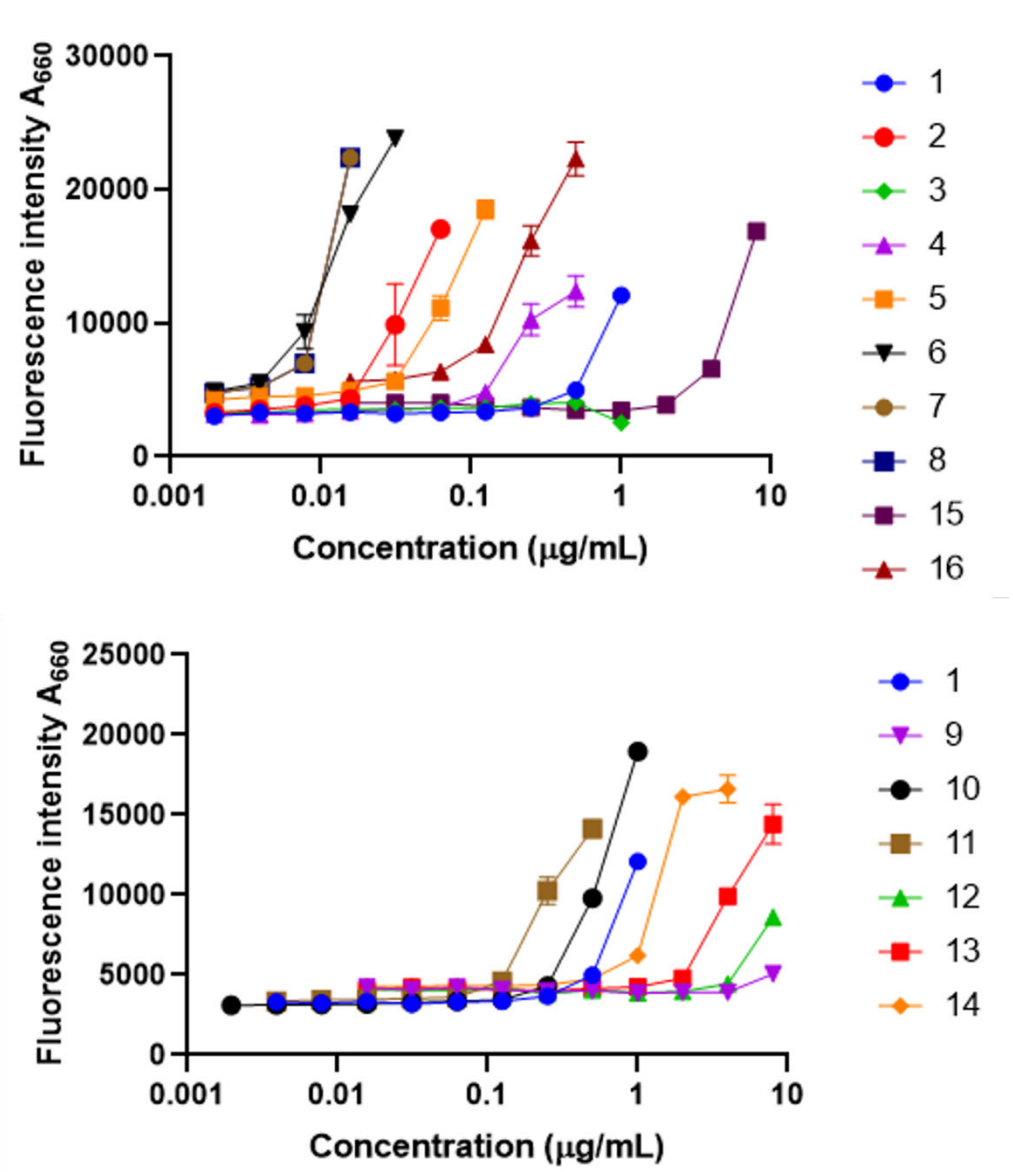

Figure S1. (A) $DiSC_3(5)$ assay of methyl chain derivatives (B) $DiSC_3(5)$ assay of Hexyl chain derivatives

Table S1. MIC and MEC of armeniaspirol analogues in $DiSC_3(5)$ assay

Compound	MIC	MEC $DiSC_3(5)$
1	4	0.5
2	1	0.03125
3	16	>1
4	4	0.25
5	1	0.5
6	2	0.125
7	0.5	0.125
8	0.5	0.125
9	>32	8
10	4	0.5
11	1	0.25
12	>32	8
13	32	4
14	16	2
15	>32	4
16	4	0.125

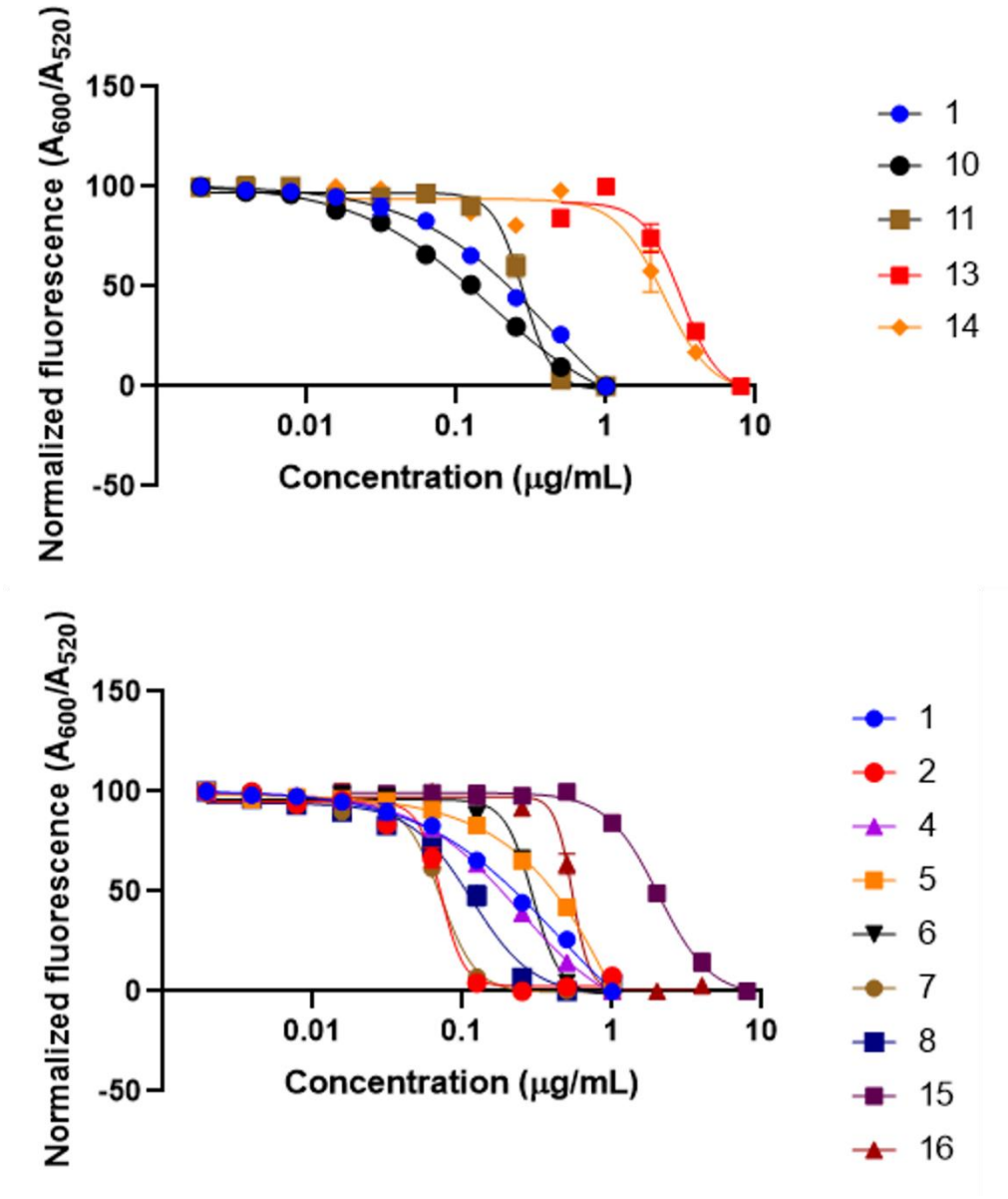

Figure S2. (A) $DiOC_2(3)$ assay of methyl chain derivatives (B) $DiOC_2(3)$ assay of hexyl chain derivatives

Table S2. MIC and EC_{50} of armeniaspirol analogues in $DiOC_2(3)$ assay

Compound	MIC (μg/ml)	$DiOC_2(3)$ EC_{50} (μg/ml)
1	4	0.42 ± 0.09
2	1	0.07 ± 0.003
3	16	> 8
4	4	0.23 ± 0.01
5	1	0.39 ± 0.03
6	2	0.30 ± 0.01
7	0.5	0.07 ± 0.002
8	0.5	0.12 ± 0.007
9	>32	> 8
10	4	0.17 ± 0.01
11	1	0.28 ± 0.008
12	>32	> 8
13	32	3.20 ± 0.25
14	16	2.45 ± 0.22
15	>32	2.04 ± 0.09
16	4	0.54 ± 0.02

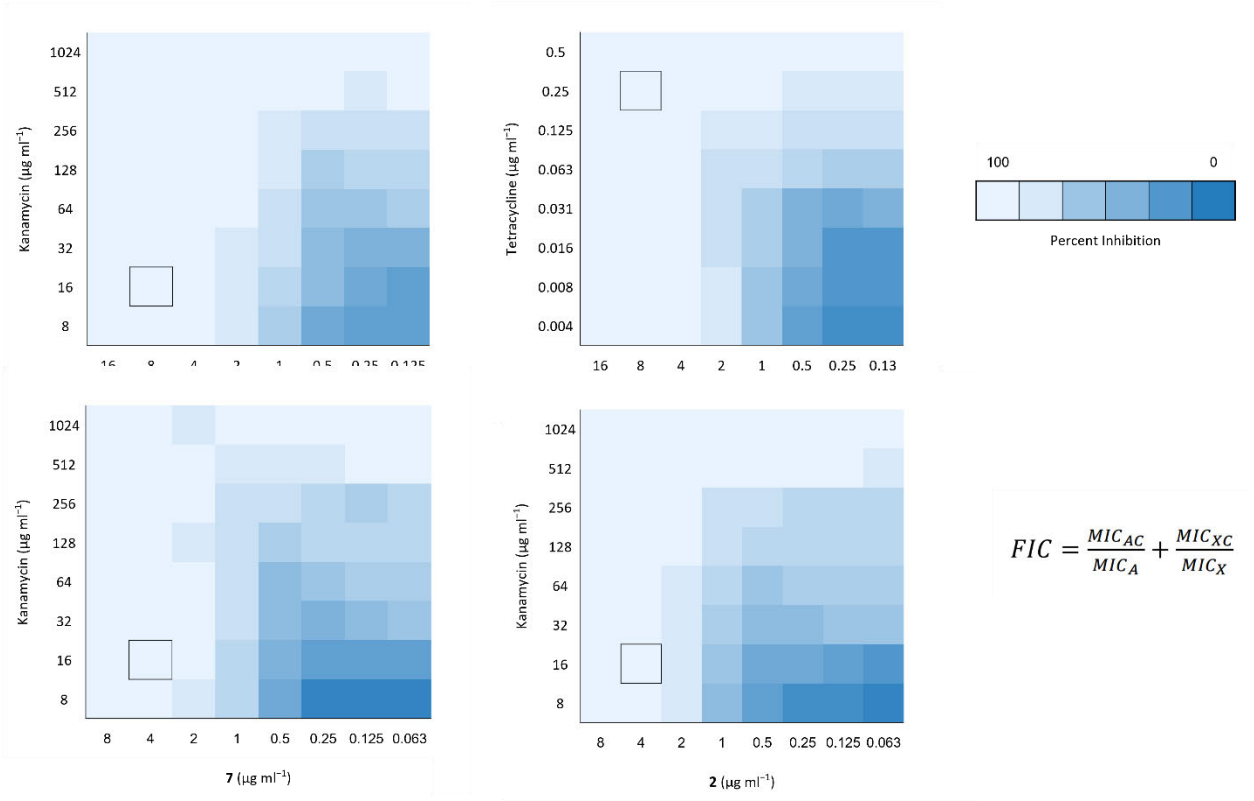

Figure S3. Checkerboard assays showing antibiotic antagonism/synergy in *E. coli ΔtolC* by **1**, **2**, and **7** with kanamycin and tetracycline. MICs of **1**, **2**, **7**, kanamycin and tetracycline alone are 8 μg mL^{-1}, 4 μg mL^{-1}, 4 μg mL^{-1}, 16 μg mL^{-1},0.25 μg mL^{-1} respectively, are highlighted on each plot by the boxed square. The fractional inhibitory concentration (FIC) index was calculated according to the equation above, where MIC_A represents the MIC of **1**,**2** or **7** alone, MIC_{AC} represents the MIC of **1**, **2** or **7** in combination with either tetracycline or kanamycin, MIC_X represents the MIC of tetracycline or kanamycin alone, MIC_{XC} represents the MIC of tetracycline or kanamycin in combination with **1**, **2** or **7**. Synergy is defined as FIC index ≤ 0.5. Antagonism is defined as FIC index ≥ 4.

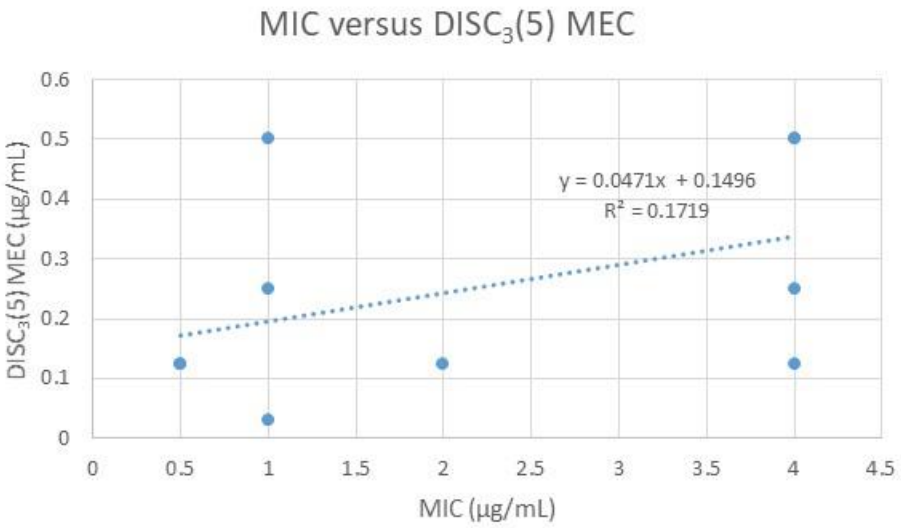

Figure S4. Plot of DiSC$_3$(5) versus MIC activity for armeniaspirol analogues with MIC potency ≤ 4 µg/mL.

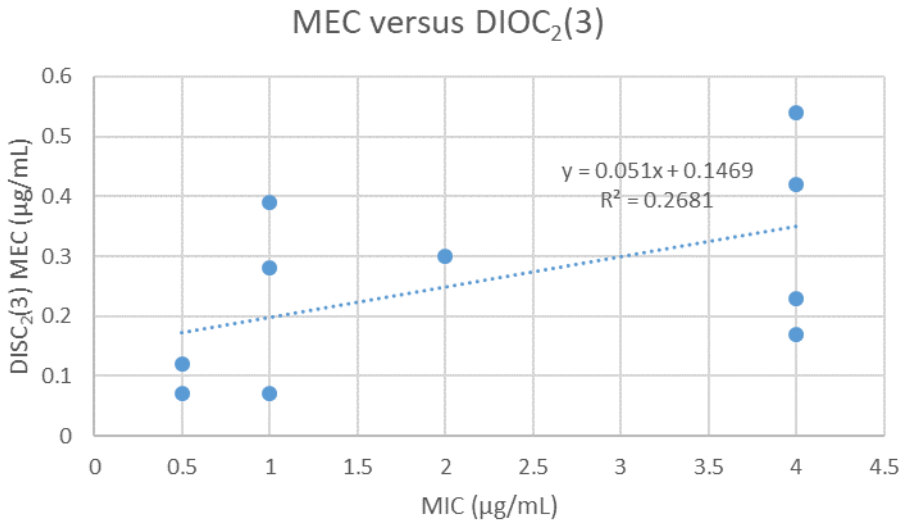

Figure S5. Plot of DiOC$_2$(3) versus MIC MEC activity for armeniaspirol analogues with MIC potency ≤ 4 µg/mL.

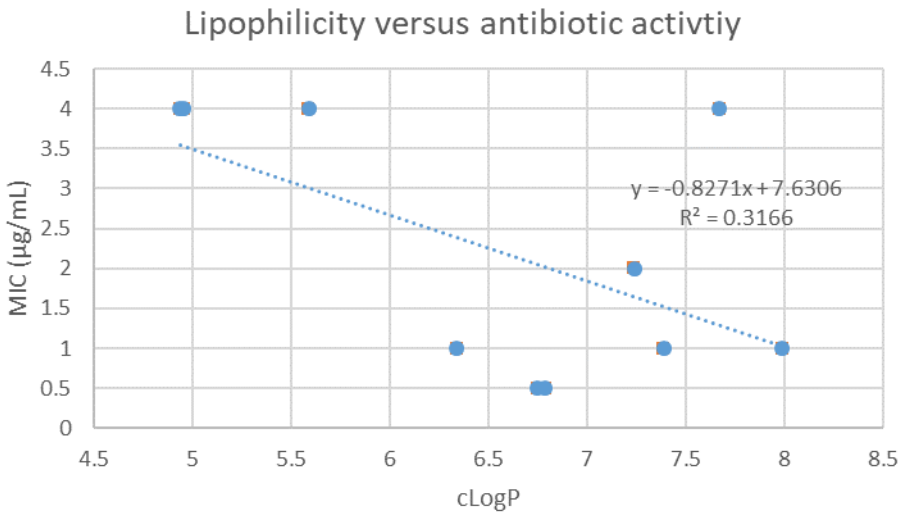

Figure S6. A plot of the lipophilicity (cLogP) versus the antibiotic activity (MIC) shows a moderate negative linear correlation that is not statistically significant as measured by the Pearson product-moment correlation ($r(10) = -0.56$, $p = 0.092$)

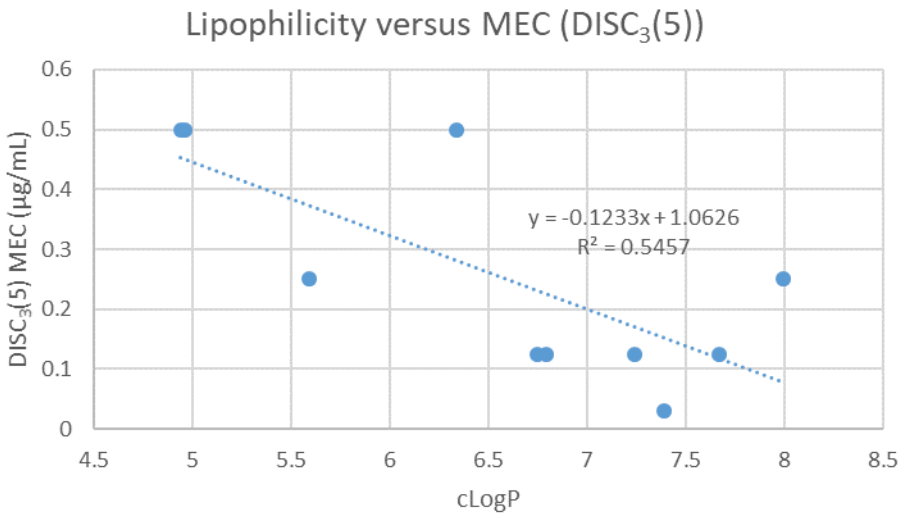

Figure S7. A plot of the lipophilicity (cLogP) versus the minimum effective concentration for disruption of membrane potential as determined by the $DiSC_3(5)$ assay shows a moderate negative linear correlation that is statistically significant as measured by the Pearson product-moment correlation ($r(10) = -0.74$, $p = 0.016$).

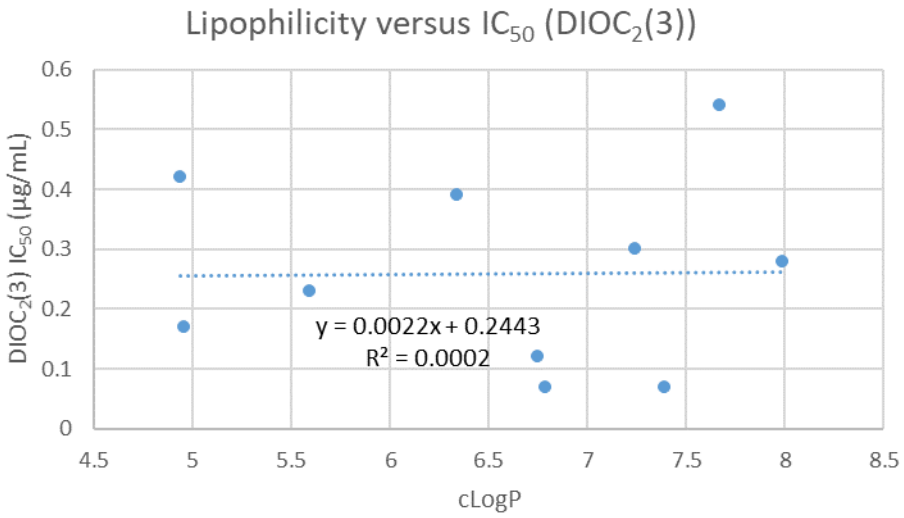

Figure S8. A plot of the lipophilicity (cLogP) versus the IC_{50} for disruption of membrane potential as determined by the $DiOC_2(3)$ assay shows no linear correlation as measured by the Pearson product-moment correlation ($r(10) = -0.016$, $p = 0.96$).

Table S3. Comparing analogues to armeniaspirol for displaying dual mechanism of action. Compounds with improved activity compared to **1** received a check.

#	Membrane disruption ($DiSC_3(5)$ MEC)	Clp protease inhibition	Antibiotic activity (MIC)	Dual mechanism of action
1	0.5	3.2 ± 0.2	4	✓
2	✓	✓	✓	✓
3	X	X	X	X
4	✓	X	X	X
5	X	✓	✓	X
6	✓	✓	✓	✓
7	✓	✓	✓	✓
8	✓	✓	✓	✓
9	X	X	X	X
10	✓	X	X	X
11	✓	✓	✓	✓
12	X	X	X	X
13	X	X	X	X
14	X	X	X	X
15	X	X	X	X
16	✓	X	X	X

Copies of ^{1}H and ^{13}C NMR spectra and MS (EI) spectra

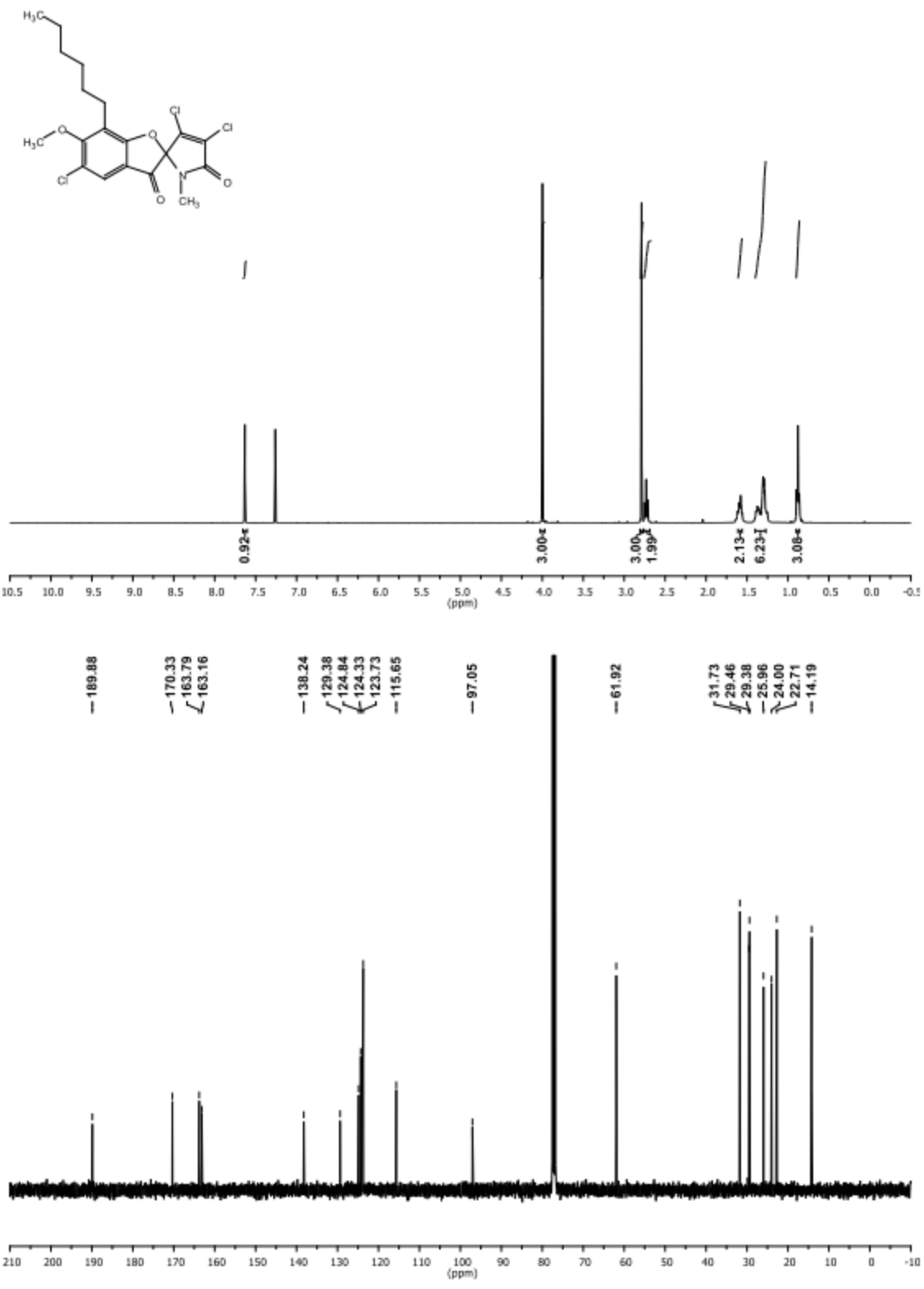
0.92
3.00
3.00
1.99
2.13
6.23
3.08
(ppm)
189.88
170.33
163.79
163.16
138.24
129.38
124.84
124.33
123.73
115.65
97.05
61.92
31.73
29.46
29.38
25.96
24.00
22.71
14.19
(ppm)

^{1}H NMR (400 MHz, $CDCl_3$) and ^{13}C NMR (100 MHz, $CDCl_3$) of **15**

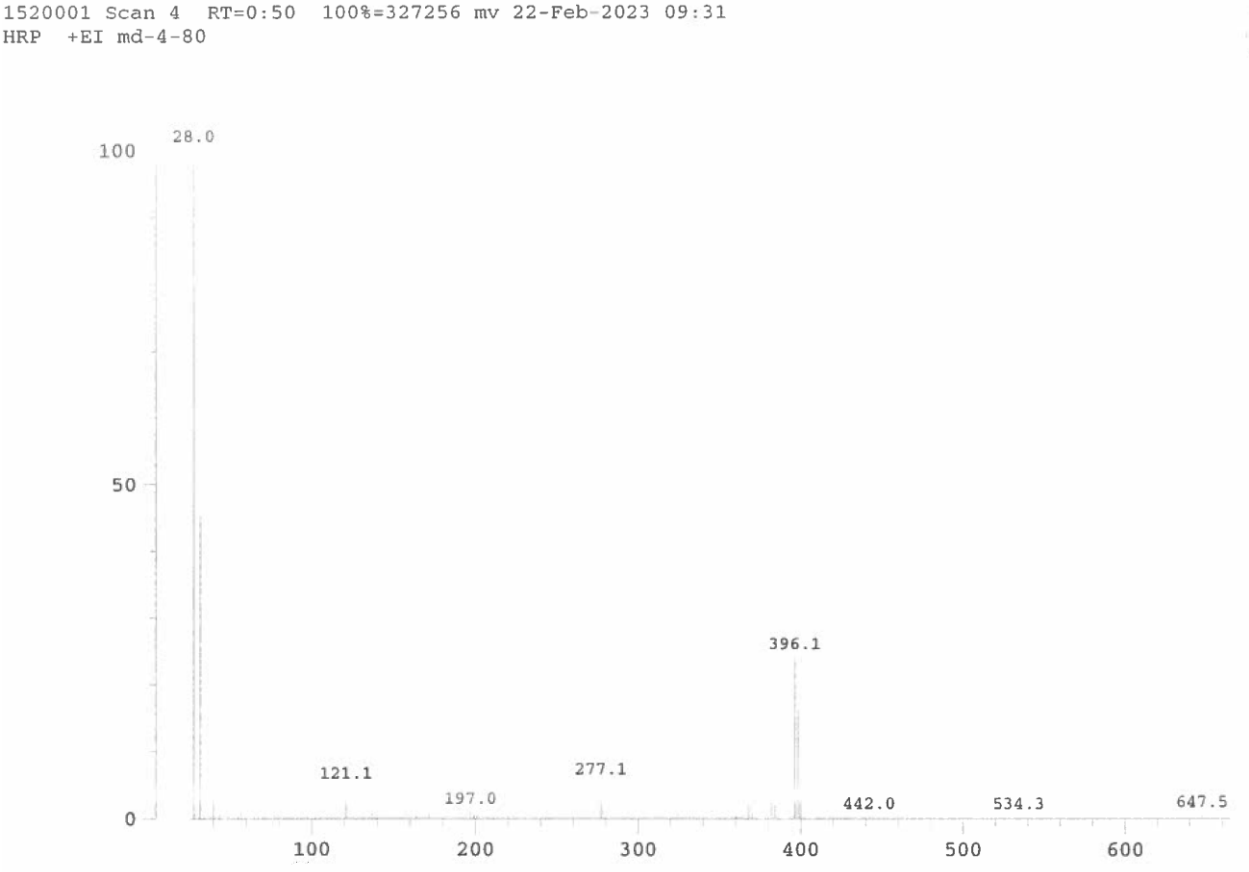

EI+ mass spectrum of **15**

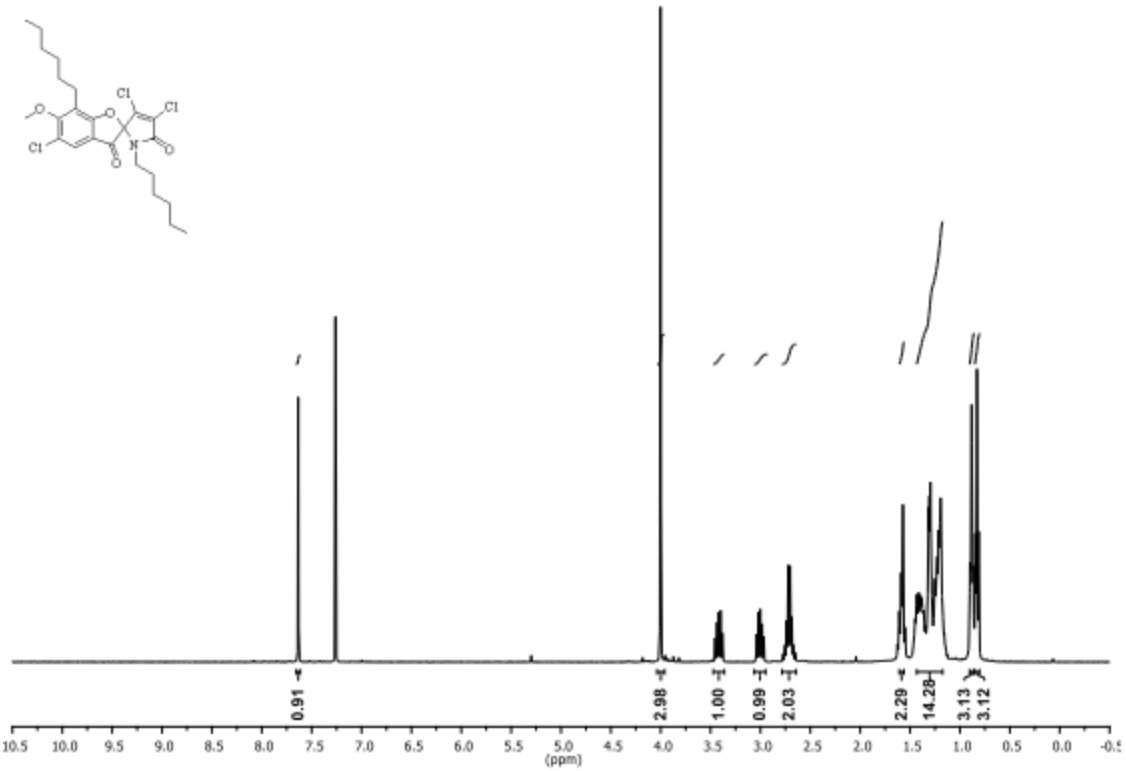
0.91
2.98
1.00
0.99
2.03
2.29
14.28
3.13
3.12
(ppm)

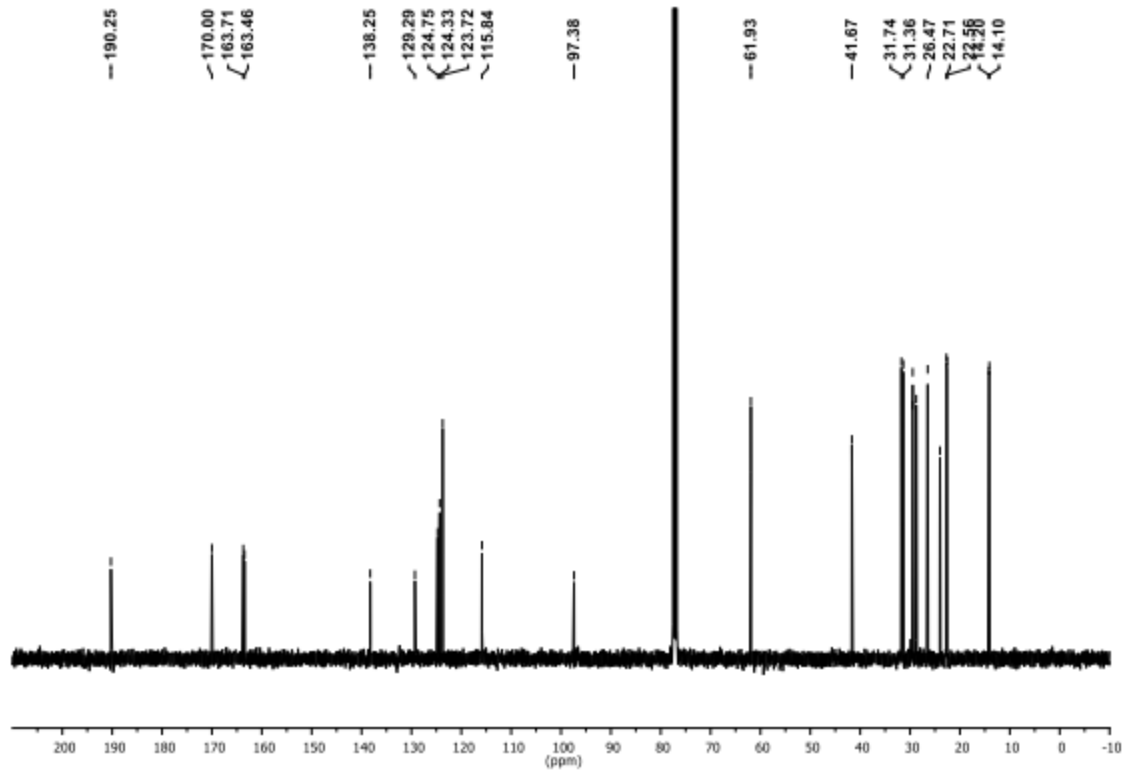
190.25
170.00
163.71
163.46
138.25
129.29
124.75
124.33
123.72
115.84
97.38
61.93
41.67
31.74
31.36
26.47
22.71
14.10
(ppm)

^{1}H NMR (400 MHz, $CDCl_3$) and ^{13}C NMR (100 MHz, $CDCl_3$) of **16**

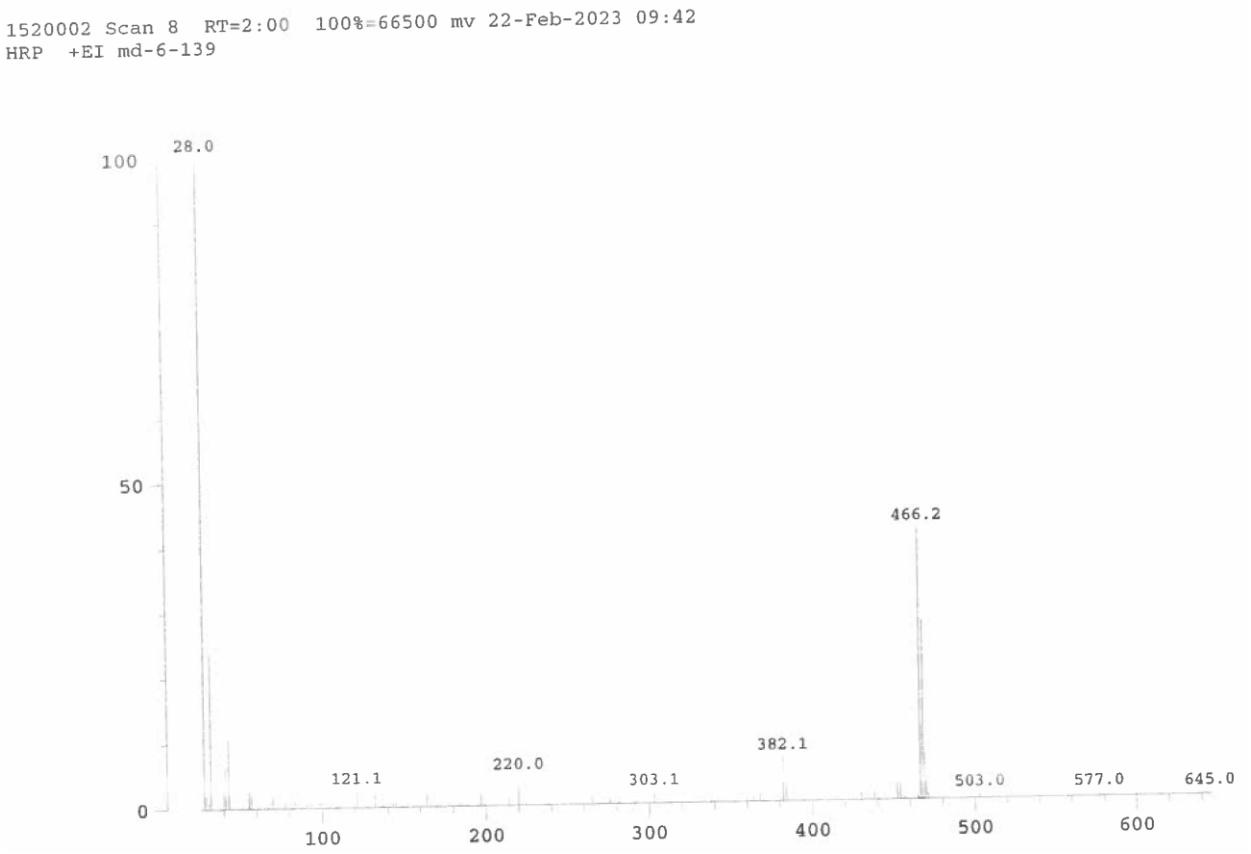

EI+ mass spectrum of **16**

References

1. Darnowski MG, Lanosky TD, Labana P, Brazeau-Henrie JT, Calvert ND, Dornan MH, Natola C, Paquette AR, Shuhendler AJ, Boddy CN. Armeniaspirol analogues with more potent Gram-positive antibiotic activity show enhanced inhibition of the ATP-dependent proteases ClpXP and ClpYQ. *RSC Med. Chem.* **13**, 436–444 (2022).

Chapter 4: Synthesis of a Constitutional Isomer of Armeniaspirol A, Pseudoarmeniaspirol A, via Lewis Acid-Mediated Rearrangement

4.1 Introduction

The research presented in this chapter was born from the efforts towards the total synthesis of armeniaspirol A. Because of unwanted late-stage chlorination of the electron rich phenyl ring, our strategies centred around early chlorination of the pyrrole. A study published in 1971 (in the *Canadian Journal of Chemistry*) by Durham and Rees caught our eye[1]. This infrequently cited paper reported the tri-chlorinated lactam structure shown in figure 4.1; however, the structural characterization was based on infrared spectroscopy and mass spectrometry-based fragmentation. We sought to confirm this structure and to develop a transform-based approach to the total synthesis of armeniaspirol using an early-stage oxidative chlorination.

Once the product was confirmed by NMR characterization and the reaction shown to be effective and scalable to deliver gram quantities of the correctly functionalized intermediate, it was then applied to our planned total synthesis of armeniaspirol. However, the synthesis was derailed by an unexpected Lewis acid mediated rearrangement in the penultimate step to yield a constitutional isomer of armeniaspirol, which we called pseudoarmeniaspirol. Extensive screening of substrates and reaction condition unfortunately could not suppress this undesired rearrangement.

With the potential utility and the limited literature precedence surrounding the oxidative chlorination of pyrrole-2-carbonyl compounds[1–3], we set out to determine what other carbonyl derivatives would undergo successful oxidation. This led to a mechanistic study to determine

why ketones result in decomposition products as opposed to esters and amides, which are effectively oxidized to the product. The instability of ketones was unexpected as the successful oxidation to yield the armeniaspirol scaffold and its analogues had been conducted countless times in our group under the same conditions.

Lastly, with the structural similarity to the natural product[4,5], pseudoarmeniaspirol and several analogues were evaluated for inhibition at known targets of armeniaspirol ClpXP, ClpYQ, and proton motive force as well as antibiotic potency in Gram-positive bacteria.

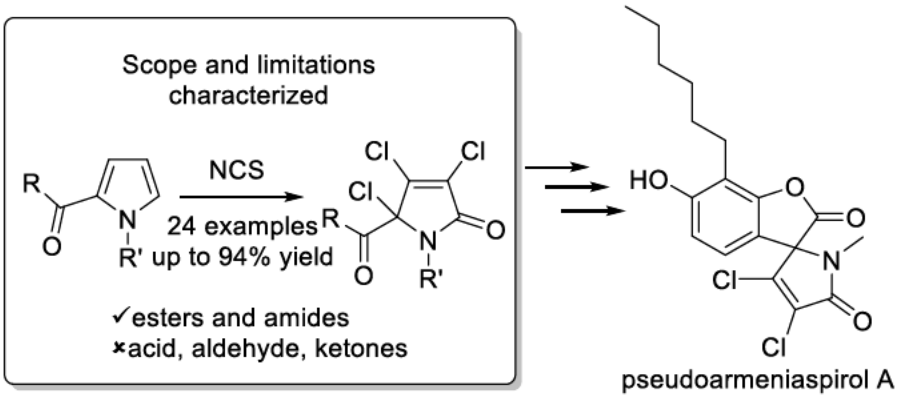

Figure 4.1 Oxidative chlorination of pyrrole-2-carbonyls used for attempted synthesis of armeniaspirol

4.2 References

1. Durham, D. G. & Rees, A. H. Chlorination of Pyrroles. Part I. *Can. J. Chem.* **49**, 136 (**1971**).
2. Birchall, G. R. & Rees, A. H. The Chlorination of Pyrroles. Part II. *Can. J. Chem.* **49**, 919 (**1971**).
3. Durham, D. G., Hughes, C. G. & Rees, A. H. The Chlorination of Pyrroles. Part III. *Can. J. Chem.* **50**, 3223–3228 (**1972**).

4. Dufour C, Wink J, Kurz M, Kogler H, Olivan H, Sablé S, Heyse W, Gerlitz M, Toti L, Nußer A, Rey A, Couturier C, Bauer A, Brönstrup M.Isolation and structural elucidation of armeniaspirols A-C: Potent antibiotics against gram-positive pathogens. *Chem. - A Eur. J.* **18**, 16123–16128 (**2012**).
5. Couturier, C., Bauer, A., Rey, A., Schroif-Dufour, C. & Broenstrup, M. Armeniaspiroles, a new class of antibacterials: Antibacterial activities and total synthesis of 5-chloro-Armeniaspirole A. *Bioorg. Med. Chem. Lett.* **22**, 6292–6296 (**2012**).

4.3 Author contributions

I synthesized all the compounds used in this study. I conducted the ClpXP assay and collected all the data regarding ClpXP inhibition. In collaboration with Taylor Lanosky, we conducted the voltage sensitive dye assays to evaluate membrane disruption by pseudoarmeniaspirol as well as MIC assays to evaluate antibiotic potency. Taylor Lanosky performed the ClpYQ kinetic assasys. I wrote the first draft of the manuscript.

4.4 Copyright

4.5 Synthesis of a constitutional isomer of armeniaspirol A, pseudoarmeniaspirol A, via Lewis acid-mediated rearrangement

Michael G. Darnowski, Taylor D. Lanosky, André R. Paquette, Christopher N. Boddy*

Department of Chemistry and Biomolecular Sciences

University of Ottawa

Ottawa, ON K1N 6N5 Canada

cboddy@uottawa.ca

Abstract

The natural product armeniaspirol possesses a unique spirocyclic *N,O*-ketal in an α,β-dichloro-α,β-unsaturated lactam scaffold that has proven to be challenging to synthesize. Herein we characterize the oxidative chlorination of pyrrole-2-carboxylate derivatives that rapidly generates this scaffold. The scope of this oxidation was extended to a series of esters and amides. Pyrrole-2-ketones could not be converted into the lactam due to an oxidative fragmentation. This result was unexpected since chloro-armeniaspirol has been synthesized via oxidative chlorination of a pyrrole-2-ketone. Examination of this successful oxidation showed the desired scaffold was accessed due to intramolecular trapping from the neighboring free phenol, preventing fragmentation. Using the product of methyl *N*-methyl pyrrole-2-carboxylate oxidation **7b**, we attempted to access the natural product armeniaspirol **2**; however, an unanticipated Lewis-acid mediated rearrangement led to formation of a constitutional isomer, pseudoarmeniaspirol A **1**. A small panel of pseudoarmeniaspirol analogues were synthesized and evaluated for antibiotic activity, inhibition of the targets of armeniaspirol, ClpXP and ClpYQ, and protonophore activity.

While pseudoarmeniaspirol shows antibiotic activity, it does not target ClpXP or ClpYQ and has less protonophore activity than the natural product.

Introduction

The natural product family of the armeniaspirols contains a unique and unusual spiro-[4.4]non-8-ene scaffold that has been challenging to generate (Figure 1A).[1,2] This *N,O*-ketal spirocyclic scaffold can be accessed from a pyrrole derivative through an oxidative chlorination strategy. Treatment of the pyrrole **3** with *N*-chlorosuccinimide (NCS) led to oxidation of the pyrrole ring and installation of the desired 3,4 dichloro-σ,β-unsaturated lactam and the spiro *N,O*-ketal, all in one operation (Figure 1B).[2,3] This reaction furnishes the core of armeniaspirol swiftly. However, it also installed an undesired chlorine at the 5-position on the electron rich aryl ring which is not present in the natural product. While this route has proven effective at synthesizing a series of analogues of **2**, a number of which showed increased antibiotic activity against Gram-positive pathogens[3], it has not yielded a total synthesis of armenaispirol. Recently however the total synthesis of (±) armeniaspirol A, **2**, was elegantly solved using an oxidative radical cross coupling and [3+2] cycloaddition (Figure 1C).[4] Herein we disclose a strategy based on an intramolecular Friedel-Crafts acylation that yields a constitutional isomer of armeniaspirol A, pseudoarmeniaspirol A, **1**, through an unexpected rearrangement (Figure 1A).

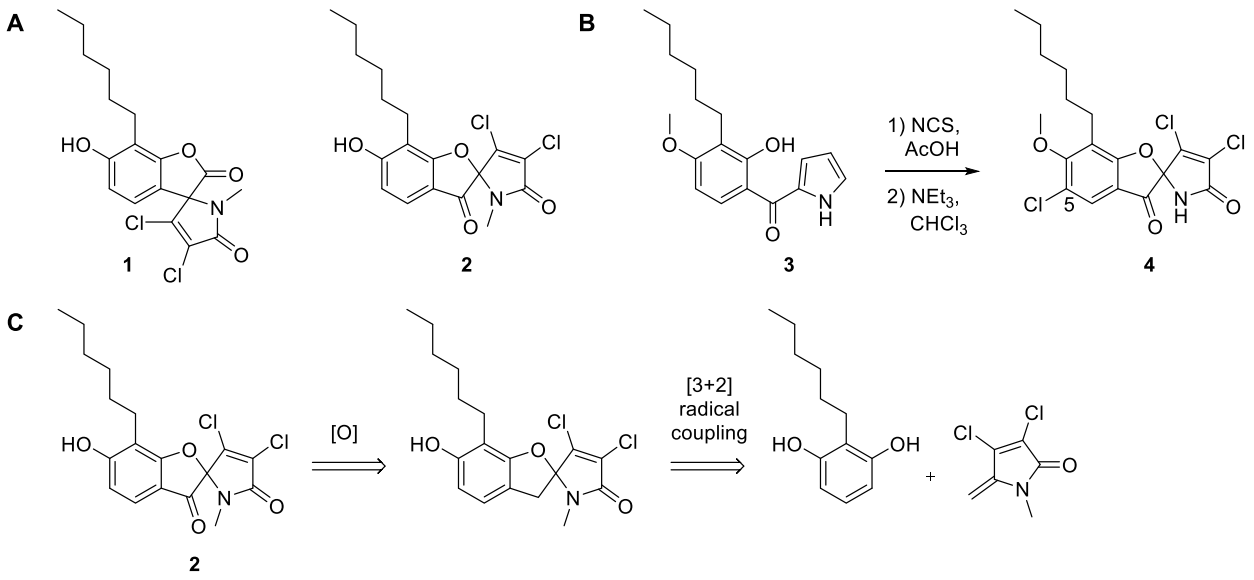

Figure 1. (A) Structures of (±) pseudoarmeniaspirol A, **1**, and (±) armeniaspirol A, **2**. (B) NCS-mediated oxidative chlorination used to generate the skeleton of armeniaspirol along with undesired chlorination at the 5 position. (C) Previous retrosynthetic disconnection of (±) armeniaspirol A.

Results and Discussion

To prevent undesired chlorination, a route where the pyrrole was oxidized to the dichloro-α,β-unsaturated lactam prior to installation of the electron rich aryl ring was envisioned. Pioneering work by Durham and Rees reported that chlorination of the methyl ester of pyrrole carboxylic acid generated a lactam with the appropriate functionalization for the synthesis of armeniaspirol A.[5] We thus envisioned installing the aryl ring after oxidation of the pyrrole and effecting an intramolecular Friedel-Crafts acylation to generate the complete framework of **2** (Figure 2).

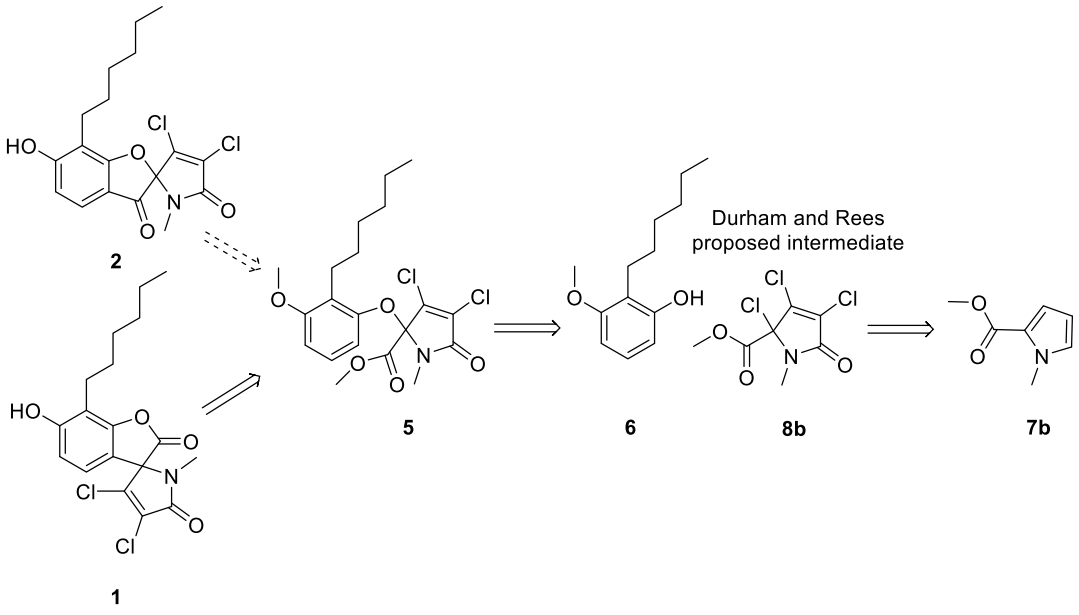

Figure 2. Retrosynthetic analysis of (±) pseudoarmeniaspirol A from early stage oxidation of pyrrole moiety.

The oxidative conversion of pyrrole carboxylic acids into α,β-unsaturated α,β-dichlorinated lactams has not been well characterized. Durham and Rees initially reported the reaction in 1971; however, their structural assignment was tentative and relied primarily on mass spectrometry fragmentation patterns.[5] Thus, we set out to investigate the scope of this key oxidative transformation by varying the substituents on the pyrrole nitrogen as well as the electron-withdrawing groups at the 2-position.

Substitution of the pyrrole nitrogen did not impact the reaction (Table 1). Esters of pyrrole-2-carboxylic acid (both *N*-H and *N*-alkyl, **7a-d**) underwent smooth oxidation to the lactam when treated with 4 equivalents of NCS. Similarly, treatment of the *N*-methyl pyrrole methyl ester with 4 equivalents of *N*-bromosuccinimide generated the corresponding brominated compound **18**. The presence of a stereogenic centre in the alkyl chain in **7e** did not impede the

NCS-mediated oxidation, though it did not significantly bias the facial selectivity of pyrrole oxidation, generating a 1:1.2 ratio of diastereomeric products. The *N*-Boc and *N*-Tosyl protected pyrroles were oxidized by NCS; however, the protecting groups were lost during the reaction (**7w-x**). To probe the substrate scope at the 2-position, a series of *N*-methyl pyrrole 2-carboxylic acid esters were screened (**7f-i**). All oxidized smoothly to the expected lactam product. Interestingly, neither the carboxylic acid, ketones, or the aldehyde yielded any of the expected product (**7l-q**).

Table 1. Scope of NCS-mediated chlorination of pyrrole 2-carbonyl compounds.

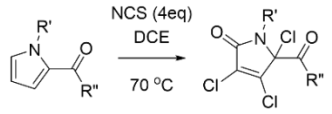

7a-x **8a-k**

Entry	R’	R”	Yield (%)
a	H	OMe	94
b	CH_3	OMe	91
c	*n*-C_6H_{13}	OMe	84
d	*n*-$C_{12}H_{25}$	OMe	81
e		OMe	78
f	CH_3		81
g	CH_3		77
h	CH_3		74
i	H		84
j	H		80
k	H		72
l	H	CH_3	nd
m	CH_3		nd
n	CH_3		nd
o	CH_3	H	nd
p	H	OH	nd
q	CH_3	CCl_3	nd
r	H		nd
s	H		nd
t	H		nd
u	H		nd
v	H		nd
w	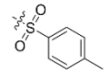	OMe	nd
x		OMe	nd

*nd = not detected.

The observation that ketones **7l-n** were not successfully oxidized was particularly surprising. In the case of armeniaspirol, which contains a ketone, NCS successfully oxidizes the pyrrole to the chlorinated lactam. A key difference between the simple pyrrole substrate and the chloro-armeniaspirol example is the trapping of the lactam γ-position by the teathered phenol (Figure 3A). This trapping is clearly important since when the phenol is protected as a methyl ether in **9**, NCS-mediated oxidation of the pyrrole leads to oxidative cleavage of the C-C bond linking the pyrrole to the ketone, resulting in **10** (Figure 3B). The oxidative cleavage is consistent with Cue and Chamberlin's observations that chlorination of a related pyrrolo-phenone leads to oxidative cleavage of the pyrrole carbonyl bond and formation of 5-chloro pyrrole.[6]

Based on our results and Cue and Chamberlin's work,[6] we propose that formation of the 5-chloropyrrolium intermediate leads to fragmentation into the 5-chloropyrrole and the acylium ion (Figure 3D, R = alkyl), which is converted into the acid on aqueous work up.[5] To test this, we investigated the oxidation of pyrrole carboxylic acid with excess NCS. We predicted that chlorination to trichloropyrrole carboxylic acid would occur followed by formation of the 5-chloropyrrolium and decarboxylation to the tetrachloropyrrole, which can be further oxidized to dichloromaleic anhydride (Figure 3C). We were pleased to see that both the tetrachloropyrrole **11** and dichloromaleic anhydride **12** were readily isolated from treatment of pyrrole 2-carboxylic acid with excess NCS. As mass spectrometry-based characterization of **11** proved challenging, [7,8] authentic **11** was generated by treating pyrrole with excess sulfuryl chloride (Figure S5).[9] This compound proved identical in all respects to **11** generated from treatment of pyrrole 2-carboxylic acid with excess NCS.

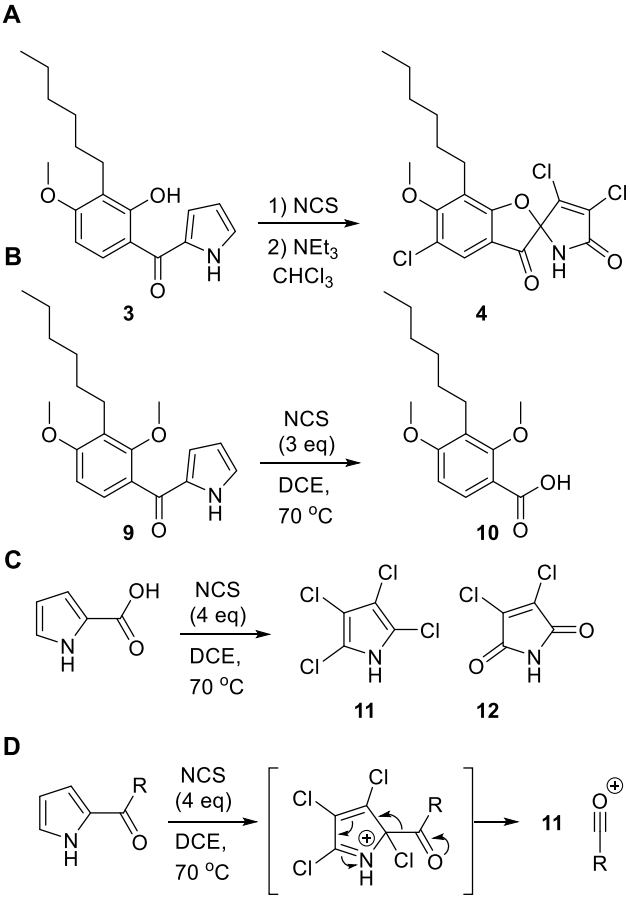

Figure 3. (A) Productive ketone oxidative chlorination via intramolecular phenol trapping. (B) Fate of protected phenol in armeniaspirol system. (C) Fate of pyrrole carboxylic acid derivative under oxidative chlorination conditions. (D) Mechanistic proposal for C-C bond fragmentation when R = alkyl. C-C bond fragmentation does not occur when R = NHR' or R = OR'.[1]

[1] An Alternative explanation for this reactivity is via addition of a nucleophile into the carbonyl to generate a tetrahedral intermediate which collapses via C-C bond cleavage to generate the pyrrole.

Based on this mechanistic analysis, we proposed that amides, like esters, should be effectively converted into the chlorinated lactams. In amides and esters, the loss of the high energy protonated alkylisocyanate ion (Figure 3D, R = NHR') and alkoxylcarbonyl cation (Figure 3D, R = OR')[10,11] (versus the acylium ions in ketone (Figure 3D, R = alkyl)) is expected to be slow, preventing unwanted C-C bond cleavage. Consistent with this hypothesis, propyl and piperidine amides were converted into the chlorinated lactams **8j-k**. The benzyl and propargylic amides **7r-s** however were not, presumably due to the oxidative cleavage of the benzyl and propargyl groups.[12] Similarly, thioesters **7u-v** were also not converted into the expected lactam due to rapid sulfur oxidation followed by decomposition.

To gain further insight into the successful oxidation of **3** into **4**, we evaluated its conversion by stepwise addition of NCS equivalents by NMR spectroscopy. Addition of three equivalents of NCS generated the trichloro intermediate **13**. Addition of another equivalent of NCS yielded an equal mixture of starting material **13** and the doubly oxidized product **14** (Figure 4). Thus, we proposed that the 4-chloropyrrolium ion is generated[13] and trapped by the neighbouring phenol to install the desired spirocyclic centre. The resulting enamine is then rapidly α-chlorinated and resulting protonated imidoyl chloride hydrolyzes yielding the lactam **14**. The formation of an equal molar ratio of starting material to product suggests that the second chlorination step is significantly faster than the first, consistent with the reactivity of the enamine versus an electron-poor pyrrole.

A published model study for the synthesis of chloro-armeniaspirol indicated a α,β,β-trichlorolactam species was the product of this oxidation.[2] However, our mechanistic hypothesis suggested the α,α,β-trichlorolactam regioisomer **14** was formed. We thus wanted to unambiguously assign the structure of the product. We therefore isolated **13** from treatment of **3**

with 3 equivalents of NCS and subjected it to a single equivalent of NCS, generating a 1:1 mixture of **13** to **14**. **14** was isolated and the structure was assigned by 1D and 2D NMR analysis confirming the regiochemistry as the α,α,β-trichlorolactam.

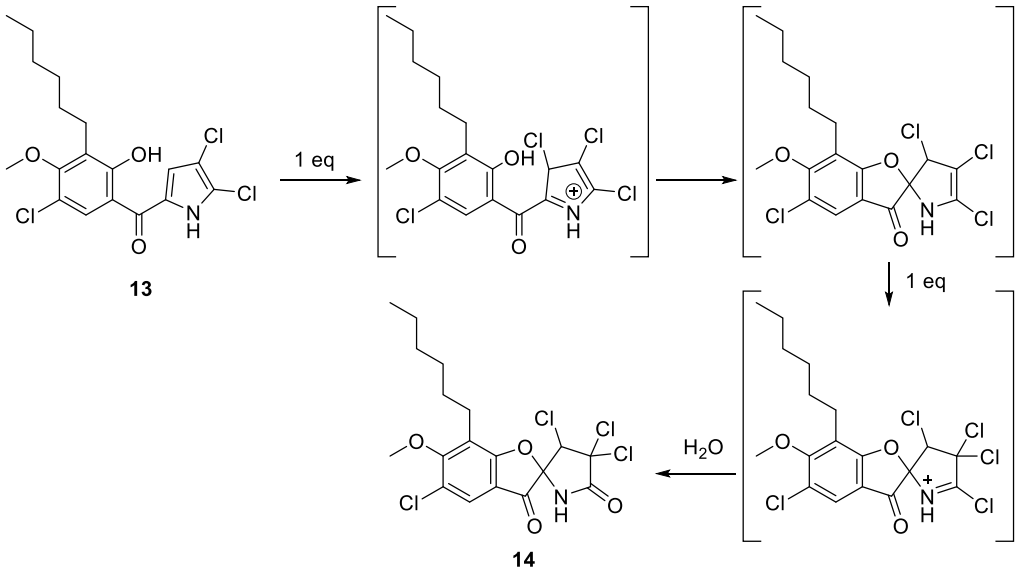

Figure 4. Proposed mechanism of pyrrole ketone oxidative chlorination on the route to (±) chloro-armeniasprol A.

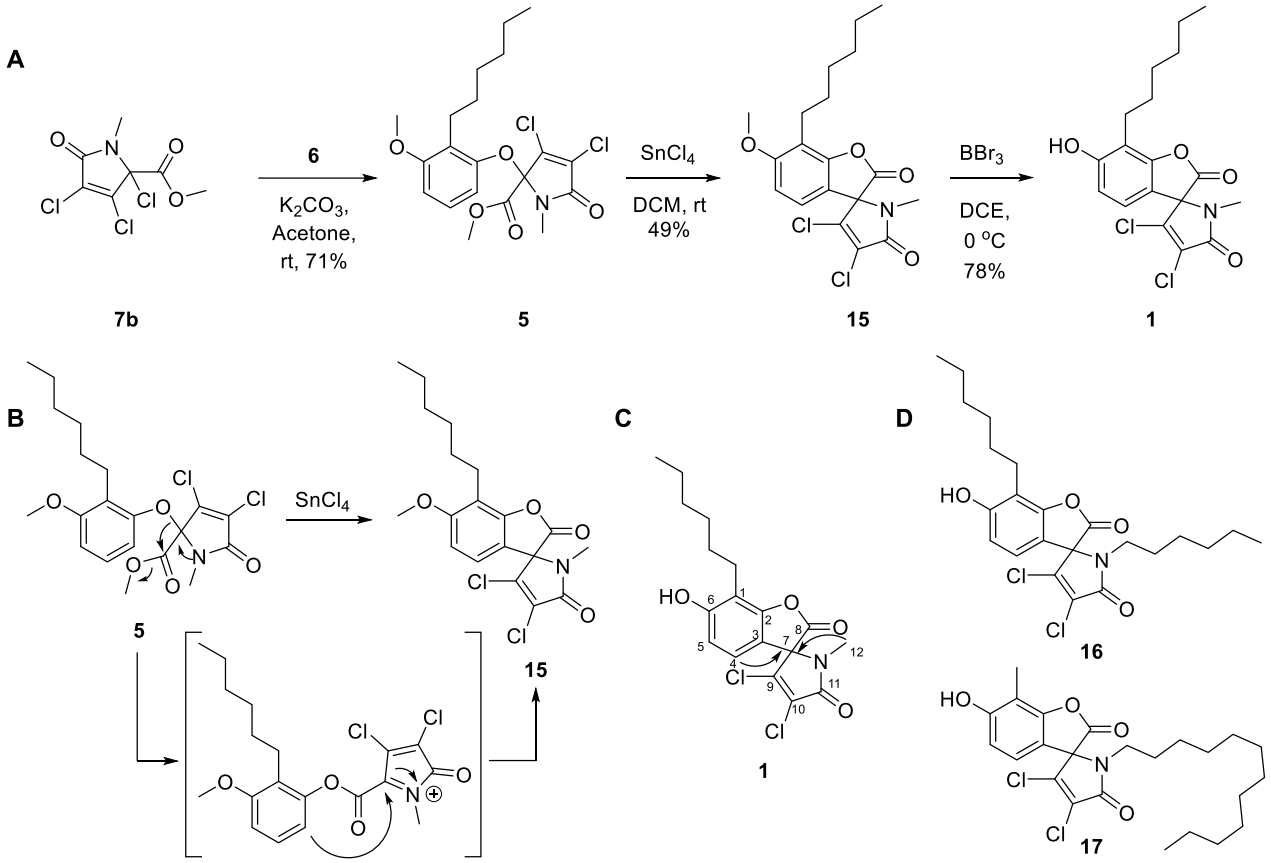

Figure 5. (A) Route to synthesis of (±)-pseudoarmeniaspirol. (B) Proposed Lewis acid-mediated skeletal rearrangement leading to pseudo-armeniaspirol skeleton.[2] (C) Key HMBC correlation in structure elucidation. (D) Analogues of pseudoarmeniaspirol.

Having evaluated the scope and mechanism of pyrrole chlorination, we had ready access to *N*-methyl lactam derivative **7b**. Treatment with 2-hexyl-3-methoxyphenol **6** and K_2CO_3

[2] Conversion of 5 to the intermediate is stepwise. A 1,2 migration of the phenolic oxygen would form a tetrahedral intermediate where methanol would leave after collapse of the tetrahedral intermediate to form the phenolic ester. The iminium ion would then be attacked by the aryl ring.

coupled the two halves of armeniaspirol and set the stage for the key Friedel-Crafts acylation.[14] All attempts to hydrolyze the methyl ester **5** resulted in decomposition. Derivatives with acid labile and fluoride sensitive esters similarly decomposed upon attempts to deprotect the acid (see Table S1). Because activated esters for the Friedel-Crafts acylation were not accessible, Lewis acid-mediated Friedel-Crafts acylation with the ester was attempted.[15,16] Tin (IV) chloride treatment led to a new product and its ^{1}H NMR spectrum was consistent with a tetrasubstituted aryl ring. Unfortunately the data were not consistent with those expected for the methyl ether of the natural product. Structural elucidation by 1D and 2D NMR analysis revealed an unexpected rearrangement had occurred generating a constitutional isomer of the desired product where the spiro-center is connected directly to the aromatic ring, in **15**. Screening a wide variety of reaction conditions, Lewis acids, and additives did not yield conditions that suppressed this unwanted migration (Table S1). Final deprotection of the aryl ether yielded pseudoarmeniaspirol A, **1**, a constitutional isomer of armeniaspirol A.

With its structural similarity to **2**, we evaluated **1** and a small panel of analogs, **16** and **17**, for biological activity. **2** is a Gram-positive antibiotic active against methicillin-resistant *Staphylococcus aureus* (MRSA). **1** displayed comparable antibiotic activity with an MIC of 4 μg/mL against MRSA USA300 (Table 2), the most common form of community-acquired MRSA infections. Synthetic chloro-armeniaspirol is known to inhibit proteolysis by recombinant purified ClpYQ *in vitro* with a K_I of 3.2 ± 0.2 μM and inhibit ClpXP activity in a cell-based assay at 1 μg/mL. **1** did not show any inhibition of ClpYQ even at 50 μM nor did it inhibit ClpXP at up to 1 μg/mL (Table 2). Lastly, armeniaspirol has been shown to possess protonophore activity. Thus, we evaluated pseudoarmeniaspirol for its ability to disrupt the proton gradient in bacterial cells using two different voltage-sensitive fluorescent dye assays. **1**

showed significantly less protonophore activity than chloro-armeniaspirol in both assays. **16** and **17** were synthesized and evaluated for antibiotic activity. Neither compound possessed relevant antibiotic activity (Table 2). Thus while **1** possesses comparable antibiotic activity to chloro-armeniaspirol, it does not appear to exert this activity through inhibition of the Clp proteases nor through disruption of the proton motive force.

In conclusion, we have elucidated the scope of pyrrole oxidative chlorination for accessing α,β-dichloro-α,β-unsaturated lactams. We have shown that oxidative C-C bond cleavage can occur in pyrroles substituted with aldehydes, ketones, or a carboxylic acid at the 2-position but does not occur with esters or amides. We show that the pyrrole oxidation in the synthesis of chloro-armeinaspirol, which occurs on a ketone-substituted pyrrole, does not lead to C-C bond cleavage due to the intramolecular trapping of a reaction intermediate by the phenol. Lastly, using the product from oxidation of the pyrrole carboxylic acid methyl ester, we generate an intermediate primed for synthesis of the armeniaspirol scaffold by a Friedel-Crafts acylation. Surprisingly this intermediate undergoes a Lewis acid-mediated rearrangement prior to electrophilic aromatic substitution, leading to a new scaffold and ultimately to a constitutional isomer of armeniaspirol that we name pseudoarmeniaspirol. While pseudoarmeniaspirol **1** is active against the Gram-positive pathogen MRSA like armeniaspirol, it does not inhibit the Clp proteases targeted by armeniaspirol nor does it act as a protonophore suggesting a different mechanism of action.

Table 2. Biological evaluation of constitutional isomers of Armeniaspirol.

	MEC_{ClpXP} (μg/mL)	**K_I ClpYQ(μM) (± std dev)**	**MIC (μg/mL)**	**$DiOC_2(3)$ IC_{50} (μg/mL)**	**$DiSC_3(5)$ EC_{50} (μg/mL)**
Cl-Arm	1	3.2 ± 0.2	4	0.169	0.5

1	>1	< 50	4	2.45	1
16	>1	< 50	>32	4.75	>1
17	>1	< 50	>32	1.82	0.25

Acknowledgements
Thanks to the John L. Holmes Mass Spectrometry Facility. This work was supported by the Natural Sciences and Engineering Research Council (NSERC) of Canada.

References

1. Dufour, C.; Wink, J.; Kurz, M.; Kogler, H.; Olivan, H.; Sablé, S.; Heyse, W.; Gerlitz, M.; Toti, L.; Nußer, A.; Rey, A.; Couturier, C.; Bauer, A.; Brönstrup, M. Isolation and Structural Elucidation of Armeniaspirols A-C: Potent Antibiotics against Gram-Positive Pathogens. *Chem. - A Eur. J.* **2012**, *18* (50), 16123–16128.
2. Couturier, C.; Bauer, A.; Rey, A.; Schroif-Dufour, C.; Broenstrup, M. Armeniaspiroles, a New Class of Antibacterials: Antibacterial Activities and Total Synthesis of 5-Chloro-Armeniaspirole A. *Bioorganic Med. Chem. Lett.* **2012**, *22* (19), 6292–6296.
3. Darnowski MG, Lanosky TD, Labana P, Brazeau-Henrie JT, Calvert ND, Dornan MH, Natola C, Paquette AR, Shuhendler AJ, Boddy CN. Armeniaspirol Analogues with More Potent Gram-Positive Antibiotic Activity Show Enhanced Inhibition of the ATP-Dependent Proteases ClpXP and ClpYQ. *RSC Med. Chem.* **2022**, *13* (4), 436–444.
4 . Arisetti, N.; Fuchs, H. L. S.; Coetzee, J.; Orozco, M.; Ruppelt, D.; Bauer, A.; Heimann, D.; Kuhnert, E.; Bhamidimarri, S. P.; Bafna, J. A.; Hinkelmann, B.; Eckel, K.; Sieber, S. A.; Müller, P. P.; Herrmann, J.; Müller, R.; Winterhalter, M.; Steinem, C.; Brönstrup, M. Total Synthesis and Mechanism of Action of the Antibiotic Armeniaspirol A. *Chem. Sci.*

2021, *12* (48), 16023–16034.

5. Durham, D. G.; Rees, A. H. Chlorination of Pyrroles. Part I. *Can. J. Chem.* **1971**, *49* (1), 136–138.
6. Cue, B. W.; Chamberlain, N. Pyoluteorin Derivatives. II. Synthetic Approaches to Pyrrole Ring Substituted Pyoluteorins. *J. Heterocycl. Chem.* **1981**, *18* (4), 667–670.
7. Ciamician, G.; Silber, P. Ueber Die Einwirkung von Unterchlorigsauren Und Unterbromigsauren Alkalien Auf Pyrrol. *Berichte der Dtsch. Chem. Gesellschaft* **1884**, *17* (2), 1743–1745.
8. El Khadem, H.; Kemler, L. A.; El-Shafei, Z. M.; Rahman, M. M. A. A.; El Sadany, S. Synthesis and Mass Spectra of N-aryl-pyrroles and Their Chlorination Products. *J. Heterocycl. Chem.* **1972**, pp 1413–1417.
9. Daniels, P. H.; Wong, J. L.; Atwood, J. L.; Canada, L. G.; Rogers, R. D. Unreactive 1-Azadiene and Reactive 2-Azadiene in Diels-Alder Reaction of Pentachloroazacyclopentadienes. *J. Org. Chem.* **1980**, *45* (3), 435–440.
10. Briggs, P. R.; Shannon, T. W. The Heat of Formation of the Methoxycarbonyl Ion. *J. Am. Chem. Soc.* July 1, **1969,** pp 4307–4309.
11. Olah, G. A.; Schilling, P.; Bollinger, J. M.; Nishimura, J. Stable Carbocations. CLXIII. Complexing Ionization, and Fragmentative Alkylcarbenium Ion Formation from Alkyl Haloformates, Thiolhaloformates, and Halosulfites with Antimony Pentafluoride. *J. Am. Chem. Soc.* **1974**, *96* (7), 2221–2228.
12. Moriyama, K.; Nakamura, Y.; Togo, H. Oxidative Debenzylation of N-Benzyl Amides and O-Benzyl Ethers Using Alkali Metal Bromide. *Org. Lett.* **2014**, *16* (14), 3812–3815.
13. Tutino, F.; Papeo, G.; Quartieri, F. Acid Catalyzed Halogen Dance on Deactivated

Pyrroles. *J. Heterocycl. Chem.* **2010**, *47* (1), 112–117.

14. Zhou, H.; Li, X.; Li, Y.; Zhu, X.; Zhang, L.; Li, J. Synthesis and Bioevaluation of 1-Phenylimidazole-4-Carboxylic Acid Derivatives as Novel Xanthine Oxidoreductase Inhibitors. *Eur. J. Med. Chem.* **2020**, *186*, 111883.
15. Nishimoto, Y.; Babu, S. A.; Yasuda, M.; Baba, A. Esters as Acylating Reagent in a Friedel-Crafts Reaction: Indium Tribromide Catalyzed Acylation of Arenes Using Dimethylchlorosilane. *J. Org. Chem.* **2008**, *73* (23), 9465–9468.
16. Chavan, S. P.; Garai, S.; Dutta, A. K.; Pal, S. Friedel-Crafts Acylation Reactions Using Esters. *European J. Org. Chem.* **2012**, No. 35, 6841–6845.
17. Shao, C.; Shi, G.; Zhang, Y.; Pan, S.; Guan, X. Palladium-Catalyzed C-H Ethoxycarbonyldifluoromethylation of Electron-Rich Heteroarenes. *Org. Lett.* **2015**, *17* (11), 2652–2655.
18. Chadwick, D. J.; Chambers, J.; Meakins, G. D.; Snowden, R. L. Esters of Furan-, Thiophen-, and N-Methylpyrrole-2-Carboxylic Acids. Bromination of Methyl Furan-2-Carboxylate, Furan-2-Carbaldehyde, and Thiophen-2-Carbaldehyde in the Presence of Aluminium Chloride. *J. Chem. Soc. Perkin Trans. 1* **1973**, 1766–1773.
19. Barker, P.; Gendler, P.; Rapoport, H. 2-(Trichloroacetyl)Pyrroles as Intermediates in the Preparation of 2, 4-Disubstituted Pyrroles. *J. Org. Chem.* **1978**, *43* (25), 4849–4853.
20. Shih, B. H.; Basha, R. S.; Lee, C. F. Nickel-Catalyzed Cross-Coupling of Aryl Redoxactive Esters with Aryl Zinc Reagents. *ACS Catal.* **2019**, *9* (10), 8862–8866.
21. Foley, L. H.; Habgood, G. J.; Gallagher, K. S. Assignment of the 13C NMR Shifts of Brominated Pyrrole Derivatives. *Magn. Reson. Chem.* **1988**, *26* (11), 1037–1038.
22. Gao, S.; Bethel, T. K.; Kakeshpour, T.; Hubbell, G. E.; Jackson, J. E.; Tepe, J. J. Substrate

Controlled Regioselective Bromination of Acylated Pyrroles Using Tetrabutylammonium Tribromide (TBABr3). *J. Org. Chem.* **2018**, *83* (16), 9250–9255.

23. Wakeham, R. J.; Taylor, J. E.; Bull, S. D.; Morris, J. A.; Williams, J. M. J. Iodide as an Activating Agent for Acid Chlorides in Acylation Reactions. *Org. Lett.* **2013**, *15* (3), 702–705.

24. Laha, J. K.; Kaur Hunjan, M.; Hegde, S.; Gupta, A. Aroylation of Electron-Rich Pyrroles under Minisci Reaction Conditions. *Org. Lett.* **2020**, *22* (4), 1442–1447.

25. Alniss, H. Y.; Witzel, I. I.; Semreen, M. H.; Panda, P. K.; Mishra, Y. K.; Ahuja, R.; Parkinson, J. A. Investigation of the Factors That Dictate the Preferred Orientation of Lexitropsins in the Minor Groove of DNA. *J. Med. Chem.* **2019**, 22, 10423-10440.

26. Sindhuja, E.; Ramesh, R.; Balaji, S.; Liu, Y. Direct Synthesis of Amides from Coupling of Alcohols and Amines Catalyzed by Ruthenium(II) Thiocarboxamide Complexes under Aerobic Conditions. *Organometallics* **2014**, *33* (16), 4269–4278.

27. Allmann, T. C.; Moldovan, R. P.; Jones, P. G.; Lindel, T. Synthesis of Hydroxypyrrolone Carboxamides Employing Selectfluor. *Chem. – A Eur. J.* **2016**, *22* (1), 111–115.

28. Borrero, N. V.; Aponick, A. Total Synthesis of Acortatarin A Using a Pd(II)-Catalyzed Spiroketalization Strategy. *J. Org. Chem.* **2012**, *77* (19), 8410–8416.

29. Loader, C. E.; Anderson, H. J. Pyrrole Chemistry. Part XI. Some Reactions of the Pyrrole Grignard Reagent with Alkyl Carbonates and Alkyl Thiocarbonates. *Can. J. Chem.* **1971**, *49* (1), 45–48.

30. Fu, J.; Wurzer, N.; Lehner, V.; Reiser, O.; Davies, H. M. L. Rh(II)-Catalyzed Monocyclopropanation of Pyrroles and Its Application to the Synthesis Pharmaceutically Relevant Compounds. *Org. Lett.* **2019**, *21* (15), 6102–6106.

31. Chen, Q.; Chen, H.; Meng, X.; Ma, Y. Lewis Acid Assisted Diels-Alder Reaction with Regio- and Stereoselectivity: Anti-1,4-Adducts with Rigid Scaffolds and Their Application in Explosives Sensing. *Org. Lett.* **2015**, *17* (20), 5016–5019.

4.6 Supporting information

Synthesis of a constitutional isomer of armeniaspirol A, pseudoarmeniaspirol A, via Lewis acid-mediated rearrangement

Michael G. Darnowski, Taylor D. Lanosky, André R. Paquette, Christopher N. Boddy*

[1]Department of Chemistry and Biomolecular Sciences, University of Ottawa

Table of Contents

Section 1. General Methods

- Clp YQ protein purification
- Peptide hydrolysis assay
- Minimum inhibitory concentration
- *Staphylococcus aureus* urease activity assay
- *Staphylococcus aureus* protonophore assay to monitor membrane depolarization assay using $DiSC_3$ (5) fluorescent dye
- *Staphylococcus aureus* protonophore assay to monitor membrane depolarization assay using $DiOC_2$ (3) fluorescent dye
- General Synthetic Protocols

Section 2. Supplemental figures and tables

- **Supplemental figure S1.** $DiSC_3$(5) fluorescence assay
- **Supplemental figure S2**. $DiOC_2$(3) fluorescence assay
- **Supplemental Figure S3.** ClpYQ inhibition curve for **1** showing fit to an IC_{50}

- **Supplemental Figure S4.** ClpYQ inhibition curve for **17** showing fit to an IC_{50}
- **Supplemental Figure S5.** Chlorination products of pyrrole-2-carboxylic acid and pyrrole for **SI6, 11, 12**
- **Supplemental Figure S6.** Synthetic scheme of pseudoarmeniaspirol analogues **1**, **16**, **17.**
- **Supplemental Figure S7.** Synthetic scheme for preparation of **SI7, SI8, 7f, 7h**
- **Supplemental Table S1.** Reaction conditions screened for hydrolysis and Lewis acid rearrangement of esters in attempts to synthesize **2**.

Section 3. Synthetic procedures and annotated NMR data of all Compounds

Section 4. Copies of ^{1}H and ^{13}C spectra

- A) **Table 1. 7a-w**
- B) **Table 1. 8a-k**
- C) Compounds on route to pseudoarmeniaspirol **(5,6,15,1)**
- D) Compounds on route to hexyl-pseudoarmeniaspirol **(SI1,SI2,16)**
- E) Compounds on route to N-dodecyl-1-methyl-pseudoarmeniaspirol **(SI5,SI3,SI4,17)**
- F) Compounds **3,4,9,10,11,12,13,14**
- G) Compounds **SI6,SI7,SI8**

References

Section 1. General Methods

ClpYQ protein purification

The ClpQ expression vector (pPL29, pET21c-based, C-terminal His tag, AmpR) was transformed into chemically competent *E. coli* BL21(DE3) for protein expression. 400 mL LB media was inoculated with 0.5% (*v/v*) of an overnight pre-culture. The culture was grown at 37 °C (200 rpm) and expression was induced with 1 mM isopropyl-1-thio-β-D-galactopyranoside at an optical density (OD_{600}) of 0.5. The culture was grown at 37 °C (200 rpm) for 4 h. The cells were pelleted at 4,000 rpm for 20 min and re-suspended in lysis buffer (50 mM Tris, 100 mM NaCl, 1 µg/mL leupeptin, 1 µg/mL pepstatin A, 1 mg/mL lysozyme, 10% glycerol, pH 8.0). Mechanical cell lysis was achieved by 3 cycles of 3 s sonication then 2 s incubation on ice followed by a 1 min incubation on ice. The cell debris was pelleted at 10,000 rpm for 60 min and the supernatant was incubated with 800 µL 50% Ni-NTA agarose resin (QIAGEN) for 30 min at 4 °C with gentle shaking. The lysate was loaded onto a column and the flow-through was collected. The resin was washed sequentially with 5 mL elution buffer (100 mM Tris, 300 mM NaCl, pH 8.0) containing 0 mM, 20 mM, 100 mM and 250 mM imidazole. Fractions were analyzed by SDS-PAGE (4-20% Mini-PROTEAN TGX Precast Gels; Bio-Rad). ClpQ-containing fractions were pooled and additionally purified by FPLC size exclusion using a Superdex 200 10/30 GL column (GE Healthcare). Buffer used in FPLC purification included 50 mM Tris, 250 mM NaCl, pH 8.0. ClpQ-containing fractions were concentrated using a 10 kDa Amicon Ultra-15 centrifugal filter unit (Millipore Sigma). The concentrated protein was stored at -80 °C with 30% (*w/w*) glycerol. The *B. subtilis* clpY gene was cloned into pET28B (N-terminal His tag, KanR).

ClpY was expressed and purified from the resulting plasmid (pPL31) as described above with the following modifications. The culture was grown at 16 °C overnight (200 rpm) post-induction. The column fraction containing the highest concentration of ClpY (with 100 mM imidazole) was additionally purified by FPLC size exclusion using a buffer containing 300 mM NaCl, 100 mM Tris, and 100 mM imidazole, pH 8.0. Imidzaole was added to the FPLC buffer to improve protein solubility since ClpY has the tendency to aggregate and must be treated carefully during purification. Accordingly, ClpY-containing fractions obtained from FPLC purification were pooled but not concentrated. All protein concentrations were determined by Bradford assay.

Peptide hydrolysis assays

Peptide hydrolysis was assayed using the Cbz-Gly-Gly-Leu-AMC (Millipore Sigma) substrate. 0.1 mL reaction assays were done in Nunc 96-well microplates for fluorescence-based assays (ThermoFisher Scientific). Assays were composed of purified bsClpQ and bsClpY protein, 0.1 M Tris (pH 8.0), 0.1 mM Cbz-GGL-AMC, 10 mM $MgCl_2$, 1 mM ATP, 1 mM TCEP, and 1 mM EDTA. A continuous assay of AMC release was monitored at 37 °C using a Synergy H4 microplate reader (BioTek). Excitation and emission for Cbz-GGL-AMC were measured at 355 nm and 460 nm, respectively. Inhibition was observed with varying concentrations of analogs.

\

General Synthetic Protocols

All reagents were purchased from Sigma-Aldrich at the highest available purity and used without further purification. All solvents were purchased from Fisher Scientific. All reactions were conducted using dry solvents under an argon atmosphere unless otherwise noted. NMR spectroscopy was performed with a Bruker Avance II, operating at 400 MHz for ^{1}H spectra, and 100 MHz for ^{13}C spectra or Bruker Avance III, with cryoprobe operating at 600 MHz for ^{1}H

spectra, and 150 MHz for ^{13}C spectra. Structural assignments were made with additional information from gCOSY, gHSQC, and gHMBC experiments. Preparatory TLC was performed using Merck Millipore 20 x 20 cm silica gel 60 F254 plates. High-resolution mass spectroscopy (HRMS) was conducted on a Micromass Q-TOF I for ESI measurements and a Kratos Concept 1S High Resolution Mass Spectrometer for EI measurements (John L. Holmes Mass Spectroscopy Facility).

Section 2. Supplemental figures and tables

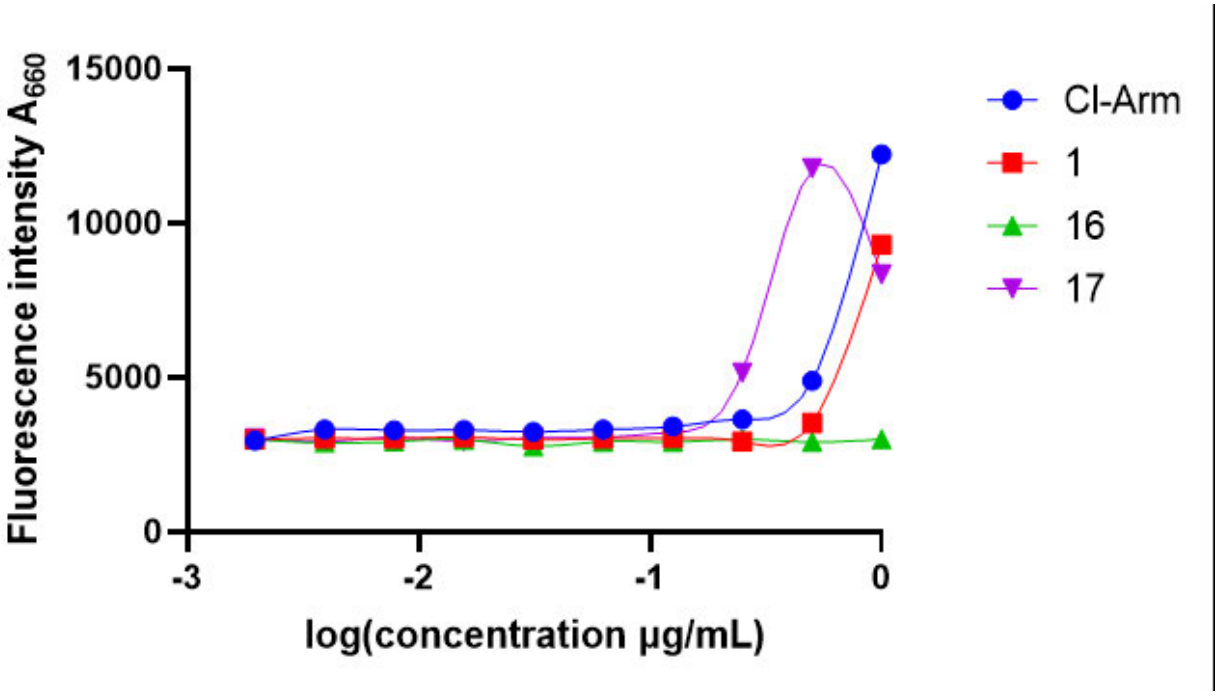

Supplemental figure S1. $DiSC_3(5)$ fluorescence assay

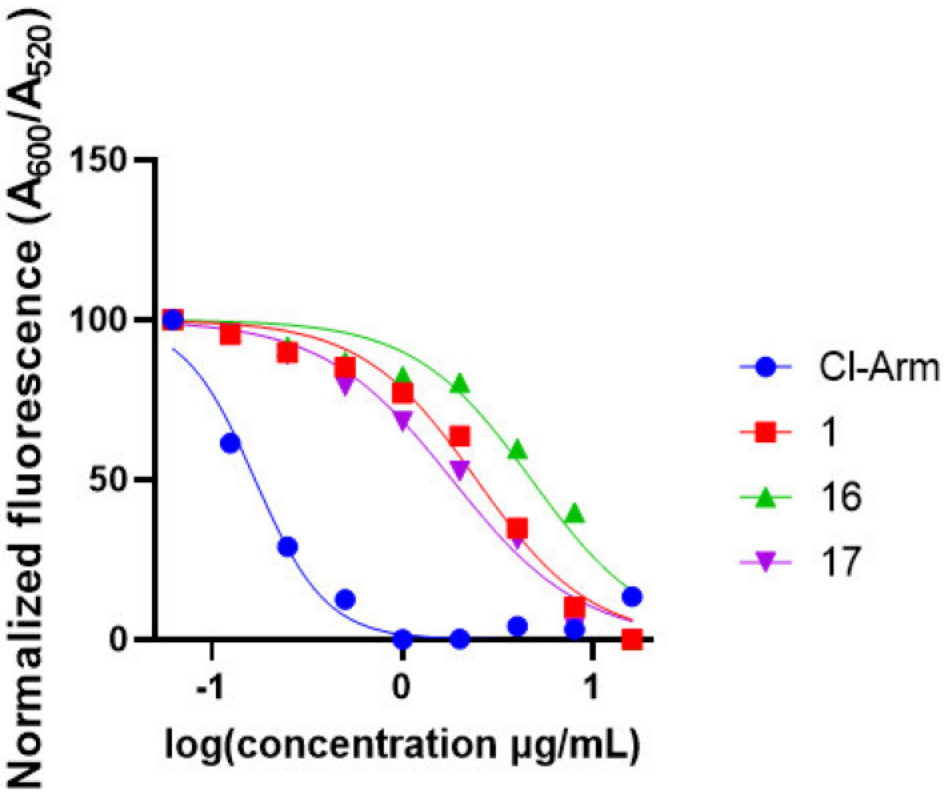

Supplemental figure S2. $DiOC_2(3)$ fluorescence assay

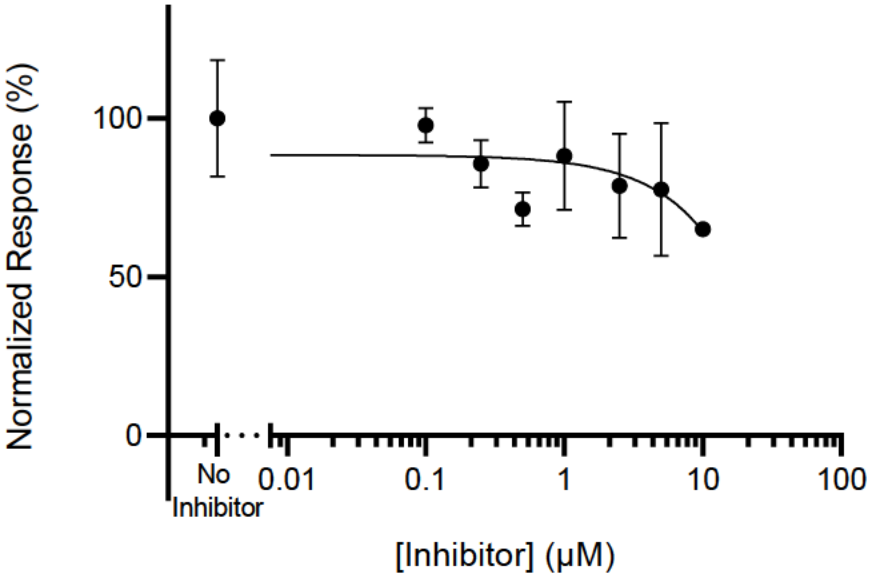

Supplemental Figure S3. ClpYQ inhibition curve for **1** showing fit to an IC_{50}

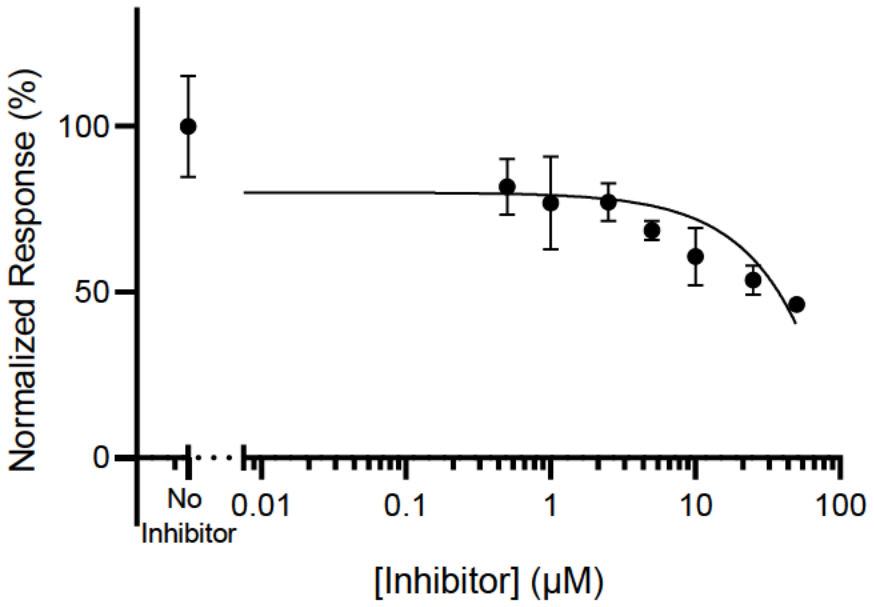

Supplemental Figure S4. ClpYQ inhibition curve for **17** showing fit to an IC_{50}

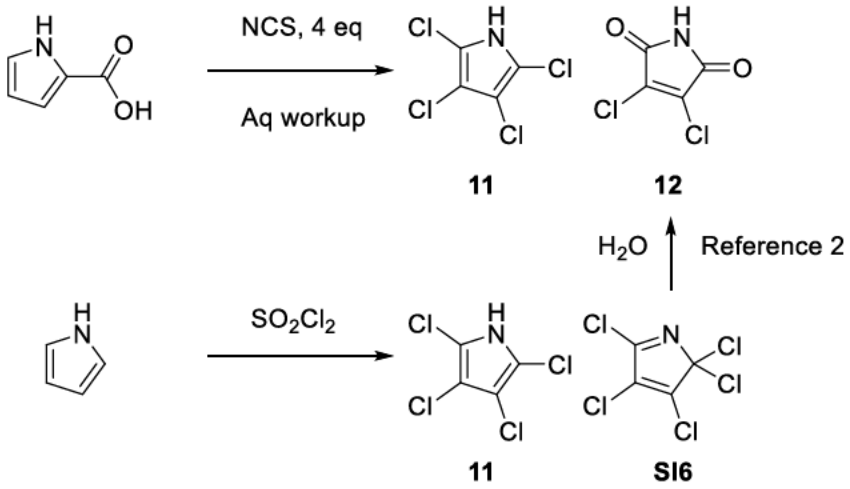

Supplemental Figure S5. Chlorination products of pyrrole-2-carboxylic acid and pyrrole **SI6,11,12**

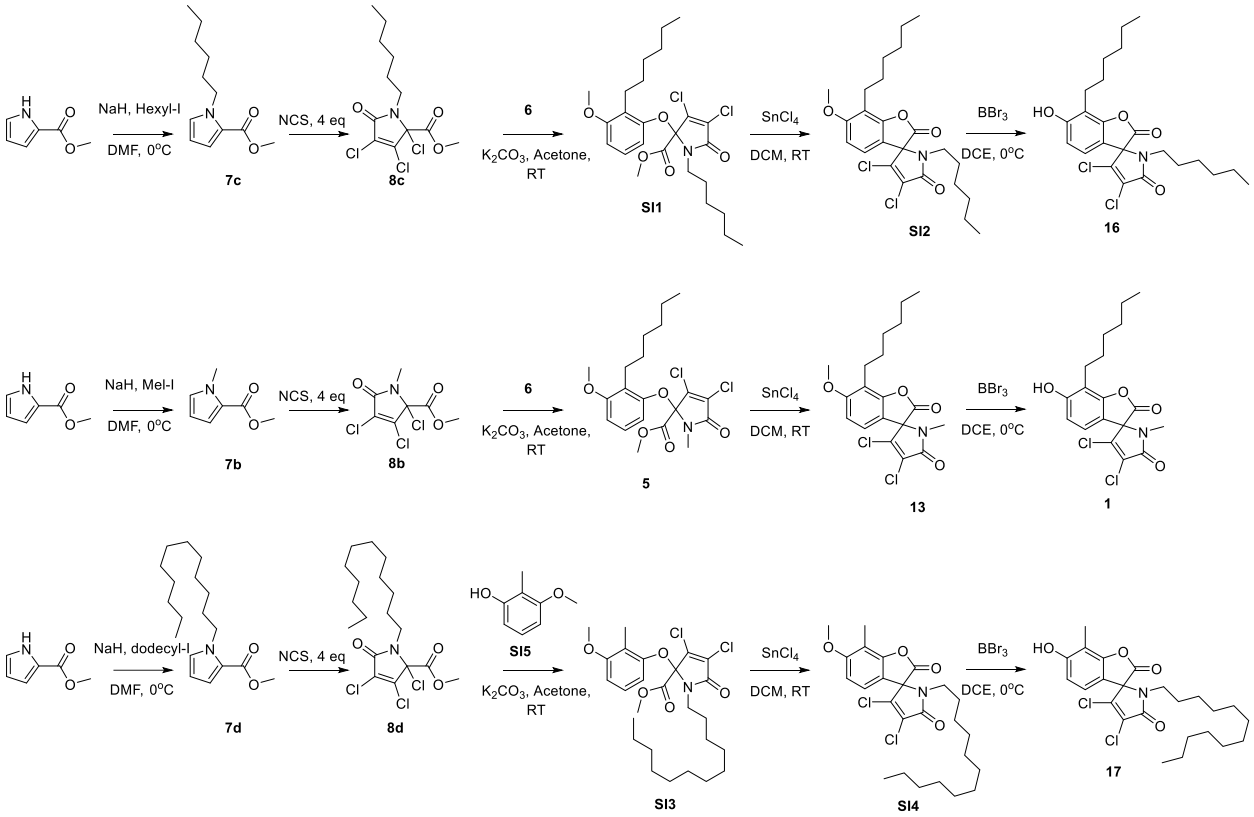

Supplemental Figure S6. Synthetic scheme of pseudoarmeniaspirol analogues **1**, **16**, **17.**

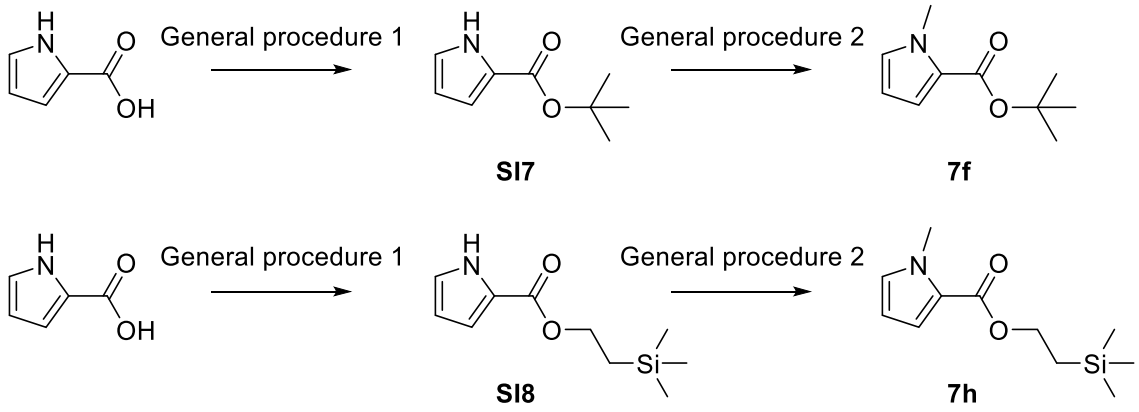

Supplemental Figure S7. Synthetic scheme for preparation of **SI7, SI8**

Supplemental Table S1. Reaction conditions screened for hydrolysis and Lewis acid rearrangement of esters in attempts to synthesize **2**.

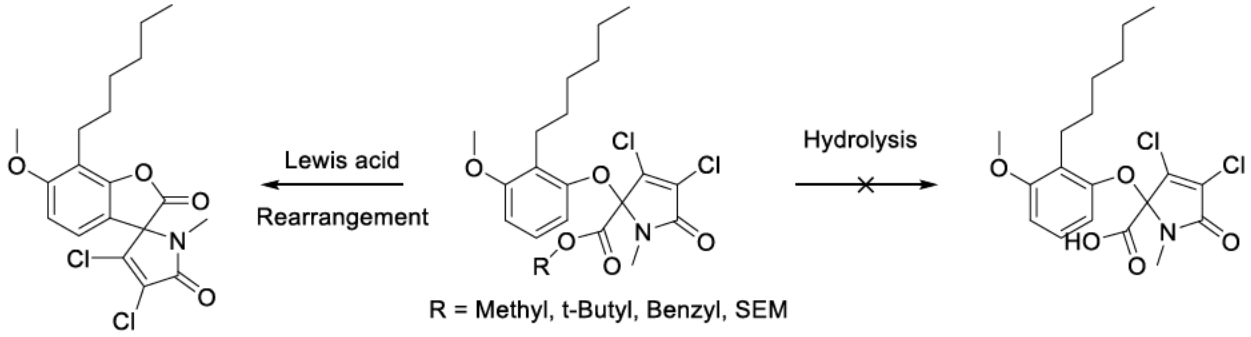

R group and entry #	Conditions	outcome	Notes
Methyl			
1	LiOH	decomposition	Various solvents and temps
2	NaOH	decomposition	Various solvents and temps
3	KOH	decomposition	
4	*p*-TsOH	decomposition	
5	AcOH	recovered SM	
6	TFA	decomposition	
7	HCl-Dioxane	decomposition	
8	SmI_2	decomposition	
9	BBr_3	decomposition	
10	$SnCl_4$	rearranged	
11	$TiCl_4$	rearranged	
12	Ti^iOPr	rearranged	

13	$AlCl_3$	rearranged	
t-Butyl			
14	10%TFA in DCM, TIPS	decomposition	**6** recovered
15	1% TFA in DCM,TIPS	decomposition	**6** recovered
16	SO_2Cl_2	recovered SM	
17	HCl / Ether	recovered SM	
18	Formic Acid	decomposition	**6** recovered
19	TESOTf, Lutidene	decomposition	**6** recovered
20	*p*-TsOH	recovered SM	
21	KOH	decomposition	
22	AcOH	recovered SM	
23	HCl / AcOH	recovered SM	
24	SiO_2, Toluene	recovered SM	
25	$SnCl_4$	rearranged	
SEM			
26	TBAF	recovered SM	
27	HF	recovered SM	
28	$SnCl_4$	rearranged	
Benzyl			
29	Pd/C, H_2	decomposition	Heat
30	Pd/C, H_2	decomposition	RT
31	Pd/C , Cyclohexene	recovered SM	

32	Pd/C, Cyclohexene	recovered SM	
33	Lindlars, H_2 50°C	recovered SM	
34	Lindlars, Cyclohexene 50°C	recovered SM	
35	$NiCl_2$-H_2O, $NaBH_4$, MeOH	decomposition	
36	$AlCl_3$, Anisole, DCM	rearranged	
37	$SnCl_4$, DCM	rearranged	

Section 3. Synthetic procedures and annotated NMR data of all Compounds

Experimental Section

General procedure 1 – Synthesis of esters amides and thioesters

At 0 °C, pyrrole-2-carboxylic acid (1.8 mmol,1 equiv) was added to a solution of 1-(3-dimethylaminopropyl)-3-ethylcarbodiimide, (2.7 mmol, 1.5 equiv) and DMAP (0.18 mmol, 0.1 equiv) in DCM (0.1 M). Then commercially available amine, alcohol, or thiol (2.16mmol, 1.2 equiv) was added to the mixture. The ice bath was removed and warmed to room temperature. After 24 h at room temperature, the solution was diluted with EtOAc (25 mL) and washed with a NH_4Cl solution. The aqueous layer was then extracted twice with EtOAc (20 mL). The combined EtOAc layers were dried with $MgSO_4$ and concentrated in vacuo. Silica gel chromatography (10-50 % EtOAc/hexanes) yielded pure amides, esters or thioesters.

General procedure 2 – Alkylation of pyrroles

At 0 °C, Methyl 1 H-pyrrole-2-carboxylate (0.8 mmol, 1 equiv) was dissolved in DMF (0.2 M). NaH (1.04 mmol, 1.3 equiv) was added and allowed to stir for 15 minutes. Commercially available alkyl halide (0.88 mmol, 1.1 equiv) was added to the mixture and the ice bath was removed and warmed to room temperature. After 3 h at room temperature the solution was diluted with EtOAc (25 mL) and washed with a NH_4Cl solution. The aqueous layer was then extracted twice with EtOAc (20 mL). The organic layer was then washed consecutively with brine. The combined EtOAc layers were dried with $MgSO_4$ and concentrated in vacuo. Silica gel chromatography (5-15 % EtOAc/Hexanes) yielded pure alkyl pyrrole esters.

General procedure 3 – Chlorination of pyrroles

Pyrrole substrate (0.3 mmol, 1 equiv) was dissolved in DCE (0.2 M). Following this, NCS (1.2 mmol, 4 equiv) was added to the mixture and heated to 70 ^oC using an oil bath and stirred over

night. The reaction was quenched with $NaHCO_3$ solution and diluted with EtOAc (25 mL). The aqueous layer was then extracted twice with EtOAc (20mL). The organic layer was then washed again with aqueous $NaHCO_3$. The combined EtOAc layers were dried with $MgSO_4$ and concentrated in vacuo. Silica gel chromatography (5-40 % EtOAc/hexanes) yielded the desired compound.

Compounds from Table 1.

Methyl N-methyl pyrrole-2-carboxylate (7b).

Prepared following general procedure 2. Compound **7b** was obtained as a colourless oil and was used without further purification (139 mg, quant). ^{1}H NMR (600 MHz, Chloroform-*d*) δ 6.93 (dd, *J* = 4.0, 1.8 Hz, 1H), 6.78 (ddd, *J* = 2.4, 1.8, 0.5 Hz, 1H), 6.11 (dd, *J* = 4.0, 2.5 Hz, 1H), 3.93 (s, 3H), 3.81 (s, 3H). ^{13}C{^{1}H} NMR (150 MHz, $CDCl_3$) δ 161.9, 129.6, 122.5, 117.9, 108.0, 51.2, 37.0. The NMR data is consistent with literature values.[17] HRMS (EI+/Magnetic sector) m/z: [M]+ calcd for $C_7H_9NO_2$: 139.0633 Found: 139.0640.

Methyl N-hexyl pyrrole-2-carboxylate (7c).

Prepared following general procedure 2. Compound **7c** was obtained as a colourless oil and used without further purification (209 mg, quant). ^{1}H NMR (600 MHz, Chloroform-*d*) δ 6.97 – 6.93 (m, 1H), 6.83 (dd, *J* = 2.5, 1.9 Hz, 1H), 6.13 – 6.08 (m, 1H), 4.33 – 4.26 (m, 2H), 3.80 (s, 3H), 1.79 – 1.71 (m, 2H), 1.29 (q, *J* = 4.5, 3.5 Hz, 6H), 0.89 – 0.86 (m, 3H).^{13}C{^{1}H} NMR (150 MHz, $CDCl_3$) δ 161.6, 128.8, 121.6, 118.2, 107.9, 51.1, 49.4, 31.8, 31.6, 26.5, 22.7, 14.2. HRMS (EI+/Magnetic sector) m/z: [M]+ calcd for $C_{12}H_{19}NO_2$: 209.1416 Found: 209.1420

Methyl N-dodecyl pyrrole-2-carboxylate (7d).

Prepared following general procedure 2. Compound **7d** was obtained as a colourless oil and was used without further purification (293 mg, quant). ^{1}H NMR (600 MHz, $CDCl_3$) δ 6.94 (dd, *J* = 3.9, 1.8 Hz, 1H), 6.83 (dd, *J* = 2.5, 1.8 Hz, 1H), 6.10 (dd, *J* = 3.9, 2.5 Hz, 1H), 4.30 – 4.26 (m, 2H), 3.80 (s, 3H), 1.78 – 1.70 (m, 2H), 1.29 – 1.21 (m, 18H), 0.88 (td, *J* = 7.1, 1.6 Hz, 3H). $^{13}C\{^{1}H\}$ NMR (150 MHz, $CDCl_3$) δ 161.5, 128.7, 121.4, 118.1, 107.8, 51.0, 49.3, 31.9, 31.7, 29.7, 29.6, 29.6, 29.6, 29.4, 29.3, 26.7, 22.7, 14.1. HRMS (EI+/Magnetic sector) m/z: [M]+ calcd for $C_{18}H_{31}NO_2$: 293.2355 Found: 293.2342.

Methyl 1-(1-ethoxy-1-oxopropan-2-yl)pyrrole-2-carboxylate (7e).

Prepared following general procedure 2. Compound **7e** was obtained as a colourless oil and used without further purification (900 mg, 91 % yield). R_f= 0.20 (10:90 EtOAc:Hexanes). ^{1}H NMR (400 MHz, $CDCl_3$) δ 7.04 (dd, *J* = 2.8, 1.8 Hz, 1H), 7.00 (dd, *J* = 3.9, 1.7 Hz, 1H), 6.21 (dd, *J* = 3.9, 2.8 Hz, 1H), 5.85 (q, *J* = 7.4 Hz, 1H), 4.19 (qd, *J* = 7.1, 1.0 Hz, 2H), 3.79 (s, 3H), 1.74 (s, 3H), 1.24 (t, *J* = 7.1 Hz, 3H). $^{13}C\{^{1}H\}$ NMR (101 MHz, $CDCl_3$) δ 171.6, 161.7, 125.9, 122.1, 118.5, 108.7, 61.5, 55.2, 51.1, 18.0, 14.1. HRMS (EI+/Magnetic sector) m/z: [M]+ calcd for $C_{11}H_{15}NO_4$: 225.1001 Found: 225.0989

***t*-butyl 1-methylpyrrole-2-carboxylate (7f).**

Prepared following general procedure 2 using **SI7**. Product **7f** was obtained as a colourless oil and used without further purification (400 mg, quant) .^{1}H NMR (400 MHz, $CDCl_3$) δ 6.87 (dd, *J* = 3.9, 1.9 Hz, 1H), 6.73 (t, *J* = 2.2 Hz, 1H), 6.08 (dd, *J* = 3.9, 2.5 Hz, 1H), 3.90 (s, 3H) 1.55 (s, 9H). $^{13}C\{^{1}H\}$ NMR (100 MHz, $CDCl_3$) δ 160.9, 128.9, 124.0, 117.4, 107.4, 80.2, 36.9, 28.5. The NMR data is consistent with literature values.[18] HRMS (EI+/Magnetic sector) m/z: [M]+ calcd for $C_{10}H_{15}NO_2$: 181.1103 found: 181.1116.

Benzyl 1-methylpyrrole-2-carboxylate (7g).

Prepared following general procedure 1. Compound **7g** was purified by silica gel chromatography (5:95 EtOAc:Hexanes) and obtained as a clear oil (120 mg, 74 % yield). R_f= 0.6 (10:90 EtOAc:Hexanes). ^{1}H NMR (400 MHz, $CDCl_3$) δ 7.44 – 7.33 (m, 5H), 7.00 (dd, *J* = 4.0, 1.8 Hz, 1H), 6.79 (t, *J* = 2.1 Hz, 1H), 6.11 (dd, *J* = 4.0, 2.5 Hz, 1H), 5.28 (s, 2H), 3.93 (s, 3H). $^{13}C\{^1H\}$ NMR (100 MHz, $CDCl_3$) δ 161.1, 136.6, 129.7, 128.5, 128.0, 127.9, 122.4, 118.1, 107.9, 65.4, 36.8. The NMR data is consistent with literature values.[19] HRMS (EI+/Magnetic sector) m/z: [M]+ calcd for $C_{13}H_{13}NO_2$: 215.0946 Found: 215.0955.

Trimethylsilyl ethyl-N-methyl pyrrole-2-carboxylate (7h).

Prepared following general procedure 2 using **SI8**. Compound **7h** was obtained as a colourless oil and was used without further purification (100 mg, 95 % yield). ^{1}H NMR (400 MHz, $CDCl_3$) δ 6.92 (dd, *J* = 4.0, 1.8 Hz, 1H), 6.77 (t, *J* = 2.2 Hz, 1H), 6.10 (dd, *J* = 4.0, 2.5 Hz, 1H), 4.43 – 4.20 (m, 2H), 3.93 (s, 3H), 1.12 – 1.05 (m, 2H), 0.07 (s, 9H). $^{13}C\{^1H\}$ NMR (100 MHz, $CDCl_3$) δ 161.6, 129.3, 122.8, 117.6, 107.7, 62.0, 36.8, 17.5, -1.4. HRMS (EI+/Magnetic sector) m/z: [M]+ calcd for $C_{11}H_{19}NO_2Si$: 225.1185 Found: 225.1187.

Phenol 1-H-pyrrole-2-carboxylate (7i).

Prepared following general procedure 1. Compound **7i** was purified by silica gel chromatography (20:80 EtOAc:Hexanes) and obtained as a white amorphous solid (275 mg, 81 % yield). R_f= 0.4 (20:80 EtOAc:Hexanes) ^{1}H NMR (400 MHz, $CDCl_3$) δ 9.90 (s, 1H), 7.50 – 7.42 (m, 2H), 7.35 – 7.24 (m, 3H), 7.22 (ddd, *J* = 3.9, 2.5, 1.5 Hz, 1H), 6.94 (td, *J* = 2.7, 1.5 Hz, 1H), 6.36 (dt, *J* = 3.8, 2.5 Hz, 1H). $^{13}C\{^1H\}$ NMR (100 MHz, $CDCl_3$) δ 160.0, 150.7, 129.6, 125.9, 124.7, 122.0, 121.8, 117.1, 110.8. The NMR data is consistent with literature values.[20]

1H-Pyrrole-2-carboxylic acid propylamide (7j).

Prepared following general procedure 1. Compound **7j** was purified by silica gel chromatography (30 % EtOAc/Hexanes) and obtained as a yellow oil (184 mg, 84 % yield). R_f= 0.35 (50:50 EtOAc:Hexanes) ^{1}H NMR (400 MHz, $CDCl_3$) δ 6.89 (td, *J* = 2.7, 1.3 Hz, 1H), 6.61 (ddd, *J* = 3.8, 2.5, 1.4 Hz, 1H), 6.30 (t, *J* = 5.9 Hz, 1H), 6.19 (dt, *J* = 3.7, 2.5 Hz, 1H), 3.43 – 3.32 (m, 2H), 1.59 (h, *J* = 7.4 Hz, 2H), 0.94 (t, *J* = 7.4 Hz, 3H). ^{13}C{^{1}H} NMR (100 MHz, $CDCl_3$) δ 161.7, 126.1, 121.7, 109.4, 109.0, 41.2, 23.1, 11.4. The NMR data is consistent with literature values.[21] HRMS (EI+/Magnetic sector) m/z: [M]+ calcd for $C_8H_{12}N_2O$: 152.0950 Found: 152.0944.

Piperidin-1-yl(1H-pyrrol-2-yl)methanone (7k).

Prepared following general procedure 1. Compound **7k** was purified by silica gel chromatography (30 % EtOAc/Hexanes) and obtained as an orange oil (170 mg, 77 % yield). R_f= 0.35 (40:60 EtOAc:Hexanes). ^{1}H NMR (400 MHz, $CDCl_3$) δ 6.87 (td, *J* = 2.7, 1.2 Hz, 1H), 6.49 (ddd, *J* = 3.8, 2.4, 1.3 Hz, 1H), 6.21 (td, *J* = 3.2, 2.2 Hz, 1H), 3.81 – 3.66 (m, 4H), 1.74 – 1.57 (m, 6H). ^{13}C{^{1}H} NMR (150 MHz, $CDCl_3$) δ 162.0, 124.8, 121.0, 111.8, 108.9, 46.0, 26.2, 24.8. The NMR data is consistent with literature values.[22] HRMS (EI+/Magnetic sector) m/z: [M]+ calcd for $C_{10}H_{14}N_2O$: 178.1106 Found: 178.1099.

(1-methyl-1H-pyrrol-2-yl)-2,2-dimethyl-1-propanone (7m).

Lithium iodide (644 mg, 4.81 mmol, 1.3 equiv) and N-methylpyrrole (0.33 mL, 3.7 mmol, 1 equiv) were added to 5 mL of anhydrous MeCN and 4 Å molecular sieves. Pivaloyl chloride (0.45 mL, 3.7 mmol, 1 equiv) was added to the solution and the mixture was immediately heated to 82^o C using an oil bath and stirred for 24 hours. The resulting mixture was cooled to room temperature and washed with DCM and $Na_2S_2O_3$ solution. The combined organic layers were dried and concentrated *in vacuo*. Compound **7m** was purified by silica gel column

chromatography (15:85 EtOAc:Hexanes) and obtained as an white amorphous solid (175 mg, 1.06 mmol, 29 % yield). R_f= 0.3 (15:85 EtOAc:Hexanes) ^{1}H NMR (400 MHz, $CDCl_3$) δ 7.25 (t, *J* = 2.0 Hz, 1H), 6.59 (dd, *J* = 2.9, 1.8 Hz, 1H), 6.51 (dd, *J* = 2.9, 2.2 Hz, 1H), 3.63 (s, 3H), 1.29 (s, 9H). ^{13}C{^{1}H} NMR (100 MHz, $CDCl_3$) δ 201.6, 127.33, 122.8, 122.1, 110.8, 43.5, 36.5, 28.2. The NMR data is consistent with literature values.[23]

(1-methyl-1H-pyrrol-2-yl)(*p*-tolyl)methanone (7n).

Lithium iodide (644 mg, 4.81 mmol, 1.3 equiv) and N-methylpyrrole (0.33 mL, 3.7 mmol, 1 equiv) were added to 5 mL of anhydrous MeCN and 4 Å molecular sieves. *p*-Toluoyl chloride (0.48 mL, 3.7 mmol. 1 equiv) was added to the solution and the mixture was immediately heated to 82^o C using an oil bath and stirred for 24 hours. The resulting mixture was cooled to room temperature and washed with DCM and $Na_2S_2O_3$ solution. The combined organic layers were dried and concentrated in vacuo. Compound **7n** was purified by silica gel column chromatography (15:85 EtOAc:Hexanes) and obtained as an white amorphous solid (175 mg, 0.879mmol, 24 % yield). R_f= 0.4 (15:85 EtOAc:Hexanes). ^{1}H NMR (400 MHz, $CDCl_3$) δ 7.82 – 7.65 (m, 2H), 7.31 – 7.19 (m, 2H), 6.91 – 6.87 (m, 1H), 6.74 (dd, *J* = 4.1, 1.7 Hz, 1H), 6.15 (dd, *J* = 4.1, 2.5 Hz, 1H), 4.02 (s, 3H), 2.42 (s, 3H). ^{13}C{^{1}H} NMR (100 MHz, $CDCl_3$) δ 186.0, 142.0, 137.2, 131.2, 130.6, 129.4, 128.8, 122.5, 108.0, 37.3, 21.6. The NMR data is consistent with literature values.[24]

1-methyl-2-trichloroacetyl-1H-pyrrole (7q).

At 0 °C, N-Methyl pyrrole (2.2 mL, 24.7 mmol, 1 equiv) was dissolved in diethyl ether (0.2 M). Trichloroacetyl chloride (2.8 mL, 24.7 mmol, 1 equiv) was added and allowed to stir overnight. The solution was diluted with EtOAc (25 mL) and washed with $NaHCO_3$ solution. The aqueous layer was then extracted twice with EtOAc (20 mL). The organic layer was then washed

consecutively with brine. The combined EtOAc layers were dried with $MgSO_4$ and concentrated *in vacuo*. Compound **7q** was obtained as a purple amorphous solid (5.5 g, 24.65 mmol, quant) and used without further purification. ^{1}H NMR (400 MHz, $CDCl_3$) δ 7.48 (dd, *J* = 4.4, 1.6 Hz, 1H), 6.98 – 6.89 (m, 1H), 6.20 (dd, *J* = 4.4, 2.4 Hz, 1H), 3.94 (s, 3H). $^{13}C\{^1H\}$ NMR (100 MHz, $CDCl_3$) δ 172.9, 133.8, 124.1, 121.8, 109.0, 96.3, 38.6. The NMR data is consistent with literature values.[25]

N-benzyl-1H-pyrrole-2-carboxamide (7r).

Prepared following general procedure 1. Compound **7r** was purified by silica gel column chromatography (40 % EtOAc/Hexanes) and was obtained as a white amorphous solid (177 mg, 83 % yield). R_f= 0.38 (40:60 EtOAc:Hexanes). ^{1}H NMR (400 MHz, $CDCl_3$) δ 7.37 – 7.21 (m, 5H), 6.83 (td, *J* = 2.7, 1.3 Hz, 1H), 6.70 – 6.61 (m, 2H), 6.19 (dt, *J* = 3.7, 2.5 Hz, 1H), 4.59 (d, *J* = 5.9 Hz, 2H). $^{13}C\{^1H\}$ NMR (100 MHz, $CDCl_3$) δ 161.6, 138.6, 128.7, 127.7, 127.5, 125.7, 122.2, 109.7, 109.6, 43.4. The NMR data is consistent with literature values.[26] HRMS (EI+/Magnetic sector) m/z: [M]+ calcd for $C_{12}H_{12}N_2O$: 200.0950. Found: 200.0965

N-(prop-2-yn-1-yl)-1H-pyrrole-2-carboxamide (7s).

Prepared following general procedure 1. Compound **7s** was purified by silica gel column chromatography (30 % EtOAc/Hexanes) and was obtained as a white amorphous solid (174 mg, 80 % yield). R_f= 0.35 (50:50 EtOAc:Hexanes). ^{1}H NMR (600 MHz, $CDCl_3$) δ 9.72 (s, 1H), 6.94 (ddd, *J* = 3.2, 2.3, 1.0 Hz, 1H), 6.60 (ddd, *J* = 3.9, 2.5, 1.3 Hz, 1H), 6.24 (dtd, *J* = 3.3, 2.6, 0.6 Hz, 1H), 6.08 (s, 1H), 4.22 (ddd, *J* = 5.5, 2.5, 0.6 Hz, 2H), 2.27 (td, *J* = 2.5, 0.6 Hz, 1H). $^{13}C\{^1H\}$ NMR (150 MHz, $CDCl_3$) δ 160.8, 122.0, 114.9, 110.0, 109.5, 79.7, 71.7, 29.1. The NMR data is consistent with literature values.[27] HRMS (EI+/Magnetic sector) m/z: [M]+ calcd for $C_8H_8N_2O$: 148.0637 Found: 148.0623.

N-methoxy-N-methylpyrrole-2-carboxamide (7t).

Prepared following general procedure 1. Compound **7t** was purified by silica gel column chromatography (40 % EtOAc/Hexanes) and was obtained as a yellow amorphous solid (120 mg, 64 % yield). R_f= 0.44 (40:60 EtOAc:Hexanes). ^{1}H NMR (400 MHz, $CDCl_3$) δ 9.73 (s, 1H), 6.93 (td, *J* = 2.8, 1.4 Hz, 1H), 6.89 (ddd, *J* = 3.8, 2.5, 1.4 Hz, 1H), 6.25 (dt, *J* = 3.8, 2.6 Hz, 1H), 3.75 (s, 3H), 3.33 (s, 3H). ^{13}C{^{1}H} NMR (100 MHz, $CDCl_3$) δ 161.4, 122.0, 114.9, 111.2 110.2, 61.1, 33.1. The NMR data is consistent with literature values.[28] HRMS (EI+/Magnetic sector) m/z: [M]+ calcd for $C_7H_{10}N_2O_2$: 154.0742 Found: 154.0744.

S-2-Pyrrolylthiobenzoat (7u).

Prepared following general procedure 1. Compound **7u** was purified by silica gel column chromatography (20 % EtOAc/Hexanes) and was obtained as a colourless oil (153 mg, 74 % yield) R_f= 0.3 (15:85 EtOAc:Hexanes). ^{1}H NMR (400 MHz, $CDCl_3$) δ 9.96 (s, 1H), 7.58 – 7.50 (m, 2H), 7.46 (tt, *J* = 3.9, 2.5 Hz, 3H), 7.16 (ddd, *J* = 3.9, 2.5, 1.4 Hz, 1H), 6.91 (td, *J* = 2.7, 1.4 Hz, 1H), 6.30 (dt, *J* = 3.9, 2.5 Hz, 1H). ^{13}C{^{1}H} NMR (100 MHz, $CDCl_3$) δ 180.3, 135.3, 129.4, 129.4, 129.1, 127.1, 124.7, 116.0, 110.9. HRMS (EI+/Magnetic sector) m/z: [M]+ calcd for $C_{11}H_9NOS$: 203.0405 Found: 203.0411.

Ethyl-2-pyrrolthiolcarboxylate (7v).

Prepared following general procedure 1. Compound **7v** was purified by silica gel chromatography (15 % EtOAc/Hexanes) and was obtained as a colourless oil (112 mg, 62 % yield). R_f= 0.33 (15:85 EtOAc:Hexanes) ^{1}H NMR (400 MHz, $CDCl_3$) δ 7.02 (ddt, *J* = 4.0, 2.8, 1.4 Hz, 2H), 6.25 (dt, *J* = 3.8, 2.5 Hz, 1H), 3.05 (q, *J* = 7.4 Hz, 2H), 1.34 (t, *J* = 7.4 Hz, 3H). ^{13}C{^{1}H} NMR (100 MHz, $CDCl_3$) δ 182.6, 130.4, 124.0, 115.3, 110.6, 22.7, 15.2. The NMR data

is consistent with literature values.[29] HRMS (EI+/Magnetic sector) m/z: [M]+ calcd for C_7H_9NOS: 155.0405 Found: 155.0415.

Methyl N-Boc-2-pyrrolecarboxylate (7x).

Methyl 1 H-pyrrole-2-carboxylate (0.20 g, 1.6 mmol, 1 equiv) was dissolved in MeCN (0.2 M). Boc_2O (0.418 g, 1.92 mmol, 1.2 equiv) and catalytic DMAP (19 mg, 0.08 mmol, 0.05 equiv) was added and allowed to stir for 4 hours at room temperature. The mixture was quenched with NH_4Cl solution and diluted with EtOAc. The aqueous layer was then extracted twice with EtOAc (20 mL). The combined EtOAc layers were dried with $MgSO_4$ and concentrated *in vacuo*. The residue was purified by silica gel column chromatography (5 % EtOAc/hexanes) to yield pure **7w** as an amorphous white solid (290 mg, 1.3 mmol, 81 % yield). R_f= 0.31 (5:95 EtOAc:hexanes). ^{1}H NMR (400 MHz, $CDCl_3$) δ 7.28 (dd, *J* = 3.1, 1.7 Hz, 1H), 6.80 (dd, *J* = 3.5, 1.7 Hz, 1H), 6.17 – 6.09 (m, 1H), 3.80 (s, 3H), 1.55 (s, 9H). $^{13}C\{^1H\}$ NMR (100 MHz, $CDCl_3$) δ 161.3, 148.4, 126.7, 125.1, 120.8, 110.1, 84.7, 51.8, 27.6. The NMR data is consistent with literature values.[30] HRMS (EI+/Magnetic sector) m/z: [M]+ calcd for $C_{11}H_{15}NO_4$: 225.1001 Found: 225.1003.

2,3,4-trichloro-5-oxo-1-H-2,5-dihydro-pyrrole-2-carboxylic acid methyl ester (8a).

Prepared following general procedure 3. Purification by silica gel chromatography (10 % EtOAc/Hexanes) yielded **8a** as a colourless oil (221 mg, 94 % yield). R_f= 0.6 (20:80 EtOAc:Hexanes) ^{1}H NMR (400 MHz, $CDCl_3$) δ 3.83 (s, 3H). $^{13}C\{^1H\}$ NMR (100 MHz, $CDCl_3$) δ 166.2, 162.0, 149.7, 127.9, 88.3, 54.9. HRMS (EI+/Magnetic sector) m/z: [M]+ calcd for $C_6H_4Cl_3NO_3$: 242.9257 Found: 242.9246.

2,3,4-trichloro-5-oxo-1-methyl-2,5-dihydro-pyrrole-2-carboxylic acid methyl ester (8b).

Prepared following general procedure 3. Purification by silica gel chromatography (10 % EtOAc/Hexanes) yielded Compound **8b** as a colourless oil (136 mg, 91 % yield). R_f= 0.4 (15:85 EtOAc:Hexanes) ^{1}H NMR (600 MHz, Chloroform-*d*) δ 3.86 (s, 3H), 3.01 (s, 3H). ^{13}C{^{1}H} NMR (150 MHz, $CDCl_3$) δ 162.57, 162.1, 142.6, 128.2, 83.4, 55.1, 26.7. HRMS (EI+/Magnetic sector) m/z: [M]+ calcd for $C_7H_6Cl_3NO_3$: 256.9413 Found:256.9422.

2,3,4-trichloro-5-oxo-1-hexyl-2,5-dihydro-pyrrole-2-carboxylic acid methyl ester (8c).

Prepared following general procedure 3. Purification by silica gel chromatography (5 % EtOAc/hexanes) yielded compound **8c** as a colourless oil (124 mg, 84 % yield). R_f= 0.25 (10:90 EtOAc:hexanes). ^{1}H NMR (600 MHz, Chloroform-*d*) δ 3.87 (s, 3H), 3.47 (t, *J* = 7.9 Hz, 2H), 1.70 – 1.55 (m, 2H), 1.33 – 1.27 (m, 6H), 0.91 – 0.86 (m, 3H). ^{13}C{^{1}H} NMR (150 MHz, $CDCl_3$) δ 163.1, 162.6, 142.7, 128.0, 83.8, 54.9, 42.3, 31.3, 27.8, 26.5, 22.5, 14.0. HRMS (EI+/Magnetic sector) m/z: [M]+ calcd for $C_{12}H_{16}Cl_3NO_3$: 327.0196 Found: 327.0201.

2,3,4-trichloro-5-oxo-1-dodecyl-2,5-dihydro-pyrrole-2-carboxylic acid methyl ester (8d).

Prepared following general procedure 3. Purification by silica gel chromatography (5 % EtOAc/hexanes) yielded compound **8d** as a colourless oil (154 mg, 81 % yield). R_f= 0.25 (5:95 EtOAc:hexanes). ^{1}H NMR (400 MHz, $CDCl_3$) δ 3.85 (s, 3H), 3.45 (t, *J* = 7.8 Hz, 2H), 1.70 – 1.47 (m, 2H), 1.25 (d, *J* = 13.0 Hz, 18H), 0.90 – 0.80 (m, 3H).^{13}C{^{1}H} NMR (100 MHz, $CDCl_3$) δ 163.1, 162.5, 142.7, 127.9, 83.8, 54.9, 42.3, 31.9, 29.6, 29.5, 29.5, 29.5, 29.3, 29.2, 27.9, 26.8, 22.7, 14.1.HRMS (EI+/Magnetic sector) m/z: [M]+ calcd for $C_{18}H_{28}Cl_3NO_3$: 411.1135 Found: 411.1140.

2,3,4-trichloro-5-oxo-1-(1-ethoxy-1-oxopropan-2-yl)-2,5-dihydro-pyrrole-2-carboxylic acid methyl ester (8e).

Prepared following general procedure 3. Purification by silica gel chromatography (25 % EtOAc/hexanes) yielded a colourless oil **8e** as an inseparable 1:1.2 mixture of diastereomers (84 mg, 78 % yield). R_f= 0.25 (10:90 EtOAc:hexanes). ^{1}H NMR (400 MHz, $CDCl_3$) δ 4.53 – 4.45 (m, 1H), 4.42 (t, *J* = 7.3 Hz, 1H), 4.23 – 4.14 (m, 4H), 3.88 (s, 3H), 3.84 (s, 2H), 1.67 (dd, *J* = 14.1, 7.4 Hz, 6H), 1.24 (td, *J* = 4.2, 2.1 Hz, 6H). ^{13}C{^{1}H} NMR (101 MHz, $CDCl_3$) δ 169.3, 169.1, 162.9, 162.6, 161.7, 161.2, 143.4, 143.3, 128.0, 82.6, 82.5, 62.0, 54.9, 54.8, 52.2, 51.8, 15.19, 15.15, 14.10, 14.06. HRMS (ESI+/Q-TOF) m/z: [M+Na]+ Calcd. For $C_{11}H_{12}Cl_3NO_5Na$ 365.9679; Found: 365.9675

2,3,4-trichloro-5-oxo-1-methyl-2,5-dihydro-pyrrole-2-carboxylic acid *t*-butyl ester (8f).

Prepared following general procedure 3. Purification by silica gel chromatography (10 % EtOAc/hexanes) yielded pure **8f** as a colourless oil (507 mg, 81 % yield). R_f= 0.34 (10 % EtOAc/hexanes) ^{1}H NMR (400 MHz, $CDCl_3$) δ, 3.01 (s, 3H), 1.46 (s, 9H). ^{13}C{^{1}H} NMR (100 MHz, $CDCl_3$) δ 162.3, 160.4, 143.0, 127.7, 86.7, 84.0, 28.0, 26.5. HRMS (EI+/Magnetic sector) m/z: [M]+ calcd for $C_{10}H_{12}Cl_3NO_3$: 298.9883 Found: 298.9892

2,3,4-trichloro-5-oxo-1-methyl-2,5-dihydro-pyrrole-2-carboxylic acid benzyl ester (8g).

Prepared following general procedure 3. Purification by silica gel chromatography (10 % EtOAc/hexanes) yielded pure **8g** as an amorphous white solid (507 mg, 77 % yield). R_f = 0.1 (10:90 EtOAc:hexanes) ^{1}H NMR (400 MHz, $CDCl_3$) δ 7.40 – 7.29 (m, 5H), 5.30 – 5.21 (m, 2H), 2.94 (s, 3H). ^{13}C{^{1}H} NMR (100 MHz, $CDCl_3$) δ 162.0, 161.9, 142.6, 133.9, 129.2, 128.9, 128.6, 128.3, 83.5, 70.0, 26.6. HRMS (EI+/Magnetic sector) m/z: [M]+ calcd for $C_{13}H_{10}Cl_3NO_3$: 332.9726 Found: 332.9736.

2,3,4-trichloro-5-oxo-1-methyl-2,5-dihydro-pyrrole-2-carboxylic acid trimethylsilylethyl ester (8h).

Prepared following general procedure 3. Purification by silica gel chromatography (10 % EtOAc/hexanes) yielded pure **8h** as a colourless oil (507 mg, 74 % yield). R_f = 0.25 (5:95 EtOAc:hexanes). ^{1}H NMR (400 MHz, $CDCl_3$) δ 4.32 – 4.23 (m, 2H), 2.97 (s, 3H), 1.02 – 0.93 (m, 2H) 0.02 (s, 9H). $^{13}C\{^1H\}$ NMR (100 MHz, $CDCl_3$) δ 162.0, 161.9, 142.7, 128.0, 83.5, 67.5, 26.5, 17.4, -1.6. HRMS (EI+/Magnetic sector) m/z: [M]+ calcd for $C_{11}H_{16}Cl_3NO_3Si$: 342.9965 Found: 342.9948.

2,3,4-trichloro-5-oxo-1-H-2,5-dihydro-pyrrole-2-carboxylic acid phenol ester (8i).

Prepared following general procedure 3. Purification by silica gel chromatography (5:95 EtOAc:Hexanes) yielded **8i** as an amorphous white solid (207 mg, 84 % yield). R_f= 0.55 (5:95 EtOAc:Hexanes) ^{1}H NMR (600 MHz, $CDCl_3$) δ 7.31 – 7.27 (m, 2H), 7.20 – 7.15 (m, 1H), 7.02 – 6.99 (m, 2H). $^{13}C\{^1H\}$ NMR (150 MHz, $CDCl_3$) δ 166.8, 160.3, 150.2, 149.5, 129.8, 128.4, 127.0, 120.8, 88.6. HRMS (EI+/Magnetic sector) m/z: [M]+ calcd for $C_{11}H_6Cl_3NO_3$: 304.9413 Found: 304.9419

2,3,4-trichloro-5-oxo-1-H-2,5-dihydro-pyrrole-2-carboxylic acid propylamide (8j).

Prepared following general procedure 3. Purification by silica gel chromatography (25 % EtOAc/Hexanes) yielded pure **8j** as an amorphous white solid (84 mg, 80 % yield). R_f = 0.4 (50:50 EtOAc:Hexanes) ^{1}H NMR (400 MHz, Acetone) δ 6.55 (s, 1H), 3.29 – 3.15 (m, 2H), 1.54 (h, *J* = 7.2 Hz, 2H), 0.89 (t, *J* = 7.4 Hz, 3H). $^{13}C\{^1H\}$ NMR (100 MHz, Acetone) δ 165.4, 164.0, 145.3, 126.4, 86.5, 41.5, 22.4, 10.7. HRMS (EI+/Magnetic sector) m/z: [M]+ calcd for $C_8H_9Cl_3N_2O_2$: 269.9730 Found:269.9721.

2,3,4-trichloro-5-oxo-1-H-2,5-dihydro-pyrrole-2-carboxylic acid piperidine amide (8k).

Prepared following general procedure 3. Purification by silica gel chromatography (25 % EtOAc/hexanes) yielded pure **8k** as an amorphous white solid (86 mg, 72 % yield). R_f= 0.45

(40:60 EtOAc:Hexanes). ^{1}H NMR (400 MHz, $CDCl_3$) δ 4.09 – 3.87 (m, 2H), 3.52 (tt, *J* = 14.5, 8.7 Hz, 2H), 1.95 – 1.36 (m, 7H). $^{13}C\{^{1}H\}$ NMR (100 MHz, $CDCl_3$) δ 165.8, 159.7, 154.3, 126.1, 87.4, 48.3, 45.0, 25.9, 25.6, 24.3. HRMS (EI+/Magnetic sector) m/z: [M]+ calcd for $C_{10}H_{11}Cl_3N_2O_2$: 295.9886 Found: 295.9874.

Methyl 2,3,4-tribromo-5-oxo-2,5-dihydro-1H-pyrrole-2-carboxylate (18).

Prepared following general procedure 3 with modification that NCS was replaced with NBS. Purification by silica gel chromatography (10 % EtOAc/hexanes) yielded the brominated analogue **18** as an orange amorphous solid (101 mg, 96 % yield). R_f= 0.4 (10:90 EtOAc:Hexanes). ^{1}H NMR (400 MHz, $CDCl_3$) δ 3.83 (s, 3H). $^{13}C\{^{1}H\}$ NMR (101 MHz, $CDCl_3$) δ 162.3, 159.9, 144.8, 124.2, 81.3, 54.9. HRMS (EI+/Magnetic sector) m/z: [M]+ calcd for $C_6H_4{}^{79}Br_2{}^{81}Br_1N_1O_2$: 360.7771. $C_6H_4{}^{79}Br_2{}^{81}Br_1N_1O_2$ Found:360.7768

Compounds from Figure 3

2-(1-hexyl-2-hydroxy-6-methoxy-3-benzoyl)-1H-pyrrole (3).

In a round-bottom flask, **9** (0.830 g, 2.63 mmol, 1.0 equiv.) was dissolved in 1,2-dichloroethane (3 mL). The solution was cooled to -20 °C using a dry ice/acetone bath. BBr_3 (3.13 mL of a 1 M solution in DCM, 3.13 mmol, 1.2 equiv.) was added dropwise, and the reaction mixture was stirred at -20 to – 10 °C for 2 hours. Subsequently, Et_3N / water was added, and the solution was extracted 3 × with EtOAc. The organic fractions were combined, washed with brine, dried over Na_2SO_4, and concentrated. The desired compound **3** (0.788 g, 99 % yield) was obtained as a yellow amorphous solid and used without purification. ^{1}H NMR (400 MHz, Acetone-d6) δ 12.76 (s, 1H), 8.05 (dd, J = 8.9, 0.9 Hz, 1H), 7.27 (ddd, J = 3.0, 2.5, 1.4 Hz, 1H), 7.05 (dtd, J = 4.2, 2.8, 1.3 Hz, 1H), 6.67 (d, J = 9.0 Hz, 1H), 6.36 (ddd, J = 3.9, 2.9, 2.0 Hz, 1H), 3.93 (s, 3H), 2.73 – 2.58 (m, 2H), 1.59 – 1.42 (m, 2H), 1.40 – 1.26 (m, 6H), 0.91 – 0.82 (m, 3H). $^{13}C\{^{1}H\}$ NMR (100

MHz, Acetone-d6) δ 186.2, 162.8, 162.0, 130.7, 130.0, 125.5, 118.5, 117.9, 113.4, 110.7, 102.2, 55.3, 31.6, 29.3, 28.6, 22.5, 22.2, 13.5. NMR data matched literature values.[3]

5-Chloro-6-methoxy-N-desmethyl armeniaspirol (4).

In a round-bottom flask, **3** (0.7 g, 2.32 mmol, 1.0 equiv) was dissolved in acetic acid (0.2 M). NCS (0.619 g, 4.64 mmol, 2.0 equiv) was added and the resulting mixture was stirred at room temperature for 2 hours. Following this, NCS (1.24 g, 9.29 mmol, 4.0 equiv) was added, and the resulting mixture was heated to 70 °C using an oil bath for 16 hours. The mixture was then quenched with a 10 % K_2CO_3 solution and extracted three times with EtOAc. The organic fractions were combined, washed with brine, dried over $MgSO_4$ and concentrated in vacuo. The resulting oil was dissolved in $CHCl_3$ (0.2M) and Et_3N (0.97 mL, 6.96 mmol, 3 equiv.) and the mixture was heated at 60 °C using an oil bath for 5 hours. The solution was cooled to room temperature, concentrated *in vacuo*, and the spiro-intermediate **4** (0.745 g, 1.78 mmol, 77 % yield) was purified from the crude mixture by silica gel column chromatography (10 % EtOAc/Hexanes) and was obtained as a yellow oil. ^{1}H NMR (400 MHz, $CDCl_3$) δ 7.60 (s, 1H), 7.55 (s, 1H), 3.97 (s, 3H), 2.70 (td, *J* = 7.5, 4.0 Hz, 2H), 1.61 – 1.55 (m, 2H), 1.36 – 1.27 (m, 6H), 0.89 – 0.86 (m, 3H). ^{13}C{^{1}H} NMR (100 MHz, $CDCl_3$) δ 189.7, 169.8, 165.4, 163.5, 140.7, 128.4, 124.6, 124.3, 123.7, 115.1, 94.09, 61.7, 31.6, 29.3, 29.3, 23.9, 22.6, 14.1. HRMS (EI+/Magnetic sector) m/z: [M]+ calcd for $C_{18}H_{18}Cl_3NO_4$: 417.0301 Found: 417.0312.

2-(1-hexyl-2'6-dimethoxy-3-benzoyl)-1H-pyrrole (9).

Pyrrole 2-carboxylic acid (0.721 g, 6.49 mmol, 2 eq) was dissolved in 10 ml of DCM. Oxalyl chloride (9.7 mL of a 2.5M solution in DCM, 19.5 mmol, 3 equiv.) was added dropwise, 1 drop of DMF was added. The following mixture was stirred for 1 hour at room temperature. The solvent was removed *en vacuo*. The intermediate acid chloride was resuspended in DCM In a

round-bottom flask, 2-hexyl-1,3-dimethoxybenzene[3] (0.50 g, 3.25 mmol, 1.0 equiv.) was added and cooled to 0 °C with an ice bath. added, followed by $SnCl_4$ (16.2 mL of a 1.0 M solution in DCM, 16.2 mmol, 5 equiv.). The mixture was stirred for 1 hour at 0 °C, then warmed to ambient temperature. The reaction mixture was quenched with a saturated $NaHCO_3$(aq) and extracted 3 × with EtOAc. The organic fractions were combined, washed with brine, dried over Na_2SO_4 and concentrated. The desired compound **9** (0.640 g, 78 % yield) was purified from the crude mixture by silica column chromatography (30 % EtOAc/Hexanes) and was obtained as a white amorphous solid. The NMR data were consistent with literature values ^{1}H NMR (400 MHz, Acetone-d6) δ 7.30 (d, *J* = 8.5 Hz, 1H), 7.19 (dq, *J* = 2.9, 1.5 Hz, 1H), 6.80 (d, J = 8.6 Hz, 1H), 6.59 (ddd, *J* = 3.8, 2.2, 1.4 Hz, 1H), 6.23 (dt, *J* = 3.8, 2.3 Hz, 1H), 3.89 (s, 3H), 3.67 (s, 3H), 2.70 – 2.57 (m, 2H), 1.52 (q, *J* = 7.7 Hz, 2H), 1.42 – 1.24 (m, 6H), 0.93 – 0.82 (m, 3H). ^{13}C{^{1}H} NMR (100 MHz, Acetone-d6) δ 183.6, 160.1, 157.5, 132.6, 128.2, 125.8, 125.2, 124.4, 118.5, 109.9, 105.1, 61.9, 55.3, 31.6, 29.4, 23.4, 22.4, 13.5. NMR data matched literature values.[3]

2,4-dimethoxy-3-hexylbenzoic acid (10).

In a round-bottom flask, **9** (42 mg, 0.127 mmol, 1.0 equiv) was dissolved in DCE (0.2 M). Following this, NCS (51 mg, 0.382 mmol, 3.0 equiv) was added and the resulting mixture was heated to 70 °C using an oil bath for 8 hours. The reaction mixture was then quenched with a 10 % HCl solution and extracted three times with EtOAc. The organic fractions were combined, washed with brine, dried over $MgSO_4$ and concentrated in vacuo. Compound **10** (23 mg, 0.087 mmol, 69 % yield) was purified from the crude mixture using silica gel column chromatography and was obtained as an amorphous white solid (35 % EtOAc/Hexanes). R_f= 0.3 (35:65 EtOAc:Hexanes). ^{1}H NMR (400 MHz, $CDCl_3$) δ 8.00 (d, *J* = 8.8 Hz, 1H), 6.78 (d, *J* = 8.8 Hz, 1H), 3.90 (d, *J* = 4.4 Hz, 6H), 2.69 – 2.56 (m, 2H), 1.57 – 1.47 (m, 2H), 1.39 – 1.27 (m, 6H),

0.93 – 0.85 (m, 3H). $^{13}C\{^{1}H\}$ NMR (100 MHz, $CDCl_3$) δ 166.0, 163.1, 158.5, 131.9, 124.9, 114.3, 107.5, 63.6, 55.9, 31.6, 29.6, 29.3, 23.9, 22.6, 14.1. HRMS (ESI+/Q-TOF) m/z: [M+Na]+ calcd for $C_{15}H_{22}O_4Na$ 289.1416. Found: 289.1428

Tetrachloropyrrole (11).

Prepared following general procedure 3, using pyrrole-2-carboxylic acid (43mg, 0.388mmol, 1 equiv) as starting material. Purification by silica gel chromatography (20 % EtOAc/Hexanes) yielded pure tetrachloropyrrole **11** as an amorphous brown solid (31 mg, 0.151 mmol, 39 % yield). R_f= 0.35 (20:80 EtOAc:Hexanes). ^{1}H NMR (600 MHz, $CDCl_3$) δ 8.19 (s, 1H). $^{13}C\{^{1}H\}$ NMR (150 MHz, $CDCl_3$) δ 110.3, 109.5. HRMS data could not be collected. All attempts to ionize **11** failed.

3,4-dichloromaleimide (12).

Prepared following general procedure 3, using pyrrole-2-carboxylic acid (43 mg, 0.388 mmol, 1 equiv) as starting material. Purification by silica gel chromatography (20 % EtOAc/Hexanes) yielded pure maleamide **12** as an amorphous white solid (27 mg, 0.163 mmol, 42 % yield). R_f= 0.27 (20:80 EtOAc:Hexanes). ^{1}H NMR (600 MHz, $CDCl_3$) δ 7.77 (s, 1H). $^{13}C\{^{1}H\}$ NMR (150 MHz, $CDCl_3$) δ 162.1, 134.2. NMR data was consistent with literature values.[31] HRMS (EI+/Magnetic sector) m/z: [M]+ calcd for $C_4H_1Cl_2NO_2$: 164.9384 Found: 164.9389

Compounds from Figure 4.

1H-4,5-dichloro-pyrrole-2-(1-hexyl-2-hydroxy-6-methoxy-3-benzoyl) (13).

In a round-bottom flask, **3** (29.5 mg, 0.097 mmol, 1.0 equiv) were dissolved in acetic acid (0.2 M). Following this, NCS (39 mg, 0.294 mmol, 3.0 equiv) was added and the resulting mixture was heated to 70 °C using an oil bath for 8 hours. The reaction mixture was then quenched with

a 10 % K_2CO_3 solution and extracted three times with EtOAc. The organic fractions were combined, washed with brine, dried over $MgSO_4$ and concentrated in vacuo. The desired compound **13,** was purified from the crude mixture using preparative TLC (15 % EtOAc/Hexanes) and was obtained as an amorphous yellow solid (32 mg, 88 % yield). ^{1}H NMR (600 MHz, $CDCl_3$) δ 11.92 (s, 1H), 7.81 (s, 1H), 6.95 (d, *J* = 2.5 Hz, 1H), 3.92 (s, 3H), 2.73 – 2.61 (m, 2H), 1.56 – 1.51 (m, 2H), 1.40 (p, *J* = 7.4 Hz, 2H), 1.34 – 1.30 (m, 4H), 0.90 – 0.87 (m, 3H). ^{13}C{^{1}H} NMR (150 MHz, $CDCl_3$) δ 183.4, 161.3, 160.0, 128.8, 127.5, 126.9, 121.3, 118.3, 118.2, 115.2, 112.8, 61.3, 31.7, 29.6, 29.3, 24.2, 22.6, 14.1. HRMS (EI+/Magnetic sector) m/z: [M]+ calcd for $C_{18}H_{20}Cl_3NO_3$: 403.0509 Found: 403.0512.

Spirocyclic-α,β,β-trichlorolactam (14).

In a round-bottom flask, **13** (16 mg, 0.0514 mmol, 1.0 equiv) were dissolved in acetic acid (0.2 M) and NCS was added (7 mg, 0.0514 mmol, 1.0 equiv). The mixture was heated to 70 °C using an oil bath for 1 hour. The reaction was quenched with 10 % Na_2CO_3 solution and the mixture was extracted three times with EtOAc. The organic fractions were combined, washed with brine, dried over $MgSO_4$, and concentrated *in vacuo*. The desired compound was purified from the crude mixture using Preparative TLC (15 % EtOAc/hexanes) affording **14** as a yellow oil (11 mg, 0.0242mmol, 47 % yield). R_f= 0.25 (17:83 EtOAc:hexanes). ^{1}H NMR (600 MHz, $CDCl_3$) δ 7.59 (s, 1H), 7.13 (s, 1H), 4.89 (s, 1H), 3.97 (s, 3H), 2.74 – 2.65 (m, 2H), 1.37 – 1.27 (m, 10H), 0.88 (q, *J* = 3.5 Hz, 3H). ^{13}C{^{1}H} NMR (150 MHz, $CDCl_3$) δ 190.8, 170.0, 166.3, 163.9, 124.8, 124.1, 123.2, 114.6, 92.4, 79.7, 68.0, 61.8, 31.5, 29.3, 28.8, 23.9, 22.5, 14.1. HRMS (EI+/Magnetic sector) m/z: [M]+ calcd for $C_{18}H_{19}Cl_4NO_4$: 453.0068 Found: 453.0081.

Compounds from Figure 5

2-hexyl-3 methoxy phenol (6).

In a round-bottom flask, 2-hexyl-1,3-dimethoxybenzene[3] (0.322 g, 1.61 mmol, 1.0 equiv) was dissolved in DCE (3 mL). The solution was cooled to -20 °C using a dry ice/acetone bath. BBr_3 (1.9 mL of a 1 M solution in DCM, 1.9 mmol, 1.2 equiv) was added dropwise, and the reaction mixture was stirred at -20 to – 10 °C for 2 hours. Subsequently, Et_3N / water was added, and the solution was extracted three times with EtOAc. The organic fractions were combined, washed with brine, dried over $MgSO_4$, and concentrated in vacuo. Purification by silica gel chromatography (10 % EtOAc/Hexanes) yielded pure compound **6** as an orange oil (243 mg, 1.31 mmol, 81 % yield). ^{1}H NMR (600 MHz, $CDCl_3$) δ 7.04 (t, *J* = 8.2 Hz, 1H), 6.50 (dd, *J* = 8.3, 1.0 Hz, 1H), 6.46 (dd, *J* = 8.1, 1.0 Hz, 1H), 4.68 – 4.61 (m, 1H), 3.82 (s, 3H), 2.67 – 2.60 (m, 2H), 1.56 – 1.49 (m, 2H), 1.38 (dddd, *J* = 13.9, 8.2, 6.1, 3.3 Hz, 2H), 1.35 – 1.30 (m, 4H), 0.93 – 0.87 (m, 3H). ^{13}C{^{1}H} NMR (150 MHz, $CDCl_3$) δ 158.6, 154.2, 126.6, 117.2, 108.2, 103.2, 55.7, 31.8, 29.5, 29.1, 23.0, 22.7, 14.2. HRMS (EI+/Magnetic sector) m/z: [M]+ calcd for $C_{13}H_{20}O_2$: 208.1463 Found: 208.1458.

***N,O*-ketal (5).**

Phenol **6** (23 mg, 0.124 mmol, 1 equiv) was suspended in acetone and K_2CO_3 (51 mg, 0.372 mmol, 3 equiv) was added and allowed to stir at room temperature for 10 minutes. **7b** (32 mg, 0.124 mmol, 1 equiv) was added and allowed to stir overnight. The mixture was filtered and concentrated in vacuo to yield pure **5** as a colourless oil (38 mg, 0.088 mmol, 71 % yield), which was used without further purification. ^{1}H NMR (400 MHz, Chloroform-*d*) δ 6.94 (t, *J* = 8.3 Hz, 1H), 6.61 (d, *J* = 8.3 Hz, 1H), 6.21 (dd, *J* = 8.4, 0.9 Hz, 1H), 3.89 (s, 3H), 3.78 (s, 3H), 2.95 (s, 3H), 2.81 (dt, *J* = 12.4, 7.5 Hz, 1H), 2.72 (dt, *J* = 12.4, 7.2 Hz, 1H), 1.58 – 1.47 (m, 2H), 1.32 (m, 6H), 0.87 (m, 3H). ^{13}C{^{1}H} NMR (100 MHz, $CDCl_3$) δ 164.3, 162.8, 158.7, 151.8, 140.5,

130.1, 126.7, 123.7, 109.2, 107.0, 93.1, 55.6, 54.1, 31.7, 29.6, 29.2, 26.2, 24.0, 22.7, 14.1. HRMS (EI+/Magnetic sector) m/z: [M]+ calcd for $C_{20}H_{25}Cl_2NO_5$: 429.1110 Found: 429.1130.

6-methoxy pseudoarmeniaspirol A (15).

N,O-ketal **5** (38 mg, 0.088 mmol, 1 equiv) was dissolved in DCM (0.05M) and a Tin (IV) chloride solution (0.264 mL of a 1 M solution in DCM, 0.0264 mmol, 3 equiv) was added dropwise. The mixture was stirred at room temperature overnight and quenched with brine. The aqueous layer was then extracted twice with EtOAc (20 mL). The combined EtOAc layers were dried with $MgSO_4$ and concentrated in vacuo. Purification by silica gel chromatography (12.5 % EtOAc/Hexanes) yielded pure **15** as a yellow oil (17 mg, 0.043 mmol, 49 % yield). R_f= 0.4 (20:80 EtOAc:Hexanes). ^{1}H NMR (400 MHz, Chloroform-*d*) δ 6.93 (d, *J* = 8.4 Hz, 1H), 6.73 (d, *J* = 8.5 Hz, 1H), 3.89 (s, 3H), 2.78 (s, 3H), 2.70 (td, *J* = 7.2, 1.5 Hz, 2H), 1.56 (d, *J* = 7.3 Hz, 2H), 1.37 – 1.27 (m, 6H), 0.91 – 0.86 (m, 3H). ^{13}C{^{1}H} NMR (100 MHz, $CDCl_3$) δ 169.3, 163.8, 161.1, 153.7, 140.6, 128.0, 122.6, 116.8, 110.5, 107.5, 73.5, 56.0, 31.6, 29.1, 28.8, 26.8, 23.6, 22.6, 14.0. HRMS (EI+/Magnetic sector) m/z: [M]+ calcd for $C_{19}H_{21}Cl_2NO_4$: 397.0848 Found 397.0844.

Pseudoarmeniaspirol A (1).

In a round-bottom flask, **15** (17 mg, 0.043 mmol, 1.0 equiv) was dissolved in DCE (0.4 M). The mixture was cooled to 0 °C using an ice bath and BBr_3 solution (0.129 mL of a 1 M solution in DCM, 0.129 mmol, 3.0 equiv) was added dropwise. The reaction was allowed to proceed for 4 hours from 0 °C to room temperature. Water was added, and the solution was extracted three times with EtOAc. The organic fractions were combined, washed with brine, dried over $MgSO_4$, and concentrated in vacuo. The final compound was purified from the crude mixture using Preparative TLC (25 % EtOAc/Hexanes) yielding **1** as a tan amorphous solid (13 mg, 78 %

yield). R_f= 0.3 (20:80 EtOAc:Hexanes). ^{1}H NMR (400 MHz, $CDCl_3$) δ 6.83 (d, *J* = 8.2 Hz, 1H), 6.72 (d, *J* = 8.2 Hz, 1H), 6.01 (s, 1H), 2.79 (s, 3H), 2.77 – 2.67 (m, 2H), 1.67 – 1.55 (m, 2H), 1.41 – 1.23 (m, 6H), 0.88 (td, *J* = 6.2, 3.7 Hz, 3H). $^{13}C\{^1H\}$ NMR (100 MHz, $CDCl_3$) δ 169.3, 164.1, 157.8, 154.2, 140.7, 127.9, 122.6, 115.1, 112.7, 110.1, 73.6, 31.6, 29.1, 28.8, 26.9, 23.7, 22.6, 14.1. HRMS (EI+/Magnetic sector) m/z: [M]+ calcd for $C_{18}H_{19}Cl_2NO_4$: 383.0691 Found 383.0659.

N-hexyl-pseudoarmeniaspirol (16).

In a round-bottom flask, **SI2** (19 mg, 0.0405 mmol, 1.0 equiv) were dissolved in DCE (0.4 M). The mixture was cooled to 0 °C using an ice bath and BBr_3 (0.122 mL of a 1 M solution in DCM, 0.122 mmol, 3.0 equiv) was added dropwise. The reaction was allowed to proceed for 4 hours from 0 °C to room temperature. Water was added, and the solution was extracted three times with EtOAc. The organic fractions were combined, washed with brine, dried over $MgSO_4$, and concentrated in vacuo. The desired compound (14 mg, 76 % yield) was purified from the crude mixture using Preparative TLC (20 % EtOAc in hexanes) yielding **16** as a white amorphous solid. R_f= 0.35 (20:80 EtOAc:Hexanes). ^{1}H NMR (600 MHz, Chloroform-*d*) δ 6.82 (d, *J* = 8.2 Hz, 1H), 6.69 (d, *J* = 8.2 Hz, 1H), 3.34 (ddd, *J* = 14.3, 8.8, 7.0 Hz, 1H), 3.09 (ddd, *J* = 14.5, 8.5, 6.2 Hz, 1H), 2.73 (t, *J* = 7.6 Hz, 2H), 1.61 (dp, *J* = 12.4, 6.7, 6.2 Hz, 4H), 1.22 – 1.11 (m, 12H), 0.91 – 0.85 (m, 3H), 0.82 (t, *J* = 7.1 Hz, 3H). $^{13}C\{^1H\}$ NMR (150 MHz, $CDCl_3$) δ 169.9, 164.2, 157.5, 154.0, 140.6, 128.0, 122.8, 114.9, 112.6, 110.7, 73.1, 42.3, 31.6, 31.1, 29.0, 28.7, 28.1, 26.2, 23.6, 22.6, 22.4, 14.1, 14.0. HRMS (EI+/Magnetic sector) m/z: [M]+ calcd for $C_{23}H_{29}Cl_2NO_4$: 453.1474 Found 453.1468.

N-dodecyl-1-methyl-pseudoarmeniaspirol (17).

In a round-bottom flask, **SI4** (16 mg, 0.033 mmol, 1.0 equiv) were dissolved in DCE (0.4 M). The mixture was cooled to 0 °C using an ice bath and BBr_3 (0.1mL of a 1 M solution in DCM, 0.1 mmol, 3.0 equiv) was added dropwise. The reaction was allowed to proceed for 4 hours from 0 °C to room temperature. Water was added, and the solution was extracted three times with EtOAc. The organic fractions were combined, washed with brine, dried over $MgSO_4$, and concentrated in vacuo. The product was purified from the crude mixture using preparative TLC (15 % EtOAc in hexanes) affording pure **17** as a colourless oil (10 mg, 0.0213 mmol, 64 % yield). R_f= 0.2 (10:90 EtOAc:Hexanes). ^{1}H NMR (600 MHz, Chloroform-*d*) δ 6.83 (d, *J* = 8.2 Hz, 1H), 6.70 (d, *J* = 8.2 Hz, 1H), 3.35 – 3.26 (m, 1H), 3.10 (ddd, *J* = 14.4, 8.0, 6.5 Hz, 1H), 2.27 (s, 3H), 1.34 – 1.14 (m, 20H), 0.91 – 0.85 (m, 3H). ^{13}C{^{1}H} NMR (150 MHz, $CDCl_3$) δ 169.8, 164.2, 157.7, 154.0, 140.5, 128.0, 122.7, 112.2, 110.8, 109.9, 73.2, 42.3, 31.9, 29.64, 29.62, 29.5, 29.37, 29.35, 29.0, 28.2, 26.6, 22.7, 14.1, 8.7. HRMS (EI+/Magnetic sector) m/z: [M]+ calcd for $C_{24}H_{31}Cl_2NO_4$: 467.1630 Found: 467.1618.

Synthesis of N-Hexyl-pseudoarmeniaspirol **16**

SI1 – N hexyl – *N,O* ketal

Phenol **6,** (20 mg, 0.1075mmol, 1 equiv) was suspended in acetone and K_2CO_3 (44mg, 0.323 mmol, 3 equiv) and allowed to stir at room temperature for 10 minutes. **8c** (35 mg, 0.1075mmol, 1 equiv) was added and allowed to stir overnight. The reaction was filtered and concentrated to yield **SI1** as a clear oil (35 mg, 0.07mmol, 65%), which was used without further purification. ^{1}H NMR (400 MHz, Chloroform-*d*) δ 6.95 (t, *J* = 8.3 Hz, 1H), 6.62 (d, *J* = 8.3 Hz, 1H), 6.23 (d, *J* = 8.3 Hz, 1H), 3.88 (s, 3H), 3.80 (s, 3H), 3.45 (dt, *J* = 13.8, 8.1 Hz, 1H), 3.37 – 3.20 (m, 1H), 2.78 (qt, *J* = 12.4, 7.6 Hz, 2H), 1.54 (dt, *J* = 16.8, 8.2 Hz, 4H), 1.43 – 1.16 (m, 14H), 0.92 – 0.81 (m,

7H). $^{13}C\{^{1}H\}$ NMR (100 MHz, $CDCl_3$) δ 164.8, 163.2, 158.6, 152.1, 140.4, 130.0, 126.6, 123.5, 109.0, 106.7, 92.8, 55.6, 54.0, 41.6, 31.8, 31.3, 29.6, 29.2, 27.8, 26.6, 23.9, 22.7, 22.5, 14.1, 13.9. HRMS (EI): Exact mass calculated for $C_{25}H_{35}Cl_2NO_5$: 499.1892 Found 499.1880.

SI2 – 6-methoxy – N-hexyl-pseudoarmeniaspirol

Compound **SI1** (35 mg, 0.07mmol, 1 equivalent) was dissolved in DCM (0.05 M) and a solution of Tin (IV) chloride solution (0.21mL of a 1M solution in DCM, 0.21mmol, 3 equiv) was added dropwise. The reaction was stirred at room temperature overnight and quenched with aqueous NaCl. The aqueous layer was then extracted twice with ethyl acetate (20 mL). The combined EtOAc layers were dried with Na_2SO_4 and concentrated *in vacuo*. Purification by silica gel chromatography (10% EtOAc/hexanes) yielded pure **SI2** as a colourless oil (19 mg, 0.0405mmol, 57% yield). R_f= 0.45 (20:80 EtOAc:hexanes). ^{1}H NMR (400 MHz, Chloroform-*d*) δ 6.90 (d, *J* = 8.4 Hz, 1H), 6.71 (d, *J* = 8.5 Hz, 1H), 3.87 (s, 3H), 3.39 – 3.27 (m, 1H), 3.06 (ddd, *J* = 14.5, 8.3, 6.3 Hz, 1H), 2.74 – 2.63 (m, 2H), 1.56 (t, *J* = 7.6 Hz, 2H), 1.33 – 1.25 (m, 10H), 1.18 – 1.12 (m, 4H), 0.86 (q, *J* = 4.5, 3.9 Hz, 3H), 0.80 (t, *J* = 6.9 Hz, 3H). $^{13}C\{^{1}H\}$ NMR (100 MHz, $CDCl_3$) δ 169.9, 164.1, 161.0, 153.6, 140.6, 128.0, 122.8, 116.7, 110.9, 107.4, 73.0, 56.0, 42.2, 31.6, 31.1, 29.0, 28.8, 28.1, 26.2, 23.6, 22.6, 22.4, 14.1, 13.9. HRMS (EI): Exact mass calculated for $C_{24}H_{31}Cl_2NO_4$: 467.1630 Found: 467.1646.

Synthesis of N-dodecyl-1-methyl-pseudoarmeniaspirol **17**

SI3 – N-dodecyl-1-methyl-N,O ketal

Phenol **SI5** (15 mg, 0.1067mmol, 1 equiv) was suspended in acetone and K_2CO_3 (44 mg, 0.32mmol 3 equiv) was added and allowed to stir at room temperature for 10 minutes. **8d** (44 mg, 0.1067mmol, 1 equiv) was added and allowed to stir overnight. The reaction was filtered

and concentrated to yield **SI3** as a colourless oil (30 mg,0.062mmol, 58%), which was used without further purification. ^{1}H NMR (600 MHz, Chloroform-*d*) δ 6.99 (t, *J* = 8.3 Hz, 1H), 6.65 (d, *J* = 8.3 Hz, 1H), 6.30 (d, *J* = 8.3 Hz, 1H), 3.91 (s, 3H), 3.84 (s, 3H), 3.47 (ddd, *J* = 15.2, 9.8, 5.9 Hz, 1H), 3.39 (ddd, *J* = 14.4, 9.8, 6.1 Hz, 1H), 2.28 (s, 3H), 1.58 (ddp, *J* = 30.6, 19.2, 6.6 Hz, 2H), 1.36 – 1.19 (m, 20H), 0.90 (t, *J* = 7.0 Hz, 3H). ^{13}C{^{1}H} NMR (150 MHz, $CDCl_3$) δ 164.9, 163.2, 158.7, 152.0, 140.2, 130.0, 126.4, 119.1, 109.9, 106.6, 92.9, 55.6, 54.1, 41.6, 31.9, 29.6, 29.6, 29.6, 29.5, 29.4, 29.2, 27.9, 27.0, 22.7, 14.1, 9.3. HRMS (EI): Exact mass calculated for $C_{26}H_{37}Cl_2NO_5$: 513.2049 Found: 513.2062.

SI4 - N-dodecyl- 1-methyl-5 methoxy-pseudoarmeniaspirol

Compound **SI3** (30 mg, 0.062mmol, 1 equiv) was dissolved in DCM (0.05 M) and a solution of Tin (IV) chloride (0.186mL of a 1M solution in DCM, 0.186mmol, 3 equiv) was added dropwise. The reaction was stirred at room temperature overnight and quenched with aqueous NaCl. The aqueous layer was then extracted twice with ethyl acetate (20 mL). The combined EtOAc layers were dried with Na_2SO_4 and concentrated *in vacuo*. Purification by silica gel chromatography (10% EtOAc/Hexane) yielded pure **SI4** as a colourless oil (16 mg, 0.033mmol, 53% yield). R_f= 0.3 (10:90 EtOAc:Hexanes). ^{1}H NMR (400 MHz, $CDCl_3$) δ 6.90 (d, *J* = 8.4 Hz, 1H), 6.70 (dd, *J* = 8.4, 3.5 Hz, 1H), 3.88 (s, 3H), 3.35 – 3.26 (m, 1H), 3.13 – 3.03 (m, 1H), 2.21 (s, 3H), 1.26 – 1.18 (m, 18H), 0.85 (t, *J* = 6.7 Hz, 5H). ^{13}C{^{1}H} NMR (100 MHz, $CDCl_3$) δ 169.8, 164.1, 161.2, 153.6, 140.6, 128.0, 122.7, 111.8, 110.9, 107.0, 73.1, 56.0, 42.3, 31.9, 29.6, 29.5, 29.3, 29.2, 28.9, 28.2, 26.5, 22.7, 14.1, 8.9. HRMS (EI): Exact mass calculated for $C_{25}H_{33}Cl_2NO_4$: 481.1787 Found: 481.1773.

SI5 – 2-methyl-3 methoxy phenol

In a round-bottom flask, commercially available 2,6 dimethoxy toluene (204mg, 1.34mmol, 1.0 equiv.) was dissolved in 1,2-dichloroethane (3 mL). The solution was cooled to -20 °C using a dry ice/acetone bath. A solution of BBr_3 (1.6mL of a 1M solution in DCM, 1.6mmol,1.2 equiv.) was added dropwise, and the reaction mixture was stirred at -20 to – 10 °C for 2 hours. Subsequently, Et_3N / water was added, and the solution was extracted 3 × with EtOAc. The organic fractions were combined, washed with brine, dried over Na_2SO_4, and concentrated. Purification by silica gel chromatography (10% EtOAc/Hexane) yielded pure compound **SI5** as a brown amorphous solid (141 mg, 1.02mmol, 76 % yield). ^{1}H NMR (400 MHz, $CDCl_3$) δ 7.05 (t, *J* = 8.2 Hz, 1H), 6.56 – 6.45 (m, 2H), 3.85 (s, 3H), 2.16 (s, 3H). $^{13}C\{^1H\}$ NMR (100 MHz, $CDCl_3$) δ 158.7, 154.5, 126.5, 112.4, 108.2, 103.2, 55.8, 8.1. The NMR data were consistent with literature values.[1]

SI6 - pentachloro-2H-pyrrole

Pyrrole (0.1g, 1.49mmol, 1 equiv) was dissolved in diethyl ether and cooled to 0ºC. Sulfuryl chloride (0754mL 8.94mmol, 6equiv.) was added and the solution was stirred overnight. The resulting solution was concentrated and upon flash chromatography (20% EtOAc/Hexane) yielded **SI6** as a brown amorphous solid. R_f= 0.5 (20:80 EtOAc:Hexanes) $^{13}C\{^1H\}$ NMR (100 MHz, $CDCl_3$) δ 164.1, 151.1, 125.4, 98.3. NMR data was consistent with literature values.[2]

SI7 - *t*-butyl 1-H-pyrrole-2-carboxylate

Prepared following general procedure 1. Compound **SI7** was purified by silica gel chromatography (15:85 EtOAc:Hexanes) and was obtained as a yellow oil (450mg, 63%) . R_f= 0.45 (15:85 EtOAc:Hexanes) ^{1}H NMR (400 MHz, $CDCl_3$) δ 6.92 (td, *J* = 2.7, 1.5 Hz, 1H), 6.85 (ddd, *J* = 3.8, 2.4, 1.5 Hz, 1H), 6.23 (dt, *J* = 3.7, 2.5 Hz, 1H), 1.58 (s, 9H). $^{13}C\{^1H\}$ NMR (150

MHz, $CDCl_3$) δ 160.5, 124.5, 122.0, 114.5, 110.2, 80.8, 28.4. The NMR data is consistent with literature values.[3] HRMS (EI): Exact mass calculated for $C_9H_{13}NO_2$: 167.0946 found: 167.0957.

SI8 – trimethylsilylethyl-1H-pyrrole-2-carboxylate

Prepared following general procedure 1. Compound **SI8** was purified by silica gel chromatography (30% EtOAc/Hexane) and was obtained as a red oil (202 mg, 74%) . R_f= 0.5 (12.5:87.5 EtOAc:Hexane) ^{1}H NMR (400 MHz, $CDCl_3$) δ 6.95 (td, *J* = 2.7, 1.5 Hz, 1H), 6.90 (ddd, *J* = 3.9, 2.5, 1.5 Hz, 1H), 6.26 (dt, *J* = 3.7, 2.6 Hz, 1H), 4.42 – 4.29 (m, 2H), 1.13 – 1.05 (m, 2H), 0.08 (s, 9H). $^{13}C\{^1H\}$ NMR (100 MHz, $CDCl_3$) δ 161.5, 123.4, 122.7, 115.0, 110.5, 62.7, 17.6, -1.3. The NMR data is consistent with literature values.[4] HRMS (EI): Exact mass calculated for $C_{10}H_{17}NO_2Si$ 211.1029: Found: 211.1046.

Section 4. Copies of ^{1}H and ^{13}C spectra – A) Table 1. 7a-w

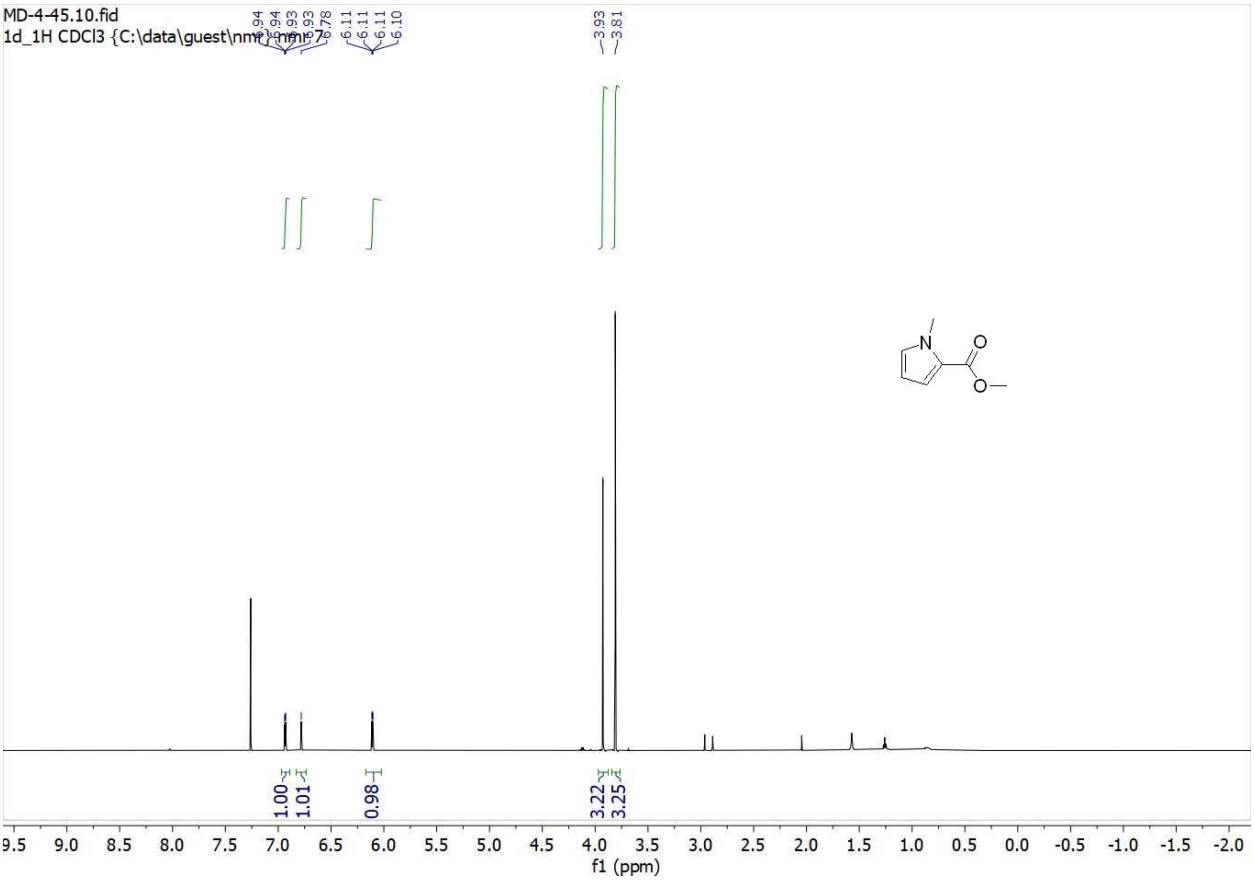

^{1}H NMR (600 MHz, $CDCl_3$) of **7b**

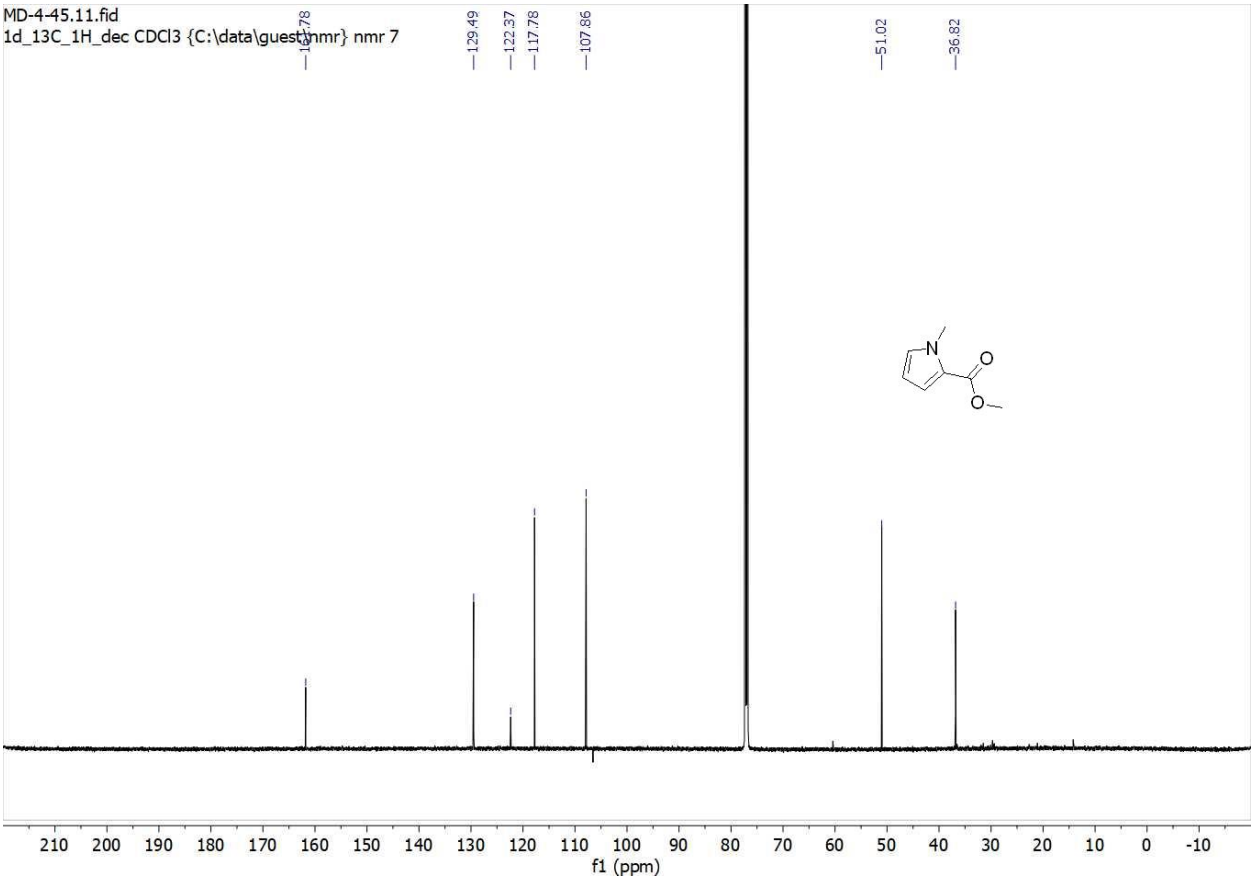

$^{13}C\{^{1}H\}$ NMR (150 MHz, $CDCl_3$) of **7b**

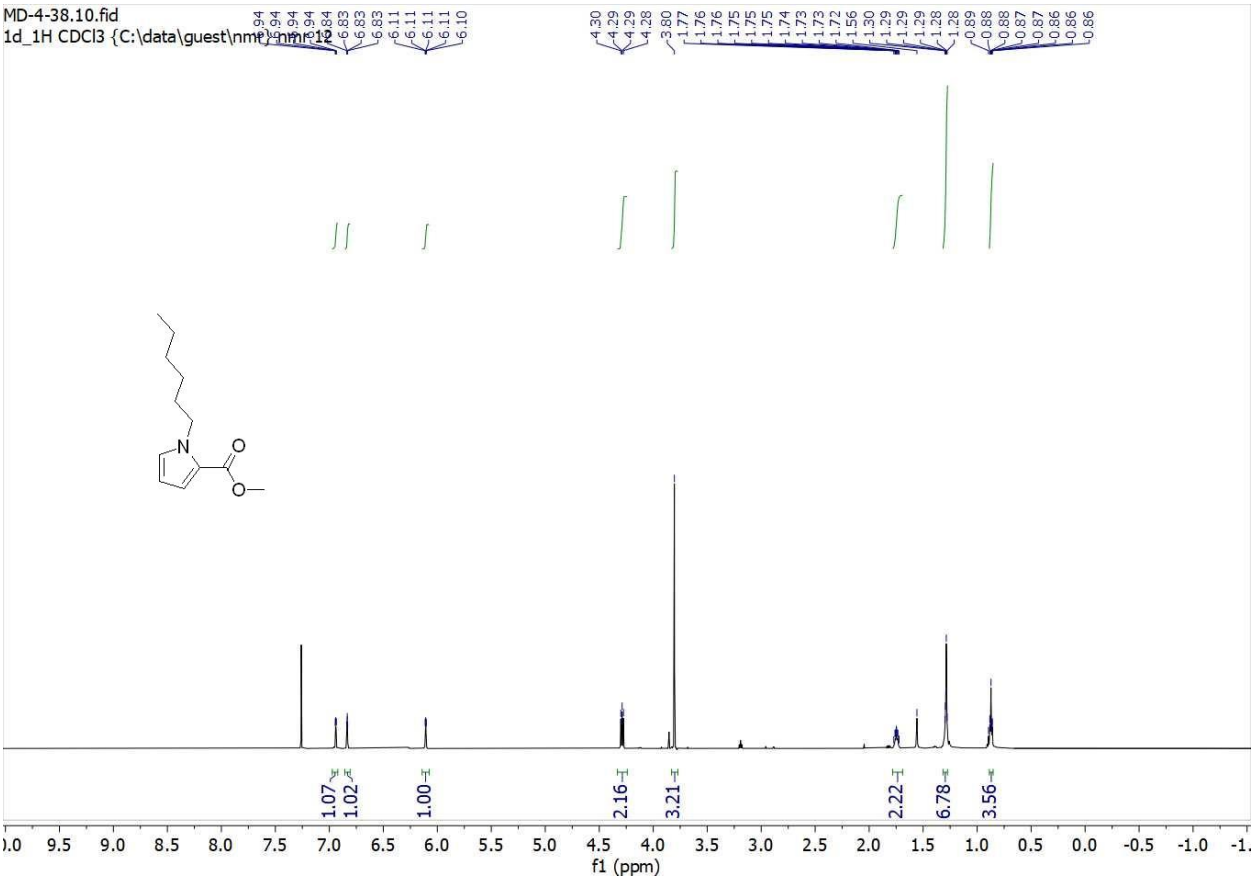

^{1}H NMR (600 MHz, $CDCl_3$) of **7c**

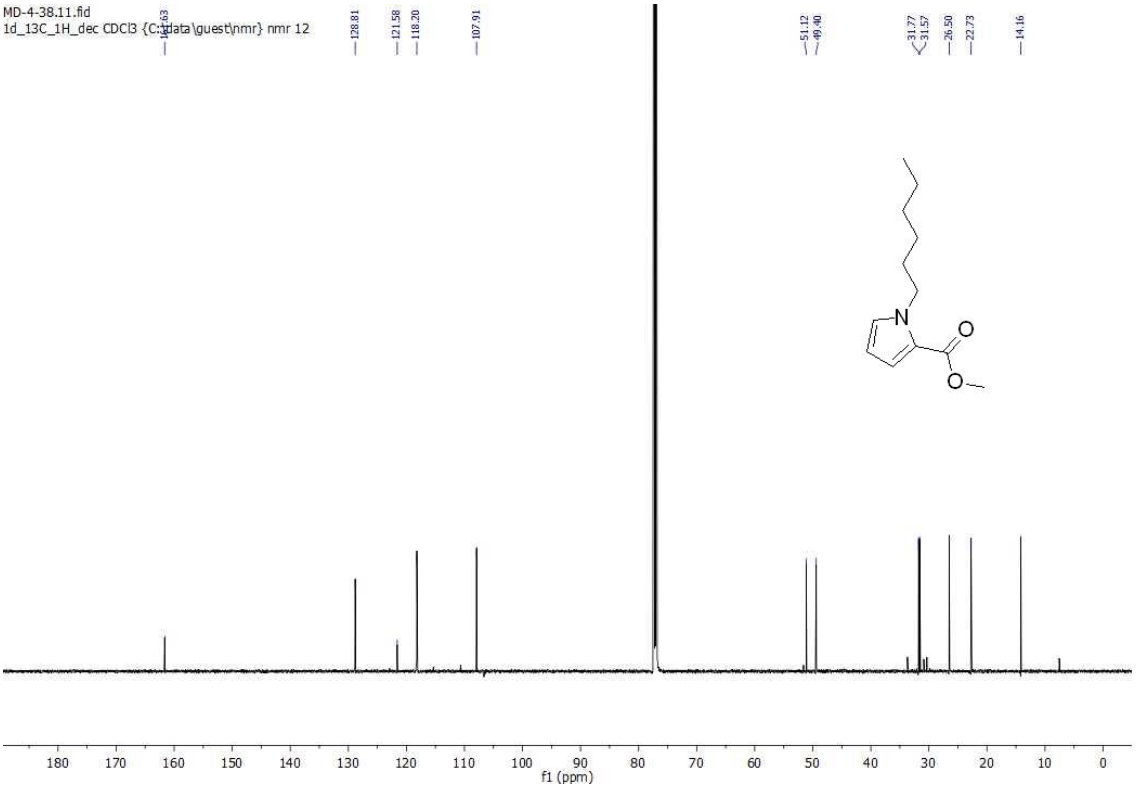

$^{13}C\{^{1}H\}$ NMR (150 MHz, $CDCl_3$) of **7c**

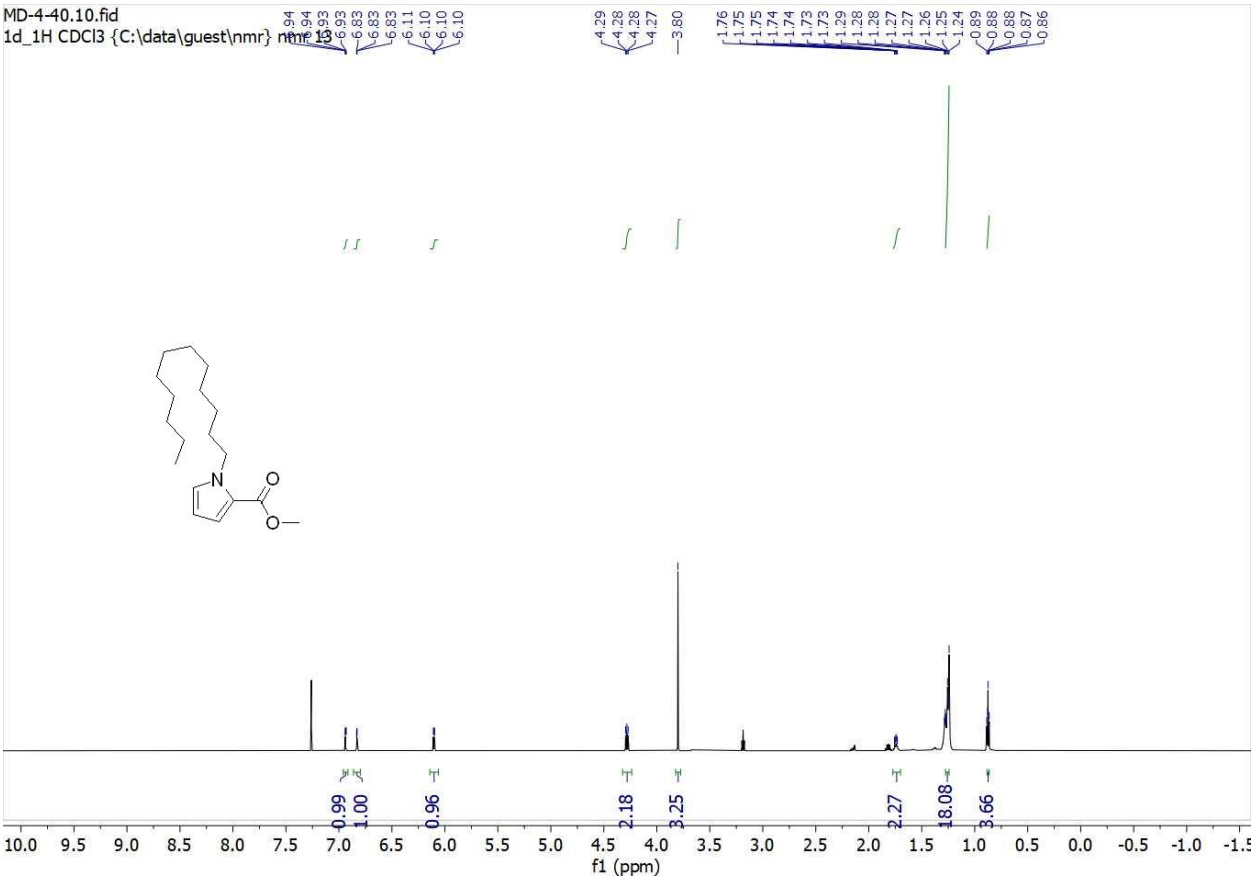

^{1}H NMR (600 MHz, $CDCl_3$) of **7d.**

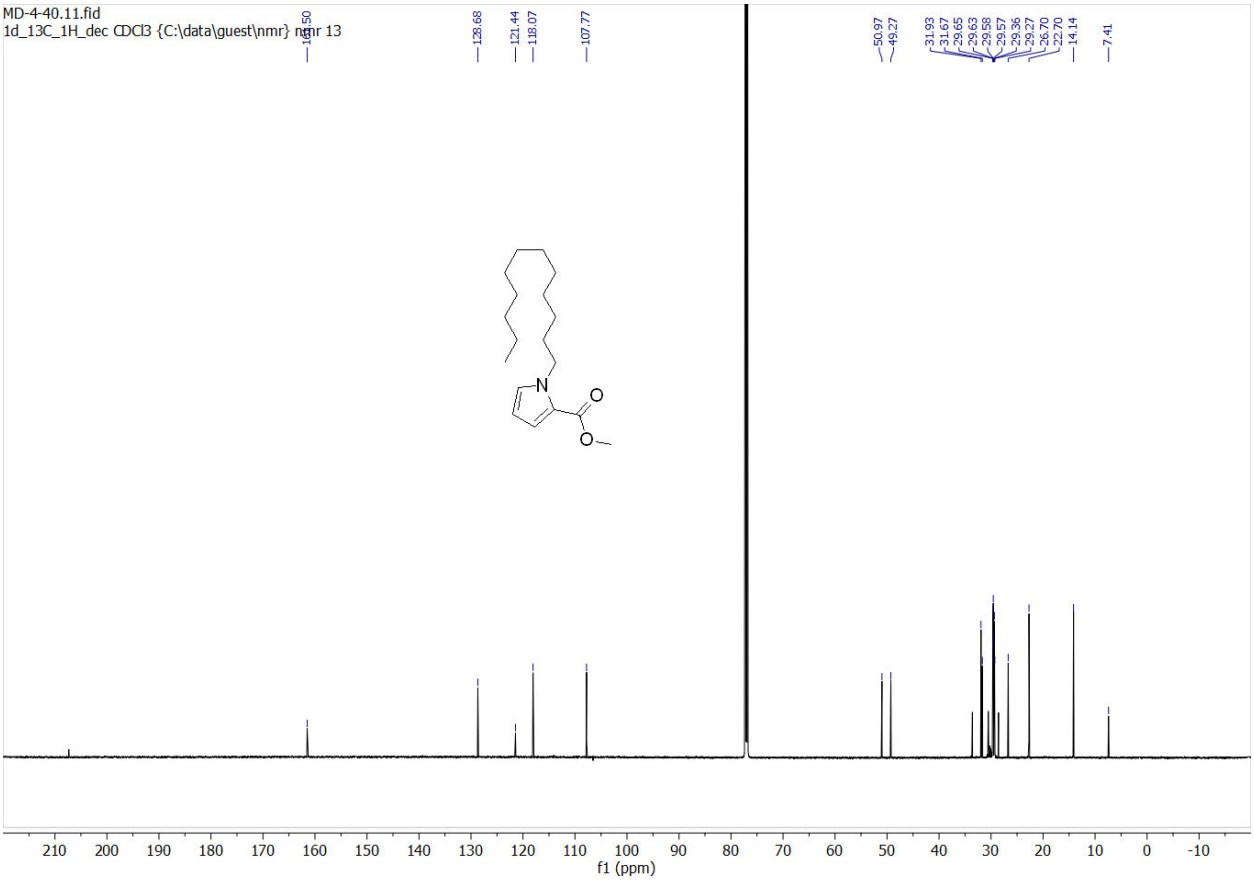

$^{13}C\{^{1}H\}$ NMR (150 MHz, $CDCl_3$) of **7d.**

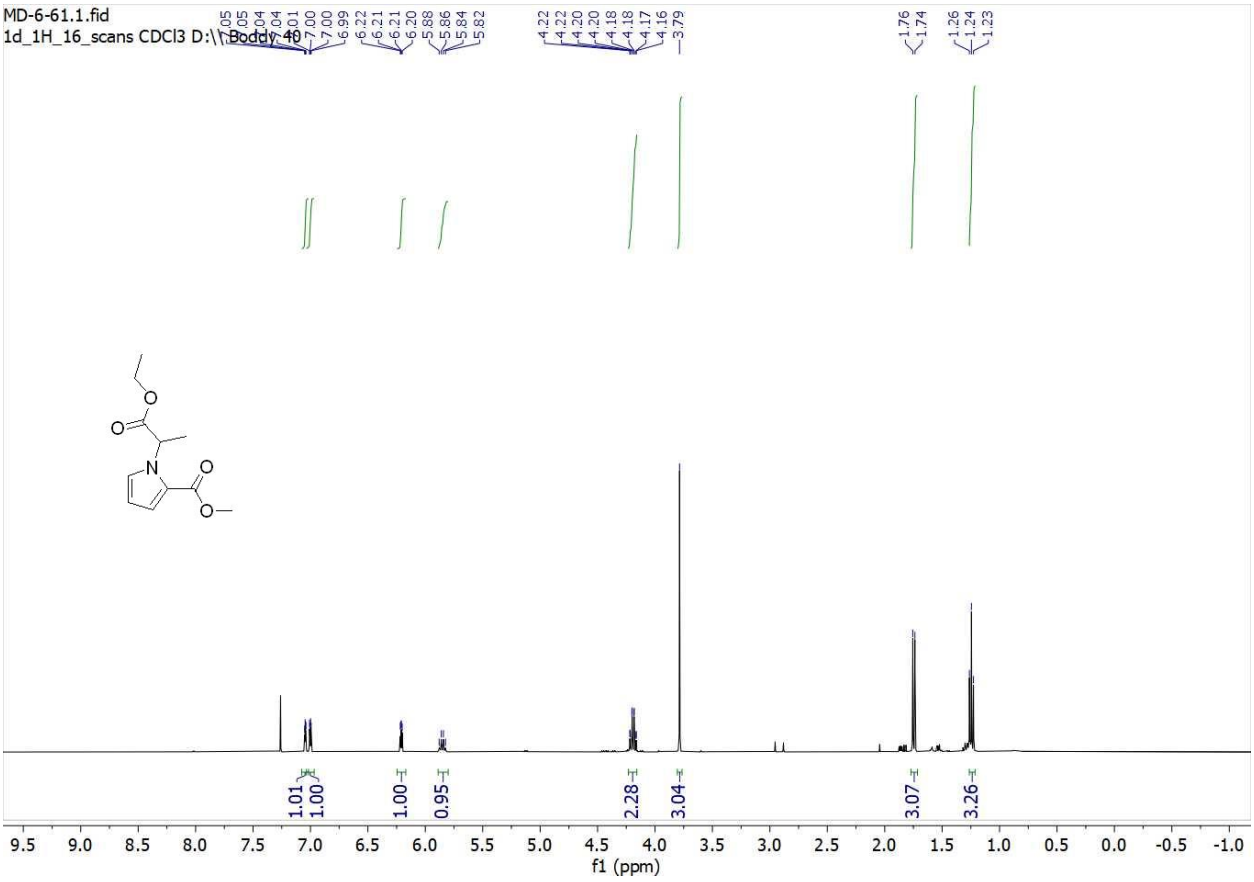

^{1}H NMR (400 MHz, $CDCl_3$) of **7e**

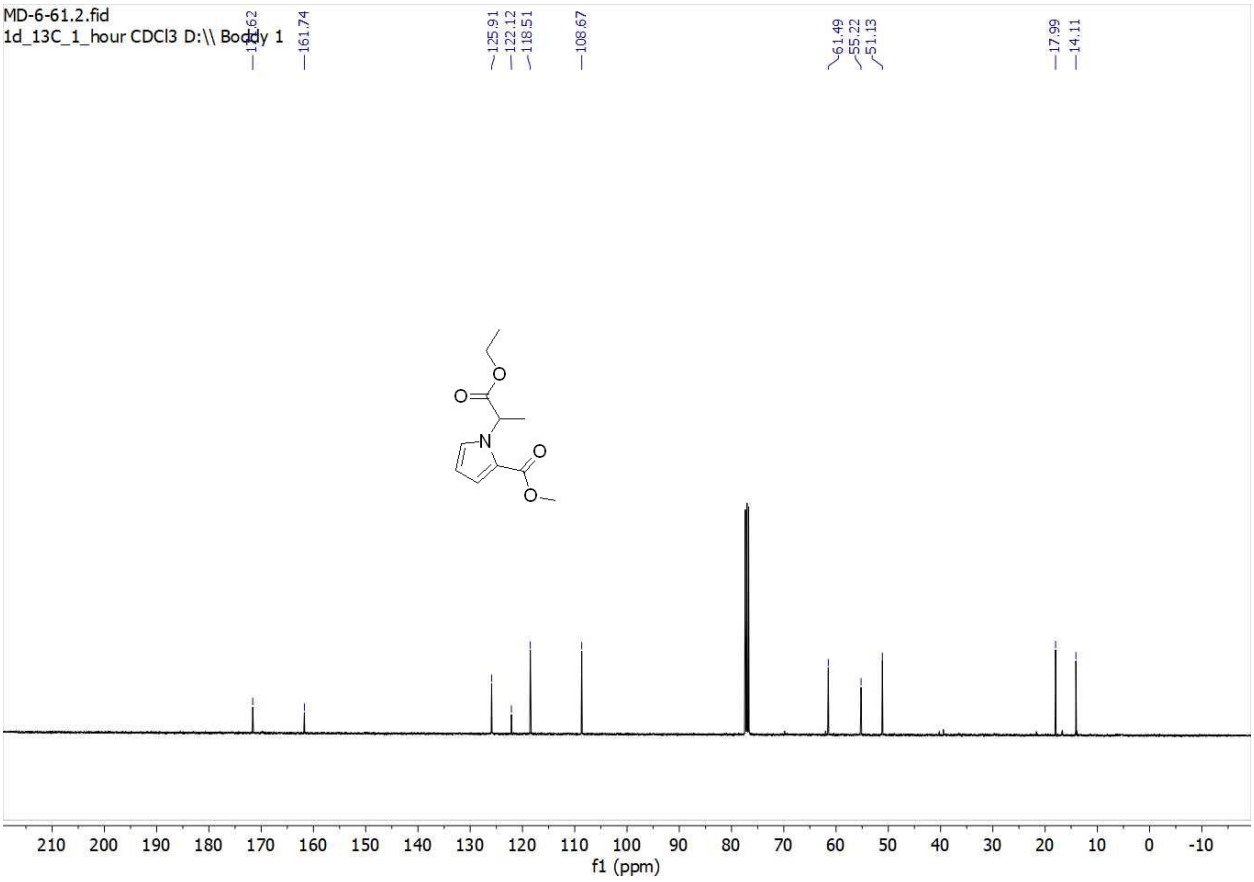

$^{13}C\{^{1}H\}$ NMR (100 MHz, $CDCl_3$) of **7e**

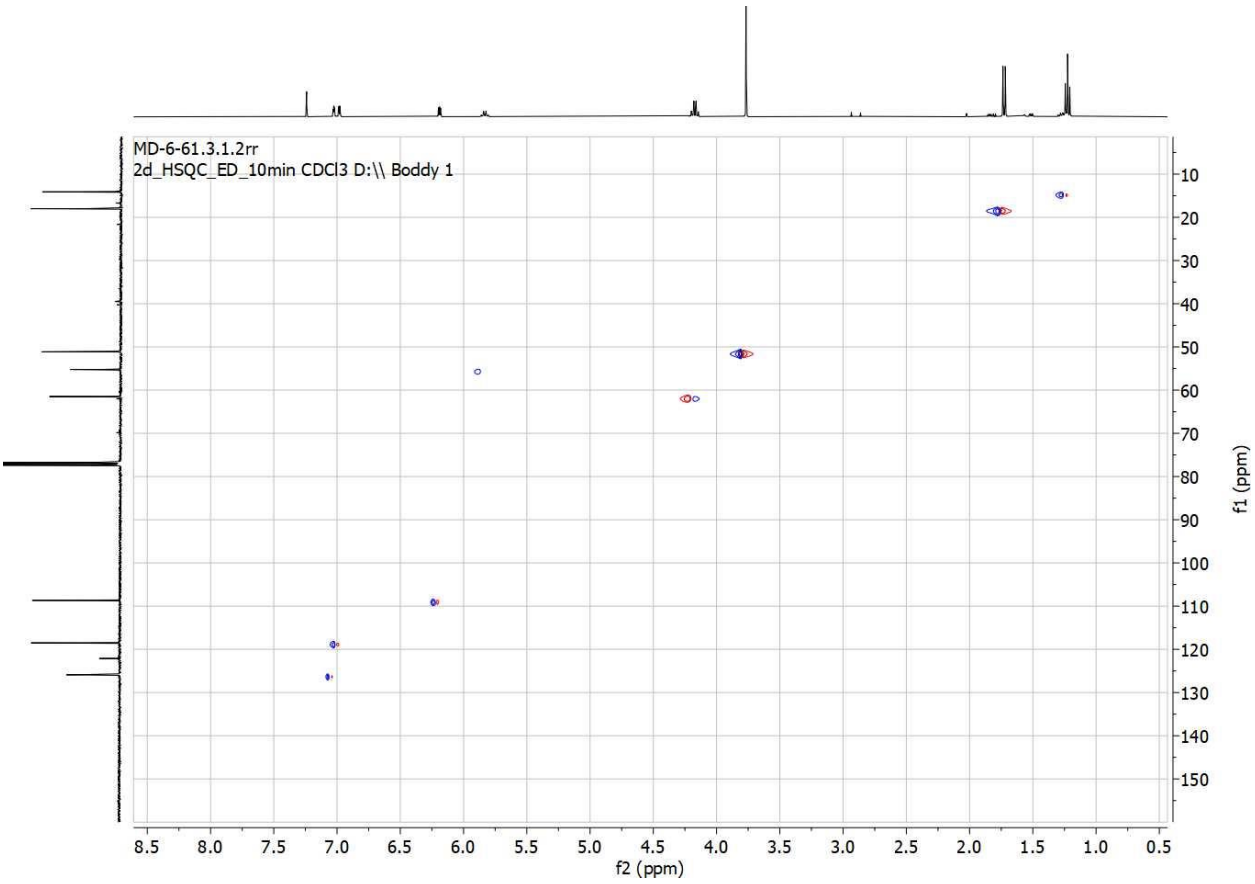

HSQC of **7e**

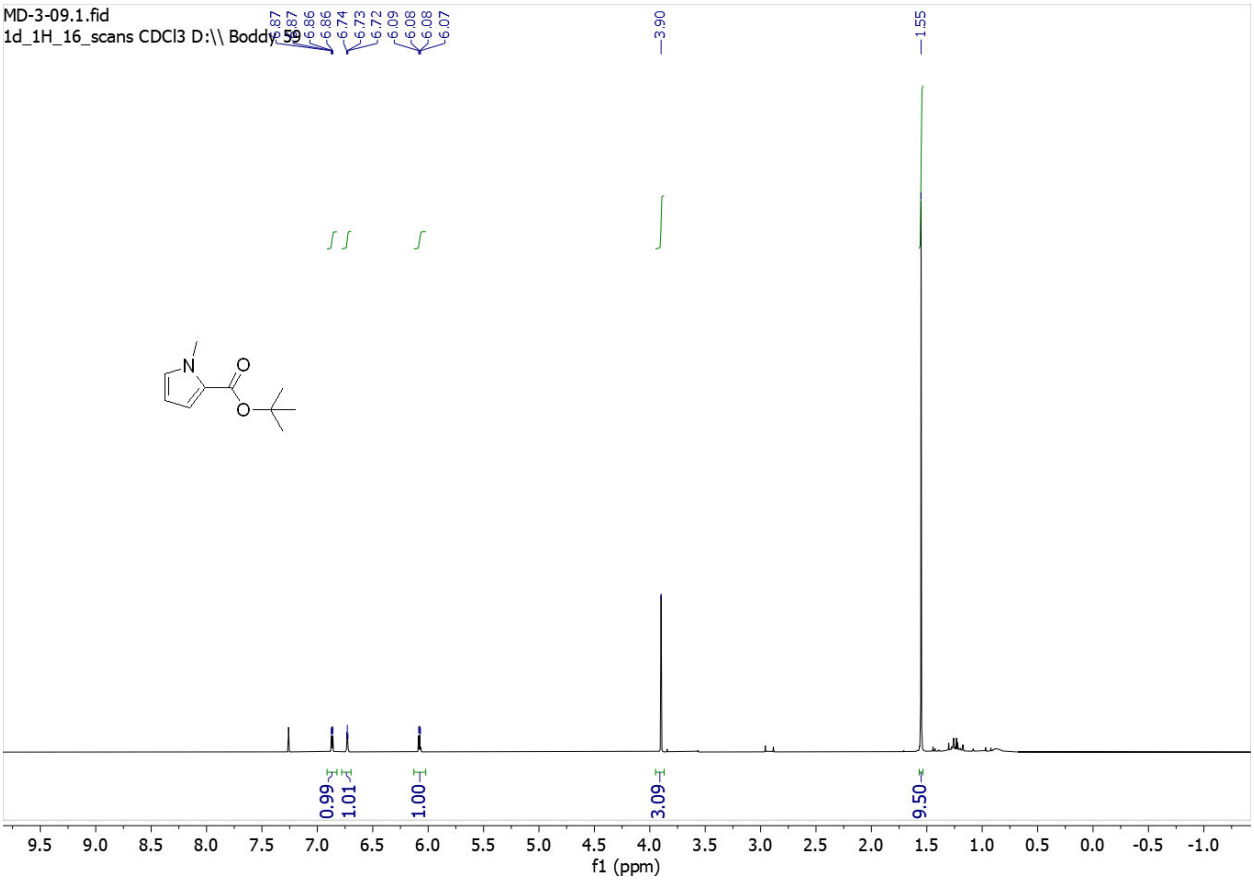

^{1}H NMR (400 MHz, $CDCl_3$), of **7f.**

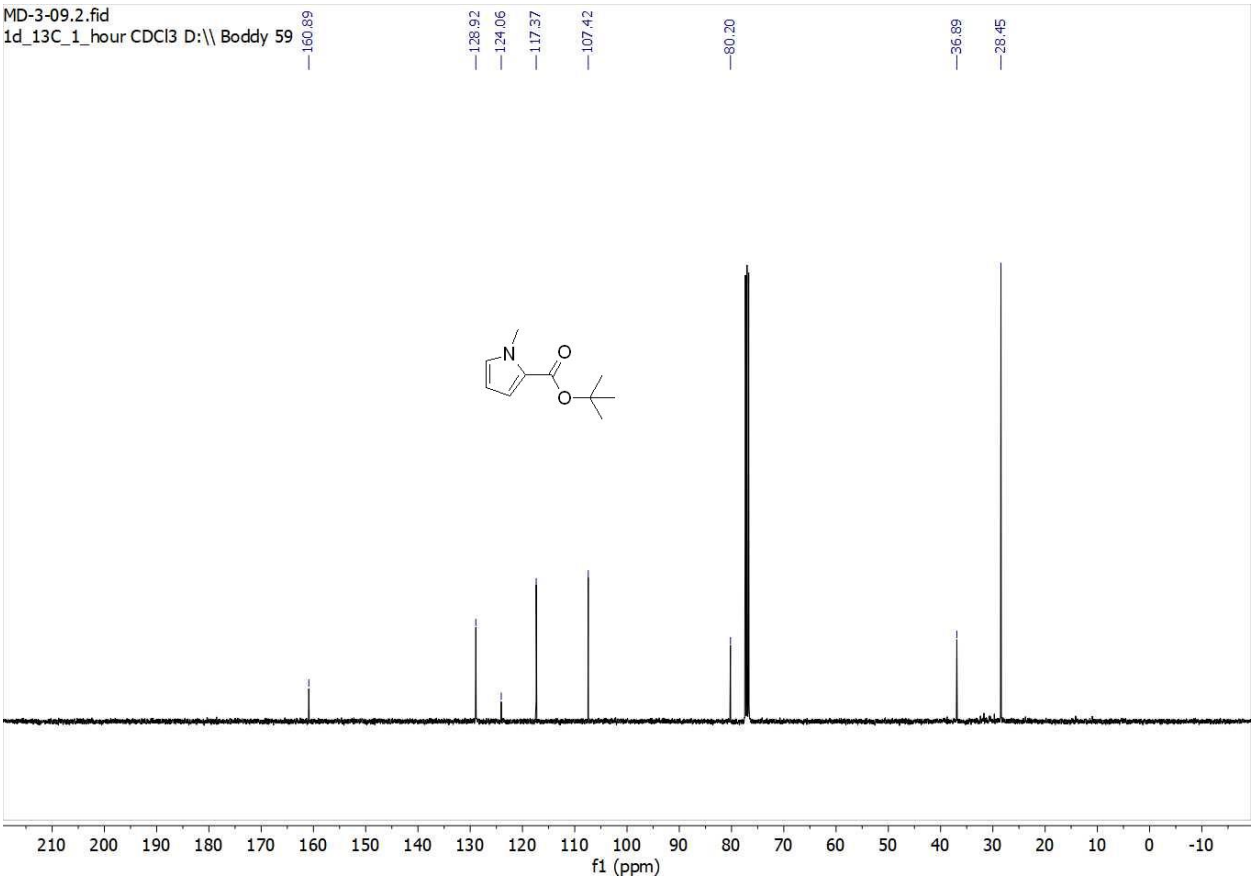

$^{13}C\{^{1}H\}$ NMR (100 MHz, $CDCl_3$) of **7f.**

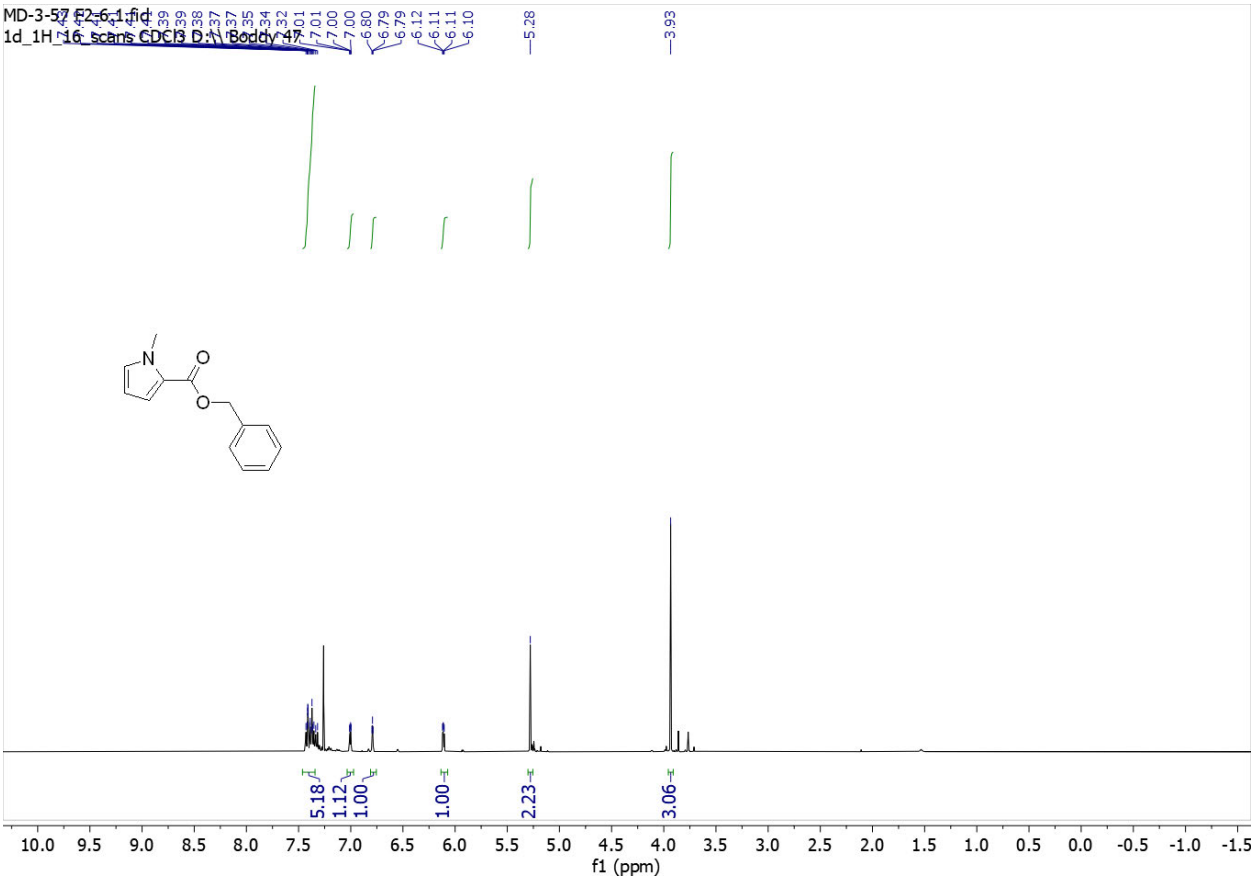

^{1}H NMR (400 MHz, $CDCl_3$) of **7g**

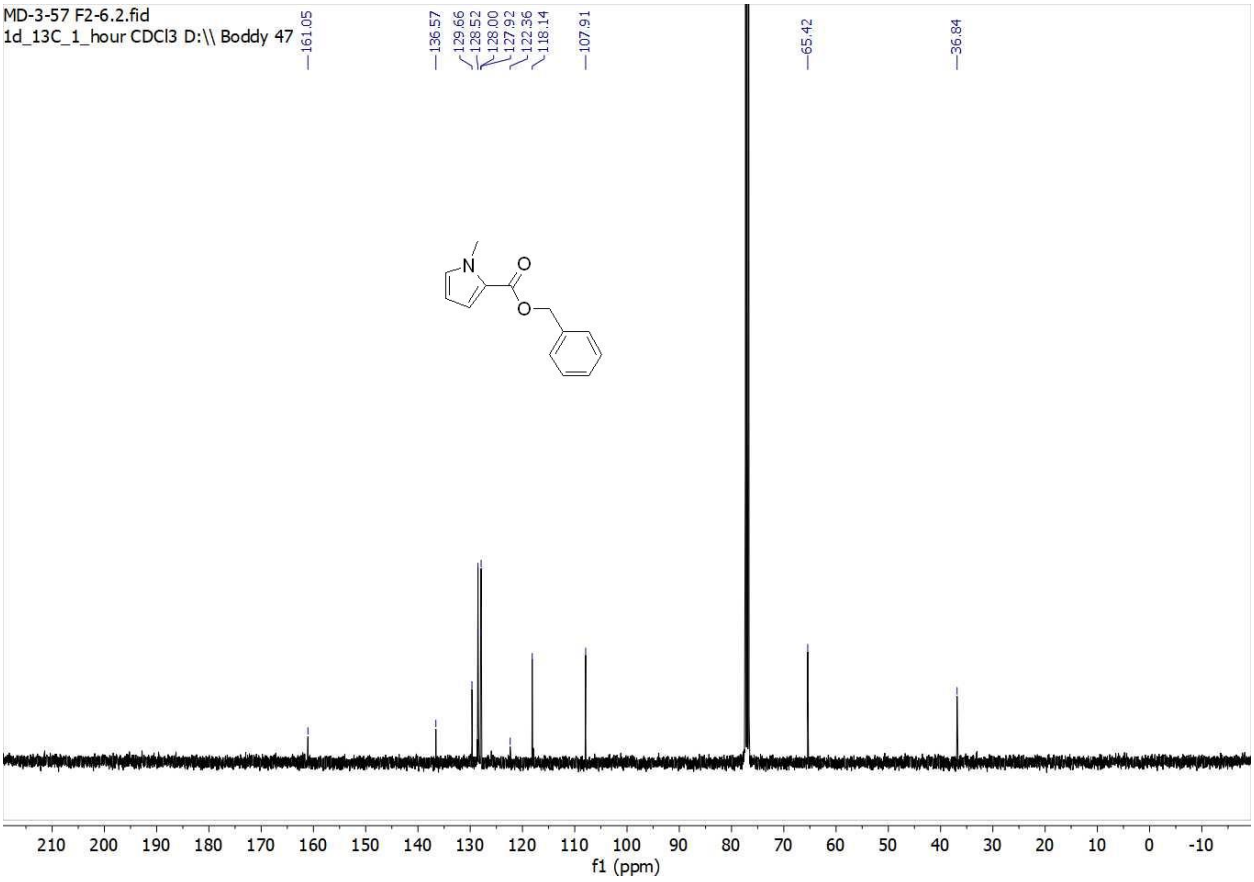

$^{13}C\{^{1}H\}$ NMR (100 MHz, $CDCl_3$) of **7g**

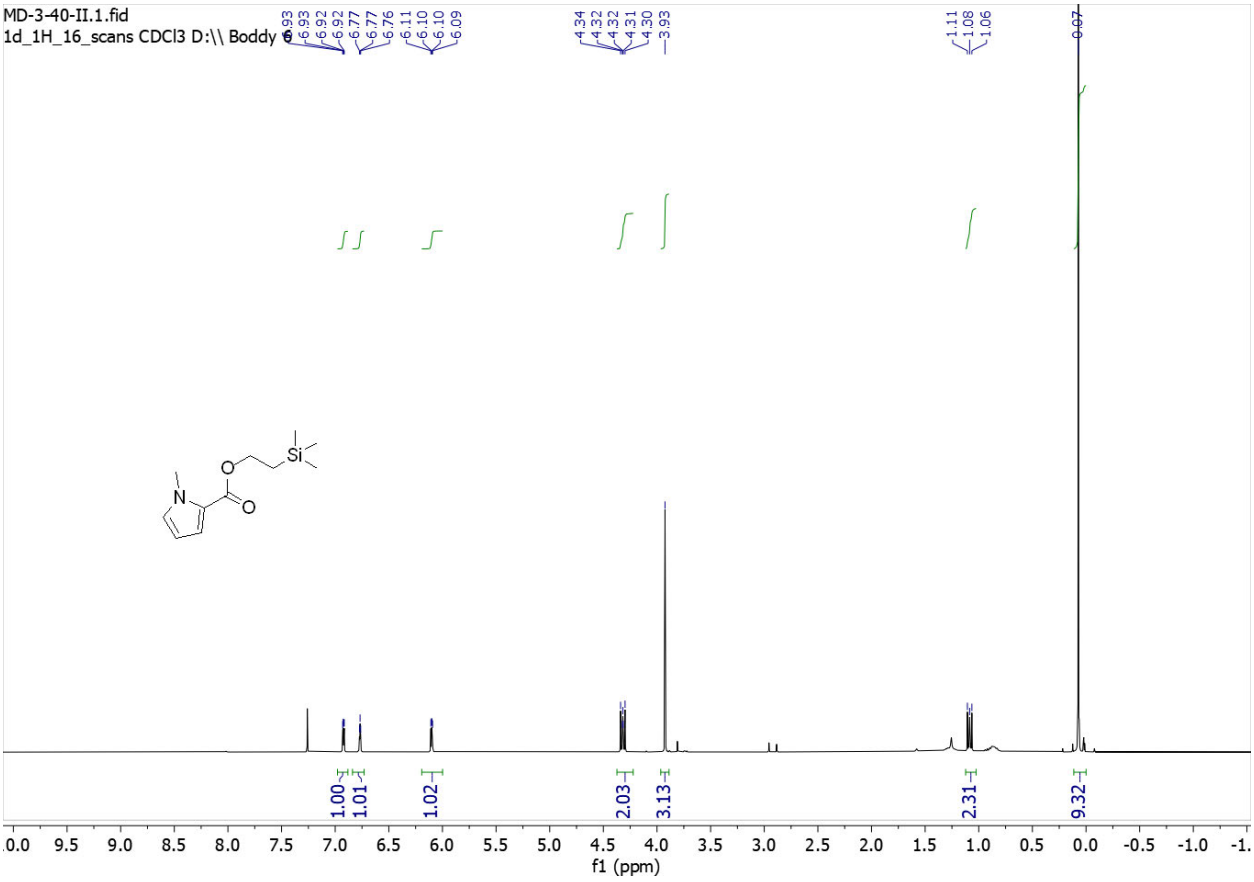

^{1}H NMR (400 MHz, $CDCl_3$) of **7h.**

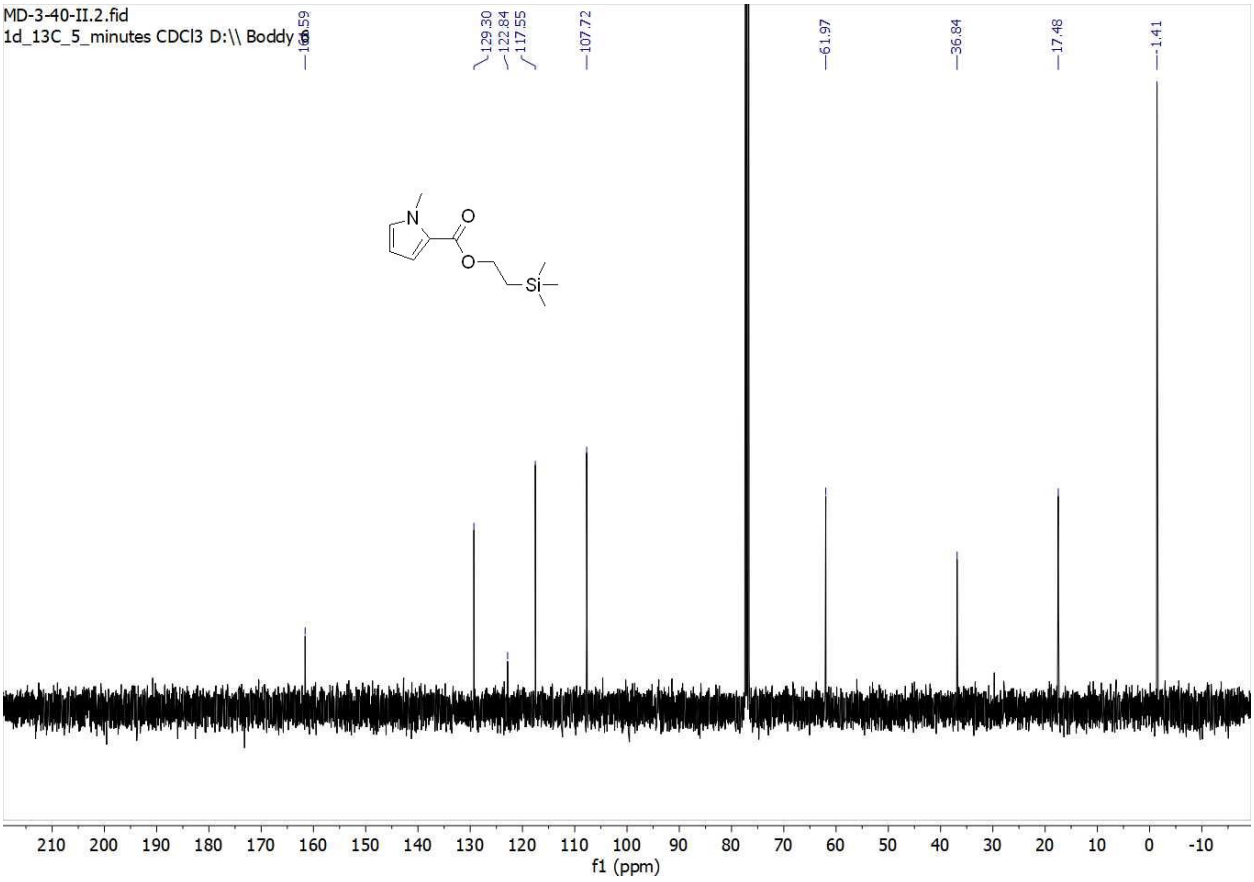

$^{13}C\{^{1}H\}$ NMR (100 MHz, $CDCl_3$) of **7h.**

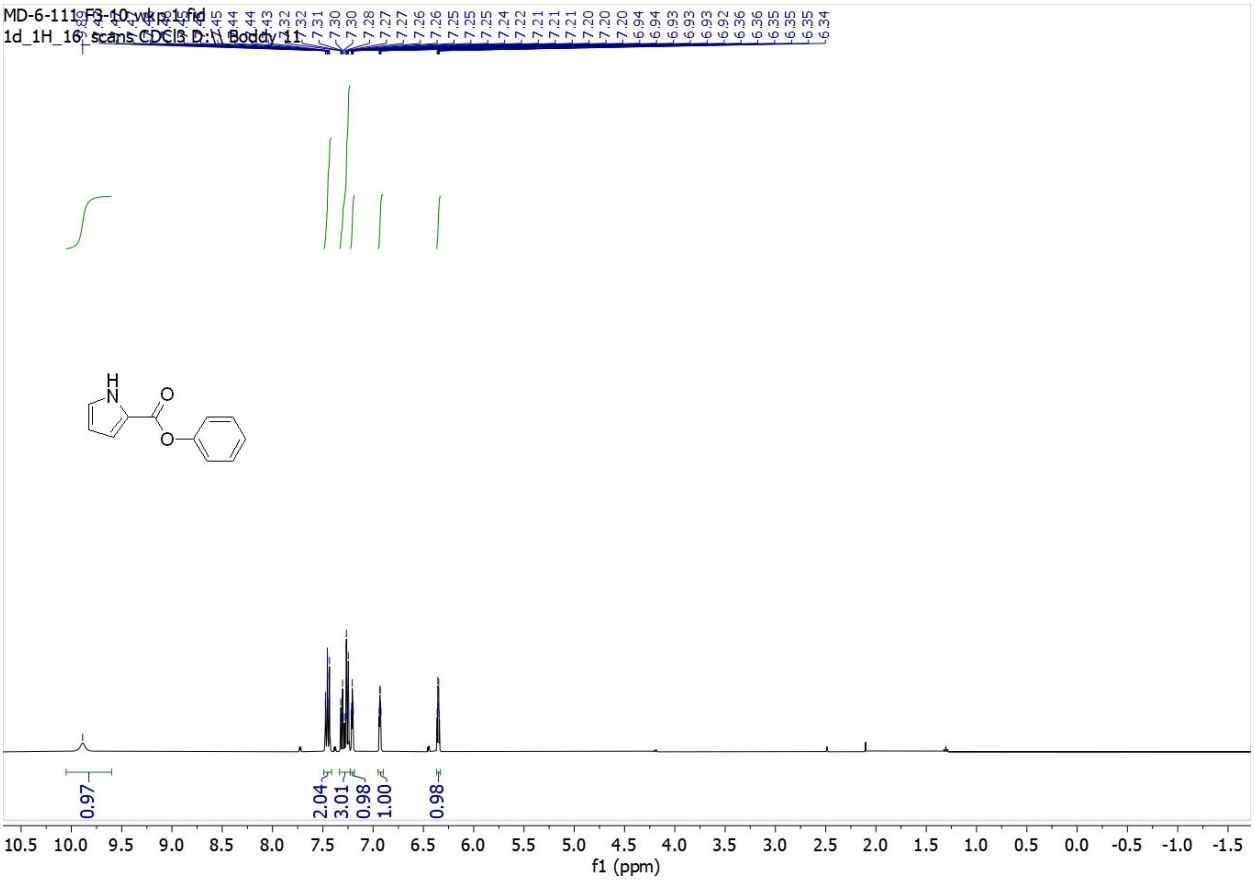

^{1}H NMR (400 MHz, $CDCl_3$) of **7i**

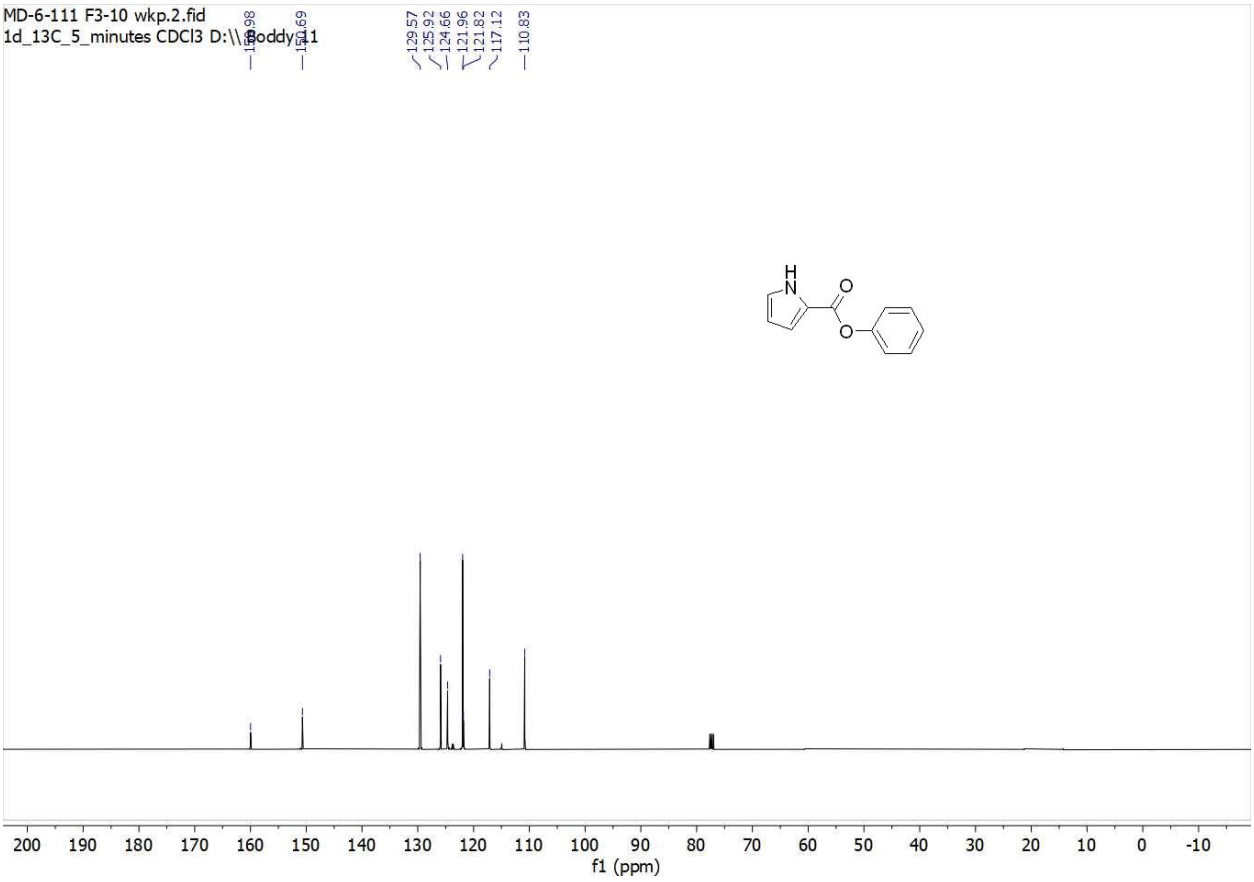

$^{13}C\{^{1}H\}$ NMR (100 MHz, $CDCl_3$) of **7i**

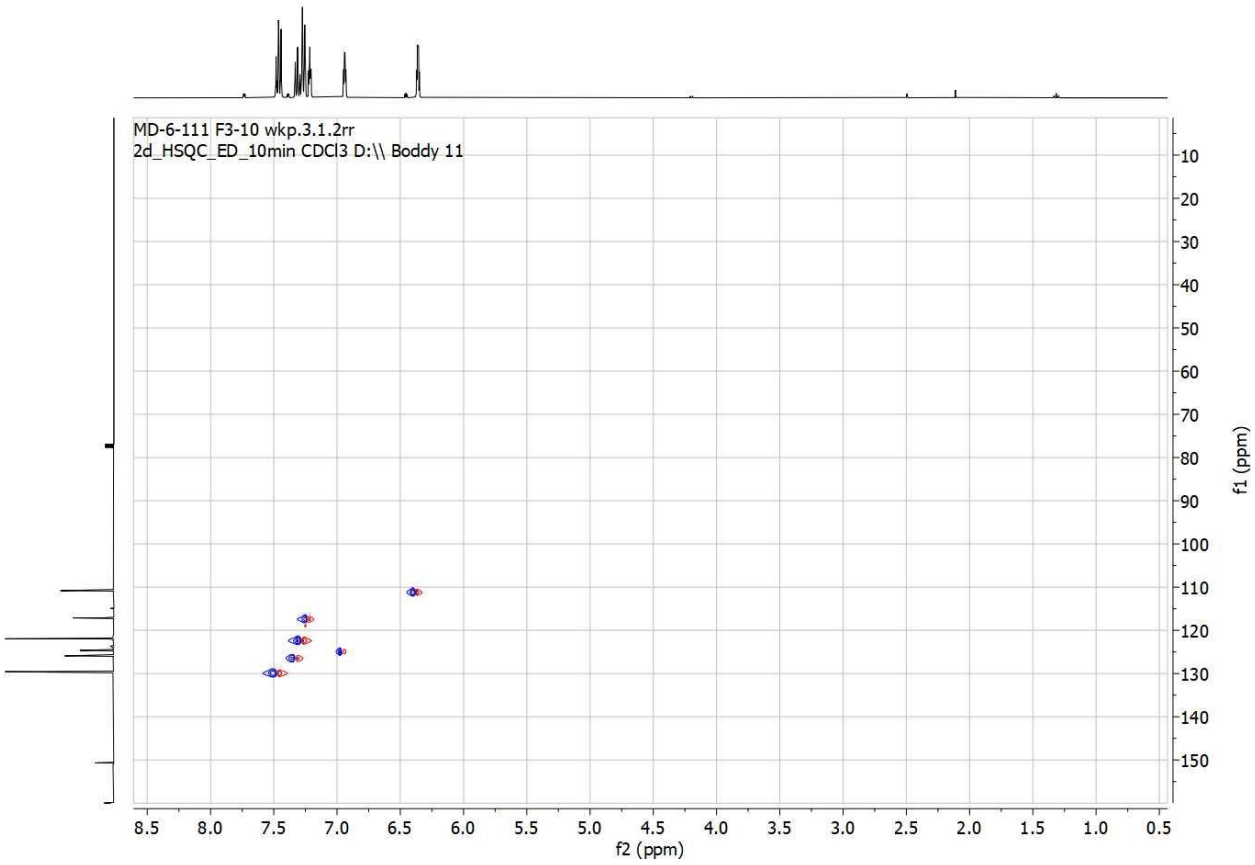
MD-6-111 F3-10 wkp.3.1.2rr
2d_HSQC_ED_10min CDCl3 D:\\ Boddy 11
f2 (ppm)
f1 (ppm)

HSQC of **7i**

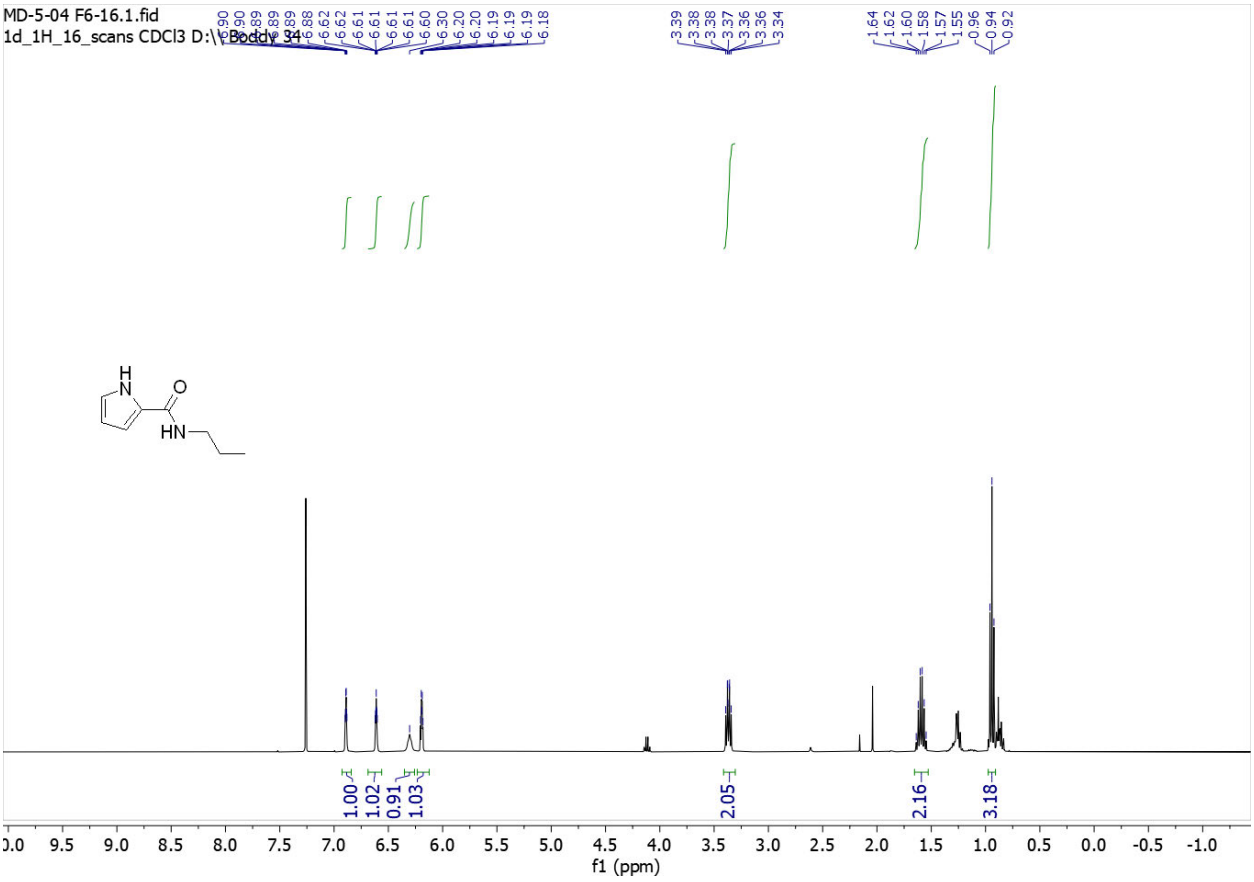

^{1}H NMR (400 MHz, $CDCl_3$) of **7j.**

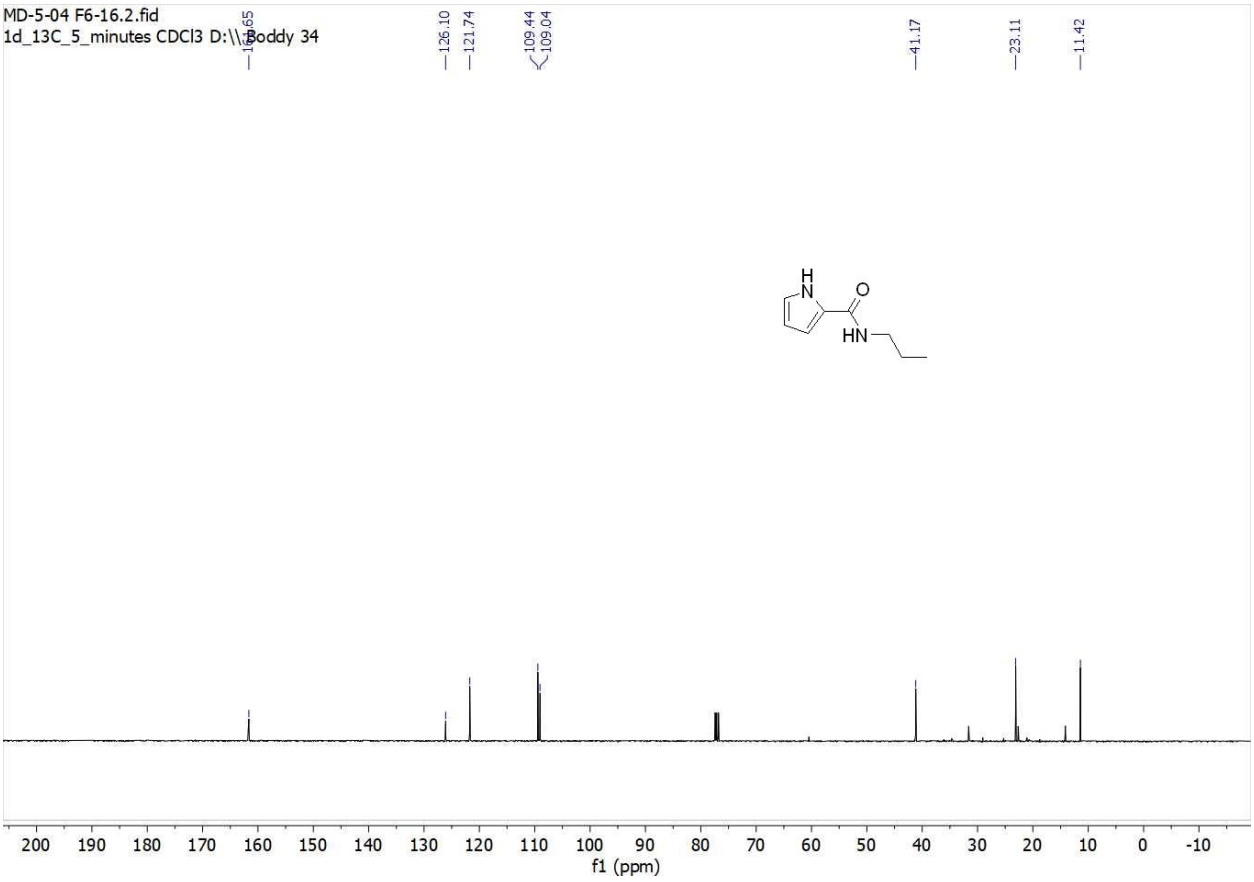

$^{13}C\{^{1}H\}$ NMR (100 MHz, $CDCl_3$) of **7j.**

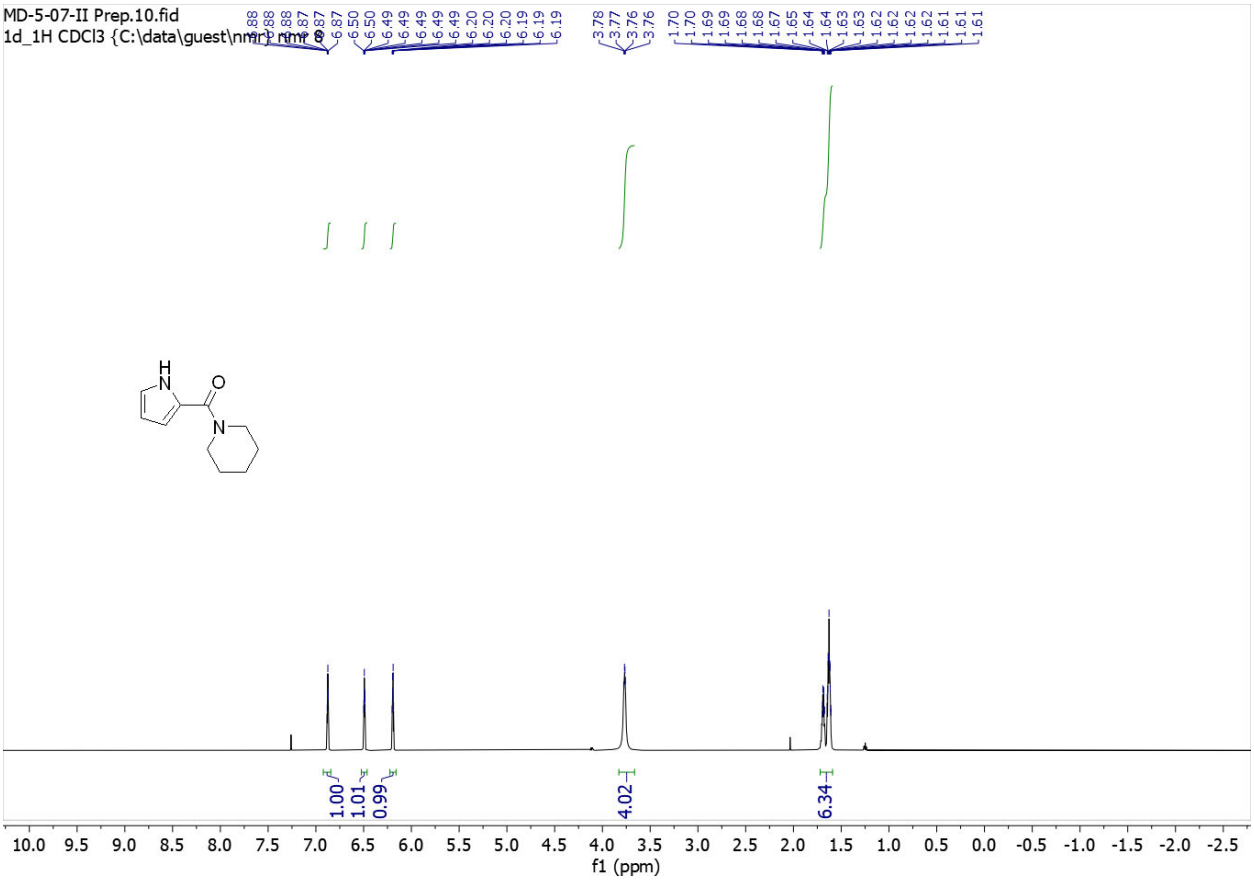

^{1}H NMR (600 MHz, $CDCl_3$) of **7k.**

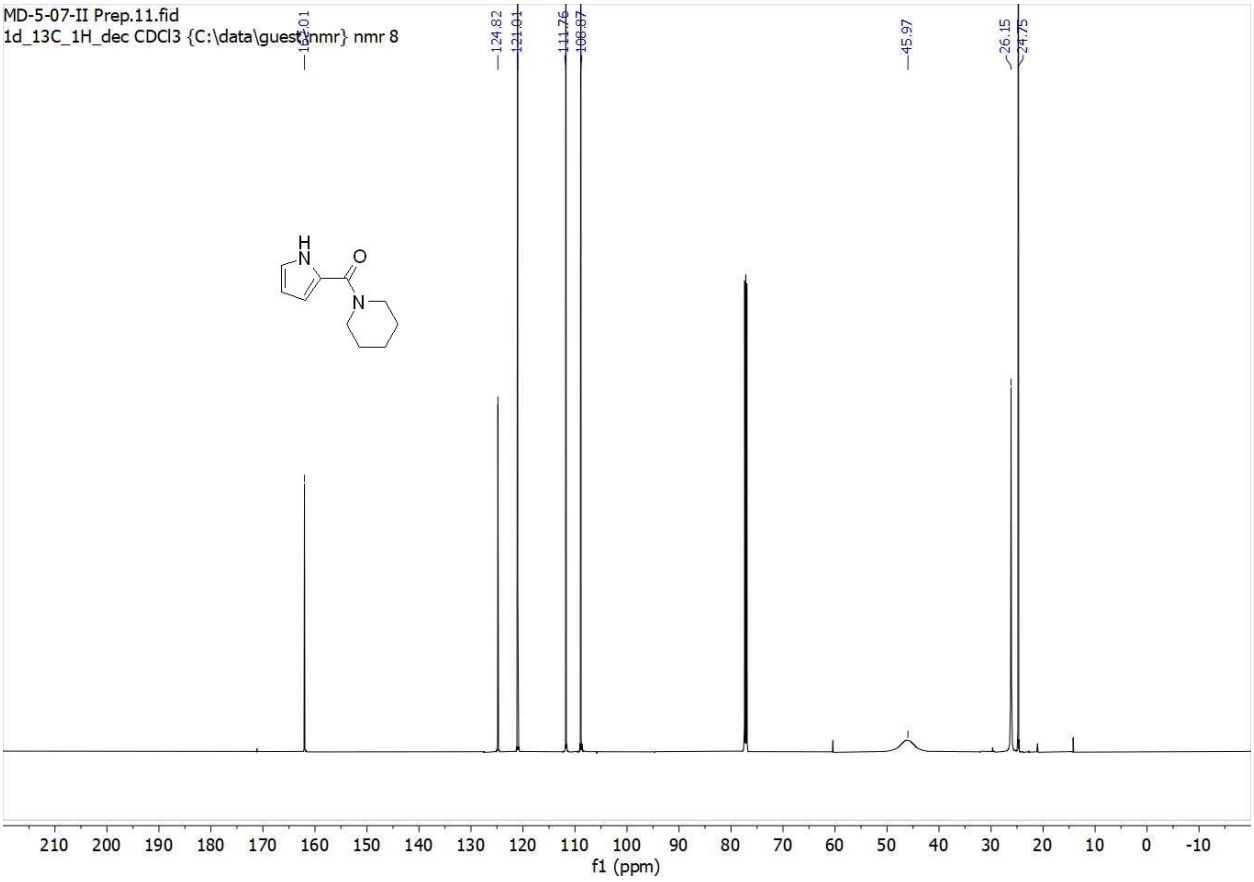

$^{13}C\{^{1}H\}$ NMR (150 MHz, $CDCl_3$) of **7k.**

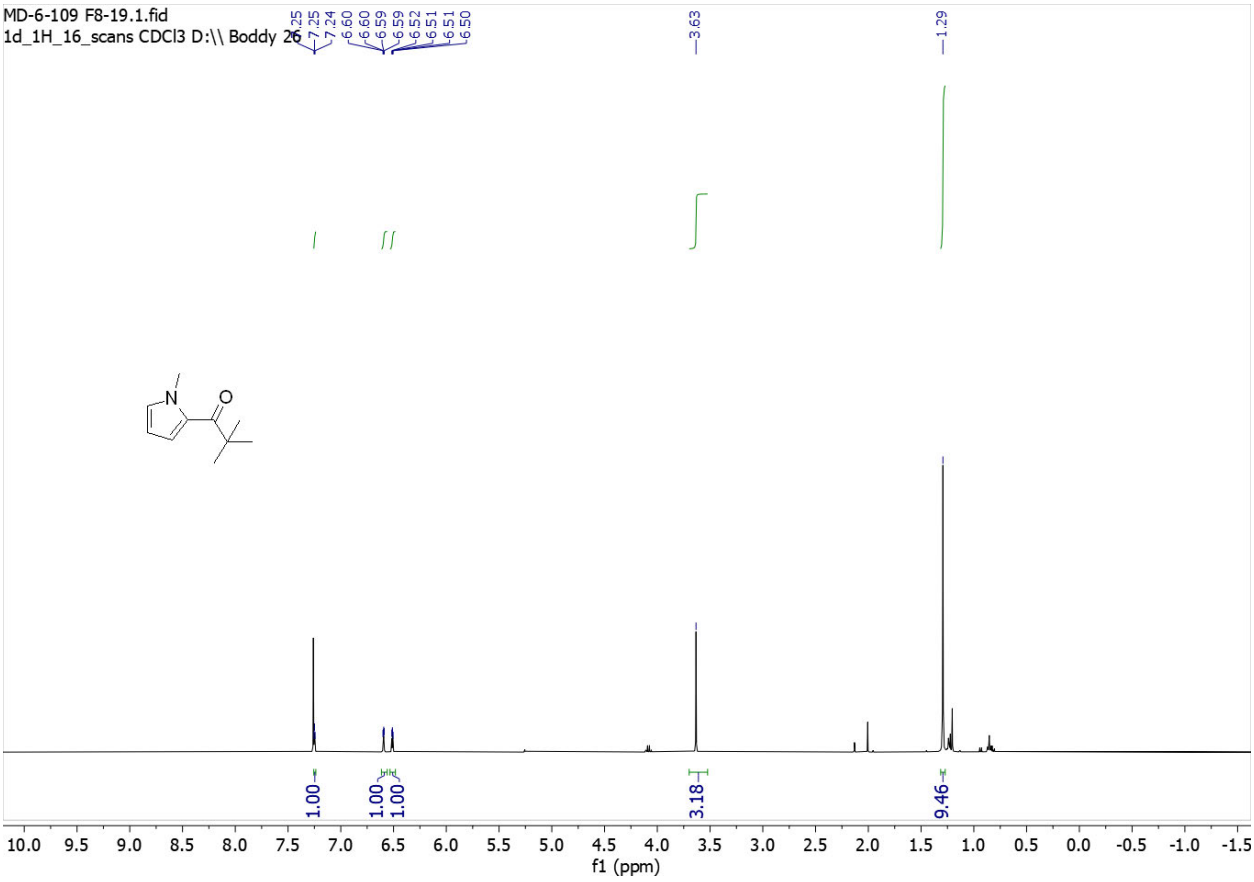

^{1}H NMR (600 MHz, $CDCl_3$) of **7m.**

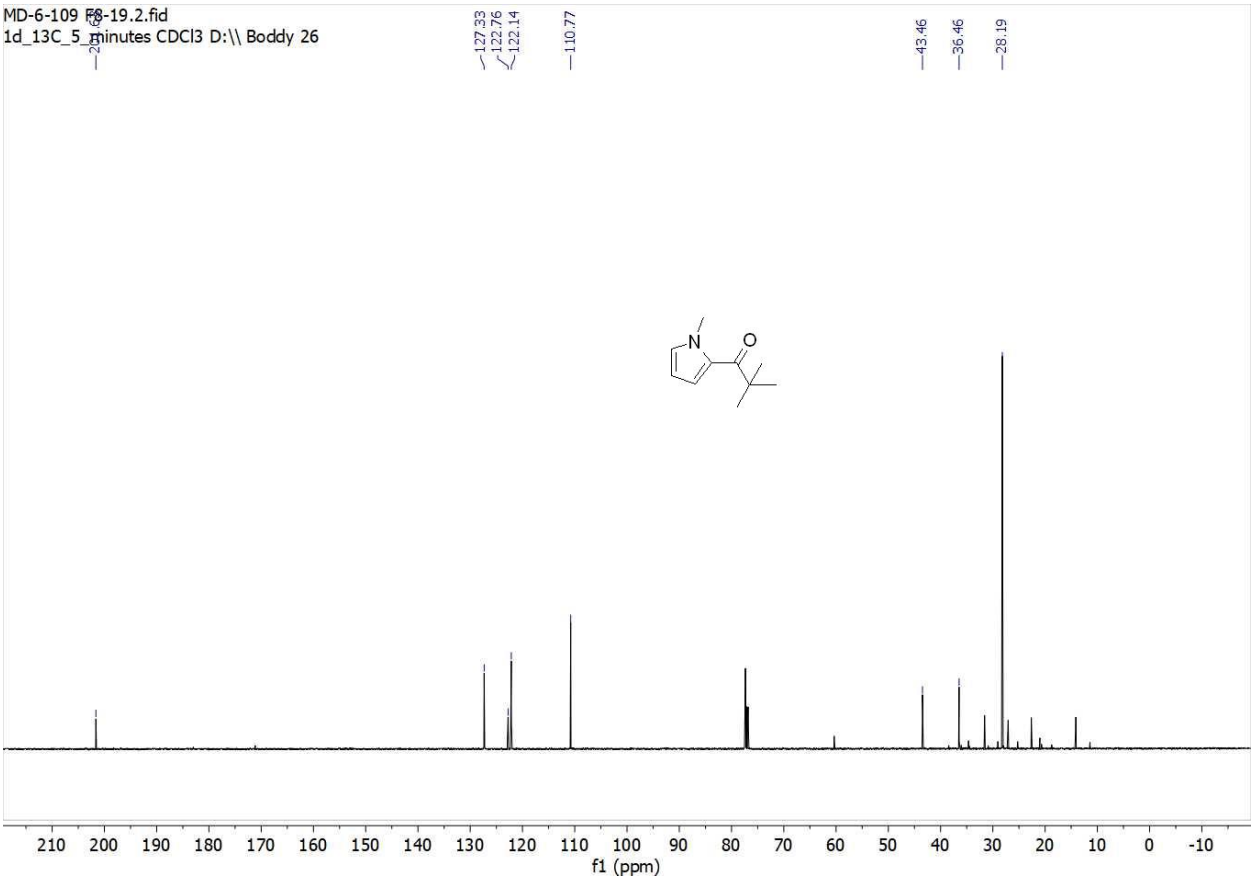

$^{13}C\{^{1}H\}$ NMR (150 MHz, $CDCl_3$) of **7m.**

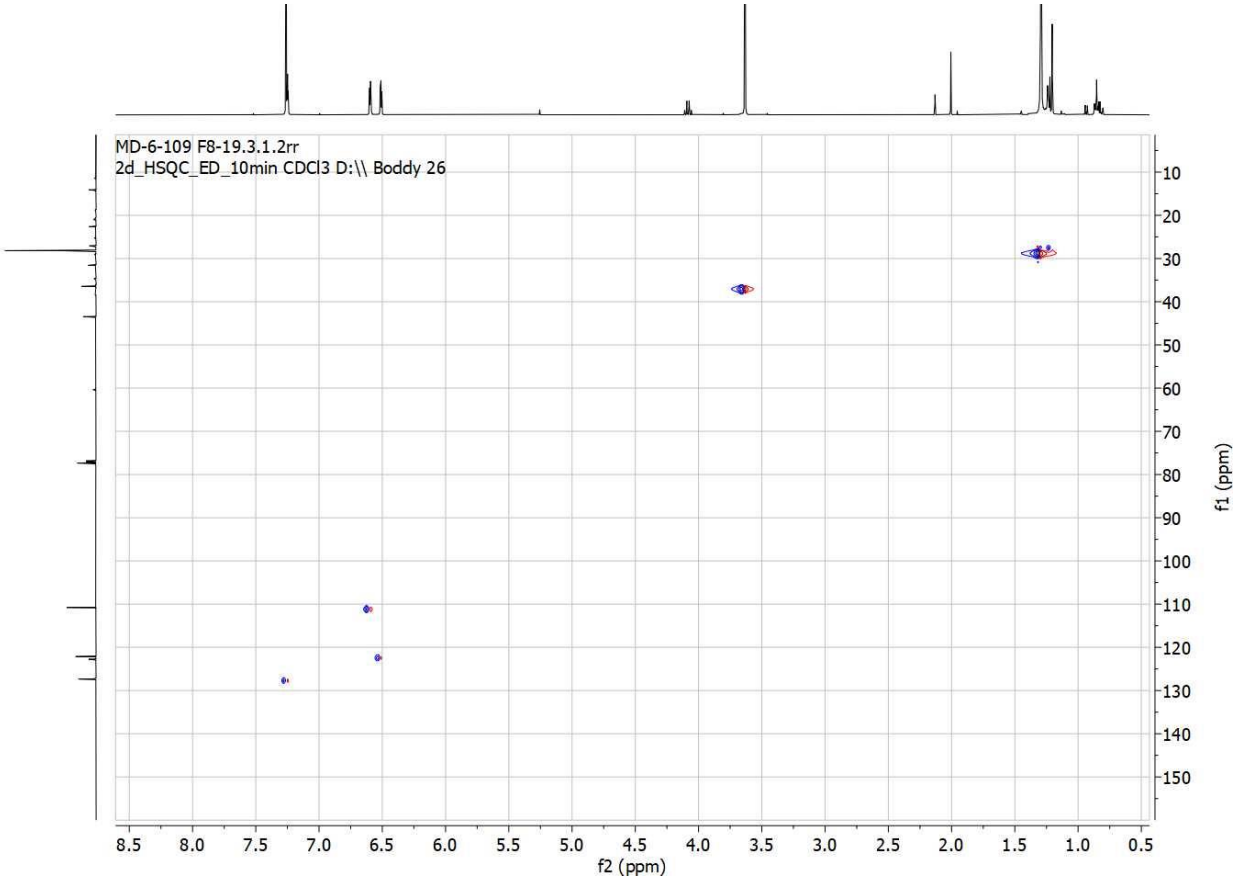
MD-6-109 F8-19.3.1.2rr
2d_HSQC_ED_10min CDCl3 D:\\ Boddy 26
f2 (ppm)
f1 (ppm)

HSQC of **7m.**

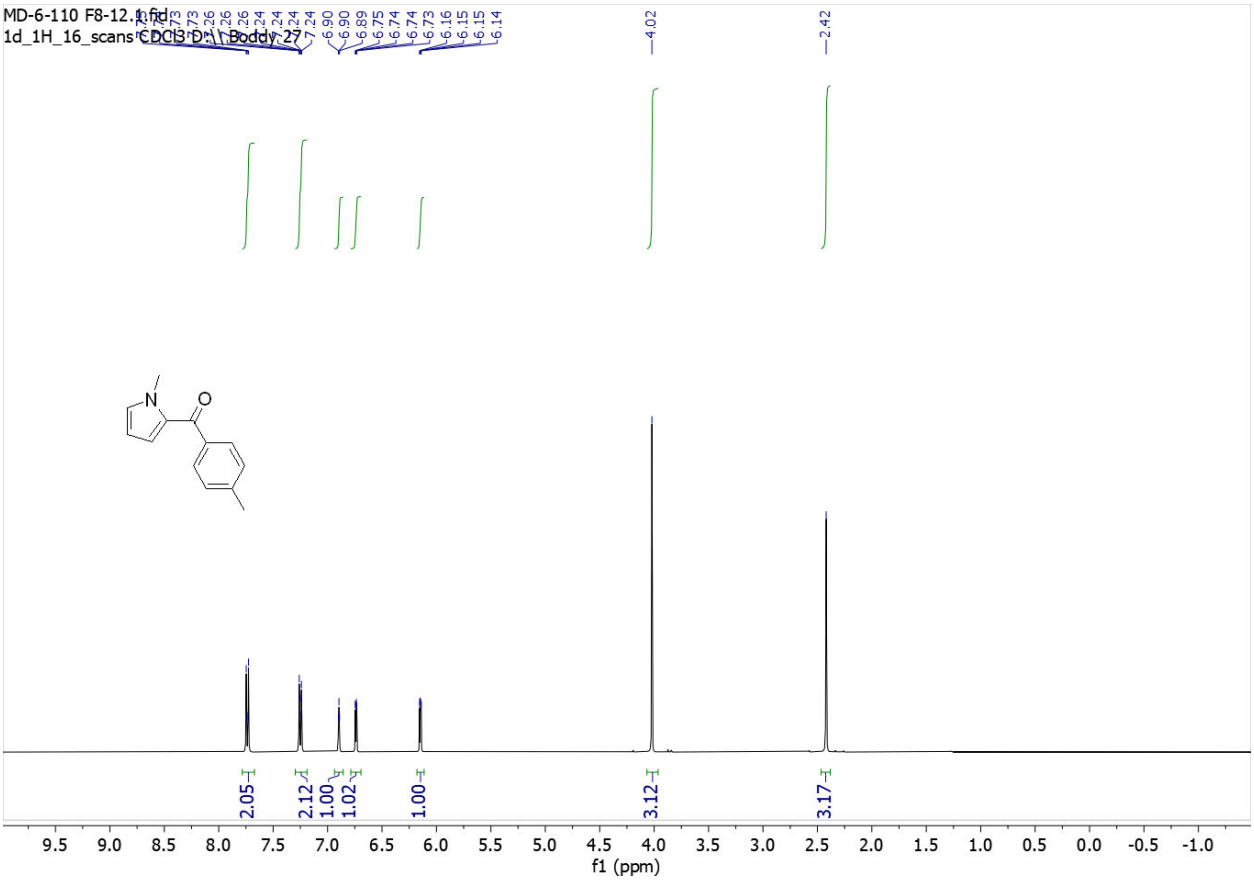

^{1}H NMR (600 MHz, $CDCl_3$) of **7n.**

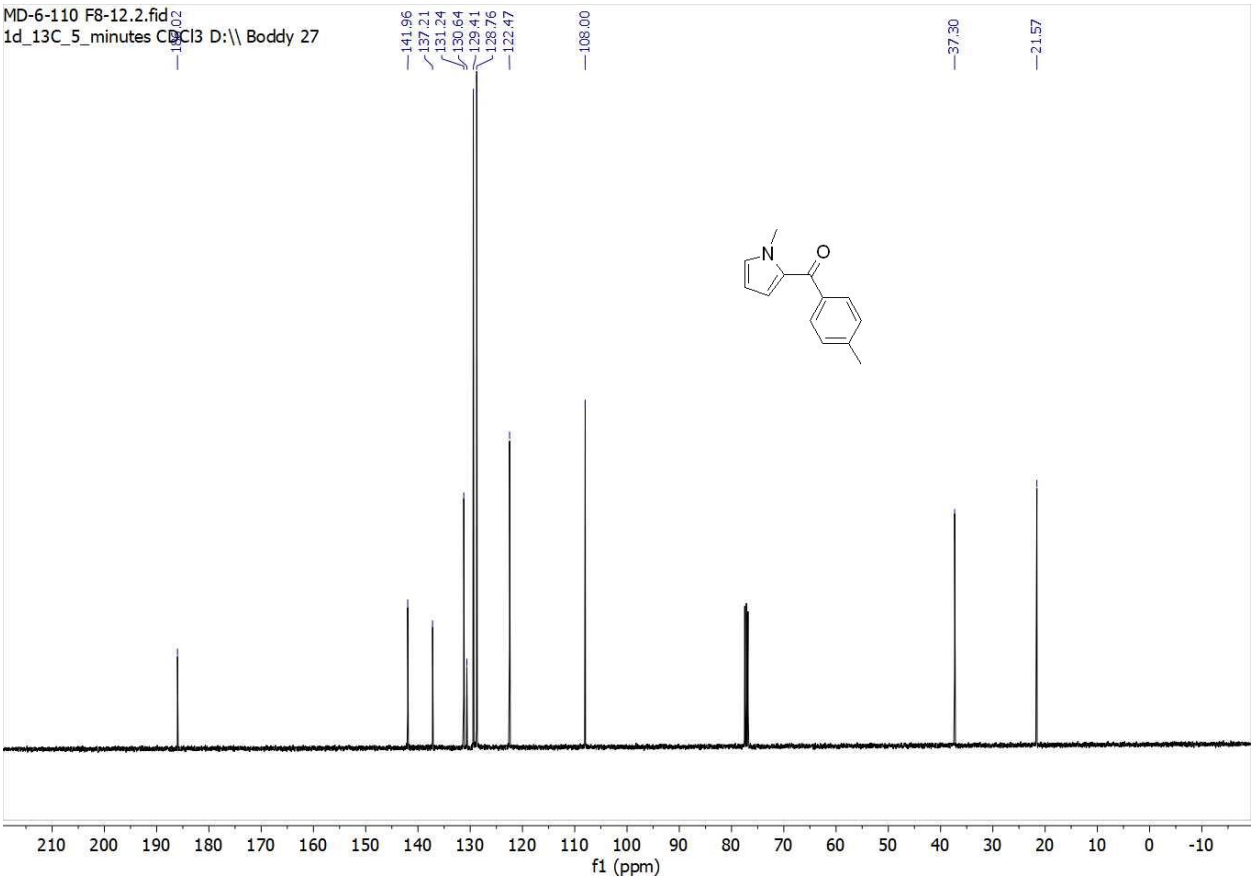

$^{13}C\{^{1}H\}$ NMR (150 MHz, $CDCl_3$) of **7n.**

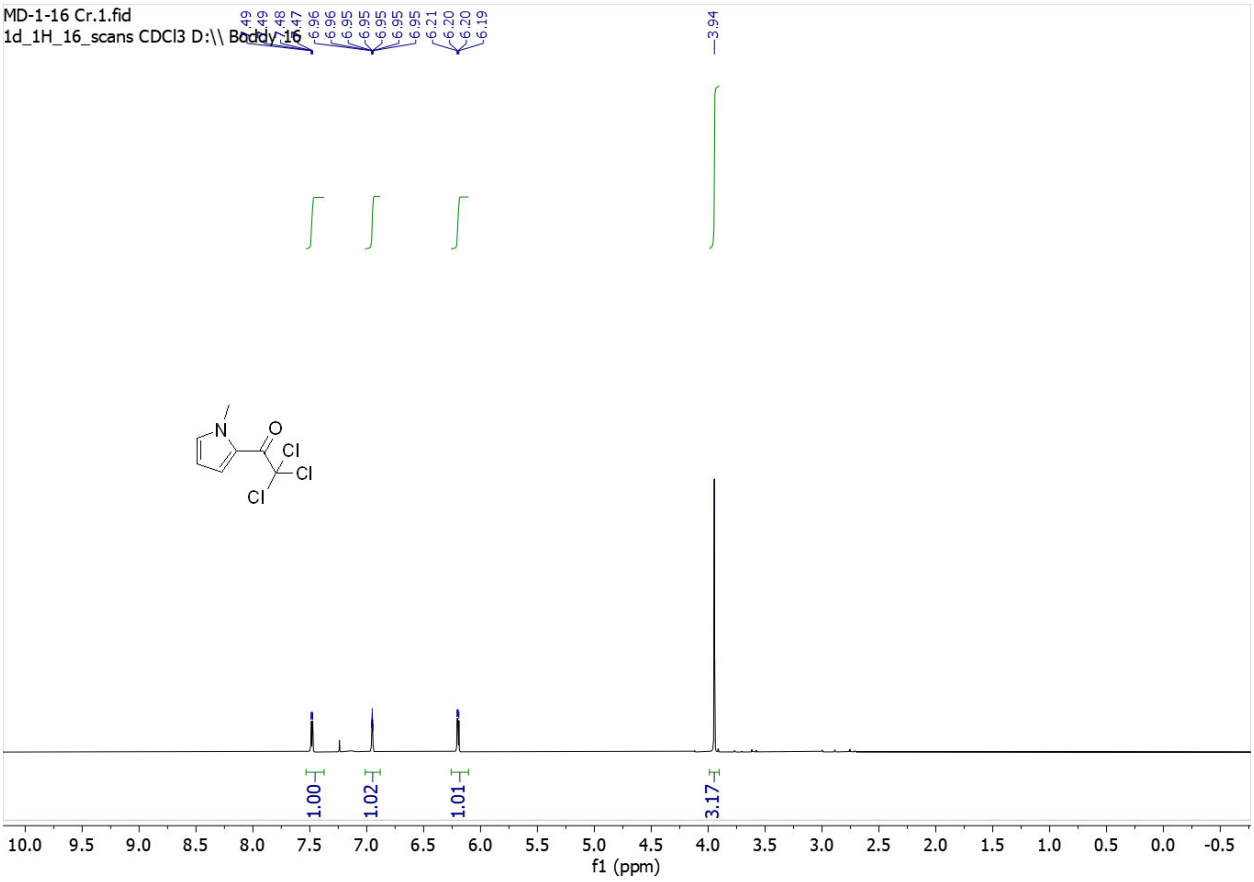

^{1}H NMR (400 MHz, $CDCl_3$) of **7q.**

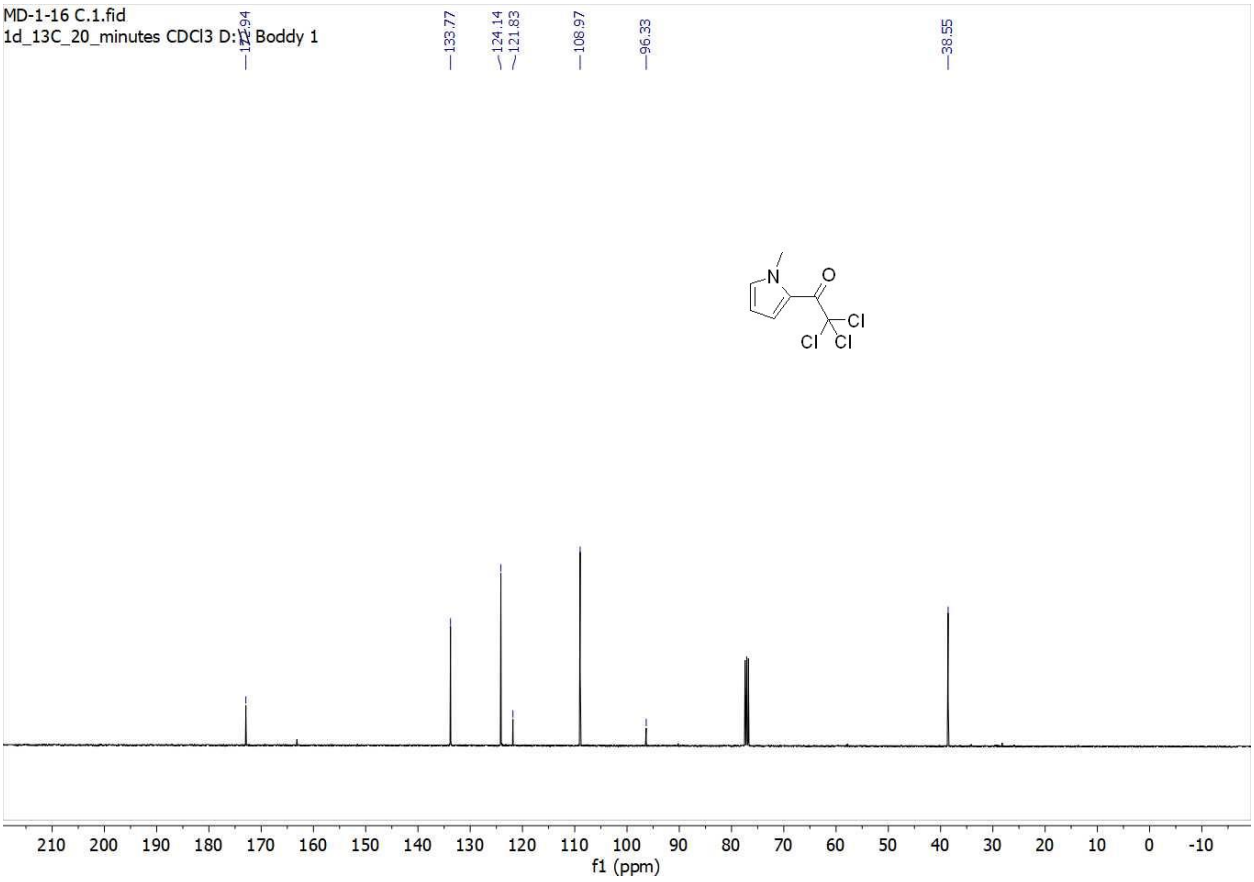

$^{13}C\{^{1}H\}$ NMR (100 MHz, $CDCl_3$) of **7q.**

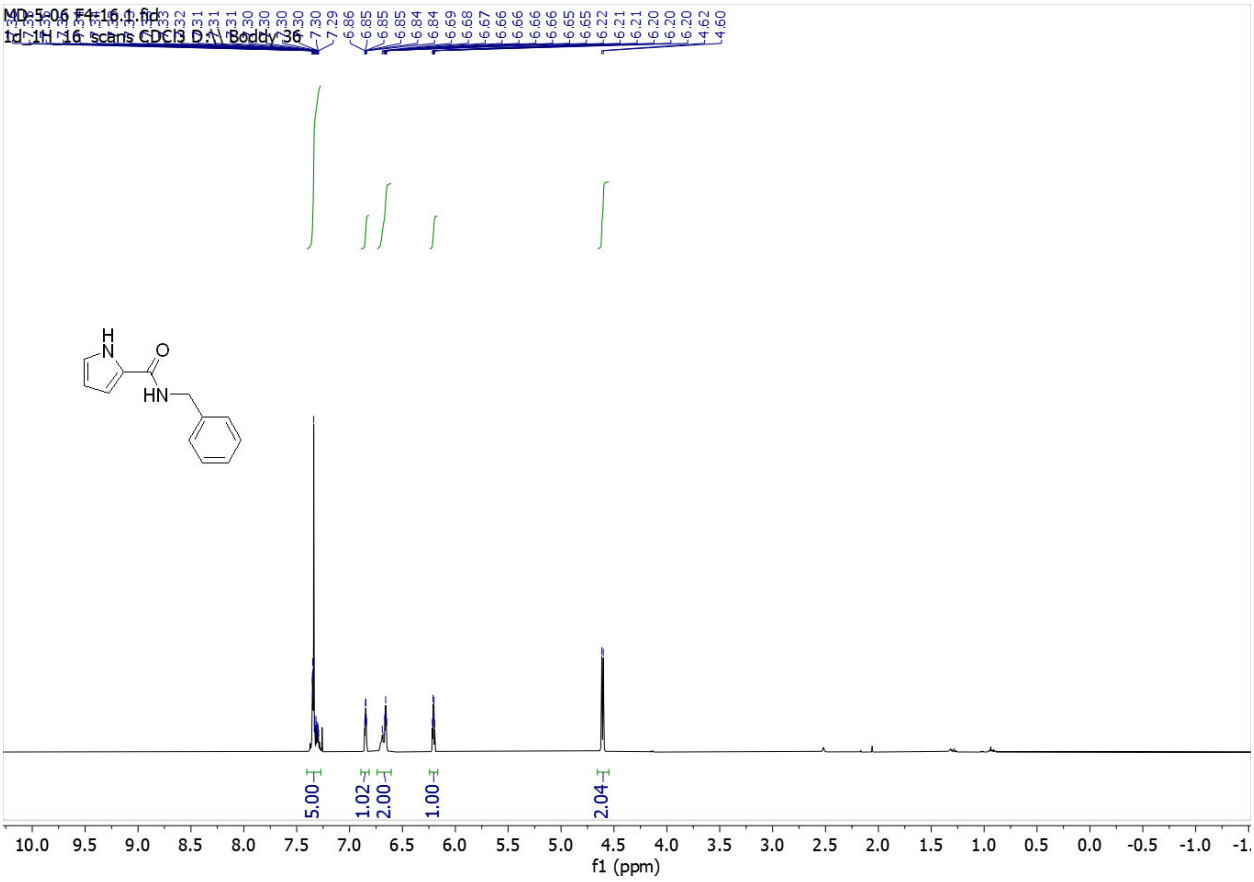

^{1}H NMR (400 MHz, $CDCl_3$) of **7r.**

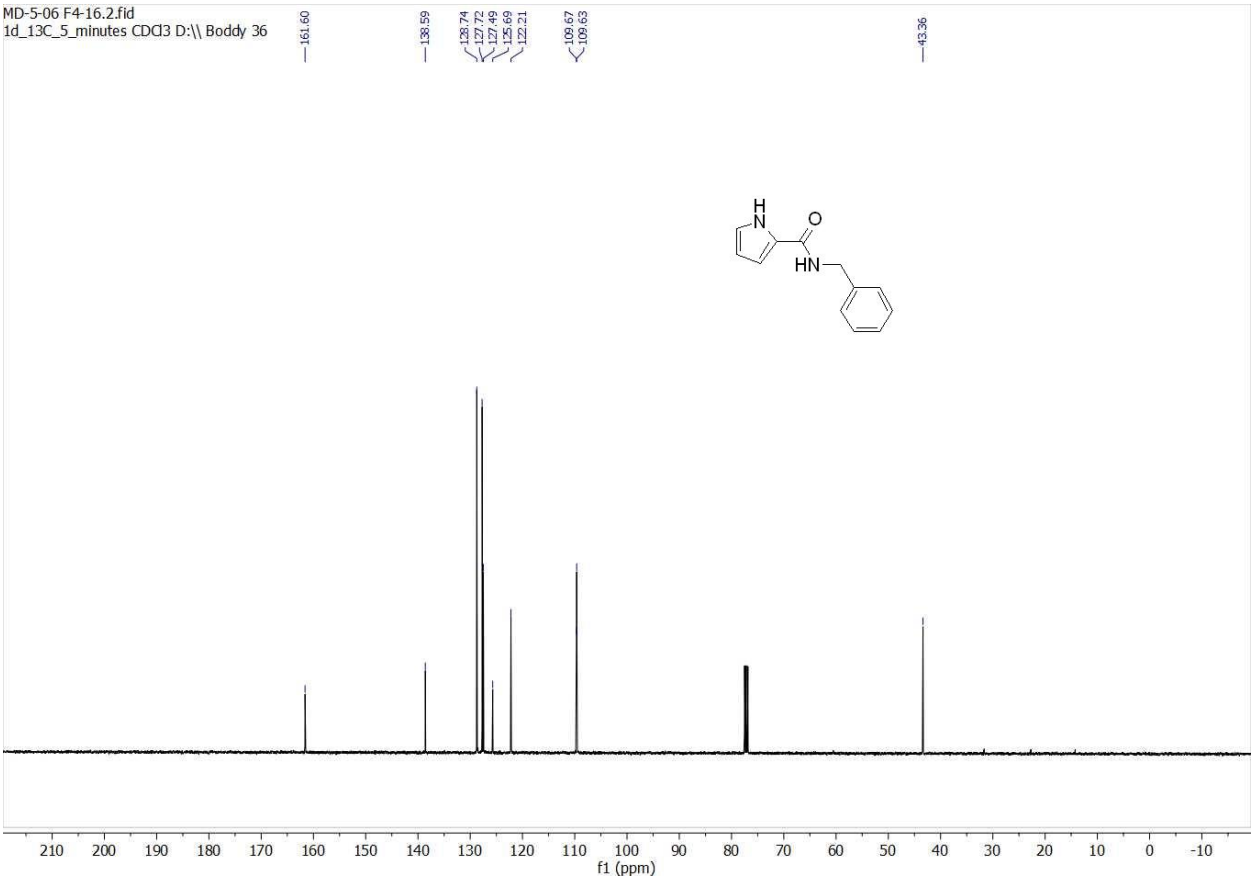

$^{13}C\{^{1}H\}$ NMR (100 MHz, $CDCl_3$) of **7r.**

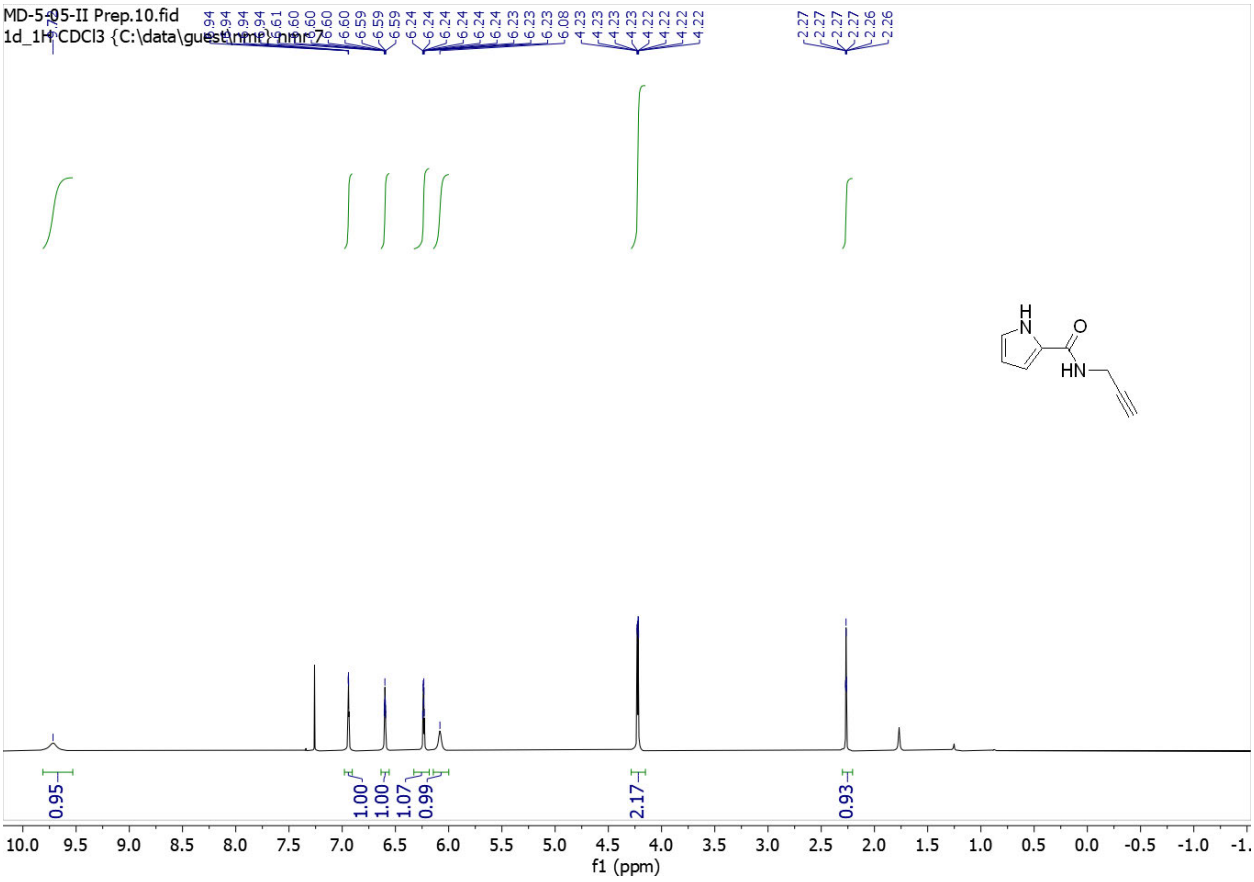

^{1}H NMR (600 MHz, $CDCl_3$) of **7s.**

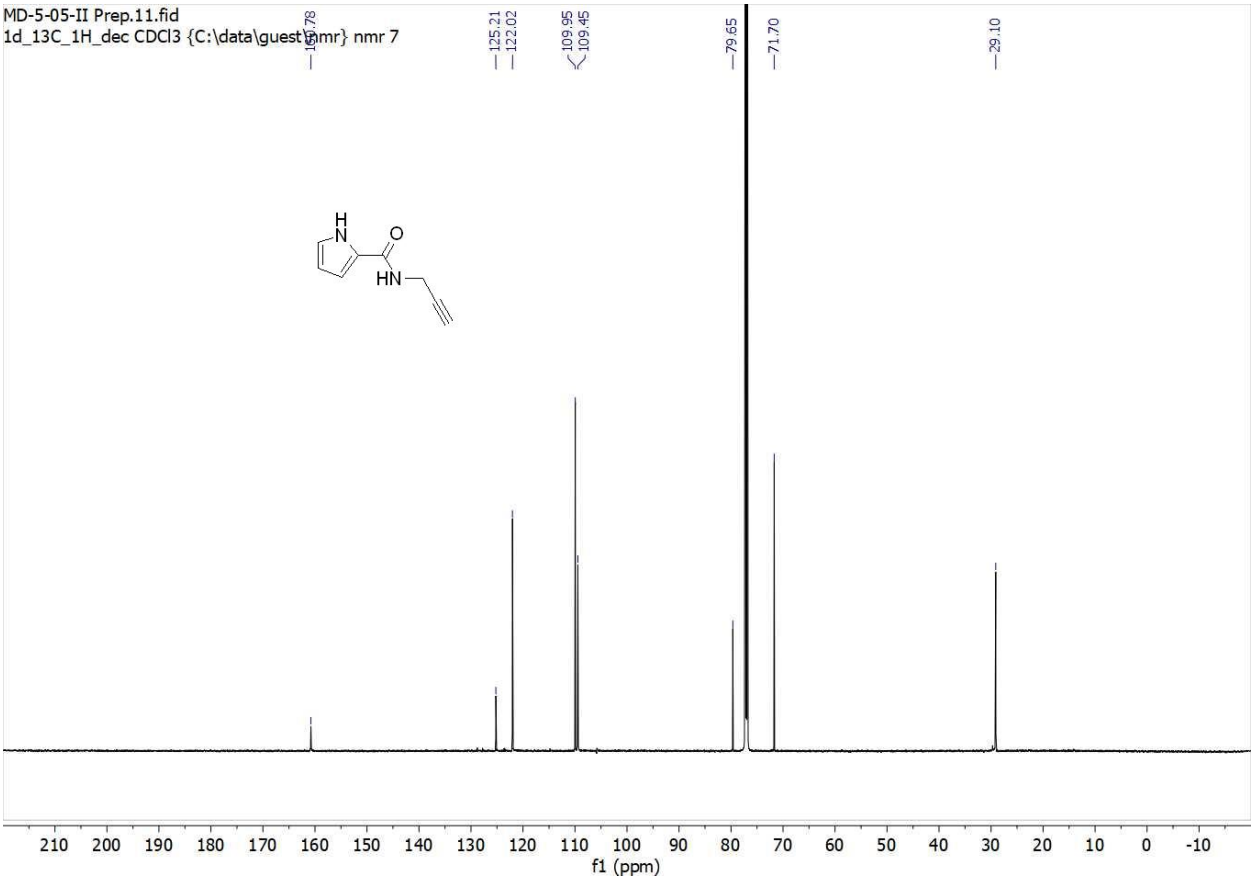

$^{13}C\{^{1}H\}$ NMR (150 MHz, $CDCl_3$) of **7s.**

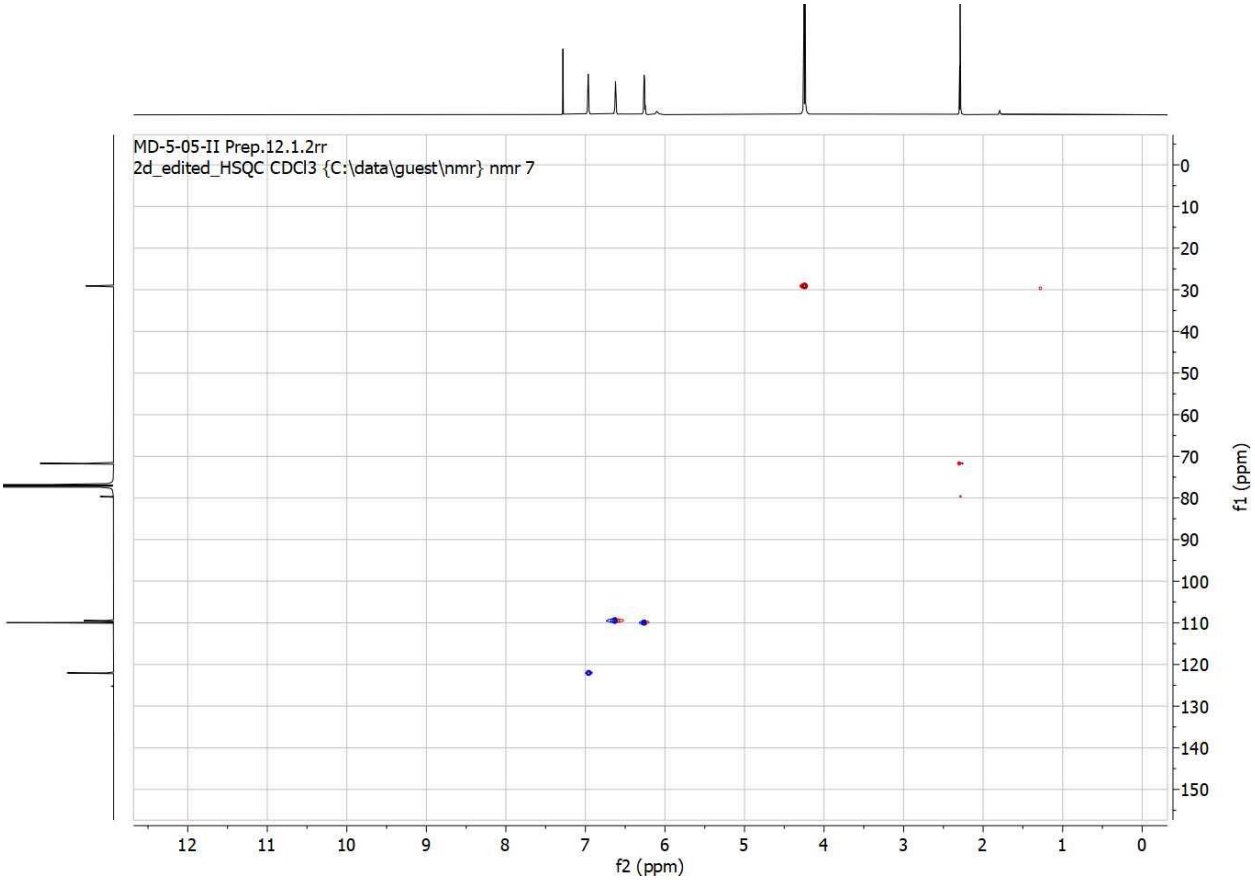
MD-5-05-II Prep.12.1.2rr
2d_edited_HSQC CDCl3 {C:\data\guest\nmr} nmr 7
f2 (ppm)
f1 (ppm)

HSQC of **7s.**

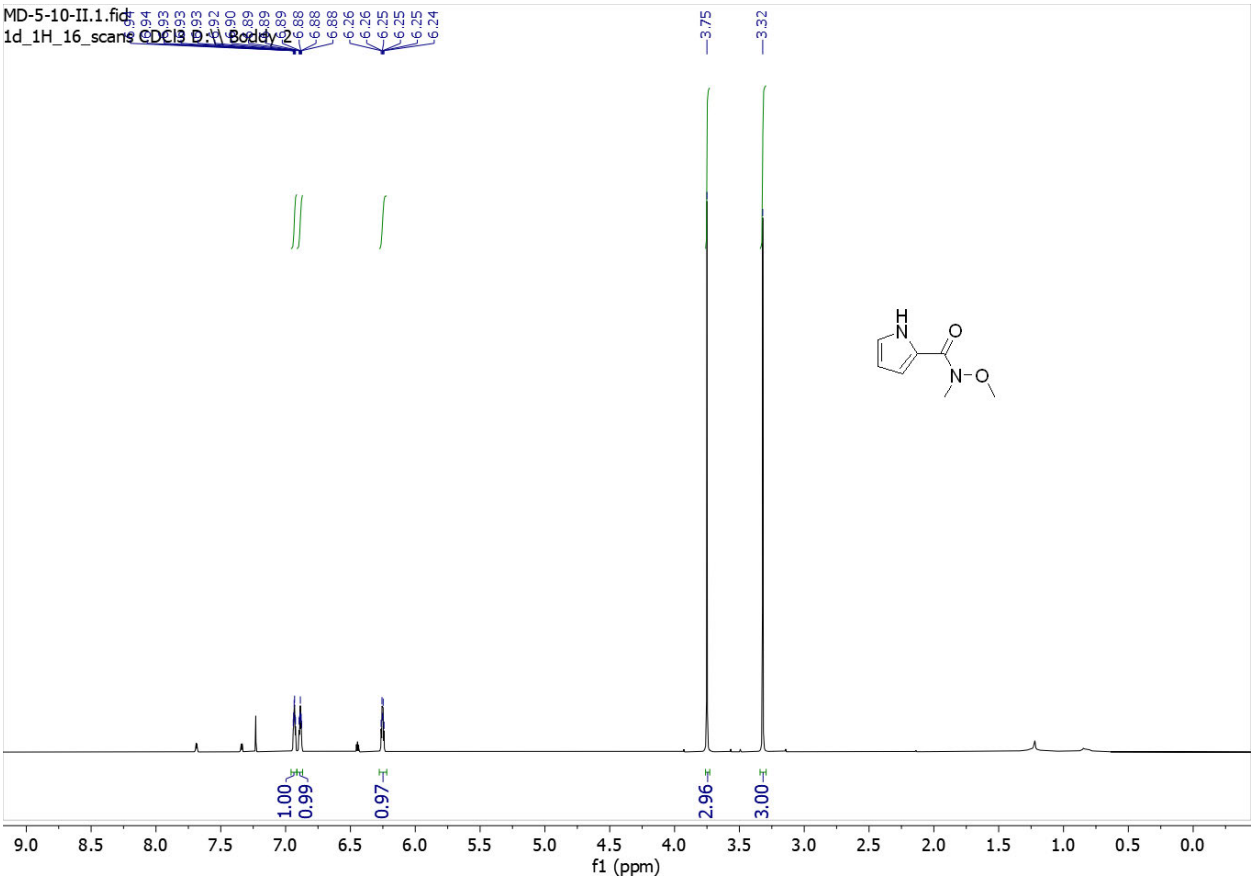

^{1}H NMR (600 MHz, $CDCl_3$) of **7t.**

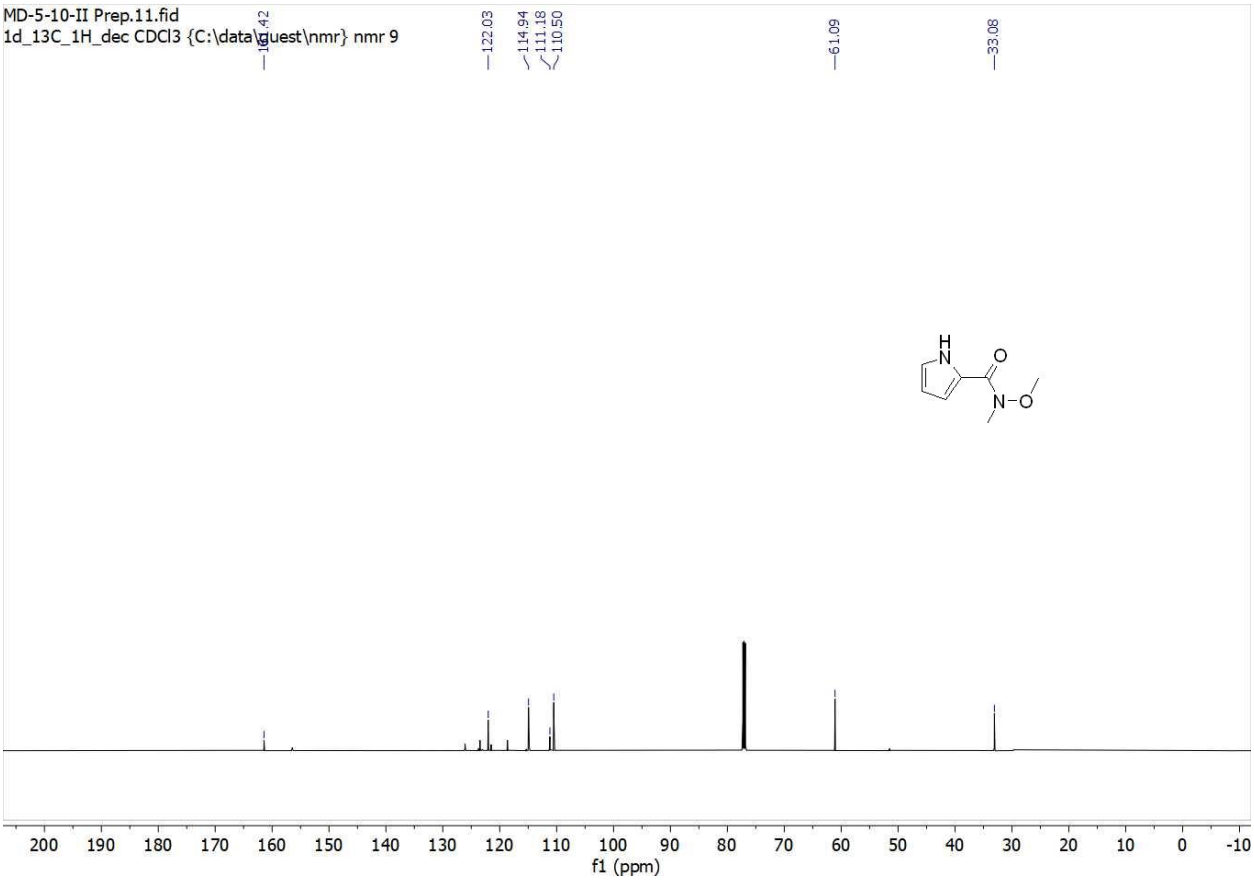

$^{13}C\{^{1}H\}$ NMR (150 MHz, $CDCl_3$) of **7t.**

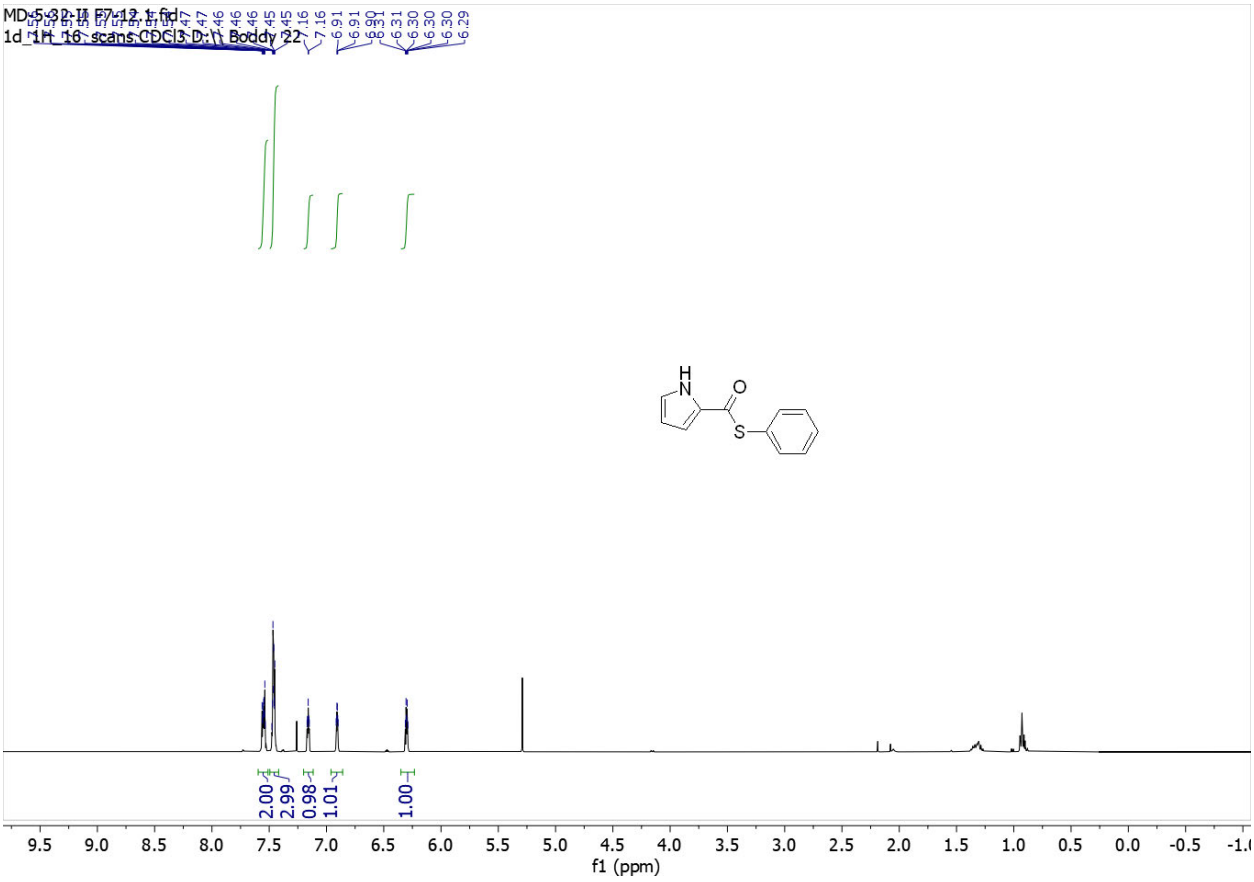

^{1}H NMR (400 MHz, $CDCl_3$) of **7u.**

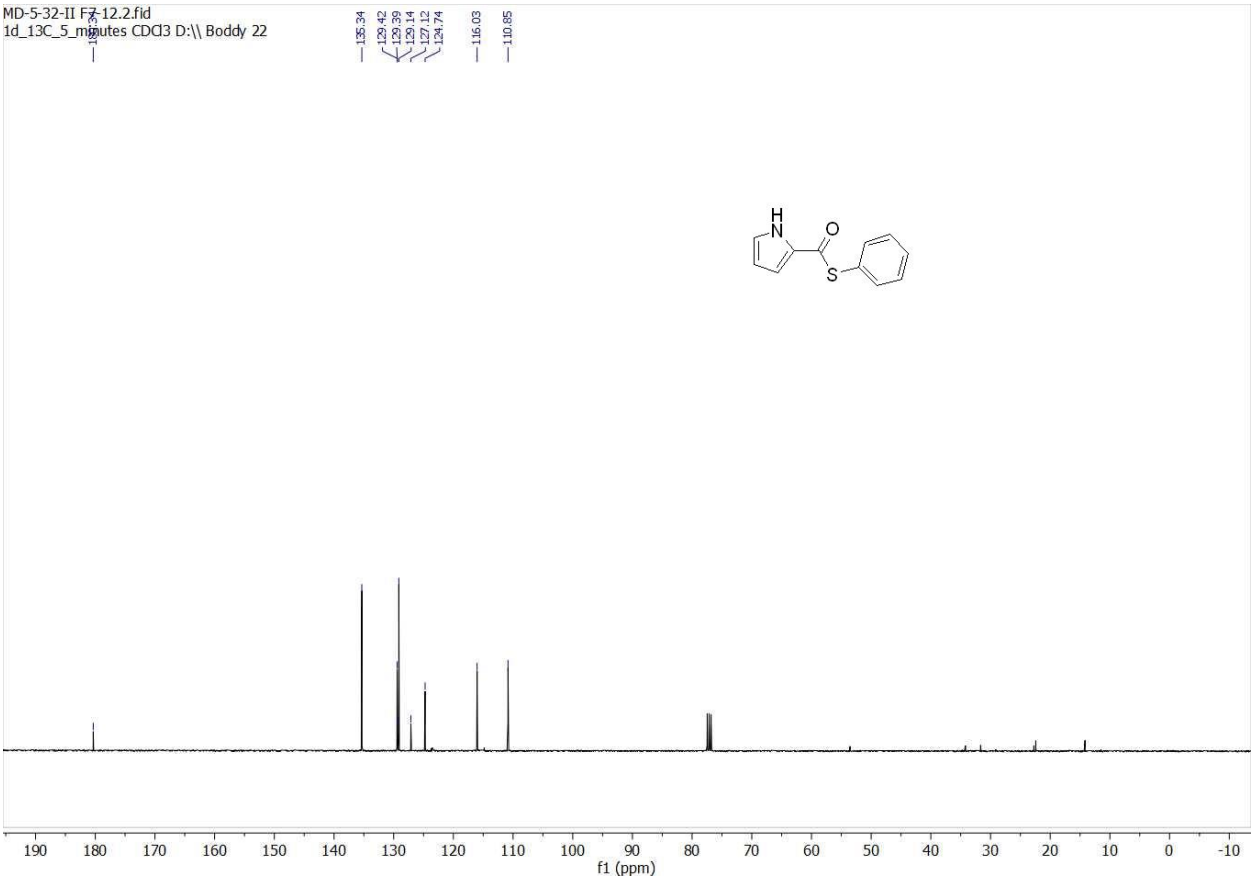

$^{13}C\{^{1}H\}$ NMR (100 MHz, $CDCl_3$) of **7u.**

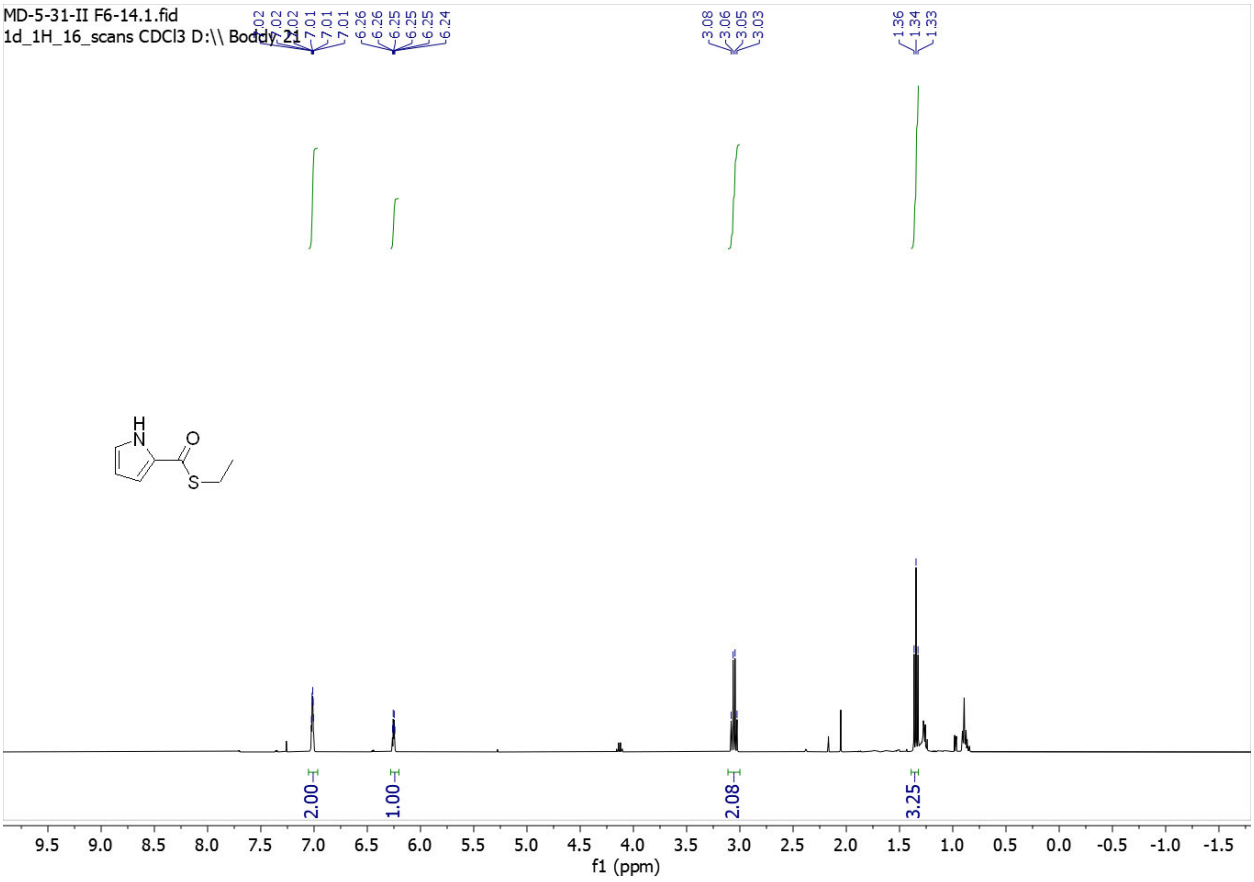

^{1}H NMR (400 MHz, $CDCl_3$) of **7v.**

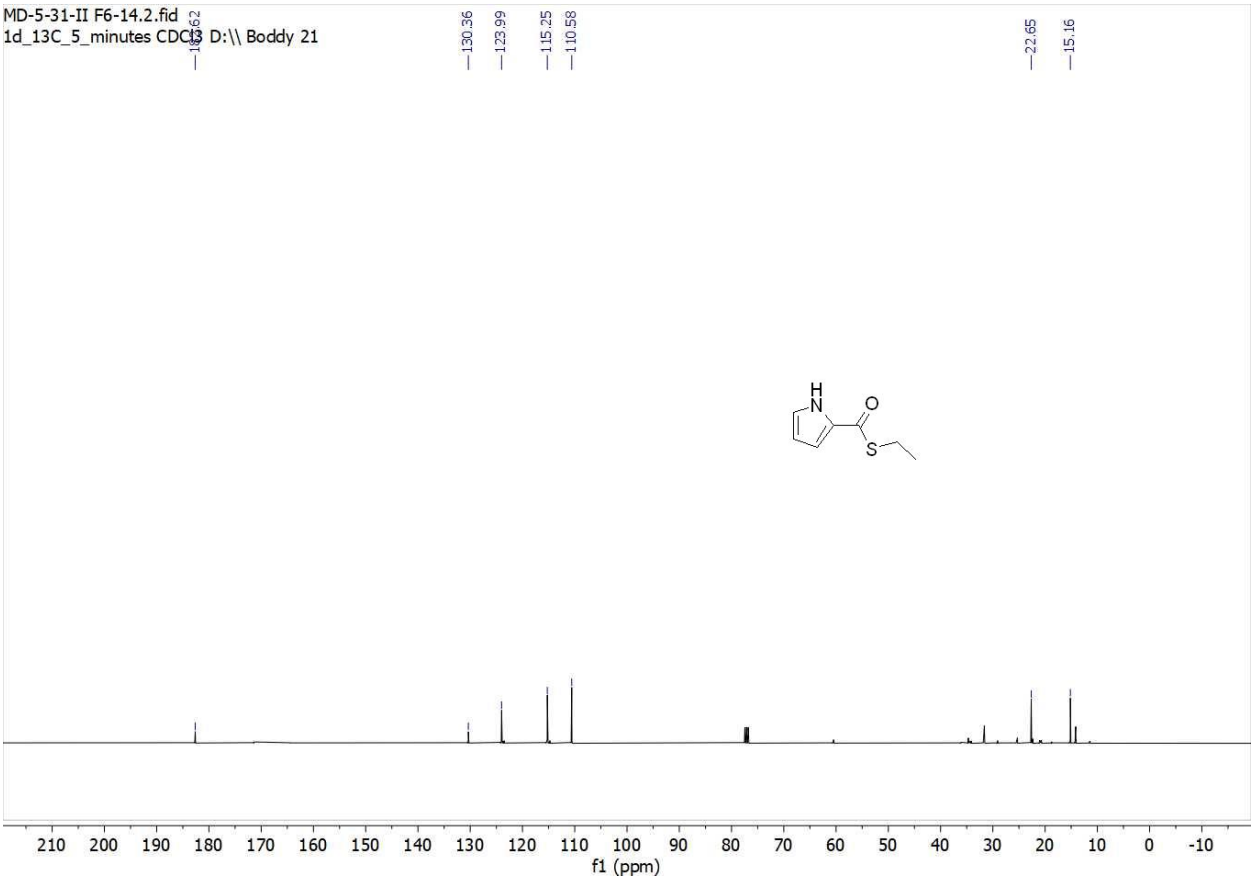

$^{13}C\{^{1}H\}$ NMR (100 MHz, $CDCl_3$) of **7v.**

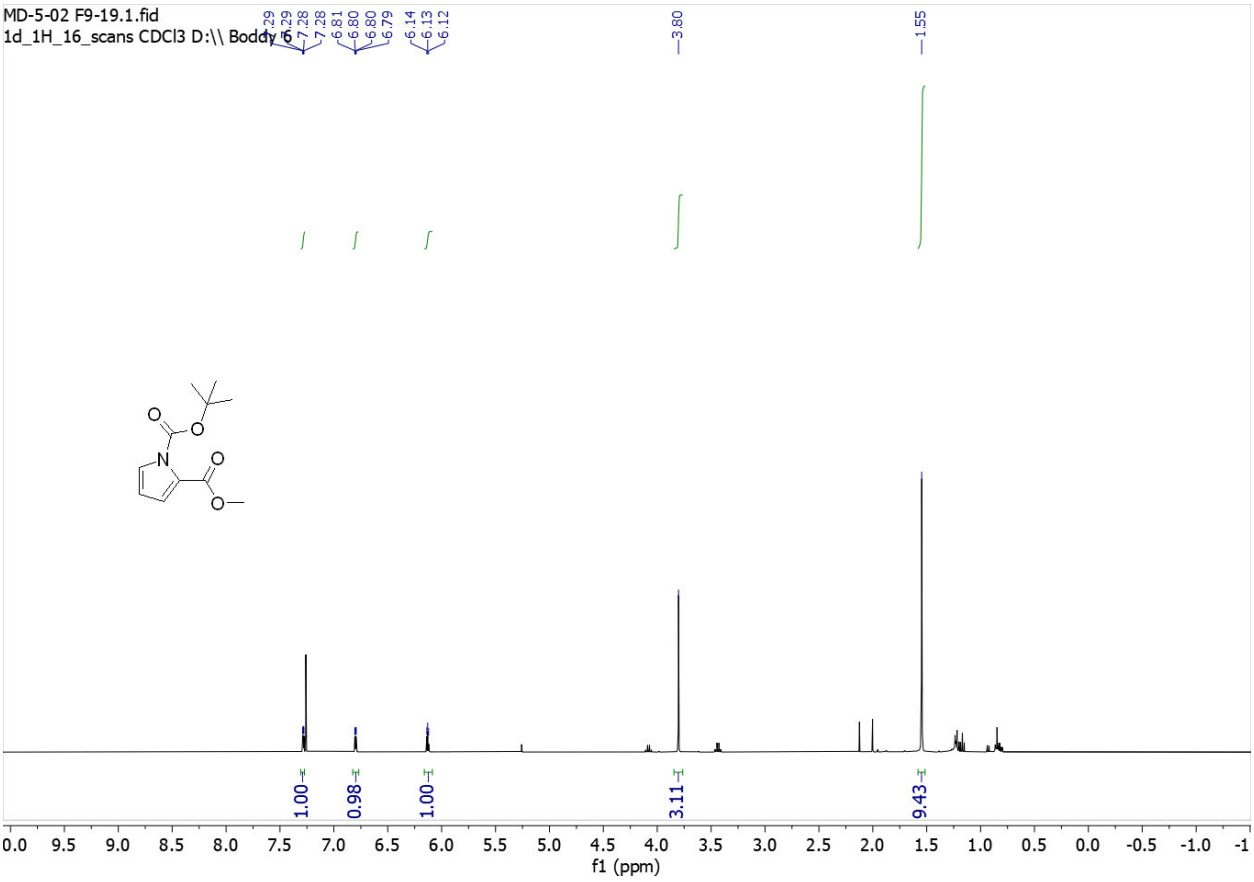

^{1}H NMR (400 MHz, $CDCl_3$) of **7x.**

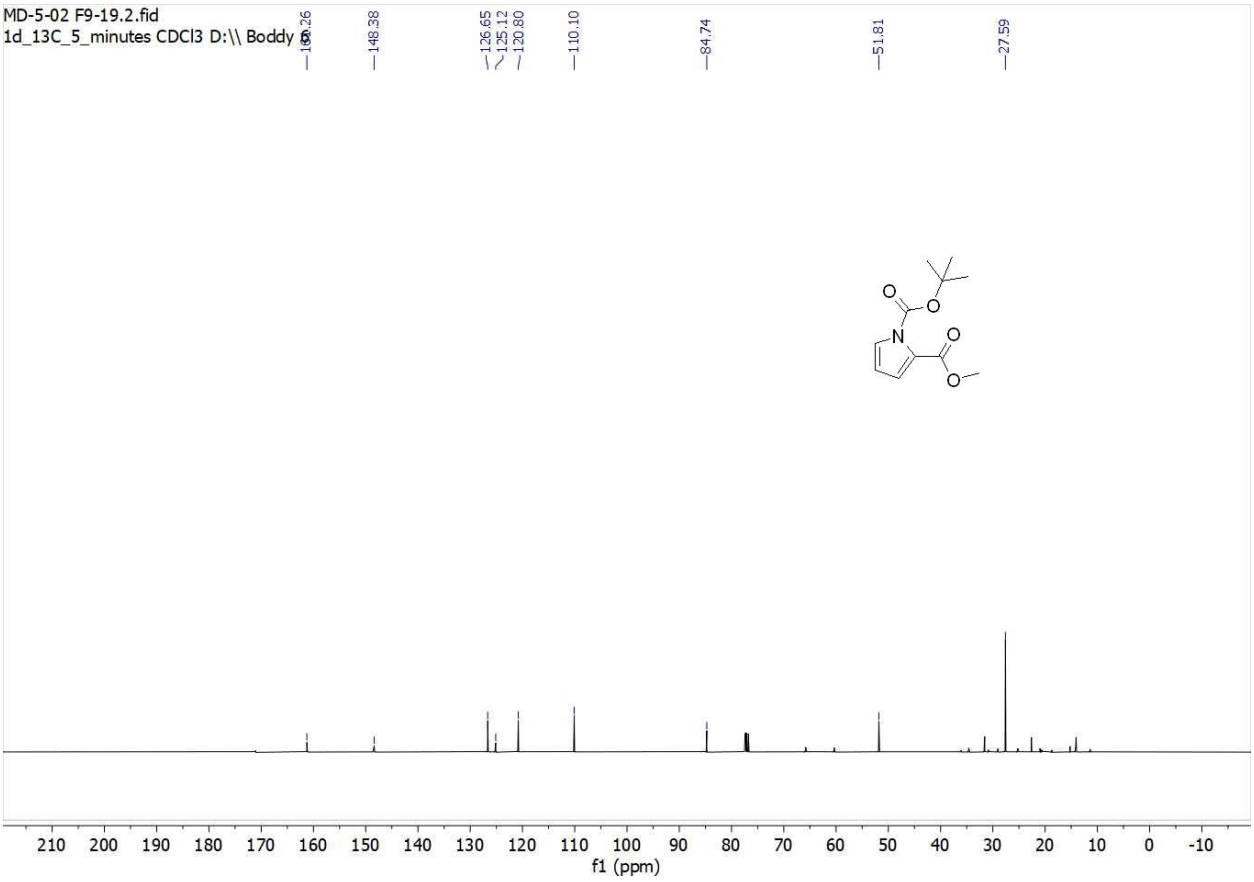

$^{13}C\{^{1}H\}$ NMR (100 MHz, $CDCl_3$) of **7x.**

Section 4. Copies of ^{1}H and ^{13}C spectra - B) **Table 1. 8a-k**

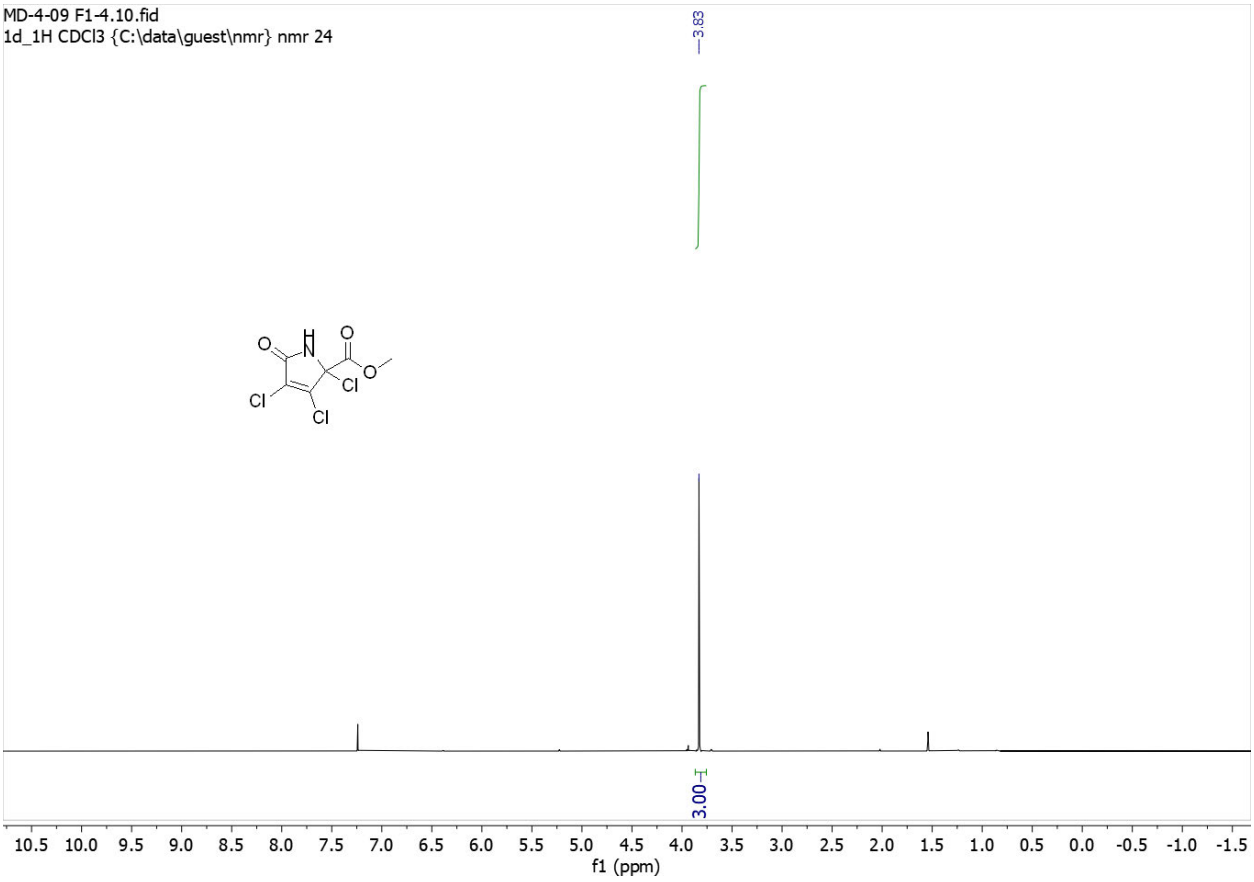

^{1}H NMR (400 MHz, $CDCl_3$) of **8a.**

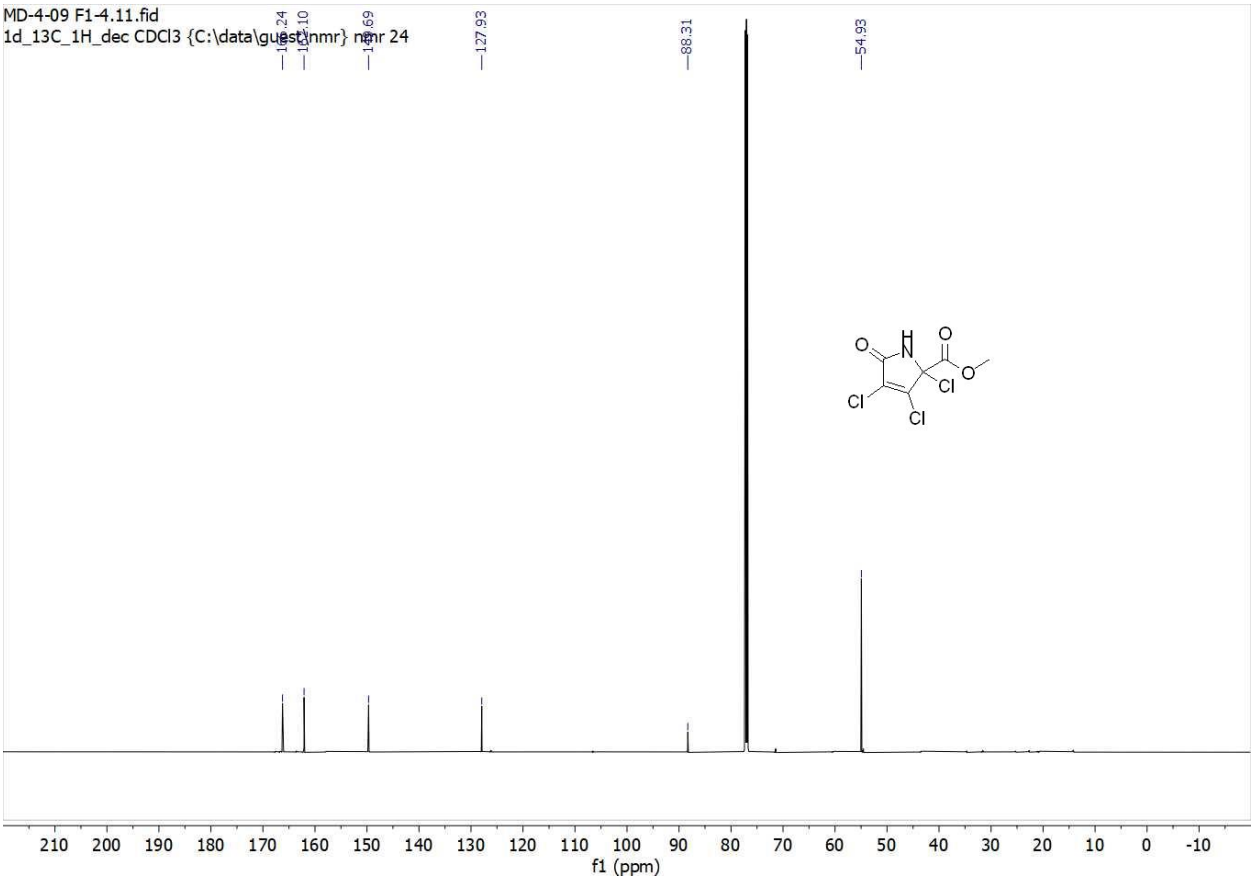

$^{13}C\{^{1}H\}$ NMR (100 MHz, $CDCl_3$) of **8a.**

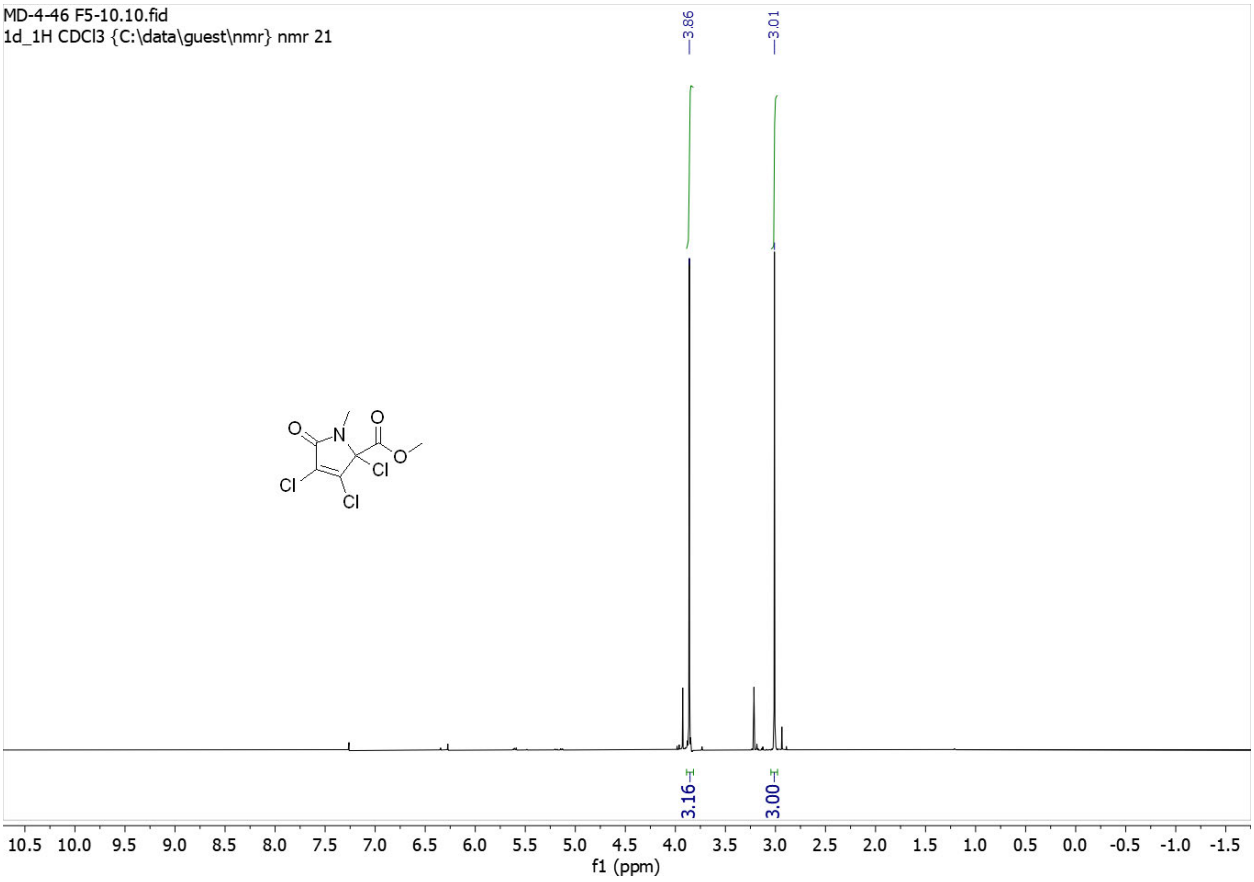

^{1}H NMR (600 MHz, $CDCl_3$) of **8b.**

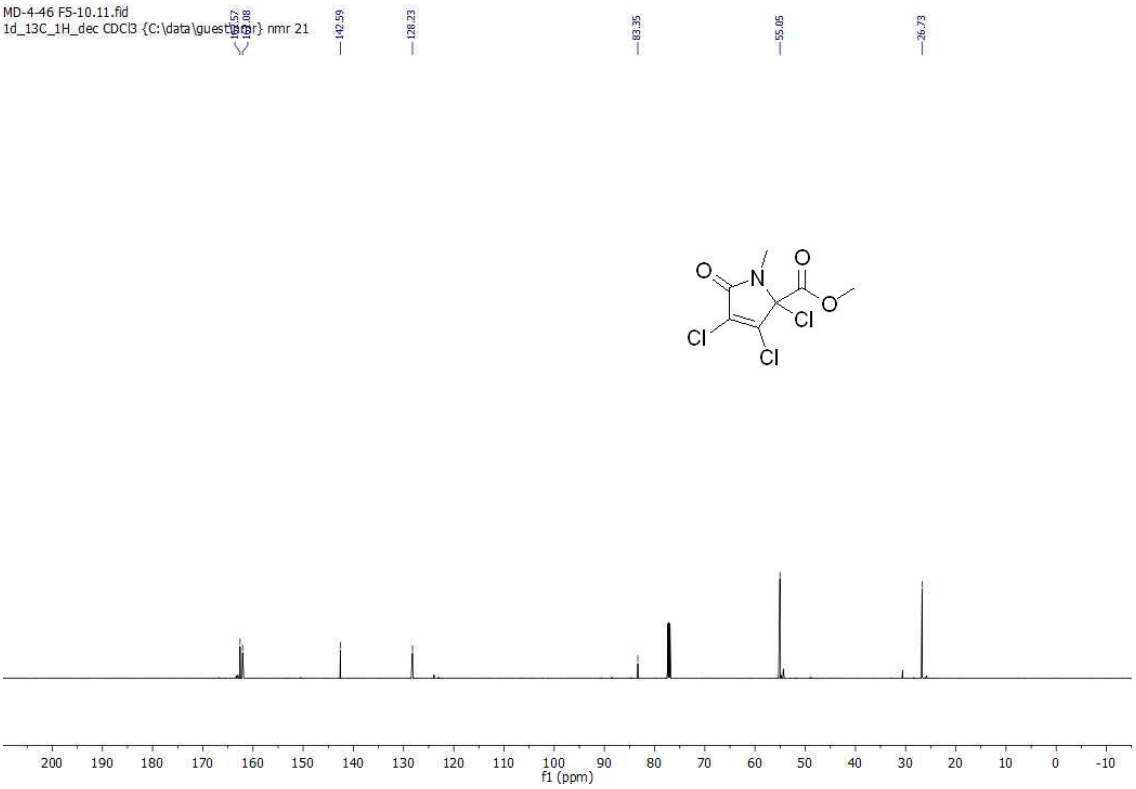

$^{13}C\{^{1}H\}$ NMR (150 MHz, $CDCl_3$) of **8b.**

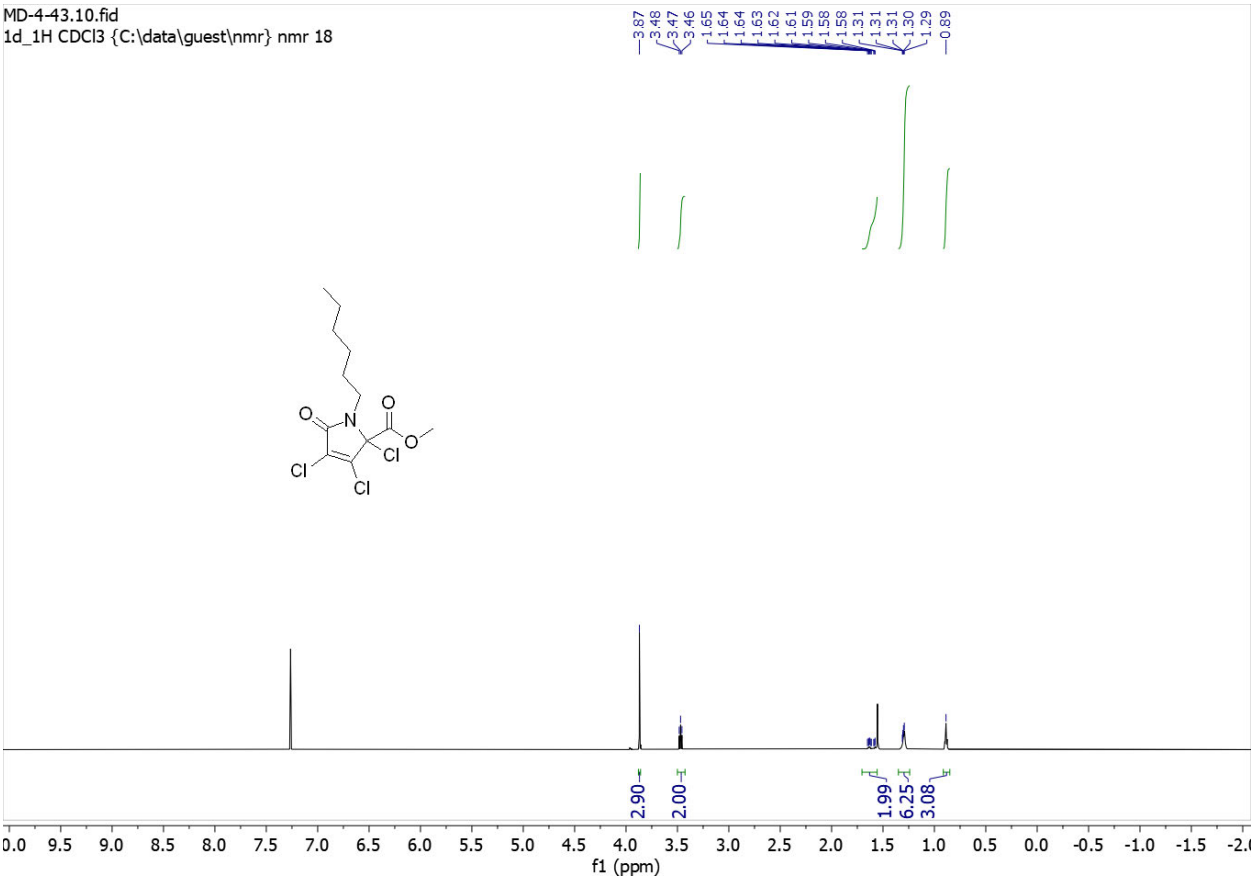

^{1}H NMR (600 MHz, $CDCl_3$) of **8c.**

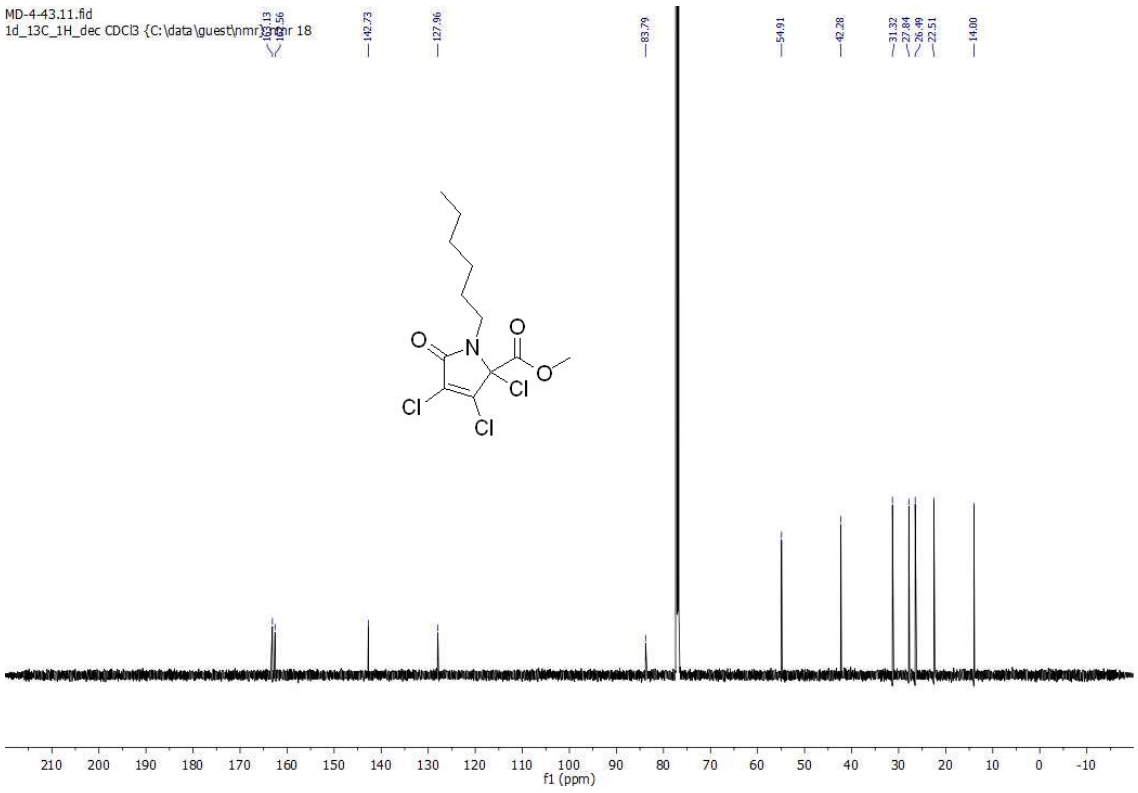

$^{13}C\{^{1}H\}$ NMR (150 MHz, $CDCl_3$) of **8c.**

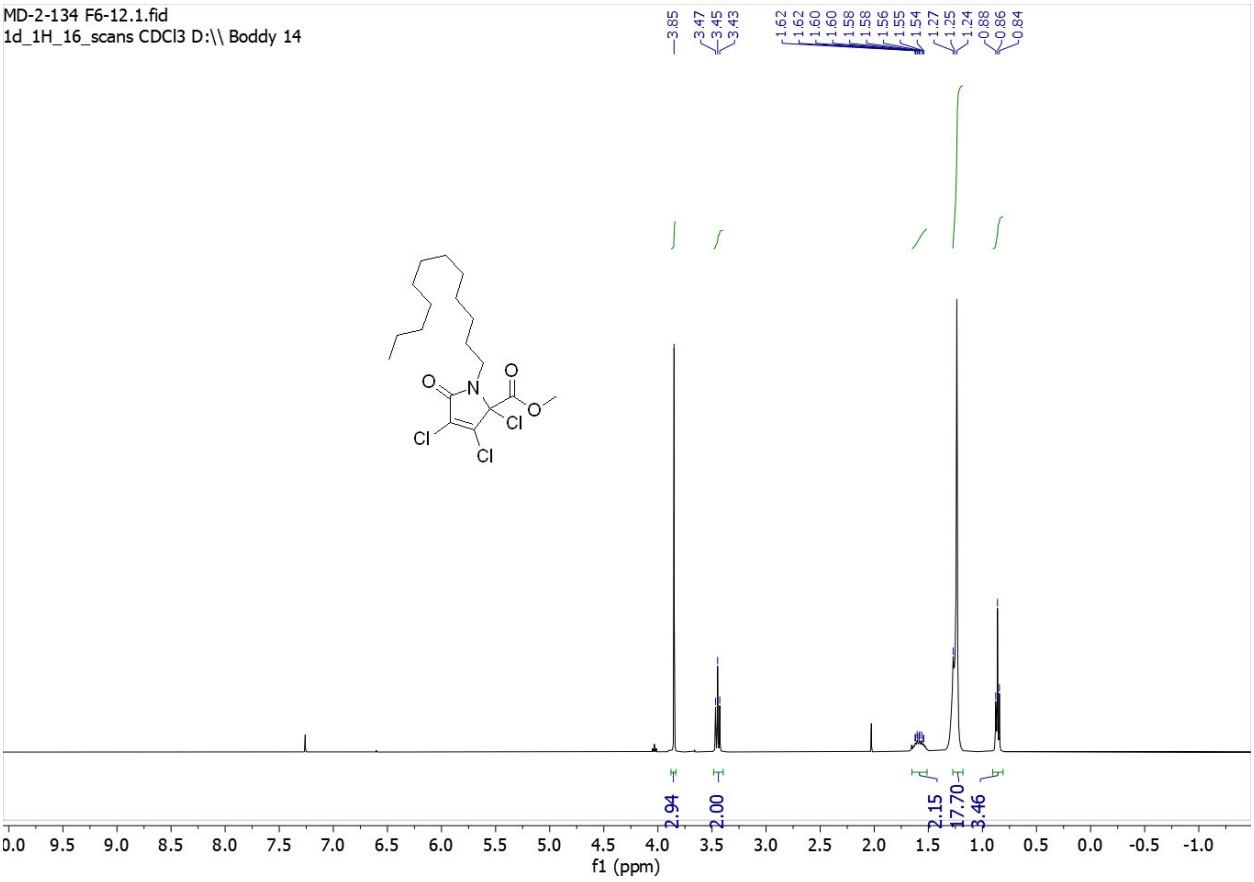

^{1}H NMR (400 MHz, $CDCl_3$) of **8d.**

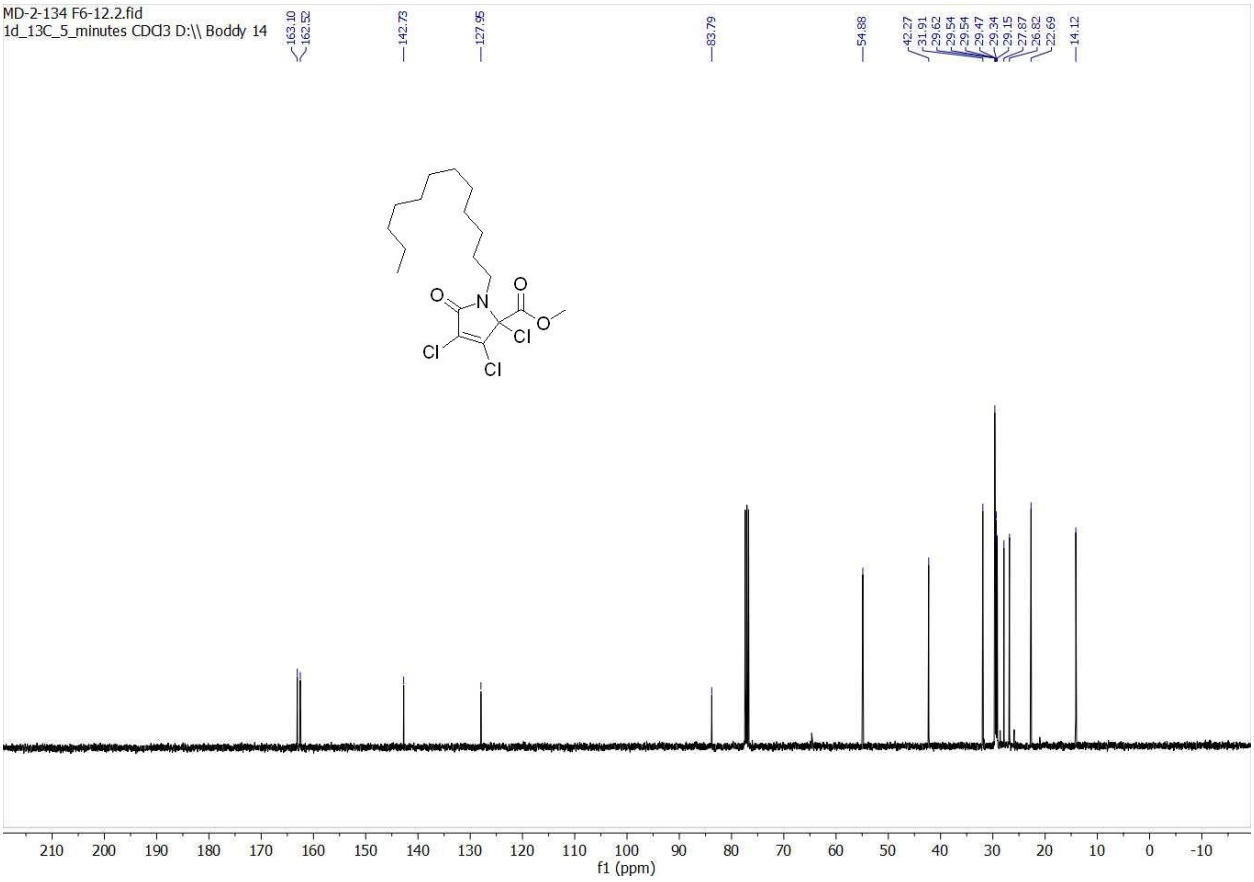

$^{13}C\{^{1}H\}$ NMR (100 MHz, $CDCl_3$) of **8d.**

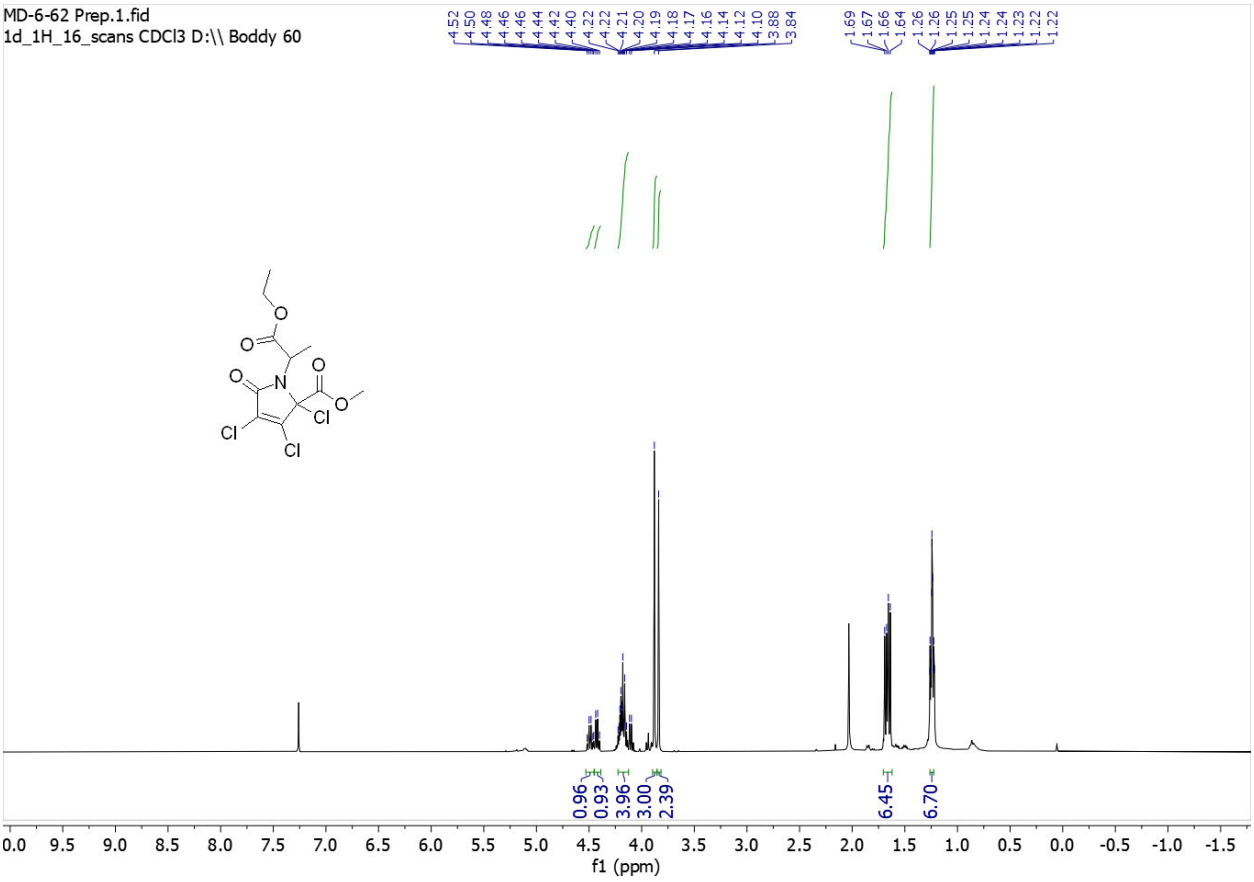

^{1}H NMR (400 MHz, $CDCl_3$) of **8e.**

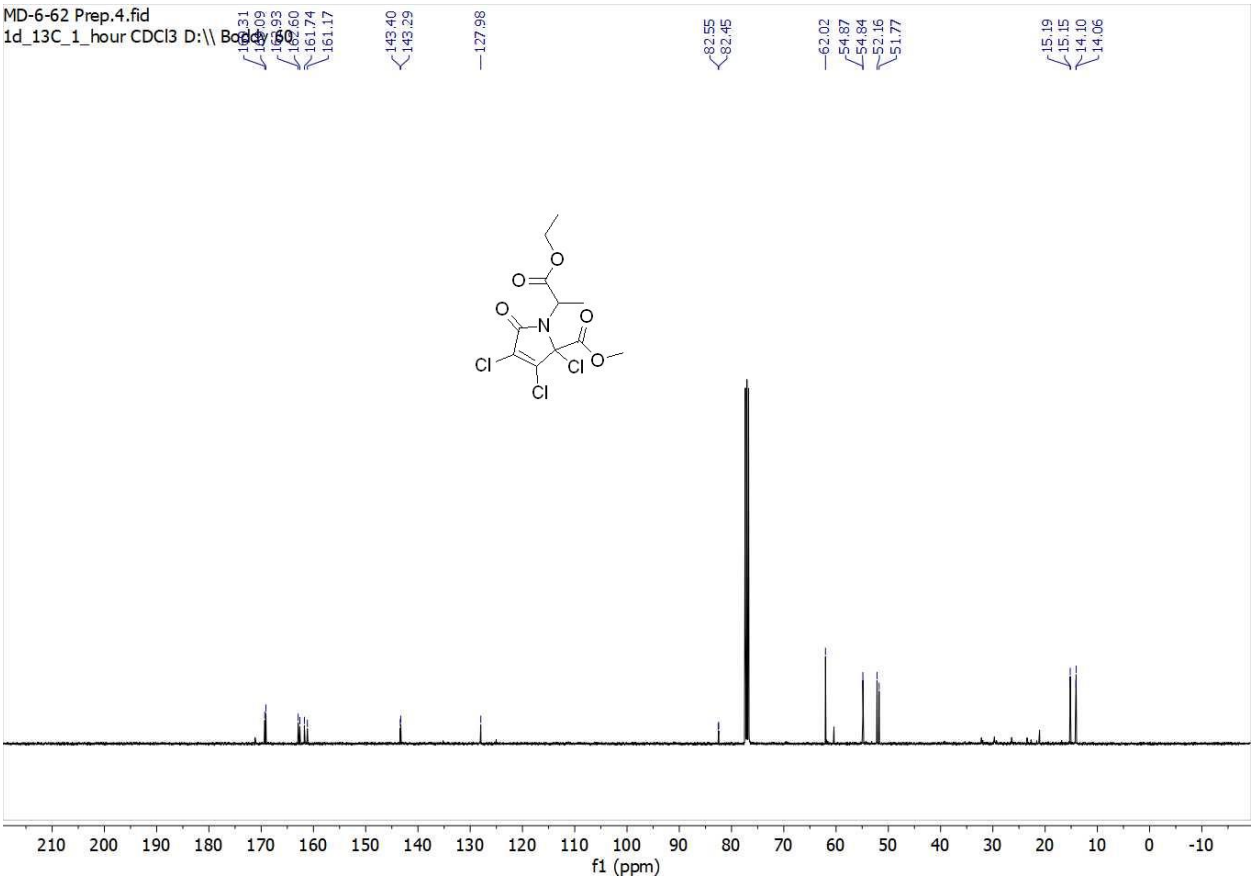

$^{13}C\{^{1}H\}$ NMR (100 MHz, $CDCl_3$) of **8e.**

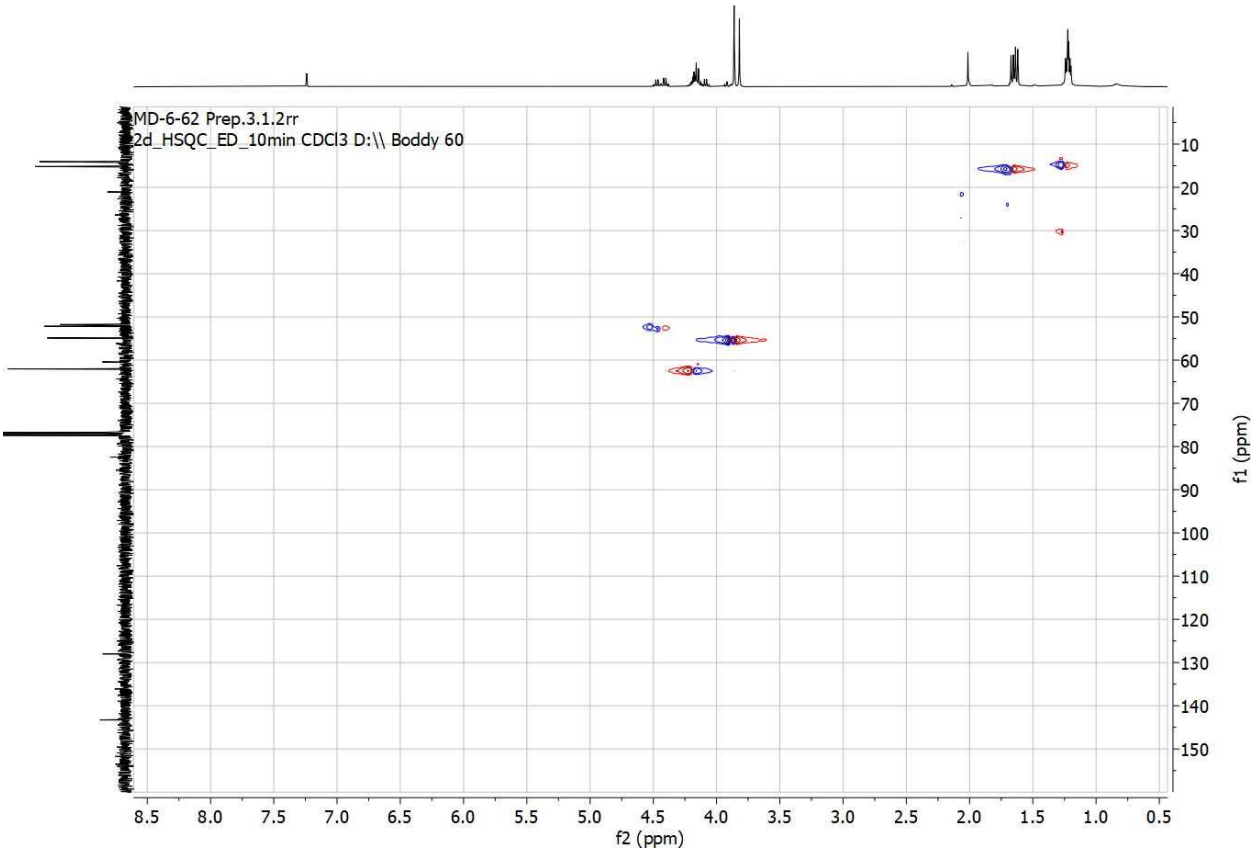
MD-6-62 Prep.3.1.2rr
2d_HSQC_ED_10min CDCl3 D:\\ Boddy 60
f2 (ppm)
f1 (ppm)

HSQC of **8e.**

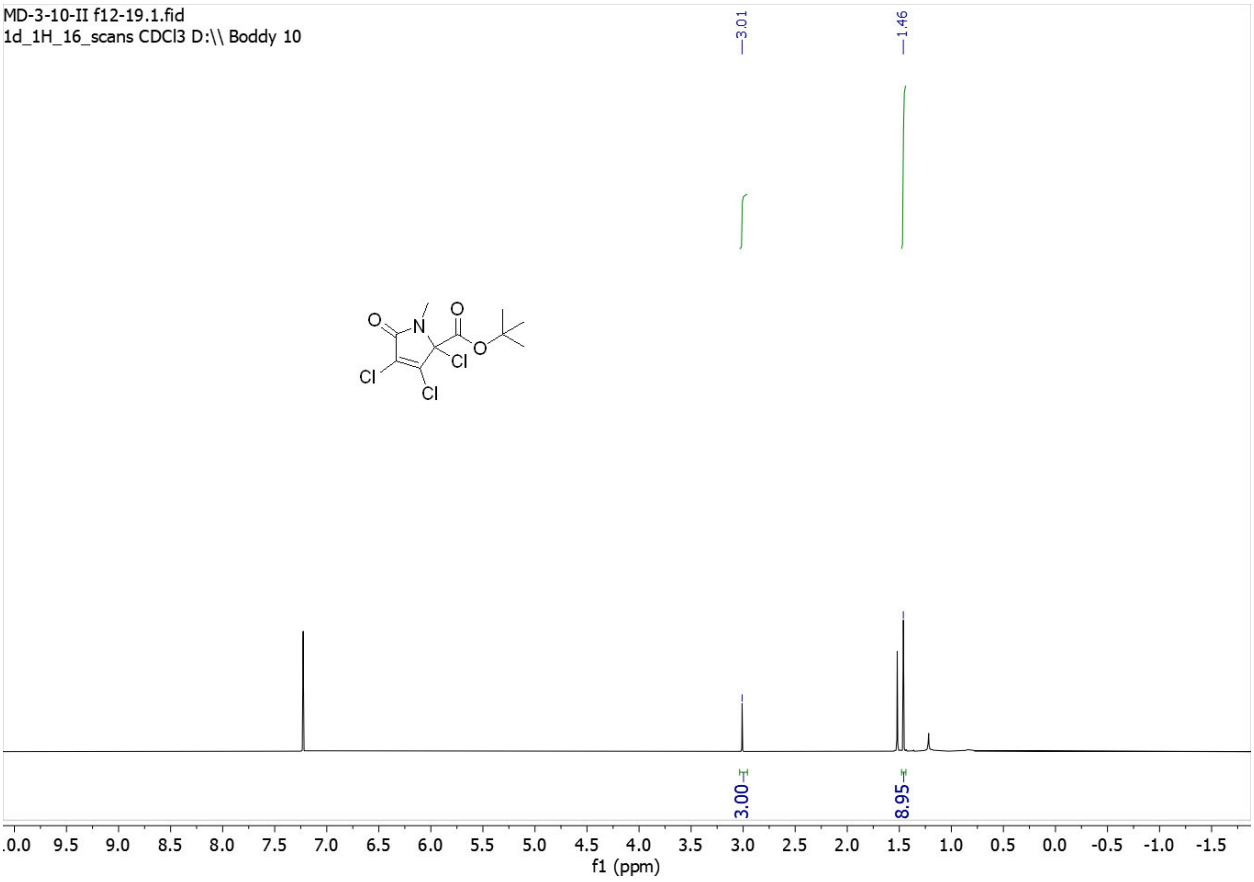

^{1}H NMR (400 MHz, $CDCl_3$) of **8f.**

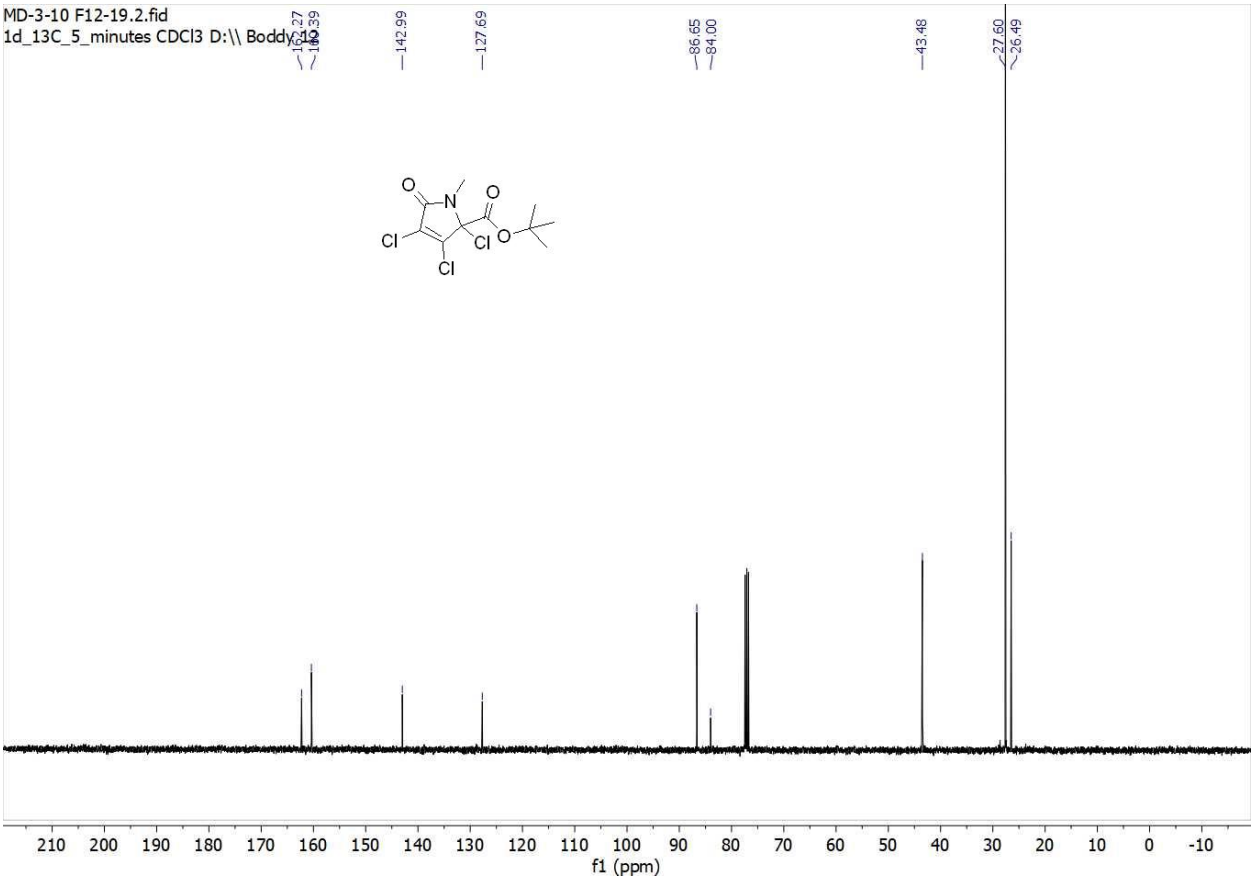

$^{13}C\{^{1}H\}$ NMR (100 MHz, $CDCl_3$) of **8f.**

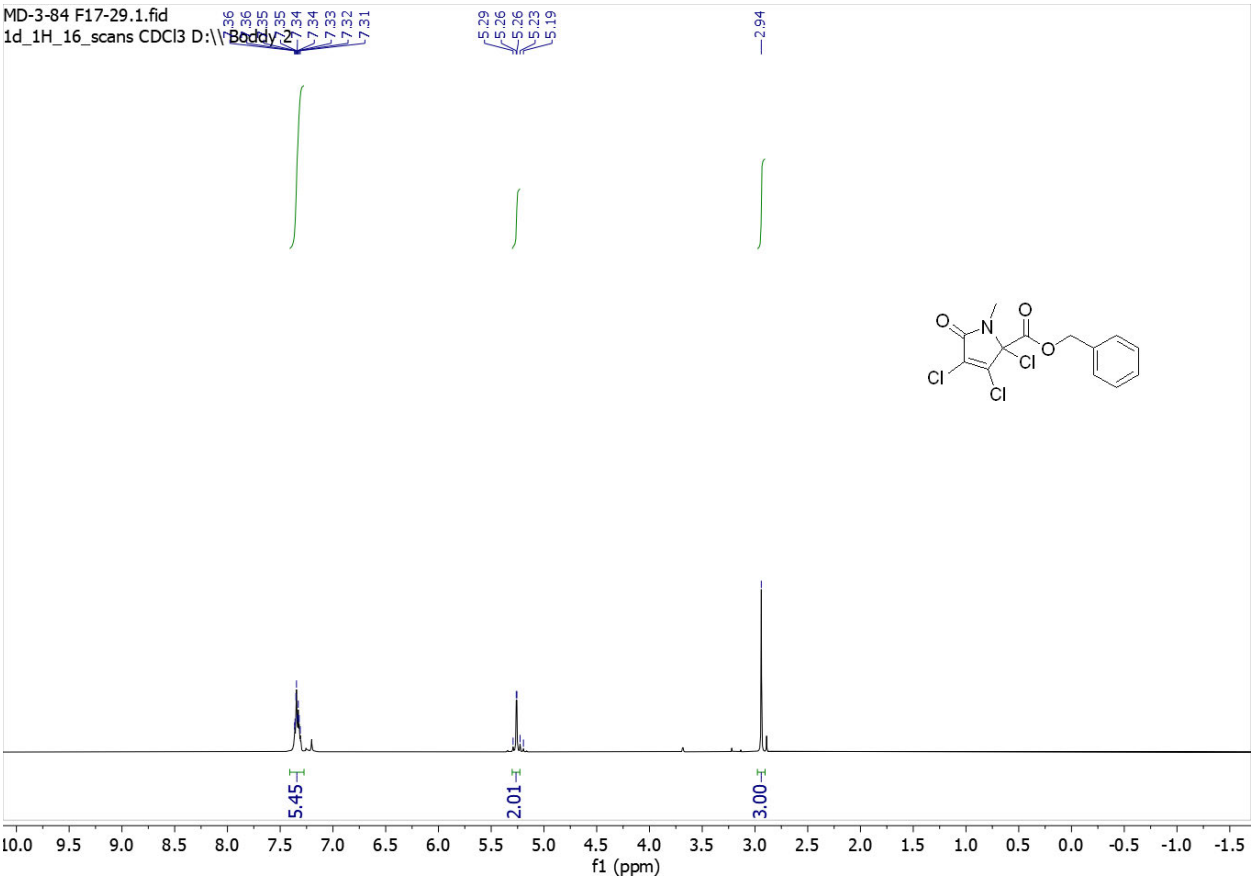

^{1}H NMR (400 MHz, $CDCl_3$) of **8g.**

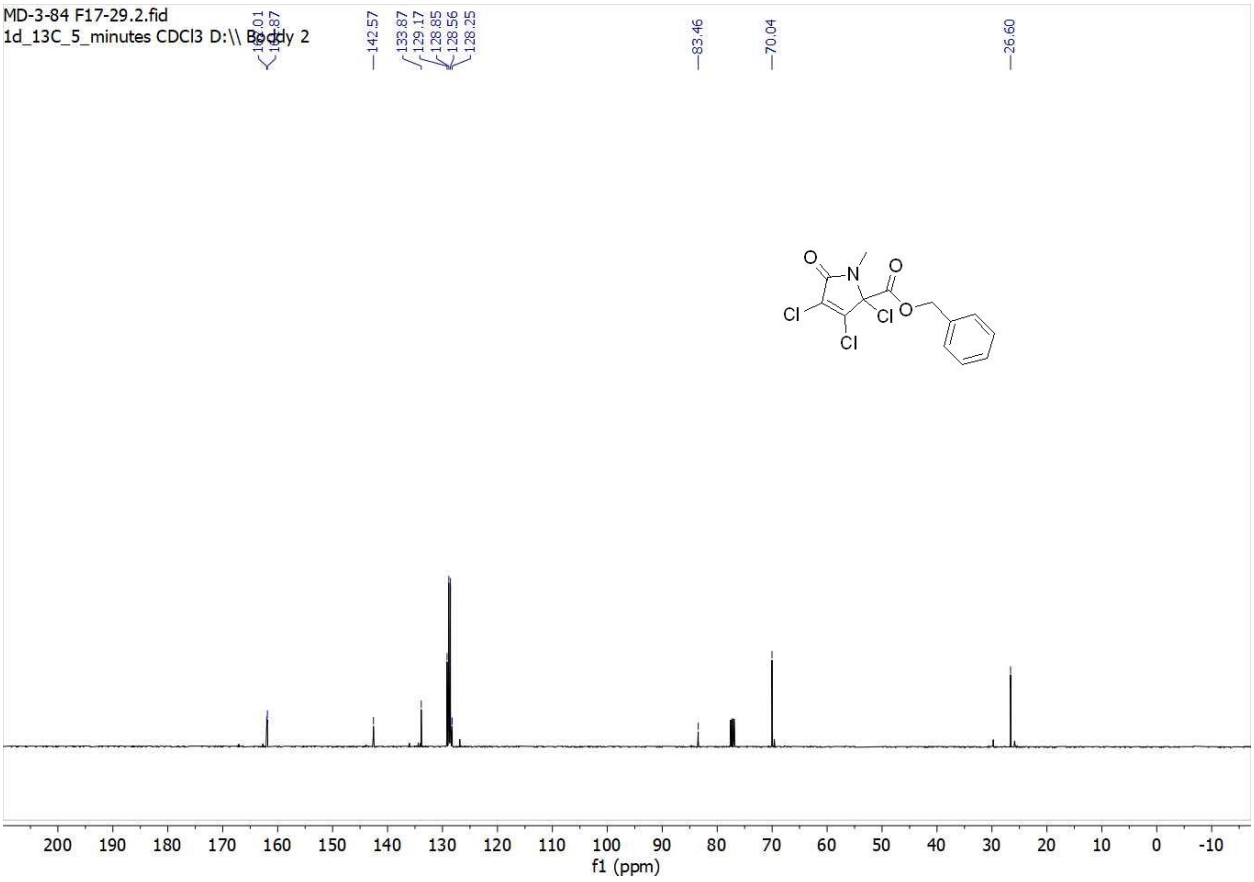

$^{13}C\{^{1}H\}$ NMR (100 MHz, $CDCl_3$) of **8g.**

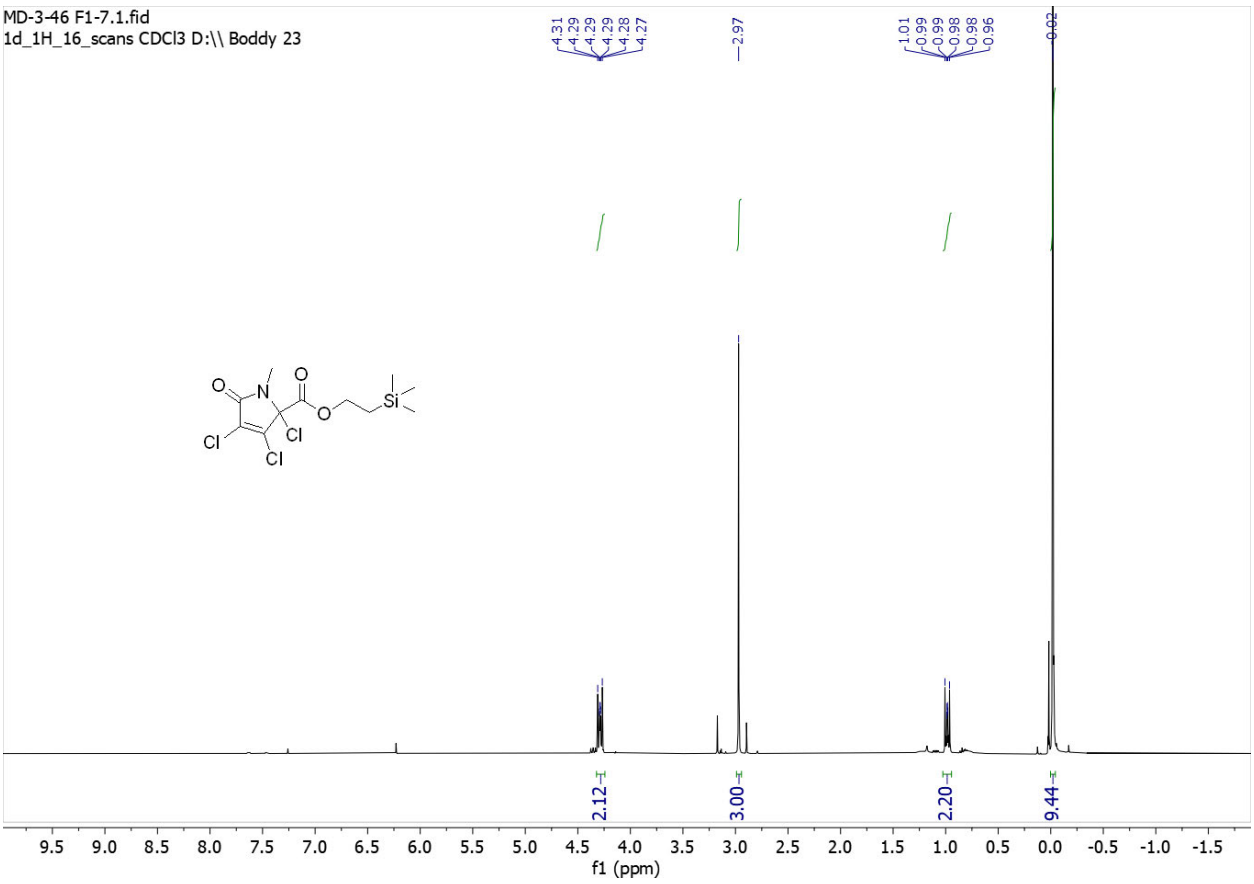

^{1}H NMR (400 MHz, $CDCl_3$) of **8h.**

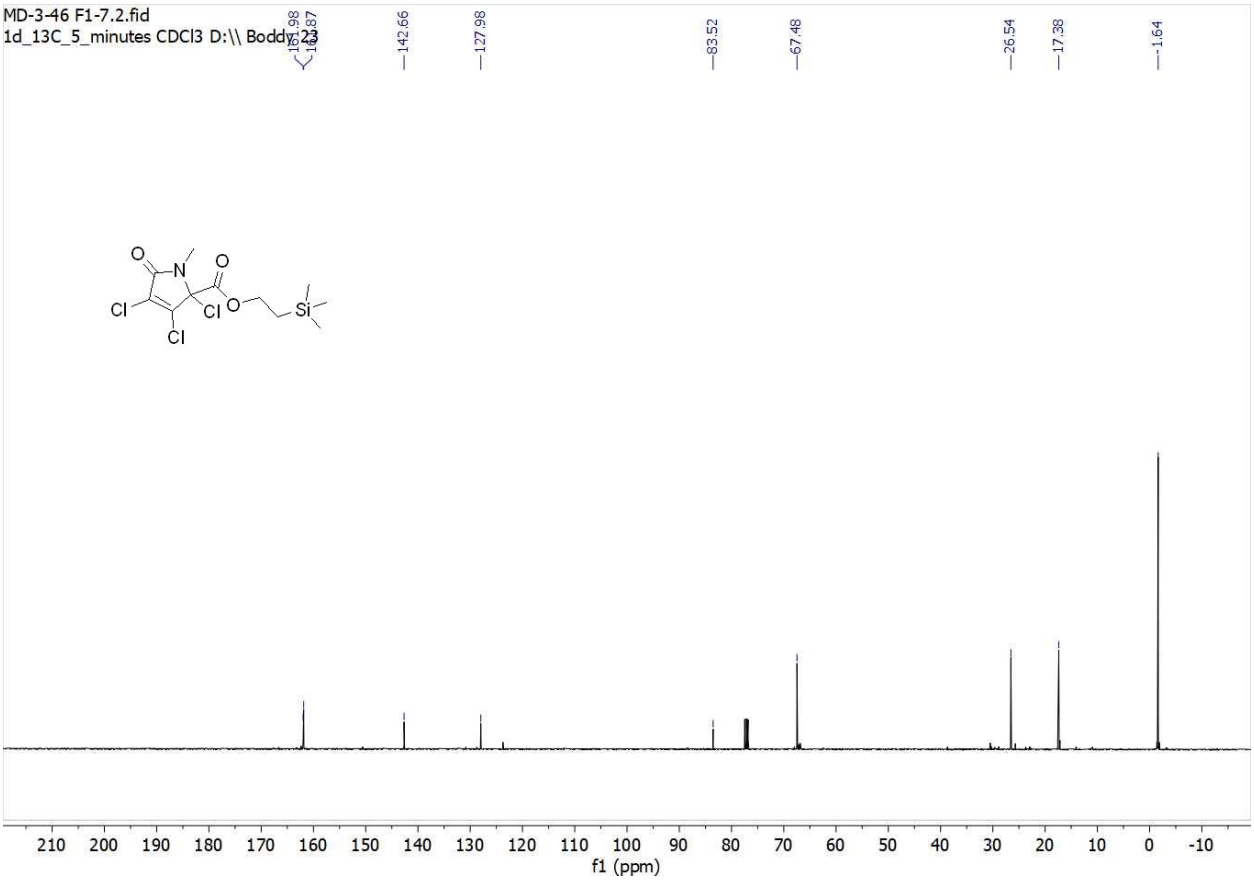

$^{13}C\{^{1}H\}$ NMR (100 MHz, $CDCl_3$) of **8h.**

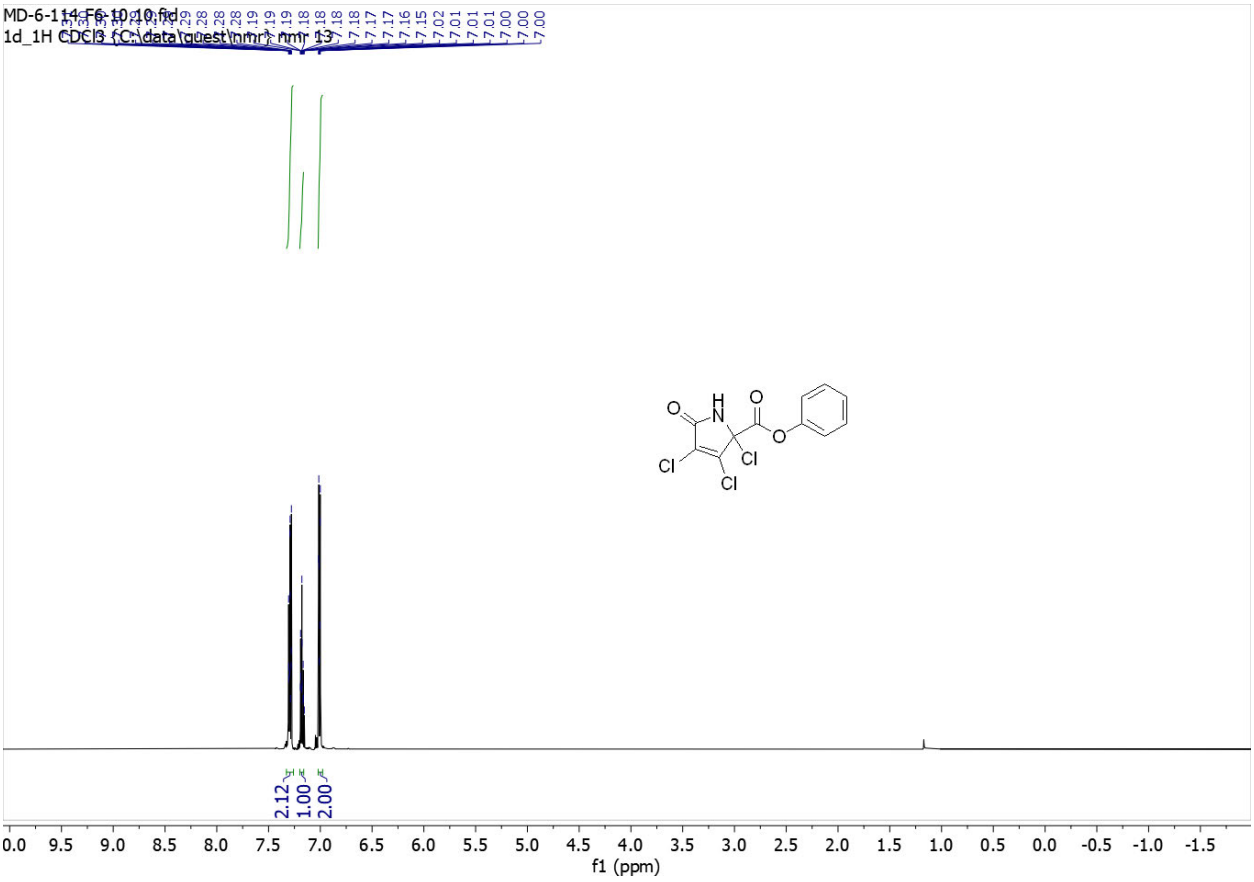

^{1}H NMR (400 MHz, $CDCl_3$) of **8i.**

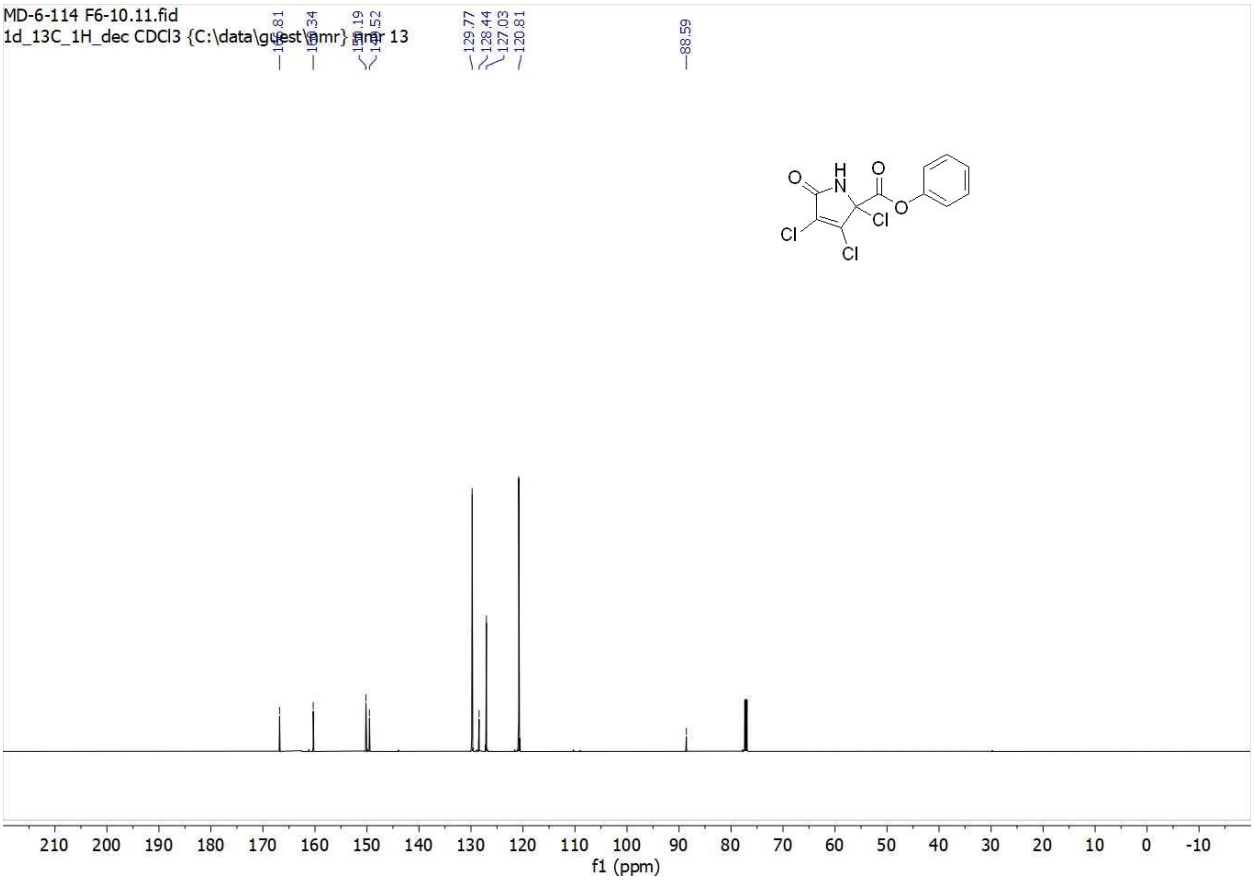

$^{13}C\{^{1}H\}$ NMR (100 MHz, $CDCl_3$) of **8i.**

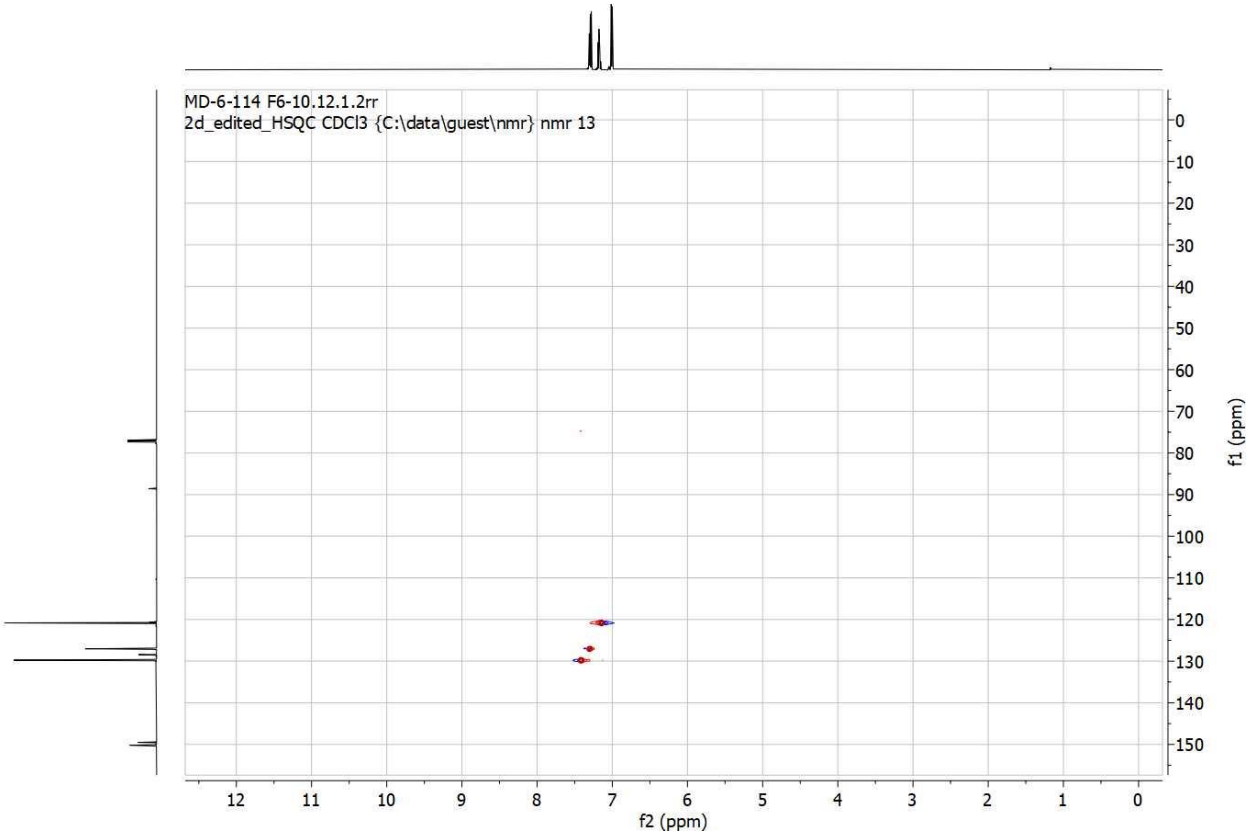
MD-6-114 F6-10.12.1.2rr
2d_edited_HSQC CDCl3 {C:\data\guest\nmr} nmr 13
f2 (ppm)
f1 (ppm)

HSQC of **8i.**

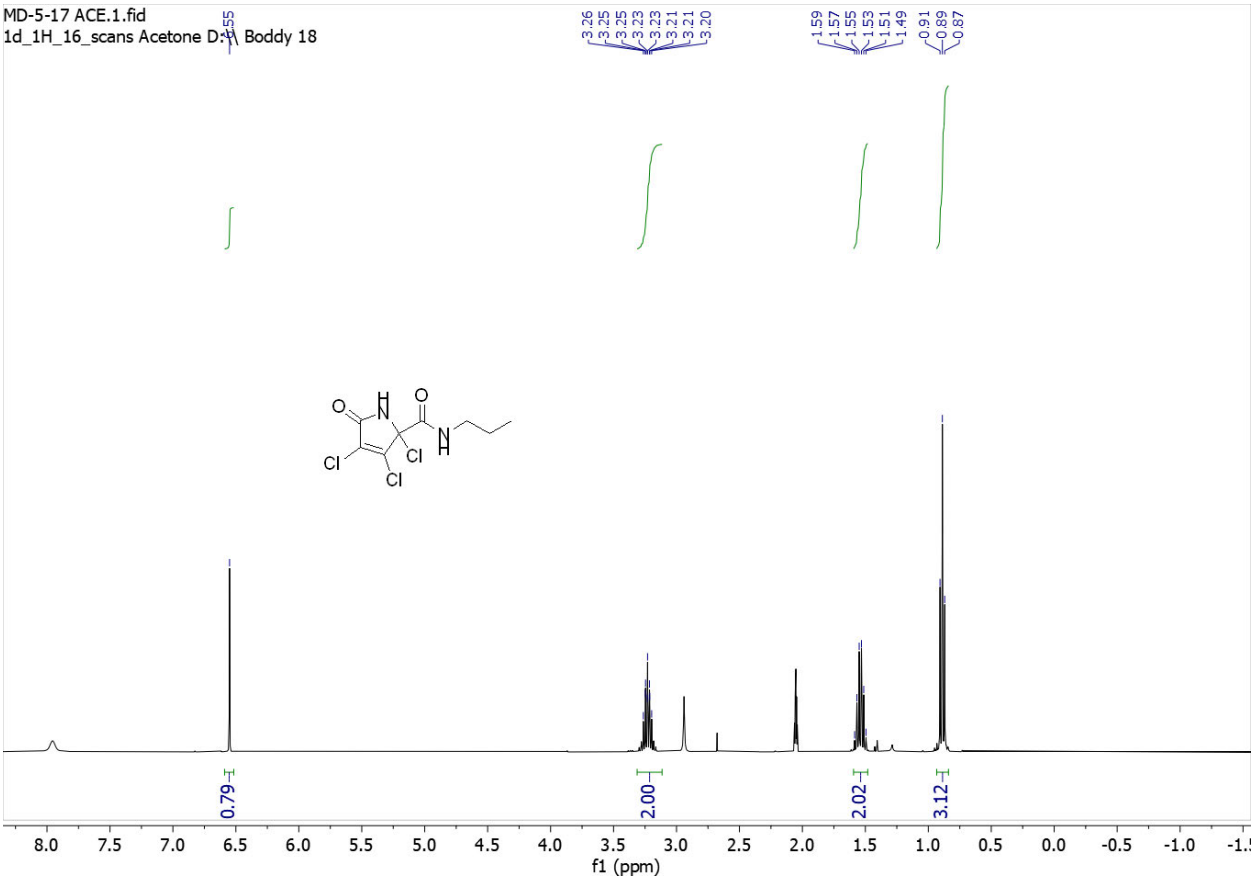

^{1}H NMR (400 MHz, *d-6* Acetone) of **8j.**

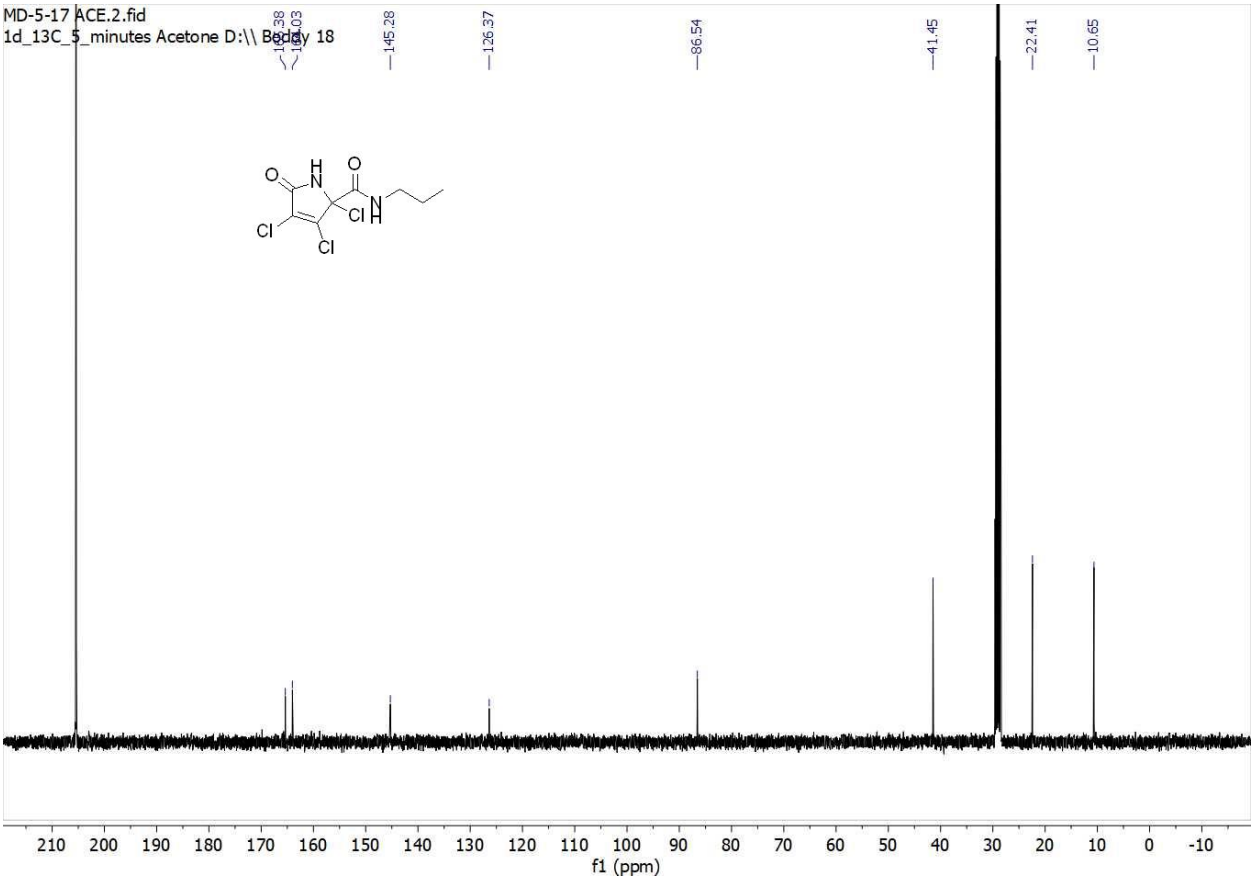

$^{13}C\{^{1}H\}$ NMR (100 MHz, *d-6* Acetone) of **8j.**

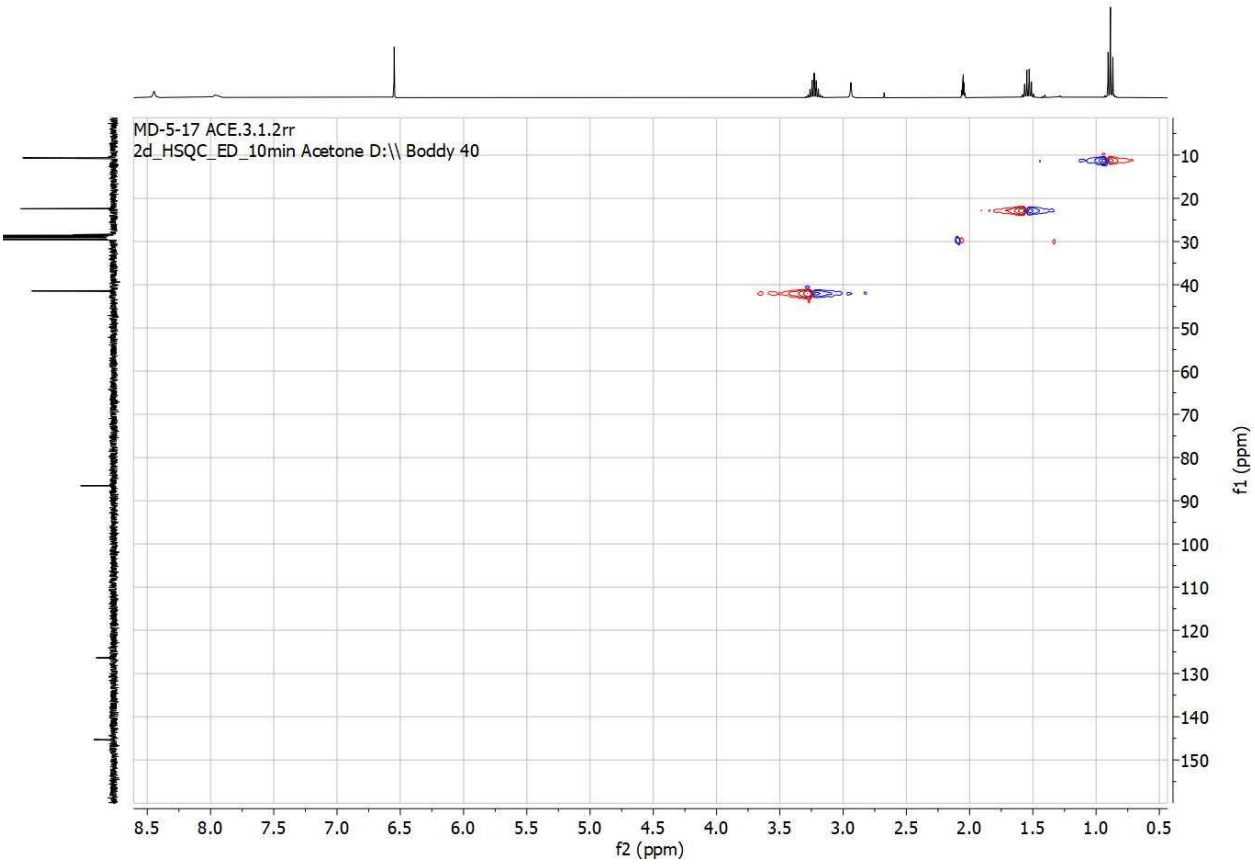
MD-5-17 ACE.3.1.2rr
2d_HSQC_ED_10min Acetone D:\\ Boddy 40
f2 (ppm)
f1 (ppm)

HSQC of **8j.**

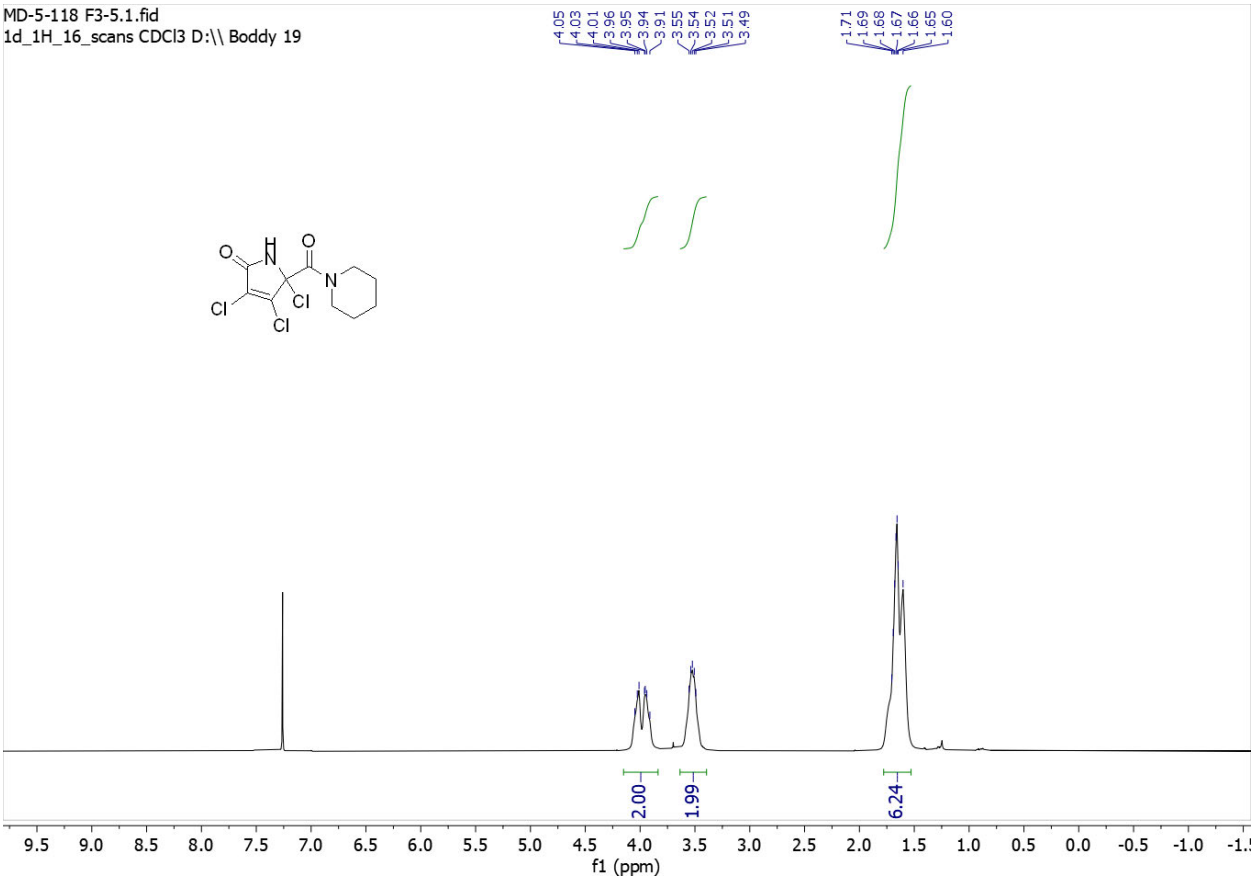

^{1}H NMR (400 MHz, $CDCl_3$) of **8k.**

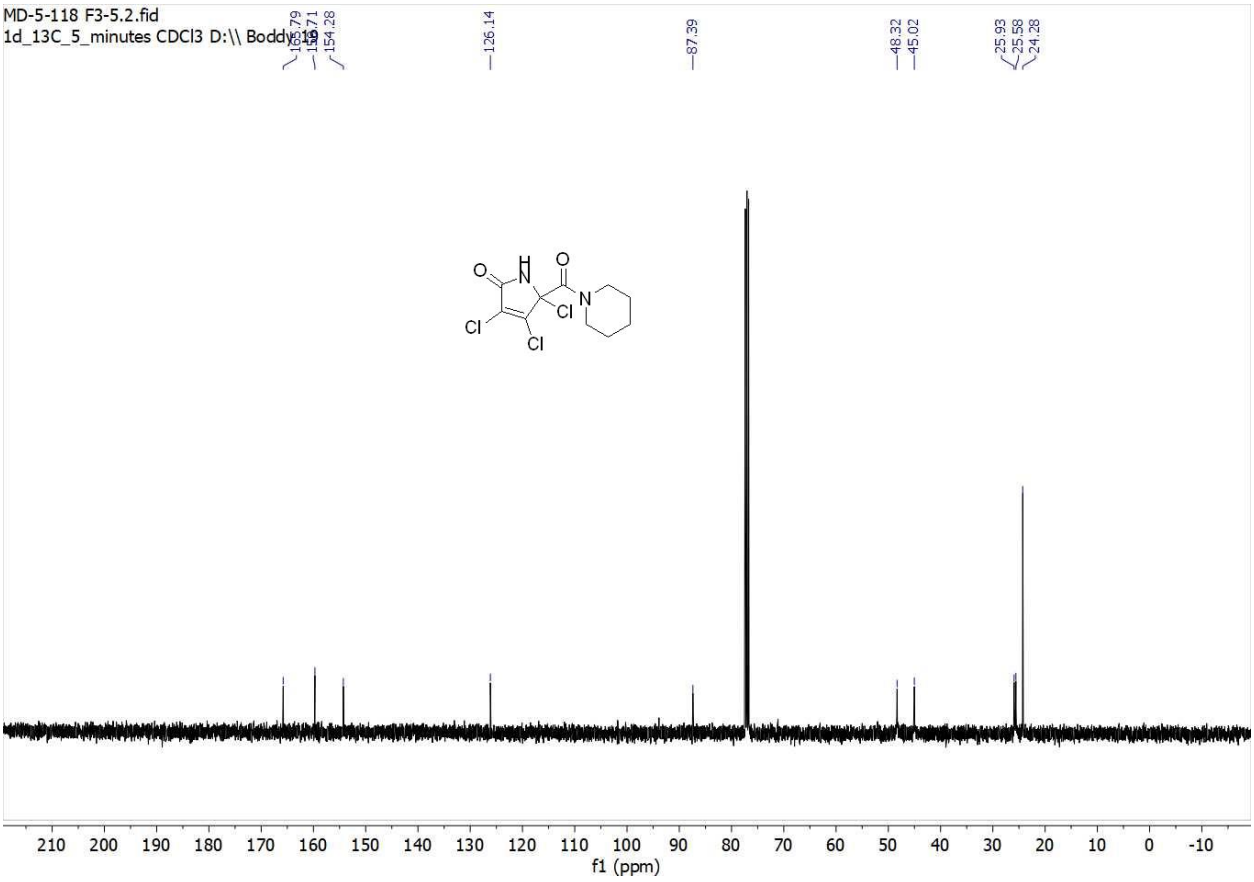

$^{13}C\{^{1}H\}$ NMR (100 MHz, $CDCl_3$) of **8k.**

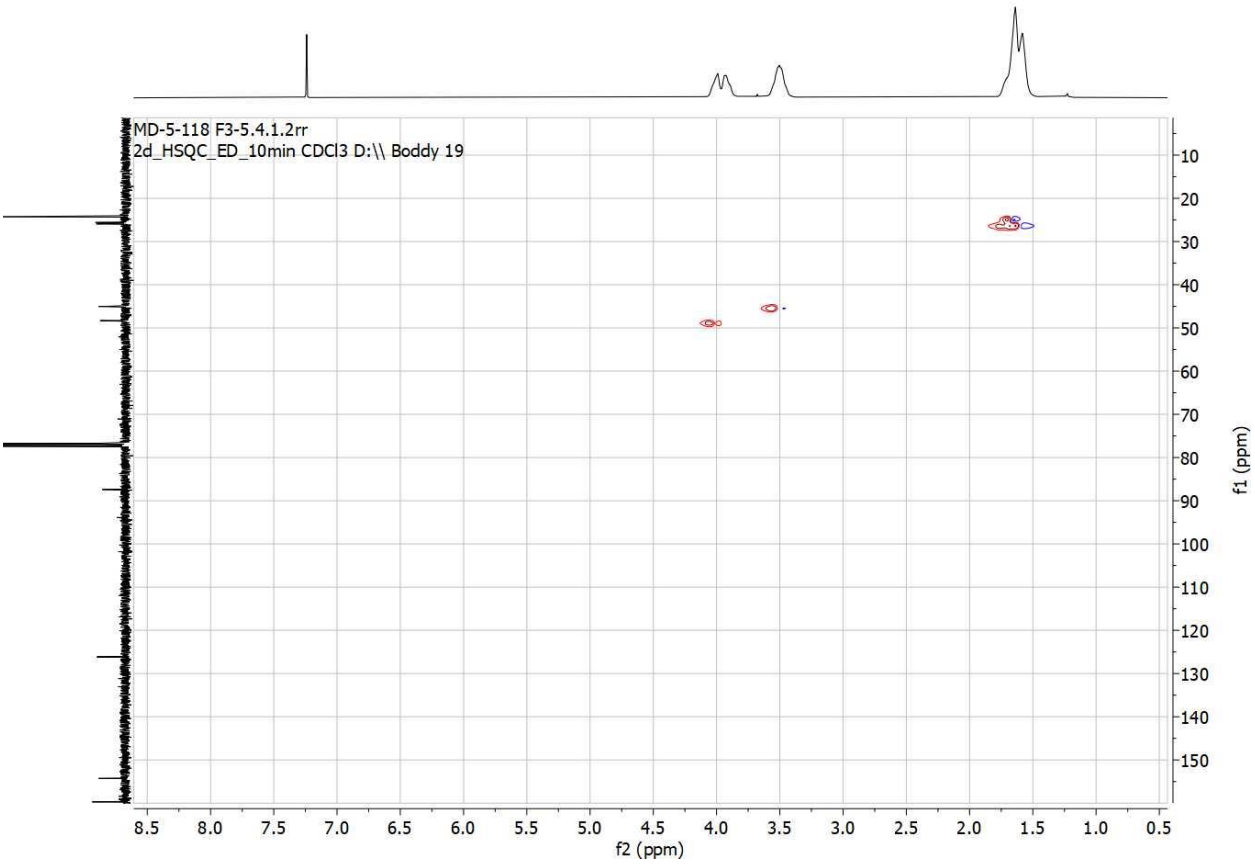
MD-5-118 F3-5.4.1.2rr
2d_HSQC_ED_10min CDCl3 D:\\ Boddy 19
f2 (ppm)
f1 (ppm)

HSQC of **8k.**

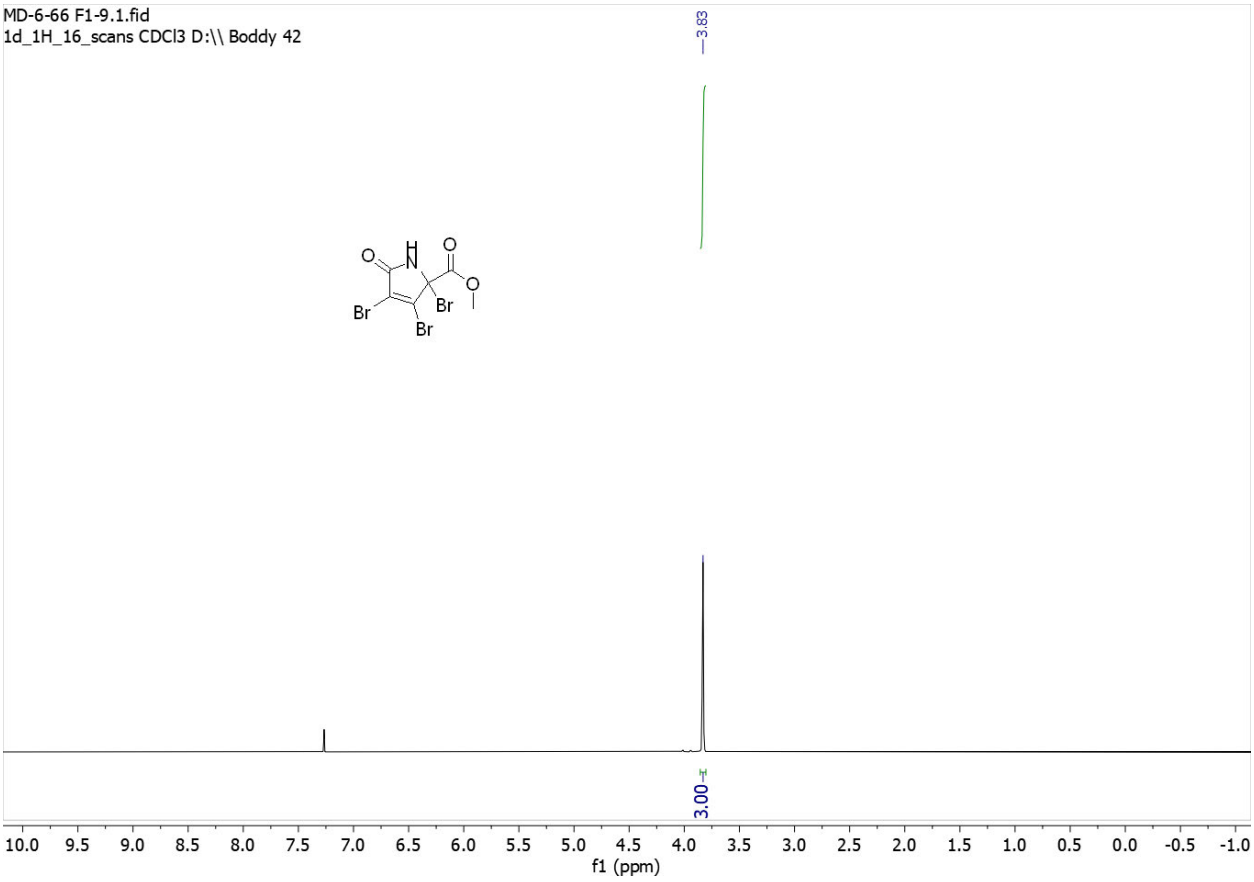

^{1}H NMR (400 MHz, $CDCl_3$) of **18** - Methyl

2,3,4-tribromo-5-oxo-2,5-dihydro-1H-pyrrole-2-carboxylate**.**

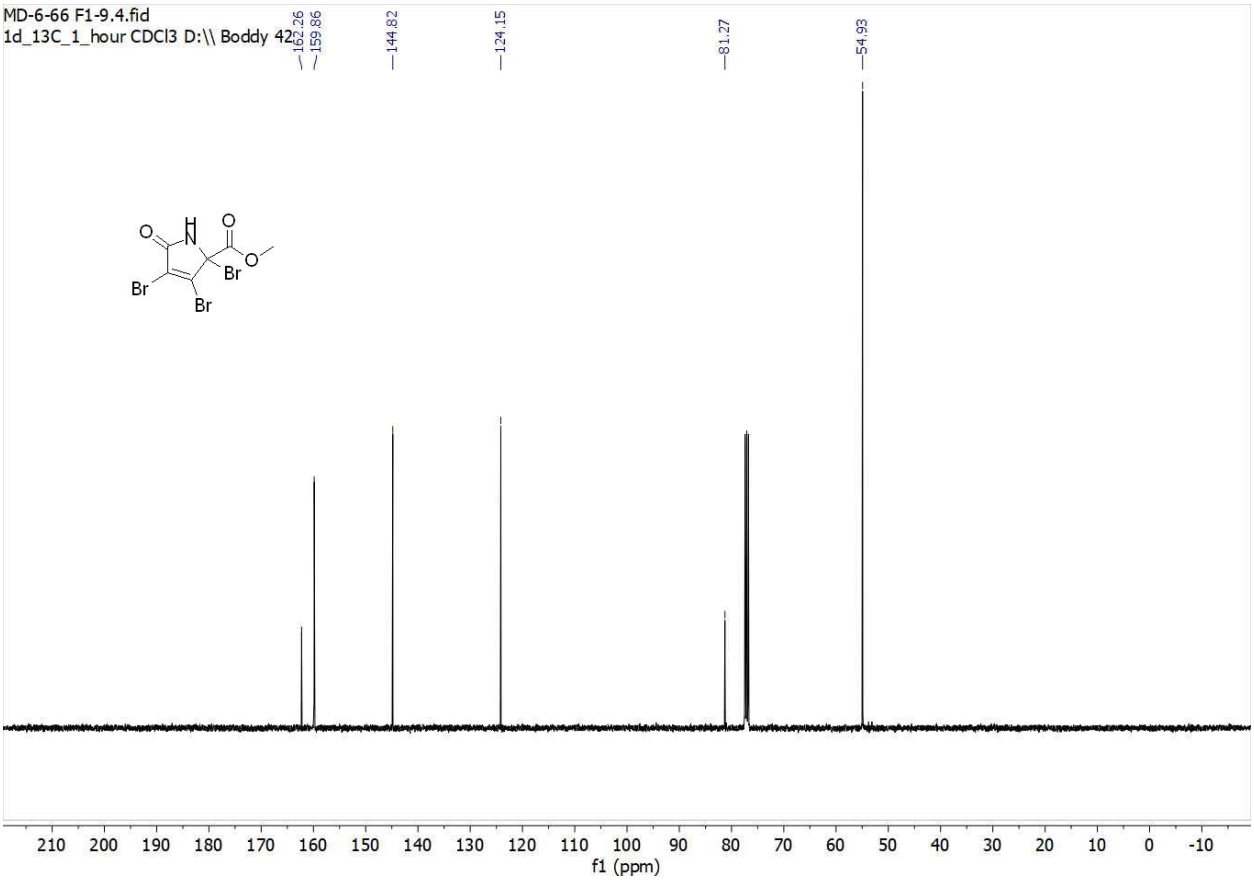

$^{13}C\{^{1}H\}$ NMR (100 MHz, $CDCl_3$) of **18** - Methyl

2,3,4-tribromo-5-oxo-2,5-dihydro-1H-pyrrole-2-carboxylate**.**

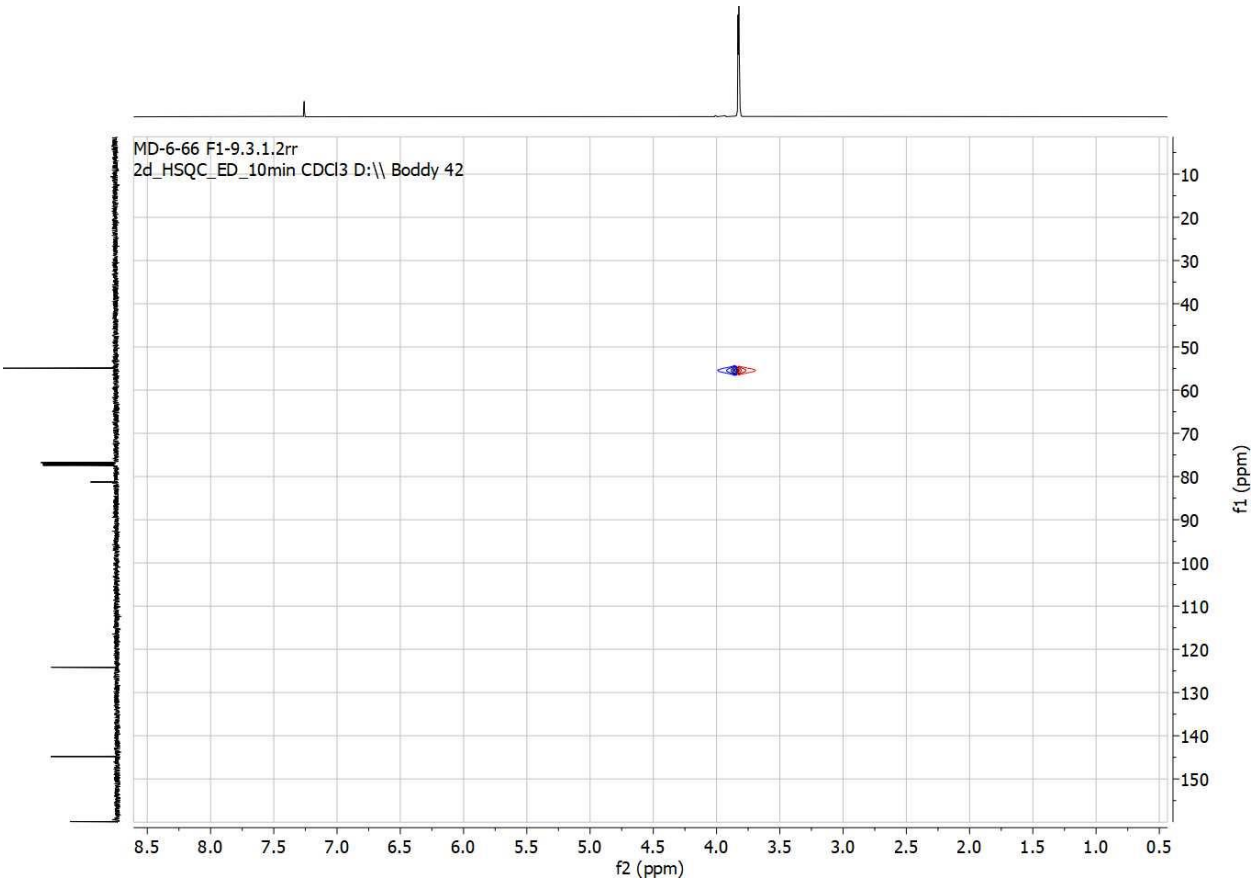

HSQC of **18** - Methyl 2,3,4-tribromo-5-oxo-2,5-dihydro-1H-pyrrole-2-carboxylate**.**

Section 4. Copies of ^{1}H and ^{13}C spectra - C) Compounds on route to pseudoarmeniaspirol **(5,6,15,1)**

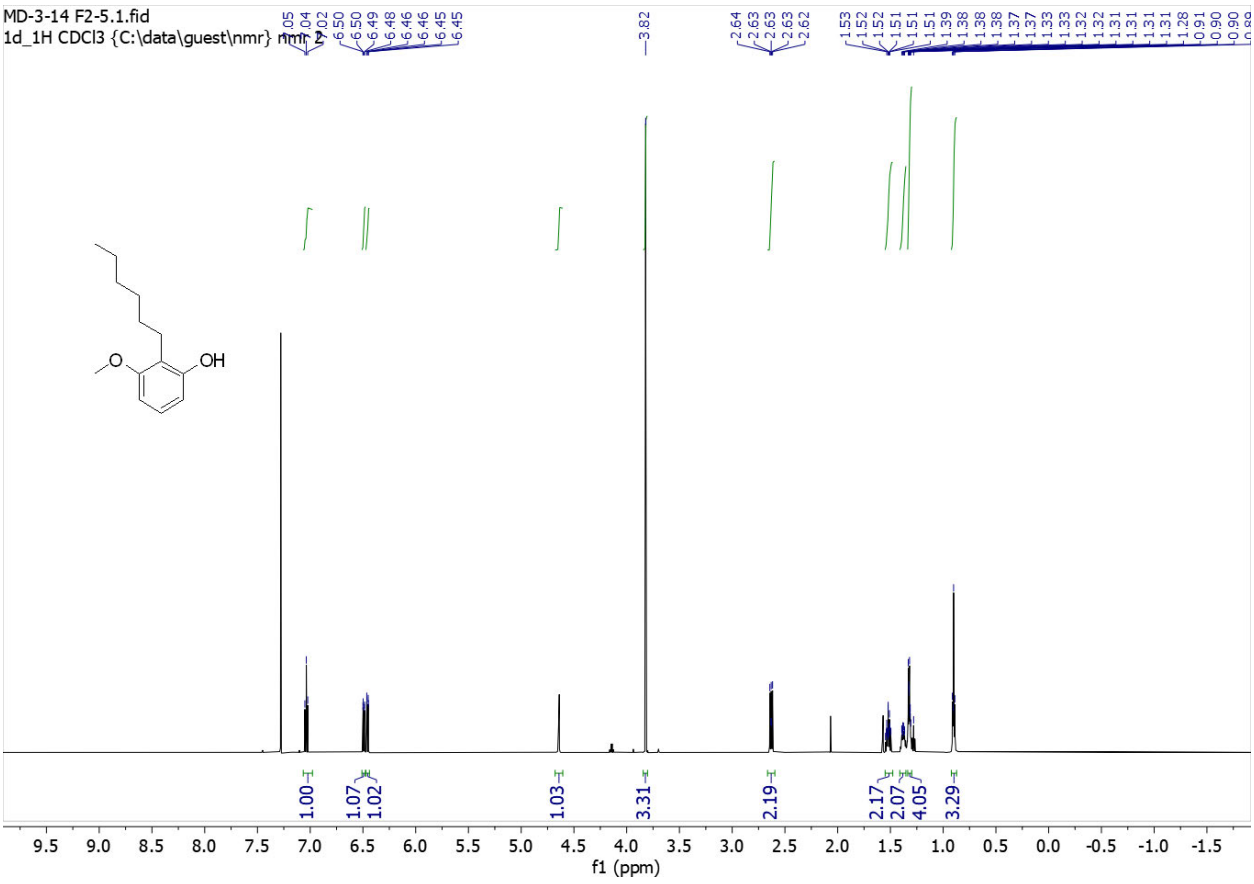

^{1}H NMR (400 MHz, $CDCl_3$) of **6**

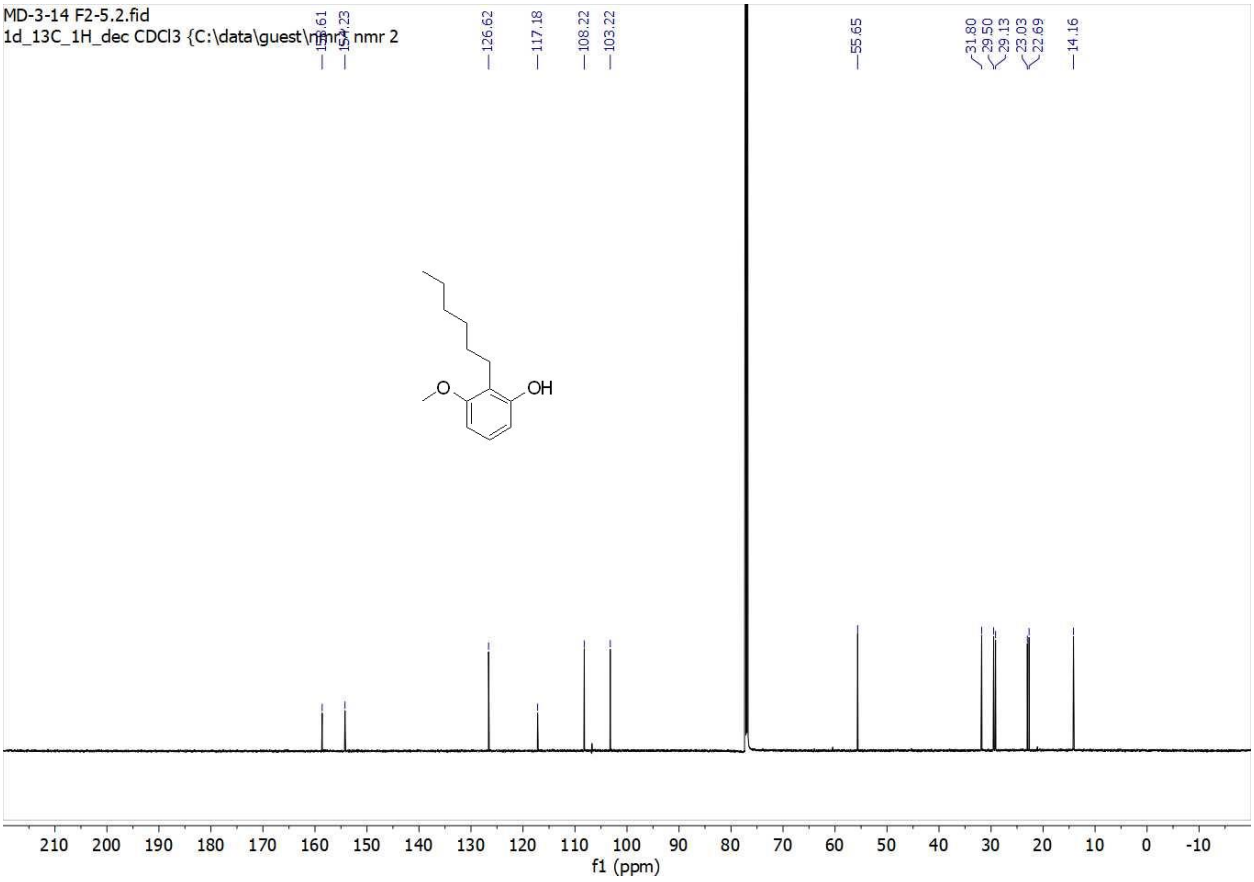

$^{13}C\{^{1}H\}$ NMR (100 MHz, $CDCl_3$) of **6**

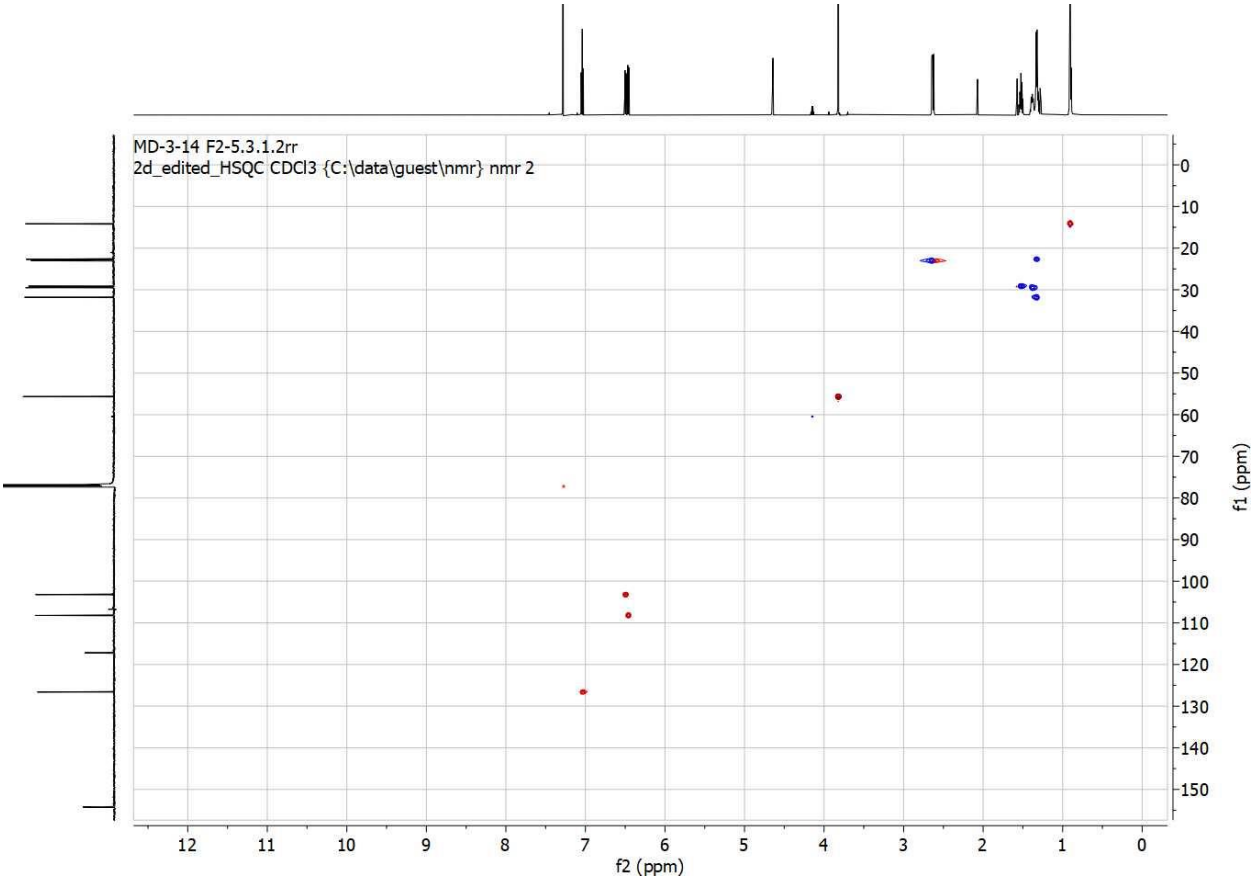
MD-3-14 F2-5.3.1.2rr
2d_edited_HSQC CDCl3 {C:\data\guest\nmr} nmr 2
f2 (ppm)
f1 (ppm)

HSQC of **6**

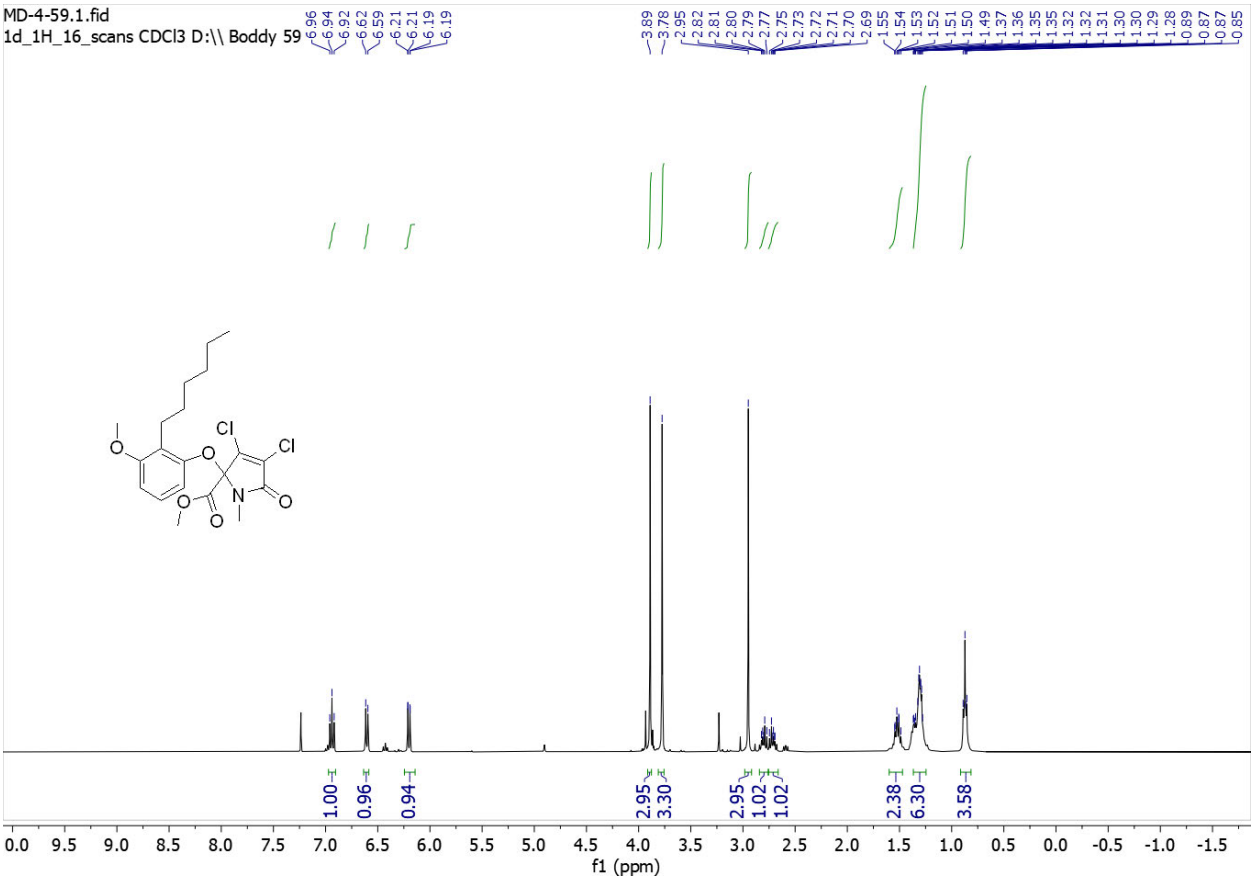

^{1}H NMR (400 MHz, $CDCl_3$) of **5**

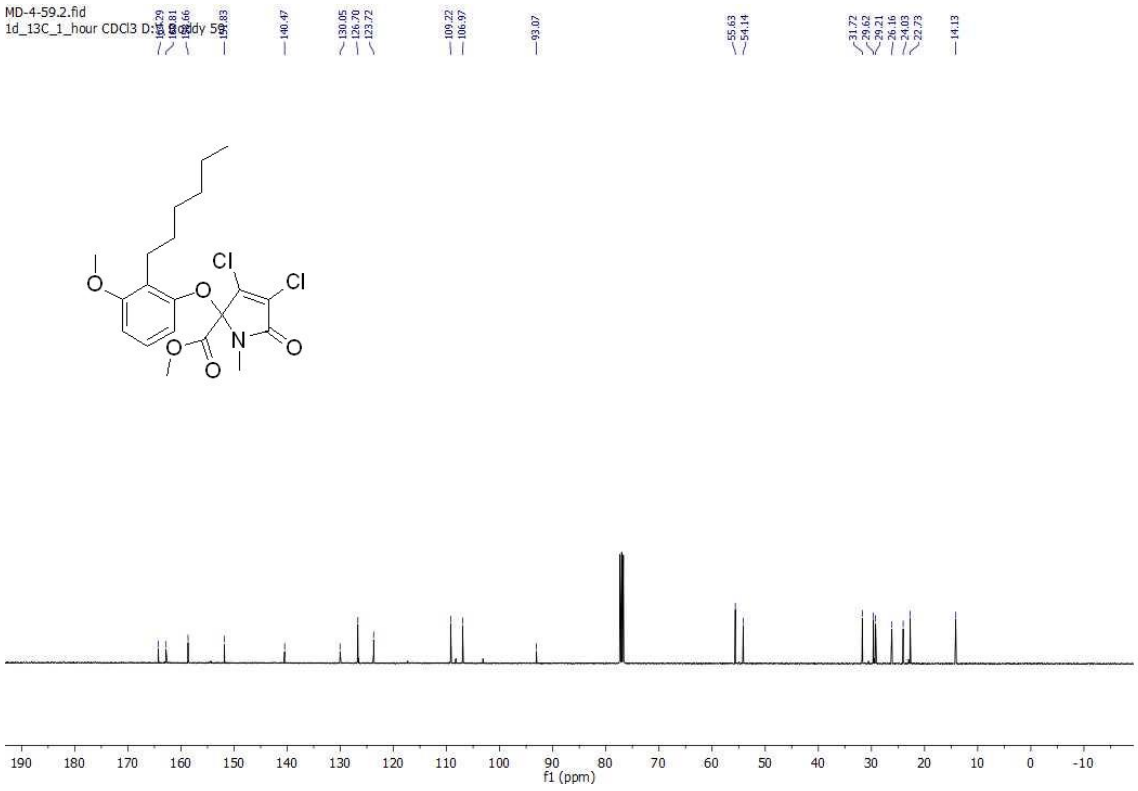

$^{13}C\{^{1}H\}$ NMR (100 MHz, $CDCl_3$) of **5**

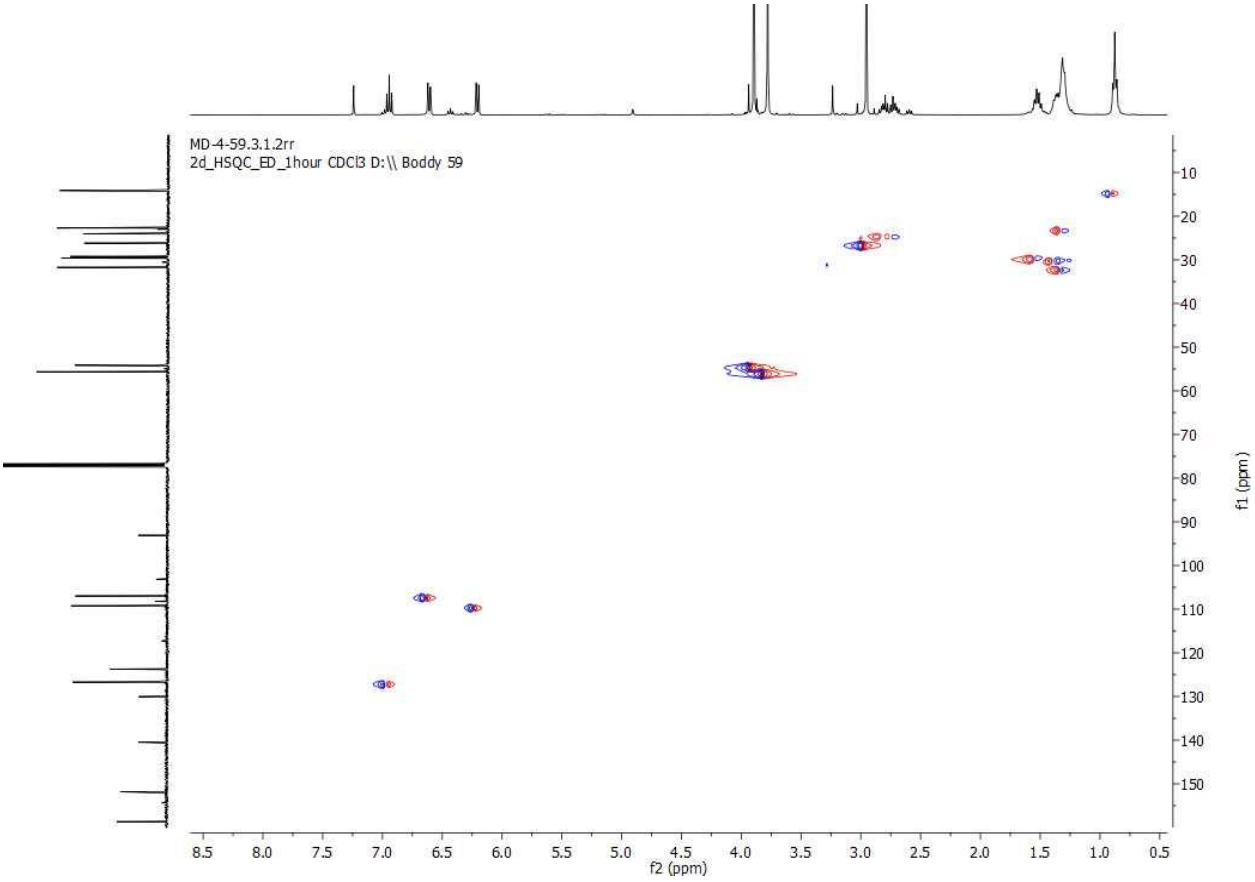

HSQC of **5**

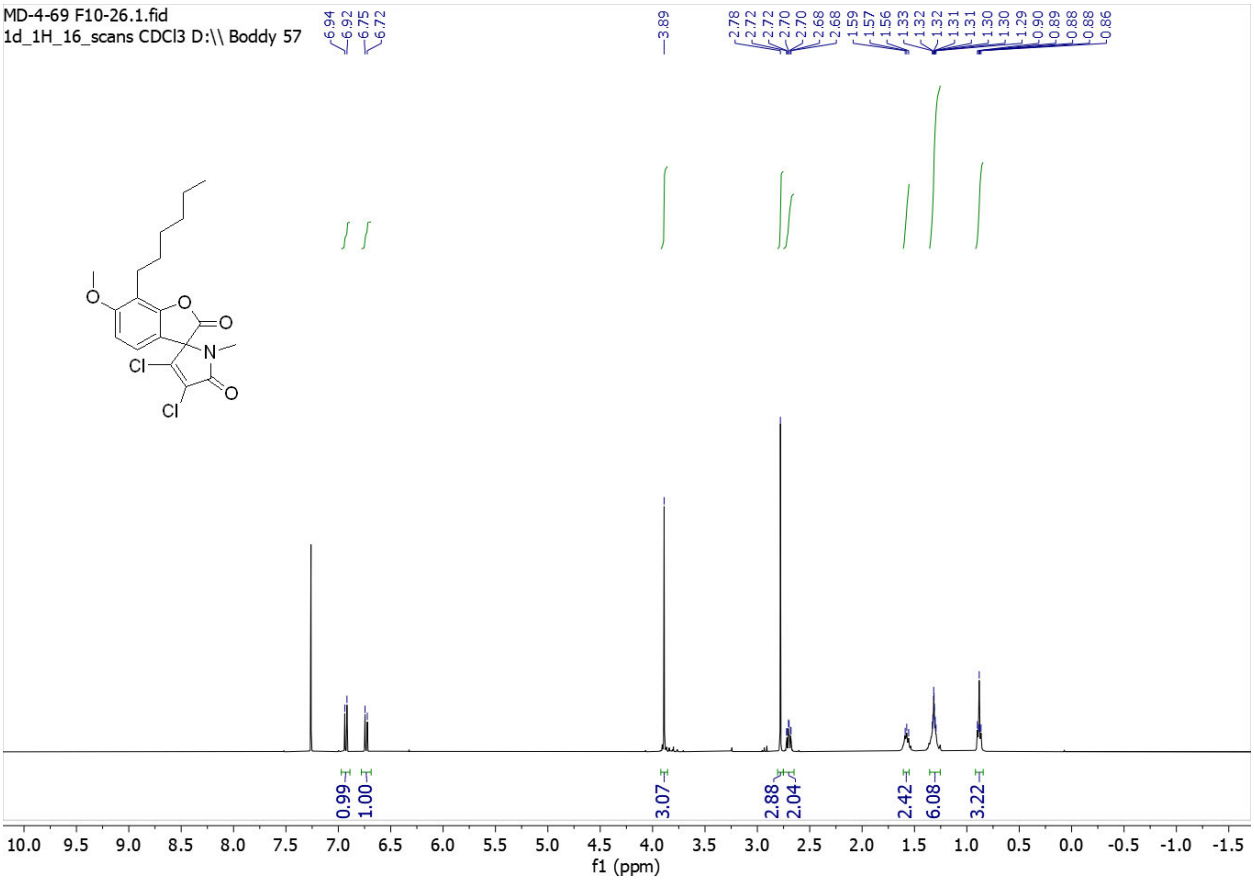

^{1}H NMR (400 MHz, $CDCl_3$) of **15**

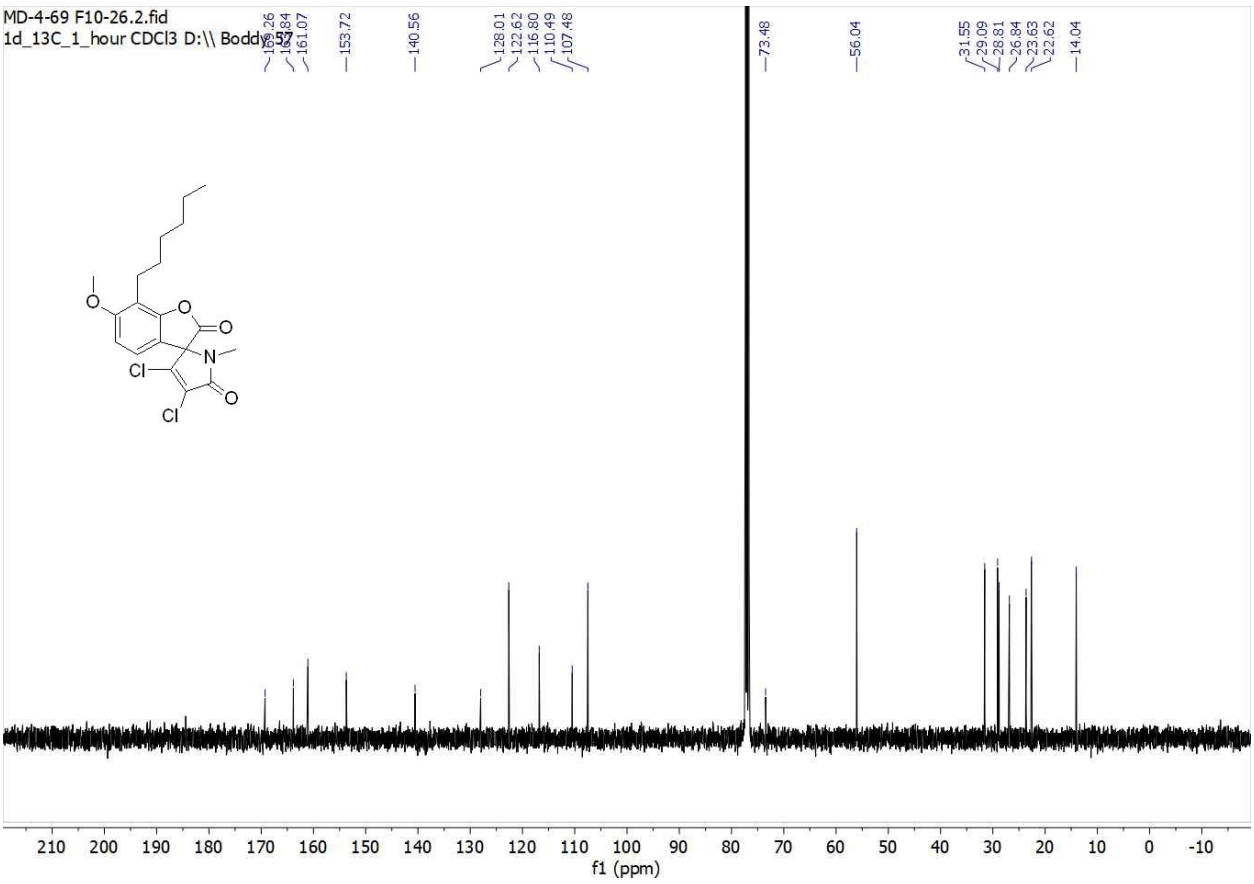

$^{13}C\{^{1}H\}$ NMR (100 MHz, $CDCl_3$) of **15**

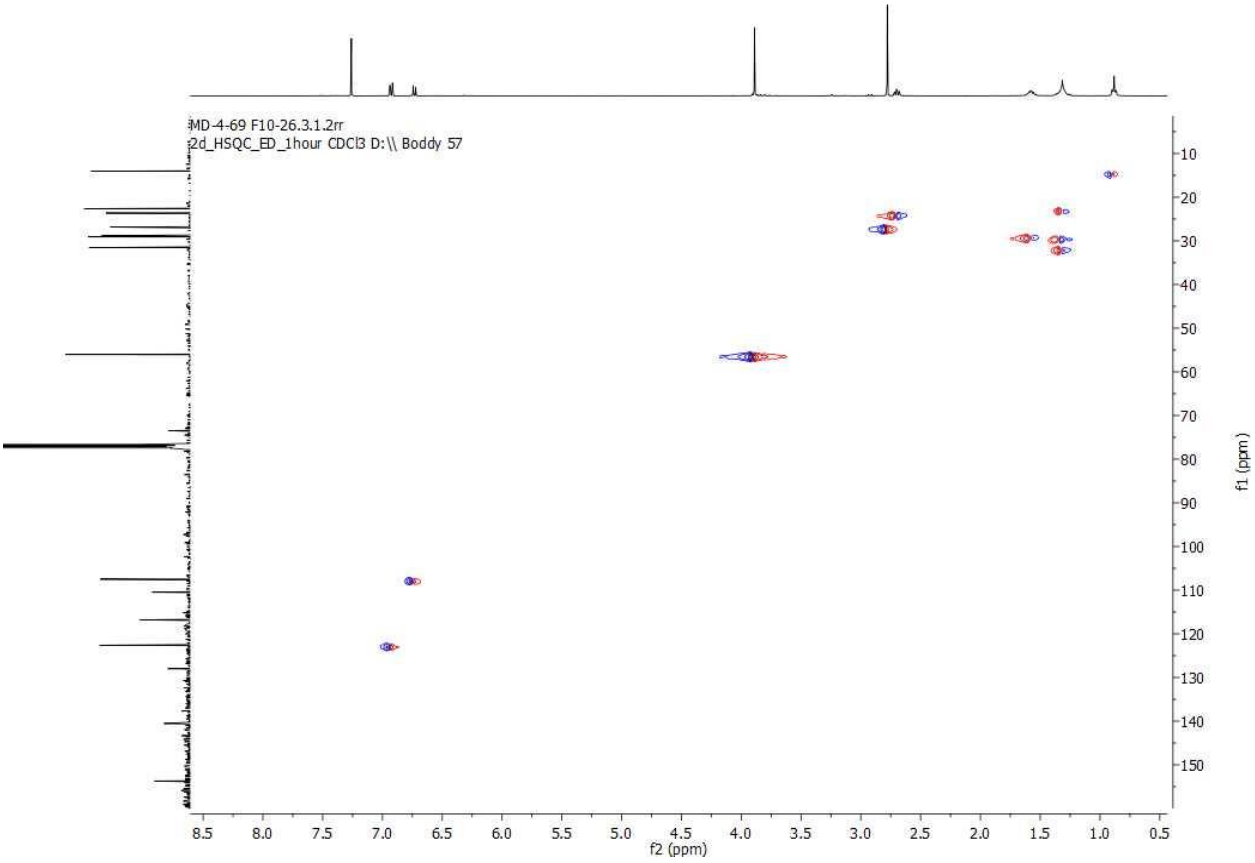
MD-4-69 F10-26.3.1.2rr
2d_HSQC_ED_1hour CDCl3 D:\\ Boddy 57
f2 (ppm)
f1 (ppm)

HSQC of **15**

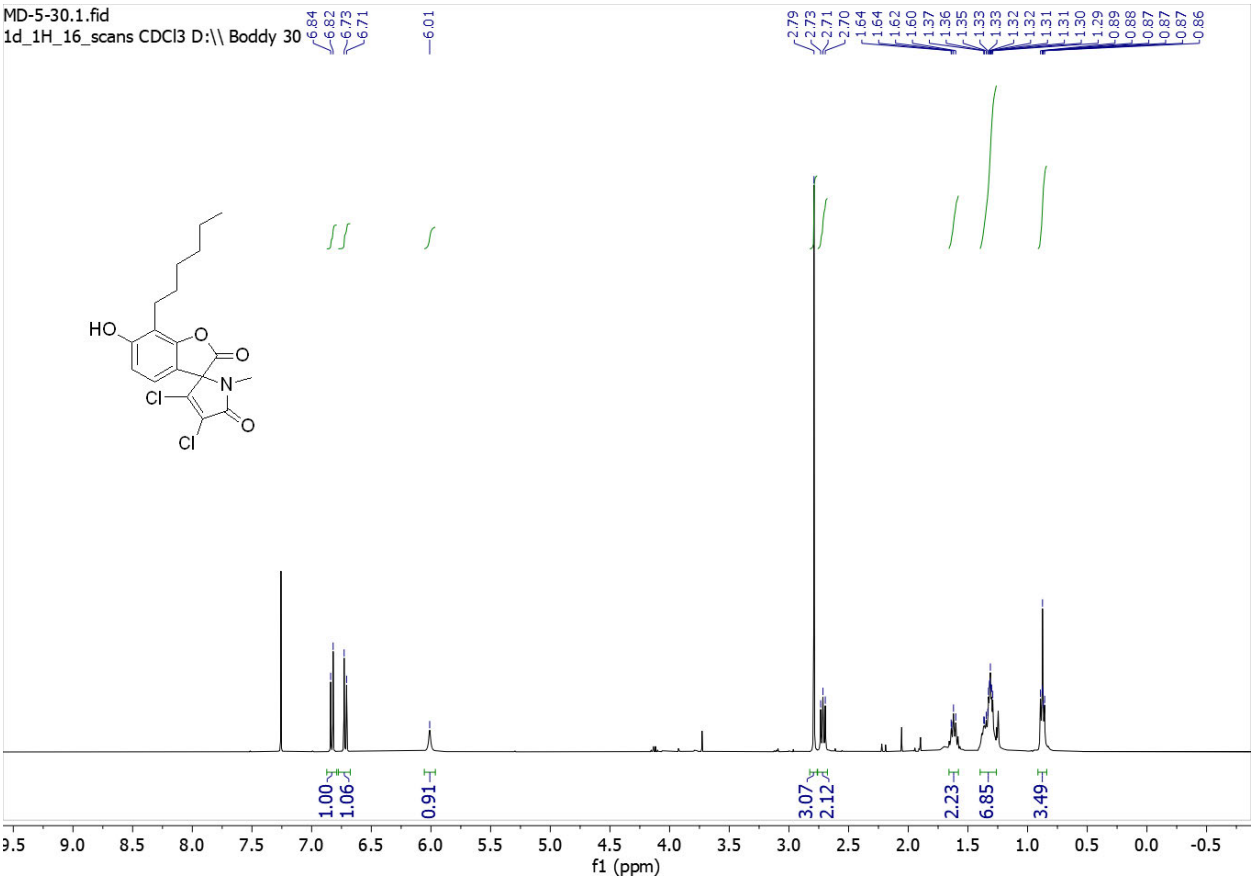

^{1}H NMR (600 MHz, $CDCl_3$) of **1**

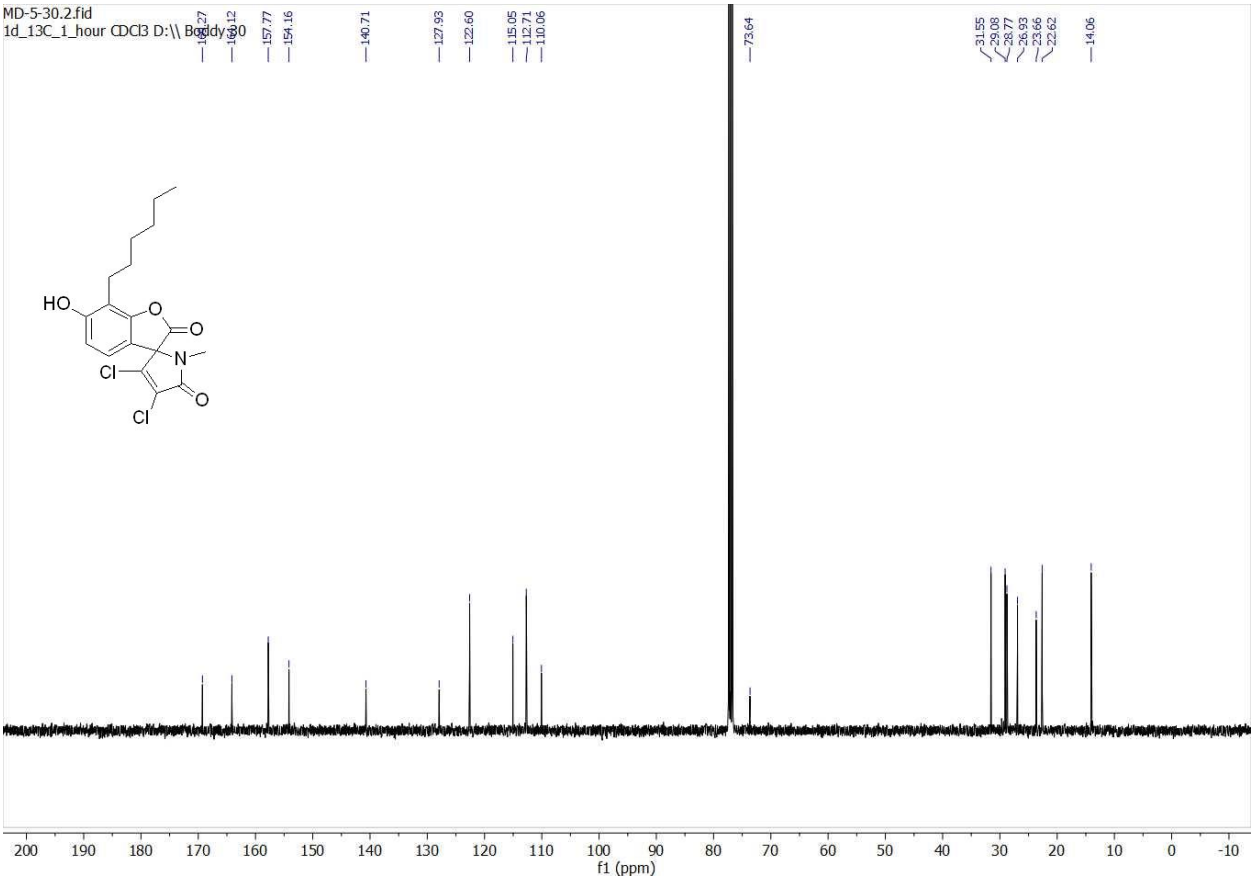

$^{13}C\{^{1}H\}$ NMR (150 MHz, $CDCl_3$) of **1**

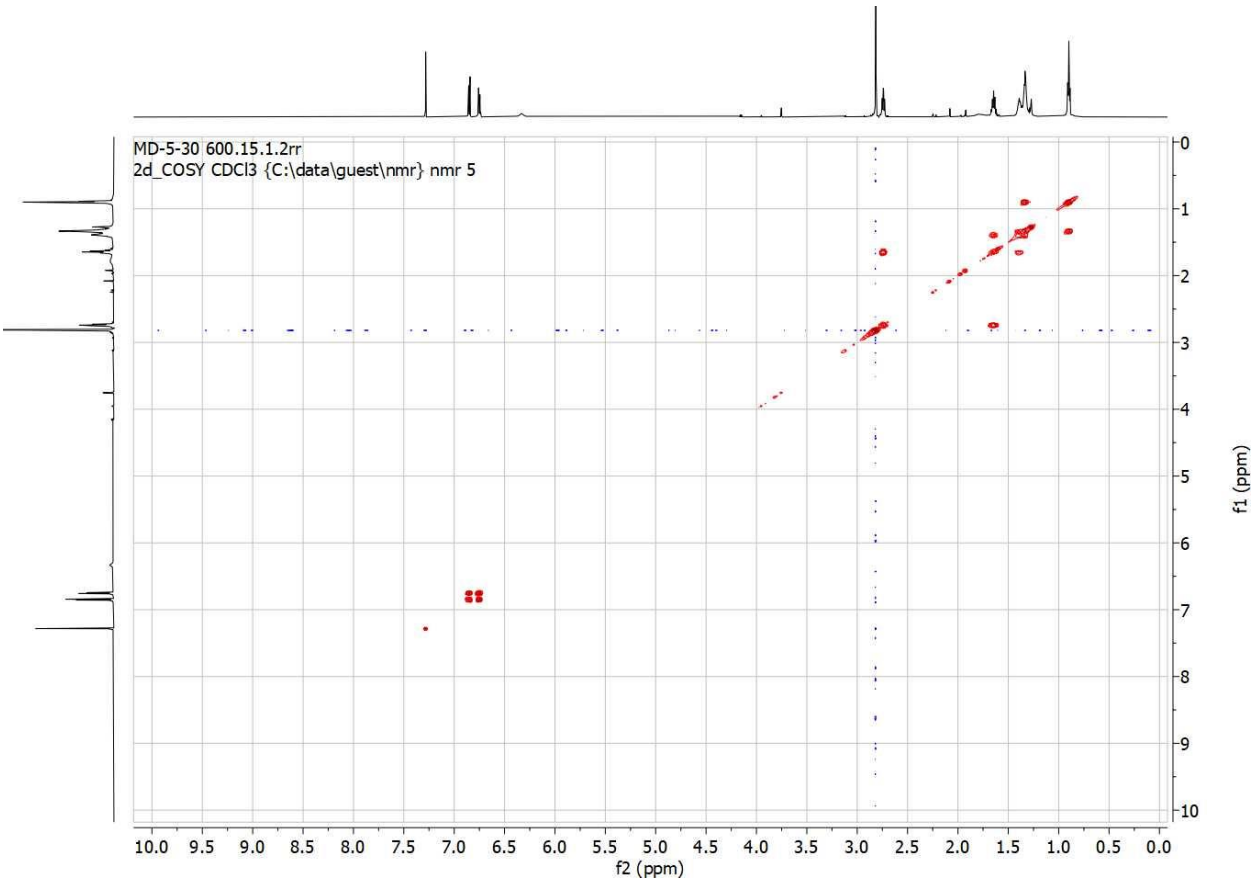
MD-5-30 600.15.1.2rr
2d_COSY CDCl3 {C:\data\guest\nmr} nmr 5
f2 (ppm)
f1 (ppm)

COSY of **1**

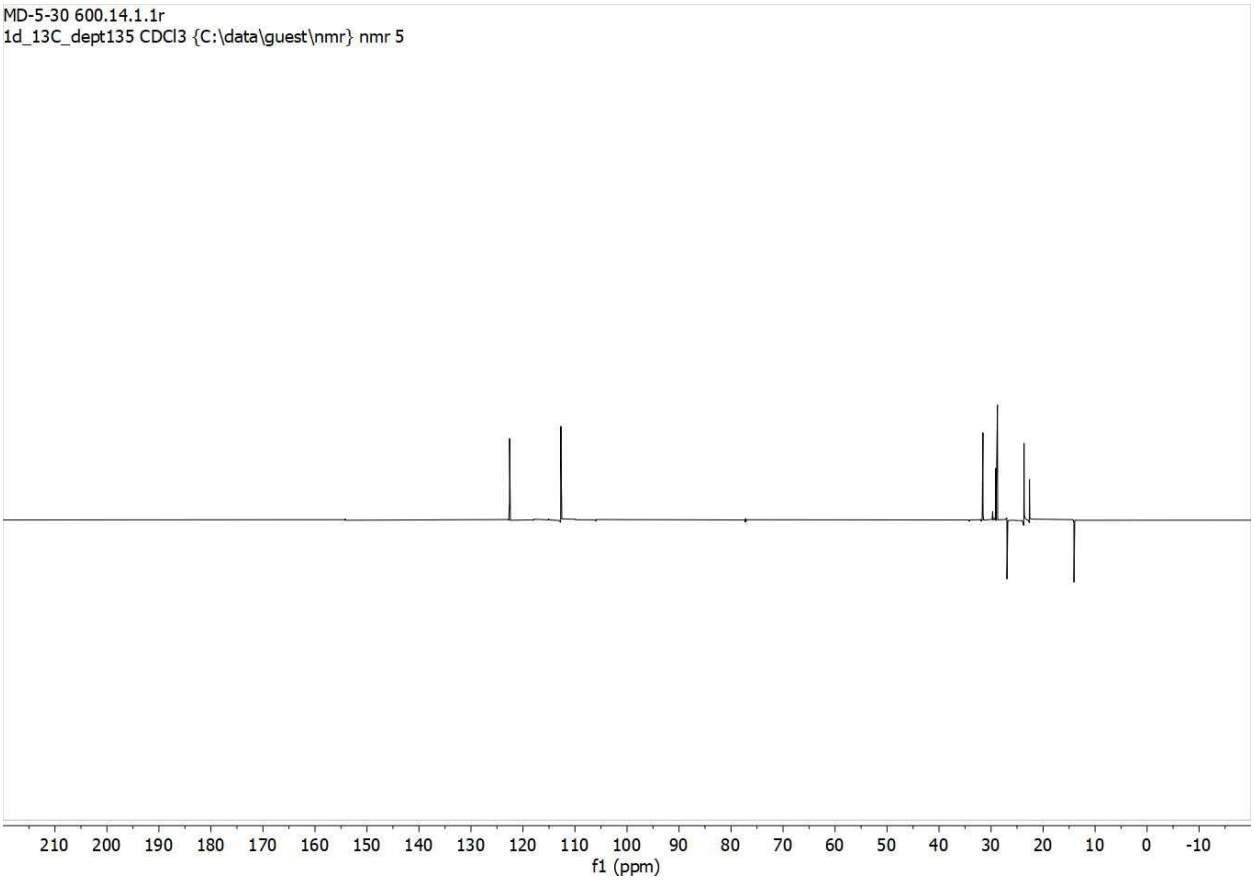
MD-5-30 600.14.1.1r
1d_13C_dept135 CDCl3 {C:\data\guest\nmr} nmr 5
210 200 190 180 170 160 150 140 130 120 110 100 90 80 70 60 50 40 30 20 10 0 -10
f1 (ppm)

DEPT135 of **1**

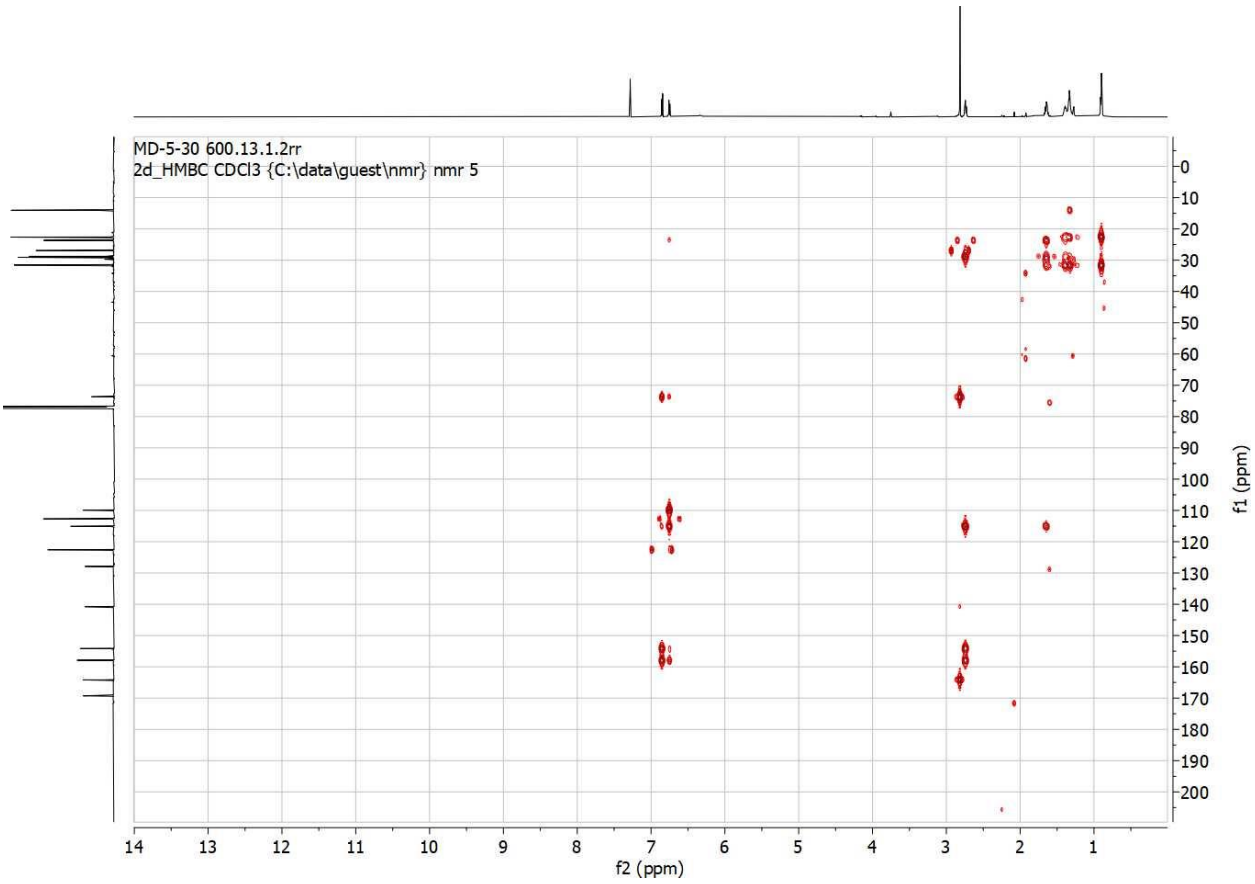
MD-5-30 600.13.1.2rr
2d_HMBC CDCl3 {C:\data\guest\nmr} nmr 5
f2 (ppm)
f1 (ppm)

HMBC of **1**

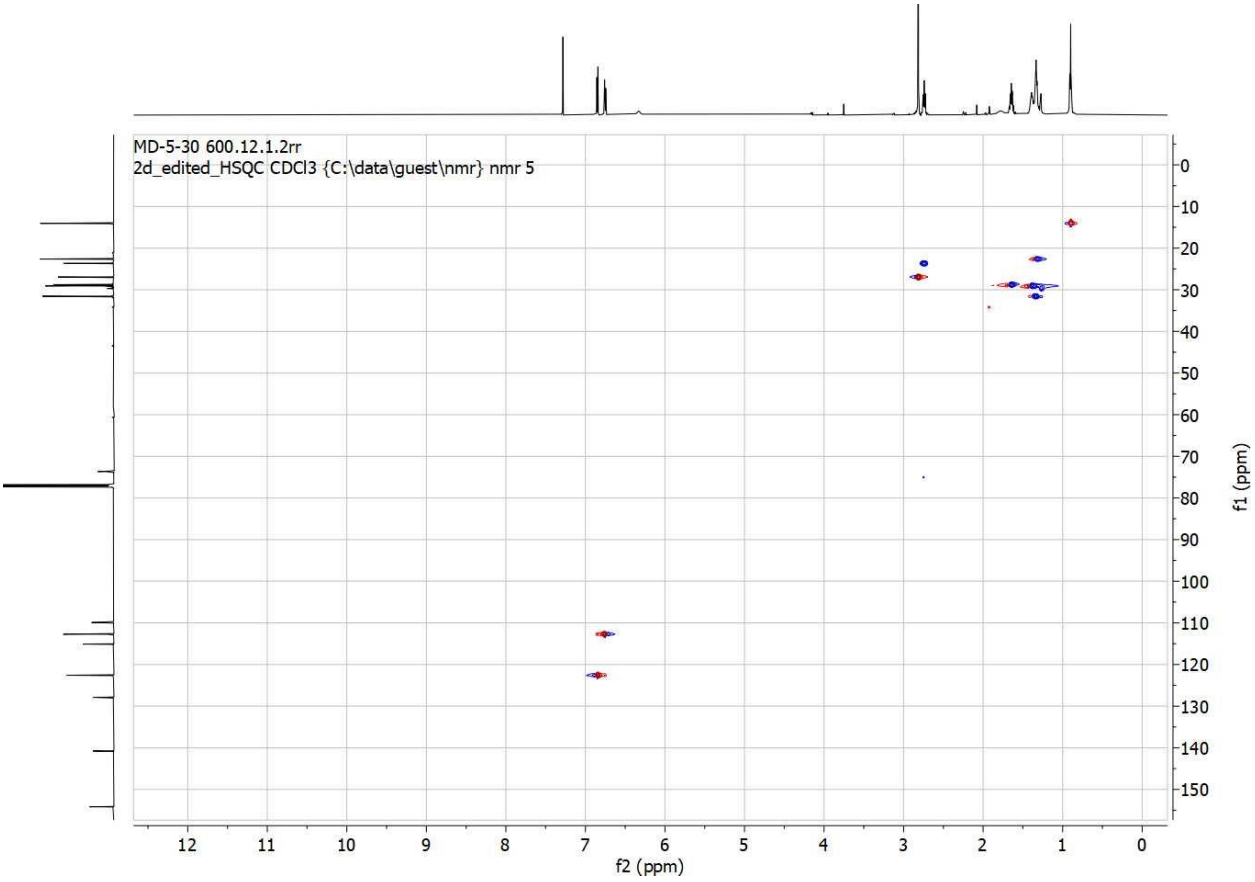
MD-5-30 600.12.1.2rr
2d_edited_HSQC CDCl3 {C:\data\guest\nmr} nmr 5
f2 (ppm)
f1 (ppm)

HSQC of **1**

Section 4. Copies of ^{1}H and ^{13}C spectra - D) Compounds on route to hexyl-pseudoarmeniaspirol **(SI1,SI2,16)**

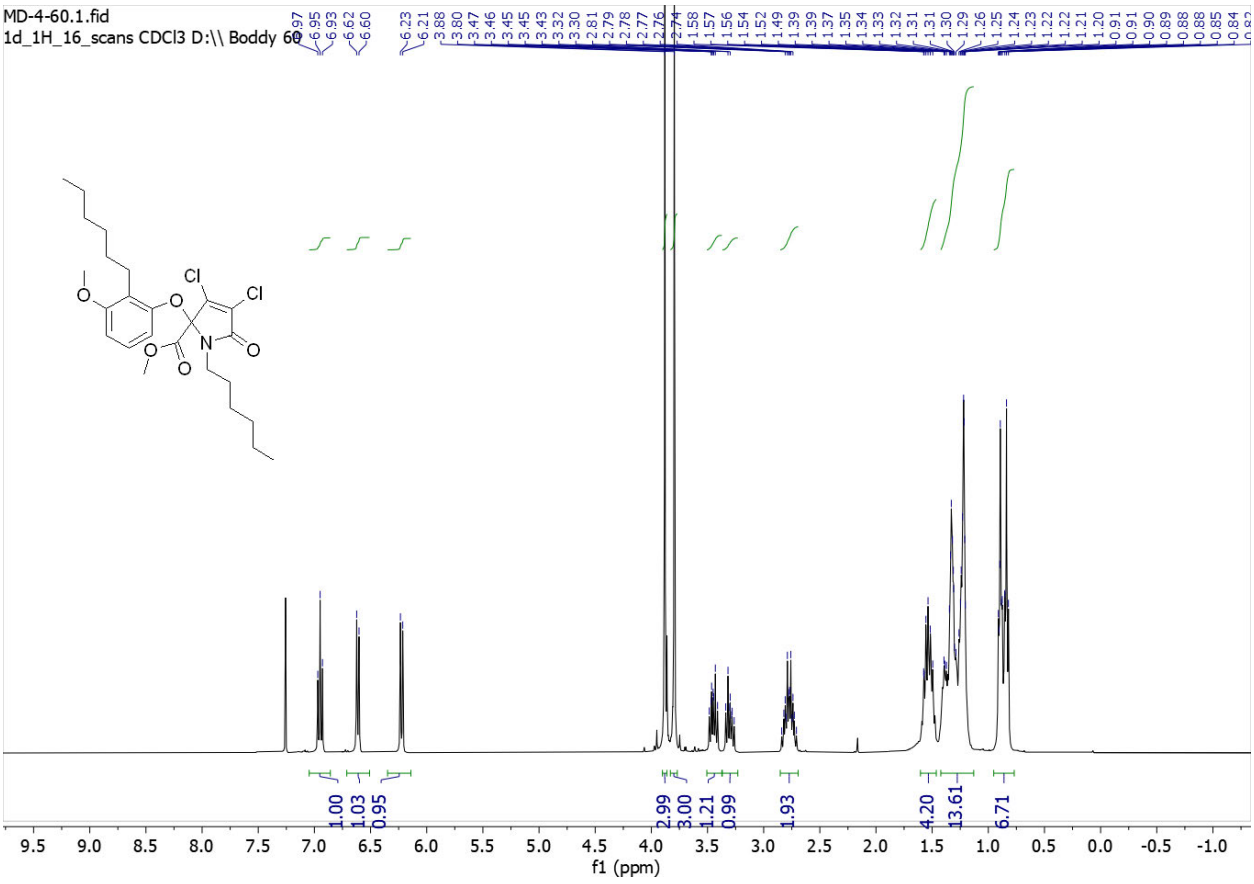

^{1}H NMR (400 MHz, $CDCl_3$) of **SI1**

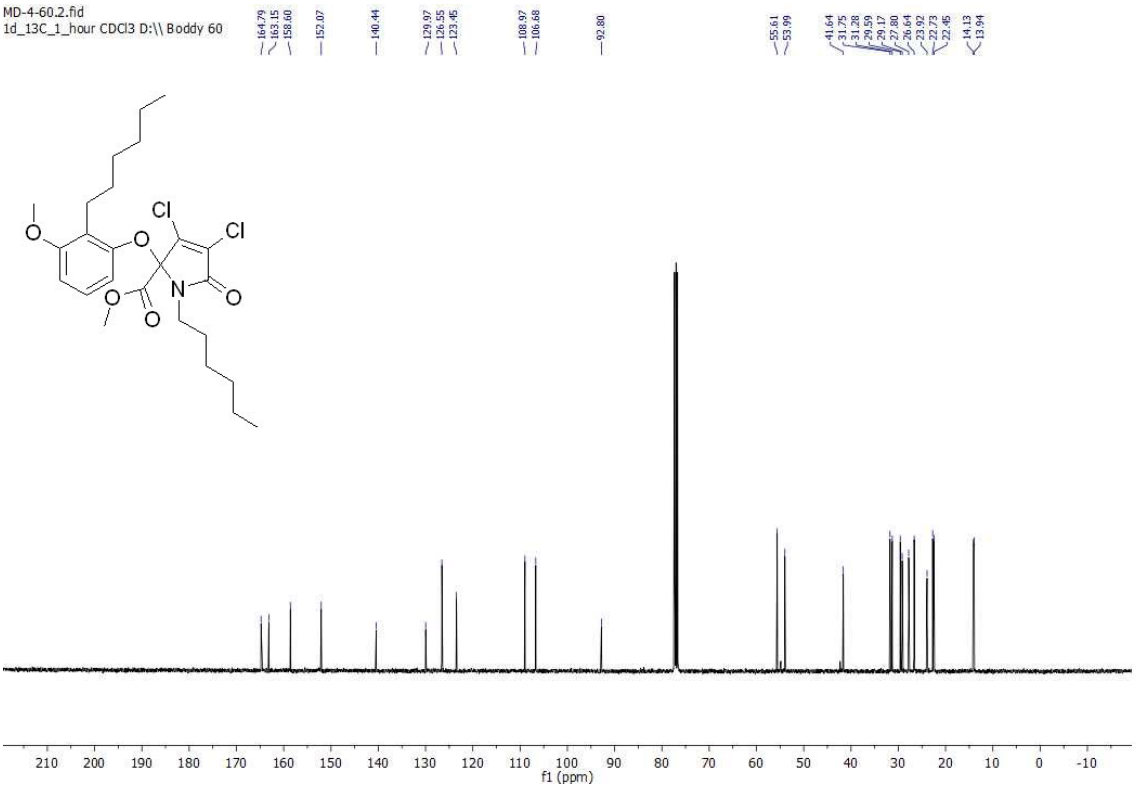

$^{13}C\{^{1}H\}$ NMR (100 MHz, $CDCl_3$) of **SI1**

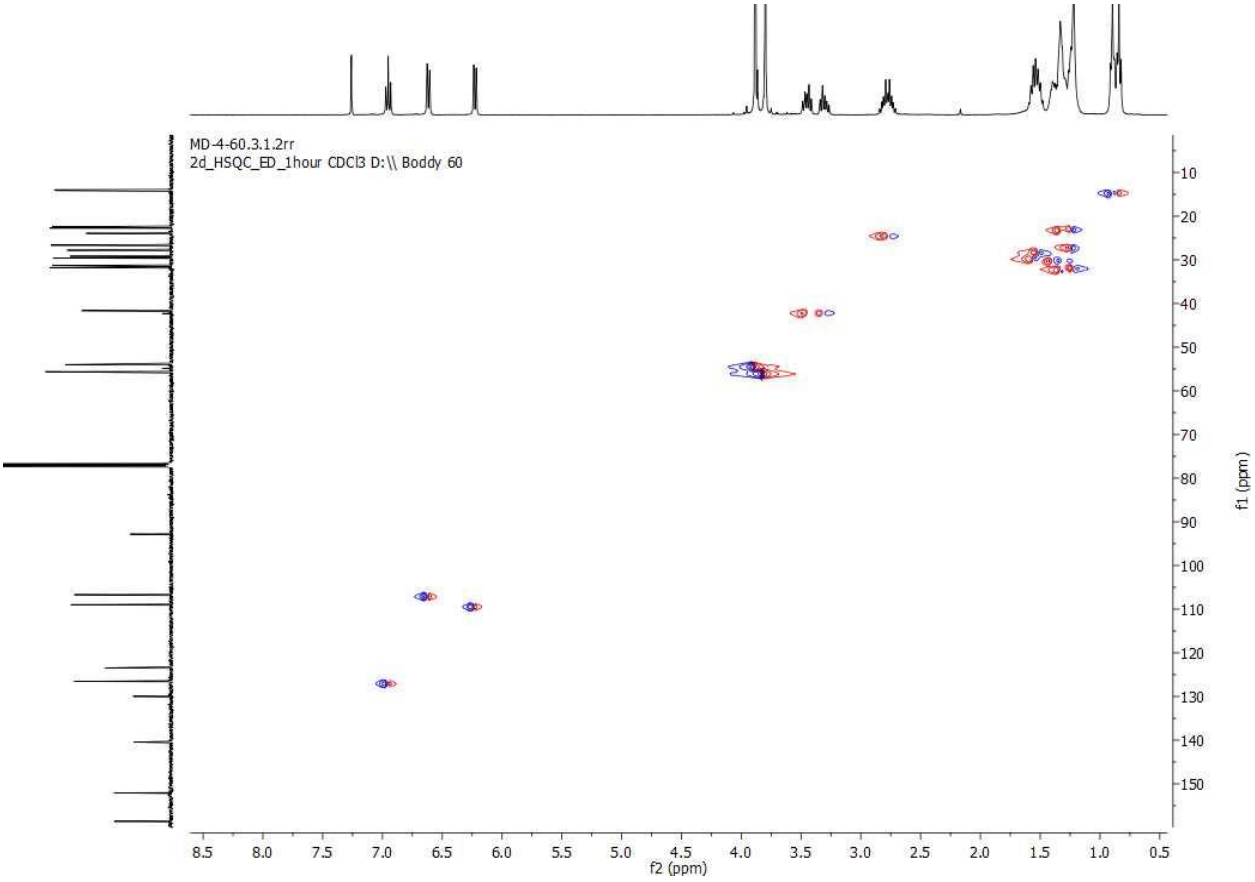

HSQC of **SI1**

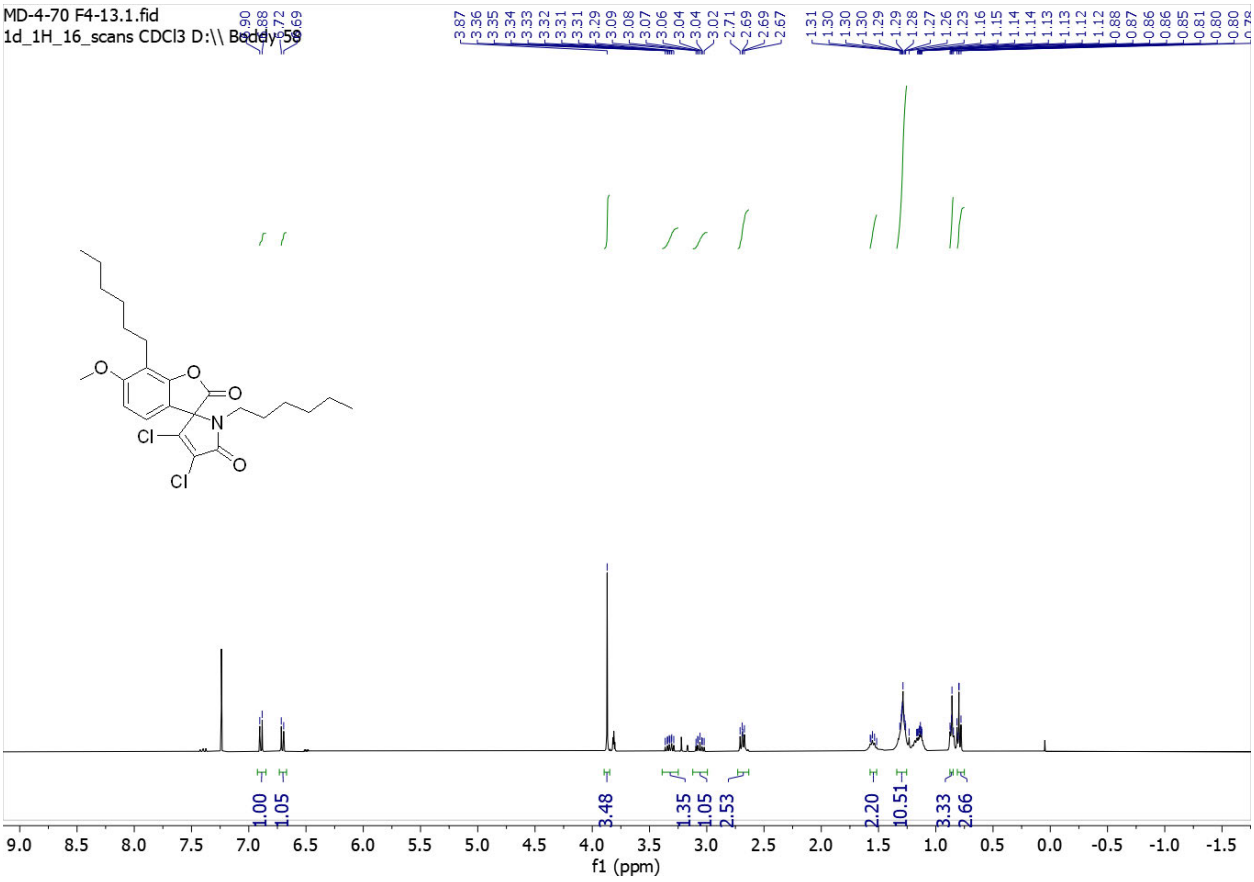

^{1}H NMR (400 MHz, $CDCl_3$) of **SI2**

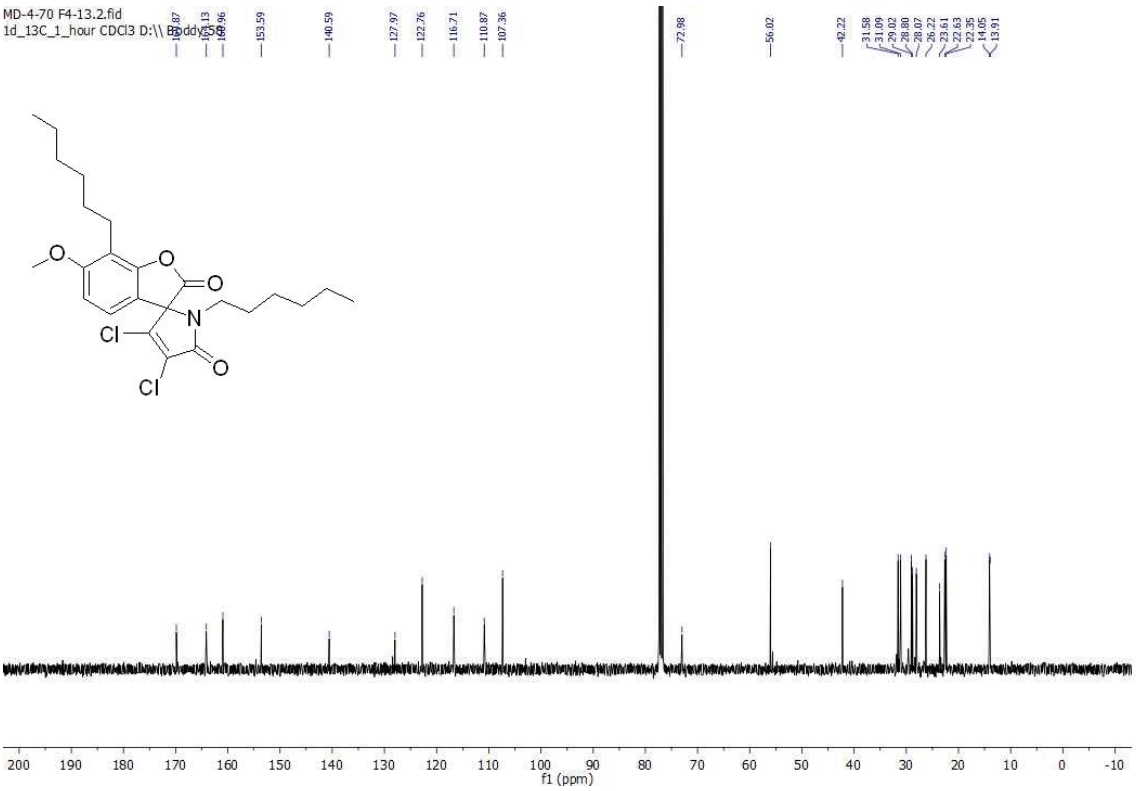

$^{13}C\{^{1}H\}$ NMR (100 MHz, $CDCl_3$) of **SI2**

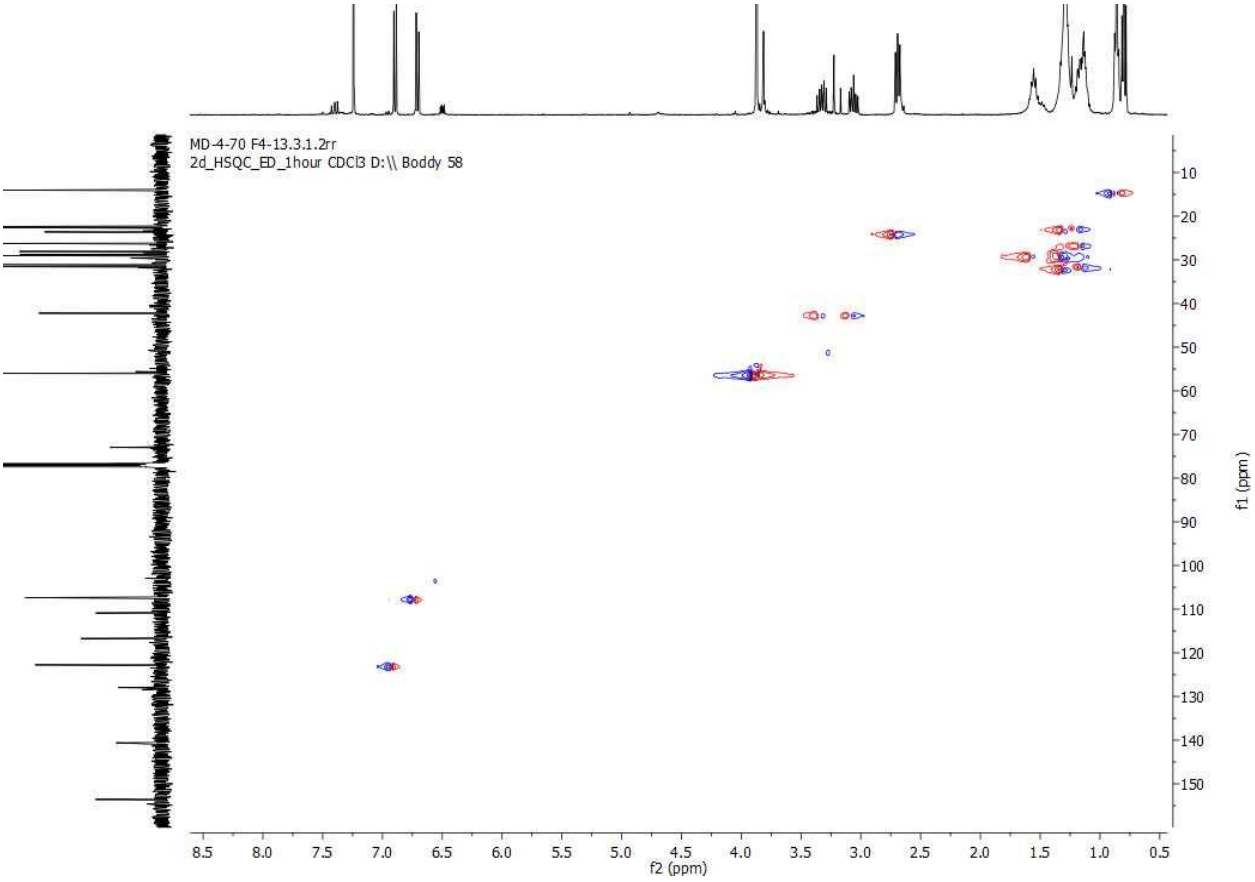
MD-4-70 F4-13.3.1.2rr
2d_HSQC_ED_1hour CDCl3 D:\\ Boddy 58
f2 (ppm)
f1 (ppm)

HSQC of **SI2**

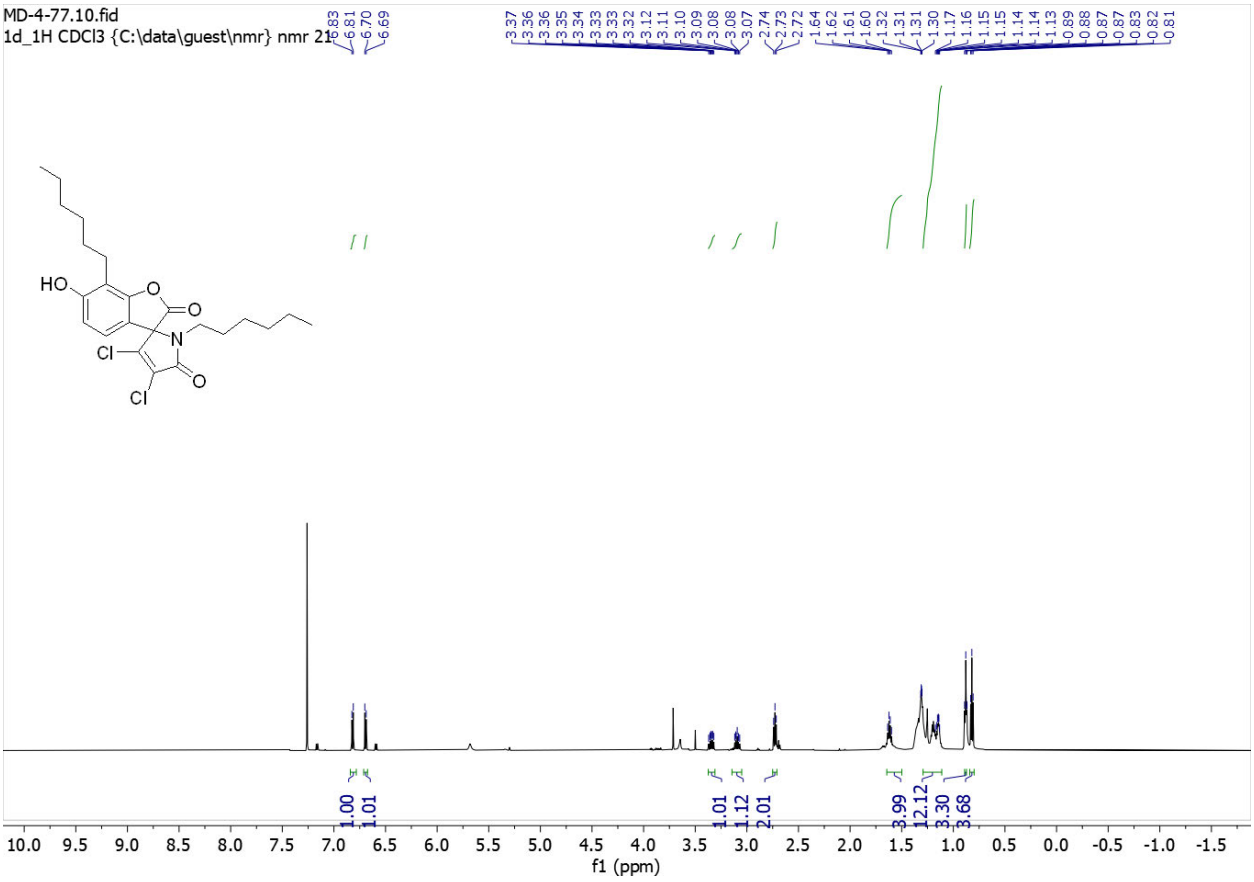

^{1}H NMR (600 MHz, $CDCl_3$) of **16**

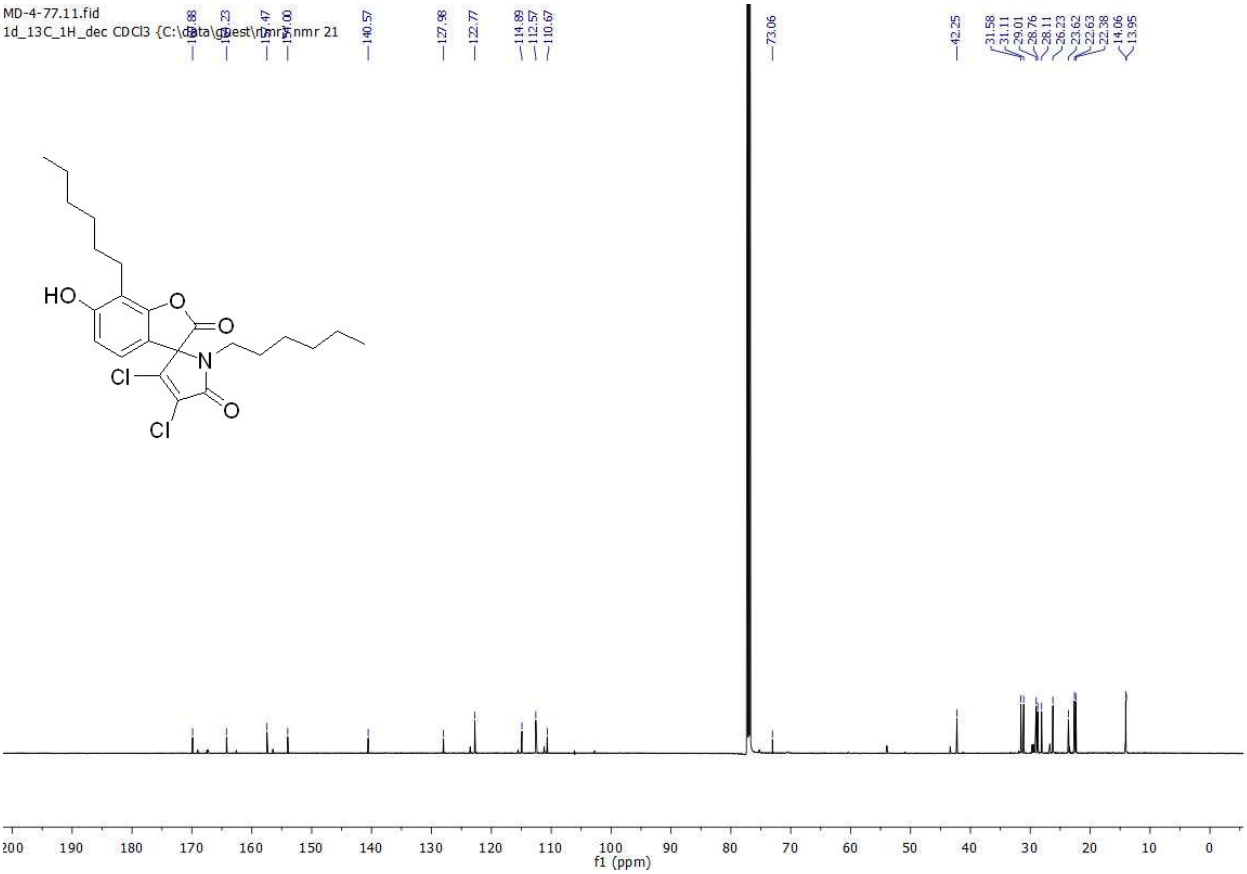

$^{13}C\{^{1}H\}$ NMR (150 MHz, $CDCl_3$) of **16**

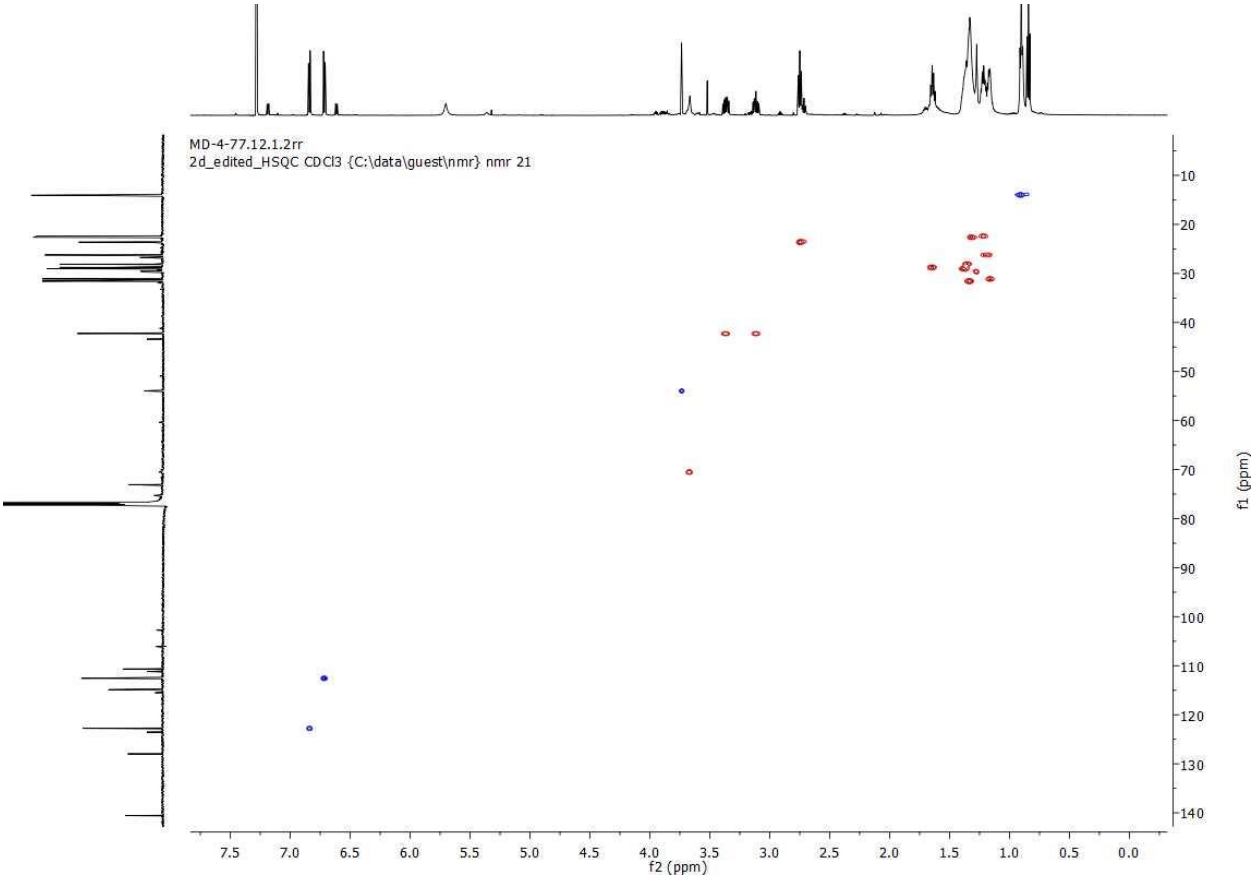
MD-4-77.12.1.2rr
2d_edited_HSQC CDCl3 {C:\data\guest\nmr} nmr 21
f1 (ppm)
f2 (ppm)

HSQC of **16**

Section 4. Copies of ^{1}H and ^{13}C spectra - E) Compounds on route to N-dodecyl-p-1-methyl-pseudoarmeniaspirol **(SI5,SI3,SI4,17)**

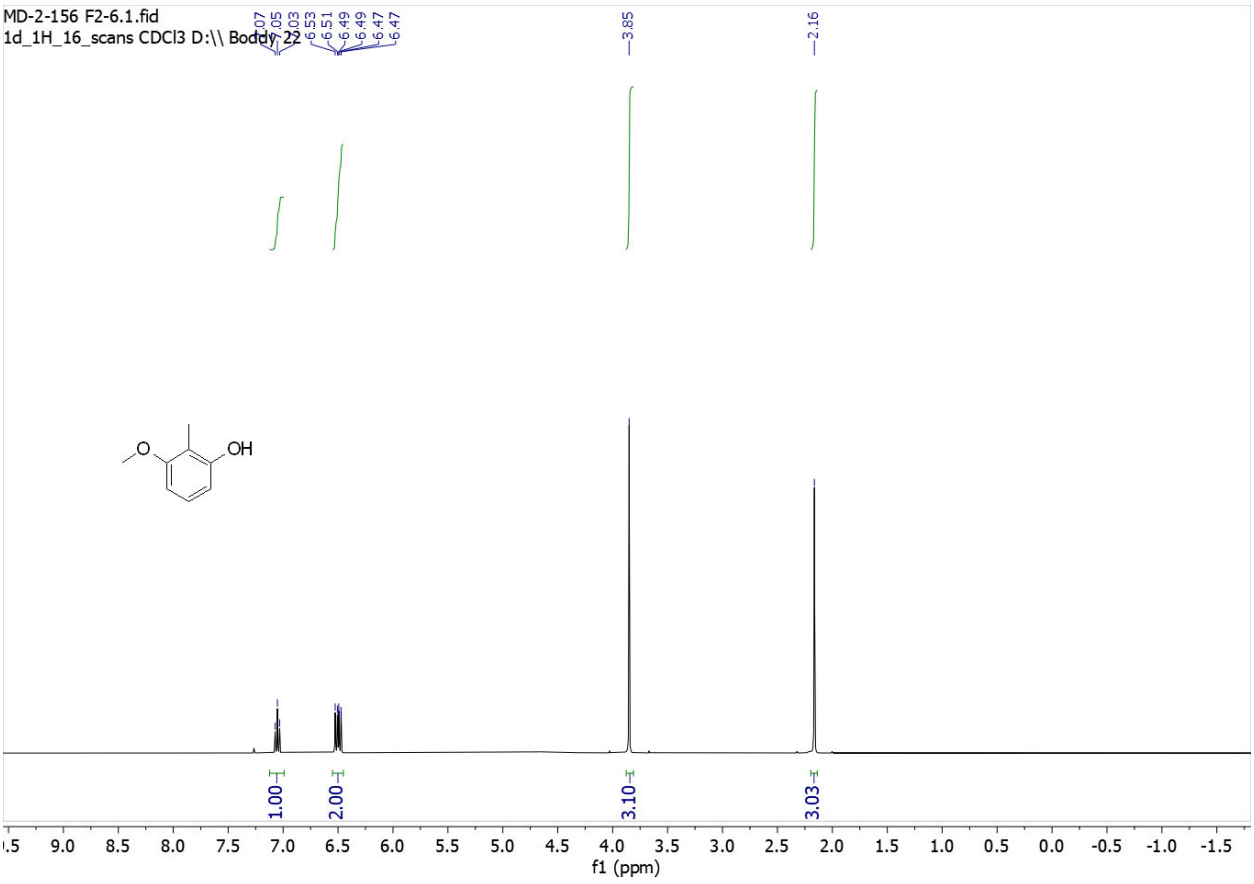

^{1}H NMR (400 MHz, $CDCl_3$) of **SI5**

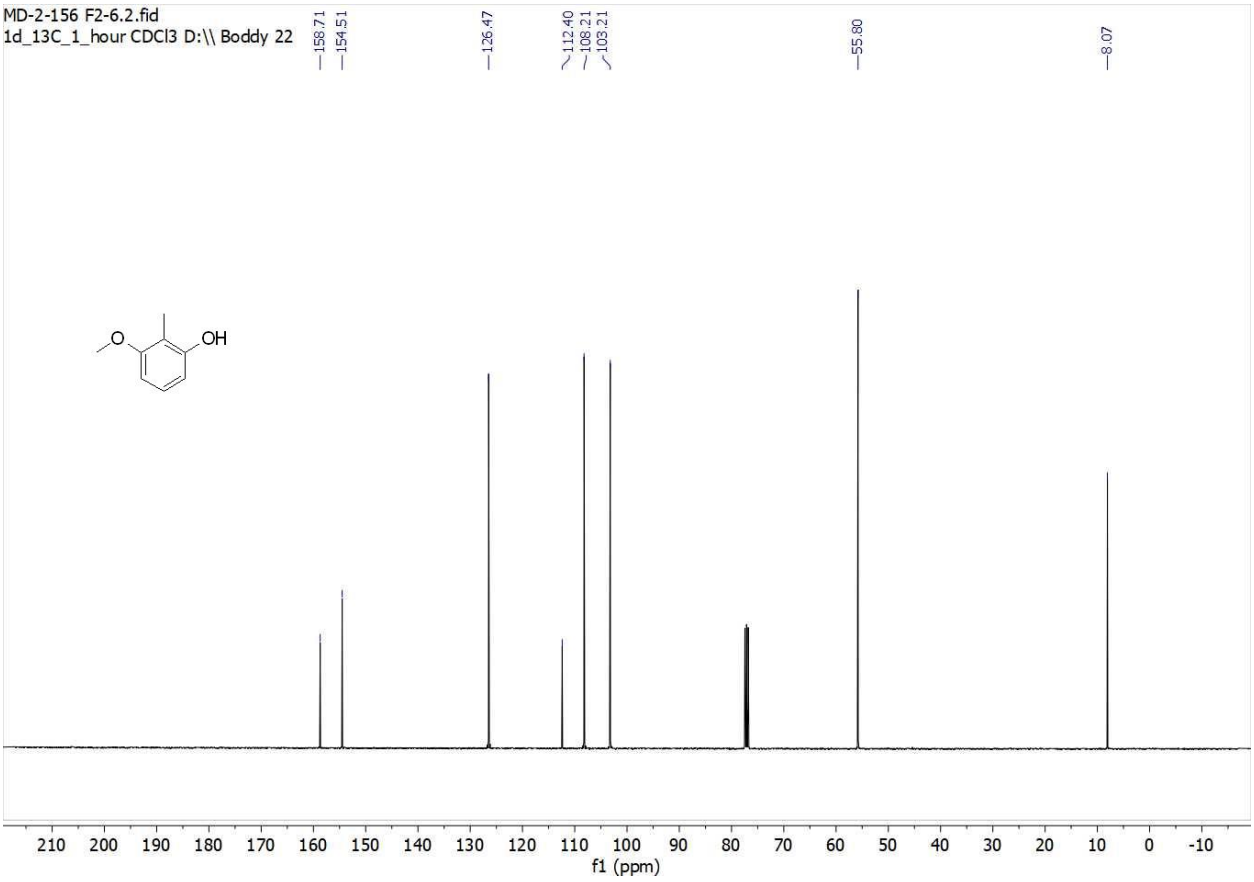

$^{13}C\{^{1}H\}$ NMR (100 MHz, $CDCl_3$) of **SI5**

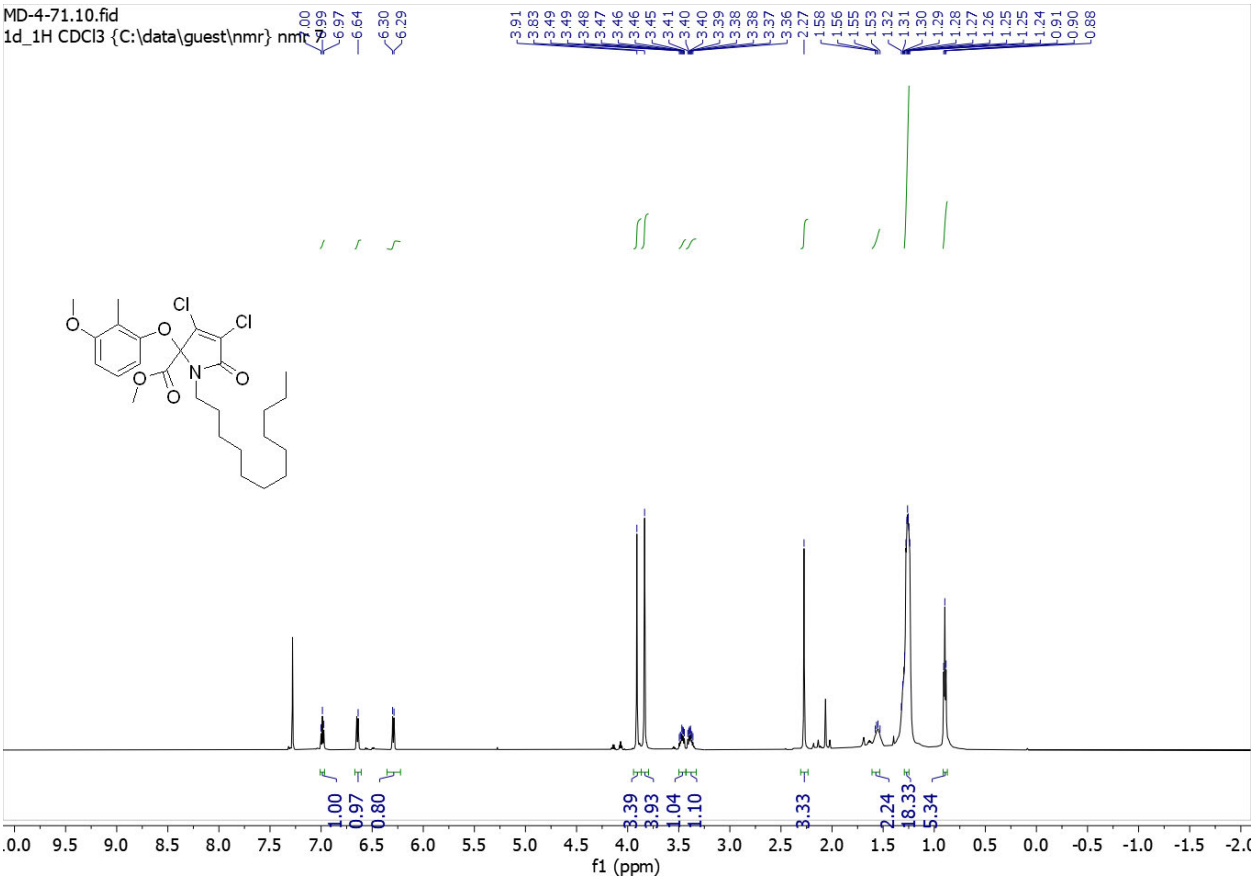

^{1}H NMR (600 MHz, $CDCl_3$) of **SI3**

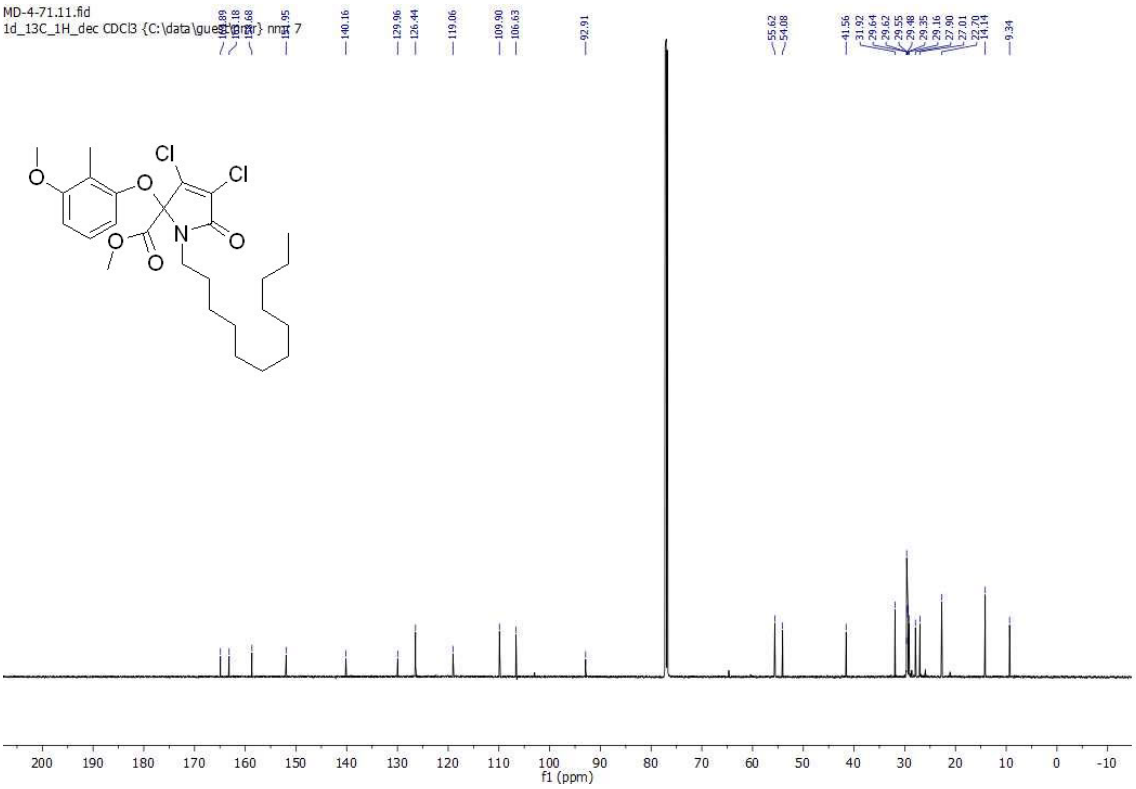

$^{13}C\{^{1}H\}$ NMR (150 MHz, $CDCl_3$) of **SI3**

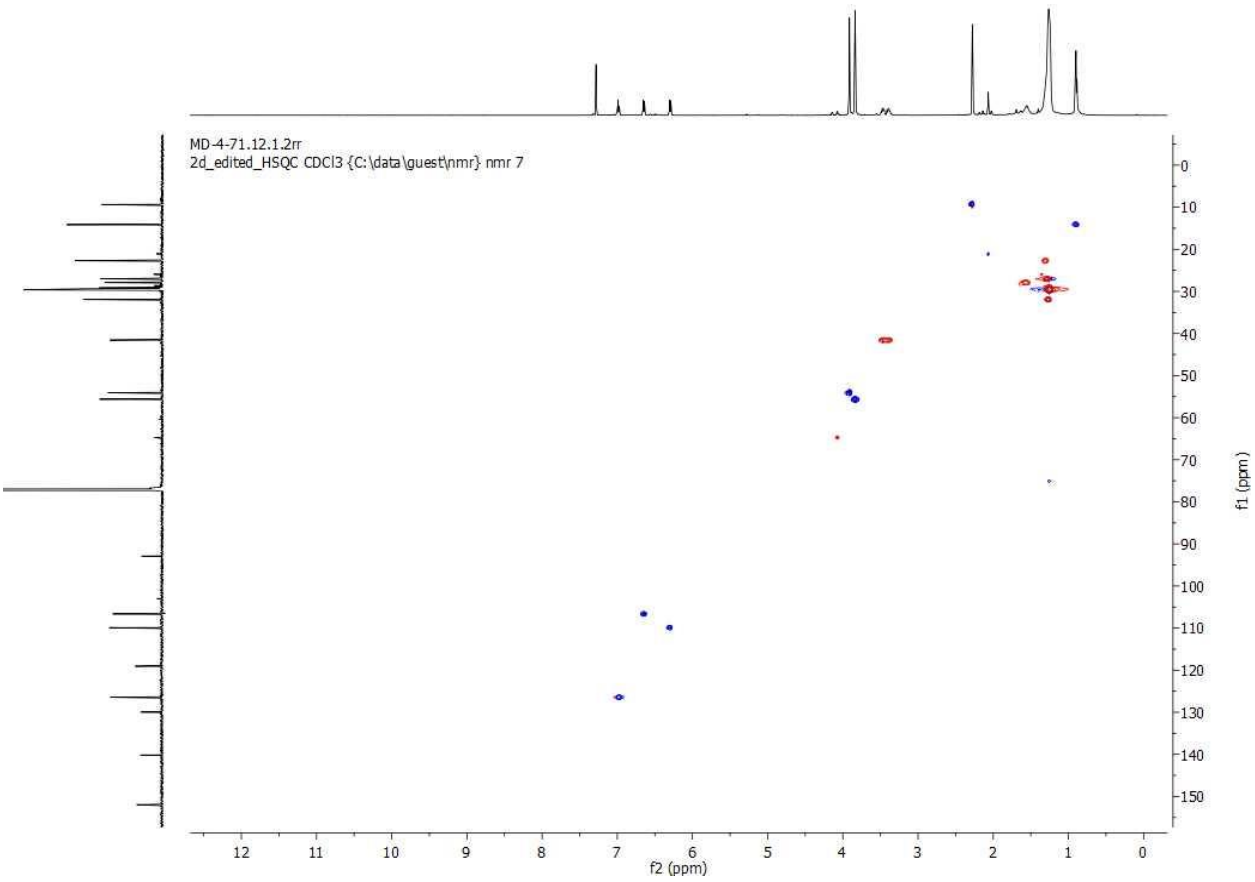
MD-4-71.12.1.2rr
2d_edited_HSQC CDCl3 {C:\data\guest\nmr} nmr 7
f2 (ppm)
f1 (ppm)

HSQC of **SI3**

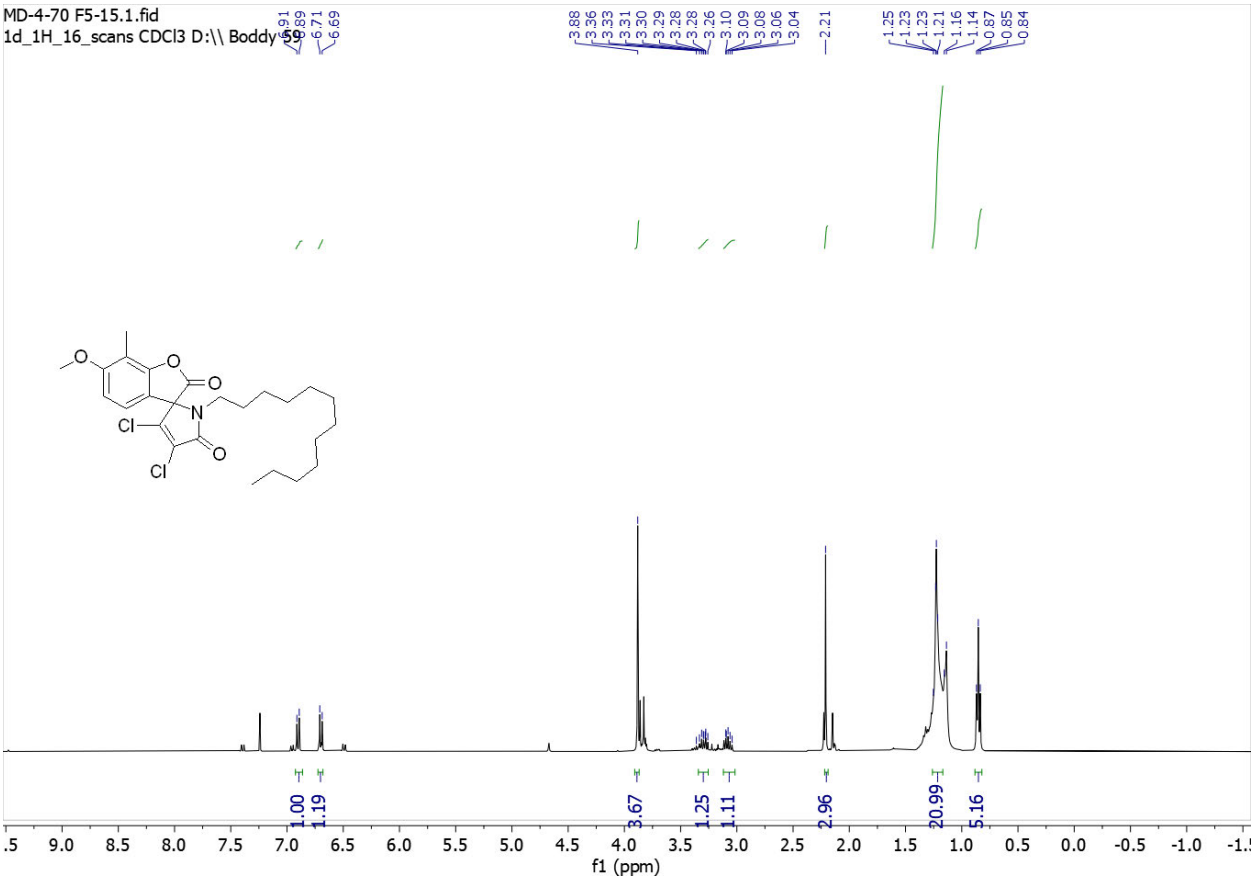

^{1}H NMR (400 MHz, $CDCl_3$) of **SI4**

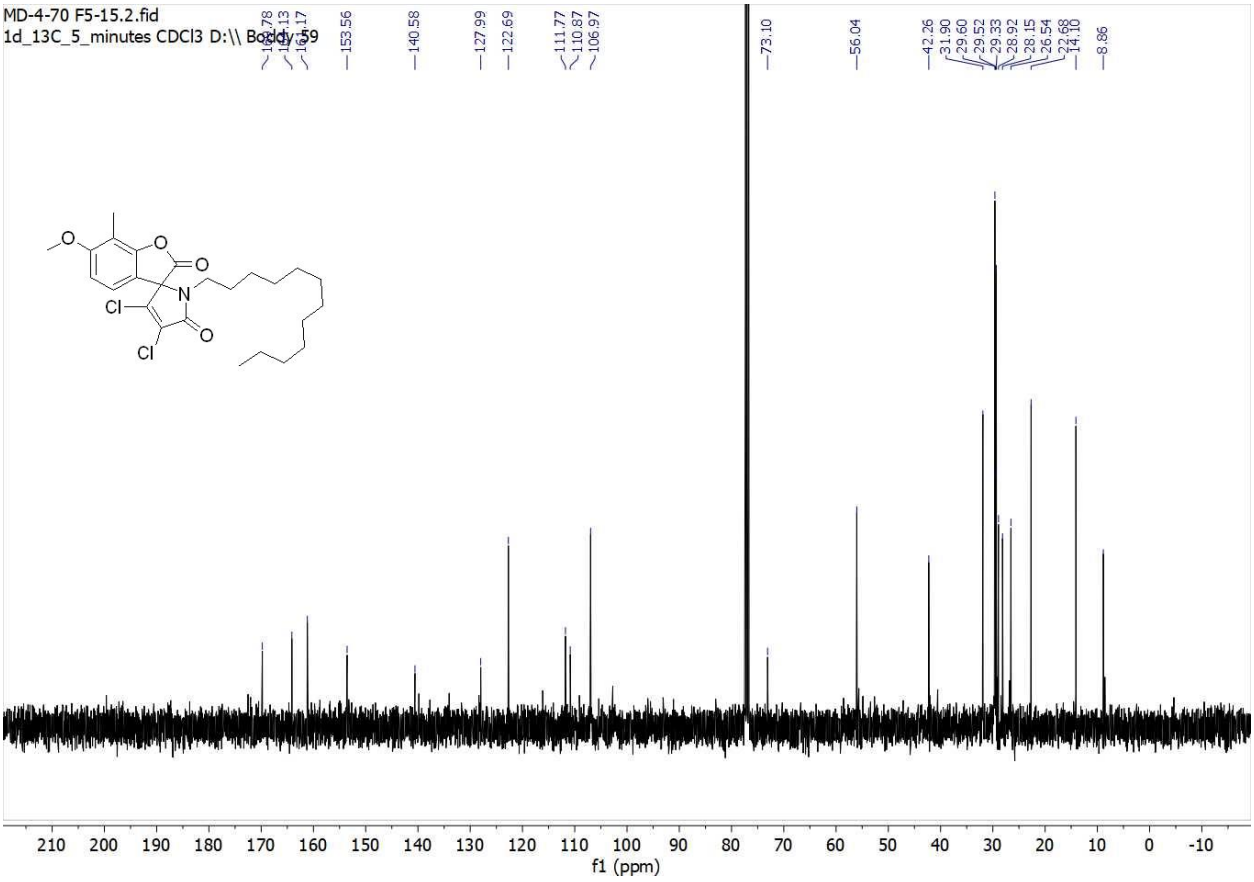

$^{13}C\{^{1}H\}$ NMR (100 MHz, $CDCl_3$) of **SI4**

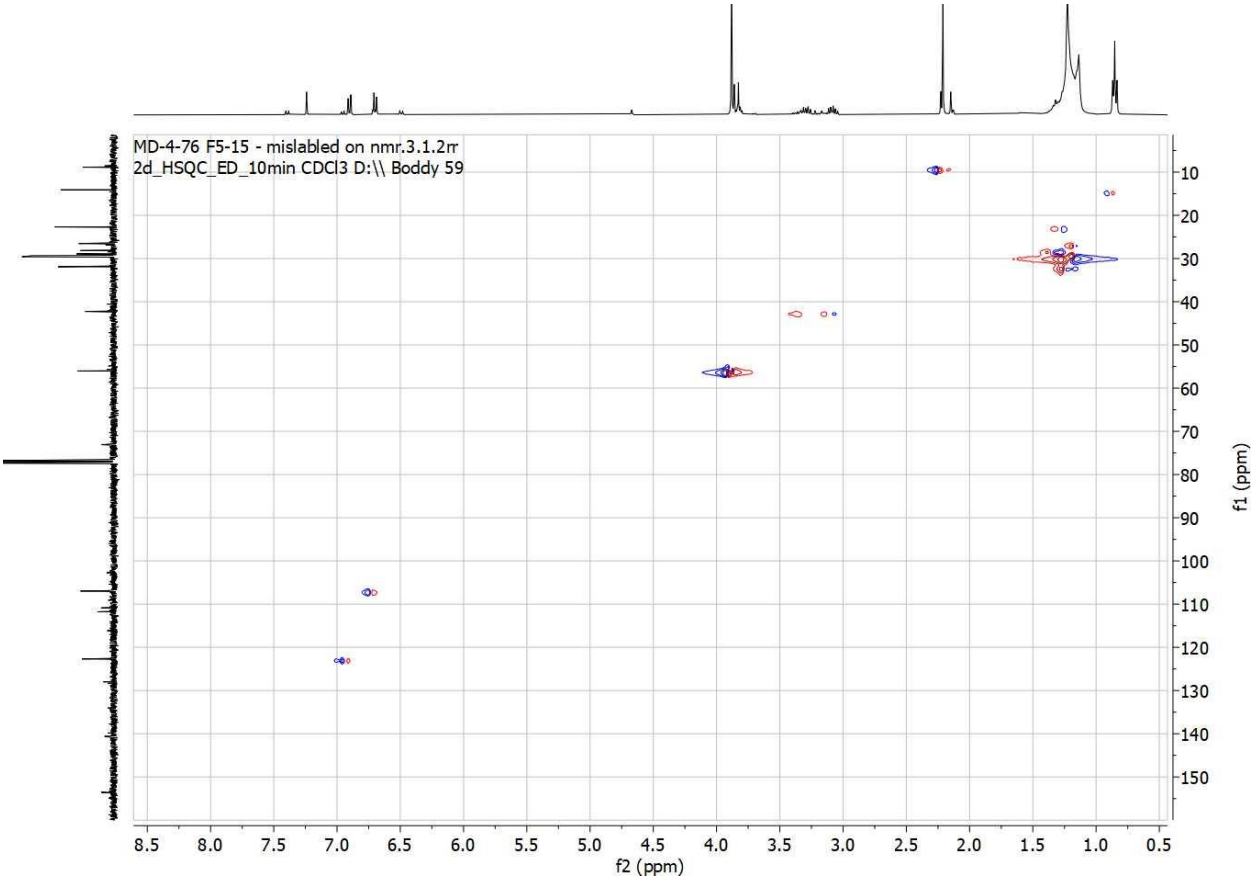
MD-4-76 F5-15 - mislabled on nmr.3.1.2rr
2d_HSQC_ED_10min CDCl3 D:\\ Boddy 59
f2 (ppm)
f1 (ppm)

HSQC of **SI4**

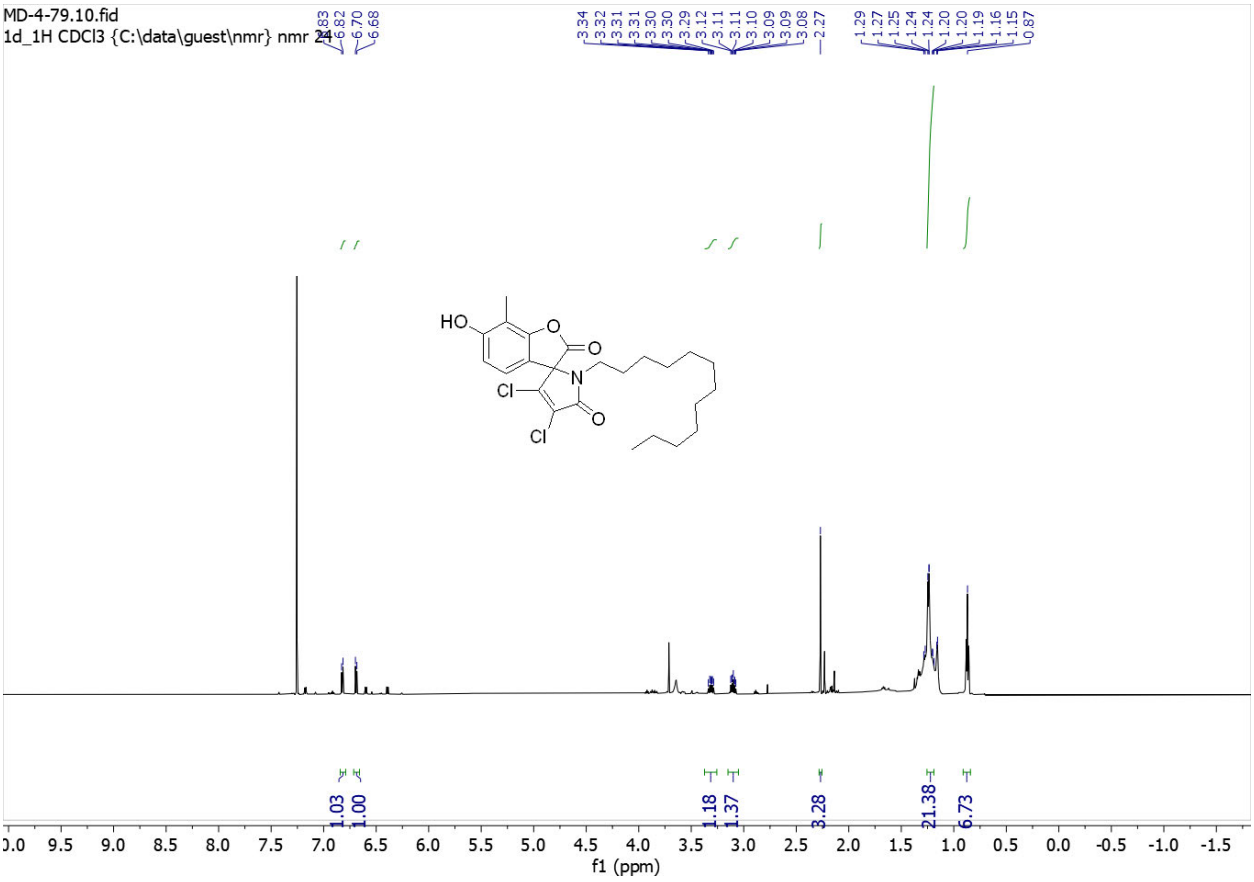

^{1}H NMR (600 MHz, $CDCl_3$) of **17**

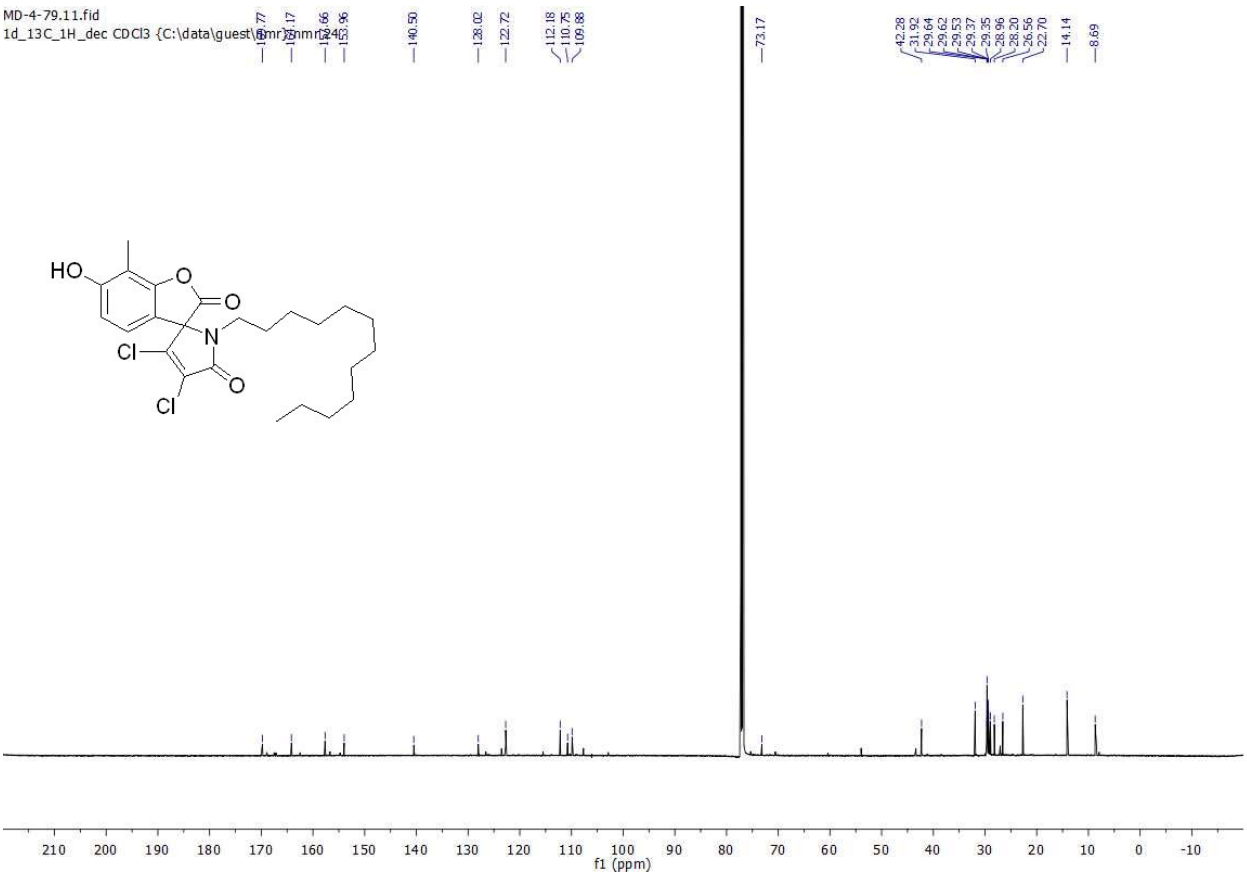

$^{13}C\{^{1}H\}$ NMR (150 MHz, $CDCl_3$) of **17**

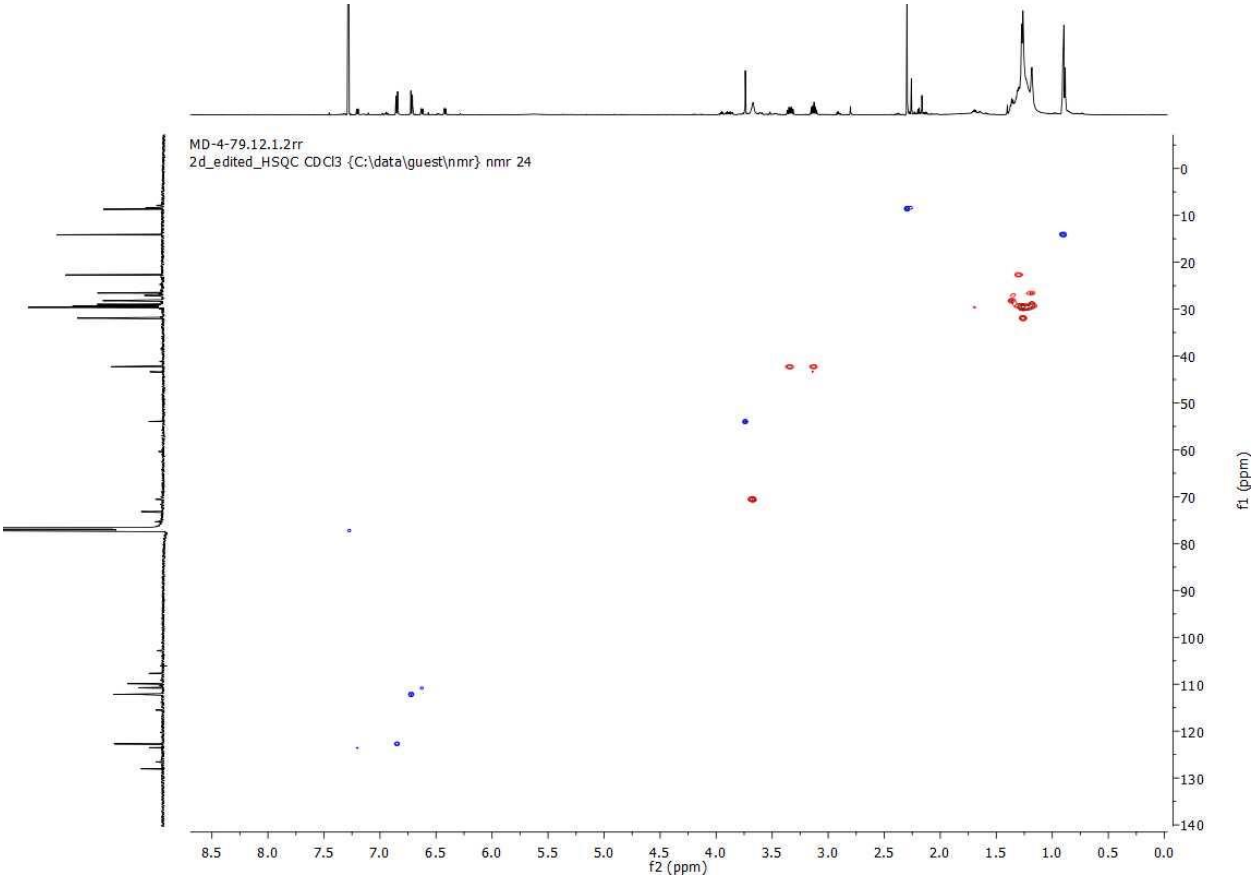
MD-4-79.12.1.2rr
2d_edited_HSQC CDCl3 {C:\data\guest\nmr} nmr 24
f2 (ppm)
f1 (ppm)

HSQC of **17**

Section 4. Copies of ^{1}H and ^{13}C spectra - F) Compounds **3,4,9,10,11,12,13,14**

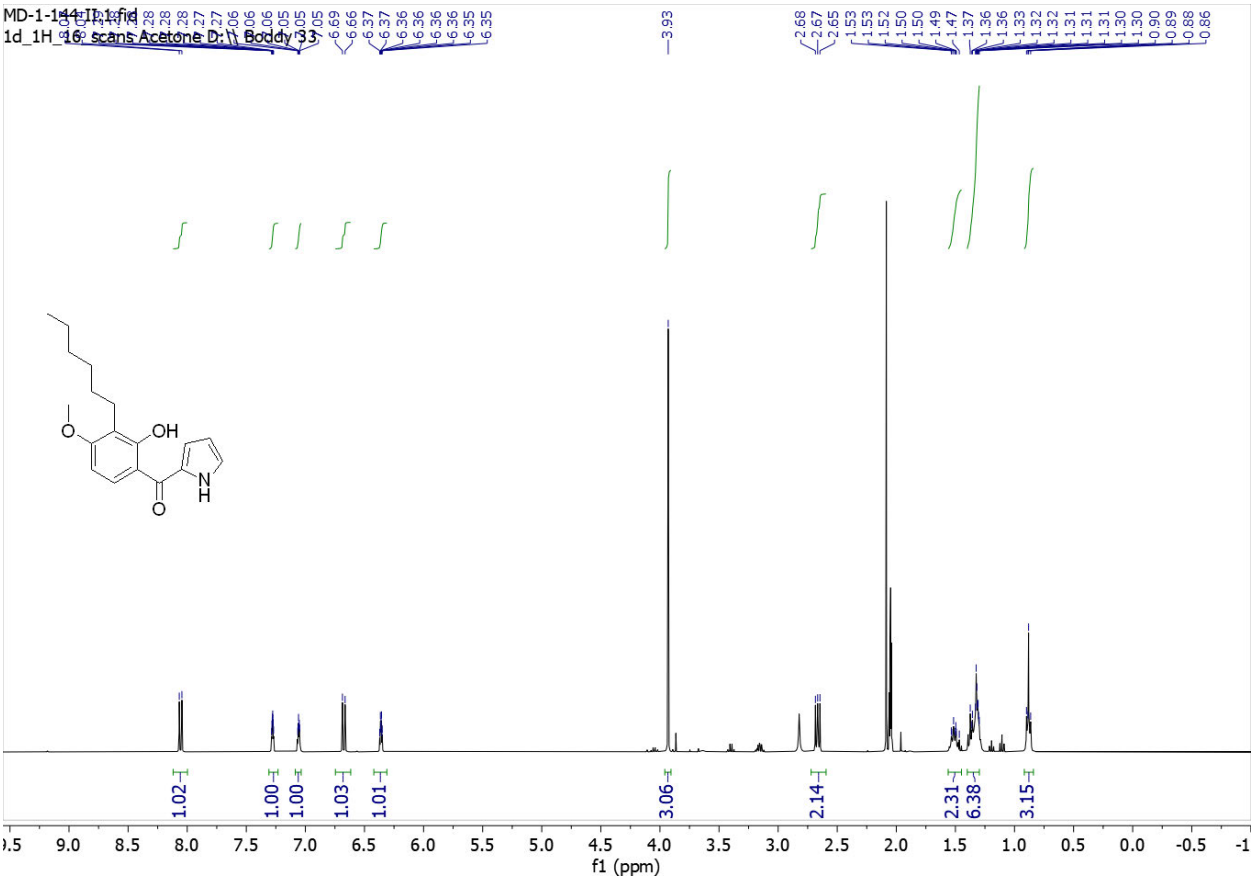

^{1}H NMR (400 MHz, $CDCl_3$) of **3**

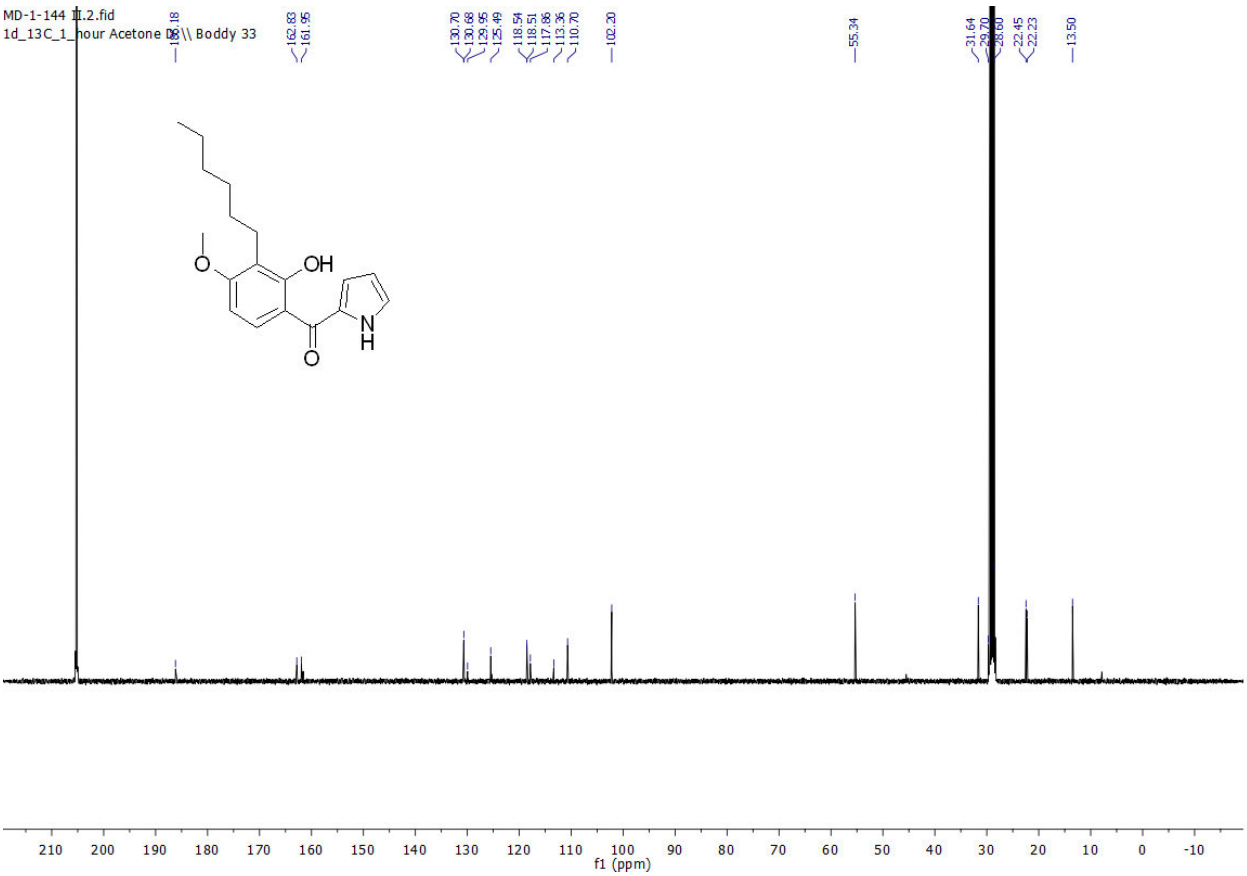

$^{13}C\{^{1}H\}$ NMR (100 MHz, $CDCl_3$) of **3**

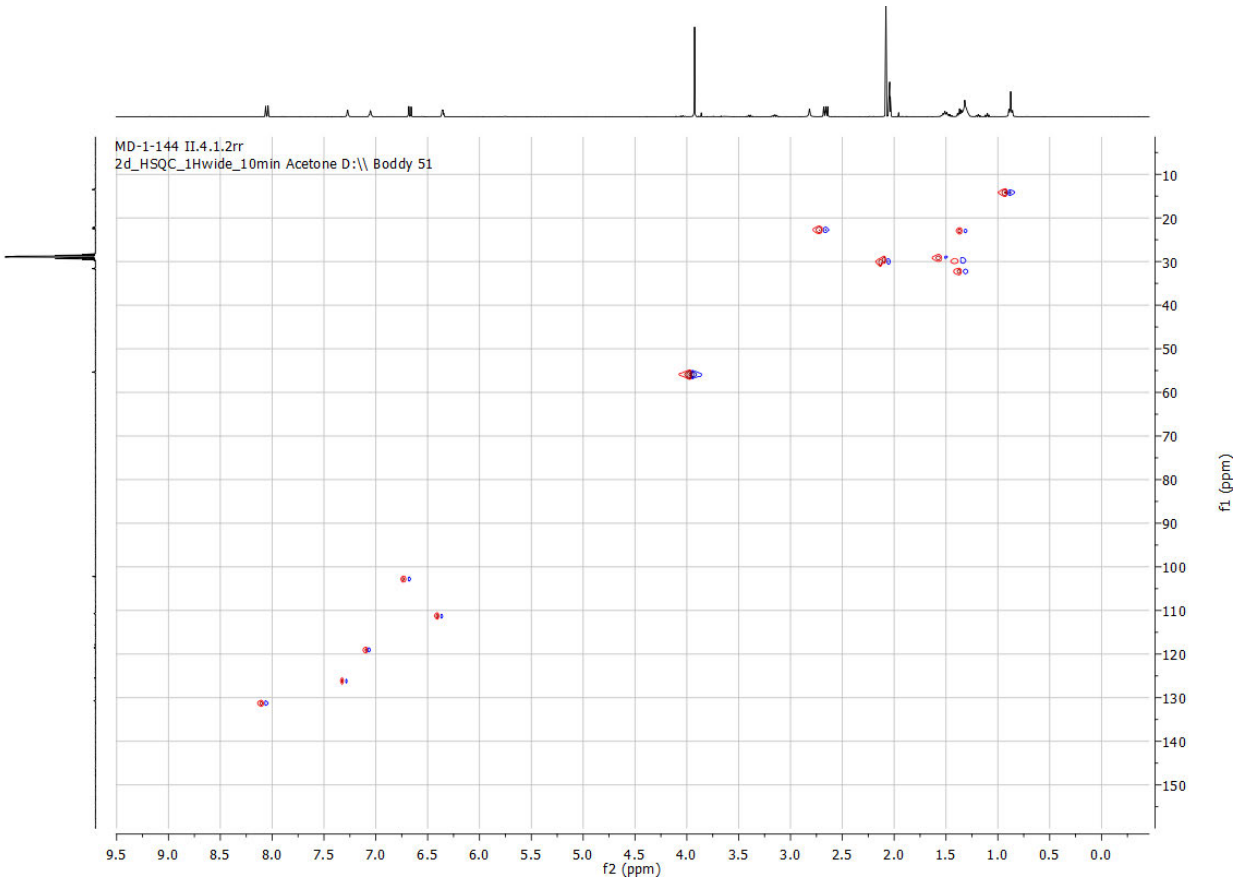
MD-1-144 II.4.1.2rr
2d_HSQC_1Hwide_10min Acetone D:\\ Boddy 51
f1 (ppm)
f2 (ppm)

HSQC of **3**

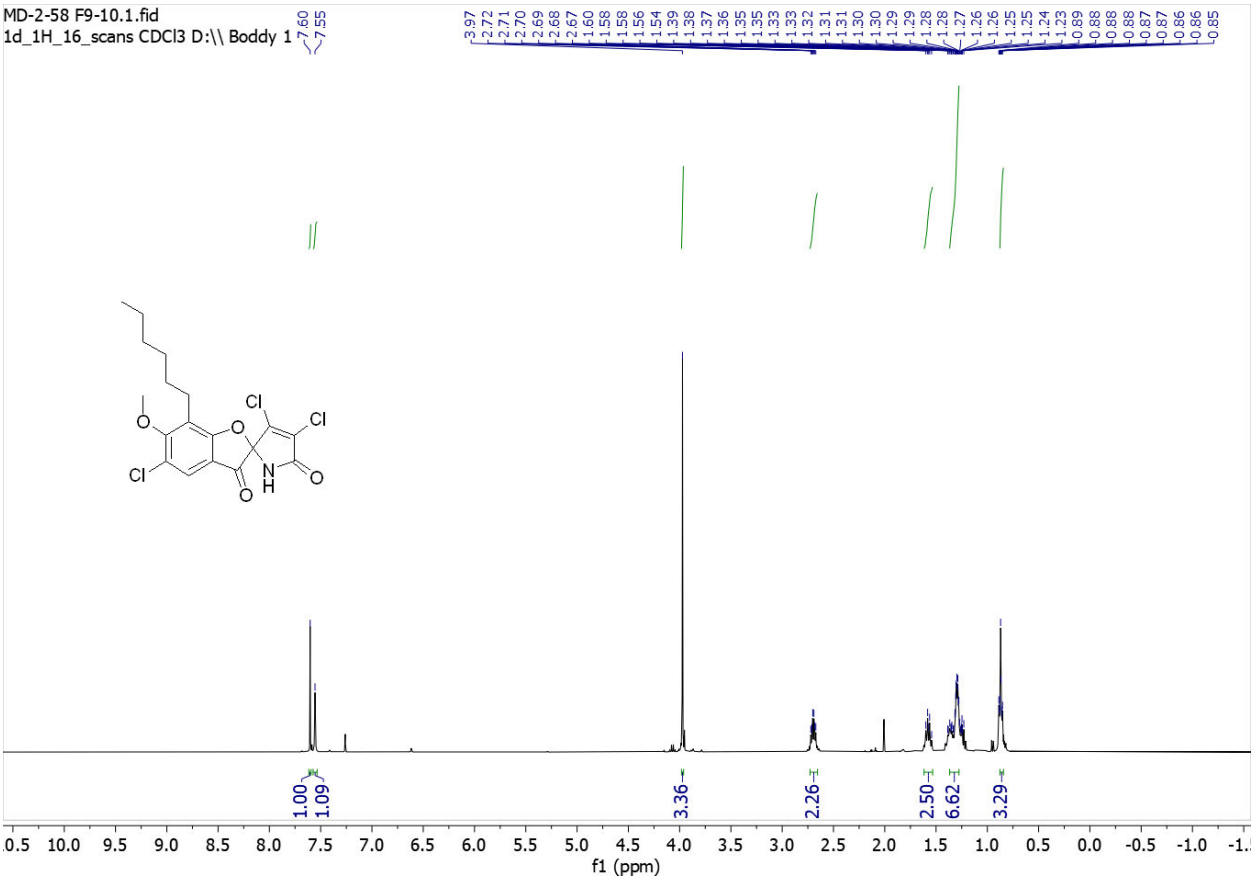

^{1}H NMR (400 MHz, $CDCl_3$) of **4**

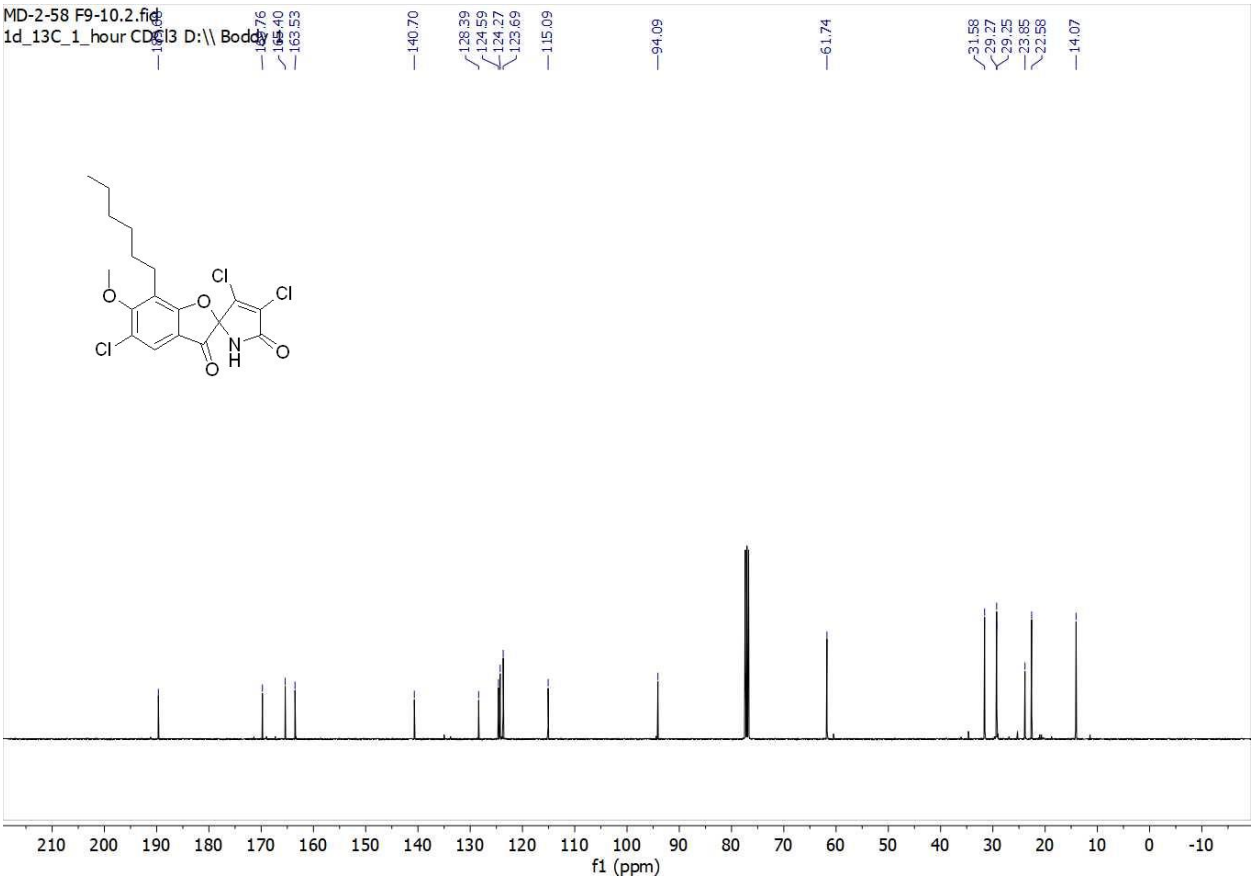

$^{13}C\{^{1}H\}$ NMR (100 MHz, $CDCl_3$) of **4**

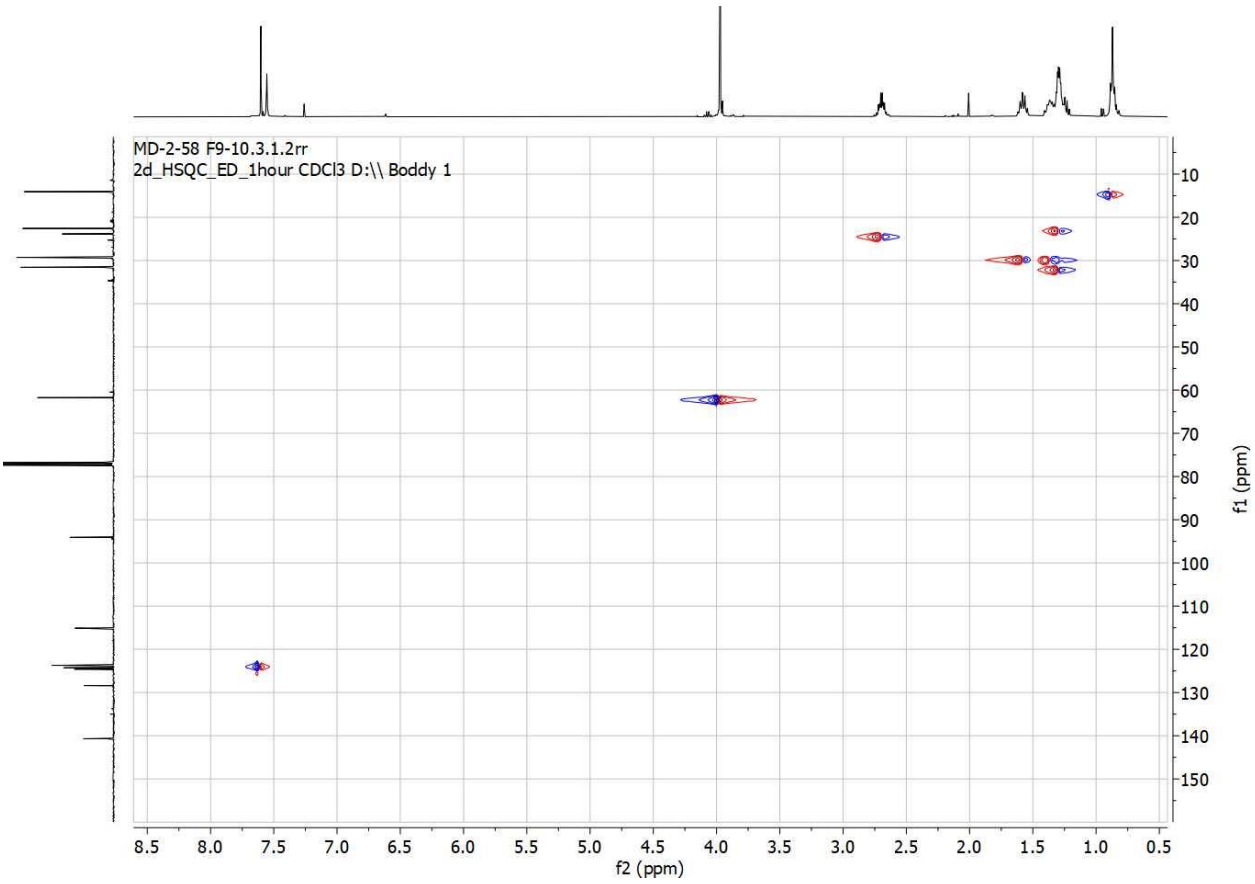

HSQC of **4**

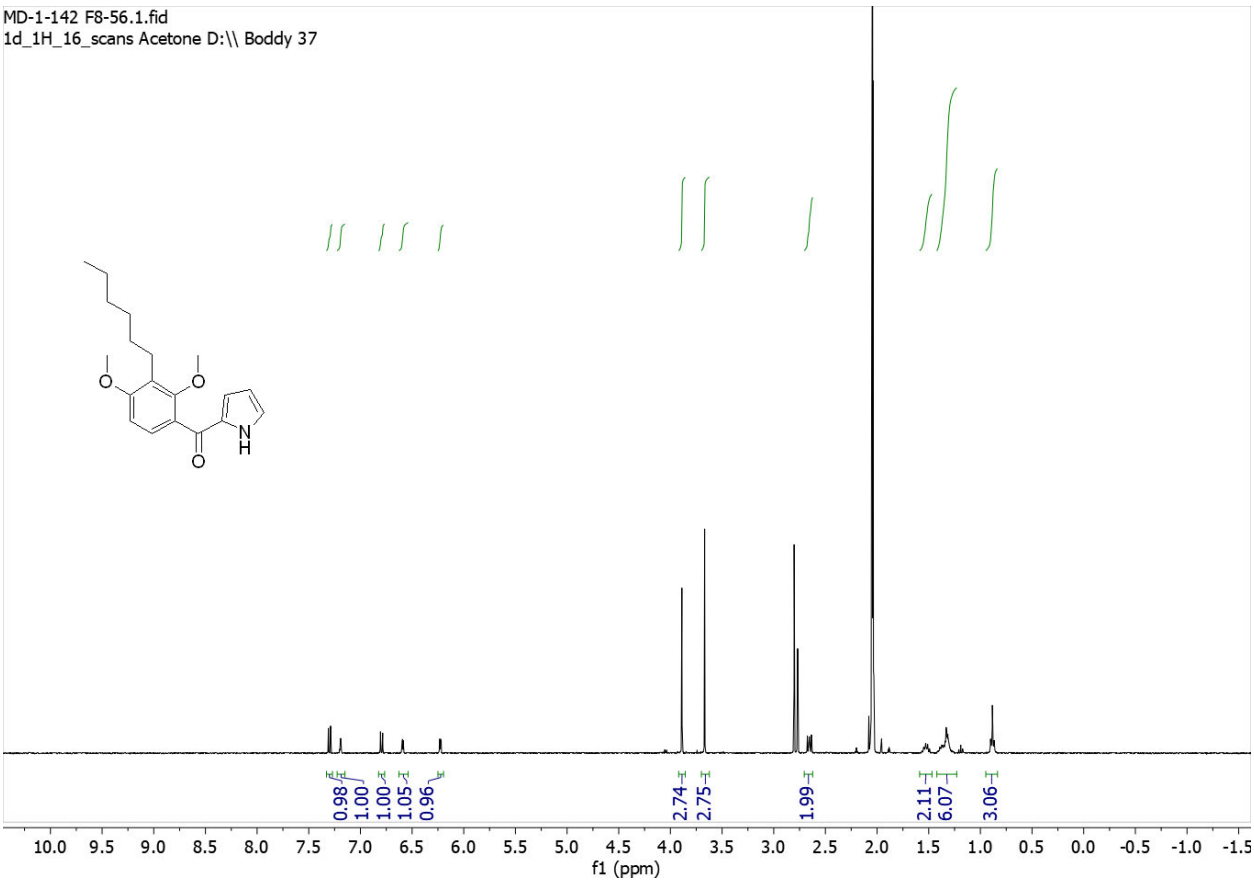

^{1}H NMR (400 MHz, $CDCl_3$) of **9**

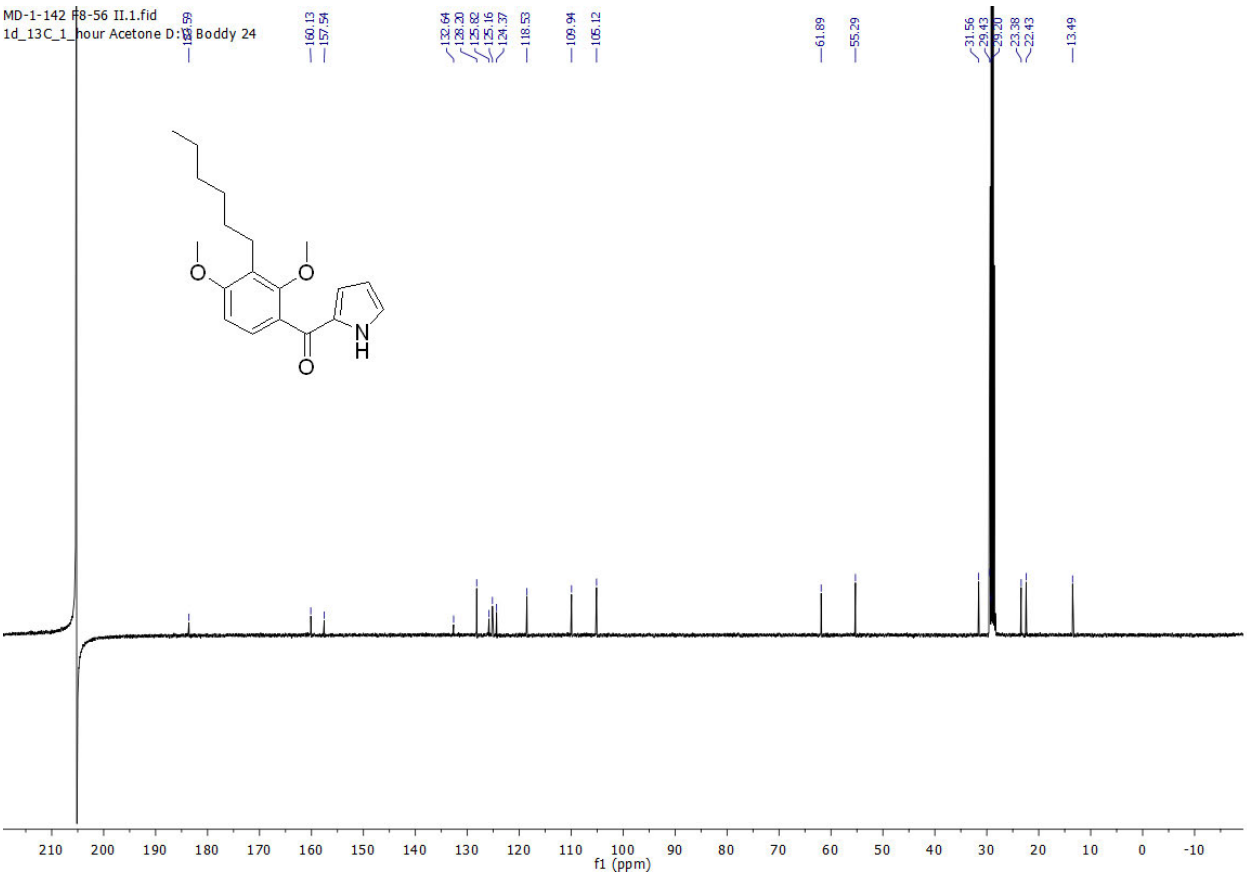

$^{13}C\{^{1}H\}$ NMR (100 MHz, $CDCl_3$) of **9**

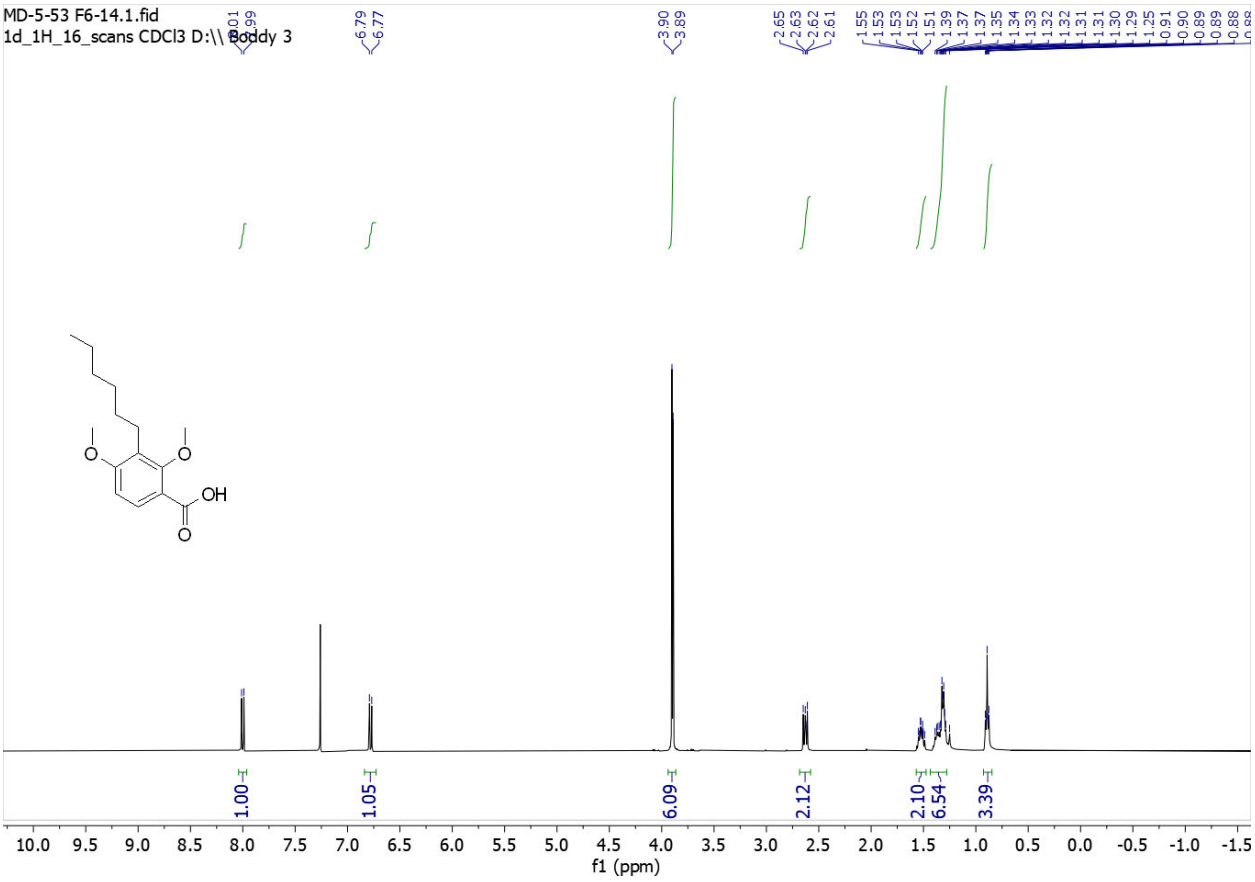

^{1}H NMR (400 MHz, $CDCl_3$) of **10**

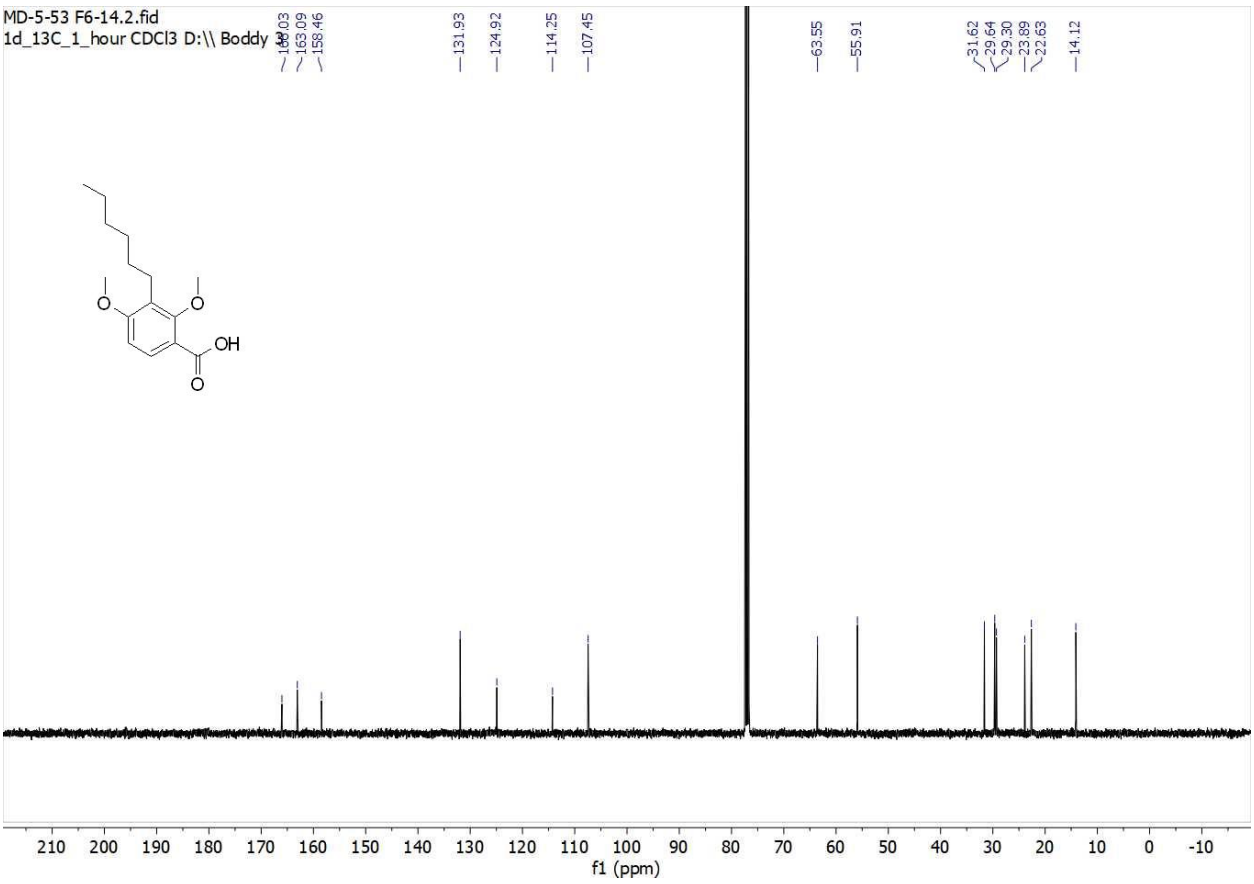

$^{13}C\{^{1}H\}$ NMR (100 MHz, $CDCl_3$) of **10**

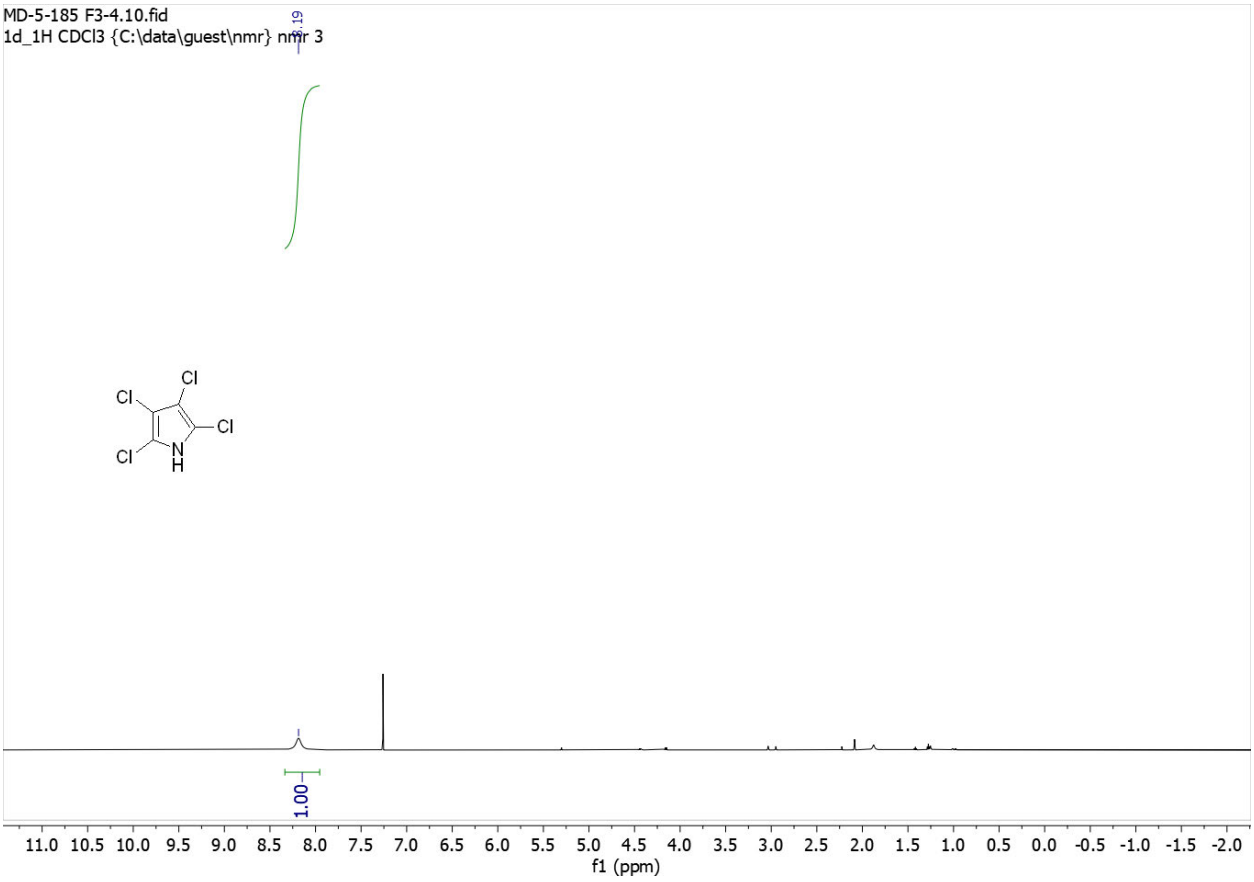

^{1}H NMR (600 MHz, $CDCl_3$) of **11**

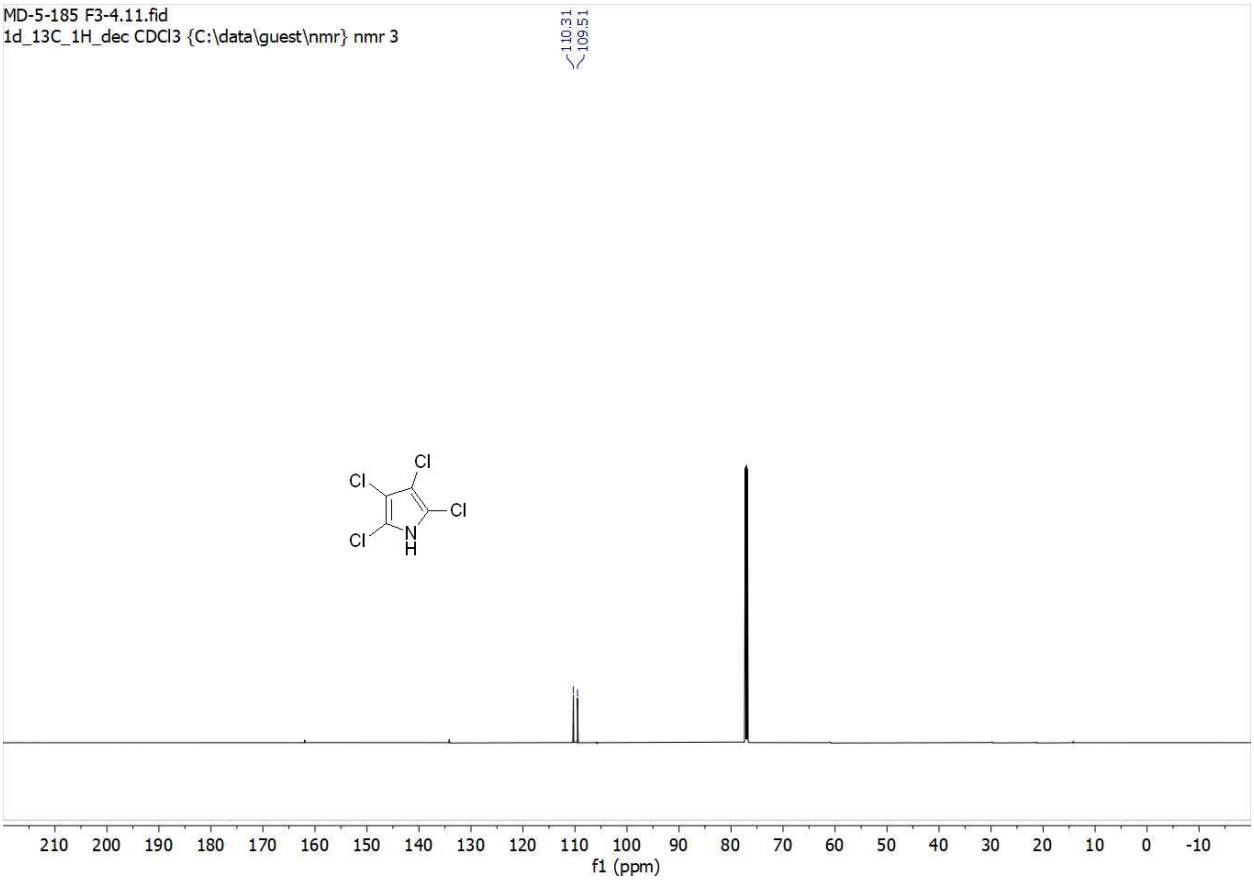

$^{13}C\{^{1}H\}$ NMR (150 MHz, $CDCl_3$) of **11**

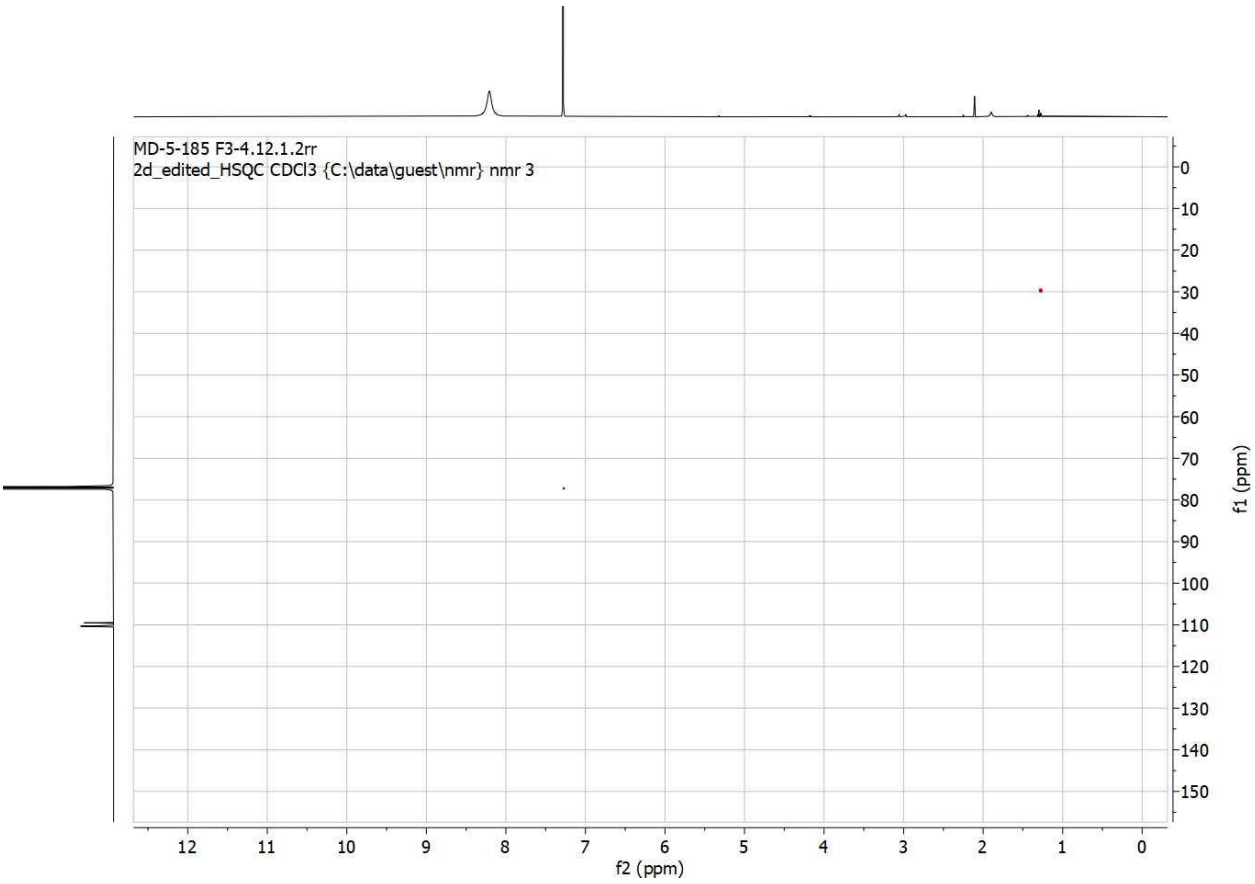
MD-5-185 F3-4.12.1.2rr
2d_edited_HSQC CDCl3 {C:\data\guest\nmr} nmr 3
f2 (ppm)
f1 (ppm)

HSQC of **11**

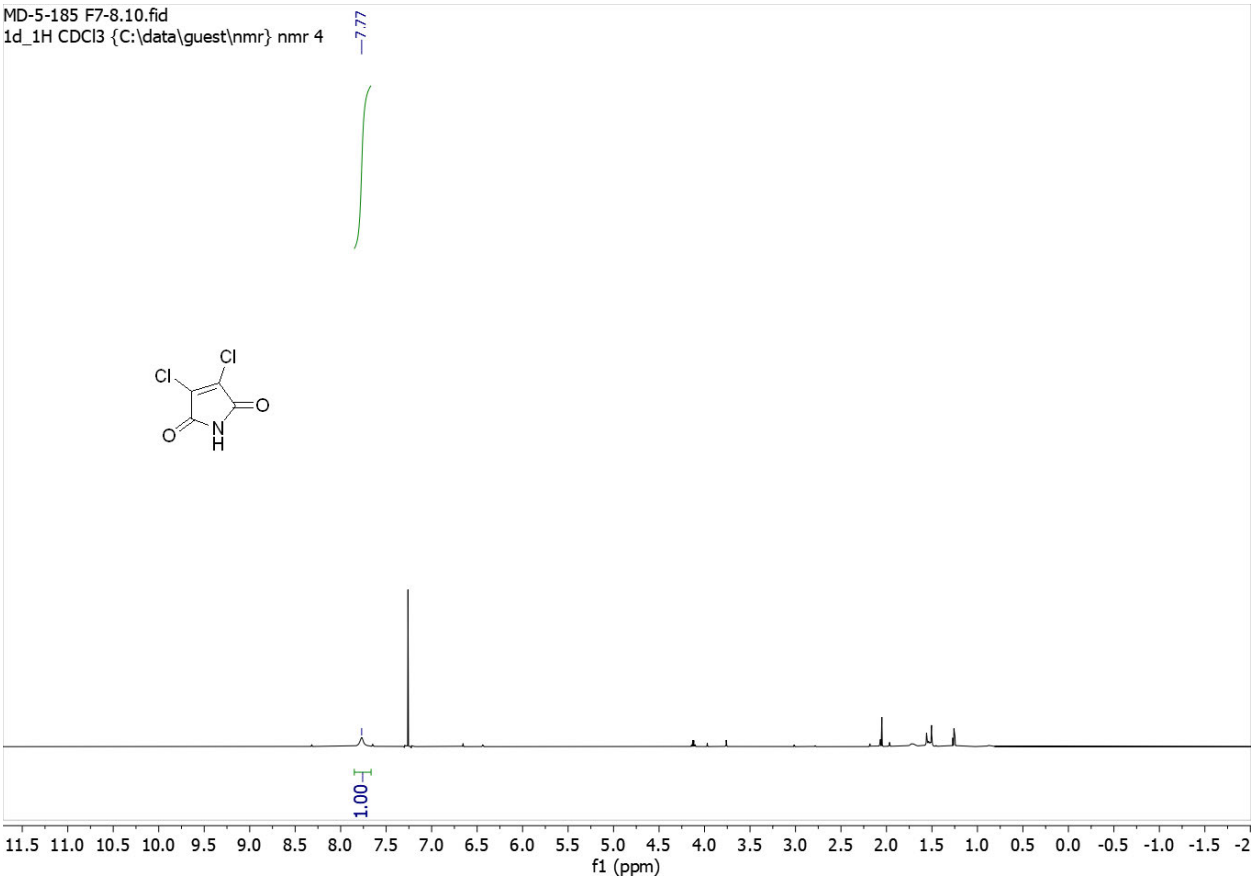

^{1}H NMR (400 MHz, $CDCl_3$) of **12**

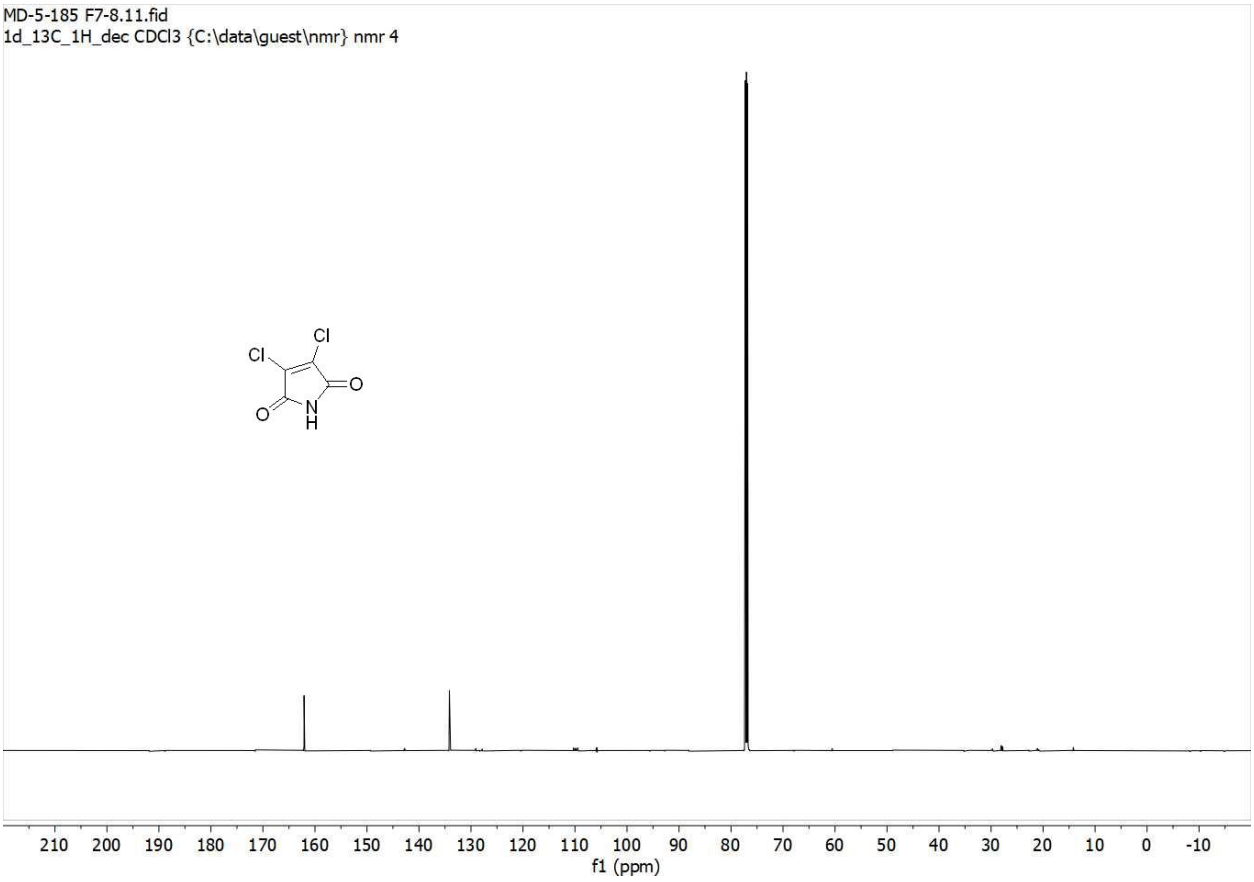

$^{13}C\{^{1}H\}$ NMR (100 MHz, $CDCl_3$) of **12**

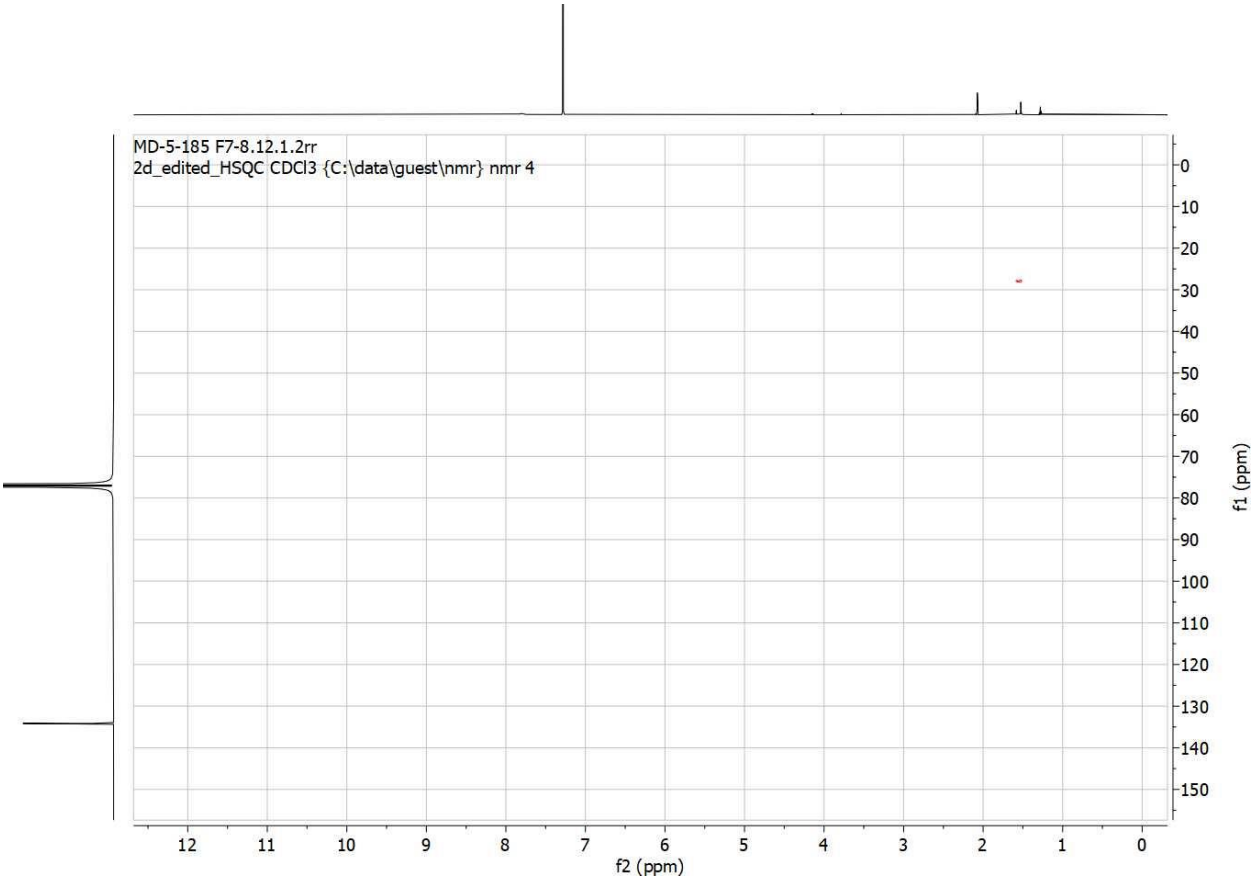
MD-5-185 F7-8.12.1.2rr
2d_edited_HSQC CDCl3 {C:\data\guest\nmr} nmr 4
f2 (ppm)
f1 (ppm)

HSQC of **12**

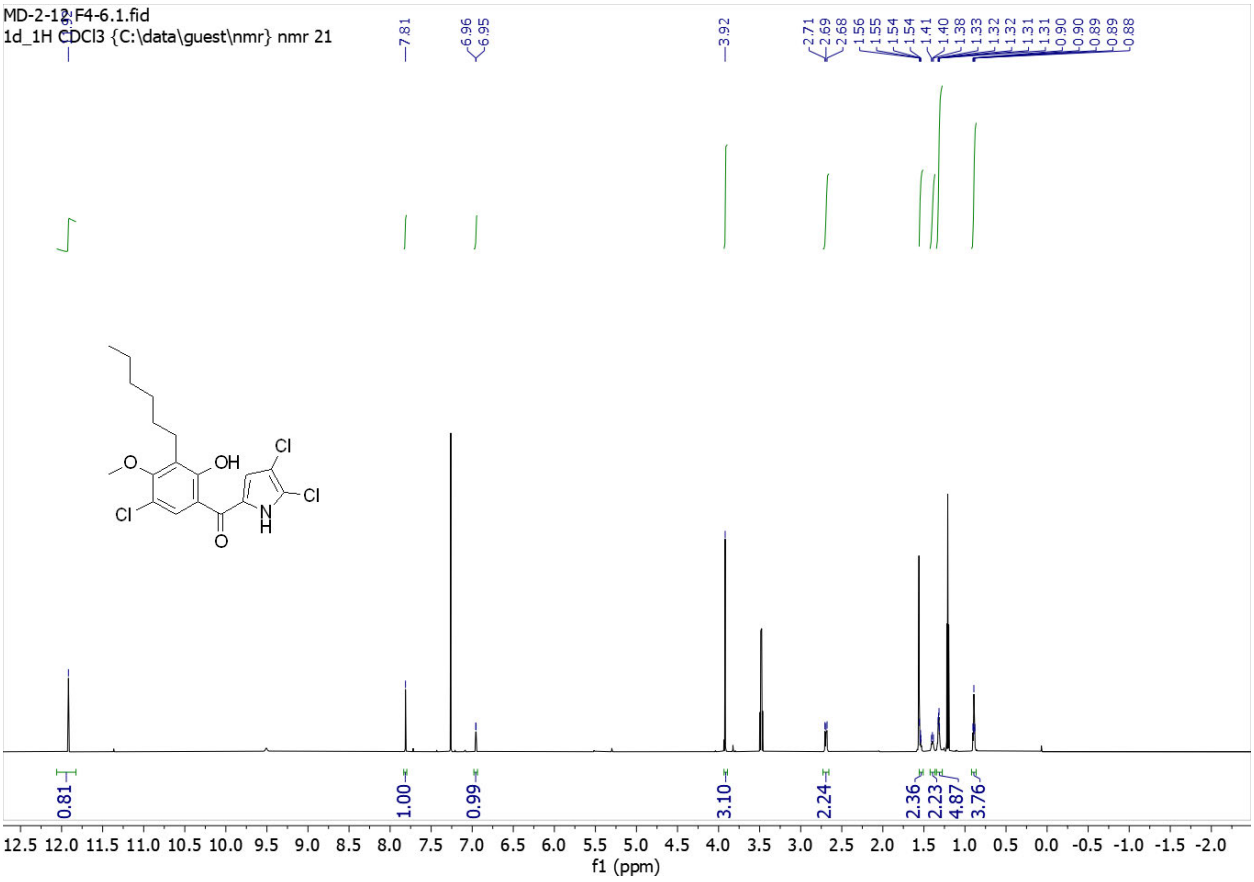

^{1}H NMR (600 MHz, $CDCl_3$) of **13**

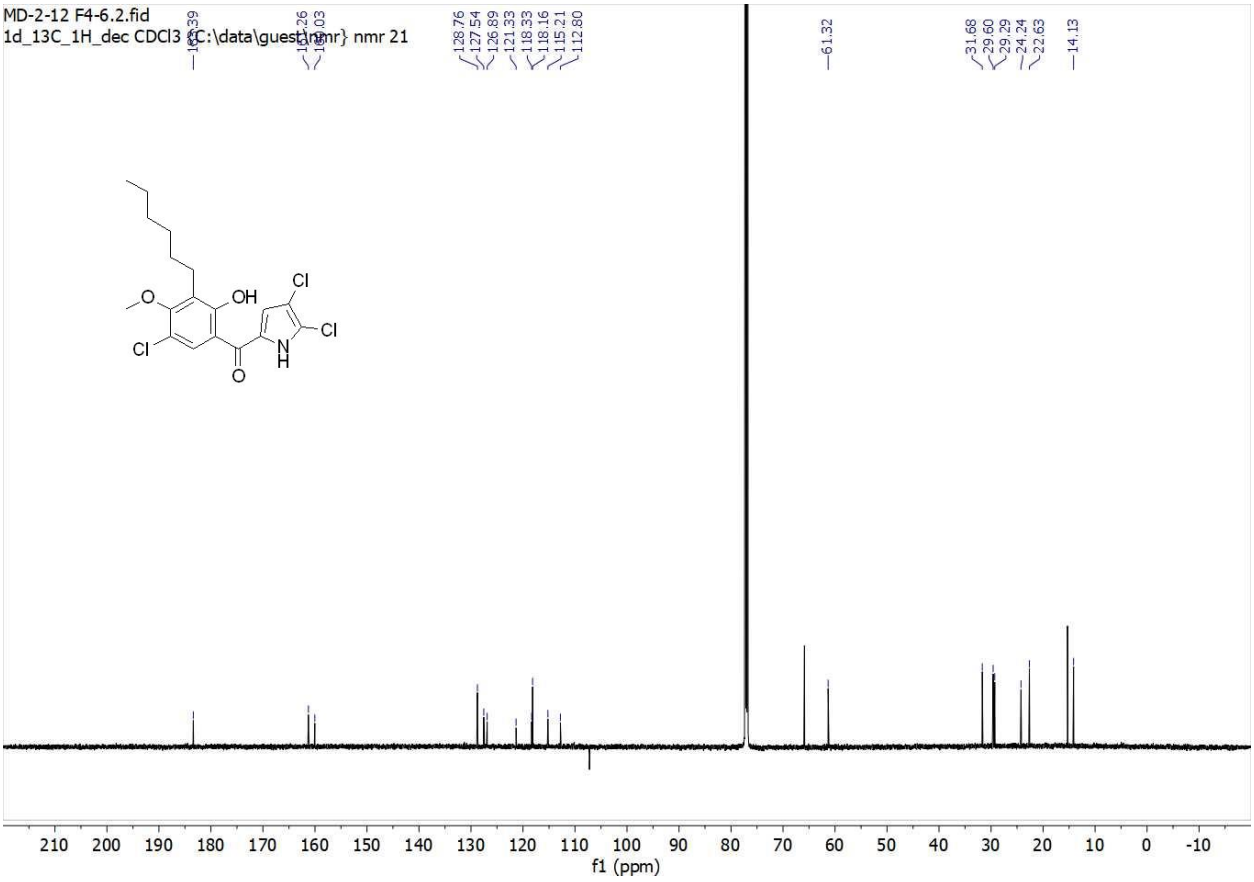

$^{13}C\{^{1}H\}$ NMR (150 MHz, $CDCl_3$) of **13**

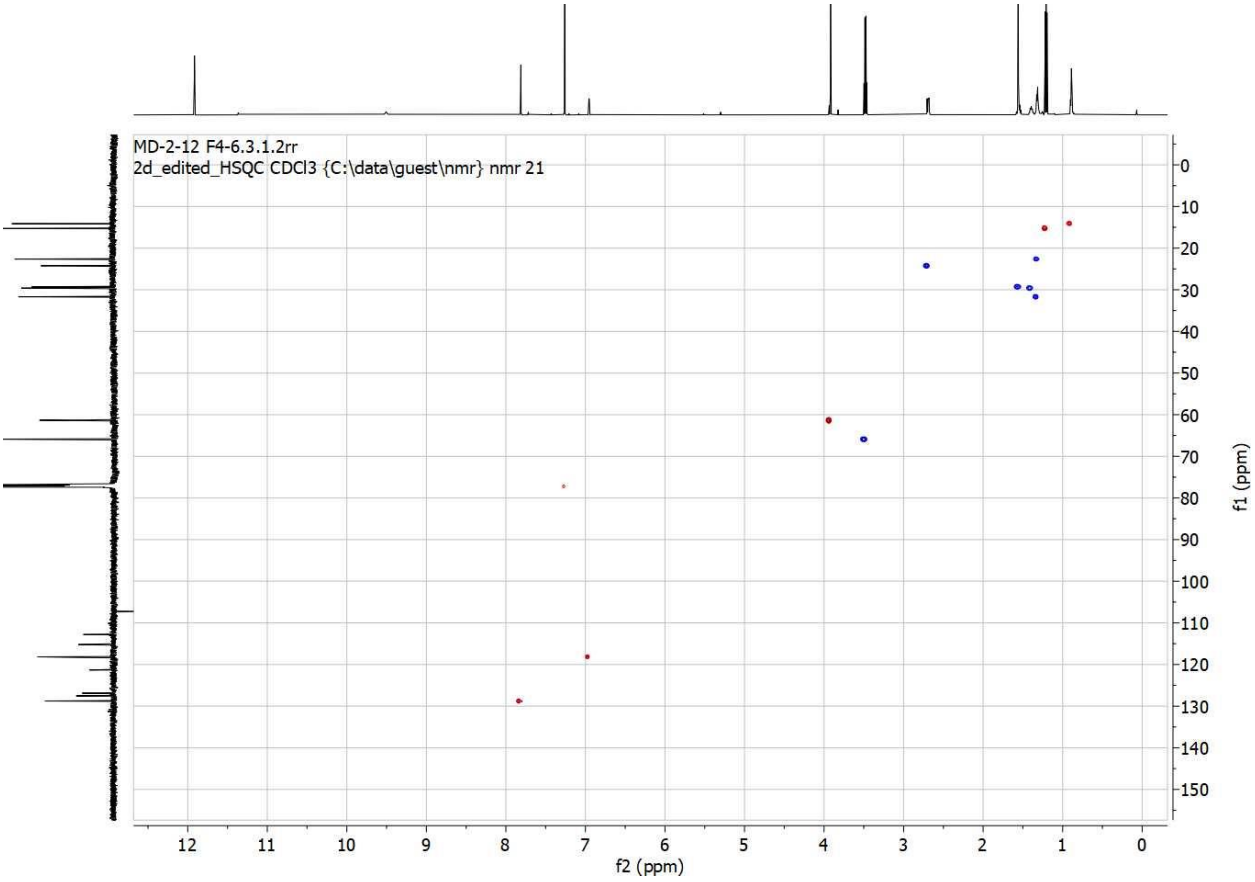
MD-2-12 F4-6.3.1.2rr
2d_edited_HSQC CDCl3 {C:\data\guest\nmr} nmr 21
f2 (ppm)
f1 (ppm)

HSQC of **13**

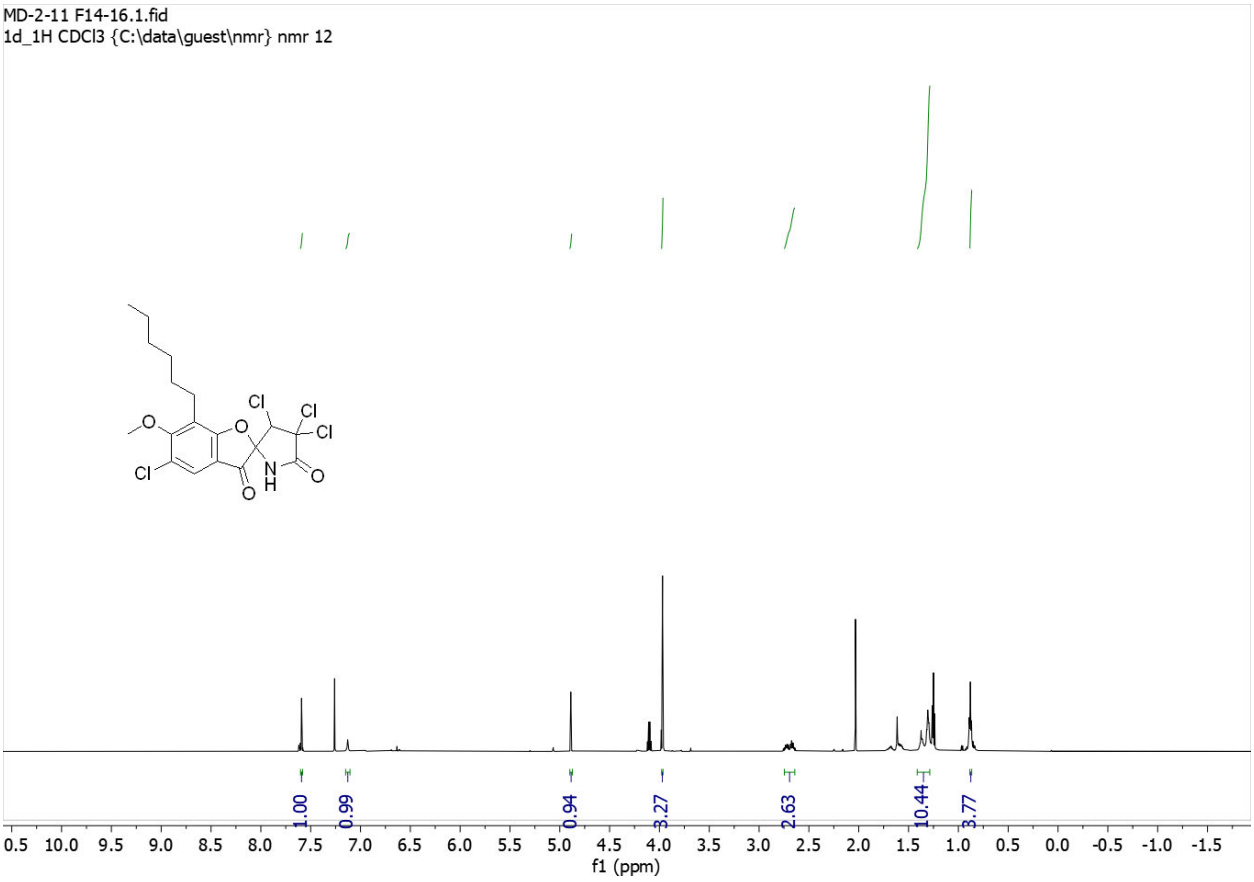

^{1}H NMR (600 MHz, $CDCl_3$) of **14**

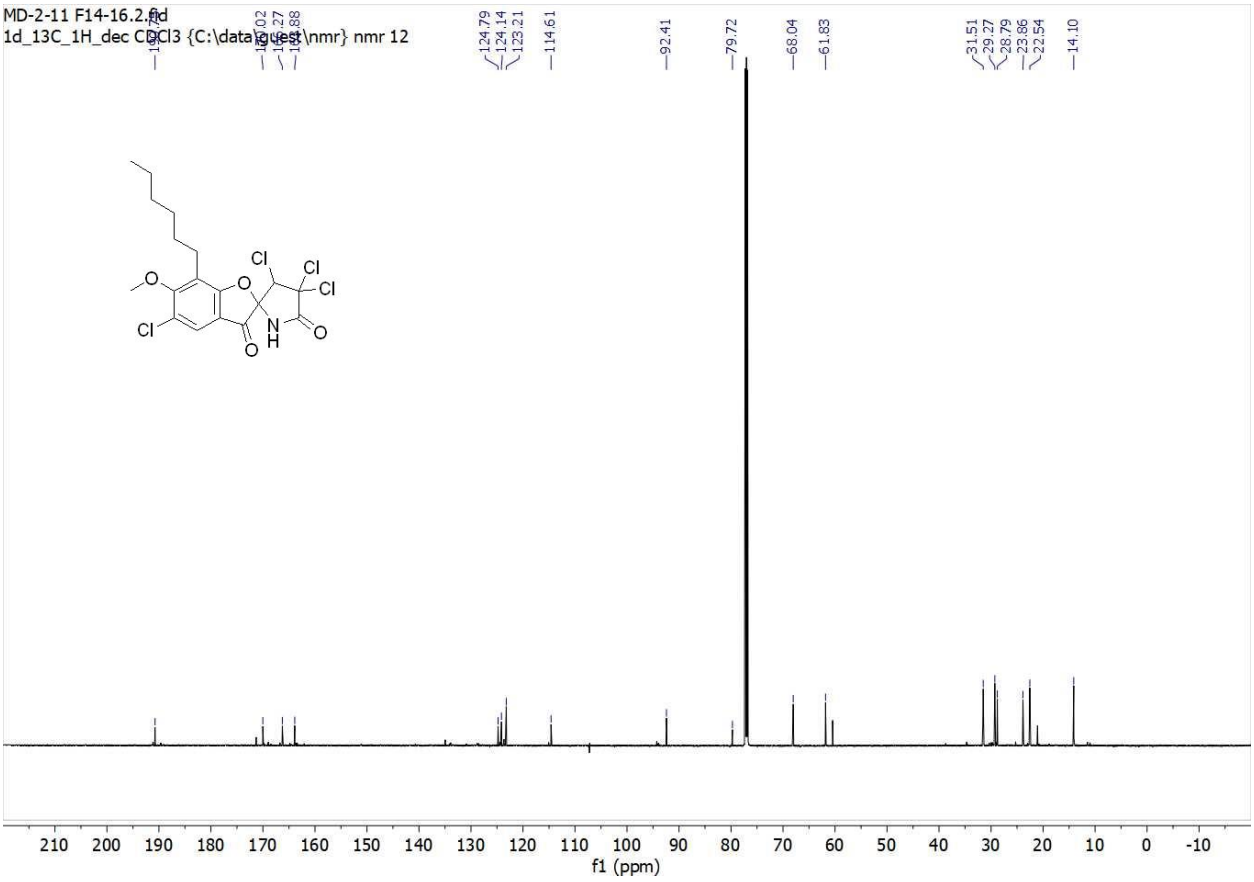

$^{13}C\{^{1}H\}$ NMR (150 MHz, $CDCl_3$) of **14**

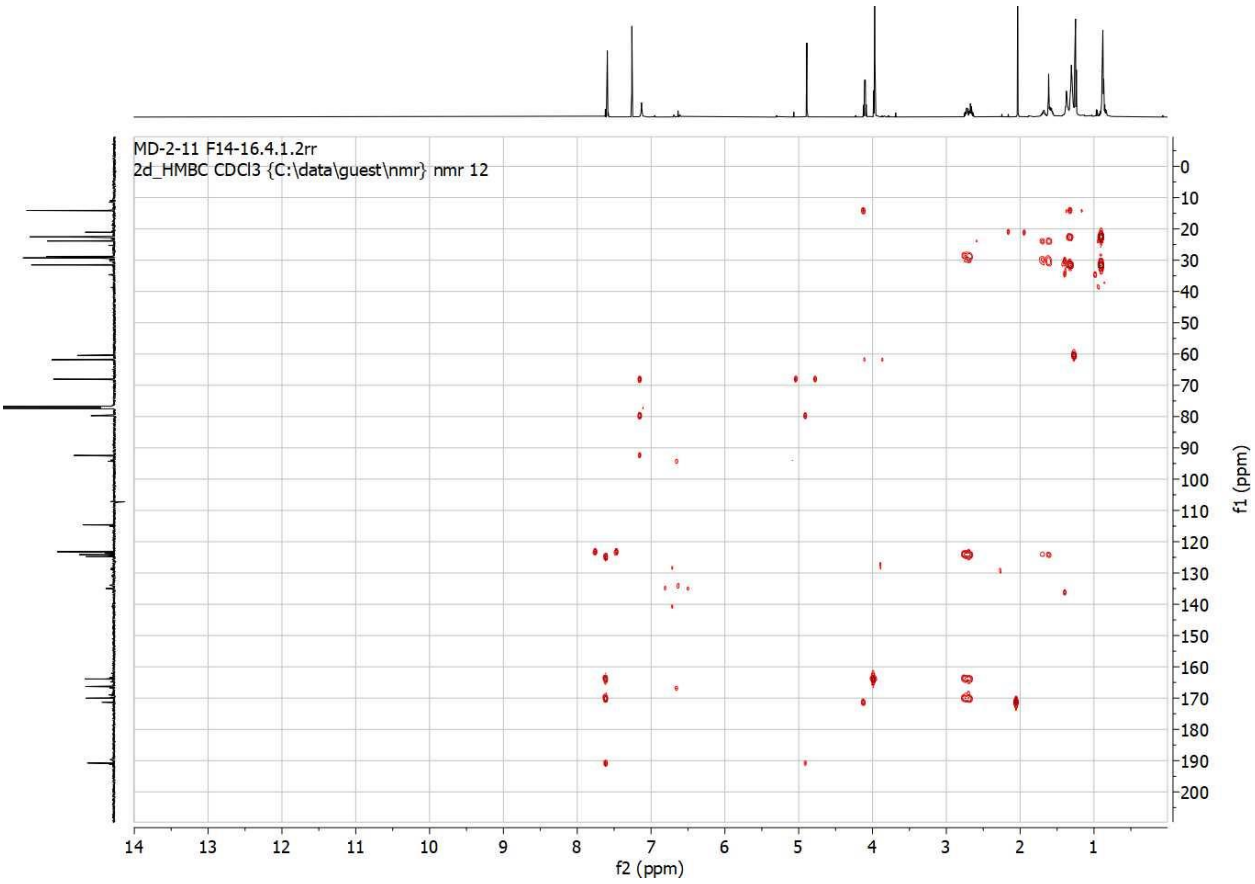
MD-2-11 F14-16.4.1.2rr
2d_HMBC CDCl3 {C:\data\guest\nmr} nmr 12
f2 (ppm)
f1 (ppm)

HMBC of **14**

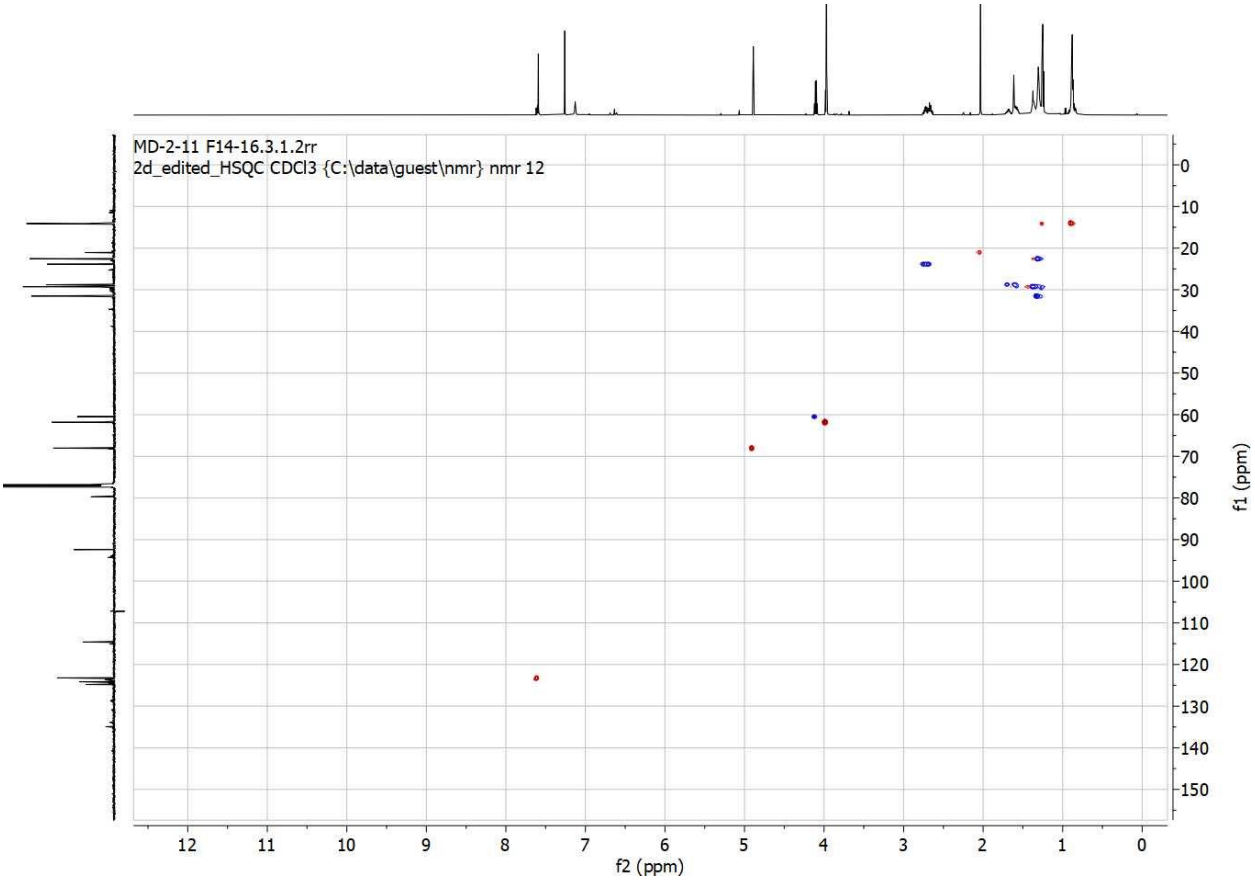
MD-2-11 F14-16.3.1.2rr
2d_edited_HSQC CDCl3 {C:\data\guest\nmr} nmr 12
f2 (ppm)
f1 (ppm)

HSQC of **14**

Section 4. Copies of ^{1}H and ^{13}C spectra - G) Compounds **SI6,SI7,SI8**

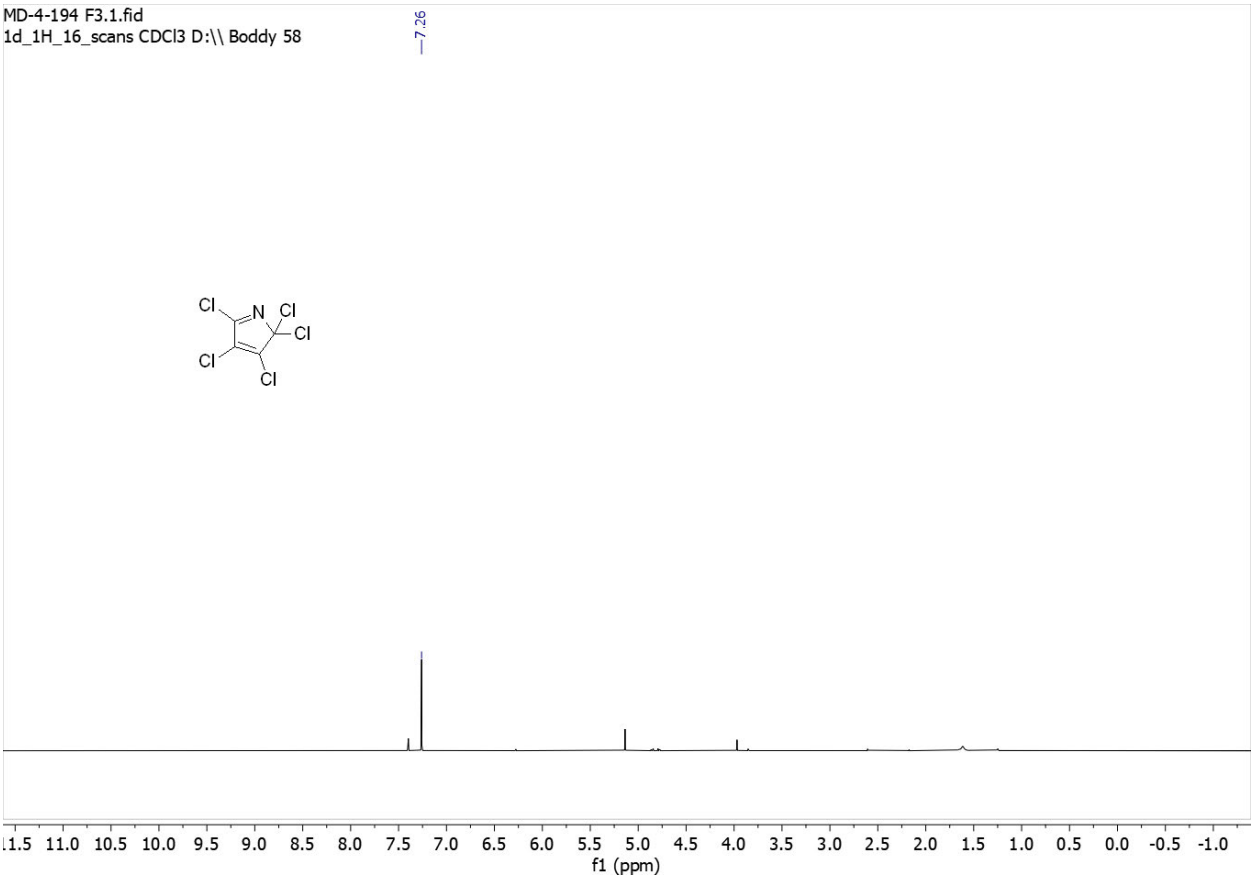

^{1}H NMR (400 MHz, $CDCl_3$) of **SI6**

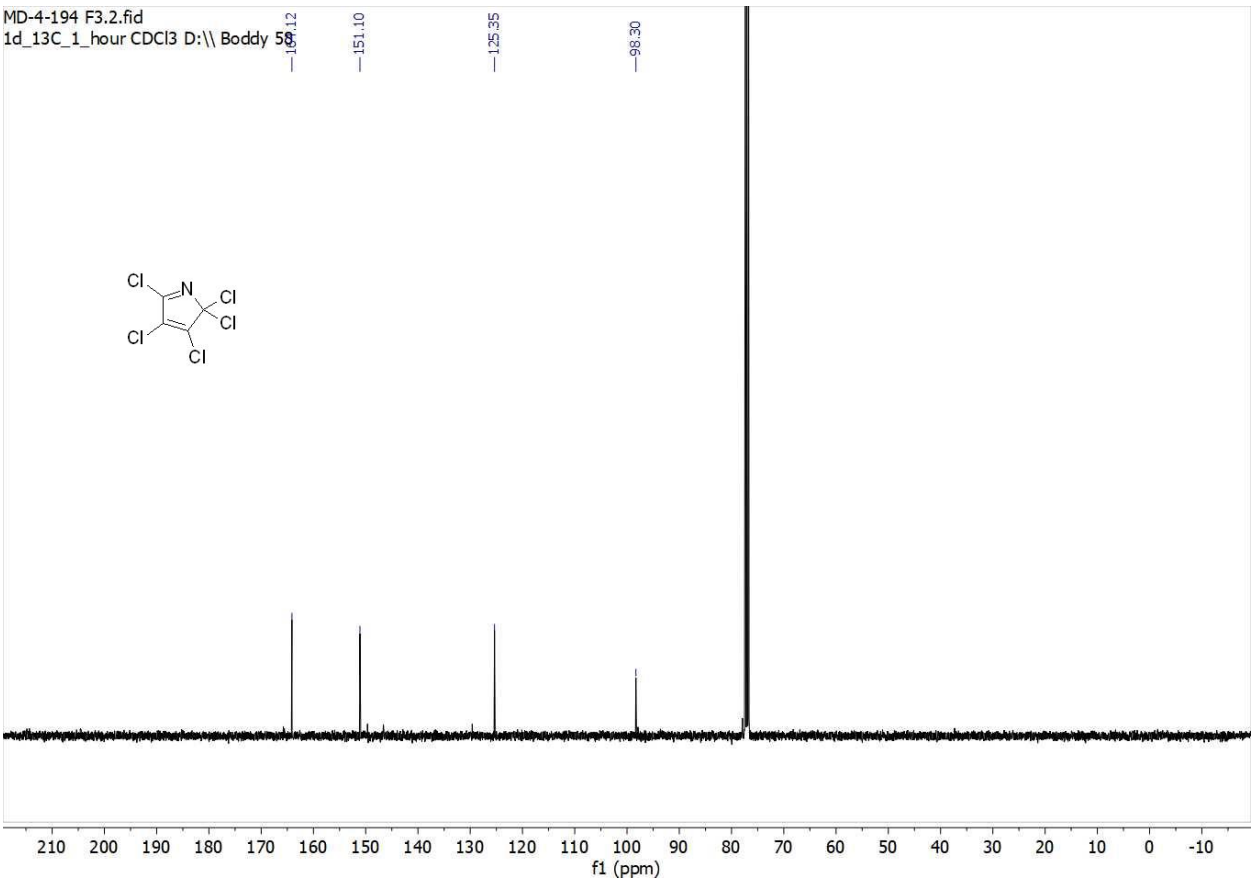

$^{13}C\{^{1}H\}$ NMR (100 MHz, $CDCl_3$) of **SI6**

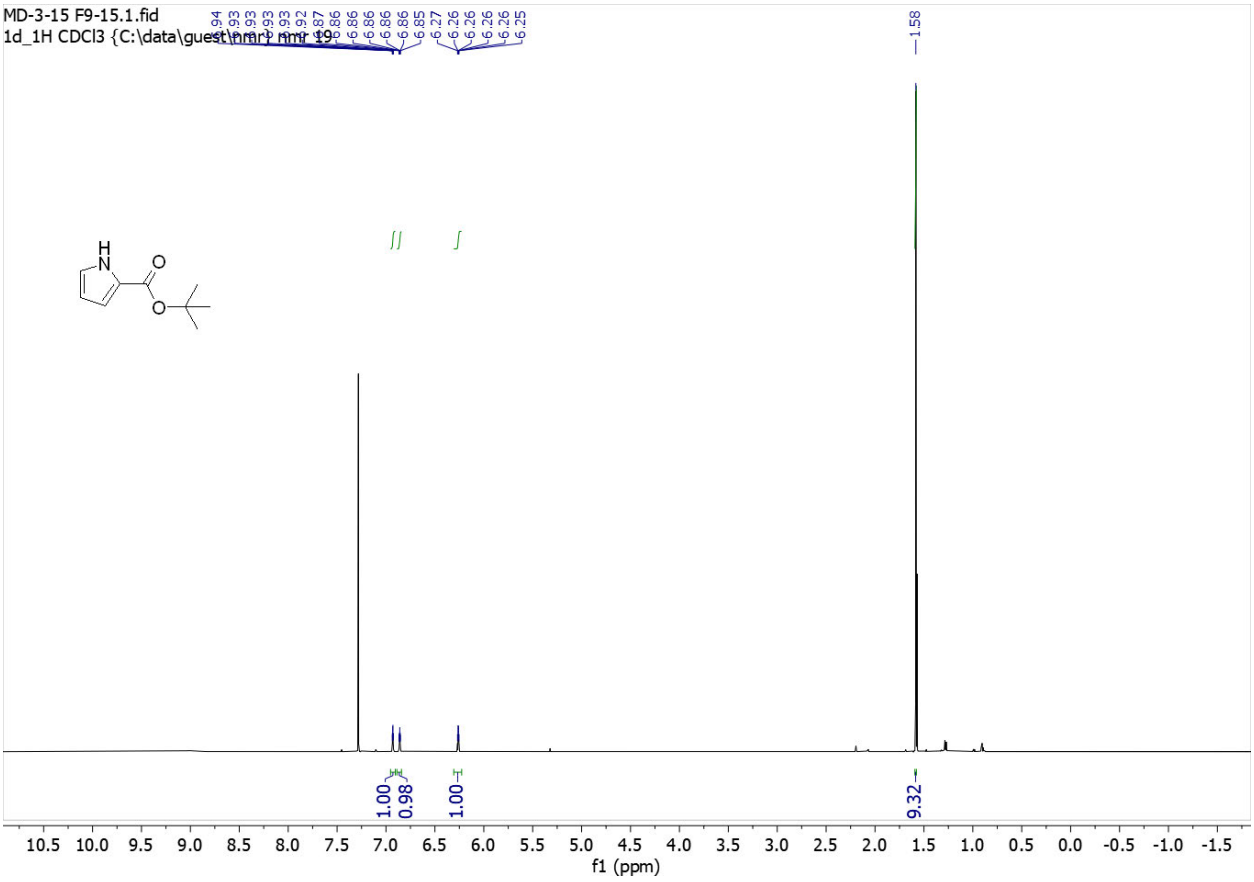

^{1}H NMR (400 MHz, $CDCl_3$) of **SI7**

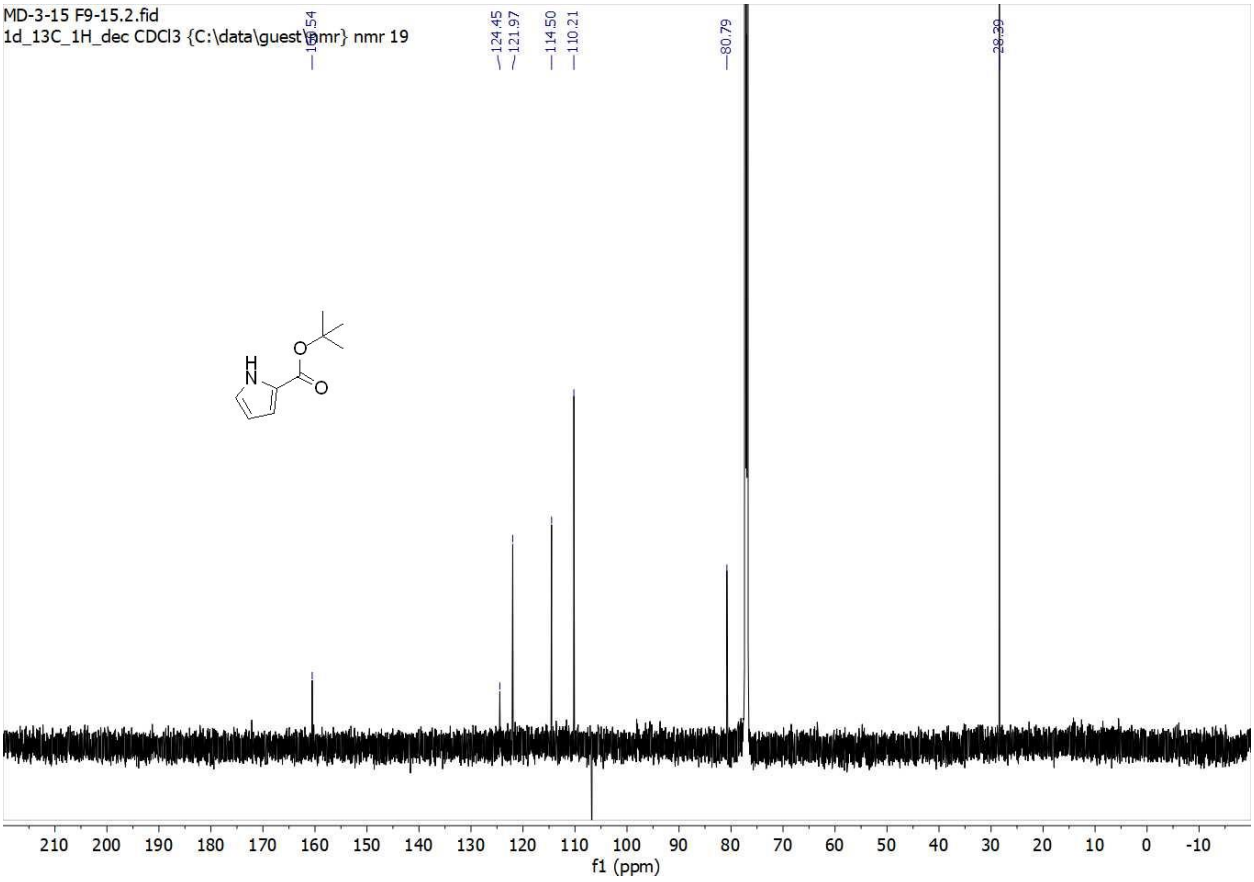

$^{13}C\{^{1}H\}$ NMR (100 MHz, $CDCl_3$) of **SI7**

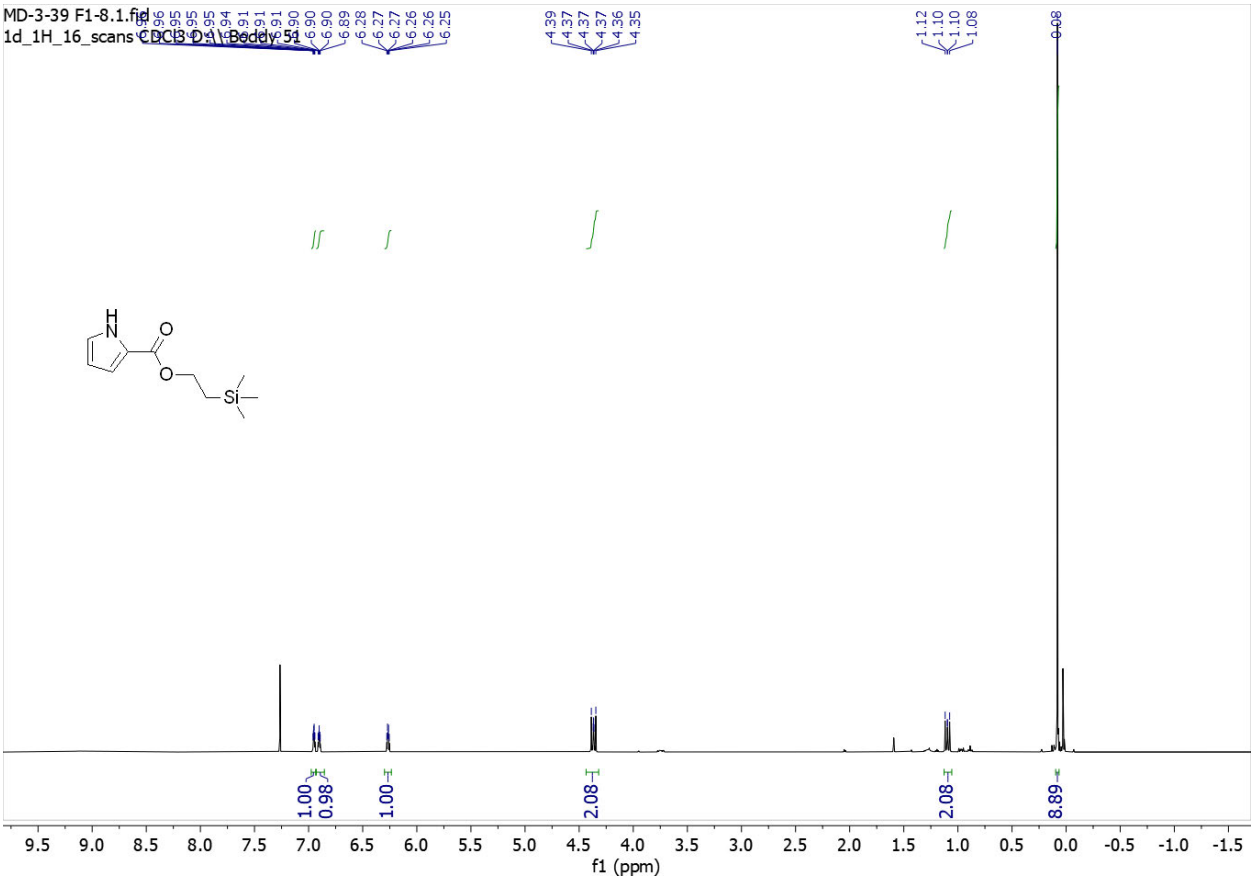

^{1}H NMR (400 MHz, $CDCl_3$) of **SI8**

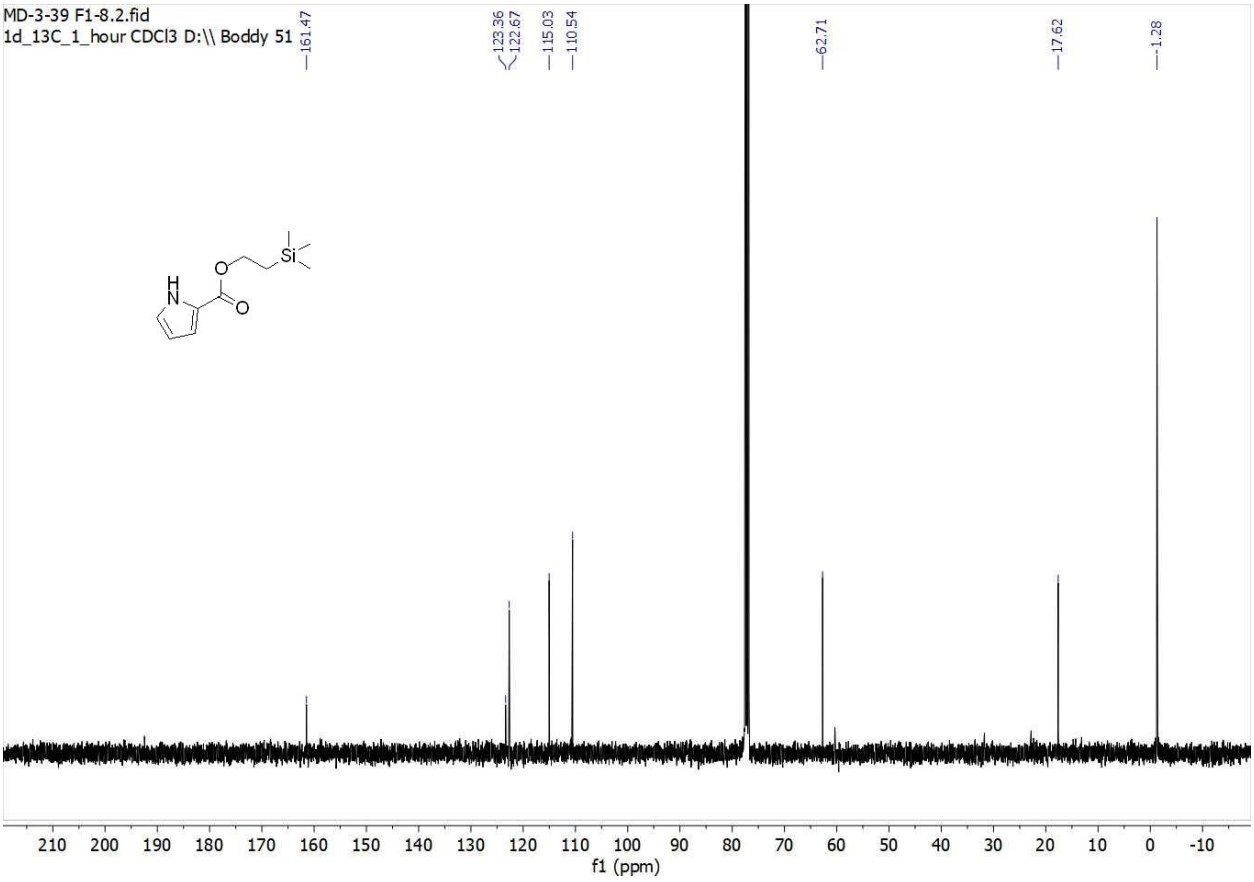

$^{13}C\{^{1}H\}$ NMR (100 MHz, $CDCl_3$) of **SI8**

References

(1) Pilevar, A.; Hosseini, A.; Šekutor, M.; Hausmann, H.; Becker, J.; Turke, K.; Schreiner, P. R. Tuning the Reactivity of Peroxo Anhydrides for Aromatic C-H Bond Oxidation. *J. Org. Chem.* **2018**, *83* (17), 10070–10079.

(2) Daniels, P. H.; Wong, J. L.; Atwood, J. L.; Canada, L. G.; Rogers, R. D. Unreactive 1-Azadiene and Reactive 2-Azadiene in Diels-Alder Reaction of Pentachloroazacyclopentadienes. *J. Org. Chem.* **1980**, *45* (3), 435–440.

(3) Liu, Y.; Lindsey, J. S. Northern-Southern Route to Synthetic Bacteriochlorins. *J. Org. Chem.* **2016**, *81* (23), 11882–11897.

(4) Reinus, B. J.; Kerwin, S. M. A Copper-Catalyzed N-Alkynylation Route to 2-Substituted N-Alkynyl Pyrroles and Their Cyclization into Pyrrolo[2,1-c]oxazin-1-ones: A Formal Total Synthesis of Peramine. *Synth.* **2017**, *49* (11), 2544.

Chapter 5: Conclusions and future directions

5.1 Overview

Development of antibiotics with novel mechanisms of action that are effective against drug resistant Gram-positive bacteria is a major unmet challenge[1–4]. My thesis work aims to address this challenge. Chapter 1 reviews the discovery, activity, initial SAR, pharmacological evaluation, mechanism of actions and the total synthesis of armeniaspirol[5–10]. Chapter 2 presents the first comprehensive medicinal chemistry study of fourteen new analogues for antibiotic activity against MRSA and VRE. This study shows that an increase in potency against both AAA+ proteases ClpXP and ClpYQ is required for an increase in antibiotic activity in cells and new analogues with 8-fold increase in potency were discovered[11]. Chapter 3 establishes that armeniaspirols exhibit a dual mechanism of action, which includes disruption of the $\Delta\Psi$ component of the PMF rather than the ΔpH[12], correcting the current literature[6] on the armeniaspirol compounds. We show that disruption of $\Delta\Psi$ of the PMF is necessary for antibiotic activity but is not a standalone mechanism for antibiotic activity. We postulate that the reduction of membrane potential could synergize with inhibition of these ATP dependent cellular targets ClpXP and ClpYQ as discussed *vide infra*. Chapter 4 details and characterizes the oxidative chlorination of pyrrole-2-carboxylate derivatives. This transformation rapidly generates the α,β-dichloro-α,β-unsaturated lactam functionality in armeniaspirol. Using the product of methyl *N*-methyl pyrrole-2-carboxylate oxidation, we attempted to access the natural product. Our efforts were derailed by an unanticipated rearrangement leading to a constitutional isomer, pseudoarmeniaspirol A[13].

5.2 State of armeniaspirol antibiotic development and outlook

Continued structure optimization in antibiotics has led to improved clinical candidates as seen in the development of penicillin analogues resulting in dicloxacillin[14] (and more recently piperacillin[15]). From the first generation of armeniaspirol analogues, the benzyl derivatives displayed 8-fold improvement in antibiotic activity against MRSA with roughly 20-fold improvement in K_i of ClpYQ. This spurred us to determine if we could continue to improve potency by generating analogues with more balanced activity at both protein targets ClpXP and ClpYQ and sufficient disruption of $\Delta\Psi$ to potentiate activity and limit emergence of resistance[11]. A second generation set of analogues of armeniaspirol were thus designed to further explore chemical space around the *N*-benzyl analogues that had shown highly potent (nM) K_i for ClpYQ. Data from our first-generation analogues also suggested that increased *N*-alkyl character led to increased ClpXP inhibition. Thus, we modified the chain length between the amide *N* and the phenyl ring and introduced branched alkyl chains into this second generation series of unpublished analogues. We expect that this will increase potency at both ClpXP and ClpYQ. A second aim of the study was to have access to a range of benzyls with varying substitution patterns that could potentially access new binding interactions with the targets as well as improve pharmacokinetic properties.

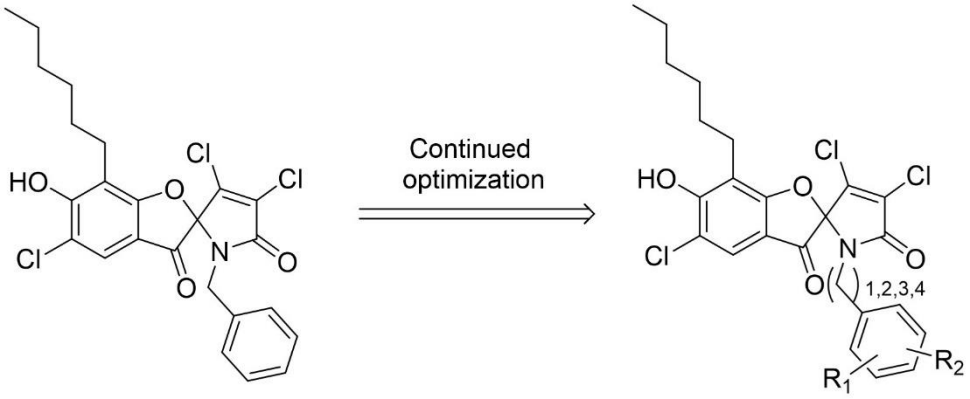

Figure 5.1 Design of second-generation aryl analogues of armeniaspirol

From preliminary MIC screens, the second-generation analogues yielded many new active compounds against MRSA. The next logical step in this follow up study would be to evaluate the activity of these analogues against the intracellular biochemical targets, ClpYQ and ClpXP and to characterize their perturbation of $\Delta\Psi$. Future directions would entail preliminary pharmacokinetics and toxicity to advance the armeniaspirols as therapeutic agents. A Liver microsomal assay should be conducted to give insights into stability as well as metabolic hot spots on the scaffold[16]. Using a PAMPA assay, the compounds should be assessed for transport across cell membranes as well as the GI tract. Recently our group used an *in vivo* activity in *Galleria mellonella* to study Gram-positive and Gram-negative bacterial infections. *Galleria mellonella* possess an innate immune response that shows similarities with that of vertebrates[17]. Developing a *Bacillus subtilis* or *S. aureus* infection model in *G. mellonella* will thus provide an ideal setting for the initial evaluation of antibiotic ability of these armeniaspirol analogues *in vivo*.

Compounds that disrupt membrane potential can often be associated with mitochondrial dysfunction in humans. Armeniaspirol and its analogues all show the ability to disrupt the

electrical potential of Gram-positive bacteria and consistent with this, at high doses in a mouse model, some cardiac side effect are observed[12,18,19]. We have begun investigating the effect of our analogues on mitochondrial function in the mouse myoblast cell line C2C12 with Prof. Harper in the Faculty of Medicine at the University of Ottawa. Preliminary data shows that the mitochondrial potential is rapidly uncoupled (disrupted) by treatment with Cl-armeniaspirol. Excitingly we have identified an analogue with potent antibiotic activity that does not rapidly uncouple mitochondria. Future work includes evaluating additional compounds and new analogues for their uncoupling of mitochondrial electron transport and oxidative phosphorylation as well as correlating reduced uncoupling with cardiotoxicity in a human induced pluripotent stem-derived cardiomyocytes microelectrode array-based assay.

With improved druglike properties in mind, future studies should focus on developing armeniaspirol analogues with lowered clogP values. The most potent analogues have clogP values of approximately 7 and Cl-armeniaspirol clogP is approximately 5. This is outside of the ideal range for developing orally bioavailable drugs. High clogP values are associated with problems including increased protein bound drug, faster metabolism and lower solubility, all of which impact a drug candidate's ability to move forward into the clinic[20]. Analogues that could be developed should include additional heteroatoms as well as bioisosteres to improve drug like properties (Figure 5.2).

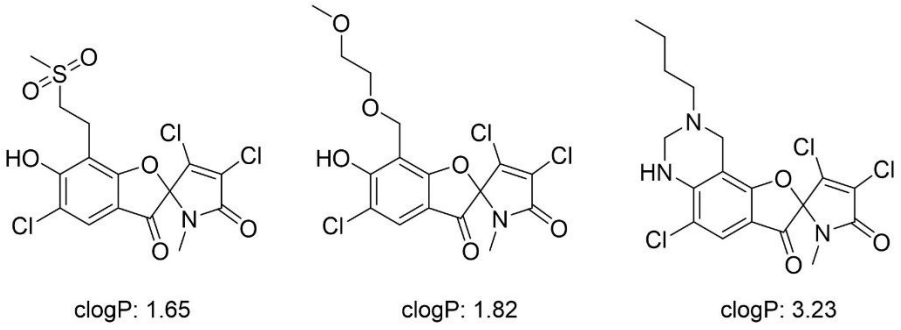

Figure 5.2 Potential future analogues of armeniaspirol with improved clogP values

5.2 Total synthesis outlook

As briefly discussed in chapter 4, many efforts had been attempted to access the complex scaffold of armeniaspirol, tThe majority centering around early-stage chlorination followed by intramolecular formation of the central ring system. For example, in the synthesis of pseudoarmeniaspirol, fragment coupling via *N*,*O*-ketal formation between a phenol and the chlorinated pyrrole carboxylic acid derivative was used with a Friedel-Crafts acylation envisioned for the annulation step leading to the central carbonyl. A particularly appealing alternative strategy for formation of the central ring is the direct oxidation of pyrrole with molecular oxygen. This would generate a reactive intermediate that could be trapped by the neighbouring phenol *in situ* yielding the lactam and *N*,*O*-ketal in one step. This strategy drew on precedent from Boger and Wasserman's work using singlet oxygen to oxidize bipyrrole compounds to α,β-unsaturated lactams and culminated in the total synthesis of D,L- and meso-isochrysohermidin (figure 5.3)[21,22].

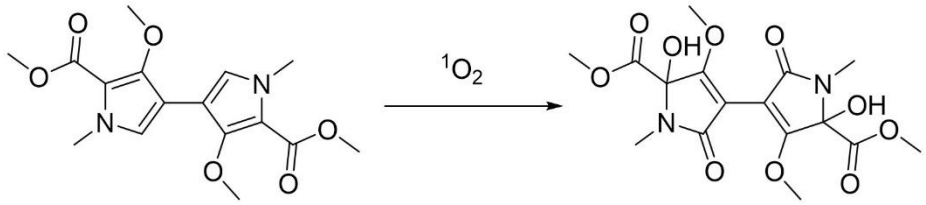

Figure 5.3 Boger and Wasserman's oxidation of pyrrole using singlet oxygen.

We were readily able to generate the inverse electron demand [4+2] substrate (Figure 5.4) to test this strategy. Treating the pyrrole with singlet oxygen generated from irradiation in the presence of the sensitizer Rose Bengal yielded the desired pyrrole oxidation as well as the cyclization forming the *N*,*O* ketal successfully, thus constructing the skeleton or armeniaspirol (Figure 5.4)[23]. However, it must be noted the reaction was hampered by low yields, inconsistent reaction times, and poor reproducibility. This is likely due to limited light penetration, causing low amounts of singlet oxygen particularly upon scaling up the reaction.

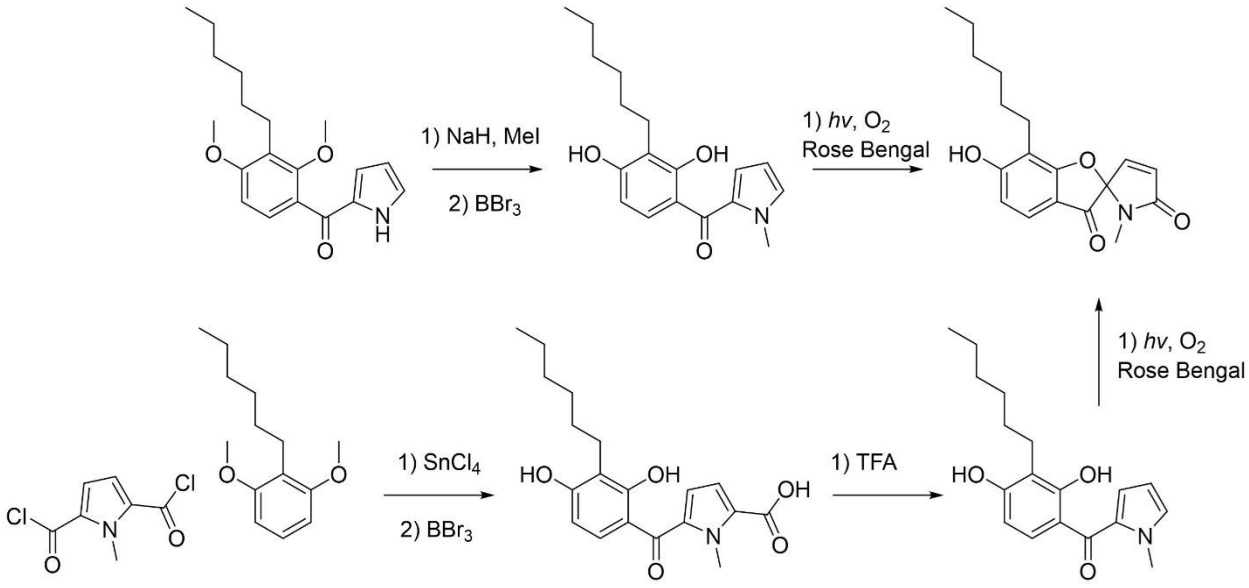

Figure 5.4 Synthesis of des-chloroarmeniaspirol using singlet oxygen

With the desired skeleton formed, we turned our attention to synthesizing 3,4 dichloro-pyrrole compounds to have the correct functionalization to access the natural product. The 3 and 4 positions of pyrroles are notoriously difficult to selectively chlorinate due greatly reduced nucleophilicity compared to 2 and 5 positions[23–26]. Additionally, 3,4-dichlorinated pyrroles, when lacking 2,5 substituents, are also prone to rapid degradation. Using aggressive chlorination reaction conditions[27], we were able to access a suitable substrate in *N*-methyl-2,5-diethyl ester-3,4-dichloro pyrrole, which we envisioned could be carried forward to the key [4+2] reaction (Figure 5.4). In a model system lacking the two chlorines, we were able to easily couple *N*-methyl-2,5-dicarboxylate pyrrole to the left side of armeniaspirol in a Friedel-Crafts acylation. This product could then be decarboxylated with TFA to yield the intermediate for the key [4+2] reaction (Figure 5.4). However, with the dichlorinated pyrrole, *N*-methyl-2,5-dicarboxylate-3,4-chloro pyrrole, this chemistry proved much more challenging. At low temperatures the hydrolysis of *N*-methyl-2,5-diethyl ester-3,4-chloro pyrrole yielded the desired diacid, which could be converted into the acid chloride for the Friedel-Crafts acylation. After rigorous screening of Lewis acids and reaction conditions, no Friedel-Crafts acylation products could be observed.

With this failed route and excess *N*-methyl-2,5-diethyl ester-3,4 chloro pyrrole in hand, we turned our attention to using the pyrrole moiety as the nucleophile in the Friedel-Crafts acylation and the left side correctly functionalized with an activated carbonyl compound as the electrophile. At elevated temperatures under basic conditions *N*-methyl-2,5-diethyl ester-3,4 dichloro pyrrole decarboxylated to yield the *N*-methyl-3,4 dichloro pyrrole[27]. This intermediate was again subjected to a screen of Lewis acid coupling conditions. Frustratingly, no reaction

conditions yielded Friedel-Crafts acylation products. Using strong bases to yield activated 2-position pyrroles were attempted to add into corresponding aryl aldehydes; however, no addition was observed (Figure 5.5).

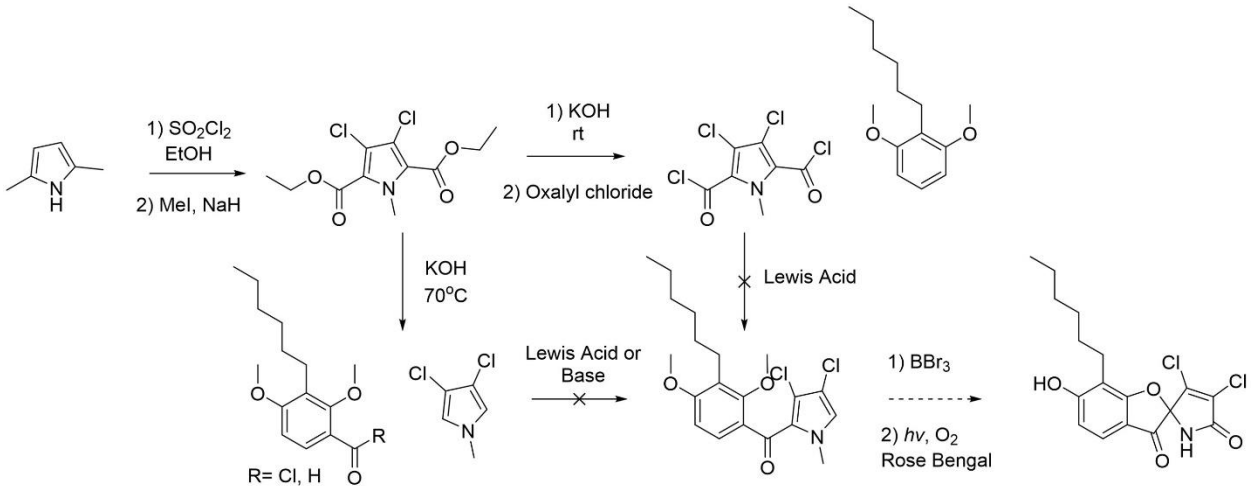

Figure 5.5 Attempts using 3,4 chlorinated pyrroles to access armeniaspirol.

The efforts toward the total synthesis of armeniaspirol have highlighted many synthetic challenges associated with the reactivity surrounding this scaffold, the first being the central spirocyclic *N,O*-ketal contained in armeniaspirol has remained very challenging to forge. All efforts relied on trapping a highly reactive oxidized pyrrole intermediate, which often resulted in degradation. Additionally, the reactivity of pyrroles in electrophilic aromatic substitution (EAS) reactions provided unexpected challenges as slight increases in temperature or reaction concentrations resulted in over substitution and degradation. The failed Friedel-Crafts reaction of the 3,4 dichlorinated pyrrole species is particularly interesting with the des-chloro compound undergoing smooth acylation. The addition of a slight EWG like Cl could potentially prevent access to the acylium ion for EAS. However, it was unexpected that increased temperatures and strong Lewis acids could not overcome this problem. Although the total synthesis of

armeniaspirol has presented many challenges, it has allowed us to further our understanding of the reactivity of pyrrole and this complex scaffold.

5.3 Perspective on the evolution and genesis of armeniaspirol

The study of evolution has been at the forefront of science since the 19th century when Darwin first wrote *The origin of species.* Evolution focuses on organism fitness with respect to a genotype or to a phenotype. According to Darwin, improved fitness leads to organisms that will leave the most copies of itself in successive generations. Examples of improved fitness leading to organism success has been well documented in evolution studies with some of the most famous examples being bird beaks and human eyes[28,29]. This evolutionary model can also be applied to secondary metabolites. The gene clusters responsible for natural product biosynthesis must be built through improvements to the fitness of the organism. In this light, the biological function of the natural product is presumably a key effector of the improved fitness. For example, the antibiotic activity of armeniaspirol could make the producing organism more fit since it could outcompete other bacteria for the limited resources in its environment.

Natural products are typically biosynthesized through the action of many genes, in some case a dozen or more. The probability of the spontaneous evolution off all dozen genes simultaneously is extremely low, yet with anyone of the genes missing the natural product is not made and the fitness of the organism not improved. Thus how do these complex gene clusters evolve? We propose that our characterization of the activity and mechanisms of action of armeniaspirol, its analogues, and some of its potential biosynthetic precursors sheds some light on this question.

Armeniaspirol is generated biosynthetically from a halogenated pyrrole precursor, which contains a high degree of structural homology to the halopyrrole compounds (Figure 5.6)[9,10]. We synthesized the biosynthetic precursors to armeniaspirol and found that they exhibit potent antibiotic activity against Gram-positive bacteria as well as the ability to disrupt the PMF.

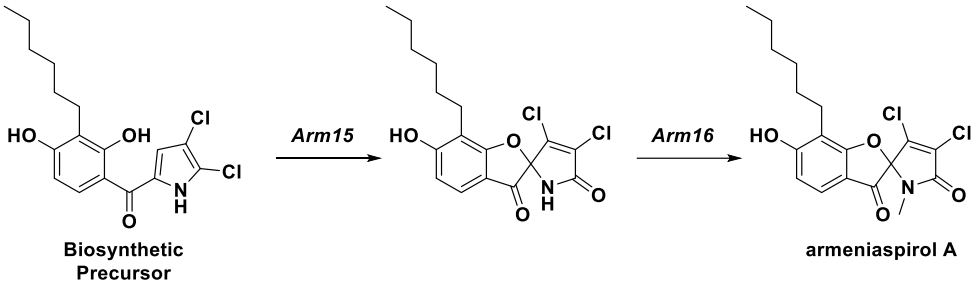

Figure 5.6 Biosynthesis of armeniaspirol containing potent antibiotic precursors.

Intriguingly, they showed no inhibition of either of the protein targets, ClpXP or ClpYQ. From a biosynthesis perspective, this preliminary data gives us insights into how the biosynthetic pathway to armeniaspirol evolved in a stepwise matter. We thus propose that a protoarmeniaspirol biosynthetic gene cluster existed that made a halopyrrole like compound. This compound was antibiotic, though via a different uncharacterized mechanism, providing an increase in fitness to the producing organism. By capturing a flavin monooxygenase capable of forming the *N*,*O*-ketal and a methyltransferase capable of methylating the pyrrole NH, a new compound with a new mechanism of action and potent antibiotic activity could be obtained[30]. Thus the protoarmeniaspirol pathway provides a potential snapshot along the stepwise pathway for the evolution of the current armeniaspirol gene cluster.

When conducting our study into both mechanisms of action of armeniaspirol, we began to contemplate the evolutionary link between armeniaspirol and its biosynthetic precursor. Based

on our hypothesis that armeniaspirol and its precursor had different mechanisms of action, we performed a synergy/antagonism assay with both compounds. Our data showed they were highly synergistic against MRSA. While this was initially surprising; from an evolutionary perspective it was reasonable. Synergy would result in a large increase in fitness since the precursor and product of a biosynthetic pathway could work together. Based on these observations, we suggest that it may be common for mid- to late-stage biosynthetic intermediates to possess different mechanisms of action as compared to the parent natural product and that these mechanisms of action may synergize, increasing the fitness boost as the pathway evolves. Intriguingly, this could be a potential evolutionary mechanism for the multiple mechanism of actions frequently seen in natural product antibiotics.

5.4 Conclusions

Overall, a more thorough SAR and mechanism of action study of armeniaspirol has been completed[11]. Forays into the total synthesis of this complex scaffold as well as reactivity of pyrrole has been further characterized and provides framework for suture chemist to leverage halogenation of pyrroles to make bioactive scaffolds[13]. Further work is needed to further confirm safety, efficacy, and toxicity of armeniaspirol, and new analogues with improved drug like characteristics could be examined. This molecule has provided a tremendous platform to improve my skills as an organic chemist and as a chemical biologist. It provided avenues into studying total synthesis, organic chemistry methodology, and medicinal chemistry.

5.5 References

1. Murray, C. J. Antimicrobial Resistance Collaborators. Global burden of bacterial

antimicrobial resistance in 2019: a systematic analysis. *Lancet* **399**, 629–655 (2022).

2. Miethke M, Pieroni M, Weber T, Brönstrup M, Hammann P, Halby L, Arimondo PB, Glaser P, Aigle B, Bode HB, Moreira R, Li Y, Luzhetskyy A, Medema MH, Pernodet JL, Stadler M, Tormo JR, Genilloud O, Truman AW, Weissman KJ, Takano E, Sabatini S, Stegmann E, Brötz-Oesterhelt H, Wohlleben W, Seemann M, Empting M, Hirsch AKH, Loretz B, Lehr CM, Titz A, Herrmann J, Jaeger T, Alt S, Hesterkamp T, Winterhalter M, Schiefer A, Pfarr K, Hoerauf A, Graz H, Graz M, Lindvall M, Ramurthy S, Karlén A, van Dongen M, Petkovic H, Keller A, Peyrane F, Donadio S, Fraisse L, Piddock LJV, Gilbert IH, Moser HE, Müller R. Towards the sustainable discovery and development of new antibiotics. *Nat. Rev. Chem*. 5 726–749 (2021).
3. de Kraker, M. E. A., Stewardson, A. J. & Harbarth, S. Will 10 Million People Die a Year due to Antimicrobial Resistance by 2050? *PLoS Med.* **13**, S71–S75 (2016).
4. Lee Ventola, C. The Antibiotic Resistance Crisis Part 1: *Causes and Threats*. vol. 40 (2015).
5. Labana, P.; Dornan, M. H.; Lafrenière, M.; Czarny, T. L.; Brown, E. D.; Pezacki, J. P.; Boddy, C. N. Armeniaspirols inhibit the AAA+ proteases ClpXP and ClpYQ leading to cell division arrest in Gram-positive bacteria. *Cell Chem. Biol.* **28**, 1703-1715.e11 (2021).
6. Arisetti N, Fuchs HLS, Coetzee J, Orozco M, Ruppelt D, Bauer A, Heimann D, Kuhnert E, Bhamidimarri SP, Bafna JA, Hinkelmann B, Eckel K, Sieber SA, Müller PP, Herrmann J, Müller R, Winterhalter M, Steinem C, Brönstrup M. Total synthesis and mechanism of action of the antibiotic armeniaspirol A. *Chem. Sci.* **12**, 16023–16034 (2021).
7. Dufour C, Wink J, Kurz M, Kogler H, Olivan H, Sablé S, Heyse W, Gerlitz M, Toti L, Nußer A, Rey A, Couturier C, Bauer A, Brönstrup M.Isolation and structural elucidation

of armeniaspirols A-C: Potent antibiotics against gram-positive pathogens. *Chem. - A Eur. J.* **18**, 16123–16128 (2012).

8. Couturier, C., Bauer, A., Rey, A., Schroif-Dufour, C. & Broenstrup, M. Armeniaspiroles, a new class of antibacterials: Antibacterial activities and total synthesis of 5-chloro-Armeniaspirole A. *Bioorg. Med. Chem. Lett.* **22**, 6292–6296 (2012).
9. Fu C, Xie F, Hoffmann J, Wang Q, Bauer A, Brönstrup M, Mahmud T, Müller RArmeniaspirol Antibiotic Biosynthesis: Chlorination and Oxidative Dechlorination Steps Affording Spiro[4.4]non-8-ene. *ChemBioChem* **20**, 764–769 (2019).
10. Qiao Y, Yan J, Jia J, Xue J, Qu X, Hu Y, Deng Z, Bi H, Zhu D. Characterization of the Biosynthetic Gene Cluster for the Antibiotic Armeniaspirols in *Streptomyces armeniacus*. *J. Nat. Prod.* 82. 318-323. (2019)
11. Darnowski, M. G. Lanosky, T. D, Labana P. Brazeau-Henrie, J. Calvert, N. Dornan, M., Natola, C. Paquette, A. R, Shuhendler, A. Boddy, C. N. Armeniaspirol analogues with more potent Gram-positive antibiotic activity show enhanced inhibition of the ATP-dependent proteases ClpXP and ClpYQ. *RSC Med. Chem.* **13**, 436–444 (2022).
12. Darnowski, M. G., Lanosky, T. D., Paquette, A. R. & Boddy, C. N. Armeniaspirol analogues disrupt the electrical potential (ΔΨ) of the proton motive force. *Bioorg. Med. Chem. Lett.* **84**, 129210 (2023).
13. Darnowski, M. G., Lanosky, T. D., Paquette, A. R. & Boddy, C. N. Synthesis of a Constitutional Isomer of Armeniaspirol A, Pseudoarmeniaspirol A, via Lewis Acid-Mediated Rearrangement. *J. Org. Chem.* ***87****, 15634* (2022).
14. Rosdahl, V. T., Frimodt-Moller, N. & Bentzon, M. W. Resistance to dicloxacillin, methicillin and oxacillin in methicillin-susceptible and methicillin-resistant

Staphylococcus aureus detected by dilution and diffusion methods. *APMIS* **97**, 715–722 (1989).

15. Vardakas, K. Z., Voulgaris, G. L., Maliaros, A., Samonis, G. & Falagas, M. E. Prolonged versus short-term intravenous infusion of antipseudomonal β-lactams for patients with sepsis: a systematic review and meta-analysis of randomised trials. *Lancet Infect. Dis.* **18**, 108–120 (2018).

16. Llona-Minguez S, Ghassemian A, Baranczewski P, Desroses M, Koolmeister T, Artursson P, Scobie M, Helleday T. Structure-metabolism-relationships in the microsomal clearance of piperazin-1-ylpyridazines. *MedChemComm* **8**, 1553–1560 (2017).

17. Paquette AR, Payne SR, McKay GA, Brazeau-Henrie JT, Darnowski MG, Kammili A, Bernal F, Mah TF, Gruenheid S, Nguyen D, Boddy CN. RpoN-Based stapled peptides with improved DNA binding suppress Pseudomonas aeruginosa virulence. *RSC Med. Chem.* **13**, 445–455 (2022).

18. Couturier, C., Bauer, A., Rey, A., Schroif-Dufour, C. & Broenstrup, M. Armeniaspiroles, a new class of antibacterials: Antibacterial activities and total synthesis of 5-chloro-Armeniaspirole A. *Bioorg. Med. Chem. Lett.* **22**, 6292–6296 (2012).

19. Dufour C, Wink J, Kurz M, Kogler H, Olivan H, Sablé S, Heyse W, Gerlitz M, Toti L, Nußer A, Rey A, Couturier C, Bauer A, Brönstrup M. Isolation and structural elucidation of armeniaspirols A-C: Potent antibiotics against gram-positive pathogens. *Chem. - A Eur. J.* **18**, 16123–16128 (2012).

20. Tsantili-Kakoulidou, A. & Demopoulos, V. J. Drug-like Properties and Fraction Lipophilicity Index as a combined metric. *ADMET DMPK* **9**, 177–190 (2021).

21. Boger, D. L. & Baldino, C. M. d,l- and meso-Isochrysohermidin: Total Synthesis and

Interstrand DNA Cross-Linking. *J. Am. Chem. Soc.* **115**, 11418–11425 (1993).

22. Wasserman, H. H., DeSimone, R. W., Boger, D. L. & Baldino, C. M. Singlet Oxygen Oxidation of Bipyrroles: Total Synthesis of d,l- and meso-Isochrysohermidin. *J. Am. Chem. Soc.* **115**, 8457–8458 (1993).

23. Kalaitzakis, D., Kouridaki, A., Noutsias, D., Montagnon, T. & Vassilikogiannakis, G. Methylene Blue as a Photosensitizer and Redox Agent: Synthesis of 5-Hydroxy-1H-pyrrol-2(5H)-ones from Furans. *Angew. Chemie - Int. Ed.* **54**, 6283–6287 (2015).

24. Birchall, G. R. & Rees, A. H. The Chlorination of Pyrroles. Part II. **49**, 919–922 (2011).

25. Durham, D. G., Hughes, C. G. & Rees, A. H. The Chlorination of Pyrroles. Part III. *Can. J. Chem.* **50**, 3223–3228 (1972).

26. Durham, D. G. & Rees, A. H. Chlorination of Pyrroles. Part I. *Can. J. Chem.* **49**, 136 (1971).

27. Gale, P. A., Navakhun, K., Camiolo, S., Light, M. E. & Hursthouse, M. B. Anion-anion assembly: A new class of anionic supramolecular polymer containing 3,4-dichloro-2,5-diamido-substituted pyrrole anion dimers. *J. Am. Chem. Soc.* **124**, 11228–11229 (2002).

28. Yang, T. R. & Martin Sander, P. The origin of the bird's beak: New insights from dinosaur incubation periods. *Biol. Lett.* **14**, (2018).

29. Schwab, I. R. The evolution of eyes: Major steps. the Keeler lecture 2017: Centenary of Keeler Ltd. *Eye* **32**, 302–313 (2018).

30. Maplestone, R. A., Stone, M. J. & Williams, D. H. The evolutionary role of secondary metabolites - a review. *Gene* **115**, 151–157 (1992).

Appendix I: Copyright information and manuscripts

Marketplace

Order Date	01-Feb-2023	Type of Use	Republish in a thesis/dissertation
Order License ID	1318577-1		
ISSN	2632-8682	Publisher	Royal Society of Chemistry
		Portion	Chapter/article

LICENSED CONTENT

Publication Title	RSC Medicinal Chemistry	Publication Type	Journal
Article Title	Armeniaspirol analogues with more potent Gram-positive antibiotic activity show enhanced inhibition of the ATP-dependent proteases ClpXP and ClpYQ.	Start Page	436
		End Page	444
		Issue	4
		Volume	13
Date	01/01/2020		
Country	United Kingdom of Great Britain and Northern Ireland		
Rightsholder	Royal Society of Chemistry		

REQUEST DETAILS

Portion Type	Chapter/article	Rights Requested	Main product
Page Range(s)	436-444	Distribution	Canada
Total Number of Pages	9	Translation	Original language of publication
Format (select all that apply)	Print, Electronic	Copies for the Disabled?	No
Who Will Republish the Content?	Academic institution	Minor Editing Privileges?	No
Duration of Use	Life of current edition	Incidental Promotional Use?	No
Lifetime Unit Quantity	More than 2,000,000	Currency	CAD

NEW WORK DETAILS

Title	SYNTHESIS AND EVALUTION OF MULTITARGET ANTIBIOTIC ARMENIASPIROL AND ANALOGUES	Institution Name	University of Ottawa
		Expected Presentation Date	2023-04-25
Instructor Name	Dr. Christopher N. Boddy		

ADDITIONAL DETAILS

Order Reference Number	N/A	**The Requesting Person/Organization to Appear on the License**	University of Ottawa

REQUESTED CONTENT DETAILS

Title, Description or Numeric Reference of the Portion(s)	RSC Medicinal Chemistry	**Title of the Article/Chapter the Portion Is From**	Armeniaspirol analogues with more potent Gram-positive antibiotic activity show enhanced inhibition of the ATP-dependent proteases ClpXP and ClpYQ.
Editor of Portion(s)	Darnowski, Michael; Lanosky, Taylor; Labana, Puneet; Brazeau-Henrie, Jordan; Calvert, Nicholas; Dornan, Mark Howard; Natola, Claudia; Paquette, Andre; Shuhendler, Adam Jason; Boddy, Christopher Noyce	**Author of Portion(s)**	Darnowski, Michael; Lanosky, Taylor; Labana, Puneet; Brazeau-Henrie, Jordan; Calvert, Nicholas; Dornan, Mark Howard; Natola, Claudia; Paquette, Andre; Shuhendler, Adam Jason; Boddy, Christopher Noyce
Volume of Serial or Monograph	13		
Page or Page Range of Portion	436-444	**Issue, if Republishing an Article From a Serial**	4
		Publication Date of Portion	2022-04-20

Marketplace Permissions General Terms and Conditions

The following terms and conditions ("General Terms"), together with any applicable Publisher Terms and Conditions, govern User's use of Works pursuant to the Licenses granted by Copyright Clearance Center, Inc. ("CCC") on behalf of the applicable Rightsholders of such Works through CCC's applicable Marketplace transactional licensing services (each, a "Service").

1) **Definitions.** For purposes of these General Terms, the following definitions apply:

"License" is the licensed use the User obtains via the Marketplace platform in a particular licensing transaction, as set forth in the Order Confirmation.

"Order Confirmation" is the confirmation CCC provides to the User at the conclusion of each Marketplace transaction. "Order Confirmation Terms" are additional terms set forth on specific Order Confirmations not set forth in the General Terms that can include terms applicable to a particular CCC transactional licensing service and/or any Rightsholder-specific terms.

"Rightsholder(s)" are the holders of copyright rights in the Works for which a User obtains licenses via the Marketplace platform, which are displayed on specific Order Confirmations.

"Terms" means the terms and conditions set forth in these General Terms and any additional Order Confirmation Terms collectively.

"User" or "you" is the person or entity making the use granted under the relevant License. Where the person accepting the Terms on behalf of a User is a freelancer or other third party who the User authorized to accept the General Terms on the User's behalf, such person shall be deemed jointly a User for purposes of such Terms.

"Work(s)" are the copyright protected works described in relevant Order Confirmations.

2) **Description of Service.** CCC's Marketplace enables Users to obtain Licenses to use one or more Works in accordance with all relevant Terms. CCC grants Licenses as an agent on behalf of the copyright rightsholder identified in the relevant Order Confirmation.

3) **Applicability of Terms.** The Terms govern User's use of Works in connection with the relevant License. In the event of any conflict between General Terms and Order Confirmation Terms, the latter shall govern. User acknowledges that Rightsholders have complete discretion whether to grant any permission, and whether to place any limitations on any grant, and that CCC has no right to supersede or to modify any such discretionary act by a Rightsholder.

4) **Representations; Acceptance.** By using the Service, User represents and warrants that User has been duly authorized by the User to accept, and hereby does accept, all Terms.

5) **Scope of License; Limitations and Obligations.** All Works and all rights therein, including copyright rights, remain the sole and exclusive property of the Rightsholder. The License provides only those rights expressly set forth in the terms and conveys no other rights in any Works

6) **General Payment Terms.** User may pay at time of checkout by credit card or choose to be invoiced. If the User chooses to be invoiced, the User shall: (i) remit payments in the manner identified on specific invoices, (ii) unless otherwise specifically stated in an Order Confirmation or separate written agreement, Users shall remit payments upon receipt of the relevant invoice from CCC, either by delivery or notification of availability of the invoice via the Marketplace platform, and (iii) if the User does not pay the invoice within 30 days of receipt, the User may incur a service charge of 1.5% per month or the maximum rate allowed by applicable law, whichever is less. While User may exercise the rights in the License immediately upon receiving the Order Confirmation, the License is automatically revoked and is null and void, as if it had never been issued, if CCC does not receive complete payment on a timely basis.

7) **General Limits on Use.** Unless otherwise provided in the Order Confirmation, any grant of rights to User (i) involves only the rights set forth in the Terms and does not include subsequent or additional uses, (ii) is non-exclusive and non-transferable, and (iii) is subject to any and all limitations and restrictions (such as, but not limited to, limitations on duration of use or circulation) included in the Terms. Upon completion of the licensed use as set forth in the Order Confirmation, User shall either secure a new permission for further use of the Work(s) or immediately cease any new use of the Work(s) and shall render inaccessible (such as by deleting or by removing or severing links or other locators) any further copies of the Work. User may only make alterations to the Work if and as expressly set forth in the Order Confirmation. No Work may be used in any way that is unlawful, including without limitation if such use would violate applicable sanctions laws or regulations, would be defamatory, violate the rights of third parties (including such third parties' rights of copyright, privacy, publicity, or other tangible or intangible property), or is otherwise illegal, sexually explicit, or obscene. In addition, User may not conjoin a Work with any other material that may result in damage to the reputation of the Rightsholder. Any unlawful use will render any licenses hereunder null and void. User agrees to inform CCC if it becomes aware of any infringement of any rights in a Work and to cooperate with any reasonable request of CCC or the Rightsholder in connection therewith.

8) **Third Party Materials.** In the event that the material for which a License is sought includes third party materials (such as photographs, illustrations, graphs, inserts and similar materials) that are identified in such material as having been used by permission (or a similar indicator), User is responsible for identifying, and seeking separate licenses (under this Service, if available, or otherwise) for any of such third party materials; without a separate license, User may not use such third party materials via the License.

9) **Copyright Notice.** Use of proper copyright notice for a Work is required as a condition of any License granted under the Service. Unless otherwise provided in the Order Confirmation, a proper copyright notice will read substantially as follows: "Used with permission of [Rightsholder's name], from [Work's title, author, volume, edition number and year of copyright]; permission conveyed through Copyright Clearance Center, Inc." Such notice must be provided in a reasonably legible font size and must be placed either on a cover page or in another location that any person, upon gaining access to the material which is the subject of a permission, shall see, or in the case of republication Licenses, immediately adjacent to the Work as used (for example, as part of a by-line or footnote) or in the place where substantially all other credits or notices for the new work containing the republished Work are located. Failure to include the required notice results in loss to the Rightsholder and CCC, and the User shall be liable to pay liquidated damages for each such failure equal to twice the use fee specified in the Order Confirmation, in addition to the use fee itself and any other fees and charges specified.

10) **Indemnity.** User hereby indemnifies and agrees to defend the Rightsholder and CCC, and their respective employees and directors, against all claims, liability, damages, costs, and expenses, including legal fees and expenses, arising out of

any use of a Work beyond the scope of the rights granted herein and in the Order Confirmation, or any use of a Work which has been altered in any unauthorized way by User, including claims of defamation or infringement of rights of copyright, publicity, privacy, or other tangible or intangible property.

11) **Limitation of Liability.** UNDER NO CIRCUMSTANCES WILL CCC OR THE RIGHTSHOLDER BE LIABLE FOR ANY DIRECT, INDIRECT, CONSEQUENTIAL, OR INCIDENTAL DAMAGES (INCLUDING WITHOUT LIMITATION DAMAGES FOR LOSS OF BUSINESS PROFITS OR INFORMATION, OR FOR BUSINESS INTERRUPTION) ARISING OUT OF THE USE OR INABILITY TO USE A WORK, EVEN IF ONE OR BOTH OF THEM HAS BEEN ADVISED OF THE POSSIBILITY OF SUCH DAMAGES. In any event, the total liability of the Rightsholder and CCC (including their respective employees and directors) shall not exceed the total amount actually paid by User for the relevant License. User assumes full liability for the actions and omissions of its principals, employees, agents, affiliates, successors, and assigns.

12) **Limited Warranties.** THE WORK(S) AND RIGHT(S) ARE PROVIDED "AS IS." CCC HAS THE RIGHT TO GRANT TO USER THE RIGHTS GRANTED IN THE ORDER CONFIRMATION DOCUMENT. CCC AND THE RIGHTSHOLDER DISCLAIM ALL OTHER WARRANTIES RELATING TO THE WORK(S) AND RIGHT(S), EITHER EXPRESS OR IMPLIED, INCLUDING WITHOUT LIMITATION IMPLIED WARRANTIES OF MERCHANTABILITY OR FITNESS FOR A PARTICULAR PURPOSE. ADDITIONAL RIGHTS MAY BE REQUIRED TO USE ILLUSTRATIONS, GRAPHS, PHOTOGRAPHS, ABSTRACTS, INSERTS, OR OTHER PORTIONS OF THE WORK (AS OPPOSED TO THE ENTIRE WORK) IN A MANNER CONTEMPLATED BY USER; USER UNDERSTANDS AND AGREES THAT NEITHER CCC NOR THE RIGHTSHOLDER MAY HAVE SUCH ADDITIONAL RIGHTS TO GRANT.

13) **Effect of Breach.** Any failure by User to pay any amount when due, or any use by User of a Work beyond the scope of the License set forth in the Order Confirmation and/or the Terms, shall be a material breach of such License. Any breach not cured within 10 days of written notice thereof shall result in immediate termination of such License without further notice. Any unauthorized (but licensable) use of a Work that is terminated immediately upon notice thereof may be liquidated by payment of the Rightsholder's ordinary license price therefor; any unauthorized (and unlicensable) use that is not terminated immediately for any reason (including, for example, because materials containing the Work cannot reasonably be recalled) will be subject to all remedies available at law or in equity, but in no event to a payment of less than three times the Rightsholder's ordinary license price for the most closely analogous licensable use plus Rightsholder's and/or CCC's costs and expenses incurred in collecting such payment.

14) **Additional Terms for Specific Products and Services.** If a User is making one of the uses described in this Section 14, the additional terms and conditions apply:

a) ***Print Uses of Academic Course Content and Materials (photocopies for academic coursepacks or classroom handouts).*** For photocopies for academic coursepacks or classroom handouts the following additional terms apply:

i) The copies and anthologies created under this License may be made and assembled by faculty members individually or at their request by on-campus bookstores or copy centers, or by off-campus copy shops and other similar entities.

ii) No License granted shall in any way: (i) include any right by User to create a substantively non-identical copy of the Work or to edit or in any other way modify the Work (except by means of deleting material immediately preceding or following the entire portion of the Work copied) (ii) permit "publishing ventures" where any particular anthology would be systematically marketed at multiple institutions.

iii) Subject to any Publisher Terms (and notwithstanding any apparent contradiction in the Order Confirmation arising from data provided by User), any use authorized under the academic pay-per-use service is limited as follows:

A) any License granted shall apply to only one class (bearing a unique identifier as assigned by the institution, and thereby including all sections or other subparts of the class) at one institution;

B) use is limited to not more than 25% of the text of a book or of the items in a published collection of essays, poems or articles;

C) use is limited to no more than the greater of (a) 25% of the text of an issue of a journal or other periodical or (b) two articles from such an issue;

D) no User may sell or distribute any particular anthology, whether photocopied or electronic, at more than one institution of learning;

E) in the case of a photocopy permission, no materials may be entered into electronic memory by User except in order to produce an identical copy of a Work before or during the academic term (or analogous period) as to which any particular permission is granted. In the event that User shall choose to retain materials that are the subject of a photocopy permission in electronic memory for purposes of producing identical copies more than one day after such retention (but still within the scope of any permission granted), User must notify CCC of such fact in the applicable permission request and such retention shall constitute one copy actually sold for purposes of calculating permission fees due; and

F) any permission granted shall expire at the end of the class. No permission granted shall in any way include any right by User to create a substantively non-identical copy of the Work or to edit or in any other way modify the Work (except by means of deleting material immediately preceding or following the entire portion of the Work copied).

iv) Books and Records; Right to Audit. As to each permission granted under the academic pay-per-use Service, User shall maintain for at least four full calendar years books and records sufficient for CCC to determine the numbers of copies made by User under such permission. CCC and any representatives it may designate shall have the right to audit such books and records at any time during User's ordinary business hours, upon two days' prior notice. If any such audit shall determine that User shall have underpaid for, or underreported, any photocopies sold or by three percent (3%) or more, then User shall bear all the costs of any such audit; otherwise, CCC shall bear the costs of any such audit. Any amount determined by such audit to have been underpaid by User shall immediately be paid to CCC by User, together with interest thereon at the rate of 10% per annum from the date such amount was originally due. The provisions of this paragraph shall survive the termination of this License for any reason.

b) ***Digital Pay-Per-Uses of Academic Course Content and Materials (e-coursepacks, electronic reserves, learning management systems, academic institution intranets).*** For uses in e-coursepacks, posts in electronic reserves, posts in learning management systems, or posts on academic institution intranets, the following additional terms apply:

i) The pay-per-uses subject to this Section 14(b) include:

A) **Posting e-reserves, course management systems, e-coursepacks for text-based content,** which grants authorizations to import requested material in electronic format, and allows electronic access to this material to members of a designated college or university class, under the direction of an instructor designated by the college or university, accessible only under appropriate electronic controls (e.g., password);

B) **Posting e-reserves, course management systems, e-coursepacks for material consisting of photographs or other still images not embedded in text,** which grants not only the authorizations described in Section 14(b)(i)(A) above, but also the following authorization: to include the requested material in course materials for use consistent with Section 14(b)(i)(A) above, including any necessary resizing, reformatting or modification of the resolution of such requested material (provided that such modification does not alter the underlying editorial content or meaning of the requested material, and provided that the resulting modified content is used solely within the scope of, and in a manner consistent with, the particular authorization described in the Order Confirmation and the Terms), but not including any other form of manipulation, alteration or editing of the requested material;

C) **Posting e-reserves, course management systems, e-coursepacks or other academic distribution for audiovisual content,** which grants not only the authorizations described in Section 14(b)(i)(A) above, but also the following authorizations: (i) to include the requested material in course materials for use consistent with Section 14(b)(i)(A) above; (ii) to display and perform the requested material to such members of such class in the physical classroom or remotely by means of streaming media or other video formats; and (iii) to "clip" or reformat the requested material for purposes of time or content management or ease of delivery, provided that such “clipping” or reformatting does not alter the underlying editorial content or meaning of the requested material and that the resulting material is used solely within the scope of, and in a manner consistent with, the particular authorization described in the Order Confirmation and the Terms. Unless expressly set forth in the relevant Order Conformation, the License does not authorize any other form of manipulation, alteration or editing of the requested material.

ii) Unless expressly set forth in the relevant Order Confirmation, no License granted shall in any way: (i) include any right by User to create a substantively non-identical copy of the Work or to edit or in any other way modify the Work (except by means of deleting material immediately preceding or following the entire portion of the Work copied or, in the case of Works subject to Sections 14(b)(1)(B) or (C) above, as described in such Sections) (ii)

permit "publishing ventures" where any particular course materials would be systematically marketed at multiple institutions.

iii) Subject to any further limitations determined in the Rightsholder Terms (and notwithstanding any apparent contradiction in the Order Confirmation arising from data provided by User), any use authorized under the electronic course content pay-per-use service is limited as follows:

A) any License granted shall apply to only one class (bearing a unique identifier as assigned by the institution, and thereby including all sections or other subparts of the class) at one institution;

B) use is limited to not more than 25% of the text of a book or of the items in a published collection of essays, poems or articles;

C) use is limited to not more than the greater of (a) 25% of the text of an issue of a journal or other periodical or (b) two articles from such an issue;

D) no User may sell or distribute any particular materials, whether photocopied or electronic, at more than one institution of learning;

E) electronic access to material which is the subject of an electronic-use permission must be limited by means of electronic password, student identification or other control permitting access solely to students and instructors in the class;

F) User must ensure (through use of an electronic cover page or other appropriate means) that any person, upon gaining electronic access to the material, which is the subject of a permission, shall see:

- a proper copyright notice, identifying the Rightsholder in whose name CCC has granted permission,
- a statement to the effect that such copy was made pursuant to permission,
- a statement identifying the class to which the material applies and notifying the reader that the material has been made available electronically solely for use in the class, and
- a statement to the effect that the material may not be further distributed to any person outside the class, whether by copying or by transmission and whether electronically or in paper form, and User must also ensure that such cover page or other means will print out in the event that the person accessing the material chooses to print out the material or any part thereof.

G) any permission granted shall expire at the end of the class and, absent some other form of authorization, User is thereupon required to delete the applicable material from any electronic storage or to block electronic access to the applicable material.

iv) Uses of separate portions of a Work, even if they are to be included in the same course material or the same university or college class, require separate permissions under the electronic course content pay-per-use Service. Unless otherwise provided in the Order Confirmation, any grant of rights to User is limited to use completed no later than the end of the academic term (or analogous period) as to which any particular permission is granted.

v) Books and Records; Right to Audit. As to each permission granted under the electronic course content Service, User shall maintain for at least four full calendar years books and records sufficient for CCC to determine the numbers of copies made by User under such permission. CCC and any representatives it may designate shall have the right to audit such books and records at any time during User's ordinary business hours, upon two days' prior notice. If any such audit shall determine that User shall have underpaid for, or underreported, any electronic copies used by three percent (3%) or more, then User shall bear all the costs of any such audit; otherwise, CCC shall bear the costs of any such audit. Any amount determined by such audit to have been underpaid by User shall immediately be paid to CCC by User, together with interest thereon at the rate of 10% per annum from the date such amount was originally due. The provisions of this paragraph shall survive the termination of this license for any reason.

c) ***Pay-Per-Use Permissions for Certain Reproductions (Academic photocopies for library reserves and interlibrary loan reporting) (Non-academic internal/external business uses and commercial document delivery).*** The License expressly excludes the uses listed in Section (c)(i)-(v) below (which must be subject to separate license from the

applicable Rightsholder) for: academic photocopies for library reserves and interlibrary loan reporting; and non-academic internal/external business uses and commercial document delivery.

i) electronic storage of any reproduction (whether in plain-text, PDF, or any other format) other than on a transitory basis;

ii) the input of Works or reproductions thereof into any computerized database;

iii) reproduction of an entire Work (cover-to-cover copying) except where the Work is a single article;

iv) reproduction for resale to anyone other than a specific customer of User;

v) republication in any different form. Please obtain authorizations for these uses through other CCC services or directly from the rightsholder.

Any license granted is further limited as set forth in any restrictions included in the Order Confirmation and/or in these Terms.

d) ***Electronic Reproductions in Online Environments (Non-Academic-email, intranet, internet and extranet).*** For "electronic reproductions", which generally includes e-mail use (including instant messaging or other electronic transmission to a defined group of recipients) or posting on an intranet, extranet or Intranet site (including any display or performance incidental thereto), the following additional terms apply:

i) Unless otherwise set forth in the Order Confirmation, the License is limited to use completed within 30 days for any use on the Internet, 60 days for any use on an intranet or extranet and one year for any other use, all as measured from the "republication date" as identified in the Order Confirmation, if any, and otherwise from the date of the Order Confirmation.

ii) User may not make or permit any alterations to the Work, unless expressly set forth in the Order Confirmation (after request by User and approval by Rightsholder); provided, however, that a Work consisting of photographs or other still images not embedded in text may, if necessary, be resized, reformatted or have its resolution modified without additional express permission, and a Work consisting of audiovisual content may, if necessary, be "clipped" or reformatted for purposes of time or content management or ease of delivery (provided that any such resizing, reformatting, resolution modification or “clipping” does not alter the underlying editorial content or meaning of the Work used, and that the resulting material is used solely within the scope of, and in a manner consistent with, the particular License described in the Order Confirmation and the Terms.

15) **Miscellaneous.**

a) User acknowledges that CCC may, from time to time, make changes or additions to the Service or to the Terms, and that Rightsholder may make changes or additions to the Rightsholder Terms. Such updated Terms will replace the prior terms and conditions in the order workflow and shall be effective as to any subsequent Licenses but shall not apply to Licenses already granted and paid for under a prior set of terms.

b) Use of User-related information collected through the Service is governed by CCC's privacy policy, available online at www.copyright.com/about/privacy-policy/.

c) The License is personal to User. Therefore, User may not assign or transfer to any other person (whether a natural person or an organization of any kind) the License or any rights granted thereunder; provided, however, that, where applicable, User may assign such License in its entirety on written notice to CCC in the event of a transfer of all or substantially all of User's rights in any new material which includes the Work(s) licensed under this Service.

d) No amendment or waiver of any Terms is binding unless set forth in writing and signed by the appropriate parties, including, where applicable, the Rightsholder. The Rightsholder and CCC hereby object to any terms contained in any writing prepared by or on behalf of the User or its principals, employees, agents or affiliates and purporting to govern or otherwise relate to the License described in the Order Confirmation, which terms are in any way inconsistent with any Terms set forth in the Order Confirmation, and/or in CCC's standard operating procedures, whether such writing is prepared prior to, simultaneously with or subsequent to the Order Confirmation, and whether such writing appears on a copy of the Order Confirmation or in a separate instrument.

e) The License described in the Order Confirmation shall be governed by and construed under the law of the State of New York, USA, without regard to the principles thereof of conflicts of law. Any case, controversy, suit, action, or

proceeding arising out of, in connection with, or related to such License shall be brought, at CCC's sole discretion, in any federal or state court located in the County of New York, State of New York, USA, or in any federal or state court whose geographical jurisdiction covers the location of the Rightsholder set forth in the Order Confirmation. The parties expressly submit to the personal jurisdiction and venue of each such federal or state court.

Last updated October 2022

CCC Marketplace

Order Number: 1330823
Order Date: 06 Mar 2023

Payment Information

Order Details

1. Bioorganic & medicinal chemistry letters

Billing Status: Open

Article: Armeniaspirol analogues disrupt the electrical potential (ΔΨ) of the proton motive force

Order License ID	1330823-1	Type of use	Republish in a thesis/dissertation
Order detail status	Completed	Publisher	PERGAMON
ISSN	0960-894X	Portion	Chapter/article

0.00 CAD
Republication Permission

LICENSED CONTENT

Publication Title	Bioorganic & medicinal chemistry letters	Country	United Kingdom of Great Britain and Northern Ireland
Article Title	Armeniaspirol analogues disrupt the electrical potential (ΔΨ) of the proton motive force	Rightsholder	Elsevier Science & Technology Journals
		Publication Type	Journal
Date	01/01/1991	Start Page	129210
Language	English		

REQUEST DETAILS

Portion Type	Chapter/article	Rights Requested	Main product and any product related to main product
Page Range(s)	129210-129213		
Total Number of Pages	4	Distribution	Worldwide

Format (select all that apply)	Print, Electronic	**Translation**	Original language of publication
Who Will Republish the Content?	Academic institution	**Copies for the Disabled?**	Yes
Duration of Use	Life of current edition	**Minor Editing Privileges?**	No
Lifetime Unit Quantity	More than 2,000,000	**Incidental Promotional Use?**	No
		Currency	CAD

NEW WORK DETAILS

Title	Armeniaspirol analogues disrupt the electrical potential (ΔΨ) of the proton motive force	**Institution Name**	University of Ottawa
		Expected Presentation Date	2023-05-01
Instructor Name	Christopher N. Boddy		

ADDITIONAL DETAILS

The Requesting Person/Organization to Appear on the License	Michael Darnowski

REQUESTED CONTENT DETAILS

Title, Description or Numeric Reference of the Portion(s)	Armeniaspirol analogues disrupt the electrical potential (ΔΨ) of the proton motive force	**Title of the Article/Chapter the Portion Is From**	Armeniaspirol analogues disrupt the electrical potential (ΔΨ) of the proton motive force
Editor of Portion(s)	Darnowski, Michael G.; Lanosky, Taylor D.; Paquette, André R.; Boddy, Christopher N.	**Author of Portion(s)**	Darnowski, Michael G.; Lanosky, Taylor D.; Paquette, André R.; Boddy, Christopher N.
Volume of Serial or Monograph	84	**Publication Date of Portion**	2023-02-27
Page or Page Range of Portion	129210		

Elsevier Science & Technology Journals Terms and Conditions

Elsevier publishes Open Access articles in both its Open Access journals and via its Open Access articles option in subscription journals, for which an author selects a user license permitting certain types of reuse without permission. Before proceeding please check if the article is Open Access on http://www.sciencedirect.com and refer to the user license for the individual article. Any reuse not included in the user license terms will require permission. You must always fully and appropriately credit the author and source. If any part of the material to be used (for example, figures) has appeared in the Elsevier publication for which you are seeking permission, with credit or acknowledgement to another source it is the responsibility of the user to ensure their reuse complies with the terms and conditions determined by the rights holder. Please contact permissions@elsevier.com with any queries.

Total Items: 1 Subtotal: 0.00 CAD

Order Total: 0.00 CAD

Marketplace Permissions General Terms and Conditions

The following terms and conditions ("General Terms"), together with any applicable Publisher Terms and Conditions, govern User's use of Works pursuant to the Licenses granted by Copyright Clearance Center, Inc. ("CCC") on behalf of the applicable Rightsholders of such Works through CCC's applicable Marketplace transactional licensing services (each, a "Service").

1) **Definitions.** For purposes of these General Terms, the following definitions apply:

"License" is the licensed use the User obtains via the Marketplace platform in a particular licensing transaction, as set forth in the Order Confirmation.

"Order Confirmation" is the confirmation CCC provides to the User at the conclusion of each Marketplace transaction. "Order Confirmation Terms" are additional terms set forth on specific Order Confirmations not set forth in the General Terms that can include terms applicable to a particular CCC transactional licensing service and/or any Rightsholder-specific terms.

"Rightsholder(s)" are the holders of copyright rights in the Works for which a User obtains licenses via the Marketplace platform, which are displayed on specific Order Confirmations.

"Terms" means the terms and conditions set forth in these General Terms and any additional Order Confirmation Terms collectively.

"User" or "you" is the person or entity making the use granted under the relevant License. Where the person accepting the Terms on behalf of a User is a freelancer or other third party who the User authorized to accept the General Terms on the User's behalf, such person shall be deemed jointly a User for purposes of such Terms.

"Work(s)" are the copyright protected works described in relevant Order Confirmations.

2) **Description of Service.** CCC's Marketplace enables Users to obtain Licenses to use one or more Works in accordance with all relevant Terms. CCC grants Licenses as an agent on behalf of the copyright rightsholder identified in the relevant Order Confirmation.

3) **Applicability of Terms.** The Terms govern User's use of Works in connection with the relevant License. In the event of any conflict between General Terms and Order Confirmation Terms, the latter shall govern. User acknowledges that Rightsholders have complete discretion whether to grant any permission, and whether to place any limitations on any grant, and that CCC has no right to supersede or to modify any such discretionary act by a Rightsholder.

4) **Representations; Acceptance.** By using the Service, User represents and warrants that User has been duly authorized by the User to accept, and hereby does accept, all Terms.

5) **Scope of License; Limitations and Obligations.** All Works and all rights therein, including copyright rights, remain the sole and exclusive property of the Rightsholder. The License provides only those rights expressly set forth in the terms and conveys no other rights in any Works

6) **General Payment Terms.** User may pay at time of checkout by credit card or choose to be invoiced. If the User chooses to be invoiced, the User shall: (i) remit payments in the manner identified on specific invoices, (ii) unless otherwise specifically stated in an Order Confirmation or separate written agreement, Users shall remit payments upon receipt of the relevant invoice from CCC, either by delivery or notification of availability of the invoice via the Marketplace platform, and (iii) if the User does not pay the invoice within 30 days of receipt, the User may incur a service charge of 1.5% per month or the maximum rate allowed by applicable law, whichever is less. While User may exercise the rights in the License immediately upon receiving the Order Confirmation, the

License is automatically revoked and is null and void, as if it had never been issued, if CCC does not receive complete payment on a timely basis.

7) **General Limits on Use.** Unless otherwise provided in the Order Confirmation, any grant of rights to User (i) involves only the rights set forth in the Terms and does not include subsequent or additional uses, (ii) is non-exclusive and non-transferable, and (iii) is subject to any and all limitations and restrictions (such as, but not limited to, limitations on duration of use or circulation) included in the Terms. Upon completion of the licensed use as set forth in the Order Confirmation, User shall either secure a new permission for further use of the Work(s) or immediately cease any new use of the Work(s) and shall render inaccessible (such as by deleting or by removing or severing links or other locators) any further copies of the Work. User may only make alterations to the Work if and as expressly set forth in the Order Confirmation. No Work may be used in any way that is unlawful, including without limitation if such use would violate applicable sanctions laws or regulations, would be defamatory, violate the rights of third parties (including such third parties' rights of copyright, privacy, publicity, or other tangible or intangible property), or is otherwise illegal, sexually explicit, or obscene. In addition, User may not conjoin a Work with any other material that may result in damage to the reputation of the Rightsholder. Any unlawful use will render any licenses hereunder null and void. User agrees to inform CCC if it becomes aware of any infringement of any rights in a Work and to cooperate with any reasonable request of CCC or the Rightsholder in connection therewith.

8) **Third Party Materials.** In the event that the material for which a License is sought includes third party materials (such as photographs, illustrations, graphs, inserts and similar materials) that are identified in such material as having been used by permission (or a similar indicator), User is responsible for identifying, and seeking separate licenses (under this Service, if available, or otherwise) for any of such third party materials; without a separate license, User may not use such third party materials via the License.

9) **Copyright Notice.** Use of proper copyright notice for a Work is required as a condition of any License granted under the Service. Unless otherwise provided in the Order Confirmation, a proper copyright notice will read substantially as follows: "Used with permission of [Rightsholder's name], from [Work's title, author, volume, edition number and year of copyright]; permission conveyed through Copyright Clearance Center, Inc." Such notice must be provided in a reasonably legible font size and must be placed either on a cover page or in another location that any person, upon gaining access to the material which is the subject of a permission, shall see, or in the case of republication Licenses, immediately adjacent to the Work as used (for example, as part of a by-line or footnote) or in the place where substantially all other credits or notices for the new work containing the republished Work are located. Failure to include the required notice results in loss to the Rightsholder and CCC, and the User shall be liable to pay liquidated damages for each such failure equal to twice the use fee specified in the Order Confirmation, in addition to the use fee itself and any other fees and charges specified.

10) **Indemnity.** User hereby indemnifies and agrees to defend the Rightsholder and CCC, and their respective employees and directors, against all claims, liability, damages, costs, and expenses, including legal fees and expenses, arising out of any use of a Work beyond the scope of the rights granted herein and in the Order Confirmation, or any use of a Work which has been altered in any unauthorized way by User, including claims of defamation or infringement of rights of copyright, publicity, privacy, or other tangible or intangible property.

11) **Limitation of Liability.** UNDER NO CIRCUMSTANCES WILL CCC OR THE RIGHTSHOLDER BE LIABLE FOR ANY DIRECT, INDIRECT, CONSEQUENTIAL, OR INCIDENTAL DAMAGES (INCLUDING WITHOUT LIMITATION DAMAGES FOR LOSS OF BUSINESS PROFITS OR INFORMATION, OR FOR BUSINESS INTERRUPTION) ARISING OUT OF THE USE OR INABILITY TO USE A WORK, EVEN IF ONE OR BOTH OF THEM HAS BEEN ADVISED OF THE POSSIBILITY OF SUCH DAMAGES. In any event, the total liability of the Rightsholder and CCC (including their respective employees and directors) shall not exceed the total amount actually paid by User for the relevant License. User assumes full liability for the actions and omissions of its principals, employees, agents, affiliates, successors, and assigns.

12) **Limited Warranties.** THE WORK(S) AND RIGHT(S) ARE PROVIDED "AS IS." CCC HAS THE RIGHT TO GRANT TO USER THE RIGHTS GRANTED IN THE ORDER CONFIRMATION DOCUMENT. CCC AND THE RIGHTSHOLDER DISCLAIM ALL OTHER WARRANTIES RELATING TO THE WORK(S) AND RIGHT(S), EITHER EXPRESS OR IMPLIED, INCLUDING WITHOUT LIMITATION IMPLIED WARRANTIES OF MERCHANTABILITY OR FITNESS FOR A PARTICULAR

PURPOSE. ADDITIONAL RIGHTS MAY BE REQUIRED TO USE ILLUSTRATIONS, GRAPHS, PHOTOGRAPHS, ABSTRACTS, INSERTS, OR OTHER PORTIONS OF THE WORK (AS OPPOSED TO THE ENTIRE WORK) IN A MANNER CONTEMPLATED BY USER; USER UNDERSTANDS AND AGREES THAT NEITHER CCC NOR THE RIGHTSHOLDER MAY HAVE SUCH ADDITIONAL RIGHTS TO GRANT.

13) **Effect of Breach.** Any failure by User to pay any amount when due, or any use by User of a Work beyond the scope of the License set forth in the Order Confirmation and/or the Terms, shall be a material breach of such License. Any breach not cured within 10 days of written notice thereof shall result in immediate termination of such License without further notice. Any unauthorized (but licensable) use of a Work that is terminated immediately upon notice thereof may be liquidated by payment of the Rightsholder's ordinary license price therefor; any unauthorized (and unlicensable) use that is not terminated immediately for any reason (including, for example, because materials containing the Work cannot reasonably be recalled) will be subject to all remedies available at law or in equity, but in no event to a payment of less than three times the Rightsholder's ordinary license price for the most closely analogous licensable use plus Rightsholder's and/or CCC's costs and expenses incurred in collecting such payment.

14) **Additional Terms for Specific Products and Services.** If a User is making one of the uses described in this Section 14, the additional terms and conditions apply:

a) ***Print Uses of Academic Course Content and Materials (photocopies for academic coursepacks or classroom handouts).*** For photocopies for academic coursepacks or classroom handouts the following additional terms apply:

i) The copies and anthologies created under this License may be made and assembled by faculty members individually or at their request by on-campus bookstores or copy centers, or by off-campus copy shops and other similar entities.

ii) No License granted shall in any way: (i) include any right by User to create a substantively non-identical copy of the Work or to edit or in any other way modify the Work (except by means of deleting material immediately preceding or following the entire portion of the Work copied) (ii) permit "publishing ventures" where any particular anthology would be systematically marketed at multiple institutions.

iii) Subject to any Publisher Terms (and notwithstanding any apparent contradiction in the Order Confirmation arising from data provided by User), any use authorized under the academic pay-per-use service is limited as follows:

A) any License granted shall apply to only one class (bearing a unique identifier as assigned by the institution, and thereby including all sections or other subparts of the class) at one institution;

B) use is limited to not more than 25% of the text of a book or of the items in a published collection of essays, poems or articles;

C) use is limited to no more than the greater of (a) 25% of the text of an issue of a journal or other periodical or (b) two articles from such an issue;

D) no User may sell or distribute any particular anthology, whether photocopied or electronic, at more than one institution of learning;

E) in the case of a photocopy permission, no materials may be entered into electronic memory by User except in order to produce an identical copy of a Work before or during the academic term (or analogous period) as to which any particular permission is granted. In the event that User shall choose to retain materials that are the subject of a photocopy permission in electronic memory for purposes of producing identical copies more than one day after such retention (but still within the scope of any permission granted), User must notify CCC of such fact in the applicable permission request and such retention shall constitute one copy actually sold for purposes of calculating permission fees due; and

F) any permission granted shall expire at the end of the class. No permission granted shall in any way include any right by User to create a substantively non-identical copy of the Work or to edit or in any other way modify the Work (except by means of deleting material immediately preceding or following the entire portion of the Work copied).

iv) Books and Records; Right to Audit. As to each permission granted under the academic pay-per-use Service, User shall maintain for at least four full calendar years books and records sufficient for CCC to determine the numbers of copies made by User under such permission. CCC and any representatives it may designate shall have the right to audit such books and records at any time during User's ordinary business hours, upon two days' prior notice. If any such audit shall determine that User shall have underpaid for, or underreported, any photocopies sold or by three percent (3%) or more, then User shall bear all the costs of any such audit; otherwise, CCC shall bear the costs of any such audit. Any amount determined by such audit to have been underpaid by User shall immediately be paid to CCC by User, together with interest thereon at the rate of 10% per annum from the date such amount was originally due. The provisions of this paragraph shall survive the termination of this License for any reason.

b) ***Digital Pay-Per-Uses of Academic Course Content and Materials (e-coursepacks, electronic reserves, learning management systems, academic institution intranets).*** For uses in e-coursepacks, posts in electronic reserves, posts in learning management systems, or posts on academic institution intranets, the following additional terms apply:

i) The pay-per-uses subject to this Section 14(b) include:

A) **Posting e-reserves, course management systems, e-coursepacks for text-based content,** which grants authorizations to import requested material in electronic format, and allows electronic access to this material to members of a designated college or university class, under the direction of an instructor designated by the college or university, accessible only under appropriate electronic controls (e.g., password);

B) **Posting e-reserves, course management systems, e-coursepacks for material consisting of photographs or other still images not embedded in text,** which grants not only the authorizations described in Section 14(b)(i)(A) above, but also the following authorization: to include the requested material in course materials for use consistent with Section 14(b)(i)(A) above, including any necessary resizing, reformatting or modification of the resolution of such requested material (provided that such modification does not alter the underlying editorial content or meaning of the requested material, and provided that the resulting modified content is used solely within the scope of, and in a manner consistent with, the particular authorization described in the Order Confirmation and the Terms), but not including any other form of manipulation, alteration or editing of the requested material;

C) **Posting e-reserves, course management systems, e-coursepacks or other academic distribution for audiovisual content,** which grants not only the authorizations described in Section 14(b)(i)(A) above, but also the following authorizations: (i) to include the requested material in course materials for use consistent with Section 14(b)(i)(A) above; (ii) to display and perform the requested material to such members of such class in the physical classroom or remotely by means of streaming media or other video formats; and (iii) to "clip" or reformat the requested material for purposes of time or content management or ease of delivery, provided that such “clipping” or reformatting does not alter the underlying editorial content or meaning of the requested material and that the resulting material is used solely within the scope of, and in a manner consistent with, the particular authorization described in the Order Confirmation and the Terms. Unless expressly set forth in the relevant Order Conformation, the License does not authorize any other form of manipulation, alteration or editing of the requested material.

ii) Unless expressly set forth in the relevant Order Confirmation, no License granted shall in any way: (i) include any right by User to create a substantively non-identical copy of the Work or to edit or in any other way modify the Work (except by means of deleting material immediately preceding or following the

entire portion of the Work copied or, in the case of Works subject to Sections 14(b)(1)(B) or (C) above, as described in such Sections) (ii) permit "publishing ventures" where any particular course materials would be systematically marketed at multiple institutions.

iii) Subject to any further limitations determined in the Rightsholder Terms (and notwithstanding any apparent contradiction in the Order Confirmation arising from data provided by User), any use authorized under the electronic course content pay-per-use service is limited as follows:

A) any License granted shall apply to only one class (bearing a unique identifier as assigned by the institution, and thereby including all sections or other subparts of the class) at one institution;

B) use is limited to not more than 25% of the text of a book or of the items in a published collection of essays, poems or articles;

C) use is limited to not more than the greater of (a) 25% of the text of an issue of a journal or other periodical or (b) two articles from such an issue;

D) no User may sell or distribute any particular materials, whether photocopied or electronic, at more than one institution of learning;

E) electronic access to material which is the subject of an electronic-use permission must be limited by means of electronic password, student identification or other control permitting access solely to students and instructors in the class;

F) User must ensure (through use of an electronic cover page or other appropriate means) that any person, upon gaining electronic access to the material, which is the subject of a permission, shall see:

- a proper copyright notice, identifying the Rightsholder in whose name CCC has granted permission,
- a statement to the effect that such copy was made pursuant to permission,
- a statement identifying the class to which the material applies and notifying the reader that the material has been made available electronically solely for use in the class, and
- a statement to the effect that the material may not be further distributed to any person outside the class, whether by copying or by transmission and whether electronically or in paper form, and User must also ensure that such cover page or other means will print out in the event that the person accessing the material chooses to print out the material or any part thereof.

G) any permission granted shall expire at the end of the class and, absent some other form of authorization, User is thereupon required to delete the applicable material from any electronic storage or to block electronic access to the applicable material.

iv) Uses of separate portions of a Work, even if they are to be included in the same course material or the same university or college class, require separate permissions under the electronic course content pay-per-use Service. Unless otherwise provided in the Order Confirmation, any grant of rights to User is limited to use completed no later than the end of the academic term (or analogous period) as to which any particular permission is granted.

v) Books and Records; Right to Audit. As to each permission granted under the electronic course content Service, User shall maintain for at least four full calendar years books and records sufficient for CCC to determine the numbers of copies made by User under such permission. CCC and any representatives it may designate shall have the right to audit such books and records at any time during User's ordinary business hours, upon two days' prior notice. If any such audit shall determine that User shall have underpaid for, or underreported, any electronic copies used by three percent (3%) or more, then User shall bear all the costs of any such audit; otherwise, CCC shall bear the costs of any such audit. Any

amount determined by such audit to have been underpaid by User shall immediately be paid to CCC by User, together with interest thereon at the rate of 10% per annum from the date such amount was originally due. The provisions of this paragraph shall survive the termination of this license for any reason.

c) ***Pay-Per-Use Permissions for Certain Reproductions (Academic photocopies for library reserves and interlibrary loan reporting) (Non-academic internal/external business uses and commercial document delivery).*** The License expressly excludes the uses listed in Section (c)(i)-(v) below (which must be subject to separate license from the applicable Rightsholder) for: academic photocopies for library reserves and interlibrary loan reporting; and non-academic internal/external business uses and commercial document delivery.

i) electronic storage of any reproduction (whether in plain-text, PDF, or any other format) other than on a transitory basis;

ii) the input of Works or reproductions thereof into any computerized database;

iii) reproduction of an entire Work (cover-to-cover copying) except where the Work is a single article;

iv) reproduction for resale to anyone other than a specific customer of User;

v) republication in any different form. Please obtain authorizations for these uses through other CCC services or directly from the rightsholder.

Any license granted is further limited as set forth in any restrictions included in the Order Confirmation and/or in these Terms.

d) ***Electronic Reproductions in Online Environments (Non-Academic-email, intranet, internet and extranet).*** For "electronic reproductions", which generally includes e-mail use (including instant messaging or other electronic transmission to a defined group of recipients) or posting on an intranet, extranet or Intranet site (including any display or performance incidental thereto), the following additional terms apply:

i) Unless otherwise set forth in the Order Confirmation, the License is limited to use completed within 30 days for any use on the Internet, 60 days for any use on an intranet or extranet and one year for any other use, all as measured from the "republication date" as identified in the Order Confirmation, if any, and otherwise from the date of the Order Confirmation.

ii) User may not make or permit any alterations to the Work, unless expressly set forth in the Order Confirmation (after request by User and approval by Rightsholder); provided, however, that a Work consisting of photographs or other still images not embedded in text may, if necessary, be resized, reformatted or have its resolution modified without additional express permission, and a Work consisting of audiovisual content may, if necessary, be "clipped" or reformatted for purposes of time or content management or ease of delivery (provided that any such resizing, reformatting, resolution modification or “clipping” does not alter the underlying editorial content or meaning of the Work used, and that the resulting material is used solely within the scope of, and in a manner consistent with, the particular License described in the Order Confirmation and the Terms.

15) **Miscellaneous.**

a) User acknowledges that CCC may, from time to time, make changes or additions to the Service or to the Terms, and that Rightsholder may make changes or additions to the Rightsholder Terms. Such updated Terms will replace the prior terms and conditions in the order workflow and shall be effective as to any subsequent Licenses but shall not apply to Licenses already granted and paid for under a prior set of terms.

b) Use of User-related information collected through the Service is governed by CCC's privacy policy, available online at www.copyright.com/about/privacy-policy/.

c) The License is personal to User. Therefore, User may not assign or transfer to any other person (whether a natural person or an organization of any kind) the License or any rights granted thereunder; provided, however, that, where applicable, User may assign such License in its entirety on written notice to CCC in the event of a transfer of all or substantially all of User's rights in any new material which includes the Work(s) licensed under this Service.

d) No amendment or waiver of any Terms is binding unless set forth in writing and signed by the appropriate parties, including, where applicable, the Rightsholder. The Rightsholder and CCC hereby object to any terms contained in any writing prepared by or on behalf of the User or its principals, employees, agents or affiliates and purporting to govern or otherwise relate to the License described in the Order Confirmation, which terms are in any way inconsistent with any Terms set forth in the Order Confirmation, and/or in CCC's standard operating procedures, whether such writing is prepared prior to, simultaneously with or subsequent to the Order Confirmation, and whether such writing appears on a copy of the Order Confirmation or in a separate instrument.

e) The License described in the Order Confirmation shall be governed by and construed under the law of the State of New York, USA, without regard to the principles thereof of conflicts of law. Any case, controversy, suit, action, or proceeding arising out of, in connection with, or related to such License shall be brought, at CCC's sole discretion, in any federal or state court located in the County of New York, State of New York, USA, or in any federal or state court whose geographical jurisdiction covers the location of the Rightsholder set forth in the Order Confirmation. The parties expressly submit to the personal jurisdiction and venue of each such federal or state court.

Last updated October 2022

RSC Medicinal Chemistry

ROYAL SOCIETY OF CHEMISTRY

RESEARCH ARTICLE

View Article Online
View Journal | View Issue

Cite this: *RSC Med. Chem.*, 2022, 13, 436

Armeniaspirol analogues with more potent Gram-positive antibiotic activity show enhanced inhibition of the ATP-dependent proteases ClpXP and ClpYQ†

Michael G. Darnowski, Taylor D. Lanosky,‡ Puneet Labana,‡ Jordan T. Brazeau Henrie,§ Nicholas D. Calvert,§ Mark H. Dornan,§ Claudia Natola,§ André R. Paquette,§ Adam J. Shuhendler and Christopher N. Boddy*

Received 5th November 2021,
Accepted 7th February 2022

DOI: 10.1039/d1md00355k

rsc.li/medchem

Antibiotics with fundamentally new mechanisms of action such as the armeniaspirols, which target the ATP-dependent proteases ClpXP and ClpYQ, must be developed to combat antimicrobial resistance. While the mechanism of action of armeniaspirol against Gram-positive bacteria is understood, little is known about the structure activity relationship for its antibiotic activity. Based on the preliminary data showing that modifications of armeniaspirol's *N*-methyl group increased antibiotic potency, we probed the structure activity relationship of *N*-alkyl armeniaspirol derivatives. A series of focused derivatives were synthesized and evaluated for antibiotic activity against clinically relevant pathogens including methicillin-resistant *Staphylococcus aureus* and vancomycin-resistant *Enterococcus*. Replacement of the *N*-methyl with *N*-hexyl, various *N*-benzyl, and *N*-phenethyl substituents led to substantial increases in antibiotic activity and potency for inhibition of both ClpYQ and ClpXP. Docking studies identified binding models for ClpXP and ClpYQ that were consistent with the inhibition data. This work confirms the role of ClpXP and ClpYQ in the mechanism of action of armeniaspirol and provides important lead compounds for further antibiotic development.

Introduction

With the constant threat of increasing antimicrobial resistance, antibiotics with fundamentally new mechanisms of action must be developed and brought to the clinic. The armeniaspirols discovered in 2012 are hybrid polyketide non-ribosomal peptide natural products produced by *Streptomyces armeniacus*[1,2] that have recently been shown to possess unique pharmacology.[3] The armeniaspirols are potent Gram-positive antibiotics active against methicillin-resistant *Staphylococcus aureus* (MRSA), penicillin-resistant *Streptococcus pneumoniae* (PRSP), and vancomycin-resistant *Enterococcus* (VRE). They competitively inhibit the ATP-dependent proteases ClpXP and ClpYQ (also known as HslVU),[3] whose combined activity is essential,[3] leading to disruption of the divisome and cell division arrest (Fig. 1A). While inhibitors of ClpP are known antivirulence compounds,

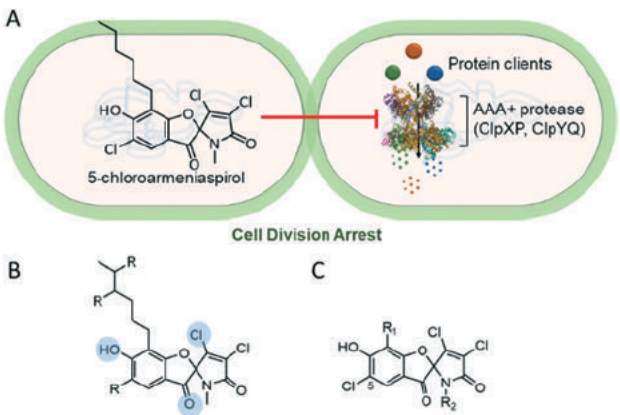

Fig. 1 Analogs of armeniaspirol to probe antibiotic activity *via* inhibition of ClpXP and ClpYQ (A) 5 chloroarmeniaspirol inhibits the ATP dependent proteases ClpXP and ClpYQ in Gram positive bacteria, which dysregulates the divisome and leads to cell division arrest. (B) Summary of structure activity relationships for armeniaspirol. Functional groups highlighted in blue are essential for antibiotic activity. *R* indicates sites amenable to substitution. (C) 5 chloroarmeniaspirol sites R_1 and R_2 were selected for detailed structure activity relationship.

† Electronic supplementary information (ESI) available. See DOI: 10.1039/d1md00355k

‡ Equal contributions.

§ Listed alphabetically.

the additional targeting of ClpYQ by armeniaspirol is unprecedented and results in antibiotic activity.

Little is known about the structure–activity relationship for antibiotic activity of armeniaspirol. Initial semi-synthesis work from the isolated natural product showed that substitution of the β-chloride with alcohols, amines, and thiols eliminated antibiotic activity as determined by minimum inhibitory concentrations (MIC).[2] Similarly alkylation of the phenol and reduction of the carbonyl abolished activity (Fig. 1B).[2] *Via* total synthesis, the *N*-methyl moiety proved amenable to replacement with a longer *N*-alkyl chain without loss of activity.[3] However no data is available on how structural modifications impact the activity against ClpXP and ClpYQ. Given that correctly balancing activity at each target is essential for development of effective and potent multi-target drugs, evaluating the impact of structural perturbations on each of these targets is thus essential.

Based on preliminary data showing that modification of armeniaspirol's *N*-methyl group increased antibiotic potency,[3] we probed the structure–activity relationship of *N*-alkyl armeniaspirol derivatives. Fourteen armeniaspirol analogues were synthesized with varying *N*-alkyl groups. To compensate for the additional lipophilic character of extending the *N*-methyl group, the aromatic hexyl chain was simplified to a methyl substituent in a subset of the analogues. All compounds were evaluated for MIC and minimum bactericidal concentration (MBC) against clinically relevant Gram-positive pathogens including MRSA USA300, the most common community acquired MRSA. Potent analogues were evaluated for activity against ClpXP in a cell-based assay and activity against ClpYQ in a biochemical assay. Highly potent armeniaspirol analogues with improved activity against ClpXP and ClpYQ were identified. These data bode well for the further development of the armeniaspirol scaffold as a Gram-positive antibiotic.

Results

The armeniaspirols and their analogues have been isolated from the producing organism,[1,4] generated through semi-synthesis,[3] and accessed *via* total synthesis.[2,3] Analogues generated from the addition of alcohols like methanol, amines such as isobutyl amine, and thiols like 2-diethylamino-ethanethiol into the Michael acceptor lack antibiotic activity against *S. aureus* in MIC assays.[1] Both diastereomers generated from reduction of the furan ring carbonyl are inactive against *S. aureus* in MIC assays.[1] Methylation of the aromatic phenol also produces inactive compounds.[1,3] However, chlorination *ortho* to the phenol is tolerated with a slight reduction in antibiotic activity as measured by MIC against MRSA.[1,3] Both the removal of the *N*-methyl[4] and substitution of it with an alkyl chain[3] produce active compounds, with installation of a *N*-hexyl chain boosting potency four fold against *Bacillus subtilis*.[3] Lastly modification of the aromatic alkyl chain *via* branching produces compounds that are comparatively potent to armeniaspirol A in MIC assays with MRSA.[1]

Based on the known structure–activity relationships, exploring modification of the lactam through *N*-alkylation appeared most promising and likely to yield compounds with improved potency. Thus we set out to diversify this position by substituting the amide N with varying alkyl groups. To evaluate the overall impact of increasing lipophilicity, which typically correlates with an increase in non-selective binding,[5] we planned two series of *N*-alkyl analogues, one with the native hexyl chain on the aromatic ring (series 1, Fig. 1C R_1 = n-C_6H_{13}) and a second with a methyl substituent (series 2, Fig. 1C R_1 = CH_3).

Synthesis of chloro-armeniaspirol analogues

The synthetic route for generation of the armeniaspirol scaffold relies on a *N*-chlorosuccinimide (NCS)-based chlorination of the pyrrole, which forms the key spirocyclic center and the dichlorinated α,β-unsaturated lactam.[2,3,6] Due to the forcing oxidative conditions, the electron rich phenyl ring is also chlorinated giving rise to 5-chloroarmeniaspirol analogues (Fig. 1C). While the 5-chloro substituent could not be selectively reduced in the presence of the dichloro-α,β-unsaturated lactam, the additional chlorination does not significantly impact the antibiotic activity as measured by MIC.[2] Thus, all analogues synthesized in this study are functionalized with a chloride in the 5-position (Fig. 2).

Diversification of the substituent on the phenyl ring (R_1) was implemented in the start of the synthesis. The hexyl chain series of analogues (series 1) were prepared *via* a lithium halogen exchange followed by a Suzuki coupling with *n*-hexyl boronic acid (Fig. 2A), while the methyl series of analogues (series 2) were prepared from commercially available 2,6-dimethoxytoluene. The two compounds were elaborated *via* parallel synthetic routes (Fig. 2B). Friedel–Crafts acylation of the electron rich aromatic with the acid chloride of pyrrole carboxylic acid, followed by selective demethylation of methoxy substituent *ortho* to the carbonyl[7] generated the key precursors for oxidative spirocyclization. NCS in acetic acid chlorinated and oxidized these intermediates generating a mixture of spirocyclic compounds with either the 2,3-dichloro-α,β-unsaturated lactam or the 2,2,3-trichloro lactam. Treatment of this mixture with triethylamine afforded the armeniaspirol scaffolds. Alkylation of the amide with a variety of electrophiles enabled diversification of each series at the R_2 site. Finally, boron tribromide deprotection of the aryl ether generated the final compounds, **1–14** (Fig. 2C).

MIC evaluation of analogues

The evaluation of antibiotic activity of armeniaspirol analogues was accomplished using the microtiter broth dilution MIC and MBC assays[8] against a panel of clinically relevant Gram-positive pathogens (Table 1). These include MRSA USA100, the primary lineage responsible for hospital

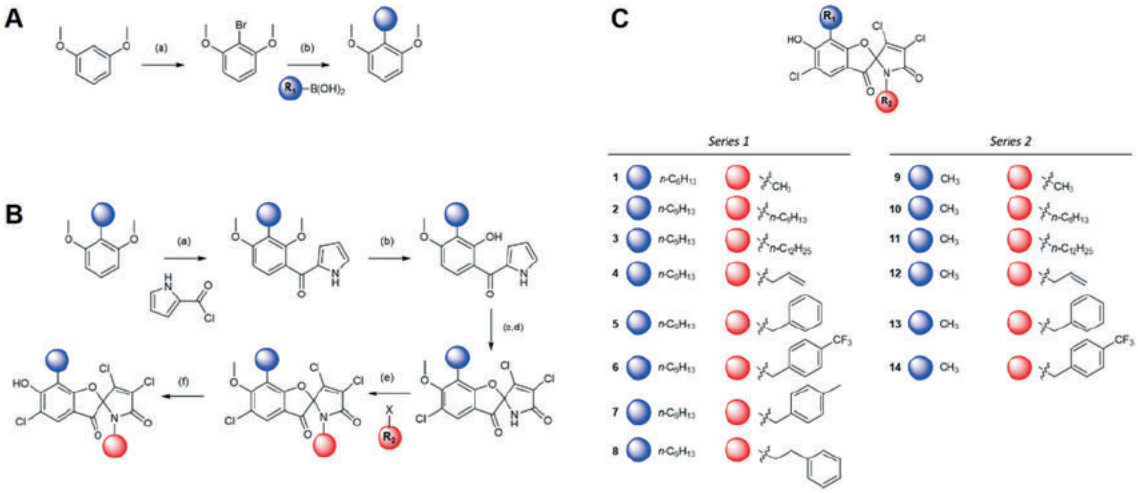

Fig. 2 Armeniaspirol analogues. (A) Synthetic route installing the hexyl chain for the starting material used for all series 1 analogues. Reagents and conditions are as follows a) *n* BuLi, Br_2 b) $Pd(OAc)_2$, SPhos, K_3PO_4. (B) Synthetic route generating series 1 and 2 analogues from dimethyl 2 methylresorcinol and dimethyl 2 hexylresorcinol. Reagents and conditions are as follows a) $SnCl_4$ b) BBr_3 c) NCS d) NEt_3 e) NaH f) BBr_3 (C) structures of series 1 and 2 analogues used in this study.

Table 1 MIC evaluation of analogues 1 14 against a panel of Gram positive and negative bacteria

	Minimum inhibitory concentration (μg mL ^{1})													
	1	**2**	**3**	**4**	**5**	**6**	**7**	**8**	**9**	**10**	**11**	**12**	**13**	**14**
Gram positive														
S. aureus IA116 USA100	4	1	8	4	1	2	1	1	>32	4	2	>32	>32	16
S. aureus MN8 USA200	4	1	16	4	1	2	0.5	0.5	>32	4	2	>32	>32	16
S. aureus LAC Fitz USA300	4	1	16	4	1	2	0.5	0.5	>32	4	1	>32	32	16
S. aureus MW2 USA400	4	1	8	4	2	2	0.5	0.5	>32	8	2	>32	32	16
E. faecalis NJ3	8	2	8	8	2	2	1	1	>32	8	0.5	>32	>32	32
Gram negative														
P. aeruginosa PA01	>32	>32	>32	>32	>32	>32	>32	>32	>32	>32	>32	>32	>32	>32

acquired MRSA infections,[9] USA200, responsible for a smaller subset of hospital acquired infections, USA300, the primary community acquired MRSA pathogen, USA400, also responsible for community acquired MRSA infections,[10,11] and the high-priority pathogen VRE. MIC were also determined with the Gram-negative pathogen *Pseudomonas aeruginosa* PA01, to determine if any analogues had expanded activity against Gram-negative bacteria.

In general the series 1 hexyl chain analogues exhibited superior potency relative to the methyl derivatives from series 2. The hexyl derivative, 2, and the benzyl derivative, 5, showed two- to four-fold more potent MICs compared to **1**. 6, the *p*-trifluorobenzyl derivative consistently showed slightly diminished potency across all strains, while the *p*-methylbenzyl derivative 7 showed some of the most potent activity in this study. Interesting its constitutional isomer 8 also showed comparable activity.

The series 2 analogues, which all possess a methyl substituent at R_1, showed little to no inhibition of bacterial growth except for **10** and **11**. **10** is the constitutional isomer of **1** and shows near identical potency across all six strains. The dodecyl derivative **11** was the most potent of all series 2 compounds and exhibited comparable MIC values to several of the best series 1 derivatives. While derivatives from series 1 were generally more potent than the derivatives from series 2, consistent with the increase in lipophilicity, the *N*-dodecyl derivative in series 2, **11**, was substantially more potent than **3**. In addition to having unique potency in series 2, **11** proved to be bactericidal differentiating it from all the other analogues. The parent compound and all other analogues were bacteriostatic as defined by having MBC greater than four times the MIC (ESI† Table S1).[12–14]

None of the compounds showed activity against the Gram-negative pathogen *P. aeruginosa*. Previous work has shown that the armeniaspirols are not active against many Gram-negative pathogens including *Acinetobacter baumannii*, *Klebsiella pneumonia*, *Salmonella typhimurium*, *Shigella dysenteriae*.[4] Interestingly while **1** does not inhibit the growth of wild-type *Escherichia coli*, it does inhibit growth of an *E. coli* Δ*tolC* mutant (ESI† Table S4), suggesting efflux may be limiting activity in Gram-negative bacteria.[15,16]

Inhibition of recombinant purified ClpYQ

Mechanistically, armeniaspirol functions *via* inhibition of both the ATP-dependent proteases ClpXP and ClpYQ.[3] We

thus evaluated the ability of analogues with enhanced MIC potency relative to 1 for their ability to inhibit peptide hydrolysis by recombinant purified ClpYQ (Table 2, ESI† Fig. S1, ESI† Table S2). Given that ClpYQ from *S. aureus* was inactive in our *in vitro* biochemical assays, inhibition kinetics were performed on the characterized *B. subtilis* ClpYQ.[3]

A clear dose response curve was observed with all compounds for ClpYQ hydrolysis of 100 μM fluorogenic substrate Cbz-GGL-AMC. While all compounds exhibited more potent inhibition of ClpYQ, 7 showed the most potent inhibition of ClpYQ, consistent with its highly potent MICs. Given that 1 was shown to be competitive inhibitor of ClpYQ proteolysis activity,[3] we applied the Cheng–Prusoff relationship to determine K_I. 7 inhibits ClpYQ with a K_I = 150 ± 20 nM.

Inhibition of ClpXP activity in *S. aureus*

To evaluate the inhibition of ClpXP, a cell-based assay was developed. Although we were able to express and purify *S. aureus* ClpXP and the closely related *B. subtilis* ClpXP, we could only achieve single turnover for proteolysis under all conditions investigated. Recombinant purified *E. coli* ClpXP was active and inhibition kinetics could be readily obtained,[3] however the orthologs from Gram-negative *E. coli* are distantly related to the *S. aureus* proteins. Thus *E. coli* ClpXP inhibition data was expected to be of limited relevance to inhibition of *S. aureus* ClpXP. Because direct ClpP inhibition increases urease activity,[3,17] we were able to determine the minimum effective concentration (MEC) of a ClpXP inhibitor required to increase urease activity above background in MRSA USA300. Thus in Christensen's media supplemented with phenol red pH indicator, inhibition of ClpXP activity in MRSA USA300 will increase urease activity, hydrolyzing the urea in the media, releasing ammonia, and leading to a colour change from yellow to red as the pH of the media is increased.[3,17]

Compounds 1–14 were analyzed for their MEC for urease activation from concentrations of 0.067 μg mL^{-1} to 1 μg mL^{-1} (ESI† Table S3). As concentrations approached the MIC (within two fold), bacterial growth slowed. In all cases however, activation of urease by ClpXP inhibition could be detected prior to growth inhibition. The potent benzyl derivatives 5–8 showed similar but improved ClpXP activity compared to 1. Compound 2 containing a hexyl group at both R_1 and R_2 showed the most potent ClpXP inhibition with a MEC of 0.067 μg mL^{-1}.

Discussion

A series of focused derivatives of the natural product antibiotic armeniaspirol were synthesized and evaluated for antibiotic activity against clinically relevant pathogens including MRSA and VRE. Analogues that were more potent than the parent compound 1 were evaluated for their ability to inhibit ClpYQ and ClpXP, the biochemical targets of armeniaspirol.[3] The derivatives focused on diversifying the *N*-methyl moiety (R_2), which proved to be highly amenable to modification. Replacement of the *N*-methyl with *N*-hexyl, various *N*-benzyl, and *N*-phenethyl substituents lead to substantial increases in antibiotic activity and potency for inhibition of both ClpYQ and ClpXP. Replacement of the hexyl chain on the aryl core of armeniaspirol (R_1) with a methyl substituent lead to a series of analogues substituted on the amide nitrogen (series 2) that were less active than the corresponding hexyl analogues (series 1), with the exception of 11.

Armeniaspirol targets both ClpXP and ClpYQ.[3] While single target inhibitors of *Sa*ClpXP are known, without the additional ClpYQ inhibition activity, these compounds are not antibiotic.[17–24] Thus this dual target action is required to intervene sufficiently in the redundant proteolytic pathways that regulate the divisome and cell division. Over half of approved antibiotics since 2015 have multitarget mechanisms

Table 2 Kinetic parameters of potent analogues

Analogue	R_1 group	R_2 group	MEC_{ClpXP} (μg mL^{-1})	K_I ClpYQ (μM) (± std dev)	MIC (USA300 μg mL^{-1})
1	*n* C_6H_{13}	CH_3	1	3.2 ± 0.2	4
2	*n* C_6H_{13}	*n* C_6H_{13}	0.067	1.3 ± 0.2	1
5	*n* C_6H_{13}	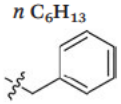	0.25	0.58 ± 0.05	1
6	*n* C_6H_{13}	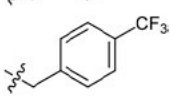	1	0.57 ± 0.10	2
7	*n* C_6H_{13}	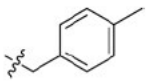	0.25	0.15 ± 0.02	0.5
8	*n* C_6H_{13}	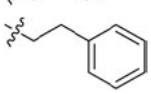	0.25	0.41 ± 0.07	0.5
11	CH_3	*n* $C_{12}H_{25}$	0.5	1.0 ± 0.2	1

of action,[25] likely due to their natural product origins.[26] Optimizing activity of compounds that inhibit multiple targets is challenging. The relevant substrate, cofactor, and allosteric regulator concentrations in the cell can impact the level of inhibition required at each target. Thus it is typically not possible to predict the optimal level of inhibition at each target for maximal effect. Structure–activity relationships at each target are needed as is a structure–activity relationship from an assay that integrates the function of both targets together. In the case of armeniaspirol analogues, the MIC assays provide the data integrating activity at both ClpYQ and ClpXP.

In general, increasing potency at either target appears to correlate with improved overall antibiotic activity. For example series 1 analogues **1**, **2**, and **7** show a steady ≈20-fold decrease in K_I for ClpYQ inhibition, which correlates with the 8-fold increase in potency as measured by MIC. Similarly, analogues **1**, **11** and **8** show a steady decrease in MEC, representative of inhibition of ClpXP, which correlates to a decrease in MIC against MRSA USA300. This data is consistent with armeniaspirol antibiotic activity being derived from both ClpXP and ClpYQ inhibition. In addition, the data suggests that inhibitory activity against both targets is balanced, since analogues that possess increased potency against ClpXP or ClpYQ, increase antibiotic activity.

Some analogues however show highly potent inhibition of one of the targets over the other. For example, **7** is a sub-micromolar inhibitor of ClpYQ (K_I = 150 ± 20 nM), however it is no more active in the MIC assays than the less potent **8** (K_I = 410 ± 70 nM) in MIC assays (MIC = 0.5 μg mL^{-1}). This is even more apparent with **2**, which shows ClpXP inhibition at 0.067 μg mL^{-1} but is no more active in MIC assays (MIC = 1.0 μg mL^{-1}) than **5**, which inhibits ClpXP at 0.25 μg mL^{-1}. These data suggest that as analogues become highly potent towards one of the targets, without significantly increasing the potency against the other, little increase in antibiotic activity is obtained.

The enhanced activity of the more lipophilic series 1 analogues over series 2 compounds raised concerns that activity was either a function of aggregation or non-specific lipophilicity-mediated affinity. To evaluate if aggregation of the analogues played a significant role in activity, the MICs for the parent compound **1** and the highly lipophilic **2** were determined in the presence of detergent. Addition of 0.01% v/v Triton X-100 had minimal impact on the MICs of either compounds against MRSA USA300 (ESI† Table S4). In further support of aggregation playing a limited role in activity, fitting of the ClpYQ does response data to an IC_{50} model where the slope could vary provided Hill coefficients of 1 to 1.5. In cases where aggregation plays a significant role in inhibition, steep slopes are frequently obtained, corresponding to Hill coefficients well below 1.5.[27] As such aggregation was not considered a major source of the increased potency observed for the more lipophilic analogues.

Careful examination of the data shows that activity is not simply a function of increased lipophilicity as the most lipophilic compounds **3** and **6** (highest cLog*P*s) were not the most potent in any of the assays. Though there does appear to be a correlation between low activity and low lipophilicity since **9** and **12**, two of the library members with the lowest clog*P* are some of the least active compounds. As the proteolytic chambers of both the ClpYQ and ClpXP must accommodate their unfolded protein clients whose hydrophobic cores are exposed, it stands to reason that moderately lipophilic inhibitors could be well suited to inhibition.

Models rationalizing the observed K_I and MEC data were generated by docking armeniaspirol into ClpP and ClpQ high resolution structures using AutoDock Vina.[28] Armeniaspirol showed two preferred binding site on the active conformation of the *S. aureus* ClpP heptamer (3V5E),[29] both of which were in the proteolytic cavity (Fig. 3 and ESI† Fig. S2A). The most frequent pose from the lowest energy docked structures showed armeniaspirol bound in the same site as seen for the binding of the ClpXP inhibitor bortezomib to *Thermus thermophilus* ClpP (6HWM, Fig. 3C).[30] Armeniaspirol, like bortezomib, H-bonds to backbone NHs at the C-terminal end of αC (ref. 30) *via* its ketone. In addition, our model shows the ketone H-bonding to the side chain of the active site Ser70. The hexyl chain engages in van der Waals interactions with the hydrophobic face of αE. Lastly the phenol of armeniaspirol H-bonds to His142 and Thr146 of αE. The second pose showed armeniaspirol bound closer to the N-terminus of ClpP, though still in the proteolytic chamber (ESI† Fig. S2A).

This ClpP binding model is in excellent accordance with the bortezomib *Tt*ClpP structure (Fig. 3C, inset 2) and is consistent with all current structure–activity relationship data. For example, both the phenol and ketone are required for antibiotic activity and in this model they both have discrete H-binding interactions with the target. Similarly, our current work shows that the hexyl chain of series 1 analogues is preferred over the methyl chain of series 2 analogues, consistent with the model showing the hexyl to be buried between αE and the loop between β6 and β7. Lastly the model shows significant space available for the *N*-methyl group to be replaced with varying *N*-alkyl groups, consistent with these *N*-alkyl analogues displaying potent inhibition of ClpP. While experimental evidence validating this model is clearly needed, it does provide for multiple testable atomic level hypothesis for inhibitor binding.

A model of armeniaspirol binding to the dodecamer of *S. aureus* ClpQ (6KUI) was also generated (Fig. 4),[31] with two main poses being observed. In the first pose (Fig. 4B) armeniaspirol is positioned at the active site, with the phenol hydrogen bonding to the active site Thr1 backbone NH and Thr29 side-chain. This pose is similar to that seen in the high resolution structure of the NLVS inhibitor bound to *Haemophilus influenzae* ClpQ (1KYI, Fig. 4C).[32] For example, Ser21 of *Hi*ClpQ, analogous to Thr29 of *Sa*ClpQ, H-bonds

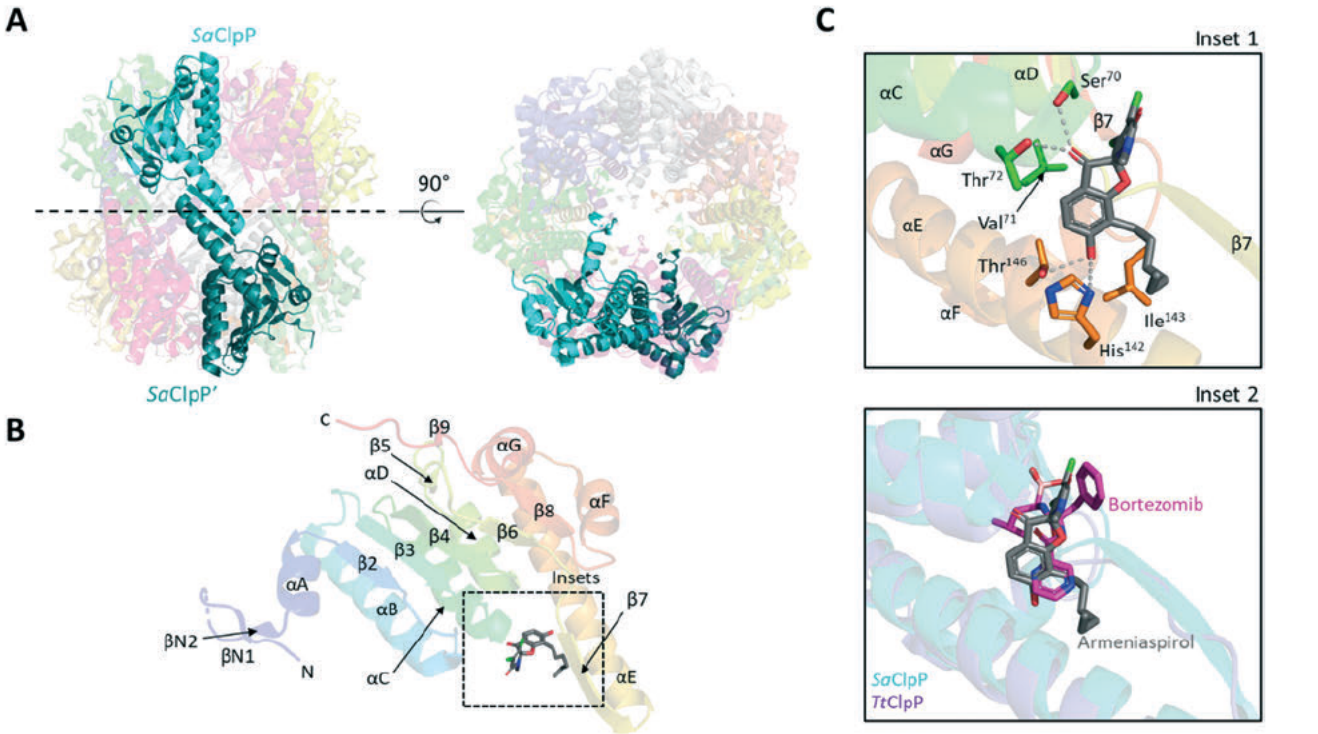

Fig. 3 Structure and docking results of *S. aureus* ClpP (3V5E). (A) Side and top views of *S. aureus* ClpP (SaClpP) tetradecamer. A single monomer per heptameric ring (transparent cartoons) are highlighted in cyan and dark cyan respectively. (B) Cartoon representation of the SaClpP monomer bound to armeniaspirol. Secondary structures are coloured in rainbow, helices are named by letters while strands are indicated by numbers. The dashed line box indicates the armeniaspirol binding site predicted by molecular docking. (C) Zoom in of armeniaspirol docking site in SaClpP. Possible residues involved in armeniaspirol binding are shown as sticks with proposed hydrogen bonds shown as grey dashed lines (inset 1). Overlay of *Thermus thermophilus* ClpP (TtClpP) bound to bortezomib (PDB: 6HWM) and SaClpP bound to armeniaspirol is shown (inset 2).

with the inhibitor. The armeniaspirol hexyl chain fits into the same S1 pocket as the aliphatic *i*Pr group from NLVS and packs against *Sa*ClpQ Val28, in an analogous fashion to *Hi*ClpQ Val20. The ketone of armeniaspirol engages with Gln32, and the amide carbonyl with Glu101, anchoring armeniaspirol in front of the active site. The second pose for armeniaspirol shows the compound bound at the interface between two protomers of one of the hexameric rings (ESI† Fig. S2B). While the ClpQ binding model agrees with known structure–activity data and the data generated from this study, it remains to be experimentally validated.

While both bortezomib and NLVS are covalent inhibitors of their respective targets ClpP and ClpQ,[30,32] **1** has been shown to be a competitive inhibitor of the peptide substrate in purified enzyme assays.[3] In the models of armeniaspirol bound to ClpP and ClpQ the electrophilic β-carbon of the α,β-unsaturated lactam is well removed from the active site nucleophiles, consistent with a competitive model for inhibition of proteolysis.

In addition to target binding, lipophilicity can impact off-target interactions.[5,33,34] In particular membrane targeting may be enhanced with increased lipophilicity. As such the hemolytic activity of **1** and two of the most potent and lipophilic analogues **2** and **8** was determined (Fig. S3†).[35] At 200 μM **1** showed less than 15% lysis of sheep erythrocytes whereas the more lipophilic **2** and **8** showed less than 5% hemolysis. Thus while lypophilic, the armeniaspirols do not destabilize mammalian red blood cell membranes at pharmacologically relevant concentrations. The toxicity of **1**, **2**, and **8** was also evaluated against human lung epithelial carcinoma (A549) cells. The cell culture cells were incubated with up to 100 μM compound, stained with calcein-AM and ethidium homodimer-1, and evaluated by both by confocal microscopy and flow cytometry to determine the fraction of viable and dead cells (Fig. S4†). All three compounds at 100 μM where indistinguishable from the vehicle control and showed a greater than 95% viable cell population.

Lipophilicity is also an important driver of protein binding, which can impact antibiotic pharmacokinetics and pharmacodynamics.[36] To evaluate the effect of protein binding on antimicrobial activity, we determined the MIC of **1** and the highly lipophilic **2** against MRSA USA300 in the presence of bovine serum albumin (Table S4†). Addition of serum suppressed antibiotic activity, consistent with a high degree of protein binding expected for these lipophilic compounds. For example, the MIC of the parent compound exceeded 32 μg mL^{-1} in the presence of BSA. However armeniaspirol is known to be active in an *in vivo* mouse model of MRSA septicaemia with 10 mg kg^{-1} i.p. delivery. Thus while this assay confirms that protein binding is a significant factor in the antibiotic activity of the armeniaspirols, the addition of serum albumin alone does

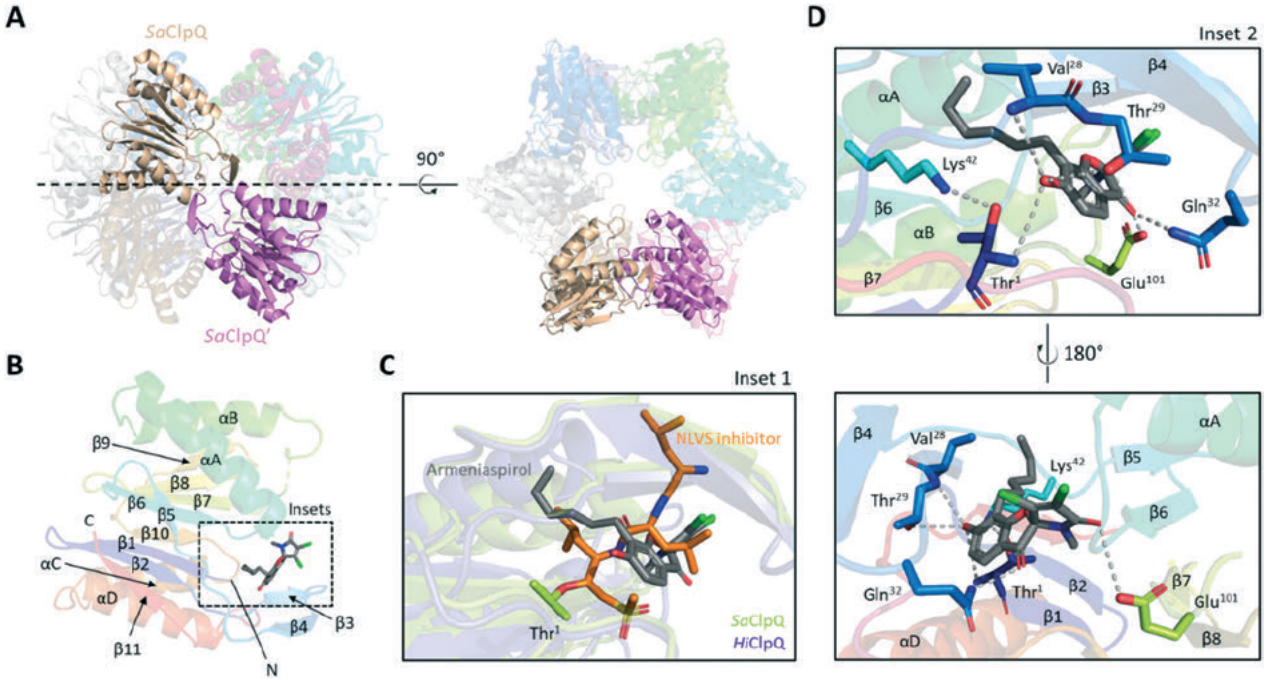

Fig. 4 Structure and docking results of *S. aureus* ClpQ (6KUI). (A) Side and top views of *S. aureus* ClpQ (*Sa*ClpQ) dodecamer. A single monomer per hexameric ring (transparent cartoons) are highlighted in sandstone and magenta respectively. (B) Cartoon representation of the *Sa*ClpQ monomer bound to armeniaspirol. Secondary structures are coloured in rainbow, helices are named by letters while strands are indicated by numbers. The dashed line box indicates the armeniaspirol binding site predicted by molecular docking. (C) Overlay of *Haemophilus influenzae* ClpQ (*Hi*ClpQ) covalently bound to a vinyl sulfone inhibitor (PDB: 1KYI) and *Sa*ClpQ bound to armeniaspirol (inset 1). (D) Zoom in of armeniaspirol docking site in *Sa*ClpQ. Possible residues involved in armeniaspirol binding are shown as sticks with proposed hydrogen bonds shown as grey dashed lines (inset 2).

not adequately model the pharmacodynamics behaviour of the drug *in vivo*.[37]

Conclusion

This study has provided new highly potent Gram-positive antibiotics active against clinically relevant strains of MRSA, including USA300 the most common community acquired MRSA infection. Our work has shown that the increased potency of analogues against ClpXP and ClpYQ correlates with increased antibiotic activity, strongly supporting the mechanism of action. We show that activity against both targets is balanced, such that increasing activity at either target increases antibiotic activity. Furthermore, while potency tracks loosely with lipophilicity, this is likely due to binding to the hydrophobic proteolysis chamber rather than non-selective binding interactions. Docking models support this hypothesis and show armeniaspirol may bind at the active site, but in a configuration that does not enable covalent modification of the active site nucleophiles, consistent with competitive inhibition of ClpXP and ClpYQ.

Author contributions

C. N. B and M. G. D. conceived of the study. M. G. D, M. H. D. and A. R. P. synthesized and characterized compounds. M. G. D., P. L. and C. N. collected MIC and MBC data. T. D. L. and P. L. collected ClpYQ inhibition data. M. G. D. collected ClpXP inhibition data. J. T. B.-H. performed docking studies. A. R. P. and M. D. collected hemolysis data. N. D. C. collected live human cell data. C. N. B. supervised and managed the study. All authors contributed to analysing data and writing and editing the manuscript.

Conflicts of interest

There are no conflicts of interest.

Acknowledgements

This work was funded by the Natural Sciences and Engineering Research Council of Canada (NSERC) (A. J. S. RGPIN 2021-03387; C. N. B RGPIN 2019-06859). The authors thank the John L. Holmes Mass Spectrometry Facility for assistance in acquiring mass spectrometry data and the University of Ottawa Faculty of Science NMR facility for assistance in collecting NMR spectra.

Notes and references

1 C. Dufour, J. Wink, M. Kurz, H. Kogler, H. Olivan, S. Sablé, W. Heyse, M. Gerlitz, L. Toti and A. Nußer, *et al.*, Isolation and structural elucidation of armeniaspirols A-C: Potent antibiotics against gram-positive pathogens, *Chem. – Eur. J.*, 2012, 18(50), 16123–16128.

2 C. Couturier, A. Bauer, A. Rey, C. Schroif-Dufour and M. Broenstrup, Armeniaspiroles, a new class of antibacterials: Antibacterial activities and total synthesis of 5-chloro-Armeniaspirole A, *Bioorg. Med. Chem. Lett.*, 2012, 22(19), 6292–6296.

3 P. Labana, M. H. Dornan, M. Lafrenière, T. L. Czarny, E. D. Brown, J. P. Pezacki and C. N. Boddy, Armeniaspirols inhibit the AAA+ proteases ClpXP and ClpYQ leading to cell division arrest in Gram-positive bacteria, *Cell Chem. Biol.*, 2021, 28(12), 1703–1715.

4 Y. Qiao, J. Yan, J. Jia, J. Xue, X. Qu, Y. Hu, Z. Deng, H. Bi and D. Zhu, Characterization of the biosynthetic gene cluster for the antibiotic armeniaspirols in streptomyces armeniacus, *J. Nat. Prod.*, 2019, 82(2), 318–323.

5 P. D. Leeson and B. Springthorpe, The influence of drug-like concepts on decision-making in medicinal chemistry, *Nat. Rev. Drug Discovery*, 2007, 6(11), 881–890.

6 D. G. Durham and A. H. Rees, Chlorination of Pyrroles. Part I, *Can. J. Chem.*, 1971, 49(1), 136–138.

7 W. Schäfer and B. Franck, Selektive Ätherspaltung von 4-Hydroxy-methoxy-chinolincarbonsäureestern, *Chem. Ber.*, 1966, 99(1), 160–164.

8 I. Wiegand, K. Hilpert and R. E. W. Hancock, Agar and broth dilution methods to determine the minimal inhibitory concentration (MIC) of antimicrobial substances, *Nat. Protoc.*, 2008, 3(2), 163–175.

9 Y. Chen, H. A. Crosby, W. F. Oosthuysen, D. J. Diekema, S. T. Kelley and A. R. Horswill, Draft genome sequence of usa100 methicillin-resistant Staphylococcus aureus strain 209, *Genome Announc.*, 2018, 6(1), e01399-17.

10 J. T. Weber, Community-associated methicillin-resistant Staphylococcus aureus, *Clin. Infect. Dis.*, 2005, 15, S269–S272.

11 J. M. King, K. Kulhankova, C. S. Stach, B. G. Vu and W. Salgado-Pabón, Phenotypes and Virulence among Staphylococcus aureus USA100, USA200, USA300, USA400, and USA600 Clonal Lineages, *mSphere*, 2016, 1(3), e00071-16.

12 M. E. Levison, Pharmacodynamics of antimicrobial drugs, *Infect. Dis. Clin. North Am.*, 2004, 451–465.

13 G. L. French, Bactericidal agents in the treatment of MRSA infections-the potential role of daptomycin, *J. Antimicrob. Chemother.*, 2006, 58, 1107–1117.

14 G. A. Pankey and L. D. Sabath, Clinical relevance of bacteriostatic versus bactericidal mechanisms of action in the treatment of gram-positive bacterial infections, *Clin. Infect. Dis.*, 2004, 38(6), 864–870.

15 I. T. Paulsen, J. H. Park, P. S. Choi and M. H. Saier, A family of gram-negative bacterial outer membrane factors that function in the export of proteins, carbohydrates, drugs and heavy metals from gram-negative bacteria, *FEMS Microbiol. Lett.*, 1997, 156(1), 1–8.

16 V. Koronakis, J. Eswaran and C. Hughes, Structure and function of TolC: the bacterial exit duct for proteins and drugs, *Annu. Rev. Biochem.*, 2004, 73, 467–489.

17 P. Gao, P. L. Ho, B. Yan, K. H. Sze, J. Davies and R. Y. T. Kao, Suppression of Staphylococcus aureus virulence by a small-molecule compound, *Proc. Natl. Acad. Sci. U. S. A.*, 2018, 115(31), 8003–8008.

18 T. Böttcher and S. A. Sieber, β-lactones as specific inhibitors of ClpP attenuate the production of extracellular virulence factors of Staphylococcus aureus, *J. Am. Chem. Soc.*, 2008, 130(44), 14400–14401.

19 E. Zeiler, V. S. Korotkov, K. Lorenz-Baath, T. Böttcher and S. A. Sieber, Development and characterization of improved β-lactone-based anti-virulence drugs targeting ClpP, *Bioorg. Med. Chem.*, 2012, 20(2), 583–591.

20 J. Krysiak, M. Stahl, J. Vomacka, C. Fetzer, M. Lakemeyer, A. Fux and S. A. Sieber, Quantitative Map of β-Lactone-Induced Virulence Regulation, *J. Proteome Res.*, 2017, 16(3), 1180–1192.

21 M. W. Hackl, M. Lakemeyer, M. Dahmen, M. Glaser, A. Pahl, K. Lorenz-Baath, T. Menzel, S. Sievers, T. Böttcher and I. Antes, *et al.*, Phenyl Esters Are Potent Inhibitors of Caseinolytic Protease P and Reveal a Stereogenic Switch for Deoligomerization, *J. Am. Chem. Soc.*, 2015, 137(26), 8475–8483.

22 A. Pahl, M. Lakemeyer, M. T. Vielberg, M. W. Hackl, J. Vomacka, V. S. Korotkov, M. L. Stein, C. Fetzer, K. Lorenz-Baath and K. Richter, *et al.*, Reversible Inhibitors Arrest ClpP in a Defined Conformational State that Can Be Revoked by ClpX Association, *Angew. Chem., Int. Ed.*, 2015, 54(52), 15892–15896.

23 M. Gersch, R. Kolb, F. Alte, M. Groll and S. A. Sieber, Disruption of oligomerization and dehydroalanine formation as mechanisms for ClpP protease inhibition, *J. Am. Chem. Soc.*, 2014, 136(4), 1360–1366.

24 C. Moreno-Cinos, K. Goossens, I. G. Salado, P. Van Der Veken, H. De Winter and K. Augustyns, ClpP protease, a promising antimicrobial target, *Int. J. Mol. Sci.*, 2019, 20(9), 2232.

25 C. Wetzel, M. Lonneman and C. Wu, Polypharmacological drug actions of recently FDA approved antibiotics, *Eur. J. Med. Chem.*, 2021, 112931.

26 T. T. Ho, Q. T. Tran and C. L. Chai, The polypharmacology of natural products, *Future Med. Chem.*, 2018, 10(11), 1361–1368.

27 B. K. Shoichet, Interpreting steep dose-response curves in early inhibitor discovery, *J. Med. Chem.*, 2006, 49(25), 7274–7277.

28 O. Trott and A. J. Olson, AutoDock Vina: Improving the speed and accuracy of docking with a new scoring function, efficient optimization, and multithreading, *J. Comput. Chem.*, 2009, 31(2), 455–461.

29 M. Gersch, A. List, M. Groll and S. A. Sieber, Insights into structural network responsible for oligomerization and activity of bacterial virulence regulator caseinolytic protease P (ClpP) protein, *J. Biol. Chem.*, 2012, 287(12), 9484–9494.

30 J. Felix, K. Weinhäupl, C. Chipot, F. Dehez, A. Hessel, D. F. Gauto, C. Morlot, O. Abian, I. Gutsche and A. Velazquez-Campoy, *et al.*, Mechanism of the allosteric activation of the ClpP protease machinery by substrates and active-site inhibitors, *Sci. Adv.*, 2019, 5(9), eaaw3818.

31 S. Jeong, J. Ahn, A. R. Kwon and N. C. Ha, Cleavage-Dependent Activation of ATP-Dependent Protease HslUV from Staphylococcus aureus, *Mol. Cells*, 2020, **43**(8), 694–704.

32 M. C. Sousa, B. M. Kessler, H. S. Overkleeft and D. B. McKay, Crystal Structure of HslUV Complexed with a Vinyl Sulfone Inhibitor: Corroboration of a Proposed Mechanism of Allosteric Activation of HslV by HslU, *J. Mol. Biol.*, 2002, **318**(3), 779–785.

33 A. L. Hopkins, J. S. Mason and J. P. Overington, Can we rationally design promiscuous drugs?, *Curr. Opin. Struct. Biol.*, 2006, **16**(1), 127–136, DOI: 10.1016/j.sbi.2006.01.013.

34 J.-U. Peters, P. Schnider, P. Mattei and M. Kansy, Pharmacological Promiscuity: Dependence on Compound Properties and Target Specificity in a Set of Recent Roche Compounds, *ChemMedChem*, 2009, **4**(4), 680–686.

35 B. C. Evans, C. E. Nelson, S. S. Yu, K. R. Beavers, A. J. Kim, H. Li, H. M. Nelson, T. D. Giorgio and C. L. Duvall, Ex vivo red blood cell hemolysis assay for the evaluation of pH-responsive endosomolytic agents for cytosolic delivery of biomacromolecular drugs, *J. Visualized Exp.*, 2013, **9**(73), e50166, DOI: 10.3791/50166.

36 M. A. Zeitlinger, H. Derendorf, J. W. Mouton, O. Cars, W. A. Craig, D. Andes and U. Theuretzbacher, Protein binding: do we ever learn?, *Antimicrob. Agents Chemother.*, 2011, **55**(7), 3067–3074, DOI: 10.1128/AAC.01433-10.

37 J. Beer, C. C. Wagner and M. Zeitlinger, Protein Binding of Antimicrobials: Methods for Quantification and for Investigation of its Impact on Bacterial Killing, *AAPS J.*, 2009, **11**(1), 1–12, DOI: 10.1208/s12248-008-9072-1.

Bioorg. Med. Chem. Lett. 84 (2023) 129210

Contents lists available at ScienceDirect

Bioorganic & Medicinal Chemistry Letters

journal homepage: www.elsevier.com/locate/bmcl

Armeniaspirol analogues disrupt the electrical potential (ΔΨ) of the proton motive force

Michael G. Darnowski [#], Taylor D. Lanosky [#], André R. Paquette, Christopher N. Boddy [*]

A B S T R A C T

The armeniaspirol family of natural product antibiotics have been shown to inhibit the ATP-dependent proteases ClpXP and ClpYQ and disrupt membrane potential through shuttling of protons across the membrane. Herein we investigate their ability to disrupt the proton motive force (PMF). We show, using a voltage sensitive, that armeniaspiols disrupt the electrical membrane potential (ΔΨ) component of the PMF and not the transmembrane proton gradient (ΔpH). Using checkerboard assays, we confirm this by showing antagonism, with kanamycin, an antibiotic that required ΔΨ for penetration. By evaluating the antibiotic activity and disruption of the PMF by sixteen armeniaspirol analogs, we find that disruption of the PMF is necessary but not sufficient for antibiotic activity. Analogs that are potent disruptors of the PMF without possessing the ability to inhibit ClpXP and ClpYQ are not potent antibiotics. Thus we propose that the armeniaspirols utilize a dual mechanism of action where they disrupt PMF and inhibit the ATP-dependent proteases ClpXP and ClpYQ. This type of dual mechanism has been observed in other natural product-based antibiotics, most notably chelocardin.

The armeniaspirol family of antibiotics are mixed polyketide non-ribosomal peptide natural products produced by the bacteria *Streptomyces armeniacus*.[1–4] They show potent antibiotic activity against Gram-positive pathogens such as methicillin-resistant *Staphylococcus aureus* (MRSA). Using a combination of chemoproteomics and *in vitro* biochemistry, armeniaspirol was shown to inhibit the AAA+ (ATPases Associated with diverse cellular Activities) bacterial proteases ClpYQ and ClpXP in the Gram-positive bacteria *Bacillus subtilis,* causing cell division arrest.[5] In addition, armeniaspirol has been reported to be a potent membrane depolarizing agent based on data from assays using voltage sensitive dyes in Gram-positive and -negative bacteria, ion conductance assays across a planar lipid bilayer, and pH-sensitive dyes encapsulated in unilamellar vesicles.[6] In this study we investigate disruption of the membrane potential by armeniaspirol and analogues thereof to refine our understanding of the mechanism of action of this class of compounds.

The proton motive force (PMF) in bacteria powers ATP synthesis and secondary active transport.[7] It consists of two components: the transmembrane electrical potential (ΔΨ) and the transmembrane proton gradient (ΔpH).[8] Proton pumps, primarily in the electron transport chain, generate the PMF. Because the bacterial cytosolic pH is kept constant, to maintain the PMF over a range of external pHs, ΔΨ can vary through the activity of cation-proton antiports[7] and metabolic proton consumption.[9] Thus ΔΨ and ΔpH work together to maintain the PMF.

Fluorescence assays based on the voltage sensitive dye $DiSC_3(5)$ can effectively distinguish between agents that disrupt ΔpH or ΔΨ of the PMF.[10] When bacteria are treated with the cationic $DiSC_3(5)$ dye, it accumulates within the membrane where its fluorescence is quenched. When the ΔΨ portion of the PMF is dissipated, the cationic dye is released into the media resulting in an increase in fluorescence. When the ΔpH is dissipated, the cell compensates by increasing ΔΨ and thus maintaining a constant PMF. This further concentrates $DiSC_3(5)$ within the membrane causing additional self quenching and an overall decrease in fluorescence.

Herein we show that the armeniaspirol family of natural products dissipate the ΔΨ of MRSA rather than shuttle protons across the membrane to dissipate ΔpH, as has been proposed.[6] Consistent with this observation, armeniaspirol has antagonistic activity when used with antibiotics that require ΔΨ for uptake and activity. Armeniaspirol analogues with the phenol protected, the proposed site for proton shuttling still disrupt membrane potential. By evaluating a number of armeniaspirol analogs[11] (Fig. 1), we show that potent disruption of the ΔΨ by this family of compounds is not sufficient for antibiotic activity. We hypothesize that disruption of ΔΨ in conjunction with inhibition of ClpXP and ClpYQ activity contributes to the overall mechanism of action of these compounds.

Excellent recent work by Arisetti and coworkers has shown that armeniaspirols disrupt the PMF.[6] They conclude that armeniaspirol is a

[#] Authors who have equally contributed to work.

https://doi.org/10.1016/j.bmcl.2023.129210
Received 24 January 2023; Received in revised form 22 February 2023; Accepted 25 February 2023
Available online 27 February 2023

protonophore, a class of molecules that can shuttle protons across the membrane, disrupting the transmembrane proton gradient ΔpH. Consistent with this hypothesis, modification of the phenol and carbonyl of armeniaspirol lead to compounds that did not disrupt the PMF, suggesting that deprotonation/protonation of the phenol, whose pKa was sufficiently lowered by electron withdrawing *p*-carbonyl substitution, was required for proton transfer across the membrane.

To evaluate if armeniaspirols were disrupting the PMF via dissipation of ΔΨ or the proton gradient ΔpH, we performed assays with the Nerstian voltage-dependent fluorescent dye $DiSC_3(5)$.[12] Valinomycin, a potent alkali cation transporter that selectively disrupts ΔΨ, leads to an increase in fluorescence when added to $DiSC_3(5)$-treated MRSA USA300 (Fig. 2a).[10,13] Like valinomycin, chloro-armeniaspirol, **1**, also showed a significant increase in fluorescence. Treatment with nigericin, which disrupts ΔpH, led to a decrease in fluorescence (Fig. 2a).[10] Based on these data, we suggest that armeniaspirols disrupt ΔΨ rather than ΔpH.

A number of antibiotics rely on either ΔΨ or ΔpH to cross bacterial cell membranes and act on their intracellular targets.[14] For example, aminoglycosides, like kanamycin, require ΔΨ for cell penetration in both Gram-positive bacteria like *S. aureus* and Gram-negatives such as *Escherichia coli*.[15] If **1** is disrupting ΔΨ, then it should act antagonistically when co-administered with kanamycin, reducing the potency of kanamycin. We thus evaluated synergy between potent armeniaspirol analogs **1**, **2,** and **7** and kanamycin in *E. coli ΔtolC*. From checkboard assays, the fractional inhibitory concentration (FIC) index for **1**, **2**, and **7** with kanamycin was >4 (Fig. 2b). FICs >4 are antagonistic,[16] further supporting the disruption of ΔΨ by armeniaspirols.

Tetracycline accumulation in *E. coli* is dependent on ΔpH.[17] A checkerboard assay of **1** with tetracycline in *E. coli Δtolc* shows no interaction (FIC 0.656, Fig. 2b). If armeniaspirols were disrupting ΔpH, then they should be antagonistic with tetracycline (FIC > 4). Our data is thus inconsistent with disruption of ΔpH by armeniaspirols. Disruption of ΔΨ is expected to result in no interaction (FIC 0.5–4) or a synergistic interaction (FIC < 0.5) between armeniaspirol and tetracycline.[18] Our data is thus consistent with disruption of ΔΨ.[19] We conclude that **1** is dissipating ΔΨ, not ΔpH.

Because **1** does not disrupt ΔpH, we hypothesized that the phenol, which is proposed to be required for protonophore activity, may not be essential to disrupt the PMF as measured by $DiSC_3(5)$ cell-based assays. We thus synthesized the methyl ether of chloro-armeniaspirol, **15**, and evaluated its ability to disrupt ΔΨ in MRSA. The free phenol, **1,** was a potent disruptor of ΔΨ, with a minimum effective concentration (MEC) of 0.5 μg/mL (Fig. 2C). However, **15** was also able to disrupt ΔΨ, though at a higher concentration with an MEC 4 μg/mL (Fig. 2C). **16**, which is the methyl ether of **2**, exhibits more potent disruption of the membrane potential than **1** (Fig. 2C). Thus, the phenol does not appear to be required for disruption of the PMF and furthermore is unlikely responsible for shuttling protons across the membrane as previously proposed.

To evaluate if disruption of the PMF is necessary and sufficient for antibiotic activity by the armeniaspirol analogs, we evaluated a panel of 16 armeniaspirol analogs, including **1** and two new analogs where the free phenol was protected as a methyl ether **15** and **16**, removing all ionizable protons. Compounds were evaluated for growth inhibitory activity against MRSA USA300 and the ability to disrupt membrane potential in MRSA USA300, as measured with $DiSC_3(5)$ and $DiOC_2(3)$, two different voltage sensitive dyes (Table 1).

If disruption of the PMF is necessary and sufficient for antibiotic activity, we hypothesized that the MIC and potency of membrane disruption should positively correlate. That is compounds that can disrupt membrane potential at lower concentrations should be antibiotic at lower concentrations. For this analysis we used all the compounds that displayed antibiotic activity (MIC ≤ 4 μg/mL) against MRSA USA300. Interestingly, the MEC required to observe membrane depolarization with $DiSC_3(5)$ shows a near-zero correlation with antibiotic activity as measured by MIC (Fig. S4). While there is a weak positive correlation between the $DiSC_3(5)$ and MIC data as measured by the Pearson product-moment correlation, it is not statistically significant (r(10) 0.41, p 0.23). Membrane depolarization as measured by the EC_{50} for change in $DiOC_2(3)$ fluorescence shows a similar near-zero correlation (Fig. S5) that is not statistically significant (r(10) 0.52, p 0.12). Interestingly, lipophilicity as evaluated by clogP did not correlated to MIC or $DiOC_2(3)$ EC_{50} values, though did correlated to $DiSC_3(5)$ MEC values (Figs. S6–S8).

Careful examination of the analogs shows that compounds with potent ability to disrupt membrane potential do not necessarily possess potent antibiotic activity. For example, **16** is able to disrupt membrane potential at 0.125 μg/mL as measured by the $DiSC_3(5)$ assay but is not antibiotic until 4 μg/mL against MRSA USA300. In contrast other compounds with the ability to disrupt membrane potential at 0.125 μg/mL, such as **7** and **8**, show potent antibiotic activity with MIC of 0.5 μg/mL. It is important to note that none of the non-antibiotic compounds (MIC > 4 μg/mL) are potent disruptors of membrane potential ($DiSC_3(5)$ MEC ≤ 0.5 μg/mL). These data are thus most consistent with the hypothesis that membrane disruption is necessary for antibiotic activity, but it is not sufficient.

Some natural product-based antibiotics have more than one mechanism of action.[20] For example tetracycline binds the 30S ribosomal subunit inhibiting protein synthesis[21] and distorts lipid organization in

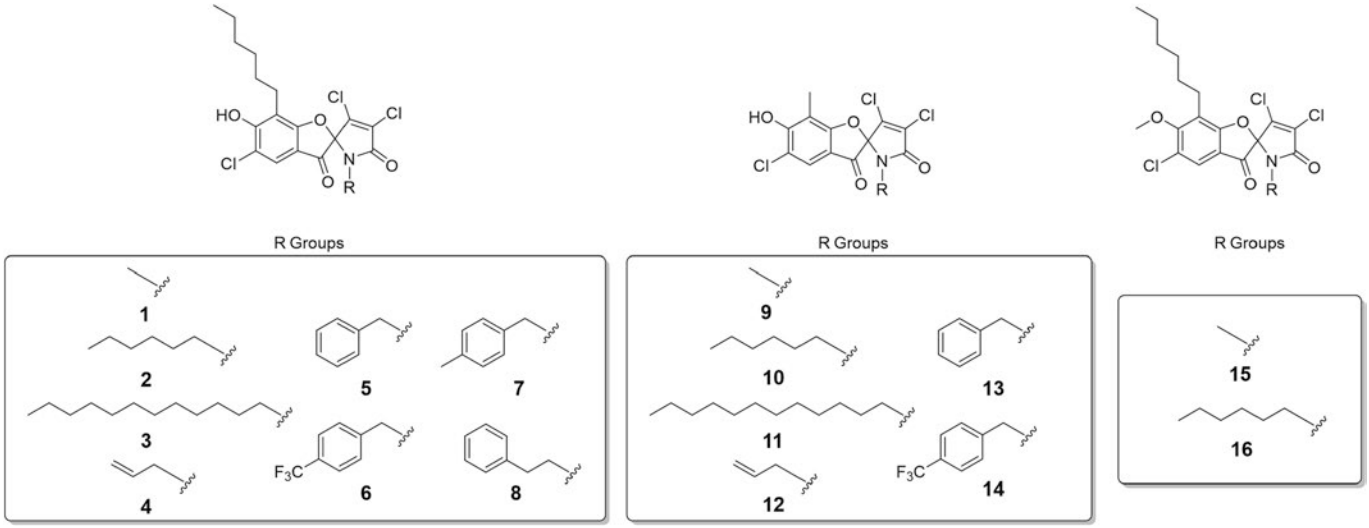

Fig. 1. The structure of the armeniaspirol analogs investigated in this study.

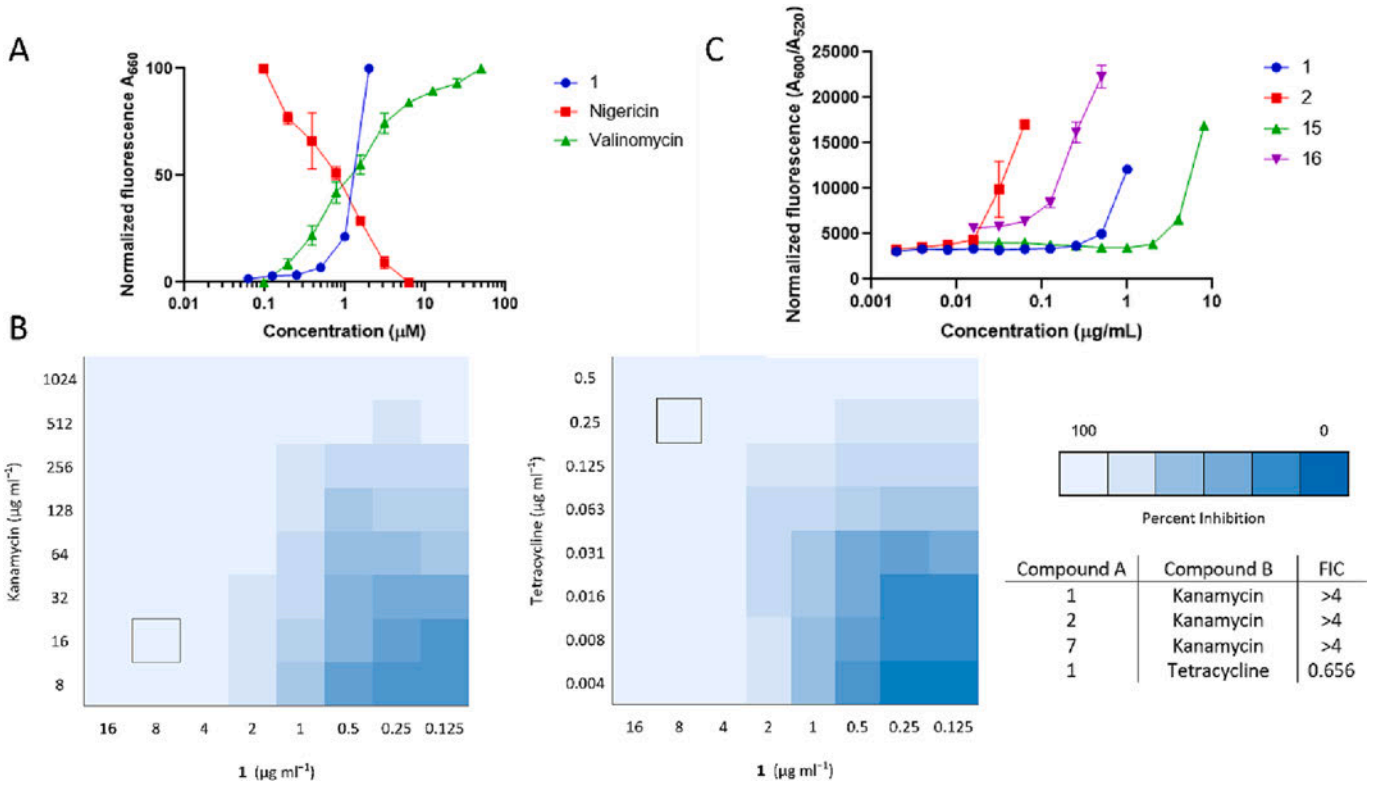

Fig. 2. 1 dissipates ΔΨ, not ΔpH. A Normalized fluorescence response of MRSA USA300 loaded with the voltage sensitive dye $DiSC_3(5)$ following treatment with 1, valinomycin, and nigericin. B Checkerboard assays showing antagonism of 1 with aminoglycoside kanamycin and no interaction of 1 and tetracycline in E. coli ΔtolC. MICs of 1, kanamycin, and tetracycline alone are 8 μg ml ^{1}, 16 μg ml ^{1}, and 0.25 μg ml ^{1}, respectively in E. coli ΔtolC (MICs are shown as the boxed square on checkerboard asssay). FIC indexes for 1, 2, and 7 with kanamycin and 1 with tetracycline are reported (see Fig. S3). C. Normalized fluorescence response of MRSA USA300 loaded with the voltage sensitive dye $DiSC_3(5)$ and treated with 1, 2, 15 and 16. 15 and 16, which lack an ionizable proton, retained ability to disrupt the PMF.

Table 1
Antibiotic, membrane disruption, and physicochemical properties of analogs.

Compound	MIC (μg/mL)	$DiSC_3(5)$ MEC (μg/mL)	$DiOC_2(3)$ EC_{50} (μg/mL) ± std error	clogP
1	4	0.5	0.42 ± 0.09	4.94
2	1	0.03125	0.07 ± 0.003	7.39
3	16	>1	>8	9.23
4	4	0.25	0.23 ± 0.01	5.59
5	1	0.5	0.39 ± 0.03	6.34
6	2	0.125	0.30 ± 0.01	7.24
7	0.5	0.125	0.07 ± 0.002	6.79
8	0.5	0.125	0.12 ± 0.007	6.75
9	>32	8	>8	2.52
10	4	0.5	0.17 ± 0.01	4.96
11	1	0.25	0.28 ± 0.01	7.99
12	>32	8	>8	3.16
13	32	4	3.20 ± 0.25	3.91
14	16	2	2.45 ± 0.22	4.81
15	>32	4	2.04 ± 0.09	5.22
16	4	0.125	0.54 ± 0.02	7.67

the membrane in a ribosome binding-independent manner.[22] The tetracycline analog chelocardin inhibits translation and causes membrane depolarization, with both mechanisms likely contributing to its antibiotic activity.[17] We thus propose that membrane depolarization and inhibition of ClpXP and ClpYQ are both required for antibiotic function of the armeniaspirol family of natural products (Table S3). Consistent with this, **16,** is not particularly antibiotic, however is a potent depolarizing agent yet shows little to no ability to inhibit ClpYQ activity in an *in vitro* assay or the ability to inhibit ClpXP in a cell-based assay. Intriguingly since ClpXP and ClpYQ are ATP-dependent proteases and membrane potential plays an essential role in ATP synthesis, it is not unreasonable to suggest that reduction of the membrane potential could synergize with inhibition of these cellular targets.

Herein we have used voltage-sensitive dyes to show that the armeniaspirol family of natural products, which are Gram-positive antibiotics, disrupt the proton motive force in MRSA USA300 by dissipating the transmembrane electrical potential (ΔΨ) rather than the proton gradient (ΔpH). This is supported by armeniaspirol acting antagonistically in checkerboard synergy assays with kanamycin, an antibiotic known to require ΔΨ for penetration in bacteria. Checkerboard assays show armeniaspirol to be indifferent when tested in a synergy assay with tetracycline, an antibiotic known to require the proton gradient to accumulate in Gram-positive bacteria. While all armeniaspirol analogs tested in this study that displayed antibiotic activity were able to disrupt membrane potential, not all compounds that disrupted membrane potential were potent antibiotics. **16** was a potent disruptor of the membrane potential but not an inhibitor of the ATP-dependent proteases ClpXP and ClpYQ, suggesting that both mechanisms may be required for antibiotic activity. This is akin to the inhibition of translation and membrane disruption of chelocardin or the inhibition of dihydrofolate reductase and membrane disruption of SCH-79797.[23] A clear benefit of this dual mechanism is that it should suppress the emergence of armeniaspirol-resistant mutants. This is borne out experimentally since armeniaspirol-resistant MRSA strains cannot be readily generated.[2]

Declaration of Competing Interest

The authors declare the following financial interests/personal relationships which may be considered as potential competing interests: Christopher N Boddy reports financial support was provided by Natural

Sciences and Engineering Research Council of Canada.

Data availability

Data will be made available on request.

Appendix A. Supplementary data

Supplementary data to this article can be found online at https://doi.org/10.1016/j.bmcl.2023.129210.

References

1 Couturier C, Bauer A, Rey A, Schroif-Dufour C, Broenstrup M. Armeniaspiroles, a new class of antibacterials: Antibacterial activities and total synthesis of 5-chloro-Armeniaspirole A. *Bioorganic Med Chem Lett*. 2012;22:6292–6296. https://doi.org/10.1016/J.BMCL.2012.06.107.

2 Dufour C, Wink J, Kurz M, et al. Isolation and structural elucidation of armeniaspirols A-C: Potent antibiotics against gram-positive pathogens. *Chem - A Eur J*. 2012;18:16123–16128. https://doi.org/10.1002/chem.201201635.

3 Fu C, Xie F, Hoffmann J, et al. Armeniaspirol antibiotic biosynthesis: chlorination and oxidative dechlorination steps affording spiro[4.4]non-8-ene. *Chembiochem*. 2019;20:764–769. https://doi.org/10.1002/CBIC.201800791.

4 Qiao Y, Yan J, Jia J, et al. Characterization of the biosynthetic gene cluster for the antibiotic armeniaspirols in Streptomyces armeniacus. *J Nat Prod*. 2019;82:318–323. https://doi.org/10.1021/acs.jnatprod.8b00753.

5 Labana P, Dornan MH, Lafrenière M, et al. Armeniaspirols inhibit the AAA+ proteases ClpXP and ClpYQ leading to cell division arrest in Gram-positive bacteria. *Cell Chem Biol*. 2021;28:1703–1715.e11. https://doi.org/10.1016/J.CHEMBIOL.2021.07.001.

6 Arisetti N, Fuchs HLS, Coetzee J, et al. Total synthesis and mechanism of action of the antibiotic armeniaspirol A. *Chem Sci*. 2021;12:16023–16034. https://doi.org/10.1039/d1sc04290d.

7 Padan E, Bibi E, Ito M, Krulwich TA. Alkaline pH homeostasis in bacteria: New insights. *Biochim Biophys Acta - Biomembr*. 2005;1717:67–88. https://doi.org/10.1016/J.BBAMEM.2005.09.010.

8 Benarroch JM, Asally M. The microbiologist's guide to membrane potential dynamics. *Trends Microbiol*. 2020;28:304–314. https://doi.org/10.1016/J.TIM.2019.12.008.

9 Guan N, Liu L. Microbial response to acid stress: mechanisms and applications. *Appl Microbiol Biotechnol*. 2020;104:51. https://doi.org/10.1007/S00253-019-10226-1.

10 Farha MA, Verschoor CP, Bowdish D, Brown ED. Collapsing the proton motive force to identify synergistic combinations against Staphylococcus aureus. *Chem Biol*. 2013;20:1168–1178. https://doi.org/10.1016/J.CHEMBIOL.2013.07.006.

11 Darnowski MG, Lanosky TD, Labana P, et al. Armeniaspirol analogues with more potent Gram-positive antibiotic activity show enhanced inhibition of the ATP-dependent proteases ClpXP and ClpYQ. *RSC Med Chem*. 2022;13:436–444. https://doi.org/10.1039/D1MD00355K.

12 Darnowski MG, Lanosky TD, Paquette AR, Boddy CN. Synthesis of a constitutional isomer of armeniaspirol A, Pseudoarmeniaspirol A, via lewis acid-mediated rearrangement. *J Org Chem*. 2022;87:15634–15643. https://doi.org/10.1021/acs.joc.2c02331.

13 King JM, Kulhankova K, Stach CS, Vu BG, Salgado-Pabón W. Phenotypes and virulence among Staphylococcus aureus USA100, USA200, USA300, USA400, and USA600 clonal lineages. *mSphere*. 2016;1. https://doi.org/10.1128/MSPHERE.00071-16.

14 Chopra I. Molecular mechanisms involved in the transport of antibiotics into bacteria. *Parasitology*. 1988;96:S25–S44. https://doi.org/10.1017/S0031182000085966.

15 Taber HW, Mueller JP, Miller PF, Arrow AS. Bacterial uptake of aminoglycoside antibiotics. *Microbiol Rev*. 1987;51:439. https://doi.org/10.1128/MR.51.4.439-457.1987.

16 Odds FC. Editorial synergy, antagonism, and what the chequerboard puts between them. *J Antimicrob Chemother*. 2003;52:1. https://doi.org/10.1093/jac/dkg301.

17 Yamaguchi A, Ohmori H, Kaneko-Ohdera M, Nomura T, Sawai T. ΔpH-dependent accumulation of tetracycline in Escherichia coli. *Antimicrob Agents Chemother*. 1991;35:53–56. https://doi.org/10.1128/AAC.35.1.53.

18 Meletiadis J, Pournaras S, Roilides E, Walsh TJ. Defining fractional inhibitory concentration index cutoffs for additive interactions based on self-drug additive combinations, Monte Carlo simulation analysis, and in vitro-in vivo correlation data for antifungal drug combinations against Aspergillus fumigatus. *Antimicrob Agents Chemother*. 2010;54:602–609. https://doi.org/10.1128/AAC.00999-09.

19 Ejim L, Farha MA, Falconer SB, et al. Combinations of antibiotics and nonantibiotic drugs enhance antimicrobial efficacy. *Nat Chem Biol*. 2011;7:348–350. https://doi.org/10.1038/nchembio.559.

20 Gray DA, Wenzel M. Multitarget approaches against multiresistant superbugs. *ACS Infect Dis*. 2020;6:1346. https://doi.org/10.1021/ACSINFECDIS.0C00001.

21 Chopra I, Roberts M. Tetracycline antibiotics: mode of action, applications, molecular biology, and epidemiology of bacterial resistance. *Microbiol Mol Biol Rev: MMBR*. 2001;65:232. https://doi.org/10.1128/MMBR.65.2.232-260.2001.

22 Wenzel M, Dekker MP, Wang B, et al. A flat embedding method for transmission electron microscopy reveals an unknown mechanism of tetracycline. *Commun Biol*. 2021;4:306. https://doi.org/10.1038/S42003-021-01809-8.

23 Martin JK, Sheehan JP, Bratton BP, et al. A dual-mechanism antibiotic kills gram-negative bacteria and avoids drug resistance. *Cell*. 2020;181:1518. https://doi.org/10.1016/J.CELL.2020.05.005.

JOC The Journal of Organic Chemistry

pubs.acs.org/joc Article

Synthesis of a Constitutional Isomer of Armeniaspirol A, Pseudoarmeniaspirol A, via Lewis Acid-Mediated Rearrangement

Michael G. Darnowski, Taylor D. Lanosky, André R. Paquette, and Christopher N. Boddy*

Cite This: J. Org. Chem. 2022, 87, 15634−15643 Read Online

ACCESS | Metrics & More | Article Recommendations | Supporting Information

ABSTRACT: The natural product armeniaspirol possesses a unique spirocyclic N,O-ketal in an α,β-dichloro-α,β-unsaturated lactam scaffold that has proved challenging to synthesize. Herein, we characterize the oxidative chlorination of pyrrole-2-carboxylate derivatives that rapidly generates this scaffold. The scope of this oxidation was extended to a series of esters and amides. Pyrrole-2-ketones could not be converted into the lactam due to an oxidative fragmentation. This result was unexpected since chloro-armeniaspirol has been synthesized via oxidative chlorination of a pyrrole-2-ketone. Examination of this successful oxidation showed that the desired scaffold was accessed due to intramolecular trapping from the neighboring free phenol, preventing fragmentation. Using the product of methyl *N*-methyl pyrrole-2-carboxylate oxidation 7b, we attempted to access the natural product armeniaspirol 2; however, an unanticipated Lewis acid-mediated rearrangement led to formation of a constitutional isomer, pseudoarmeniaspirol A 1. A small panel of pseudoarmeniaspirol analogues was synthesized and evaluated for antibiotic activity, inhibition of the targets of armeniaspirol, ClpXP and ClpYQ, and protonophore activity. While pseudoarmeniaspirol shows antibiotic activity, it does not target ClpXP or ClpYQ and has less protonophore activity than the natural product.

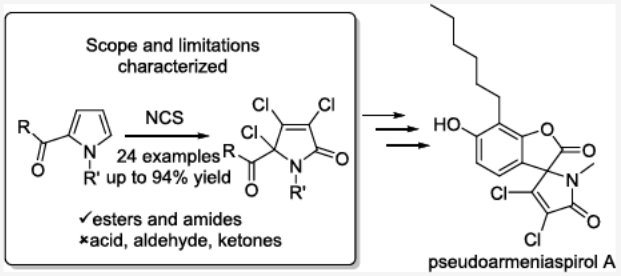

INTRODUCTION

The natural product family of the armeniaspirols contains a unique and unusual spiro-[4.4]non-8-ene scaffold that has been challenging to generate (Figure 1A).[1,2] This N,O-ketal spirocyclic scaffold can be accessed from a pyrrole derivative through an oxidative chlorination strategy. Treatment of the pyrrole 3 with N-chlorosuccinimide (NCS) leads to oxidation of the pyrrole ring and installation of the desired 3,4-dichloro-σ,β-unsaturated lactam and the spiro N,O-ketal, all-in-one operation (Figure 1B).[2,3] This reaction furnishes the core of armeniaspirol swiftly. However, it also installed an undesired chlorine at the 5-position on the electron-rich aryl ring, which is not present in the natural product. While this route has proven effective at synthesizing a series of analogs of 2, a number of which showed increased antibiotic activity against Gram-positive pathogens,[3] it has not yielded a total synthesis of armenaispirol. Recently however, the total synthesis of (±)-armeniaspirol A, 2, was elegantly solved using an oxidative radical cross coupling and [3 + 2] cycloaddition (Figure 1C).[4] Herein, we disclose a strategy based on an intramolecular Friedel−Crafts acylation that yields a constitutional isomer of armeniaspirol A, pseudoarmenaispirol A, 1, through an unexpected rearrangement (Figure 1A).

RESULTS AND DISCUSSION

To prevent undesired chlorination, a route where the pyrrole was oxidized to the dichloro-α,β-unsaturated lactam prior to installation of the electron rich aryl ring was envisioned. Pioneering work by Durham and Rees reported that chlorination of the methyl ester of pyrrole carboxylic acid generated a lactam with the appropriate functionalization for the synthesis of armeniaspirol A.[5] We thus envisioned installing the aryl ring after oxidation of the pyrrole and effecting an intramolecular Friedel−Crafts acylation to generate the complete framework of 2 (Figure 2).

The oxidative conversion of pyrrole carboxylic acids into α,β-unsaturated α,β-dichlorinated lactams has not been well characterized. Durham and Rees initially reported the reaction in 1971; however, their structural assignment was tentative and relied primarily on mass spectrometry fragmentation patterns.[5] Thus, we set out to investigate the scope of this key oxidative transformation by varying the substituents on the pyrrole nitrogen as well as the electron-withdrawing groups at the 2-position.

Substitution of the pyrrole nitrogen did not impact the reaction (Table 1). Esters of pyrrole-2-carboxylic acid (both NH and N-alkyl, 7a−d) underwent smooth oxidation to the lactam when treated with 4 equivalents of NCS. Similarly, treatment of

Received: September 28, 2022
Published: November 2, 2022

https://doi.org/10.1021/acs.joc.2c02331
J. Org. Chem. 2022, 87, 15634−15643

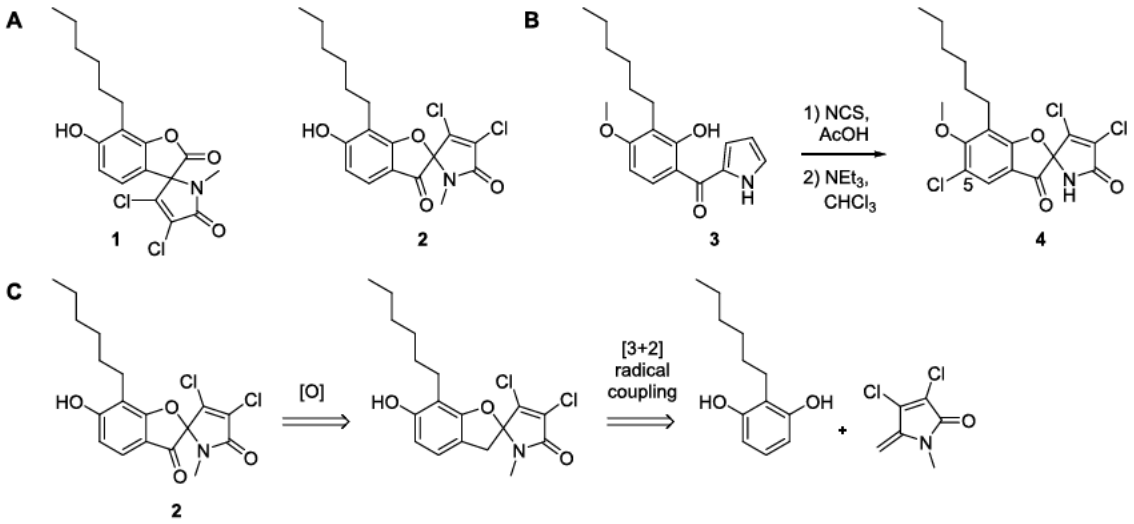

Figure 1. (A) Structures of (±)-pseudoarmeniaspirol A, **1**, and (±)-armeniaspirol A, **2**. (B) NCS-mediated oxidative chlorination used to generate the skeleton of armeniaspirol along with undesired chlorination at the 5 position. (C) Previous retrosynthetic disconnection of (±)-armeniaspirol A.

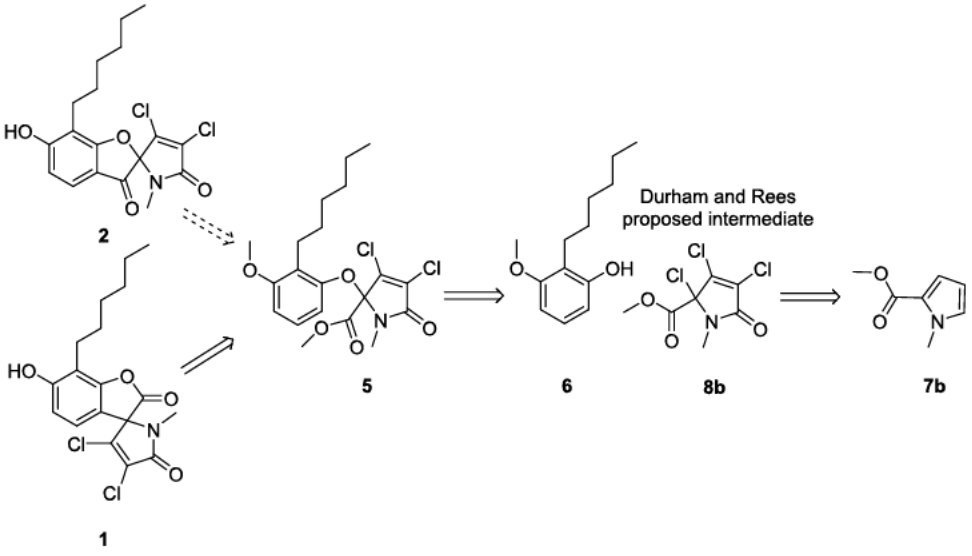

Figure 2. Retrosynthetic analysis of (±)-pseudoarmeniaspirol A from early stage oxidation of the pyrrole moiety.

the *N*-methyl pyrrole methyl ester with 4 equivalents of N-bromosuccinimide generated the corresponding brominated compound **18**. The presence of a stereogenic center in the alkyl chain in **7e** did not impede the NCS-mediated oxidation, though it did not significantly bias the facial selectivity of pyrrole oxidation, generating a 1:1.2 ratio of diastereomeric products. The *N*-Boc and *N*-tosyl protected pyrroles were oxidized by NCS; however, the protecting groups were lost during the reaction **7w–x**. To probe the substrate scope at the 2-position, a series of *N*-methyl pyrrole 2-carboxylic acid esters were screened, **7f–i**. All oxidized smoothly to the expected lactam product. Interestingly, neither the carboxylic acid, ketones, or the aldehyde yielded any of the expected product **7l–q**.

The observation that ketones **7l–n** were not successfully oxidized was particularly surprising. In the case of armeniaspirol, which contains a ketone, NCS successfully oxidizes the pyrrole to the chlorinated lactam. A key difference between the simple pyrrole substrate and the chloro-armeniaspirol example is the trapping of the lactam γ-position by the intramolecular phenol (Figure 3A). This trapping is clearly important since when the intramolecular phenol is protected as a methyl ether in **9**, NCS-mediated oxidation of the pyrrole leads to oxidative cleavage of the C–C bond linking the pyrrole to the ketone, resulting in **10** (Figure 3B). The oxidative cleavage is consistent with Cue and Chamberlin's observations that chlorination of a related pyrrolophenone leads to oxidative cleavage of the pyrrole carbonyl bond and formation of 5-chloro pyrrole.[6]

Based on our results and Cue and Chamberlin's work,[6] we propose that formation of the 5-chloropyrrolium intermediate leads to fragmentation into the 5-chloropyrrole and the acylium ion (Figure 3D, R = alkyl), which is converted into the acid on aqueous work up.[5] To test this, we investigated the oxidation of pyrrole carboxylic acid with excess NCS. We predicted that chlorination to trichloropyrrole carboxylic acid would occur followed by formation of the 5-chloropyrrolium and decarboxylation to the tetrachloropyrrole, which can be further oxidized to dichloromaleic anhydride (Figure 3C). We were pleased to see that both the tetrachloropyrrole **11** and dichloromaleic anhydride **12** were readily isolated from treatment of pyrrole 2-carboxylic acid with excess NCS. As mass spectrometry-based

https://doi.org/10.1021/acs.joc.2c02331
J. Org. Chem. 2022, 87, 15634–15643

Table 1. Scope of NCS-Mediated Chlorination of Pyrrole 2-Carbonyl Compounds[a]

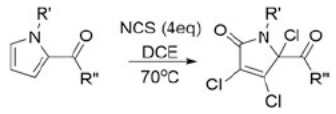

Entry	R′	R″	Yield (%)
a	H	O	94
b	CH_3	O	91
c	n-C_6H_{13}	O	84
d	n-$C_{12}H_{25}$	O	81
e	O	O	78
f	CH_3	O	81
g	CH_3	O	77
h	CH_3	O Si	74
i	H	O	84
j	H	N H	80
k	H	N	72
l	H	CH_3	nd
m	CH_3		nd
n	CH_3		nd
o	CH_3	H	nd
p	H	OH	nd
q	CH_3	CCl_3	nd
r	H	N H	nd
s	H	N H	nd
t	H	N O	nd
u	H	S	nd
v	H	S	nd
w	O S O	O	nd
x	O O O	O	nd

[a]nd = not detected.

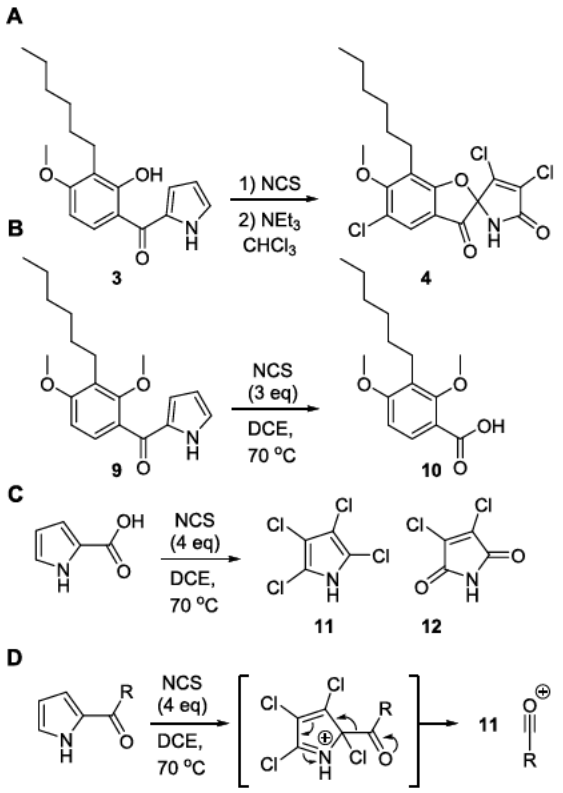

Figure 3. (A) Productive ketone oxidative chlorination via intramolecular phenol trapping. (B) Fate of protected phenol in the armeniaspirol system. (C) Fate of pyrrole carboxylic acid derivative under oxidative chlorination conditions. (D) Mechanistic proposal for C−C bond fragmentation when R = alkyl. C−C bond fragmentation does not occur when R = NHR′ or R = OR′.

characterization of **11** proved challenging,[7,8] authentic **11** was generated by treating pyrrole with excess sulfuryl chloride (Figure S5).[9] This compound proved identical in all respect to **11** generated from treatment of pyrrole 2-carboxylic acid with excess NCS.

Based on this mechanistic analysis, we proposed that amides, like esters, should be effectively converted into the chlorinated lactams. In amides and esters, the loss of the high energy alkylisocyanate ion (Figure 3D, R = NHR′) and alkoxylcarbonyl cation (Figure 3D, R = OR′)[10,11] (versus the acylium ions in ketone (Figure 3D, R = alkyl)) is expected to be slow, preventing unwanted C−C bond cleavage. Consistent with this hypothesis, propyl and piperidine amides were converted into the chlorinated lactams **8j,k**. The benzyl and propargylic amides **7r,s** however were not, presumably due to the oxidative cleavage of the benzyl and propargyl groups.[12] Similarly, thioesters **7u,v** were also not converted into the expected lactam due to rapid sulfur oxidation followed by decomposition.

To gain further insight into the successful oxidation of **3** into **4**, we evaluated its conversion by stepwise addition of NCS equivalents by NMR spectroscopy. Addition of three equivalents of NCS generated the trichloro intermediate **13**. Addition of another equivalent of NCS yielded an equal mixture of starting material **13** and the doubly oxidized product **14** (Figure 4). Thus, we proposed that the 4-chloropyrrolium ion is generated[13] and trapped by the neighboring phenol to install the desired spirocyclic center. The resulting enamine is then rapidly α-chlorinated, and the resulting protonated imidoyl chloride hydrolyzes, yielding the lactam **14**. The formation of an equal molar ratio of starting material to product suggests that the second chlorination step is significantly faster than the first,

https://doi.org/10.1021/acs.joc.2c02331
J. Org. Chem. 2022, 87, 15634−15643

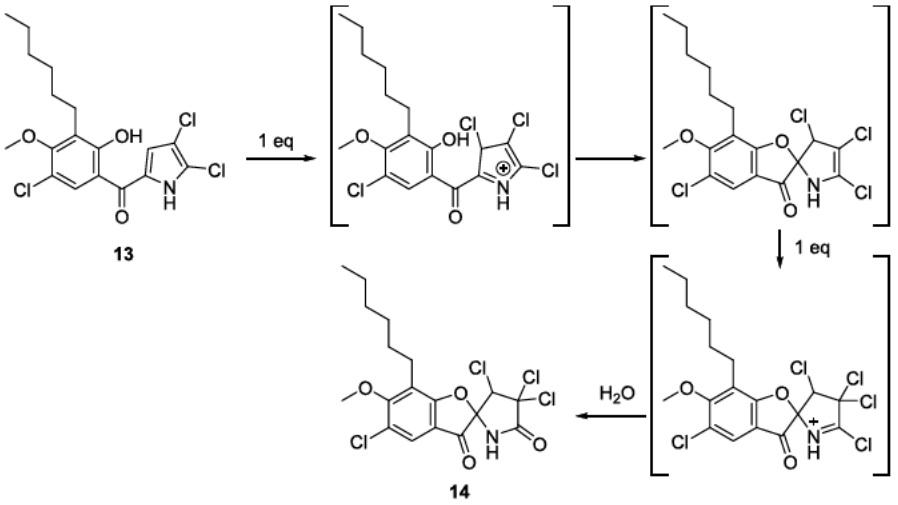

Figure 4. Proposed mechanism of pyrrole ketone oxidative chlorination on the route to (±)-chloro-armeniasprol A.

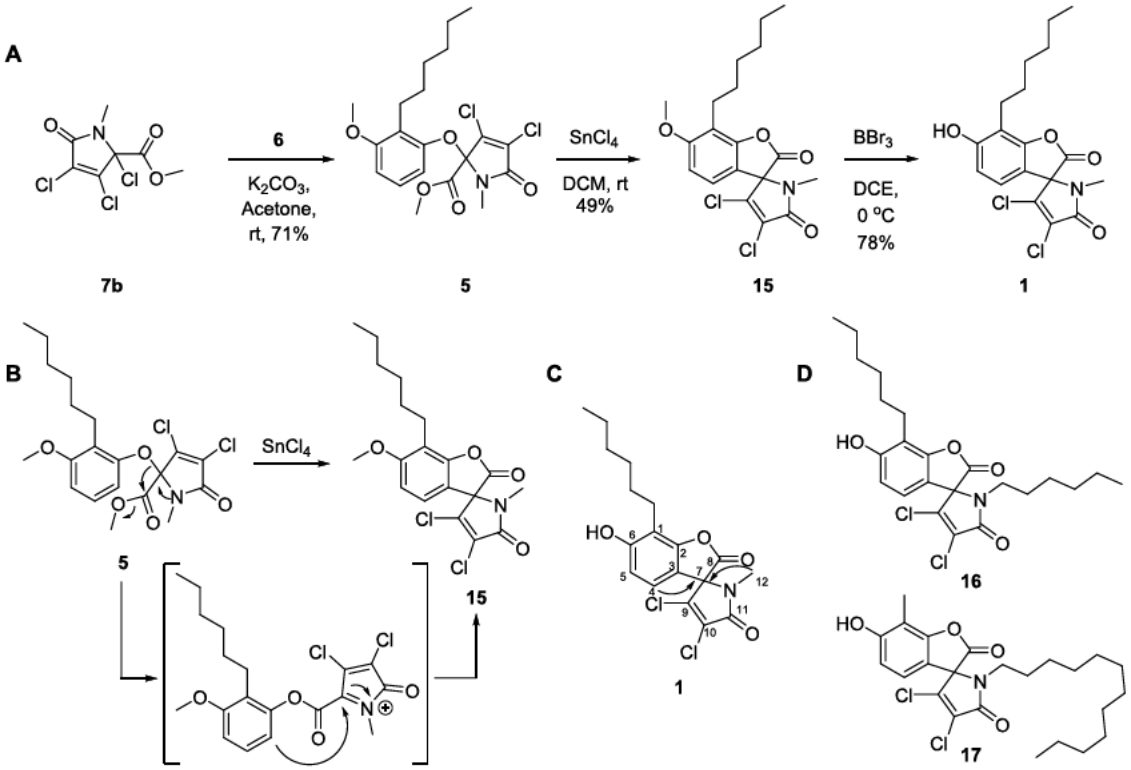

Figure 5. (A) Route to synthesis of (±)-pseudoarmeniaspirol. (B) Proposed Lewis acid-mediated skeletal rearrangement leading to the pseudoarmeniaspirol skeleton. (C) Key HMBC correlation in structure elucidation. (D) Analogues of pseudoarmeniaspirol.

consistent with the reactivity of the enamine versus an electron-poor pyrrole.

A published model study for the synthesis of chloro-armeniaspirol indicated an α,β,β-trichlorolactam species was the product of this oxidation.[2] However, our mechanistic hypothesis suggested the α,α,β-trichlorolactam regioisomer **14** was formed. We thus wanted to unambiguously assign the structure of the product. We therefore isolated **13** from treatment of **3** with 3 equivalents of NCS and subjected it to a single equivalent of NCS, generating a 1:1 mixture of **13** to **14**. **14** was isolated, and the structure was assigned by 1D and 2D NMR analysis, confirming the regiochemistry as the α,α,β-trichlorolactam.

Having evaluated the scope and mechanism of pyrrole chlorination, we had ready access to *N*-methyl lactam derivative **7b**. Treatment with 2-hexyl-3-methoxyphenol **6** and K_2CO_3 coupled the two halves of armeniaspirol and set the stage for the key Friedel–Crafts acylation (Figure 5).[14] All attempts to hydrolyze the methyl ester **5** resulted in decomposition. Derivatives with acid-labile and fluoride-sensitive esters similarly decomposed upon attempts to deprotect the acid (see Table S1). Because activated esters for the Friedel–Crafts acylation were not accessible, Lewis acid-mediated Friedel–Crafts acylation with the ester was attempted.[15,16] Tin(IV) chloride treatment led to a new product, and its ^{1}H NMR spectra was consistent with a tetrasubstituted aryl ring. Unfortunately the data was not consistent with that expected for the methyl ether

https://doi.org/10.1021/acs.joc.2c02331
J. Org. Chem. 2022, 87, 15634−15643

of the natural product. Structural elucidation by 1D and 2D NMR analysis revealed an unexpected rearrangement had occurred generating a constitutional isomer of the desired product where the spiro-center is connected directly to the aromatic ring, in **15**. Screening a wide variety of reaction conditions, Lewis acids, and additives did not yield conditions that suppressed this unwanted migration (Table S1). Final deprotection of the aryl ether yielded pseudoarmeniaspirol A, **1**, a constitutional isomer of armeniaspirol A.

With its structural similarity to **2**, we evaluated **1** and a small panel of analogs, **16** and **17**, for biological activity. **2** is a Gram-positive antibiotic active against methicillin-resistant *Staphylococcus aureus* (MRSA). **1** displayed comparable antibiotic activity with an MIC 4 μg/mL against MRSA USA300 (Table 2), the most common form of community-acquired MRSA

Table 2. Biological Evaluation of Constitutional Isomers of Armeniaspirol

	MEC_{ClpXP} (μg/mL)	K_I ClpYQ (μM) ($\pm$ std dev)	MIC (μg/mL)	$DiOC_2(3)$ IC_{50} (μg/mL)	$DiSC_3(5)$ EC_{50} (μg/mL)
Cl-Arm	1	3.2 $\pm$ 0.2	4	0.169	0.5
1	>1	<50	4	2.45	1
16	>1	<50	>32	4.75	>1
17	>1	<50	>32	1.82	0.25

infections. Synthetic chloro-armeniaspirol is known to inhibit proteolysis by recombinant purified ClpYQ *in vitro* with a K_I of 3.2 $\pm$ 0.2 μM and inhibit ClpXP activity in a cell-based assay at 1 μg/mL. **1** did not show any inhibition of ClpYQ even at 50 μM nor did it inhibit ClpXP at up to 1 μg/mL (Table 2). Lastly, armeniaspirol has been shown to possess protonophore activity. Thus, we evaluated pseudoarmeniaspirol for its ability to disrupt the proton gradient in bacterial cells using two different voltage-sensitive fluorescent dye assays. **1** showed significantly less protonophore activity than chloro-armeniaspirol in both assays. **16** and **17** were synthesized and evaluated for antibiotic activity. Neither compound possessed relevant antibiotic activity (Table 2). Thus, while **1** possesses comparable antibiotic activity to chloro-armeniaspirol, it does not appear to exert this activity through inhibition of the Clp proteases nor through disruption of the proton motive force.

In conclusion, we have elucidated the scope of pyrrole oxidative chlorination for accessing α,β-dichloro-α,β-unsaturated lactams. We have shown that oxidative C−C bond cleavage can occur in pyrroles substituted with aldehydes, ketones, or a carboxylic acid at the 2-position but does not occur with esters or amides. We show that the pyrrole oxidation in the synthesis of chloro-armeinaspirol, which occurs on a ketone-substituted pyrrole, does not lead to C-C bond cleavage due to the intramolecular trapping of a reaction intermediate by the phenol. Lastly, using the product from oxidation of the pyrrole carboxylic acid methyl ester, we generate an intermediate primed for synthesis of the armeniaspirol scaffold by a Friedel-Crafts acylation. Surprisingly this intermediate undergoes a Lewis acid-mediated rearrangement prior to electrophilic aromatic substitution, leading to a new scaffold and ultimately to a constitutional isomer of armenaispirol that we name pseudoarmeniaspirol. While pseudoarmeniaspirol **1** is active against the Gram-positive pathogen MRSA like armeniaspirol, it does not inhibit the Clp proteases targeted by armeniaspirol nor does it act as a protonophore, suggesting a different mechanism of action.

EXPERIMENTAL SECTION

General Procedure 1 − Synthesis of Esters, Amides, and Thioesters. At 0 °C, pyrrole-2-carboxylic acid (1.8 mmol, 1 equiv) was added to a solution of 1-(3-dimethylaminopropyl)-3-ethylcarbodiimide (2.7 mmol, 1.5 equiv) and DMAP (0.18 mmol, 0.1 equiv) in DCM (0.1 M). Then, commercially available amine, alcohol, or thiol (2.16 mmol, 1.2 equiv) was added to the mixture. The ice bath was removed and warmed to room temperature. After 24 h at room temperature, the solution was diluted with EtOAc (25 mL) and washed with a NH_4Cl solution. The aqueous layer was then extracted twice with EtOAc (20 mL). The combined EtOAc layers were dried with $MgSO_4$ and concentrated in vacuo. Silica gel chromatography (10−50% EtOAc/hexanes) yielded pure amides, esters, or thioesters.

General Procedure 2 − Alkylation of Pyrroles. At 0 °C, methyl-1*H*-pyrrole-2-carboxylate (0.8 mmol, 1 equiv) was dissolved in DMF (0.2 M). NaH (1.04 mmol, 1.3 equiv) was added and allowed to stir for 15 min. Commercially available alkyl halide (0.88 mmol, 1.1 equiv) was added to the mixture, and the ice bath was removed and warmed to room temperature. After 3 h at room temperature, the solution was diluted with EtOAc (25 mL) and washed with a NH_4Cl solution. The aqueous layer was then extracted twice with EtOAc (20 mL). The organic layer was then washed consecutively with brine. The combined EtOAc layers were dried with $MgSO_4$ and concentrated in vacuo. Silica gel chromatography (5−15% EtOAc/hexanes) yielded pure alkyl pyrrole esters.

General Procedure 3 − Chlorination of Pyrroles. The pyrrole substrate (0.3 mmol, 1 equiv) was dissolved in DCE (0.2 M). Following this, NCS (1.2 mmol, 4 equiv) was added to the mixture and heated to 70 °C using an oil bath and stirred overnight. The reaction was quenched with $NaHCO_3$ solution and diluted with EtOAc (25 mL). The aqueous layer was then extracted twice with EtOAc (20 mL). The organic layer was then washed again with aqueous $NaHCO_3$. The combined EtOAc layers were dried with $MgSO_4$ and concentrated in vacuo. Silica gel chromatography (5−40% EtOAc/hexanes) yielded the desired compound.

*Compounds from Table 1. Methyl-N-methyl-pyrrole-2-carboxylate (**7b**).* Prepared following general procedure 2. Compound **7b** was obtained as a clear oil and was used without further purification (139 mg, quant). ^{1}H NMR (600 MHz, chloroform-*d*) δ 6.93 (dd, J = 4.0, 1.8 Hz, 1H), 6.78 (ddd, J = 2.4, 1.8, 0.5 Hz, 1H), 6.11 (dd, J = 4.0, 2.5 Hz, 1H), 3.93 (s, 3H), 3.81 (s, 3H). ^{13}C{^{1}H} NMR (150 MHz, $CDCl_3$) δ 161.9, 129.6, 122.5, 117.9, 108.0, 51.2, 37.0. The NMR data is consistent with literature values.[17] HRMS (EI+/magnetic sector) m/z: [M] + calcd for $C_7H_9NO_2$: 139.0633 Found: 139.0640.

*Methyl-N-hexyl-pyrrole-2-carboxylate (**7c**).* Prepared following general procedure 2. Compound **7c** was obtained as a clear oil and used without further purification (209 mg, quant). ^{1}H NMR (600 MHz, chloroform-*d*) δ 6.97−6.93 (m, 1H), 6.83 (dd, J = 2.5, 1.9 Hz, 1H), 6.13−6.08 (m, 1H), 4.33−4.26 (m, 2H), 3.80 (s, 3H), 1.79−1.71 (m, 2H), 1.29 (q, J = 4.5, 3.5 Hz, 6H), 0.89−0.86 (m, 3H). ^{13}C{^{1}H} NMR (150 MHz, $CDCl_3$) δ 161.6, 128.8, 121.6, 118.2, 107.9, 51.1, 49.4, 31.8, 31.6, 26.5, 22.7, 14.2. HRMS (EI+/magnetic sector) m/z: [M] + calcd for $C_{12}H_{19}NO_2$: 209.1416 Found: 209.1420.

*Methyl-N-dodecyl-pyrrole-2-carboxylate (**7d**).* Prepared following general procedure 2. Compound **7d** was obtained as a clear oil and was used without further purification (293 mg, quant). ^{1}H NMR (600 MHz, $CDCl_3$) δ 6.94 (dd, J = 3.9, 1.8 Hz, 1H), 6.83 (dd, J = 2.5, 1.8 Hz, 1H), 6.10 (dd, J = 3.9, 2.5 Hz, 1H), 4.30−4.26 (m, 2H), 3.80 (s, 3H), 1.78−1.70 (m, 2H), 1.29−1.21 (m, 18H), 0.88 (td, J = 7.1, 1.6 Hz, 3H). ^{13}C{^{1}H} NMR (150 MHz, $CDCl_3$) δ 161.5, 128.7, 121.4, 118.1, 107.8, 51.0, 49.3, 31.9, 31.7, 29.7, 29.6, 29.6, 29.6, 29.4, 29.3, 26.7, 22.7, 14.1. HRMS (EI+/magnetic sector) m/z: [M] + calcd for $C_{18}H_{31}NO_2$: 293.2355 Found: 293.2342.

*Methyl-1-(1-ethoxy-1-oxopropan-2-yl)pyrrole-2-carboxylate (**7e**).* Prepared following general procedure 2. Compound **7e** was obtained as a clear oil and used without further purification (900 mg, 91% yield). R_f = 0.20 (10:90 EtOAc:hexanes). ^{1}H NMR (400 MHz, $CDCl_3$) δ 7.04 (dd, J = 2.8, 1.8 Hz, 1H), 7.00 (dd, J = 3.9, 1.7 Hz, 1H), 6.21 (dd, J = 3.9, 2.8 Hz, 1H), 5.85 (q, J = 7.4 Hz, 1H), 4.19 (qd, J = 7.1, 1.0 Hz, 2H), 3.79 (s, 3H), 1.74 (s, 3H), 1.24 (t, J = 7.1 Hz, 3H).

https://doi.org/10.1021/acs.joc.2c02331
J. Org. Chem. 2022, 87, 15634−15643

$^{13}C\{^1H\}$ NMR (101 MHz, $CDCl_3$) δ 171.6, 161.7, 125.9, 122.1, 118.5, 108.7, 61.5, 55.2, 51.1, 18.0, 14.1. HRMS (EI+/magnetic sector) m/z: [M] + calcd for $C_{11}H_{15}NO_4$: 225.1001 Found: 225.0989.

*t-Butyl-1-methylpyrrole-2-carboxylate (**7f**).* Prepared following general procedure 2 using **SI7**. Product **7f** was obtained as a clear oil and used without further purification (400 mg, quant). ^1H NMR (400 MHz, $CDCl_3$) δ 6.87 (dd, J = 3.9, 1.9 Hz, 1H), 6.73 (t, J = 2.2 Hz, 1H), 6.08 (dd, J = 3.9, 2.5 Hz, 1H), 3.90 (s, 3H) 1.55 (s, 9H). $^{13}C\{^1H\}$ NMR (100 MHz, $CDCl_3$) δ 160.9, 128.9, 124.0, 117.4, 107.4, 80.2, 36.9, 28.5. The NMR data is consistent with literature values.[18] HRMS (EI +/magnetic sector) m/z: [M] + calcd for $C_{10}H_{15}NO_2$: 181.1103 found: 181.1116.

*Benzyl-1-methylpyrrole-2-carboxylate (**7g**).* Prepared following general procedure 1. Compound **7g** was purified by silica gel chromatography (5:95 EtOAc:hexanes) and obtained as a clear oil (120 mg, 74% yield). R_f = 0.6 (10:90 EtOAc:hexanes). ^1H NMR (400 MHz, $CDCl_3$) δ 7.44−7.33 (m, 5H), 7.00 (dd, J = 4.0, 1.8 Hz, 1H), 6.79 (t, J = 2.1 Hz, 1H), 6.11 (dd, J = 4.0, 2.5 Hz, 1H), 5.28 (s, 2H), 3.93 (s, 3H). $^{13}C\{^1H\}$ NMR (100 MHz, $CDCl_3$) δ 161.1, 136.6, 129.7, 128.5, 128.0, 127.9, 122.4, 118.1, 107.9, 65.4, 36.8. The NMR data is consistent with literature values.[19] HRMS (EI+/magnetic sector) m/z: [M] + calcd for $C_{13}H_{13}NO_2$: 215.0946 Found: 215.0955.

*Trimethylsilyl-ethyl-N-methyl-pyrrole-2-carboxylate (**7h**).* Prepared following general procedure 2 using **SI8**. Compound **7h** was obtained as a clear oil and was used without further purification (100 mg, 95% yield). ^1H NMR (400 MHz, $CDCl_3$) δ 6.92 (dd, J = 4.0, 1.8 Hz, 1H), 6.77 (t, J = 2.2 Hz, 1H), 6.10 (dd, J = 4.0, 2.5 Hz, 1H), 4.43−4.20 (m, 2H), 3.93 (s, 3H), 1.12−1.05 (m, 2H), 0.07 (s, 9H). $^{13}C\{^1H\}$ NMR (100 MHz, $CDCl_3$) δ 161.6, 129.3, 122.8, 117.6, 107.7, 62.0, 36.8, 17.5, −1.4. HRMS (EI+/magnetic sector) m/z: [M] + calcd for $C_{11}H_{19}NO_2Si$: 225.1185 Found: 225.1187.

*Phenol-1H-pyrrole-2-carboxylate (**7i**).* Prepared following general procedure 1. Compound **7i** was purified by silica gel chromatography (20:80 EtOAc:hexanes) and obtained as a white amorphous solid (275 mg, 81% yield). R_f = 0.4 (20:80 EtOAc:hexanes). ^1H NMR (400 MHz, $CDCl_3$) δ 9.90 (s, 1H), 7.50−7.42 (m, 2H), 7.35−7.24 (m, 3H), 7.22 (ddd, J = 3.9, 2.5, 1.5 Hz, 1H), 6.94 (td, J = 2.7, 1.5 Hz, 1H), 6.36 (dt, J = 3.8, 2.5 Hz, 1H). $^{13}C\{^1H\}$ NMR (100 MHz, $CDCl_3$) δ 160.0, 150.7, 129.6, 125.9, 124.7, 122.0, 121.8, 117.1, 110.8. The NMR data is consistent with literature values.[20]

*1H-Pyrrole-2-carboxylic Acid Propylamide (**7j**).* Prepared following general procedure 1. Compound **7j** was purified by silica gel chromatography (30% EtOAc/hexanes) and obtained as a yellow oil (184 mg, 84% yield). R_f = 0.35 (50:50 EtOAc:hexanes) ^1H NMR (400 MHz, $CDCl_3$) δ 6.89 (td, J = 2.7, 1.3 Hz, 1H), 6.61 (ddd, J = 3.8, 2.5, 1.4 Hz, 1H), 6.30 (t, J = 5.9 Hz, 1H), 6.19 (dt, J = 3.7, 2.5 Hz, 1H), 3.43−3.32 (m, 2H), 1.59 (h, J = 7.4 Hz, 2H), 0.94 (t, J = 7.4 Hz, 3H). $^{13}C\{^1H\}$ NMR (100 MHz, $CDCl_3$) δ 161.7, 126.1, 121.7, 109.4, 109.0, 41.2, 23.1, 11.4. The NMR data is consistent with literature values.[21] HRMS (EI+/magnetic sector) m/z: [M] + calcd for $C_8H_{12}N_2O$: 152.0950 Found: 152.0944.

*Piperidin-1-yl(1H-pyrrol-2-yl)methanone (**7k**).* Prepared following general procedure 1. Compound **7k** was purified by silica gel chromatography (30% EtOAc/hexanes) and obtained as an orange oil (170 mg, 77% yield). R_f = 0.35 (40:60 EtOAc:hexanes). ^1H NMR (400 MHz, $CDCl_3$) δ 6.87 (td, J = 2.7, 1.2 Hz, 1H), 6.49 (ddd, J = 3.8, 2.4, 1.3 Hz, 1H), 6.21 (td, J = 3.2, 2.2 Hz, 1H), 3.81−3.66 (m, 4H), 1.74−1.57 (m, 6H). $^{13}C\{^1H\}$ NMR (150 MHz, $CDCl_3$) δ 162.0, 124.8, 121.0, 111.8, 108.9, 46.0, 26.2, 24.8. The NMR data is consistent with literature values.[22] HRMS (EI+/magnetic sector) m/z: [M] + calcd for $C_{10}H_{14}N_2O$: 178.1106 Found: 178.1099.

*(1-Methyl-1H-pyrrol-2-yl)-2,2-dimethyl-1-propanone (**7m**).* Lithium iodide (644 mg, 4.81 mmol, 1.3 equiv) and *N*-methylpyrrole (0.33 mL, 3.7 mmol, 1 equiv) were added to 5 mL of anhydrous MeCN and 4 Å molecular sieves. Pivaloyl chloride (0.45 mL, 3.7 mmol, 1 equiv) was added to the solution, and the mixture was immediately heated to 82 °C using an oil bath and stirred for 24 h. The resulting mixture was cooled to room temperature and washed with DCM and $Na_2S_2O_3$ solution. The combined organic layers were dried and concentrated in vacuo. Compound **7m** was purified by silica gel column chromatography (15:85 EtOAc:hexanes) and obtained as an white amorphous solid (175 mg, 1.06 mmol, 29% yield). R_f = 0.3 (15:85 EtOAc:hexanes) ^1H NMR (400 MHz, $CDCl_3$) δ 7.25 (t, J = 2.0 Hz, 1H), 6.59 (dd, J = 2.9, 1.8 Hz, 1H), 6.51 (dd, J = 2.9, 2.2 Hz, 1H), 3.63 (s, 3H), 1.29 (s, 9H). $^{13}C\{^1H\}$ NMR (100 MHz, $CDCl_3$) δ 201.6, 127.33, 122.8, 122.1, 110.8, 43.5, 36.5, 28.2. The NMR data is consistent with literature values.[23]

*(1-Methyl-1H-pyrrol-2-yl)(p-tolyl)methanone (**7n**).* Lithium iodide (644 mg, 4.81 mmol, 1.3 equiv) and *N*-methylpyrrole (0.33 mL, 3.7 mmol, 1 equiv) were added to 5 mL of anhydrous MeCN and 4 Å molecular sieves. *p*-Toluoyl chloride (0.48 mL, 3.7 mmol, 1 equiv) was added to the solution and the mixture was immediately heated to 82 °C using an oil bath and stirred for 24 h. The resulting mixture was cooled to room temperature and washed with DCM and $Na_2S_2O_3$ solution. The combined organic layers were dried and concentrated in vacuo. Compound **7n** was purified by silica gel column chromatography (15:85 EtOAc:hexanes) and obtained as a white amorphous solid (175 mg, 0.879 mmol, 24% yield). R_f = 0.4 (15:85 EtOAc:hexanes). ^1H NMR (400 MHz, $CDCl_3$) δ 7.82−7.65 (m, 2H), 7.31−7.19 (m, 2H), 6.91−6.87 (m, 1H), 6.74 (dd, J = 4.1, 1.7 Hz, 1H), 6.15 (dd, J = 4.1, 2.5 Hz, 1H), 4.02 (s, 3H), 2.42 (s, 3H). $^{13}C\{^1H\}$ NMR (100 MHz, $CDCl_3$) δ 186.0, 142.0, 137.2, 131.2, 130.6, 129.4, 128.8, 122.5, 108.0, 37.3, 21.6. The NMR data is consistent with literature values.[24]

*1-Methyl-2-trichloroacetyl-1H-pyrrole (**7q**).* At 0 °C, *N*-methylpyrrole (2.2 mL, 24.7 mmol, 1 equiv) was dissolved in diethyl ether (0.2 M). Trichloroacetyl chloride (2.8 mL, 24.7 mmol, 1 equiv) was added and allowed to stir overnight. The solution was diluted with EtOAc (25 mL) and washed with $NaHCO_3$ solution. The aqueous layer was then extracted twice with EtOAc (20 mL). The organic layer was then washed consecutively with brine. The combined EtOAc layers were dried with $MgSO_4$ and concentrated in vacuo. Compound **7q** was obtained as a purple amorphous solid (5.5 g, 24.65 mmol, quant) and used without further purification. ^1H NMR (400 MHz, $CDCl_3$) δ 7.48 (dd, J = 4.4, 1.6 Hz, 1H), 6.98−6.89 (m, 1H), 6.20 (dd, J = 4.4, 2.4 Hz, 1H), 3.94 (s, 3H). $^{13}C\{^1H\}$ NMR (100 MHz, $CDCl_3$) δ 172.9, 133.8, 124.1, 121.8, 109.0, 96.3, 38.6. The NMR data is consistent with literature values.[25]

*N-Benzyl-1H-pyrrole-2-carboxamide (**7r**).* Prepared following general procedure 1. Compound **7r** was purified by silica gel column chromatography (40% EtOAc/hexanes) and was obtained as a white amorphous solid (177 mg, 83% yield). R_f = 0.38 (40:60 EtOAc:hexanes). ^1H NMR (400 MHz, $CDCl_3$) δ 7.37−7.21 (m, 5H), 6.83 (td, J = 2.7, 1.3 Hz, 1H), 6.70−6.61 (m, 2H), 6.19 (dt, J = 3.7, 2.5 Hz, 1H), 4.59 (d, J = 5.9 Hz, 2H). $^{13}C\{^1H\}$ NMR (100 MHz, $CDCl_3$) δ 161.6, 138.6, 128.7, 127.7, 127.5, 125.7, 122.2, 109.7, 109.6, 43.4. The NMR data is consistent with literature values.[26] HRMS (EI +/magnetic sector) m/z: [M] + calcd for $C_{12}H_{12}N_2O$: 200.0950. Found: 200.0965.

*N-(Prop-2-yn-1-yl)-1H-pyrrole-2-carboxamide (**7s**).* Prepared following general procedure 1. Compound **7s** was purified by silica gel column chromatography (30% EtOAc/hexanes) and was obtained as a white amorphous solid (174 mg, 80% yield). R_f = 0.35 (50:50 EtOAc:hexanes). ^1H NMR (600 MHz, $CDCl_3$) δ 9.72 (s, 1H), 6.94 (ddd, J = 3.2, 2.3, 1.0 Hz, 1H), 6.60 (ddd, J = 3.9, 2.5, 1.3 Hz, 1H), 6.24 (dtd, J = 3.3, 2.6, 0.6 Hz, 1H), 6.08 (s, 1H), 4.22 (ddd, J = 5.5, 2.5, 0.6 Hz, 2H), 2.27 (td, J = 2.5, 0.6 Hz, 1H). $^{13}C\{^1H\}$ NMR (150 MHz, $CDCl_3$) δ 160.8, 122.0, 114.9, 110.0, 109.5, 79.7, 71.7, 29.1. The NMR data is consistent with literature values.[27] HRMS (EI+/magnetic sector) m/z: [M] + calcd for $C_8H_8N_2O$: 148.0637 Found: 148.0623.

*N-Methoxy-N-methylpyrrole-2-carboxamide (**7t**).* Prepared following general procedure 1. Compound **7t** was purified by silica gel column chromatography (40% EtOAc/hexanes) and was obtained as a yellow amorphous solid (120 mg, 64% yield). R_f = 0.44 (40:60 EtOAc:hexanes). ^1H NMR (400 MHz, $CDCl_3$) δ 9.73 (s, 1H), 6.93 (td, J = 2.8, 1.4 Hz, 1H), 6.89 (ddd, J = 3.8, 2.5, 1.4 Hz, 1H), 6.25 (dt, J = 3.8, 2.6 Hz, 1H), 3.75 (s, 3H), 3.33 (s, 3H). $^{13}C\{^1H\}$ NMR (100 MHz, $CDCl_3$) δ 161.4, 122.0, 114.9, 111.2110.2, 61.1, 33.1. The NMR data is consistent with literature values.[28] HRMS (EI+/magnetic sector) m/z: [M] + calcd for $C_7H_{10}N_2O_2$: 154.0742 Found: 154.0744.

*S-2-Pyrrolylthiobenzoat (**7u**).* Prepared following general procedure 1. Compound **7u** was purified by silica gel column chromatog-

https://doi.org/10.1021/acs.joc.2c02331
J. Org. Chem. 2022, 87, 15634−15643

raphy (20% EtOAc/hexanes) and was obtained as a clear oil (153 mg, 74% yield) R_f = 0.3 (15:85 EtOAc:hexanes). ^{1}H NMR (400 MHz, $CDCl_3$) δ 9.96 (s, 1H), 7.58−7.50 (m, 2H), 7.46 (tt, J = 3.9, 2.5 Hz, 3H), 7.16 (ddd, J = 3.9, 2.5, 1.4 Hz, 1H), 6.91 (td, J = 2.7, 1.4 Hz, 1H), 6.30 (dt, J = 3.9, 2.5 Hz, 1H). $^{13}C\{^1H\}$ NMR (100 MHz, $CDCl_3$) δ 180.3, 135.3, 129.4, 129.4, 129.1, 127.1, 124.7, 116.0, 110.9. HRMS (EI+/magnetic sector) m/z: [M] + calcd for $C_{11}H_9NOS$: 203.0405 Found: 203.0411.

*Ethyl-2-pyrrolthiolcarboxylate (**7v**).* Prepared following general procedure 1. Compound **7v** was purified by silica gel chromatography (15% EtOAc/hexanes) and was obtained as a clear oil (112 mg, 62% yield). R_f = 0.33 (15:85 EtOAc:hexanes) ^{1}H NMR (400 MHz, $CDCl_3$) δ 7.02 (ddt, J = 4.0, 2.8, 1.4 Hz, 2H), 6.25 (dt, J = 3.8, 2.5 Hz, 1H), 3.05 (q, J = 7.4 Hz, 2H), 1.34 (t, J = 7.4 Hz, 3H). $^{13}C\{^1H\}$ NMR (100 MHz, $CDCl_3$) δ 182.6, 130.4, 124.0, 115.3, 110.6, 22.7, 15.2. The NMR data is consistent with literature values.[29] HRMS (EI+/magnetic sector) m/z: [M] + calcd for C_7H_9NOS: 155.0405 Found: 155.0415.

*Methyl-N-Boc-2-pyrrolecarboxylate (**7x**).* Methyl-1*H*-pyrrole-2-carboxylate (0.20 g, 1.6 mmol, 1 equiv) was dissolved in MeCN (0.2 M). Boc_2O (0.418 g, 1.92 mmol, 1.2 equiv) and catalytic DMAP (19 mg, 0.08 mmol, 0.05 equiv) was added and allowed to stir for 4 h at room temperature. The mixture was quenched with NH_4Cl solution and diluted with EtOAc. The aqueous layer was then extracted twice with EtOAc (20 mL). The combined EtOAc layers were dried with $MgSO_4$ and concentrated in vacuo. The residue was purified by silica gel column chromatography (5% EtOAc/hexanes) to yield pure **7w** as an amorphous white solid (290 mg, 1.3 mmol, 81% yield). R_f = 0.31 (5:95 EtOAc:hexanes). ^{1}H NMR (400 MHz, $CDCl_3$) δ 7.28 (dd, J = 3.1, 1.7 Hz, 1H), 6.80 (dd, J = 3.5, 1.7 Hz, 1H), 6.17−6.09 (m, 1H), 3.80 (s, 3H), 1.55 (s, 9H). $^{13}C\{^1H\}$ NMR (100 MHz, $CDCl_3$) δ 161.3, 148.4, 126.7, 125.1, 120.8, 110.1, 84.7, 51.8, 27.6. The NMR data is consistent with literature values.[30] HRMS (EI+/magnetic sector) m/z: [M] + calcd for $C_{11}H_{15}NO_4$: 225.1001 Found: 225.1003.

*2,3,4-Trichloro-5-oxo-1H-2,5-dihydropyrrole-2-carboxylic Acid Methyl Ester (**8a**).* Prepared following general procedure 3. Purification by silica gel chromatography (10% EtOAc/hexanes) yielded **8a** as a clear oil (221 mg, 94% yield). R_f = 0.6 (20:80 EtOAc:hexanes) ^{1}H NMR (400 MHz, $CDCl_3$) δ 3.83 (s, 3H). $^{13}C\{^1H\}$ NMR (100 MHz, $CDCl_3$) δ 166.2, 162.0, 149.7, 127.9, 88.3, 54.9. HRMS (EI+/magnetic sector) m/z: [M] + calcd for $C_6H_4Cl_3NO_3$: 242.9257 Found: 242.9246.

*2,3,4-Trichloro-5-oxo-1-methyl-2,5-dihydro-pyrrole-2-carboxylic Acid Methyl Ester (**8b**).* Prepared following general procedure 3. Purification by silica gel chromatography (10% EtOAc/hexanes) yielded Compound **8b** as a clear oil (136 mg, 91% yield). R_f = 0.4 (15:85 EtOAc:hexanes) ^{1}H NMR (600 MHz, chloroform-*d*) δ 3.86 (s, 3H), 3.01 (s, 3H). $^{13}C\{^1H\}$ NMR (150 MHz, $CDCl_3$) δ 162.57, 162.1, 142.6, 128.2, 83.4, 55.1, 26.7. HRMS (EI+/magnetic sector) m/z: [M] + calcd for $C_7H_6Cl_3NO_3$: 256.9413 Found:256.9422.

*2,3,4-Trichloro-5-oxo-1-hexyl-2,5-dihydropyrrole-2-carboxylic Acid Methyl Ester (**8c**).* Prepared following general procedure 3. Purification by silica gel chromatography (5% EtOAc/hexanes) yielded compound **8c** as a clear oil (124 mg, 84% yield). R_f = 0.25 (10:90 EtOAc:hexanes). ^{1}H NMR (600 MHz, chloroform-*d*) δ 3.87 (s, 3H), 3.47 (t, J = 7.9 Hz, 2H), 1.70−1.55 (m, 2H), 1.33−1.27 (m, 6H), 0.91−0.86 (m, 3H). $^{13}C\{^1H\}$ NMR (150 MHz, $CDCl_3$) δ 163.1, 162.6, 142.7, 128.0, 83.8, 54.9, 42.3, 31.3, 27.8, 26.5, 22.5, 14.0. HRMS (EI+/magnetic sector) m/z: [M] + calcd for $C_{12}H_{16}Cl_3NO_3$: 327.0196 Found: 327.0201.

*2,3,4-Trichloro-5-oxo-1-dodecyl-2,5-dihydropyrrole-2-carboxylic Acid Methyl Ester (**8d**).* Prepared following general procedure 3. Purification by silica gel chromatography (5% EtOAc/hexanes) yielded compound **8d** as a clear oil (154 mg, 81% yield). R_f = 0.25 (5:95 EtOAc:hexanes). ^{1}H NMR (400 MHz, $CDCl_3$) δ 3.85 (s, 3H), 3.45 (t, J = 7.8 Hz, 2H), 1.70−1.47 (m, 2H), 1.25 (d, J = 13.0 Hz, 18H), 0.90−0.80 (m, 3H).$^{13}C\{^1H\}$ NMR (100 MHz, $CDCl_3$) δ 163.1, 162.5, 142.7, 127.9, 83.8, 54.9, 42.3, 31.9, 29.6, 29.5, 29.5, 29.5, 29.3, 29.2, 27.9, 26.8, 22.7, 14.1.HRMS (EI+/magnetic sector) m/z: [M] + calcd for $C_{18}H_{28}Cl_3NO_3$: 411.1135 Found: 411.1140.

*2,3,4-Trichloro-5-oxo-1-(1-ethoxy-1-oxopropan-2-yl)-2,5-dihydro-pyrrole-2-carboxylic Acid Methyl Ester (**8e**).* Prepared following general procedure 3. Purification by silica gel chromatography (25% EtOAc/hexanes) yielded a clear oil **8e** as an inseparable 1:1.2 mixture of diastereomers (84 mg, 78% yield). R_f = 0.25 (10:90 EtOAc:hexanes). ^{1}H NMR (400 MHz, $CDCl_3$) δ 4.53−4.45 (m, 1H), 4.42 (t, J = 7.3 Hz, 1H), 4.23−4.14 (m, 4H), 3.88 (s, 3H), 3.84 (s, 2H), 1.67 (dd, J = 14.1, 7.4 Hz, 6H), 1.24 (td, J = 4.2, 2.1 Hz, 6H). $^{13}C\{^1H\}$ NMR (101 MHz, $CDCl_3$) δ 169.3, 169.1, 162.9, 162.6, 161.7, 161.2, 143.4, 143.3, 128.0, 82.6, 82.5, 62.0, 54.9, 54.8, 52.2, 51.8, 15.19, 15.15, 14.10, 14.06. HRMS (ESI+/Q-TOF) m/z: [M + Na] + Calcd. For $C_{11}H_{12}Cl_3NO_5Na$ 365.9679; Found: 365.9675.

*2,3,4-Trichloro-5-oxo-1-methyl-2,5-dihydro-pyrrole-2-carboxylic Acid t-Butyl Ester (**8f**).* Prepared following general procedure 3. Purification by silica gel chromatography (10% EtOAc/hexanes) yielded pure **8f** as a clear oil (507 mg, 81% yield). R_f = 0.34 (10% EtOAc/Hexane) ^{1}H NMR (400 MHz, $CDCl_3$) δ, 3.01 (s, 3H), 1.46 (s, 9H). $^{13}C\{^1H\}$ NMR (100 MHz, $CDCl_3$) δ 162.3, 160.4, 143.0, 127.7, 86.7, 84.0, 28.0, 26.5. HRMS (EI+/magnetic sector) m/z: [M] + calcd for $C_{10}H_{12}Cl_3NO_3$: 298.9883 Found: 298.9892.

*2,3,4-Trichloro-5-oxo-1-methyl-2,5-dihydro-pyrrole-2-carboxylic Acid Benzyl Ester (**8g**).* Prepared following general procedure 3. Purification by silica gel chromatography (10% EtOAc/hexanes) yielded pure **8g** as an amorphous white solid (507 mg, 77% yield). R_f = 0.1 (10:90 EtOAc:hexanes) ^{1}H NMR (400 MHz, $CDCl_3$) δ 7.40−7.29 (m, 5H), 5.30−5.21 (m, 2H), 2.94 (s, 3H). $^{13}C\{^1H\}$ NMR (100 MHz, $CDCl_3$) δ 162.0, 161.9, 142.6, 133.9, 129.2, 128.9, 128.6, 128.3, 83.5, 70.0, 26.6. HRMS (EI+/magnetic sector) m/z: [M] + calcd for $C_{13}H_{10}Cl_3NO_3$: 332.9726 Found: 332.9736.

*2,3,4-Trichloro-5-oxo-1-methyl-2,5-dihydro-pyrrole-2-carboxylic Acid Trimethylsilylethyl Ester (**8h**).* Prepared following general procedure 3. Purification by silica gel chromatography (10% EtOAc/hexanes) yielded pure **8 h** as a clear oil (507 mg, 74% yield). R_f = 0.25 (5:95 EtOAc:hexanes). ^{1}H NMR (400 MHz, $CDCl_3$) δ 4.32−4.23 (m, 2H), 2.97 (s, 3H), 1.02−0.93 (m, 2H) 0.02 (s, 9H). $^{13}C\{^1H\}$ NMR (100 MHz, $CDCl_3$) δ 162.0, 161.9, 142.7, 128.0, 83.5, 67.5, 26.5, 17.4, −1.6. HRMS (EI+/magnetic sector) m/z: [M] + calcd for $C_{11}H_{16}Cl_3NO_3Si$: 342.9965 Found: 342.9948.

*2,3,4-Trichloro-5-oxo-1H-2,5-dihydropyrrole-2-carboxylic Acid Phenol Ester (**8i**).* Prepared following general procedure 3. Purification by silica gel chromatography (5:95 EtOAc: hexanes) yielded **8i** as an amorphous white solid (207 mg, 84% yield). R_f = 0.55 (5:95 EtOAc:hexanes) ^{1}H NMR (600 MHz, $CDCl_3$) δ 7.31−7.27 (m, 2H), 7.20−7.15 (m, 1H), 7.02−6.99 (m, 2H). $^{13}C\{^1H\}$ NMR (150 MHz, $CDCl_3$) δ 166.8, 160.3, 150.2, 149.5, 129.8, 128.4, 127.0, 120.8, 88.6. HRMS (EI+/magnetic sector) m/z: [M] + calcd for $C_{11}H_6Cl_3NO_3$: 304.9413 Found: 304.9419.

*2,3,4-Trichloro-5-oxo-1H-2,5-dihydropyrrole-2-carboxylic Acid Propylamide (**8j**).* Prepared following general procedure 3. Purification by silica gel chromatography (25% EtOAc/hexanes) yielded pure **8j** as an amorphous white solid (84 mg, 80% yield). R_f = 0.4 (50:50 EtOAc:hexanes) ^{1}H NMR (400 MHz, Acetone) δ 6.55 (s, 1H), 3.29−3.15 (m, 2H), 1.54 (h, J = 7.2 Hz, 2H), 0.89 (t, J = 7.4 Hz, 3H). $^{13}C\{^1H\}$ NMR (100 MHz, Acetone) δ 165.4, 164.0, 145.3, 126.4, 86.5, 41.5, 22.4, 10.7. HRMS (EI+/magnetic sector) m/z: [M] + calcd for $C_8H_9Cl_3N_2O_2$: 269.9730 Found:269.9721.

*2,3,4-Trichloro-5-oxo-1H-2,5-dihydropyrrole-2-carboxylic Acid Piperidine Amide (**8k**).* Prepared following general procedure 3. Purification by silica gel chromatography (25% EtOAc/hexanes) yielded pure **8k** as an amorphous white solid (86 mg, 72% yield). R_f = 0.45 (40:60 EtOAc:hexanes). ^{1}H NMR (400 MHz, $CDCl_3$) δ 4.09−3.87 (m, 2H), 3.52 (tt, J = 14.5, 8.7 Hz, 2H), 1.95−1.36 (m, 7H). $^{13}C\{^1H\}$ NMR (100 MHz, $CDCl_3$) δ 165.8, 159.7, 154.3, 126.1, 87.4, 48.3, 45.0, 25.9, 25.6, 24.3. HRMS (EI+/magnetic sector) m/z: [M] + calcd for $C_{10}H_{11}Cl_3N_2O_2$: 295.9886 Found: 295.9874.

*Methyl-2,3,4-tribromo-5-oxo-2,5-dihydro-1H-Pyrrole-2-Carboxylate (**18**).* Prepared following general procedure 3 with modification that NCS was replaced with NBS. Purification by silica gel chromatography (10% EtOAc/hexanes) yielded the brominated analog **18** as an orange amorphous solid (101 mg, 96% yield). R_f = 0.4 (10:90 EtOAc:hexanes). ^{1}H NMR (400 MHz, $CDCl_3$) δ 3.83 (s, 3H). $^{13}C\{^1H\}$ NMR (101 MHz, $CDCl_3$) δ 162.3, 159.9, 144.8, 124.2, 81.3, 54.9.

https://doi.org/10.1021/acs.joc.2c02331
J. Org. Chem. 2022, 87, 15634−15643

HRMS (EI+/magnetic sector) m/z: [M] + calcd for $C_6H_4{}^{79}Br_2{}^{81}Br_1N_1O_2$: 360.7771. $C_6H_4{}^{79}Br_2{}^{81}Br_1N_1O_2$ Found:360.7768.

*Compounds from Figure 3. 2-(1-Hexyl-2-hydroxy-6-methoxy-3-benzoyl)-1H-pyrrole (**3**).* In a round-bottom flask, **9** (0.830 g, 2.63 mmol, 1.0 equiv) was dissolved in 1,2-dichloroethane (3 mL). The solution was cooled to −20 °C using a dry ice/acetone bath. BBr_3 (3.13 mL of a 1 M solution in DCM, 3.13 mmol, 1.2 equiv) was added dropwise, and the reaction mixture was stirred at −20 to −10 °C for 2 h. Subsequently, Et_3N/water was added, and the solution was extracted 3 × with EtOAc. The organic fractions were combined, washed with brine, dried over Na_2SO_4, and concentrated. The desired compound **3** (0.788 g, 99% yield) was obtained as a yellow amorphous solid and used without purification. ^{1}H NMR (400 MHz, acetone-d_6) δ 12.76 (s, 1H), 8.05 (dd, J = 8.9, 0.9 Hz, 1H), 7.27 (ddd, J = 3.0, 2.5, 1.4 Hz, 1H), 7.05 (dtd, J = 4.2, 2.8, 1.3 Hz, 1H), 6.67 (d, J = 9.0 Hz, 1H), 6.36 (ddd, J = 3.9, 2.9, 2.0 Hz, 1H), 3.93 (s, 3H), 2.73−2.58 (m, 2H), 1.59−1.42 (m, 2H), 1.40−1.26 (m, 6H), 0.91−0.82 (m, 3H). ^{13}C{^{1}H} NMR (100 MHz, acetone-d_6) δ 186.2, 162.8, 162.0, 130.7, 130.0, 125.5, 118.5, 117.9, 113.4, 110.7, 102.2, 55.3, 31.6, 29.3, 28.6, 22.5, 22.2, 13.5. NMR data matched literature values.[3]

*5-Chloro-6-methoxy-N-desmethyl Armeniaspirol (**4**).* In a round-bottom flask, **3** (0.7 g, 2.32 mmol, 1.0 equiv) was dissolved in acetic acid (0.2 M). NCS (0.619 g, 4.64 mmol, 2.0 equiv) was added, and the resulting mixture was stirred at room temperature for 2 h. Following this, NCS (1.24 g, 9.29 mmol, 4.0 equiv) was added, and the resulting mixture was heated to 70 °C using an oil bath for 16 h. The mixture was then quenched with a 10% K_2CO_3 solution and extracted three times with EtOAc. The organic fractions were combined, washed with brine, dried over $MgSO_4$, and concentrated in vacuo. The resulting oil was dissolved in $CHCl_3$ (0.2 M) and Et_3N (0.97 mL, 6.96 mmol, 3 equiv), and the mixture was heated at 60 °C using an oil bath for 5 h. The solution was cooled to room temperature and concentrated in vacuo, and the spiro-intermediate **4** (0.745 g, 1.78 mmol, 77% yield) was purified from the crude mixture by silica gel column chromatography (10% EtOAc/hexanes) and was obtained as a yellow oil. ^{1}H NMR (400 MHz, $CDCl_3$) δ 7.60 (s, 1H), 7.55 (s, 1H), 3.97 (s, 3H), 2.70 (td, J = 7.5, 4.0 Hz, 2H), 1.61−1.55 (m, 2H), 1.36−1.27 (m, 6H), 0.89−0.86 (m, 3H). ^{13}C{^{1}H} NMR (100 MHz, $CDCl_3$) δ 189.7, 169.8, 165.4, 163.5, 140.7, 128.4, 124.6, 124.3, 123.7, 115.1, 94.09, 61.7, 31.6, 29.3, 29.3, 23.9, 22.6, 14.1. HRMS (EI+/magnetic sector) m/z: [M] + calcd for $C_{18}H_{18}Cl_3NO_4$: 417.0301 Found: 417.0312.

*2-(1-Hexyl-2′6-dimethoxy-3-benzoyl)-1H-pyrrole (**9**).* Pyrrole 2-carboxylic acid (0.721 g, 6.49 mmol, 2 equiv) was dissolved in 10 mL of DCM. Oxalyl chloride (9.7 mL of a 2.5 M solution in DCM, 19.5 mmol, 3 equiv) was added dropwise, and 1 drop of DMF was added. The following mixture was stirred for 1 h at room temperature. The solvent was removed in vacuo. The intermediate acid chloride was resuspended in DCM in a round-bottom flask, and 2-hexyl-1,3-dimethoxybenzene[3] (0.50 g, 3.25 mmol, 1.0 equiv) was added and cooled to 0 °C with an ice bath followed by $SnCl_4$ (16.2 mL of a 1.0 M solution in DCM, 16.2 mmol, 5 equiv). The mixture was stirred for 1 h at 0 °C and then warmed to ambient temperature. The reaction mixture was quenched with a saturated $NaHCO_3$(aq) and extracted 3× with EtOAc. The organic fractions were combined, washed with brine, dried over Na_2SO_4, and concentrated. The desired compound **9** (0.640 g, 78% yield) was purified from the crude mixture by silica column chromatography (30% EtOAc/hexanes) and was obtained as a white amorphous solid. The NMR data were consistent with literature values ^{1}H NMR (400 MHz, acetone-d_6) δ 7.30 (d, J = 8.5 Hz, 1H), 7.19 (dq, J = 2.9, 1.5 Hz, 1H), 6.80 (d, J = 8.6 Hz, 1H), 6.59 (ddd, J = 3.8, 2.2, 1.4 Hz, 1H), 6.23 (dt, J = 3.8, 2.3 Hz, 1H), 3.89 (s, 3H), 3.67 (s, 3H), 2.70−2.57 (m, 2H), 1.52 (q, J = 7.7 Hz, 2H), 1.42−1.24 (m, 6H), 0.93−0.82 (m, 3H). ^{13}C{^{1}H} NMR (100 MHz, acetone-d_6) δ 183.6, 160.1, 157.5, 132.6, 128.2, 125.8, 125.2, 124.4, 118.5, 109.9, 105.1, 61.9, 55.3, 31.6, 29.4, 23.4, 22.4, 13.5. NMR data matched literature values.[3]

*2,4-Dimethoxy-3-hexylbenzoic Acid (**10**).* In a round-bottom flask, **9** (42 mg, 0.127 mmol, 1.0 equiv) was dissolved in DCE (0.2 M). Following this, NCS (51 mg, 0.382 mmol, 3.0 equiv) was added and the resulting mixture was heated to 70 °C using an oil bath for 8 h. The reaction mixture was then quenched with a 10% HCl solution and extracted three times with EtOAc. The organic fractions were combined, washed with brine, dried over $MgSO_4$, and concentrated in vacuo. Compound **10** (23 mg, 0.087 mmol, 69% yield) was purified from the crude mixture using silica gel column chromatography and was obtained as an amorphous white solid (35% EtOAc/hexanes). R_f = 0.3 (35:65 EtOAc:hexanes). ^{1}H NMR (400 MHz, $CDCl_3$) δ 8.00 (d, J = 8.8 Hz, 1H), 6.78 (d, J = 8.8 Hz, 1H), 3.90 (d, J = 4.4 Hz, 6H), 2.69−2.56 (m, 2H), 1.57−1.47 (m, 2H), 1.39−1.27 (m, 6H), 0.93−0.85 (m, 3H). ^{13}C{^{1}H} NMR (100 MHz, $CDCl_3$) δ 166.0, 163.1, 158.5, 131.9, 124.9, 114.3, 107.5, 63.6, 55.9, 31.6, 29.6, 29.3, 23.9, 22.6, 14.1. HRMS (ESI +/Q-TOF) m/z: [M + Na] + calcd for $C_{15}H_{22}O_4Na$ 289.1416. Found: 289.1428.

*Tetrachloropyrrole (**11**).* Prepared following general procedure 3, using pyrrole-2-carboxylic acid (43 mg, 0.388 mmol, 1 equiv) as the starting material. Purification by silica gel chromatography (20% EtOAc/hexanes) yielded pure tetrachloropyrrole **11** as an amorphous brown solid (31 mg, 0.151 mmol, 39% yield). R_f = 0.35 (20:80 EtOAc:hexanes). ^{1}H NMR (600 MHz, $CDCl_3$) δ 8.19 (s, 1H). ^{13}C{^{1}H} NMR (150 MHz, $CDCl_3$) δ 110.3, 109.5. HRMS data could not be collected. All attempts to ionize **11** failed.

*3,4-Dichloromaleimide (**12**).* Prepared following general procedure 3, using pyrrole-2-carboxylic acid (43 mg, 0.388 mmol, 1 equiv) as the starting material. Purification by silica gel chromatography (20% EtOAc/hexanes) yielded pure maleamide **12** as an amorphous white solid (27 mg, 0.163 mmol, 42% yield). R_f = 0.27 (20:80 EtOAc:hexanes). ^{1}H NMR (600 MHz, $CDCl_3$) δ 7.77 (s, 1H). ^{13}C{^{1}H} NMR (150 MHz, $CDCl_3$) δ 162.1, 134.2. NMR data was consistent with literature values.[31] HRMS (EI+/magnetic sector) m/z: [M] + calcd for $C_4H_1Cl_2NO_2$: 164.9384 Found: 164.9389.

*Compounds from Figure 4. 1H-4,5-dichloropyrrole-2-(1-hexyl-2-hydroxy-6-methoxy-3-benzoyl) (**13**).* In a round-bottom flask, **3** (29.5 mg, 0.097 mmol, 1.0 equiv) was dissolved in acetic acid (0.2 M). Following this, NCS (39 mg, 0.294 mmol, 3.0 equiv) was added and the resulting mixture was heated to 70 °C using an oil bath for 8 h. The reaction mixture was then quenched with a 10% K_2CO_3 solution and extracted three times with EtOAc. The organic fractions were combined, washed with brine, dried over $MgSO_4$, and concentrated in vacuo. The desired compound **13** was purified from the crude mixture using Preparative TLC (15% EtOAc/hexanes) and was obtained as an amorphous yellow solid (32 mg, 88% yield). ^{1}H NMR (600 MHz, $CDCl_3$) δ 11.92 (s, 1H), 7.81 (s, 1H), 6.95 (d, J = 2.5 Hz, 1H), 3.92 (s, 3H), 2.73−2.61 (m, 2H), 1.56−1.51 (m, 2H), 1.40 (p, J = 7.4 Hz, 2H), 1.34−1.30 (m, 4H), 0.90−0.87 (m, 3H). ^{13}C{^{1}H} NMR (150 MHz, $CDCl_3$) δ 183.4, 161.3, 160.0, 128.8, 127.5, 126.9, 121.3, 118.3, 118.2, 115.2, 112.8, 61.3, 31.7, 29.6, 29.3, 24.2, 22.6, 14.1. HRMS (EI+/magnetic sector) m/z: [M] + calcd for $C_{18}H_{20}Cl_3NO_3$: 403.0509 Found: 403.0512.

*Spirocyclic-α,β,β-trichlorolactam (**14**).* In a round-bottom flask, **13** (16 mg, 0.0514 mmol, 1.0 equiv) was dissolved in acetic acid (0.2 M) and NCS was added (7 mg, 0.0514 mmol, 1.0 equiv). The mixture was heated to 70 °C using an oil bath for 1 h. The reaction was quenched with 10% Na_2CO_3 solution and the mixture was extracted three times with EtOAc. The organic fractions were combined, washed with brine, dried over $MgSO_4$, and concentrated in vacuo. The desired compound was purified from the crude mixture using Preparative TLC (15% EtOAc/hexanes) affording **14** as a yellow oil (11 mg, 0.0242 mmol, 47% yield). R_f = 0.25 (17:83 EtOAc:hexanes). ^{1}H NMR (600 MHz, $CDCl_3$) δ 7.59 (s, 1H), 7.13 (s, 1H), 4.89 (s, 1H), 3.97 (s, 3H), 2.74−2.65 (m, 2H), 1.37−1.27 (m, 10H), 0.88 (q, J = 3.5 Hz, 3H). ^{13}C{^{1}H} NMR (150 MHz, $CDCl_3$) δ 190.8, 170.0, 166.3, 163.9, 124.8, 124.1, 123.2, 114.6, 92.4, 79.7, 68.0, 61.8, 31.5, 29.3, 28.8, 23.9, 22.5, 14.1. HRMS (EI +/magnetic sector) m/z: [M] + calcd for $C_{18}H_{19}Cl_4NO_4$: 453.0068 Found: 453.0081.

*Compounds from Figure 5. 2-Hexyl-3-methoxyphenol (**6**).* In a round-bottom flask, 2-hexyl-1,3-dimethoxybenzene[3] (0.322 g, 1.61 mmol, 1.0 equiv) was dissolved in DCE (3 mL). The solution was cooled to −20 °C using a dry ice/acetone bath. BBr_3 (1.9 mL of a 1 M solution in DCM, 1.9 mmol, 1.2 equiv) was added dropwise, and the reaction mixture was stirred at −20 to − 10 °C for 2 h. Subsequently,

https://doi.org/10.1021/acs.joc.2c02331
J. Org. Chem. 2022, 87, 15634−15643

Et_3N/water was added, and the solution was extracted three times with EtOAc. The organic fractions were combined, washed with brine, dried over $MgSO_4$, and concentrated in vacuo. Purification by silica gel chromatography (10% EtOAc/hexanes) yielded pure compound **6** as an orange oil (243 mg, 1.31 mmol, 81% yield). ^{1}H NMR (600 MHz, $CDCl_3$) δ 7.04 (t, J = 8.2 Hz, 1H), 6.50 (dd, J = 8.3, 1.0 Hz, 1H), 6.46 (dd, J = 8.1, 1.0 Hz, 1H), 4.68−4.61 (m, 1H), 3.82 (s, 3H), 2.67−2.60 (m, 2H), 1.56−1.49 (m, 2H), 1.38 (dddd, J = 13.9, 8.2, 6.1, 3.3 Hz, 2H), 1.35−1.30 (m, 4H), 0.93−0.87 (m, 3H). ^{13}C{^{1}H} NMR (150 MHz, $CDCl_3$) δ 158.6, 154.2, 126.6, 117.2, 108.2, 103.2, 55.7, 31.8, 29.5, 29.1, 23.0, 22.7, 14.2. HRMS (EI+/magnetic sector) m/z: [M] + calcd for $C_{13}H_{20}O_2$: 208.1463 Found: 208.1458.

N,O-Ketal (5). Phenol **6** (23 mg, 0.124 mmol, 1 equiv) was suspended in acetone and K_2CO_3 (51 mg, 0.372 mmol, 3 equiv) was added and allowed to stir at room temperature for 10 min. **7b** (32 mg, 0.124 mmol, 1 equiv) was added and allowed to stir overnight. The mixture was filtered and concentrated in vacuo to yield pure **5** as a clear oil (38 mg, 0.088 mmol, 71% yield), which was used without further purification. ^{1}H NMR (400 MHz, chloroform-*d*) δ 6.94 (t, J = 8.3 Hz, 1H), 6.61 (d, J = 8.3 Hz, 1H), 6.21 (dd, J = 8.4, 0.9 Hz, 1H), 3.89 (s, 3H), 3.78 (s, 3H), 2.95 (s, 3H), 2.81 (dt, J = 12.4, 7.5 Hz, 1H), 2.72 (dt, J = 12.4, 7.2 Hz, 1H), 1.58−1.47 (m, 2H), 1.32 (m, 6H), 0.87 (m, 3H). ^{13}C{^{1}H} NMR (100 MHz, $CDCl_3$) δ 164.3, 162.8, 158.7, 151.8, 140.5, 130.1, 126.7, 123.7, 109.2, 107.0, 93.1, 55.6, 54.1, 31.7, 29.6, 29.2, 26.2, 24.0, 22.7, 14.1. HRMS (EI+/magnetic sector) m/z: [M] + calcd for $C_{20}H_{25}Cl_2NO_5$: 429.1110 Found: 429.1130.

6-Methoxy Pseudoarmeniaspirol A (15). N,O-Ketal **5** (38 mg, 0.088 mmol, 1 equiv) was dissolved in DCM (0.05 M), and a tin(IV) chloride solution (0.264 mL of a 1 M solution in DCM, 0.0264 mmol, 3 equiv) was added dropwise. The mixture was stirred at room temperature overnight and quenched with brine. The aqueous layer was then extracted twice with EtOAc (20 mL). The combined EtOAc layers were dried with $MgSO_4$ and concentrated in vacuo. Purification by silica gel chromatography (12.5% EtOAc/hexanes) yielded pure **15** as a yellow oil (17 mg, 0.043 mmol, 49% yield). R_f = 0.4 (20:80 EtOAc:hexanes). ^{1}H NMR (400 MHz, chloroform-*d*) δ 6.93 (d, J = 8.4 Hz, 1H), 6.73 (d, J = 8.5 Hz, 1H), 3.89 (s, 3H), 2.78 (s, 3H), 2.70 (td, J = 7.2, 1.5 Hz, 2H), 1.56 (d, J = 7.3 Hz, 2H), 1.37−1.27 (m, 6H), 0.91−0.86 (m, 3H). ^{13}C{^{1}H} NMR (100 MHz, $CDCl_3$) δ 169.3, 163.8, 161.1, 153.7, 140.6, 128.0, 122.6, 116.8, 110.5, 107.5, 73.5, 56.0, 31.6, 29.1, 28.8, 26.8, 23.6, 22.6, 14.0. HRMS (EI+/magnetic sector) m/z: [M] + calcd for $C_{19}H_{21}Cl_2NO_4$: 397.0848 Found 397.0844.

Pseudoarmeniaspirol A (1). In a round-bottom flask, **15** (17 mg, 0.043 mmol, 1.0 equiv) was dissolved in DCE (0.4 M). The mixture was cooled to 0 °C using an ice bath and BBr_3 solution (0.129 mL of a 1 M solution in DCM, 0.129 mmol, 3.0 equiv) was added dropwise. The reaction was allowed to proceed for 4 h from 0 °C to room temperature. Water was added, and the solution was extracted three times with EtOAc. The organic fractions were combined, washed with brine, dried over $MgSO_4$, and concentrated in vacuo. The final compound was purified from the crude mixture using preparative TLC (25% EtOAc/hexanes) yielding **1** as a tan amorphous solid (13 mg, 78% yield). R_f = 0.3 (20:80 EtOAc:hexanes). ^{1}H NMR (400 MHz, $CDCl_3$) δ 6.83 (d, J = 8.2 Hz, 1H), 6.72 (d, J = 8.2 Hz, 1H), 6.01 (s, 1H), 2.79 (s, 3H), 2.77−2.67 (m, 2H), 1.67−1.55 (m, 2H), 1.41−1.23 (m, 6H), 0.88 (td, J = 6.2, 3.7 Hz, 3H). ^{13}C{^{1}H} NMR (100 MHz, $CDCl_3$) δ 169.3, 164.1, 157.8, 154.2, 140.7, 127.9, 122.6, 115.1, 112.7, 110.1, 73.6, 31.6, 29.1, 28.8, 26.9, 23.7, 22.6, 14.1. HRMS (EI+/magnetic sector) m/z: [M] + calcd for $C_{18}H_{19}Cl_2NO_4$: 383.0691 Found 383.0659.

N-Hexyl-Pseudoarmeniaspirol (16). In a round-bottom flask, **SI2** (19 mg, 0.0405 mmol, 1.0 equiv) was dissolved in DCE (0.4 M). The mixture was cooled to 0 °C using an ice bath and BBr_3 (0.122 mL of a 1 M solution in DCM, 0.122 mmol, 3.0 equiv) was added dropwise. The reaction was allowed to proceed for 4 h from 0 °C to room temperature. Water was added, and the solution was extracted three times with EtOAc. The organic fractions were combined, washed with brine, dried over $MgSO_4$, and concentrated in vacuo. The desired compound (14 mg, 76% yield) was purified from the crude mixture using preparative TLC (20% EtOAc in hexanes) yielding **16** as a white amorphous solid. R_f = 0.35 (20:80 EtOAc:hexanes). ^{1}H NMR (600 MHz, chloroform-*d*) δ 6.82 (d, J = 8.2 Hz, 1H), 6.69 (d, J = 8.2 Hz, 1H), 3.34 (ddd, J = 14.3, 8.8, 7.0 Hz, 1H), 3.09 (ddd, J = 14.5, 8.5, 6.2 Hz, 1H), 2.73 (t, J = 7.6 Hz, 2H), 1.61 (dp, J = 12.4, 6.7, 6.2 Hz, 4H), 1.22−1.11 (m, 12H), 0.91−0.85 (m, 3H), 0.82 (t, J = 7.1 Hz, 3H). ^{13}C{^{1}H} NMR (150 MHz, $CDCl_3$) δ 169.9, 164.2, 157.5, 154.0, 140.6, 128.0, 122.8, 114.9, 112.6, 110.7, 73.1, 42.3, 31.6, 31.1, 29.0, 28.7, 28.1, 26.2, 23.6, 22.6, 22.4, 14.1, 14.0. HRMS (EI+/magnetic sector) m/z: [M] + calcd for $C_{23}H_{29}Cl_2NO_4$: 453.1474 Found 453.1468.

N-Dodecyl-1-methyl-pseudoarmeniaspirol (17). In a round-bottom flask, **SI4** (16 mg, 0.033 mmol, 1.0 equiv) was dissolved in DCE (0.4 M). The mixture was cooled to 0 °C using an ice bath and BBr_3 (0.1 mL of a 1 M solution in DCM, 0.1 mmol, 3.0 equiv) was added dropwise. The reaction was allowed to proceed for 4 h from 0 °C to room temperature. Water was added, and the solution was extracted three times with EtOAc. The organic fractions were combined, washed with brine, dried over $MgSO_4$, and concentrated in vacuo. The product was purified from the crude mixture using Preparative TLC (15% EtOAc in hexanes) affording pure **17** as a clear oil (10 mg, 0.0213 mmol, 64% yield). R_f = 0.2 (10:90 EtOAc:hexanes). ^{1}H NMR (600 MHz, chloroform-*d*) δ 6.83 (d, J = 8.2 Hz, 1H), 6.70 (d, J = 8.2 Hz, 1H), 3.35−3.26 (m, 1H), 3.10 (ddd, J = 14.4, 8.0, 6.5 Hz, 1H), 2.27 (s, 3H), 1.34−1.14 (m, 20H), 0.91−0.85 (m, 3H). ^{13}C{^{1}H} NMR (150 MHz, $CDCl_3$) δ 169.8, 164.2, 157.7, 154.0, 140.5, 128.0, 122.7, 112.2, 110.8, 109.9, 73.2, 42.3, 31.9, 29.64, 29.62, 29.5, 29.37, 29.35, 29.0, 28.2, 26.6, 22.7, 14.1, 8.7. HRMS (EI+/magnetic sector) m/z: [M] + calcd for $C_{24}H_{31}Cl_2NO_4$: 467.1630 Found: 467.1618.

■ ASSOCIATED CONTENT

Data Availability Statement

The data underlying this study are available in the published article and its online supplementary material.

Supporting Information

The Supporting Information is available free of charge at https://pubs.acs.org/doi/10.1021/acs.joc.2c02331.

General methods, ^{1}H and ^{13}C NMR spectra of all compounds, synthetic procedures and annotated data for supplemental compounds, procedures for characterization of biological data, supporting Figures S1−S7 and supporting Table S1 (PDF)

■ AUTHOR INFORMATION

Corresponding Author

https://pubs.acs.org/10.1021/acs.joc.2c02331

Notes

The authors declare no competing financial interest.

https://doi.org/10.1021/acs.joc.2c02331
J. Org. Chem. 2022, 87, 15634−15643

■ ACKNOWLEDGMENTS

Thanks to the John L. Holmes Mass Spectrometry Facility. This work was supported by the Natural Sciences and Engineering Research Council (NSERC) of Canada.

■ REFERENCES

(1) Dufour, C.; Wink, J.; Kurz, M.; Kogler, H.; Olivan, H.; Sablé, S.; Heyse, W.; Gerlitz, M.; Toti, L.; Nußer, A.; Rey, A.; Couturier, C.; Bauer, A.; Brönstrup, M. Isolation and Structural Elucidation of Armeniaspirols A-C: Potent Antibiotics against Gram-Positive Pathogens. *Chem. - Eur. J.* **2012**, *18*, 16123−16128.

(2) Couturier, C.; Bauer, A.; Rey, A.; Schroif-Dufour, C.; Broenstrup, M. Armeniaspiroles, a New Class of Antibacterials: Antibacterial Activities and Total Synthesis of 5-Chloro-Armeniaspirole A. *Bioorg. Med. Chem. Lett.* **2012**, *22*, 6292−6296.

(3) Darnowski, M. G.; Lanosky, T. D.; Labana, P.; Brazeau-Henrie, J. T.; Calvert, N. D.; Dornan, M. H.; Natola, C.; Paquette, A. R.; Shuhendler, A. J.; Boddy, C. N. Armeniaspirol Analogues with More Potent Gram-Positive Antibiotic Activity Show Enhanced Inhibition of the ATP-Dependent Proteases ClpXP and ClpYQ. *RSC Med. Chem.* **2022**, *13*, 436−444.

(4) Arisetti, N.; Fuchs, H. L. S.; Coetzee, J.; Orozco, M.; Ruppelt, D.; Bauer, A.; Heimann, D.; Kuhnert, E.; Bhamidimarri, S. P.; Bafna, J. A.; Hinkelmann, B.; Eckel, K.; Sieber, S. A.; Müller, P. P.; Herrmann, J.; Müller, R.; Winterhalter, M.; Steinem, C.; Brönstrup, M. Total Synthesis and Mechanism of Action of the Antibiotic Armeniaspirol A. *Chem. Sci.* **2021**, *12*, 16023−16034.

(5) Durham, D. G.; Rees, A. H. Chlorination of Pyrroles. Part I. *Can. J. Chem.* **1971**, *49*, 136−138.

(6) Cue, B. W., Jr.; Chamberlain, N. Pyoluteorin Derivatives. II. Synthetic Approaches to Pyrrole Ring Substituted Pyoluteorins. *J. Heterocycl. Chem.* **1981**, *18*, 667−670.

(7) Ciamician, G.; Silber, P. Ueber Die Einwirkung von Unterchlorigsauren Und Unterbromigsauren Alkalien Auf Pyrrol. *Ber. Dtsch. Chem. Ges.* **1884**, *17*, 1743−1745.

(8) El Khadem, H.; Kemler, L. A.; El-Shafei, Z. M.; Rahman, M. M. A. A.; El Sadany, S. Synthesis and Mass Spectra of N-aryl-pyrroles and Their Chlorination Products. *J. Heterocyclic Chem.* **1972**, 1413−1417.

(9) Daniels, P. H.; Wong, J. L.; Atwood, J. L.; Canada, L. G.; Rogers, R. D. Unreactive 1-Azadiene and Reactive 2-Azadiene in Diels-Alder Reaction of Pentachloroazacyclopentadienes. *J. Org. Chem.* **1980**, *45*, 435−440.

(10) Briggs, P. R.; Shannon, T. W. Heat of formation of the methoxycarbonyl ion. *J. Am. Chem. Soc.* **1969**, *91*, 4307−4309.

(11) Olah, G. A.; Schilling, P.; Bollinger, J. M.; Nishimura, J. Stable Carbocations. CLXIII. Complexing Ionization, and Fragmentative Alkylcarbenium Ion Formation from Alkyl Haloformates, Thiolhaloformates, and Halosulfites with Antimony Pentafluoride. *J. Am. Chem. Soc.* **1974**, *96*, 2221−2228.

(12) Moriyama, K.; Nakamura, Y.; Togo, H. Oxidative Debenzylation of N-Benzyl Amides and O-Benzyl Ethers Using Alkali Metal Bromide. *Org. Lett.* **2014**, *16*, 3812−3815.

(13) Tutino, F.; Papeo, G.; Quartieri, F. Acid Catalyzed Halogen Dance on Deactivated Pyrroles. *J. Heterocycl. Chem.* **2010**, *47*, 112−117.

(14) Zhou, H.; Li, X.; Li, Y.; Zhu, X.; Zhang, L.; Li, J. Synthesis and Bioevaluation of 1-Phenylimidazole-4-Carboxylic Acid Derivatives as Novel Xanthine Oxidoreductase Inhibitors. *Eur. J. Med. Chem.* **2020**, *186*, No. 111883.

(15) Nishimoto, Y.; Babu, S. A.; Yasuda, M.; Baba, A. Esters as Acylating Reagent in a Friedel-Crafts Reaction: Indium Tribromide Catalyzed Acylation of Arenes Using Dimethylchlorosilane. *J. Org. Chem.* **2008**, *73*, 9465−9468.

(16) Chavan, S. P.; Garai, S.; Dutta, A. K.; Pal, S. Friedel-Crafts Acylation Reactions Using Esters. *Eur. J. Org. Chem* **2012**, *2012*, 6841−6845.

(17) Shao, C.; Shi, G.; Zhang, Y.; Pan, S.; Guan, X. Palladium-Catalyzed C-H Ethoxycarbonyldifluoromethylation of Electron-Rich Heteroarenes. *Org. Lett.* **2015**, *17*, 2652−2655.

(18) Chadwick, D. J.; Chambers, J.; Meakins, G. D.; Snowden, R. L. Esters of Furan-, Thiophen-, and *N*-Methylpyrrole-2-Carboxylic Acids. Bromination of Methyl Furan-2-Carboxylate, Furan-2-Carbaldehyde, and Thiophen-2-Carbaldehyde in the Presence of Aluminium Chloride. *J. Chem. Soc., Perkin Trans. 1* **1973**, *0*, 1766−1773.

(19) Barker, P.; Gendler, P.; Rapoport, H. 2-(Trichloroacetyl)-Pyrroles as Intermediates in the Preparation of 2, 4-Disubstituted Pyrroles. *J. Org. Chem.* **1978**, *43*, 4849−4853.

(20) Shih, B. H.; Basha, R. S.; Lee, C. F. Nickel-Catalyzed Cross-Coupling of Aryl Redoxactive Esters with Aryl Zinc Reagents. *ACS Catal.* **2019**, *9*, 8862−8866.

(21) Foley, L. H.; Habgood, G. J.; Gallagher, K. S. Assignment of the ^{13}C NMR Shifts of Brominated Pyrrole Derivatives. *Magn. Reson. Chem.* **1988**, *26*, 1037−1038.

(22) Gao, S.; Bethel, T. K.; Kakeshpour, T.; Hubbell, G. E.; Jackson, J. E.; Tepe, J. J. Substrate Controlled Regioselective Bromination of Acylated Pyrroles Using Tetrabutylammonium Tribromide (TBABr3). *J. Org. Chem.* **2018**, *83*, 9250−9255.

(23) Wakeham, R. J.; Taylor, J. E.; Bull, S. D.; Morris, J. A.; Williams, J. M. J. Iodide as an Activating Agent for Acid Chlorides in Acylation Reactions. *Org. Lett.* **2013**, *15*, 702−705.

(24) Laha, J. K.; Kaur Hunjan, M.; Hegde, S.; Gupta, A. Aroylation of Electron-Rich Pyrroles under Minisci Reaction Conditions. *Org. Lett.* **2020**, *22*, 1442−1447.

(25) Alniss, H. Y.; Witzel, I. I.; Semreen, M. H.; Panda, P. K.; Mishra, Y. K.; Ahuja, R.; Parkinson, J. A. Investigation of the Factors That Dictate the Preferred Orientation of Lexitropsins in the Minor Groove of DNA. *J. Med. Chem.* **2019**, 10423.

(26) Sindhuja, E.; Ramesh, R.; Balaji, S.; Liu, Y. Direct Synthesis of Amides from Coupling of Alcohols and Amines Catalyzed by Ruthenium(II) Thiocarboxamide Complexes under Aerobic Conditions. *Organometallics* **2014**, *33*, 4269−4278.

(27) Allmann, T. C.; Moldovan, R. P.; Jones, P. G.; Lindel, T. Synthesis of Hydroxypyrrolone Carboxamides Employing Selectfluor. *Chem. - Eur. J.* **2016**, *22*, 111−115.

(28) Borrero, N. V.; Aponick, A. Total Synthesis of Acortatarin A Using a Pd(II)-Catalyzed Spiroketalization Strategy. *J. Org. Chem.* **2012**, *77*, 8410−8416.

(29) Loader, C. E.; Anderson, H. J. Pyrrole Chemistry. Part XI. Some Reactions of the Pyrrole Grignard Reagent with Alkyl Carbonates and Alkyl Thiocarbonates. *Can. J. Chem.* **1971**, *49*, 45−48.

(30) Fu, J.; Wurzer, N.; Lehner, V.; Reiser, O.; Davies, H. M. L. Rh(II)-Catalyzed Monocyclopropanation of Pyrroles and Its Application to the Synthesis Pharmaceutically Relevant Compounds. *Org. Lett.* **2019**, *21*, 6102−6106.

(31) Chen, Q.; Chen, H.; Meng, X.; Ma, Y. Lewis Acid Assisted Diels-Alder Reaction with Regio- and Stereoselectivity: Anti-1,4-Adducts with Rigid Scaffolds and Their Application in Explosives Sensing. *Org. Lett.* **2015**, *17*, 5016−5019.

https://doi.org/10.1021/acs.joc.2c02331
J. Org. Chem. 2022, 87, 15634−15643